APRIL 1969

ANCHAM

# ANALYTICAL CHEMISTRY

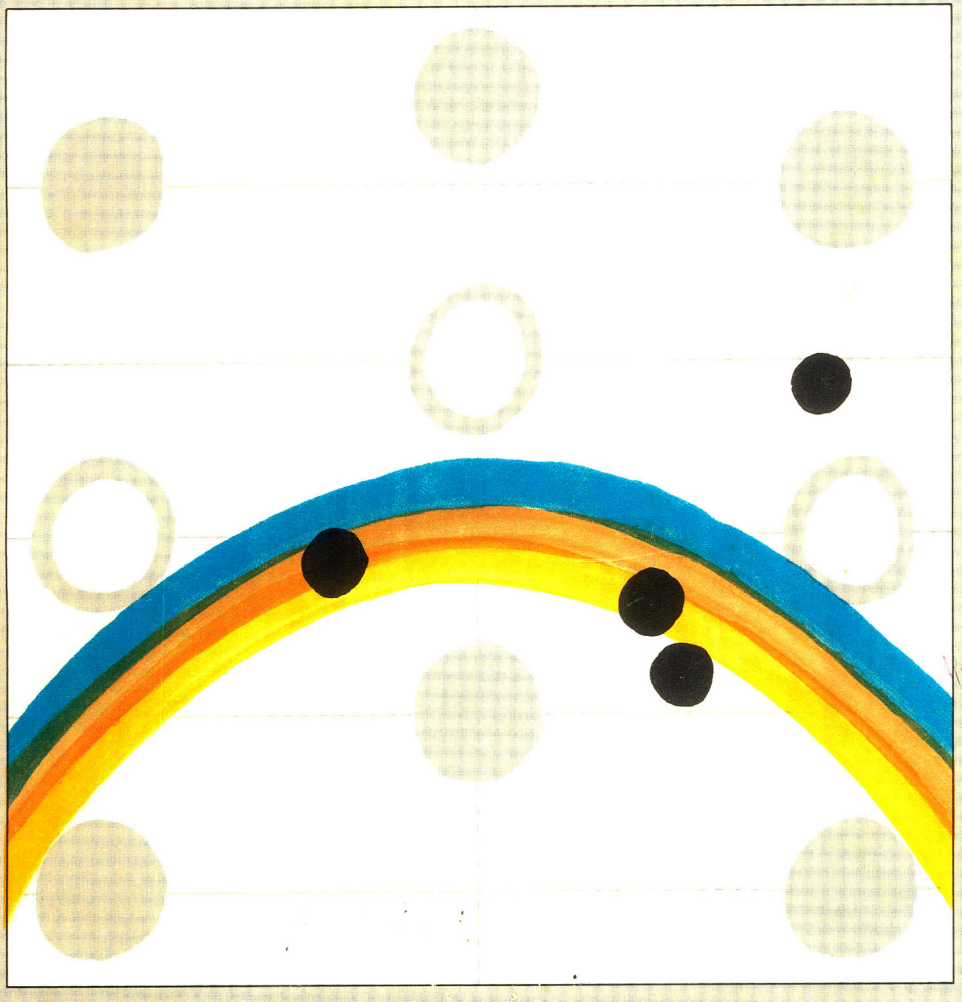

*Rutherford Scattering and Channeling—A Useful Combination for Chemical Analysis of Surfaces . . . Page 26 A*

# GET THE LATEST FACTS ON THE NEW AAA-3

The Atomic Analyzer™ is a superior, precision, reliable, compact, versatile spectrophotometer. It is capable of analyzing metals and semi-metals in absorption, emission, and fluorescence modes. Its "flexibly" designed sampling compartment accepts many different burner systems. A triple lamp-bank maintains two lamps on pre-warm, one in operation. A high-resolution monochromator, solid state electronics, 1x, 5x, 10x, and 20x scale expansion, wide scan speed range, 7½" scale, tautband meter, and many other features make the AAA-3 the most useable instrument of its kind available. Full service back-up. For our latest brochure, circle reader service number or write direct.




AZTEC Instruments, Inc.
132 Water Street, South Norwalk, Conn. 06854

Manufactured under license from Commonwealth Scientific and Industrial Research Organization, Australia

See ACS Laboratory Guide for All Products/Sales Office
Circle No. 21 on Readers' Service Card

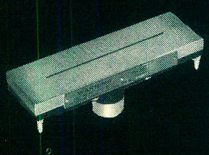

**BURNERS**
Standard Solutions Nebulizers . . .

complete line for Atomic Absorption and Atomic Emission



**HOLLOW CATHODE LAMPS**
Full line of lamps kept in stock, available for immediate delivery

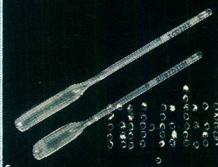

**ELECTRODELESS DISCHARGE LAMPS**
Immediate delivery of electrodeless discharge lamps — some 35 elements

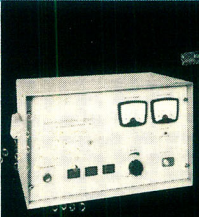

**MICROWAVE GENERATORS**
These units are designed for use in both atomic absorption and atomic fluorescence

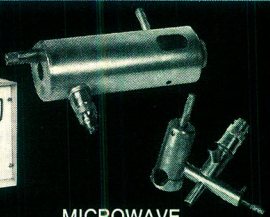

MICROWAVE CAVITIES
Two cavities are available for use with the microwave generator and electrodeless discharge lamps . . .

# This new Amino Acid Analyzer is now running sample #72

## (The operator hasn't been needed since the start of #1)

And when she comes back she'll appreciate again just how complete a job we've done on the new Beckman Model 121 Automatic Amino Acid Analyzer. We figured that, since our Analyzers are already in a class by themselves, our *fully automatic* version should be something special. It is.

The 121 uses all the basic "innards" of the proven Model 120C, but does 2½ to 3 times as many analyses. It can use any methodology – single or multi-column. With the two-column protein hydrolyzate method, 36 complete analyses (72 samples) can be run over a weekend. The programmer is so versatile that you can change from one method to a completely different one in seconds.

With the 121, you also get the finest field service in the instrumentation field and access to a cadre of knowledgeable applications research people to call on for any answers you need. We work hard to make the finest amino acid analyzers in the world, and we work hard to back them up.

For full information on the 121, the 120C and the modular 116, write Spinco Division, Palo Alto, Calif. 94304 for brochure SB-333.

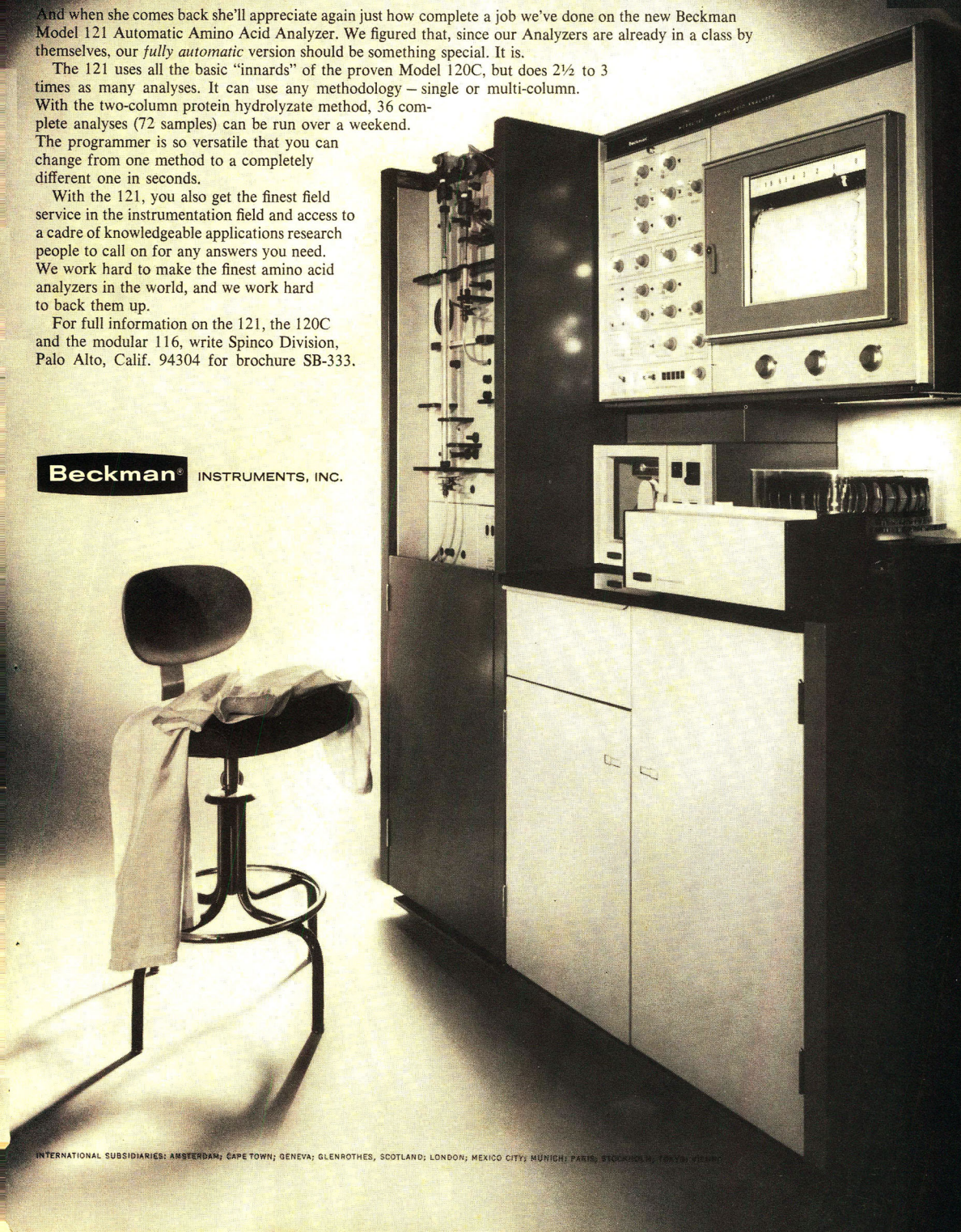

Beckman® INSTRUMENTS, INC.

INTERNATIONAL SUBSIDIARIES: AMSTERDAM; CAPE TOWN; GENEVA; GLENROTHES, SCOTLAND; LONDON; MEXICO CITY; MUNICH; PARIS; STOCKHOLM; TOKYO; VIENNA

VOLUME 41, NO. 4 APRIL 1969

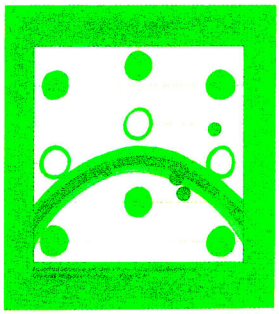

This Month's Cover. The possibilities of Rutherford scattering and channeling in chemical analysis of surfaces are discussed in the Report for Analytical Chemists. The channeling effect is depicted on the cover. See Page 26 A.

© Copyright 1969

by the American Chemical Society

MANUSCRIPT REQUIREMENTS published in December 1968 issue, page 2269, outlines scope and copy requirements to be observed in preparing manuscripts for consideration. Manuscript (4 copies) should be submitted to ANALYTICAL CHEMISTRY, 1155 Sixteenth St., N.W., Washington, D. C. 20036.

The American Chemical Society assumes no responsibility for the statements and opinions advanced by contributors to its publications. Views expressed in the editorials are those of the editors and not necessarily represent the official position of the American Chemical Society.

1969 Subscription Rates

| | 1 yr. | 2 yr. | 3 yr. |
|---|---|---|---|
| Members, domestic and foreign | $ 4.00 | $ 7.00 | $10.00 |
| Nonmembers, domestic and Canada | 5.00 | 9.00 | 12.00 |
| Nonmembers, foreign except Canada | 15.00 | 27.50 | 40.00 |

Postage: Canada and Pan-American Union, $2.50; foreign, $3.50. Single copies: current, $2.00 except Annual Reviews and Laboratory Guide issues, $3.00 each. Postage: Canada and Pan-American Union, $0.15; foreign, $0.20. Rates for back issues and volumes are available from Special Issues Sales Dept., 1155 Sixteenth St., N.W., Washington, D. C. Claims for missing numbers will not be allowed if received more than 60 days from date of mailing plus time normally required for postal delivery of journal and claim. No claims allowed because of failure to notify the Subscription Service Department of a change of address or because copy is "missing from files."

Published monthly with Review Issue added in April and a Laboratory Guide in July by the American Chemical Society, from 20th and Northampton Sts., Easton, Pa. 18042; Executive Offices, Editorial Headquarters, and Subscription Service Department, 1155 Sixteenth St., N.W., Washington, D. C. 20036; Advertising Office, 430 Park Ave., New York, N.Y. 10022. ANALYTICAL CHEMISTRY and other ACS periodicals are available on microfilm. For information write to: MICROFILM, Special Issues Sales, American Chemical Society, 1155 Sixteenth St., N.W., Washington, D.C. 20036.

Second class postage paid at Easton Pa.

CHANGE OF ADDRESS: Notify Subscription Service Department, American Chemical Society, 1155 Sixteenth St., N.W., Washington, D. C. 20036. Such notification should include both old and new addresses, with ZIP code numbers, and be accompanied by mailing label from a recent issue. Allow four weeks for change to become effective.

ANCHAM

# ANALYTICAL CHEMISTRY

Contents

**REPORT FOR ANALYTICAL CHEMISTS**

Rutherford scattering and channeling as a means of chemical analysis is discussed by Drs. Mackintosh and Davies of Atomic Energy of Canada **26 A**

**NEWS**

The 22nd Annual Summer Symposium on Analytical Chemistry, which deals with modern instrumental techniques for elemental analysis, will be held June 11 to 13, at the University of Georgia, Athens, Ga. The program for the 20th Mid-America Symposium on Spectroscopy, May 12 to 15, Chicago, Ill. is given **45 A**

**BOOK REVIEWS**

Books on reagent chemicals, NMR spectroscopy, microanalysis, polarography, and the molecular structure aspects of NMR (French) are reviewed by David H. Freeman, J. L. Sudmeier, E. W. D. Huffman, J. J. Lingane, and J. P. Laurent, respectively **87 A**

**EDITORS' COLUMN**

The first set of 1000 evaluated infrared spectra prepared under supervision of the Joint Committee on Atomic and Molecular Physical Data is now available; **Analytical Chemistry's** Editor is on sabbatical in Europe **97 A**

**INSTRUMENTATION**

R. D. Conlon of Nester/Faust discusses liquid chromatography detectors; Ralph Mueller comments **107 A**

**EDITORIAL**

A five-year collective index covering the years 1964 through 1968 will be available to **Analytical Chemistry** subscribers by midyear 1969 **553**

**Author Index** **6 A**

**Briefs** **11 A**

**Calendar of Events** **72 A**

**New Chemicals** **139 A**

**Future Articles** **154 A**

**Manufacturers' Literature** **140 A**

**New Products** **123 A**

**Readers' Information Service** **119 A**

**Scheduled Technical Courses** **70 A**

← Circle No. 97 on Readers Service Card

**Interfacially Active Acids in a California Crude Oil. Isolation of Carboxylic Acids and Phenols.** W. K. Seifert and W. G. Howells 554

**Effect of Phenols on the Interfacial Activity of Crude Oil (California) Carboxylic Acids and the Identification of Carbazoles and Indoles.** W. K. Seifert 562

**Sulfur Compound Type Distributions in Petroleum Using an In-Line Reactor or Pyrolysis Combined with Gas Chromatography and a Microcoulometric Sulfur Detector.** Harry V. Drushel 569

**Composition of Asphalt Based on Generic Fractionation, Using Solvent Deasphaltening, Elution–Adsorption Chromatography, and Densimetric Characterization.** L. W. Corbett 576

**Relative Oxygen Absorption and Volatility Properties of Submicron Films of Asphalt Using the Quartz Crystal Microbalance.** W. H. King, Jr., and L. W. Corbett 580

**Mechanism of Trace Counterion Transport through Ion-Exchange Membranes.** W. J. Blaedel, T. J. Haupert, and M. A. Evenson 583

**On Rapid Laboratory Dialysis.** L. C. Craig and Hao-Chia Chen 590

**Spectrophotometric Reaction Rate Method for Determination of Bismuth Using a Dimeric Heteropolymolybdate.** L. G. Hargis 597

**Use of Ion Selective Electrodes in Enzymic Analysis. Cation Electrodes for Deaminase Enzyme Systems.** G. G. Guilbault, R. K. Smith, and J. G. Montalvo, Jr. 600

**An Automatic Multiple-Column Gas Chromatographic Analysis of Methanol Synthesis Reaction Mixtures.** R. L. Burnett 606

**Rapid and Selective Method for the Spectrophotometric Determination of Niobium.** R. Villarreal and S. A. Barker 611

**Design of Membrane-Covered Polarographic Gas Detectors.** D. P. Lucero 613

**Electrochemical Reduction of Benzil in Alkaline Methanol–Water Solution.** H. E. Stapelfeldt and S. P. Perone 623

**Photo-Electrochemical Behavior of Benzil. Potentiostatic Monitoring Following Flash-Photolysis.** H. E. Stapelfeldt and S. P. Perone 628

**Polarographic Irreversibility of the Copper (II) Pyrophosphate System.** G. W. Higgins and P. E. Sturrock 633

**Electrochemical Reduction Products of Chromium (VI) in Molten Lithium Chloride–Potassium Chloride Eutectic.** J. H. Propp and H. A. Laitinen 644

**Quantitative Determination of 1-Naphthylamine and 2-Naphthylamine in Cigarette Smoke.** Y. Masuda and D. Hoffmann 650

**Electrochemical Kinetics of the Ferri–Ferrocyanide Couple on Platinum.** P. H. Daum and C. G. Enke 653

**Improved Resolution in High-Sensitivity Dual-Label Gas Radiochromatography.** P. J. Thomas and H. J. Dutton 657

**Quantitative Aspects of Nuclear Quadrupole Resonance Spectrometry of Inorganics and Minerals.** H. D. Schultz and C. Karr, Jr. 661

## Notes

**Cation Exchange. Separation–X-Ray Spectrometric Determination of Scandium in Plutonium.** E. A. Hakkila, R. G. Hurley, and G. R. Waterbury 665

**Infrared Spectra of Compounds Separated by Thin-Layer Chromatography Using a Potassium Bromide Micropellet Technique.** W. J. de Klein 667

**Radiochemical Determination of Technetium-99 in Environmental Water Samples.** N. W. Golchert and J. Sedlet 669

**Solvent Sublation of Iron(III)–Chloride by Tri-n-Octylamine.** J. Elhanan and B. L. Karger 671

**Derivative Spectrometry and Its Application to the Analysis of Unresolved Bands.** I. G. McWilliam 674

**Anion Determination with Ion Selective Electrodes Using Gran's Plots. Application to Fluoride.** Arnaldo Liberti and Marco Mascini 676

**Correction: Spectrophotometric Determination of Trace Amounts of Silver (I).** M. T. El-Ghamry and R. W. Frei 610

## Aids for Analytical Chemists

**Qualitative Thin-Layer Chromatography of Some Irritants.** W. D. Ludemann, M. H. Stutz, and S. Sass 679

**A Simple Micropelleting Technique.** W. J. de Klein and K. Ulbert 682

**Diamond-Windowed Cell for Spectrophotometry of Molten Fluoride Salts.** L. M. Toth, J. P. Young, and G. P. Smith 683

**Technique for Obtaining Absorption Spectra of Insoluble Metal Chelate Polymers.** P. S. Shetty and Q. Fernando 685

**A Modified Differential Scanning Calorimeter Technique Utilizing a Quenched Polymer Reference Material.** C. R. Foltz and P. V. McKinney 687

ห้องสมุด กรมวิทยาศาสตร์
3 ธ.ค. 2512

# SCINTILLATION COUNTING?

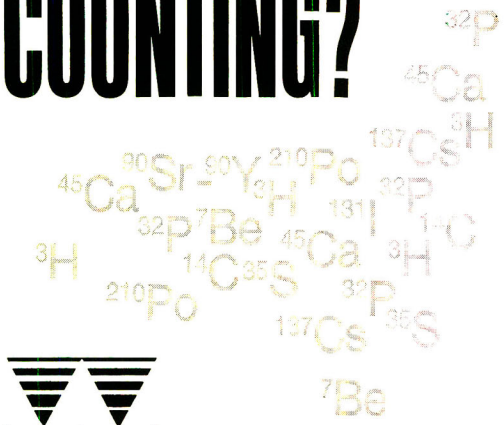


Whatman®

## GLASS FIBER PAPERS

In liquid scintillation counting of filtered materials, all filtration media may look alike, but only Whatman Glass Fiber Filter Papers allow high counting efficiency, by eliminating quenching of the radiation or absorption of the scintillation encountered with other filtration media. Glass Fiber Papers also have the ability to absorb twice as much material, letting you work with larger samples . . . at one-tenth the cost of other filtration media.

Whatman Glass Fiber Filter Papers offer a unique combination of properties: fast flow rate, finer particle retention, high resistance to chemical attack, and temperature stability . . . making them ideal for water and sewage analysis . . . cell harvesting . . . bacterial filtration . . . clinical sampling . . . dust sampling and gas testing. They are made entirely from borosilicate glass microfibers, without the addition of organic fibers or binders of any kind.

*For further information, call or write for our free Glass Fiber Filter Paper Data Sheet.*

reeve angel

H. Reeve Angel & Co., Inc.—Sole Distributor in North America
9 Bridewell Place, Clifton, New Jersey 07014
Phone: (201) 773-5800

® Whatman is the registered trademark of W & R Balston, Ltd., Maidstone, Kent, England

**Circle No. 2 on Readers' Service Card**




## Author Index


| | | | |
|---|---|---|---|
| Barker, S. A. | 611 | Laitinen, H. A. | 644 |
| Blaedel, W. J. | 583 | Liberti, A. | 676 |
| Burnett, R. L. | 606 | Lucero, D. P. | 613 |
| | | Ludemann, W. D. | 679 |
| Chen, H.-C. | 590 | | |
| Corbett, L. W. | 576, 580 | McKinney, P. V. | 687 |
| Craig, L. C. | 590 | McWilliam, I. G. | 674 |
| | | Mascini, M. | 676 |
| Daum, P. H. | 653 | Masuda, Y. | 650 |
| Drushel, H. V. | 569 | Montalvo, J. G., Jr. | 600 |
| Dutton, H. J. | 657 | | |
| | | Perone, S. P. | 623, 628 |
| Elhanan, J. | 671 | Propp, J. H. | 644 |
| Enke, C. G. | 653 | | |
| Evenson, M. A. | 583 | Sass, S. | 679 |
| | | Schultz, H. D. | 661 |
| Fernando, Q. | 685 | Sedlet, J. | 669 |
| Foltz, C. R. | 687 | Seifert, W. K. | 554, 562 |
| | | Shetty, P. S. | 685 |
| Golchert, N. W. | 669 | Smith, G. P. | 683 |
| Guilbault, G. G. | 600 | Smith, R. K. | 600 |
| | | Stapelfeldt, H. E. | 623, 628 |
| Hakkila, E. A. | 665 | Sturrock, P. E. | 633 |
| Hargis, L. G. | 597 | Stutz, M. H. | 679 |
| Haupert, T. J. | 583 | | |
| Higgins, G. W. | 633 | Thomas, P. J. | 657 |
| Hoffmann, D. | 650 | Toth, L. M. | 683 |
| Howells, W. G. | 554 | | |
| Hurley, R. G. | 665 | Ulbert, K. | 682 |
| | | Villarreal, R. | 611 |
| Karger, B. L. | 671 | | |
| Karr, C., Jr. | 661 | Waterbury, G. R. | 665 |
| King, W. H., Jr. | 580 | | |
| de Klein, W. J. | 667, 682 | Young, J. P. | 683 |



**ANALYTICAL CHEMISTRY**

A-page Reprints 1969

**BIND important A-page material with original research papers**

Volume 41 A-page reprints will include the Reports for Analytical Chemists, Instrumentation Columns, Book Reviews, Editors' Columns, and other features.

Orders may be placed now for delivery in January 1970

Price for set of A-page reprints is $3

Send name and address to ACS and reserve your set of A-page reprints

TO: Special Issues Sales
American Chemical Society
1155 Sixteenth St., N.W.
Washington, D.C. 20036

Bills will be mailed when reprints are available for distribution

gilford®

# UV—VIS SPECTROPHOTOMETERS

GILFORD INSTRUMENT LABORATORIES, INC.
OBERLIN, OHIO 44074

## *FLEXIBILITY . . .*

### *to match your growing needs in . . .*

- *analytical ultracentrifuge patterns*
- *rapid sampling*
- *data logging systems*

VISIT OUR EXHIBIT — FASEB MEETINGS
SPACES T4, 5 & U4, 5—ATLANTIC CITY

## SCAN ANALYTICAL ULTRA-CENTRIFUGE PATTERNS OR POLYACRYLAMIDE GELS

Gilford "building block" accessories such as the Model 2410 Linear Transport provide extra flexibility to meet your growing needs. The Model 2410 can handle such materials as photographic emulsions, polyacrylamide gels cylinders and slabs for analysis, possibly with your own spectrophotometer. The materials can be analyzed in both the UV and VIS, as the monochromator provides energy throughout this range.

The need for complex single-purpose instruments is eliminated.



(ACTUAL SIZE)

## RACK AFTER RACK OF SAMPLES PROCESSED SIMPLY AND RAPIDLY

The vacuum operated Gilford Model 2443 Rapid Sampling System requires samples of only 0.7 ml. and can process over 300 per hour. The cuvette remains in the measuring beam for both filling and cleaning. Sample handling and cuvette breakage are minimized. The Kel-F construction is chemically inert.

Samples can be analyzed with either UV or VIS energy, as the Model 2443 is adaptable to Gilford UV-VIS Spectrophotometers, and certain quality monochromators.

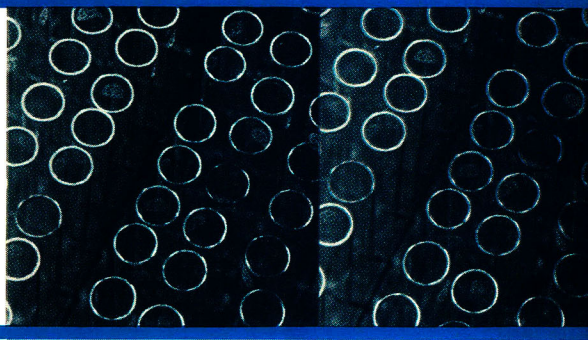

## TIME SHARE COMPUTER ANALYSIS WITH THE GILFORD DATA LOGGING SYSTEM

Analog to digital conversion, digital multiplexing, and the conversion to punch tape provide you with data that can then be transmitted to a computer.

A demonstration of enzyme rate analysis by a time share computer will be made at our FASEB exhibit. The Gilford Data Logging System will take the four enzymes under study and convert absorbance and time data into computer acceptable form. This data will then be transmitted by computer link (com-share) to a computer facility. The results will be returned to the exhibit floor via teletype.

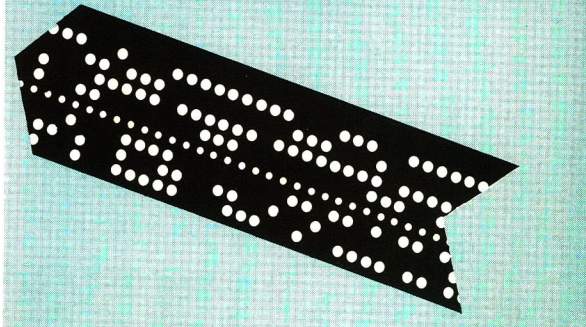

Circle No. 44 on Readers' Service Card
See ACS Laboratory Guide for All Products/Sales Office

# FULLY AUTOMATIC UNATTENDED

# CHN+O

102 AS-E

## DETERMINATIONS with

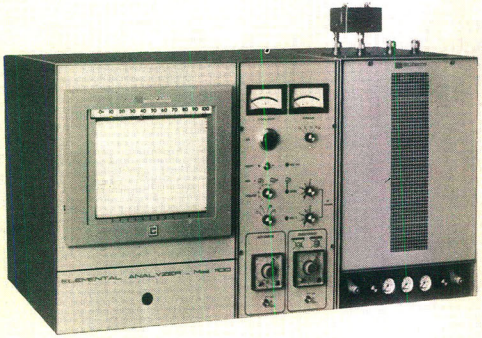

## CARLO ERBA MOD. 1100 ELEMENTAL ANALYZER

A UNIQUE MULTISEATS SAMPLE INJECTOR PLUS A SPECIAL DESIGNED DUAL REACTOR-COLUMN TEAM WITH A NOVEL DYNAMIC COMBUSTION IN OXYGEN ENRICHED ATMOSPHERE TECHNIQUE ARE THE OUTSTANDING FEATURES OF THIS NEW TRULY AUTOMATIC ANALYZER.

YOU HAVE ONLY TO LOAD THE SAMPLE MAGAZINE, SWITCH THE INSTRUMENT « ON » AND

**23 CHN DETERMINATIONS IN FOUR HOURS**
or:
**23 CHN+O DETERMINATIONS IN SIX HOURS**

WILL BE, STEP BY STEP, AUTOMATICALLY PROCESSED.

FOR MORE INFORMATIONS, PLEASE ASK FOR DT CHN+O

CARLO ERBA
SCIENTIFIC INSTRUMENTS DIVISION

VIA CARLO IMBONATI, 24
I 20159 - MILANO

Circle No. 42 on Readers' Service Card

# FREE!

## 16-PAGE CATALOG ON TEFLON LABWARE

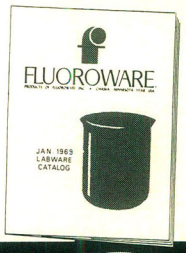


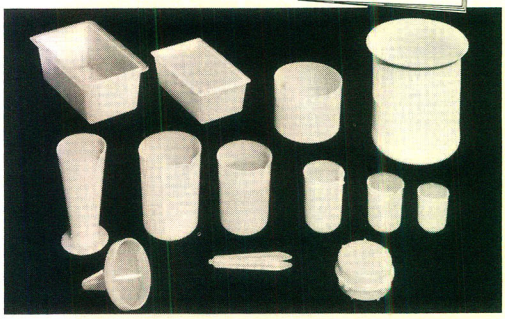

Fluoroware labware is made of FEP Teflon*, the closest thing there is to an ideal labware material—inert, useable at extreme temperatures, unwettable and unbreakable. And Fluoroware knows the secret of molding Teflon into perfect shapes with good see-through properties.

Write for a copy of Fluoroware's "Labware Catalog", including information on its physical and chemical properties.

*DuPont Trademark

FLUOROWARE.
Chaska, Minnesota 55318 • Phone 612-448-3131

Circle No. 120 on Readers' Service Card

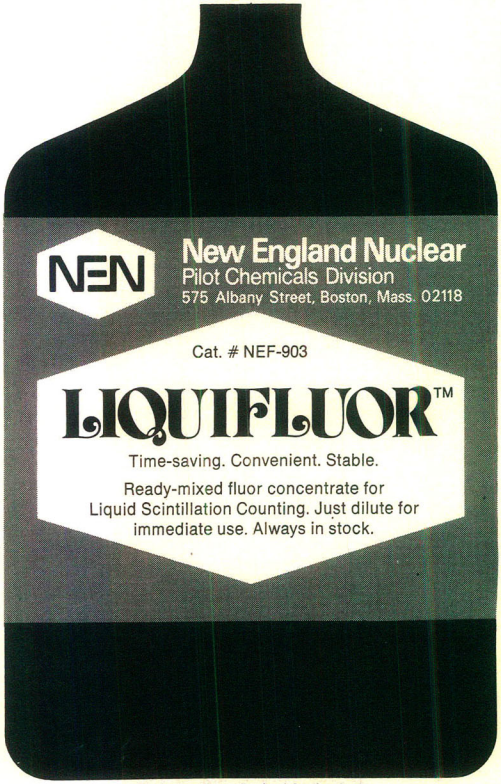


Circle No. 135 on Readers' Service Card

# The Simple Photometer

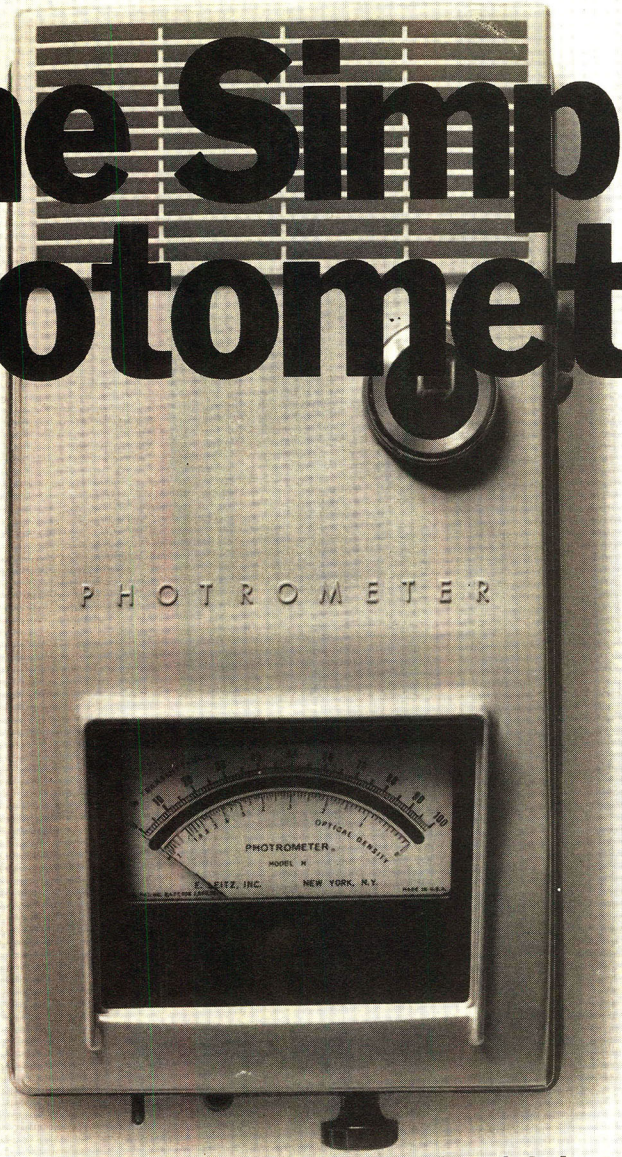


**(All the sophistication is on the *inside*, where it belongs.)**

The Leitz® Model M Photrometer® is so very simple to operate. All you do is turn one knob to make one adjustment. That's all. No mathematics. No complicated controls. It's pre-calibrated for 40 determinations; for test results, you simply check the meter reading against the calibration tables in the hardcover handbook that comes with every instrument.

What's more, this fine photometer is consistently stable... astonishingly accurate. Two of the Leitz quality features that are responsible: a built-in voltage stabilizer; light bulbs, with soldered leads and two-prong plugs, that are individually tested for the right filament alignment.

Over 27,000 Leitz Photrometers are now in use. For more information, write to Leitz.



A square precision cuvette containing distilled water or a "blank" is placed in the Photrometer and the meter needle is set at 100.

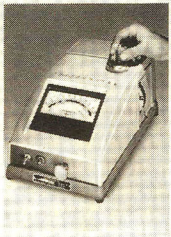

The standardizing cuvette or the "blank" is immediately replaced with the cuvette containing the unknown and the meter is then read.



The operator refers to the appropriate table in the handbook which indicates the concentration of the unknown for the particular meter reading.

Leitz®

E. Leitz, Inc., 468 Park Avenue South, New York, N.Y. 10016

69768

# Mettler automatic thermal instruments give you

## 1. melting and boiling points objectively
## 2. precise control in thermal microscopy
## 3. dropping points electronically

### Melting and Boiling Points by the Numbers

**1** Our melting/boiling point instrument, the Mettler FP-1, automatically runs melting and boiling point tests and displays results on its digital readout panel. All you do is (1) select a heating rate, (2) insert the sample, (3) press the "start" lever, (4) read the objective results to 0.1°C on the readout panel. You do not have to make subjective choices of the melting or boiling temperature, nor must you "eyeball" and apply corrections to mercury-in-glass thermometers.

### Up to 50 mpd/hr

From 30 to 50 melting point determinations can be done per hour with the FP-1, depending on the heating rate. Any of five heating rates can be selected: 10°C/min for quick survey work; 1°, 2°, 3°C/min for routine tests or where a precision of 0.5°C is adequate, and 0.2°C/min for precise determinations to a reproducibility of ±0.1°C.

### Take Three

You can make three melting point determinations simultaneously, thus identifying crystalline compounds by mixed melting point determinations in one rapid operation. Used with a standard time-base recorder, the Mettler FP-1 can provide curves showing changes in light transmission as sample temperature increases. This technique is

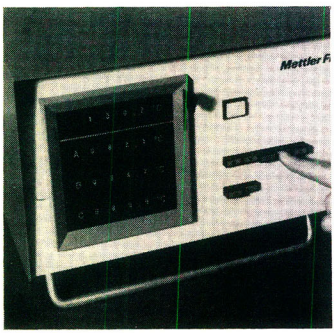

Digital readout of temperatures

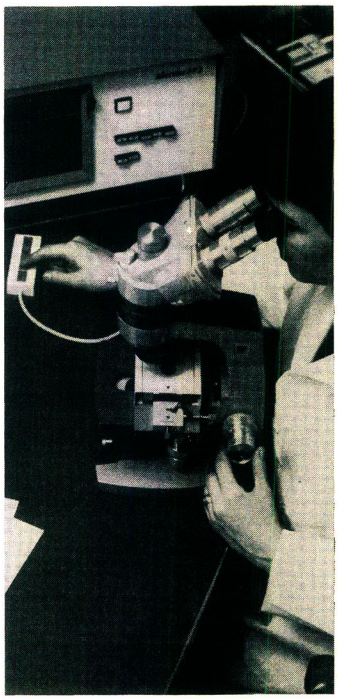

Pushbutton control of thermal events

useful in measuring melting ranges; in the construction of phase diagrams; and in analyzing the purity of compounds.

### Thermal Microscopy

**2** For thermal microanalyses, attach the Mettler FP-2 to your microscope and take fingertip command of the thermal process. You never lose visual contact with the sample because the FP-2 has a pushbutton controller to increase, decrease or maintain sample temperature at a precise value. With the same controller you can record the exact temperature at which any three thermal events occur. These include beginning of melt, end of melt, phase change, or any of several conditions in the crystallization process. Temperatures are recorded in digital form on an indicator panel. The top digital indicator shows the temperature of the sample chamber. The indicators below it record the three individual temperature events you selected. These studies in thermal microscopy can be conducted at the same five heating rates available with the FP-1.

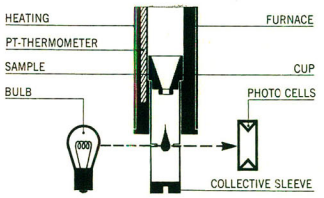


Determines dropping points electronically

### Good at the First Drop

**3** The Mettler FP-3 automatically determines dropping points of lubricating greases, ointments and edible fats in just a few minutes. The procedure conforms to the ASTM D-566 and D-2265 test specifications. When the first drop of grease to fall from a heated sample cup crosses a light beam, the dropping point is registered on the digital readout panel. The FP-3 is simple to operate: select desired temperature program, put sample cup in furnace and read dropping point. Up to 12 dropping point determinations can be conducted per hour over a temperature range of −20°C to +300°C. Heating rates are also selectable and include 0.2, 1.0, 2.0, 3.0 and 10.0°C/min rates. Accuracy of temperature indication at a heating rate of 0.2°C/min is ±0.1°C. Reproducibility (at 0.2°C/min) is ±0.2°C.

If you want to take the subjectivity out of your melting, boiling, or dropping point determinations, ask Mettler for FP-1 and FP-3 literature. Need precise control in your thermal microanalyses? Request literature on the Mettler FP-2. Or request a demonstration or trial in your own lab of these instruments. Write Mettler Instrument Corporation, 20 Nassau Street, Princeton, New Jersey 08540.

Mettler®

Circle No. 57 on Readers' Service Card
See ACS Laboratory Guide for All Products/Sales Office

# Carbohydrate chromatography... now automatic!

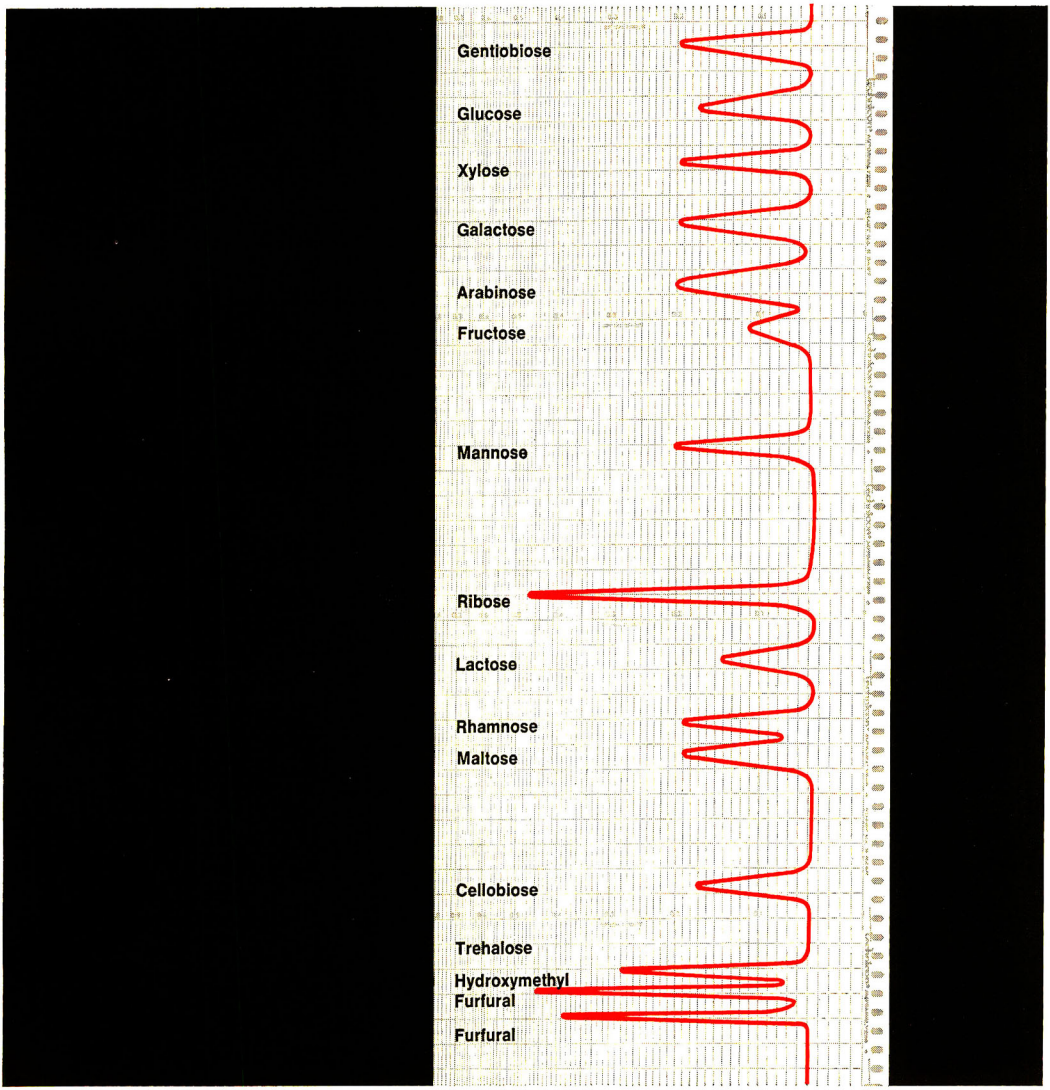


■ The 15-sugar chromatogram reproduced about one-sixth size above was produced on the new, automated Technicon® Sugar Chromatography System in 7½ hours. Notice that furfural, hydroxymethylfurfural, pentoses, hexoses, and disaccharides are well resolved.

■ This new system is uniquely sensitive (to 1 microgram of ribose, for example).

■ If the ability to quickly separate and quantitate a mixture of carbohydrates would help your work, please write for our 6-page booklet and a typical chromatogram.

**TECHNICON CORPORATION • Tarrytown, New York 10591**

T.M.

Circle No. 148 on Readers' Service Card

See ACS Laboratory Guide for All Products/Sales Office

# an old friend gets a face lifting

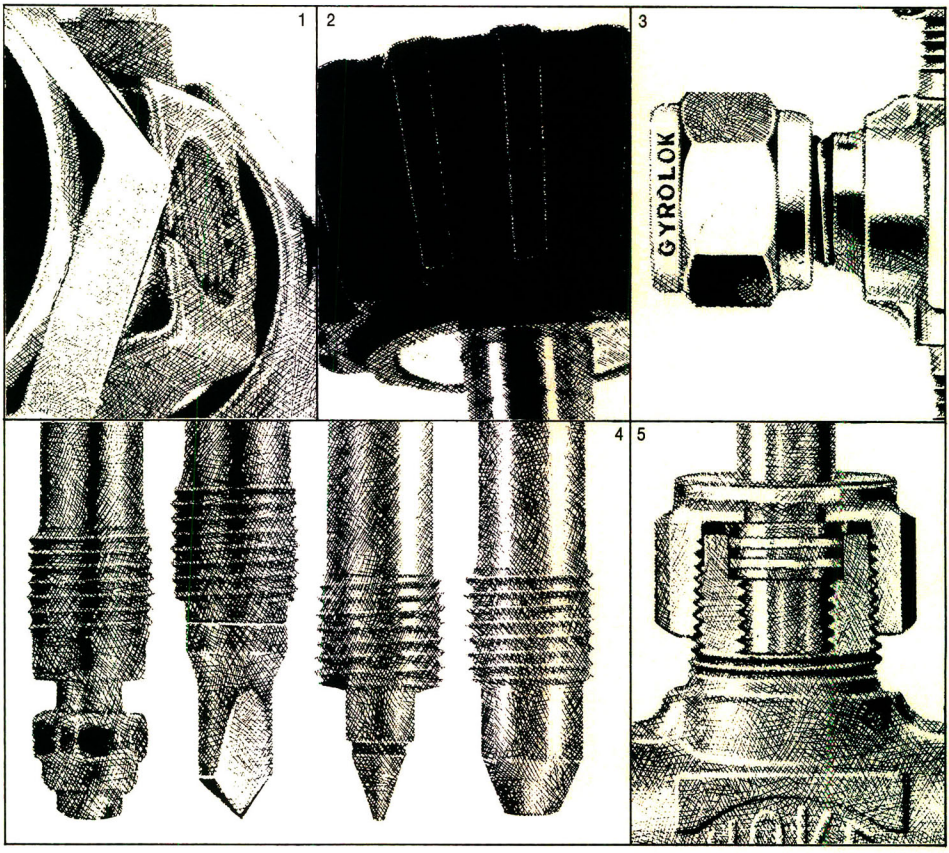


Our line of multi-purpose 300 series forged needle valves are the by-word in the industry. If you're an oldtimer, you probably know that we make them in brass, 303 and 316 stainless, monel, and aluminum, in both straight and angle patterns.

But did you realize that we've streamlined the body flats for easier installation (1), used a new easy to grip handle (2), and added our own Gyrolok® tube fitting connections (3) to an already long list of pipe ended models?

On the inside, you'll find that we now offer a choice of four stem points (4), each designed to control precisely the flow required in your application, be it fine metering or positive shut-off. As for the valve packing (5), our exclusive Dyna-Pak (wafers of TFE & metal) comes in all models with O-rings available as an option. And if you're a panel mounting enthusiast, all models can be mounted.

For more information about these and other varieties, ask your nearby Hoke-Gyrolok distributor for a copy of our Miniature Valve Catalog or write to us directly.

*See our catalog in the Fluid System Section of Sweet's Industrial Catalog.*

**HOKE INCORPORATED • ONE TENAKILL PARK • CRESSKILL, NEW JERSEY**

HOKE

Circle No. 47 on Readers' Service Card
See ACS Laboratory Guide for All Products/Sales Office

Circle No. 157 on Readers' Service Card →

# A C BRIEFS

Highlights
of Articles in
This Issue

### Interfacially Active Acids in a California Crude Oil. Isolation of Carboxylic Acids and Phenols

The isolation, separation and preliminary identification of the most active fractions are reported in this first part of a study to determine the chemical structure of the compounds in these particular fractions.

**WOLFGANG K. SEIFERT and W. GLENN HOWELLS,** Chevron Research Co., Richmond, Calif. 94802

Anal. Chem., 41, 554 (1969)

### The Effect of Phenols on the Interfacial Activity of Crude Oil (California) Carboxylic Acids and the Identification of Carbazoles and Indoles

This second part of the study explores the quantitative relation between carboxylic acid content and interfacial activity, along with the effect of phenols on this activity.

**WOLFGANG K. SEIFERT,** Chevron Research Co., Richmond, Calif. 94802

Anal. Chem., 41, 562 (1969)

### Sulfur Compound Type Distributions in Petroleum Using an In-Line Reactor or Pyrolysis Combined with Gas Chromatography and a Microcoulometric Sulfur Detector

The method reported has an analysis time of 1 hour. Precision for each of the sulfur types is within 2 or 3% based on the total sulfur content.

**HARRY V. DRUSHEL,** Esso Research Laboratories, Humble Oil and Refining Laboratories, P.O. Box 2226, Baton Rouge, La. 70821

Anal. Chem., 41, 569 (1969)

### Composition of Asphalt Based on Generic Fractionation, Using Solvent Deasphaltening, Elution–Adsorption Chromatography, and Densimetric Characterization

The method involves solvent deasphaltening for recovery of asphaltenes, followed by elution–adsorption chromatography to yield saturates, naphthene-aromatics, and polar-aromatics. Average chemical structures are defined by densimetric characterization.

**L. W. CORBETT,** Esso Research & Engineering Co., P.O. Box 51, Linden, N.J. 07036

Anal. Chem., 41, 576 (1969)

### Relative Oxygen Absorption and Volatility Properties of Submicron Films of Asphalt Using the Quartz Crystal Microbalance

Changes in the mass of a 0.3-$\mu$ film deposited on a piezoelectric quartz crystal, caused by the uptake of oxygen or by its volatilization are detected and recorded by measuring the change in oscillation frequency.

**W. H. KING, Jr., and L. W. CORBETT,** Esso Research and Engineering Co., Linden, N.J. 07036

Anal. Chem., 41, 580 (1969)

### Mechanism of Trace Counterion Transport through Ion-Exchange Membranes

An equation for the flux of a trace counterion between two solutions separated by an ion-exchange membrane is derived and experimentally verified.

**W. J. BLAEDEL, T. J. HAUPERT, and M. A. EVENSON,** Chemistry Department, University of Wisconsin, Madison, Wis. 53706

Anal. Chem., 41, 583 (1969)

### On Rapid Laboratory Dialysis

An improved countercurrent "thin-film" dialysis column which will clear the tritium count in tritiated water on a single pass requiring 6–8 min to the extent of at least six orders of magnitude is described.

**LYMAN C. CRAIG and HAO-CHIA CHEN,** The Rockefeller University, New York, N.Y. 10021

Anal. Chem., 41, 590 (1969)

### Spectrophotometric Reaction Rate Method for Determination of Bismuth Using a Dimeric Heteropolymolybdate

The relative precision for the analysis of 4 ppm bismuth is better than 0.5% and of 0.04 ppm bismuth, the lower concentration limit, better than 10%. The method is simple and requires only 20–60 seconds of reaction time.

**L. G. HARGIS,** Department of Chemistry, Louisiana State University in New Orleans, New Orleans, La. 70122

Anal. Chem., 41, 597 (1969)

### Use of Ion Selective Electrodes in Enzymic Analysis. Cation Electrodes for Deaminase Enzyme Systems

The response, selectivity, and use of the cation electrode for determination of $NH_4^+$ activity have been investigated in a study of the kinetics of deaminase enzyme systems. A precision and accuracy of about 2.5% for all substrates and enzymes are reported.

**G. G. GUILBAULT, R. K. SMITH, and J. G. MONTALVO, Jr.,** Chemistry Department, Louisiana State University in New Orleans, New Orleans, La. 70122

Anal. Chem., 41, 600 (1969)

### An Automatic, Multiple-Column Gas Chromatographic Analysis of Methanol Synthesis Reaction Mixtures

A multiple-column automatic process chromatographic analysis is described for handling the diverse products encountered during the synthesis of methanol by CO hydrogenation.

**ROBERT L. BURNETT,** Chevron Research Co., Richmond, Calif. 94802

Anal. Chem., 41, 606 (1969)

# New!
# Tri-Carb® Automatic Sample Oxidizer

## Combusts 40 $^3H$ Samples an hour for Liquid Scintillation Counting

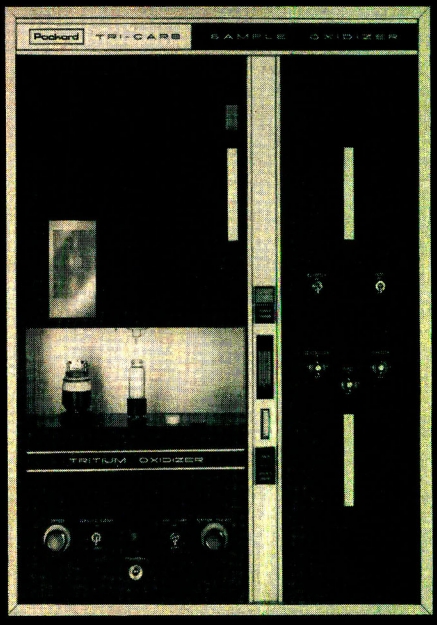


Packard

Say goodbye to time-consuming and troublesome methods of preparing tritium samples for liquid scintillation counting. The new Model 300 Tri-Carb Sample Oxidizer does the work automatically, at a rate that makes the method practical for virtually every experiment involving tritium as a tracer.

The Tri-Carb Sample Oxidizer provides recoveries of 97-99%+, with routine achievement of 1% standard deviation. (This can be reduced to 0.3% in many cases, making the deviation essentially that resulting from dispensing errors and counting statistics.) Count rates from the same sample are 25% to 100% higher than those obtained with classical methods.

The new instrument, based on the Kaartinen patents*, combines the speed of closed system flame combustion with the advantage of unlimited tritium sample size. The only manual operations are positioning of the sample and counting vial, and pushbutton initiation of the combustion process. The balance of the cycle—including addition of scintillator—is carried out through automatic sequencing within the Sample Oxidizer.

Nitrogen purging is used to eliminate oxygen quenching, and because no manual handling is necessary during the cycle, the method is relatively insensitive to the working habits of the operator. Thus, a high degree of sample standardization is achieved.

For complete specifications write for Bulletin 300Q to Packard Instrument Company, Inc., 2200 Warrenville Road, Downers Grove, Illinois 60515 or Packard Instrument International S.A., Talstrasse 39, 8001 Zurich, Switzerland.

*Dr. Niilo Kaartinen, Dept. of Physiology, University of Turku, Finland

A SUBSIDIARY OF AMBAC INDUSTRIES, INC. AMBAC

Circle No. 64 on Readers' Service Card

### Rapid and Selective Method for the Spectrophotometric Determination of Niobium

The color intensity of a Nb–BPHA–SCN complex in toluene is measured at 365 mμ. Beer's law is obeyed from 0 to 50 μg Nb; the relative precision of the method is ±3% at the 0.01% Nb level in uranium-fissium alloy.

**ROBERT VILLARREAL and SPENCE A. BARKER,** Argonne National Laboratory, Idaho Division, Idaho Falls, Idaho 83401

Anal. Chem., 41, 611 (1969)

### Design of Membrane-Covered Polarographic Gas Detectors

Reported are the fundamental principles and techniques in the design of membrane-covered polarographic gas detectors for measuring the partial pressure of a particular molecular species present in gas mixtures and/or dissolved in liquids.

**DANIEL P. LUCERO,** Electro-Analytical Transducer Corporation, Fullerton, Calif. 92633

Anal. Chem., 41, 613 (1969)

### Electrochemical Reduction of Benzil in Alkaline Methanol–Water Solution

DME polarography, stationary electrode polarography, and step functional controlled-potential electrolysis are used to provide qualitative and quantitative characterization of the benzil reduction process in alkaline solution.

**H. E. STAPELFELDT and S. P. PERONE,** Department of Chemistry, Purdue University, Lafayette, Ind. 47907

Anal. Chem., 41, 623 (1969)

### Photo-Electrochemical Behavior of Benzil. Potentiostatic Monitoring Following Flash-Photolysis

Electrochemical monitoring techniques have been applied to the study of rapid secondary photolytic processes following flash-irradiation of benzil solutions.

**H. E. STAPELFELDT, and S. P. PERONE,** Department of Chemistry, Purdue University, Lafayette, Ind. 47907

Anal. Chem., 41, 628 (1969)

### Polarographic Irreversibility of the Copper (II) Pyrophosphate System

The true heterogeneous rate constant for electron transfer has been determined to be $1.8 \times 10^{-1}$ at pH 9, and $3.8 \times 10^{-1}$ at pH 3. The rate of electron transfer is therefore always polarographically reversible.

**GIBSON W. HIGGINS,** Wabash College, Crawfordsville, Ind. 47933, and **PETER E. STURROCK,** Georgia Institute of Technology, Atlanta, Ga. 30332

Anal. Chem., 41, 633 (1969)

### Electrochemical Reduction Products of Chromium (VI) Molten Lithium Chloride–Potassium Chloride Eutectic

The chemical composition and structure of the reduction product of chromate in the presence of Mg(II) are investigated. The thermal and pressure stability of the compound are also studied.

**J. H. PROPP and H. A. LAITINEN,** Department of Chemistry and Chemical Engineering, University of Illinois, Urbana, Ill. 61801

Anal. Chem., 41, 644 (1969)

### Quantitative Determination of 1-Naphthylamine and 2-Naphthylamine in Cigarette Smoke

The mainstream of an 85-mm U.S. nonfilter cigarette contains 27 ng of 1-naphthylamine and 22 ng of 2-naphthylamine. The latter represents the first isolation of a known bladder carcinogen from a non-occupational respiratory environment, but no biological significance can yet be determined.

**YOSHITO MASUDA and DIETRICH HOFFMANN,** Division of Environmental Cancerigenesis, Sloan-Kettering Institute for Cancer Research, New York, N.Y. 10021

Anal. Chem., 41, 650 (1969)

### Electrochemical Kinetics of the Ferri–Ferrocyanide Couple on Platinum

Charge transfer kinetics are measured by the current impulse technique. The degree of oxidation of the Pt electrode strongly affects the measured heterogeneous rate constant but not the transfer coefficient.

**P. H. DAUM and C. G. ENKE,** Chemistry Department, Michigan State University, East Lansing, Mich. 48823

Anal. Chem., 41, 653 (1969)

### Improved Resolution in High-Sensitivity Dual-Label Gas Radiochromatography

This paper describes the application of digital computer techniques to speed the analysis of counting data, to improve the sensitivity and resolution of the analysis, and to plot the individual isotopic curves.

**PAUL J. THOMAS and H. J. DUTTON,** Northern Regional Research Laboratory, Peoria, Ill. 61604

Anal. Chem., 41, 657 (1969)

### Quantitative Aspects of Nuclear Quadrupole Resonance Spectrometry of Inorganics and Minerals

NQR is used for spectrometric analyses of synthetic mixtures and natural ores. The operating parameters for the instrument and the effect of the physical state of the sample for quantitative use are determined.

**HARRY D. SCHULTZ and CLARENCE KARR, Jr.,** Morgantown Coal Research Center, Bureau of Mines, U.S. Department of the Interior, Morgantown, W.Va. 26505

Anal. Chem., 41, 661 (1969)

DSTDP?

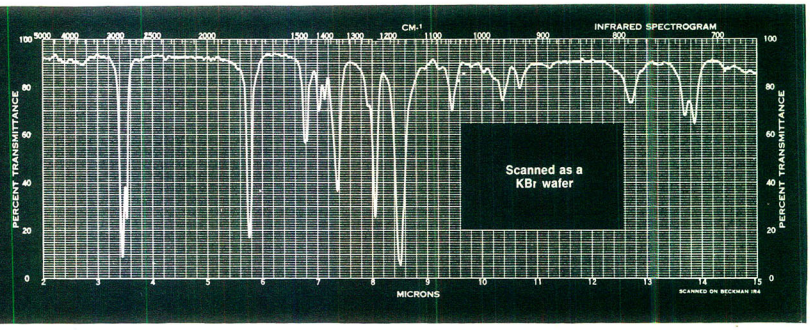


DLTDP?

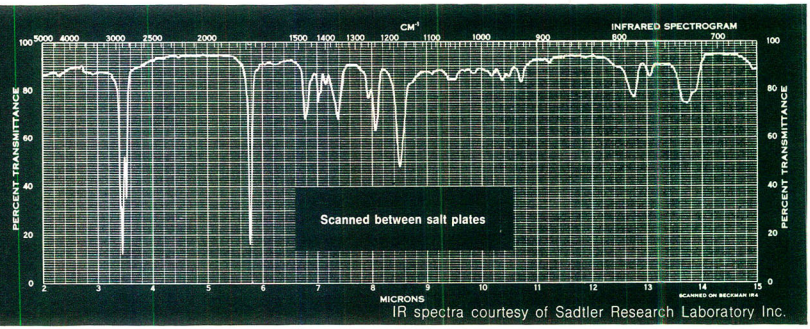


IR spectra courtesy of Sadtler Research Laboratory Inc.

## Only the liquid chromatographer knows for sure.

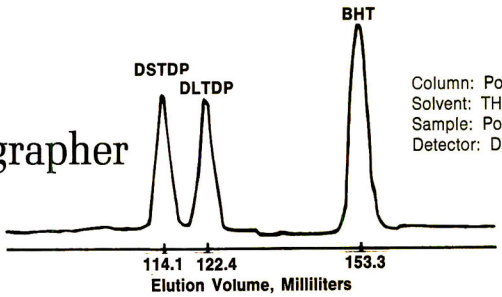


Column: Poragel A
Solvent: THF @ 1 ml/min
Sample: Polymer additive mixture
Detector: Differential refractometer

Identifying unknown compounds with closely matching IR spectra used to be one of the knottiest problems in analytical chemistry. Combining liquid chromatography with IR, however, makes the solution a routine operation.

Take the two spectra shown above. They represent two compounds (distearylthiodipropionate and dilaurylthiodipropionate) that would be extraordinarily difficult to differentiate by traditional methods. But the ALC-100 fast liquid chromatograph will separate them for you by molecular size differences. And provide you with the ultra-pure fractions you need to do subsequent IR testing for functional group identification. In addition, the response of the ALC-100's detector is a measure of the concentration of each compound present.

Together, the two techniques give you accurate molecular structure confirmation: a sort of poor man's mass spectrometer.

Far from being a limited technique, the combination of LC and IR lends itself to a diversity of analytical applications associated with the identification of unknown compounds, reaction products and by-products, additives, and impurities. A recent paper[1] on the subject discusses a variety of these problems and amply demonstrates how well the LC/IR technique solves them.

If you'd like more information, write us for a copy of the above-mentioned paper. We have some literature on the latest advances in fast liquid chromatography that you might also find interesting. Waters Associates, Inc., 61 Fountain Street, Framingham, Mass. 01701.

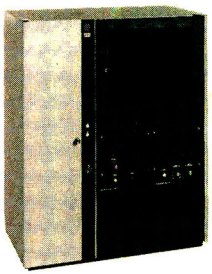

WATERS ASSOCIATES

4337

[1] "Analytical Synergism: Gel Permeation Chromatography + Infrared Spectrometry Attack Complex Organic Mixtures." H. L. Spell, Dow Chemical Company, presented at ASTM E-19 committee, Cincinnati, Ohio, Sept. 25, 1968.

Circle No. 83 on Readers' Service Card

See ACS Laboratory Guide for All Products/Sales Office

## Notes

### Cation Exchange Separation–X-Ray Spectrometric Determination of Scandium in Plutonium

A rapid method for determining scandium present in concentrations between 0.05 and 0.4% in alloys with plutonium is reported. The relative standard deviation is approximately 2% for determining 50 to 400 μg of scandium.

**E. ARNOLD HAKKILA, RONALD G. HURLEY, and GLENN R. WATERBURY,** The Los Alamos Scientific Laboratory, University of California, Los Alamos, N.M. 87544

Anal. Chem., 41, 665 (1969)

### Infrared Spectra of Compounds Separated by Thin-Layer Chromatography Using a Potassium Bromide Micropellet Technique

Contamination partly imposes on this technique the lower limit of amount of compound that can be treated; this limit ranges from 1–2 μg for relatively nonpolar compounds to 10–20 μg for strongly hydrogen-bonded compounds.

**W. J. de KLEIN,** Laboratory of Organic Chemistry, State University of Leiden, Leiden, The Netherlands

Anal. Chem., 41, 667 (1969)

### Radiochemical Determination of Technetium-99 in Environmental Water Samples

With the radiochemical procedure described, technetium-99 can be determined at levels as low as 0.5 dpm per liter of water, especially in naturally-occurring water. Large numbers of environmental water samples can be analyzed.

**NORBERT W. GOLCHERT and JACOB SEDLET,** Argonne National Laboratory, Argonne, Ill. 60439

Anal. Chem., 41, 669 (1969)

### Solvent Sublation of Iron (III)–Chloride by Tri-n- Octylamine

The solvent sublation of ferric ion from hydrochloric acid–dioxane aqueous solutions into anisole by tri-*n*-octylamine are studied. A possible extraction process mechanism is suggested.

**JACOB ELHANAN and BARRY L. KARGER,** Department of Chemistry, Northeastern University, Boston, Mass. 02115

Anal. Chem., 41, 671 (1969)

### Derivative Spectrometry and Its Application to the Analysis of Unresolved Bands

An oscillating plate differentiator is used in conjunction with a Grubb-Parsons type S.4 infrared monochromator in the reported derivative technique for the quantitative analysis of unresolved bands.

**I. G. McWILLIAM,** Central Research Laboratories, Imperial Chemical Industries of Australia and New Zealand Ltd., Newson Street, Ascot Vale, Victoria 3032, Australia

Anal. Chem., 41, 674 (1969)

### Anion Determination with Ion Selective Electrodes Using Gran's Plots. Application to Fluoride

The described method, permitting the weighting of several data points, is more accurate than a single point direct potentiometry measurement and yields satisfactory results for a number of applications.

**ARNALDO LIBERTI and MARCO MASCINI,** Istituto Chimica Analitica, Universitá di Roma, Rome, Italy

Anal. Chem., 41, 676 (1969)

## Aids for Analytical Chemists

### Qualitative Thin-Layer Chromatography of Some Irritants

**WILLIAM D. LUDEMANN, MARTIN H. STUTZ, and SAMUEL SASS,** Chemical Research Laboratory, Edgewood Arsenal, Md. 21010

Anal. Chem., 41, 679 (1969)

### A Simple Micropelleting Technique

**W. J. de KLEIN and K. ULBERT,** Laboratory of Organic Chemistry, State University of Leiden, Leiden, The Netherlands

Anal. Chem., 41, 682 (1969)

### Diamond-Windowed Cell for Spectrophotometry of Molten Fluoride Salts

**L. M. TOTH, J. P. YOUNG, and G. P. SMITH,** Oak Ridge National Laboratory, Oak Ridge, Tenn. 37830

Anal. Chem., 41, 683 (1969)

### Technique for Obtaining Absorption Spectra of Insoluble Metal Chelate Polymers

**P. S. SHETTY and QUINTUS FERNANDO,** Department of Chemistry, University of Arizona, Tucson, Ariz. 85721

Anal. Chem., 41, 685 (1969)

### A Modified Differential Scanning Calorimeter Technique Utilizing a Quenched Polymer Reference Material

**CARL R. FOLTZ and PAUL V. McKINNEY,** Armstrong Cork Company, Lancaster, Pa. 17604

Anal. Chem., 41, 687 (1969)

# In the field, or in the lab.






# Here's the pH meter that travels with you to the job.

Indoors, our model PBL plugs into the line; outside, you switch on the batteries (and detach the line cord if it's in the way). With its strong steel case, taut-band meter, and solid state circuitry, the rugged PBL is indifferent to the trials of travel.

Put it down flat, stand it on end, or prop it at an angle with the handle. It reads accurately in all these positions. A support rod, which mounts to either side of the case, pivots through 360° to put the electrodes where you want them.

Add to all this a full complement of operating facilities—pH and MV ranges, two-point calibration, Karl Fischer circuitry, recorder output, provision for automatic temperature control—and you have a lot of pH meter for $215.

Write us, or ask your Sargent-Welch representative for full details. 8-228




SARGENT-WELCH

*Scientific instruments, apparatus, chemicals.*
Sargent-Welch Scientific Company
4647 Foster Ave.; Chicago, Ill. 60630

Chicago/Anaheim, Calif./Birmingham
Cincinnati/Cleveland/Dallas/Denver
Detroit/Springfield, N.J./Toronto, Canada

**Circle No. 146 on Readers' Service Card**

**See ACS Laboratory Guide for All Products/Sales Office**

# A few months ago you'd have said impossible.

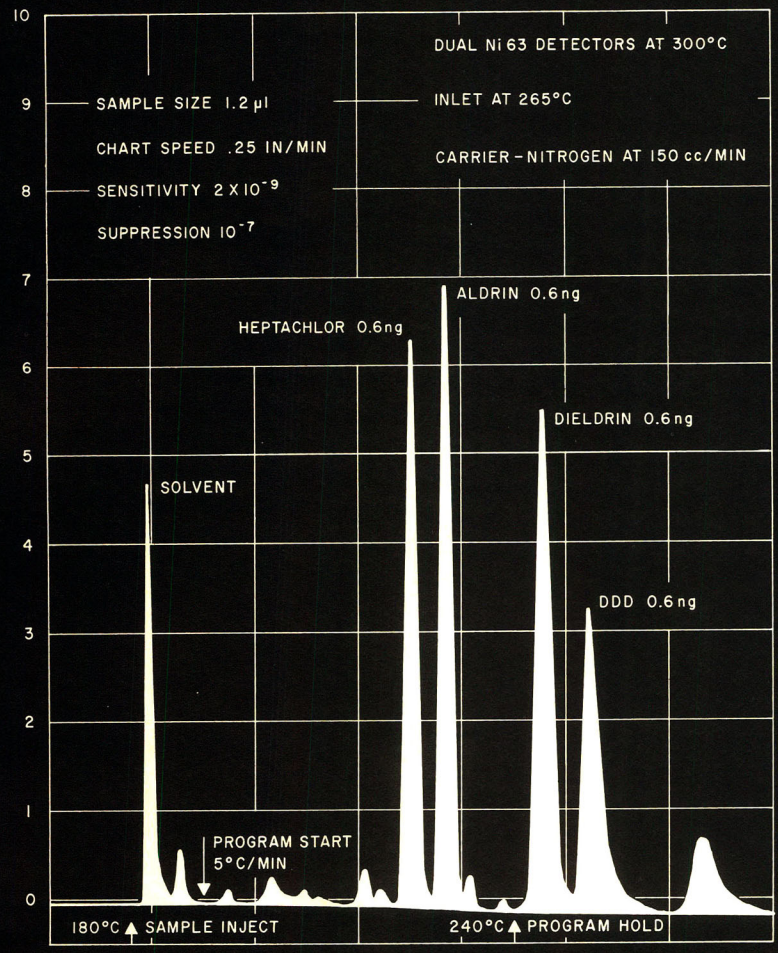


## (And you'd have been right.)

Until we came up with our dual-electron capture detector, it was impossible to run a temperature program as shown above. You know what happened when you tried it. You got base line shifts of such great magnitude that the method was obviated. But with this new Bendix lab chromatograph, you can temperature-program with little or no effect on base line within ranges of ambient to 300° C.

The key to this new unit is our dual-electron capture detector (nickel-63). Both cells are held at exact isothermal conditions with matched background currents. Using the dual-column method, one column acts as the reference and is routed to one of the detector cells which acts as the reference detector. The other receives the sample.

You'll see improved separations and be able to use the full sensitivity of this technique in obtaining quantitative and qualitative measurements. Make it possible. Get the facts. Write: The Bendix Corporation, Process Instruments Division, Ronceverte, West Virginia 24970.

**Bendix**

Circle No. 99 on Readers' Service Card
See ACS Laboratory Guide for All Products/Sales Office

# the next giant step in laboratory automation

# ...now...for less than $16,

The HP Model 7600A Chromatograph System is a truly automatic analytical system that takes over the traditional work of the chromatographer from sample measurement and injection to computation.

Capable of making replicate runs of as many as 36 different liquid samples *completely unattended,* the 7600A System relieves the analyst of all the repetitive chores that have until now occupied most of his time and releases him for more creative work.

Moreover, the 7600A System does these tasks more accurately, consistently and reliably than the most skilled technician . . . and at a fraction of the cost.

The Model 7600A Chromatograph System does its work in four stages:

**Automatic Sample Measurement and Injection.** Preload the 7600A with as many as 36 samples, set the controls and push the start button . . . then let the 7600A automatically clean the syringe, measure the selected sample volume and inject it into the gas chromatograph . . . repeating the process in replicate (if desired) for each of the 36 samples . . . automatically.

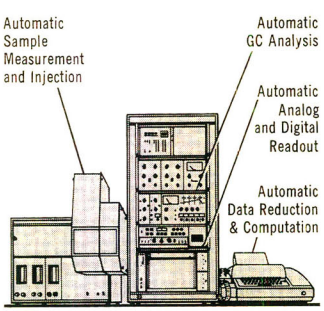


**Automatic GC Analysis.** Preset all pertinent GC run conditions —detector parameters, temperatures, oven program, gas flow rates—and the 7600A guides the GC through the program, resets it for the next run, and repeats the cycle . . . automatically.

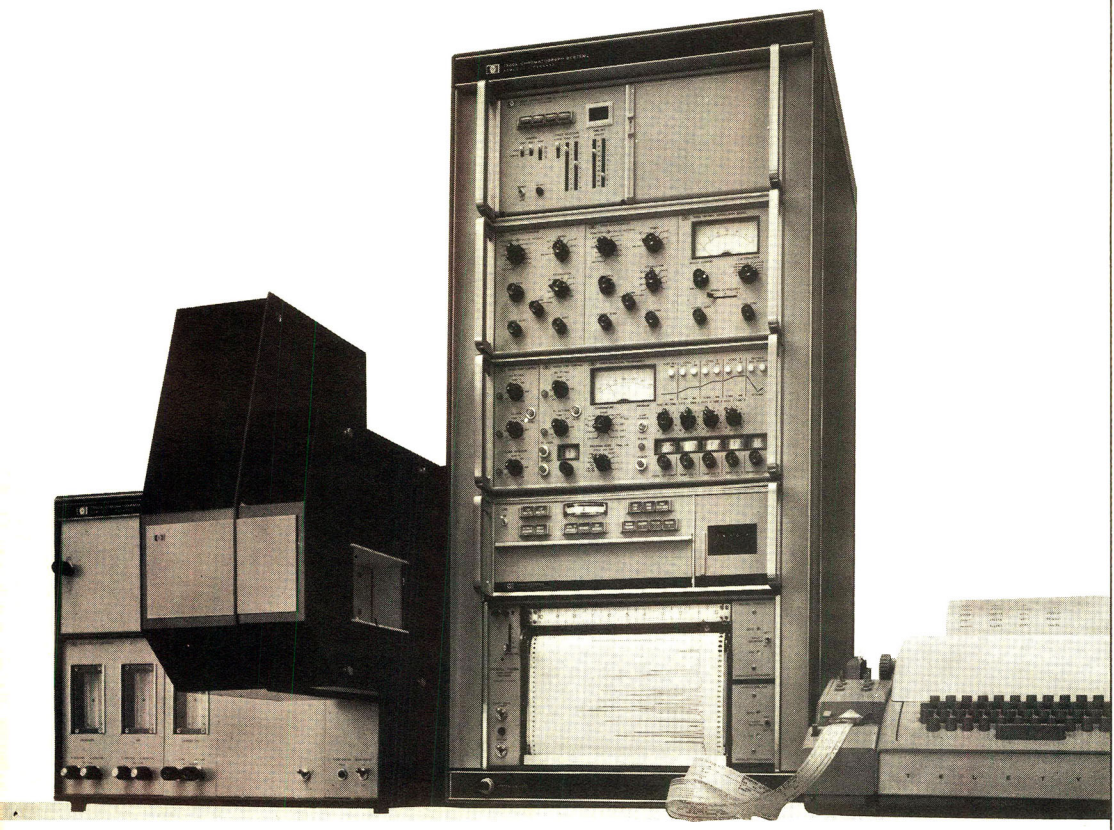

**Automatic Analog and Digital Readout.** With every sample run, the 7600A produces not only a full-size chromatogram (analog readout) but also prints a digital record of the integration of the area under each peak, the retention time for each peak, and the total area count for the run.

**Automatic Data Reduction and Computation.** The 7600A System also produces a computer-compatible punched tape record of the GC analysis (optional). This information can be fed to any standard time-shared computer terminal along with a conversational BASIC program that requires no special computer know-how on the part of the chromatographer . . . to provide a computer printout of the computer-calculated qualitative and quantitative analysis and statistical summary . . . automatically and immediately.

The 7600A System makes the analyst so efficient that in a moderately busy laboratory, he can pay-out the full system cost in a few months. Savings accrue not only from reduced manpower requirements for sample measurement and injection, chromatograph "watching", analytical computation and data reduction, all of which are now completely automatic . . . but also from increased usage of equipment overnight and on weekends, which the 7600A renders fully feasible.

For more information, write or call your local HP sales office. Prices start under $16,000.

Hewlett-Packard, Route 41, Avondale, Pennsylvania 19311. In Europe: 1217 Meyrin-Geneva, Switzerland.

HEWLETT hp PACKARD

ANALYTICAL INSTRUMENTS

43910

## New Jarrell-Ash Instrumentation for

# Atomic and Molecular Spectrochemistry

**750 Direct Reader.** This model features rapid, direct determinations of up to 30 elements with high sensitivity and precision. It requires normal room temperature and humidity control. Insensitive to vibration and shock, it can be operated by semiskilled personnel. Applications include analyses of wear metals in lube oils, plating solutions, ferrous and nonferrous metals, mineral samples, ores and slags and other analyses normally done by optical emission spectroscopy. Circle No. 208 on Reader's Service Card.

**Betaprobe X-ray Emission Spectrometer.** This direct-electron X-ray spectrometer analyzes up to 10 elements either simultaneously or sequentially. It was designed for nondestructive sample analysis of a wide range of elements (carbon to uranium on Periodic Chart) in both low and high concentration. Easy to operate, this unit determines many elements in concentration ranges as low as .005%. Circle No. 209 on Reader's Service Card.

**Portable Materials Analyzer.** A unique light-weight (only 48 lb) unit, this analyzer provides concentration analyses of many sample types—solid, liquid, powder and slurry in ten seconds time per element. The X-ray fluorescence tool is capable of measuring up to six elements in each sample. The entire unit is basically comprised of a table-mounted analyzer with radioisotope source and readout control section. Circle No. 210 on Reader's Service Card.

**Laser-Raman System.** Major features of this instrument are: Double Czerny-Turner Monochromator; stable high-intensity He-Ne, Kr, or Ar laser mounted in unit simultaneously; thermoelectrically cooled S-20 phototube detector; photon-counting detection system; and extra-large sample compartment. The entire system is housed in one completely accessible cabinet. Circle No. 211 on Reader's Service Card.

**Quarter-Meter Monochromator.** A versatile, low-cost monochromator for use in classroom or industrial lab, it offers fast, good resolution (2A) and high aperture ratio (f/3.6). This unit covers a spectral range from the ultraviolet to infrared, has a digital wavelength readout and sells for far less than conventional models. Circle No. 212 on Reader's Service Card.

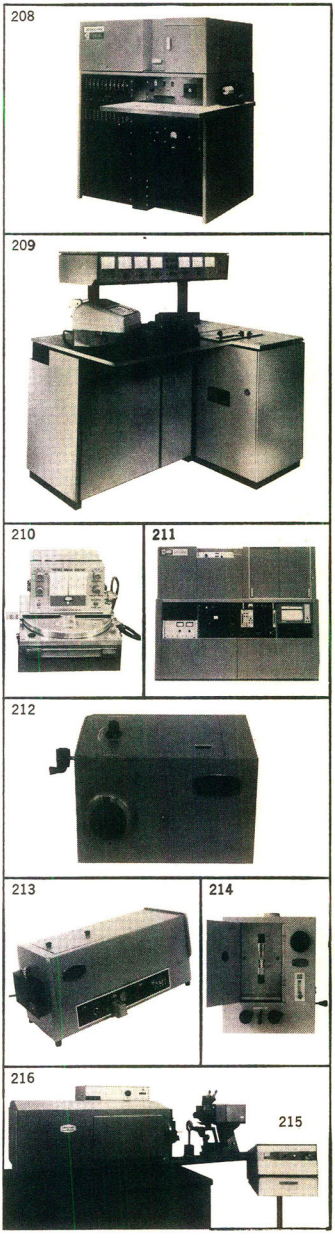


Jarrell Ash

**DIVISION OF FISHER SCIENTIFIC CO.**

See ACS Laboratory Guide for All Products/Sales Office

**Half-Meter Ebert Scanning Spectrometer.** This spectrometer is a dependable scanning monochromator that covers a wide spectral range (UV to IR), with excellent resolution (.2A) and high aperture ratio (f/8.7). An eight-speed reversible electrical wavelength drive provides scanning speeds from 2 to 500A/minute. Readout is directly in angstroms, and an optional camera accessory provides photographic capabilities. Circle No. 213 on Reader's Service Card.

**The Spectroscopist's Arc Stand** features bilateral electrode openings to ensure perfect alignment irrespective of electrode diameter, polarizing viewing window, and water-cooling attachment. Stand accepts many special-purpose accessories including Petrey Stand, Stallwood and O'Connell jets, and rotating disc electrode. Circle No. 214 on Reader's Service Card.

**Mark II Laser Microprobe.** The ideal tool for fast, nondestructive spectrographic analysis of conductive and nonconductive samples. A microscope is used to focus a neodymium laser beam; a 180 microsecond laser burst vaporizes the preselected spot (as small as 20$\mu$). The resulting vapor plume rises between crossed electrodes. As the electrical gap is closed, the added energy raises sample temperature to emissive level, and the resultant radiation passes into a spectrograph to be recorded. Applications include analyses of metals, ceramics, semiconductors, mineral and geological samples, photographic emulsions and biological samples. Circle No. 215 on Reader's Service Card.

**Fast Spectrograph/Spectrometer.** An ideal companion for the Laser Microprobe, the 1.0-meter Fast Spectrograph is able to work with and record short-duration and/or weak-light sources. It is equipped with a camera accepting 4" x 10" photographic plates, and records 2000 A of First Order spectra in one exposure. Excellent resolution (0.12A) is displayed over the entire 10 inches of spectra. Accessories adapt the unit for spectrum scanning and for photoelectric detection of up to 15 spectral lines simultaneously. Circle No. 216 on Reader's Service Card.



## See our four new tubes for small scale technique?

Our new tube looks like a tissue homogenizer. And it is. Until it's used as a centrifuge tube. Except when it becomes a reaction vessel. You probably thought it was a sample storage tube. And it is, also. That's four-use flexibility.

We call it the Kontes Microflex® Tube.

What you're looking at is an internally tapered container made of glass with a threaded neck, optional closures, and an especially thick, heavy base for stability and magnification of sample.

As a tissue homogenizer, the tube needs only a matching tapered pestle. And there's an added benefit: tissue sample can be separated from liquid by centrifugation right in the same container. No sample loss from vessel transferring.

For a completely inert reaction vessel use the Teflon* faced rubber liner and screw cap.

In sample storage, the tapered receptacle makes near-total sample retrieval possible via a bevelled syringe needle through the silicone septum and diaphragm screw cap.

Total capacity is 0.3 ml; cone capacity is 0.1 ml. Overall height is 35mm. Microflex Tubes come packed twelve to a box—a reusable plastic storage box. That's equal to forty-eight of anything else.

For complete information contact your Kontes representative or write direct.

®Trademark of Kontes Glass Co.
*Trademark of DuPont

**KONTES**
Vineland, New Jersey

Regional Distributors: **KONTES OF ILLINOIS,** Franklin Park, Illinois. **KONTES OF CALIFORNIA,** Berkeley, California

**Circle No. 128 on Readers' Service Card**

See ACS Laboratory Guide for All Products/Sales Office

# NEW "SGA" CATALOG




1528 Pages
Size 8"x10"

## Two Catalogs Combined Into One!

Over 30,000 stock items are listed in this new comprehensive laboratory supply catalog.

Like our previous catalog 66, this new edition contains two separate volumes bound together for your convenience. The 1124-page *General Section* lists thousands of modern scientific instruments, apparatus, appliances and general laboratory glassware and supplies. The 340-page *Inter-Joint Section* covers our entire line of interchangeable glassware. A 64-page cross-referenced index separates the two sections. General information is given in the 8-page preface.

To receive this valuable buying guide (mailed without charge), please write to us on your official letterhead.

- *Easy to Use*
- *Numbers in Sequence*
- *Page Headings Alphabetized*
- *Thousands of Illustrations*
- *Helpful Tables and Charts*
- *Cross-referenced Index*

SCIENTIFIC GLASS APPARATUS CO., INC.
BLOOMFIELD, NEW JERSEY

LABORATORY...
♦ APPARATUS
♦ INSTRUMENTS
♦ CHEMICALS
♦ GLASSWARE

**Branches:** Boston 16 Mass. • Danbury Conn. • Elk Grove Village Ill. • Fullerton Calif. • Philadelphia 2 Penna. • Silver Spring Md. • Syracuse 2 N. Y.

Circle No. 77 on Readers' Service Card
See ACS Laboratory Guide for All Products/Sales Office

Circle No. 154 on Readers' Service Card →
See ACS Laboratory Guide for All Products/Sales Office →

# Varian custom tailors 100 variations from six basic series of recorders.

Your custom-fitting choices include: Single or Dual channels, 10-inch or 5-inch chart widths, various types of input configurations, chart speeds (up to 8), 19-inch rack, portable or bench top mounting and a full line of capability-stretching options and accessories.

Design features that make the Varian Recorder line a choice selection: hermetically sealed slidewire, modular construction, full scale zero and zero suppression and solid state circuitry.

Some things don't vary: economy in both price and reliable service (your Varian man won't change the subject when you mention it). As a look through our catalog will attest, in the general laboratory Recorder field, variation begins and ends with Varian.

Write Recorder Product Manager, Varian Aerograph, Walnut Creek, Calif., 94598, Georgetown, Ontario, Canada; Zug, Switzerland.



varian aerograph

# This is the lowest-priced combination GC and TOF mass spectrometer in the U.S.

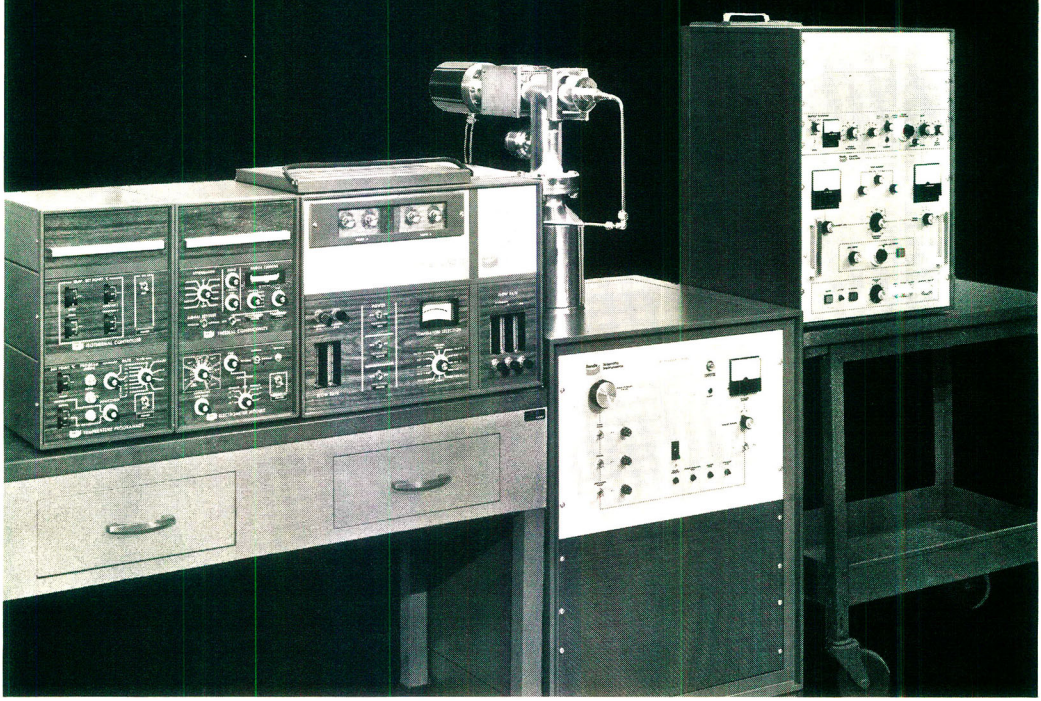

**But that may be your last reason for specifying it.**

You'll probably specify this Bendix GC/Time-of-Flight mass spectrometer because it has the most reliable and sensitive GC in the business with the widest dynamic range. Or because the TOF mass spectrometer is the fastest. Or because the entire system is completely solid state. Or because of its flexibility. (You'll find it useful for difficult polymers, amino acids, biological toxins, pesticides, narcotics, carbohydrate derivatives, much more.) Or because it's especially useful in areas of investigation where samples are minute and of short duration, particularly in natural product chemistry.

The fact it's the lowest priced combination system in the U.S. may seem almost incidental. Until you compare the price. For more information write: The Bendix Corporation, Scientific Instruments and Equipment Division, 1775 Mt. Read Boulevard, Rochester, New York 14603.

**Bendix**

Circle No. 100 on Readers' Service Card

See ACS Laboratory Guide for All Products/Sales Office

# Introducing the NEW 1072 Signal Averaging Computer...

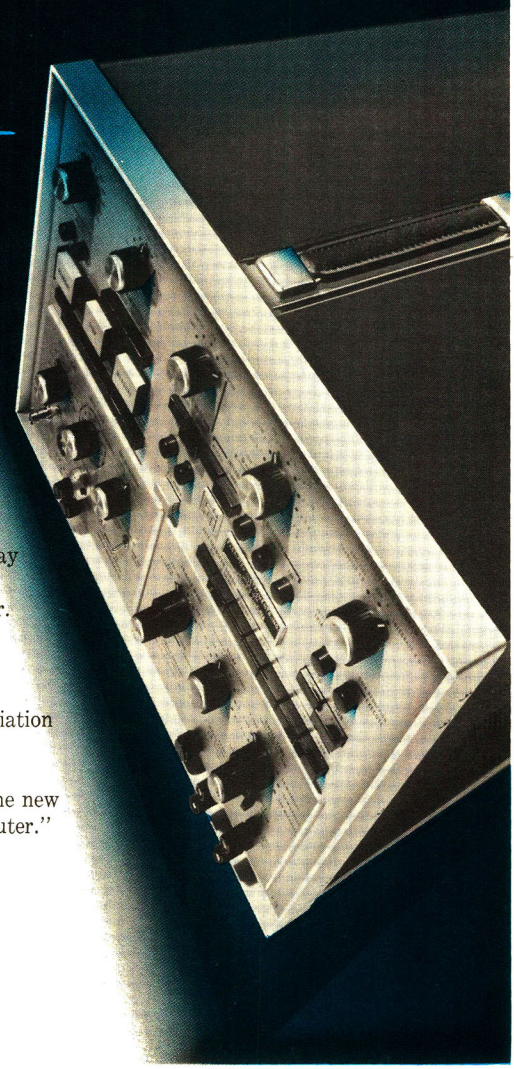

## a new standard of excellence from Fabri-Tek

Featuring: 20 microseconds/address sweep speeds with 9-bit resolution • Decimal number CRT display of address and data values • Expandable memory. • Hardwire interface to a general purpose computer. • Wide variety of measurement plug-ins.

Data modification capabilities including: additive and subtractive transfer • addition and subtraction of constants • integration and differentiation • normalization and curve smoothing.

Complete systems from less than $9,600.

For complete details please request your copy of the new "Guide to the Series 1070 Signal Averaging Computer."

Will be shown at Booth I-110, FASEB Meeting, April 14-18, 1969.

**FABRI-TEK Instruments, Inc.**

Dept. A-4, 5225 Verona Road, Madison, Wisconsin 53711. Phone: 608/238-8476
IN CANADA: Ahearn & Soper Limited, 844 Caledonia Road, Toronto 19, Ont.
Tel. (416) 789-4325—Telex 02-2757 Branches in Montreal and Vancouver

**Circle No. 198 on Readers' Service Card**

# Rutherford Scattering and Channeling— A Useful Combination for Chemical Analysis of Surfaces

**W. D. Mackintosh and J. A. Davies**
*Atomic Energy of Canada Limited, Chalk River Nuclear Laboratories*

THE INTERACTION of accelerated ions with solids provides a number of techniques for the chemical analysis of surface layers. Probably the simplest of these is the use of wide-angle elastic or Rutherford scattering, but, although several such scattering investigations have been reported (*1–6*), the method has not found very wide acceptance. However, the picture is now changing rapidly—primarily because of the widespread use (*7–8*) of elastic scattering for studying the channeling behavior of accelerated ion beams in single crystals. As a by-product of these channeling studies, we find that the elastic scattering yield can give valuable information not only on the number of impurity atoms in the crystal surface but also on their lattice location within the unit cell. Furthermore, channeling enhances considerably the sensitivity of the analysis, particularly in the case of low-mass impurities. This Report reviews the theory and practice of the elastic scattering method, and describes how channeling can be used to assist the chemical analyst.

### Theory

When a beam of monoenergetic particles strikes a surface, some will be scattered from the material, losing energy in an amount proportional to the mass of the atom struck. Further, the number of particles so scattered is a function of the number of atoms present. Hence, by measuring the energy and counting the number of the energing particles, the identity and number of atoms in the solid can be determined.

The energy of the emergent particles $E_1$ is related to the incident energy $E_0$ by the equation

$$E_1 = k^2 E_0$$

where

$$k = \frac{M_1 \cos\theta_s + M_2}{M_1 + M_2} \qquad (1)$$

$M_1$ is the mass of the incident ion, $M_2$ the mass of the struck atom, and $\theta_s$ is the laboratory scattering angle (Figure 1).

This equation holds only for scattering from surface atoms. If the incident particle does not suffer scattering in the surface layer, it will lose energy by ionization and excitation processes as it proceeds to lower layers. Thus, just before being scattered, it will have an energy $E_0'$. The scattered particle will also be slowed down on its way back to the surface and will emerge with an energy $E_1'$. If the rate of energy loss by the slowing down processes is given by the stopping power $S$, then the energy of a particle emerging from a depth $x$ below the surface is expressed by

$$\left[E_0 - \int_0^{\frac{x}{\cos\theta_1}} S_1 dl_1\right] k^2 - \int_0^{\frac{x}{\cos\theta_2}} S_2 dl_2 \qquad (2)$$

where the first and second integrals are the energy losses along the incoming and outgoing trajectories $l_1$ and $l_2$. $S_1$ and $S_2$, the mean values of the stopping power, depend on the energy of the particle; in the case of single crystals, $S_1$ also depends on whether or not the beam is channeled. The geometric relationships between $\theta_1$, $\theta_2$ and $\theta_s$ are illustrated in Figure 1.

Some facts relevant to the use of elastic scattering for analysis can be inferred from these equations:

(1) If a beam of monoenergetic particles strikes a thick polycrystalline or amorphous solid, the energy spectrum of the elastically scattered particles is similar to that shown for silicon in Figure 2. It is characterized by a sloping plateau terminated by a sharp edge. The sharp edge represents the energy $E_1$ obtained by scattering from the surface layers; its position is determined by the masses of the incident particle $M_1$ and scattering atoms $M_2$ (in this case the masses of the helium ion and silicon atom respectively), according to Equation 1. The slope of the spectrum edge is

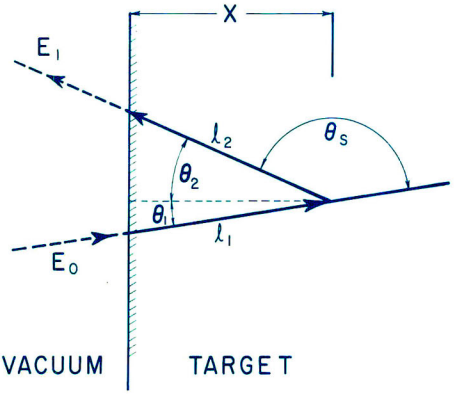


Figure 1. Schematic diagram showing the geometric relationship of the various angles involved in the elastic scattering equations

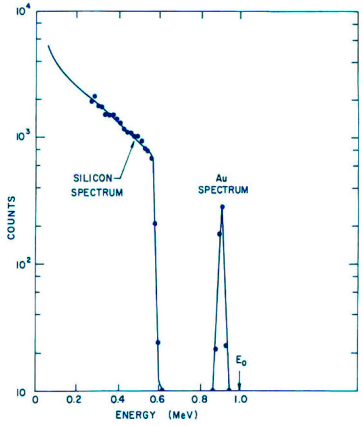


Figure 2. Energy spectrum of helium ions scattered from a silicon target whose surface had been contaminated with ~1 mono-layer (0.5 μg/cm²) of gold

due to the finite resolution of the detector. Counts recorded at lower energies are derived from particles scattered from progressively greater depths. As $x$ increases, the energy $E_1'$ decreases according to Equation 2.

(2) If the thick solid is covered with a thin (~100 Å or less) film of atoms of greater mass than the substrate, a spectrum similar in shape to that shown for gold on silicon in Figure 2 is obtained. At energies above the silicon edge, a sharp peak is observed due to scattering from the heavy gold atoms on the surface; its position also is given by Equation 1, where $M_2$ is now the mass of the gold atom. If the gold film had been much thicker (~0.1 μm or more) the width of the peak would have increased in the direction of lower energy. At the same time the edge of the substrate would have retreated to lower energies because $E_0'$, the energy of the particle entering the substrate, would have been decreased significantly by the stopping power of the surface film.

(3) Conversely if the solid is covered with a thin film of an element whose mass is less than that of the substrate, the peak representing its energy distribution is superimposed on the plateau, (*cf.* Figure 7). For such a combination the scattering technique is not particularly useful except (as we shall see later on) in the case of single crystals.

(4) Equation 1 indicates that the energy difference between the impurity peak and the edge of the plateau increases with the mass $M_1$ of the incident particle. For optimum resolution, the projectile mass should be selected so that particles lose approximately 50% of their initial energy on being scattered through the chosen scattering angle.

(5) Mass resolution also improves with increase of scattering angle $\theta_s$, although, as will be seen later, this must be compromised with a decrease in yield.

(6) Increasing the energy of the incident particle would appear to improve the differentiation of masses, particularly at large scattering angles, but this also decreases the yield. Furthermore at higher energies the chance of the incident particle undergoing a nuclear reaction rather than scattering increases. In these cases, not only is the particle lost, but the secondary particle produced in the reaction may be detected and contribute to the count rate. In general, penetration of the Coulomb barrier at modest energies, *i.e.*, <2 MeV, is less likely the greater the masses of the incident and target particles; however, no safe guide lines can be laid down.

(7) The difference in energy of particles scattered from two elements of similar mass number is very small, for example approximately 5 keV between manganese and iron for a 1.6 MeV helium beam. A typical solid state detector has an energy resolution around 20 keV and hence cannot be used in this case, unless much higher energies are employed.

We will now consider the relationship between the numbers of atoms present in a target and the number of scattered particles detected. The scattering probability, $d\sigma$, into the solid angle, $d\Omega$, is given by the Rutherford scattering formula

$$\frac{d\sigma}{d\Omega} = 1.3\times10^{-27}\left(\frac{Z_1Z_2}{E}\right)^2 \cdot \left(\frac{M_1+M_2}{M_2}\right)^2 \cdot \frac{1}{\sin^4\theta_s/2} \text{ cm}^2/\text{sr} \qquad (3)$$

where $Z_1$ and $Z_2$ are the atomic numbers of the incoming particle and target atom, respectively; $M_1$ and $M_2$ are their masses; $E$ is the energy (in MeV) of the particle before being scattered; and $\theta_s$ is the scattering angle. The scattered yield per coulomb can be directly calculated from this equation.

It follows from this equation:

(1) The higher the atomic number of the target atoms, the greater is the number of counts per unit time. This again favors the analysis of heavy elements on or in light matrixes. Conversely when the analysis of a light element on a heavier substrate is attempted not only are the impurity counts superimposed on the substrate plateau (as a consequence of Equation 3), but the relative cross sections are in the wrong direction, thereby worsening the statistics.

(2) Small scattering angles enhance the sensitivity, but at the expense of poorer mass resolution.

(3) Equation 3 is valid for the outer layer of a target only. As we have already seen, when the incident particle traverses a number of atomic layers before being scattered, its energy is decreased by the stopping power of the material. Thus the scattering cross section for nuclides located some distance below the surface is increased somewhat. An expression relating the yield of scattered particles to the depth and to the stopping power is given in Reference (*2*).

### Equipment

For most analysts using elastic scattering methods, the choice of accelerator has presumably rested on what was accessible. Most work has been carried out with Van de Graaff accelerators, particularly the 2 MeV machines. The energy spread at the target is low, typically $\pm 0.1\%$ of the mean energy. Beam currents up to 10 $\mu$A are obtainable; for most scattering experiments $\sim 10^{-2}$ $\mu$a is sufficient. The use of higher energy Van de Graaff machines has been reported (*4*) and one 600 keV heavy ion accelerator (*7*). Turkevich (*6*) used an $\alpha$-emitting source of $^{242}Cm$ for his experiments, but he had to meet the exacting requirements of transporting the entire apparatus to the moon (Surveyor lunar missions September 1967 and January 1968).

The forms of target chambers and target holders vary greatly, but a few guidelines for design can be set down. It is useful to have one port of the target chamber designed to take several different forms of target holders that can be interchanged. If the setup is to be used for charged particle activation analysis as well, another port capable of accepting interchangeable detectors is also good practice. The solid-state detector for elastic scattering analysis should be mounted so that the observed scattering angle can be altered.

We have found it convenient to use three different types of target holder. One has provision for fastening samples to the outer circumference of a disk which can be rotated from outside the chamber without breaking the vacuum, thereby bringing successive samples into the beam. Another has provision for moving a sample across the beam so that concentration gradients in a surface plane may be located and determined. The traverse is 3 cm in each direction. The third holder is a goniometer having two independent axes of rotation so that any desired crystallographic axis or plane of a single crystal may be oriented with respect to the incoming beam. All three devices enable the sample to be electrically insulated from the rest of the chamber. The sample is connected to a current integrator.

When one irradiation must be exactly comparable to another (irradiations of a sample and a comparative standard), the method for measuring the integrated beam current must account for ions scattered from the target and for secondary electron emission (*1,4,5*), at MeV energies, however, their effects are usually quite small ($\leq 10\%$).

Two quite different systems for detection and energy measurement of the scattered particles have been used. Most common is the combination of a small, high resolution solid state detector with a multichannel pulse height analyzer. Such detectors are inexpensive and readily available. They also subtend a large solid angle and thus make it possible for enough counts for good statistics to be accumulated at low beam currents—thereby minimizing sputtering and excessive heating of the target. The solid state detectors have typically a resolution of approximately 20 keV FWHM at 1 MeV, and hence cannot distinguish between elements whose masses differ by $<20\%$. In addition we have found it convenient to use three or four single-channel analyzers and scalers in parallel to the multi-channel pulse height analyzer so that data in selected channels can be recorded separately.

The alternative detector system, a high resolution magnetic or electrostatic spectrometer gives considerably better mass resolution particularly at low energies, and can almost distinguish between the isotopes of an element (*1*). However, such instruments are much less sensitive, require much higher beam currents, and are not so readily available.

### Quantitative Analysis

One important advantage of the elastic scattering technique, compared to other methods such as activation analysis, is that quantitative analyses can be obtained from a single measurement without having to prepare any comparative standards—provided the bombardment is carried out at energies where the Rutherford scattering law (Equation 3) is valid. Under such circumstances, the number $n_i$ of counts observed in an impurity peak (*cf.* Figure 2) is related to the number $N_i$ of impurity atoms/cm$^2$ of surface as follows

$$n_i = f Z_i^2 N_i (it) \qquad (4)$$

where $Z_i$ is the atomic number of the impurity, $(it)$ is the integrated beam current, and $f$ is a constant that depends only on the scattering angle, the geometry of the detector, and the energy and atomic number of the projectile.

Similarly, the number, $n_s$, of counts in one channel of the substrate spectrum (measured just beneath the surface) is related to the number, $N_s$, of substrate atoms contributing to that channel by

$$n_s = f Z_s^2 N_s (it) \qquad (5)$$

Consequently,

$$\frac{n_i}{n_s} = \frac{Z_i^2}{Z_s^2} \cdot \frac{N_i}{N_s} \qquad (6)$$

or

$$N_i = \frac{n_i}{n_s} \left( \frac{Z_s}{Z_i} \right)^2 \cdot N_s \qquad (7)$$

The $\frac{n_i}{n_s}$ is evaluated directly from the observed energy spectrum, and

$n_s$, the number of substrate atoms contributing to a given channel can be easily calculated provided the rate of energy loss $dE/dx$ in the substrate is known. This method of analysis eliminates the need not only for comparative standards but also for precise measurement of the integrated beam current. Hence the problems of secondary electron emission, etc., are completely avoided. Its success depends, of course, on the validity of the Rutherford scattering law, but with 1–2 MeV helium (or heavier ions) as projectiles this assumption does not introduce significant error. With protons, however, or with higher energy projectiles, resonance effects can cause serious departures from the Rutherford law. In such cases, the more conventional procedure of using a comparative standard should be adopted.

The preparation of comparative standards when necessary, is relatively easy. Films can be produced by such processes as electrodeposition, evaporation or thermal decomposition of organic vapors. The thickness can be obtained by various methods, for example, by weighing and by such devices as counting deposits prepared from radioactive materials of known specific activity. References to such procedure are given by Semmler, Tribby, and Brugger (*3*). The substrate does not interfere with the elastic scattering yield of these surface layers, but it is advisable to deposit the film on the same material as the sample to be analyzed; otherwise, the secondary particle yields may differ and give integrated beam current readings which are not comparable. Further, the total count rate may differ sufficiently that dead time losses would have to be evaluated and corrections applied.

### Applications

Most of the successful quantitative applications reported in the literature are concerned with the determination of thin films on substrates of lower mass. Rubin (*1*) used 2 MeV protons plus a magnetic spectrometer to analyze steel surfaces that had been exposed to an explosion. He observed peaks which were identified (by Equation 1) as silver/antimony and lead/mercury and calculated the concentrations. Samples of electrostatically precipitated aerosols on aluminum foil were similarly analyzed and carbon, oxygen, silicon, and sulfur were found. The oxygen, sulfur, and silicon peaks corresponded to deposits of 5, 0.13, and 0.3 $\mu g/cm^2$, respectively. The carbon peak was disregarded because of the well known buildup of carbon on targets by evaporation of hydrocarbons from diffusion pumps.

Anders (*5*) reported the determination of silver on glass surfaces in amounts ranging from 10 to 49 $\mu g/cm^2$ and chromium on magnesium from 20 to 150 $\mu g/cm^2$. He also used 2 MeV protons but detection and energy analysis was performed with a solid state detector and pulse height analyzer. Peisach (*4*), bombarding with $He^+$, found 1–10 $\mu g/cm^2$ gold on aluminum. Elastic scattering of $\alpha$ particles and activation by the same particles provided Patterson, Turkevitch, and co-workers the means for analyzing the lunar surfaces (*9*).

In our laboratories, we have determined as little as 0.003 $\mu g/cm^2$ of gold and copper on the surface of wafers cut from single crystals of silicon (*10*). The objective of the analysis was to see if contaminants from etching or treatment solutions used in the production of solid state devices were adsorbed on the wafers and if so, to determine how the amount of deposit varies with (i) the concentration of contaminant in solution, (ii) the orientation of the crystallographic surface, and (iii) the conductivity and resistivity type of the wafer. Thus, there were many samples to analyze, yet each required less than 10 minutes, employing a beam current of 5 nA. No comparative standard was irradiated because the incident beam of $He^+$ at 1 MeV produced no nuclear reaction to interfere with the count of the elastically scattered particles. The number of contaminant atoms was obtained by relating the relative yields through their $Z^2$ dependence. (Equation 7).

Another practical application in our laboratories was the determination of zirconium on mild steel surfaces. The zirconium had been dissolved in a liquid metal coolant circulating in mild steel piping and was intended to inhibit corrosion by deposition on the steel. Radioactive zirconium deposits of known specific activity were used for calibration.

Sippel (*2*) has described an elegant application. From the energy spectrum of emitted particles, he determined a concentration gradient of gold diffused into copper. In this way, much thinner diffusion depth could be studied than by the mechanical and chemical sectioning techniques usually employed. A similar procedure has been used by Powers (*11*) to study the concentration profile of heavier ions implanted into Be, C, and Al targets.

### Elastic Scattering in a Single Crystal—Channeling

We will now consider how—in a single crystal substrate—the channeling phenomenon can be utilized by the analyst to extend the applications of the scattering technique.

A fast-moving charged particle, entering a crystal lattice within a small predictable angle of a close-

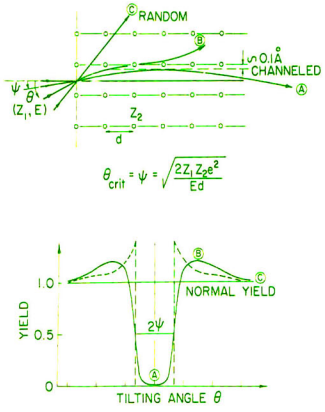


Figure 3. The influence of crystal lattice on the motion of energetic charged particles. Upper Part: Charged particle trajectories for several typical values of $\theta$, the angle between the incident beam and a close-packed atomic row. Lower Part: Angular dependence of the yield for any process requiring impact parameters <0.1 A. The dotted curve shows the predicted angular dependence for a perfect nonvibrating lattice. Taken from Reference (14)

ห้องสมุด กรมวิทยาศาสตร์

packed atomic row or plane, becomes channeled—*i.e.*, it becomes steered by successive gentle collisions, and is thereby prevented from having violent collisions with individual lattice atoms. In other words, as long as it remains channeled, a particle will not undergo elastic scattering; hence, the observed yield will be reduced drastically from that obtained on bombarding the crystal along a random direction. This phenomenon can serve as a tool for studying certain properties of crystalline material. Some of these are of direct interest to the chemical analyst.

Lindhard (*12*) has provided an accurate theoretical description of the actual steering mechanism. The principles involved are summarized in Figure 3. One can distinguish three different types of particle trajectory. An energetic charged particle, moving through a lattice within a predictable critical angle of an atomic row (or plane), is steered by successive gentle collisions (trajectory *A*), and is thereby prevented from entering a forbidden region around each lattice row. The radius of this forbidden cylinder is given by the Thomas-Fermi screening distance, $a$, which is typically 0.1–0.2 Å. When the incident angle $\theta$ is much larger than $\psi$, the particle has no "feeling" for the existence of a lattice, and so has a random trajectory (trajectory *C*). There is also an intermediate region (viz. when $\theta$ is only slightly larger than $\psi$) in which the particle trajectory (trajectory *B*) actually has a slightly enhanced probability of being close to the atomic rows and, hence, of undergoing violent collisions; however, this region is not quantitatively reproducible, and so is not of much use to the analyst.

The lower part of Figure 3 illustrates the predicted orientation dependence of the yield curve for any close-encounter process (*i.e.*, a process having an impact parameter less than $a$). Experimental investigations of wide-angle Rutherford scattering (*7*) have verified that such large attenuations do occur. The agreement between the predicted and measured orientation dependence is quite reasonable (*13*), as can be seen in Figure 4.

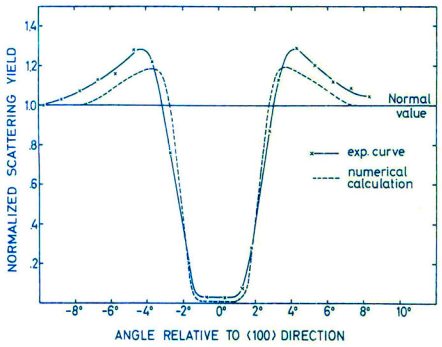


Figure 4. Experimental and calculated dip in Rutherford scattering yield for 480 keV protons incident along a ⟨100⟩ direction of a tungsten crystal. Taken from Reference (13)

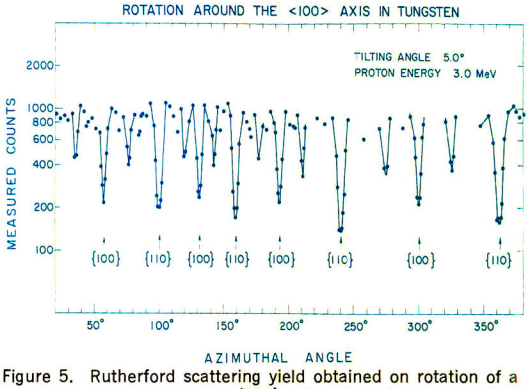


Figure 5. Rutherford scattering yield obtained on rotation of a tungsten crystal around the ⟨100⟩ axis with a tilt angle of 5.0° between the rotation axis and the incident proton beam (incident energy 3.0 MeV)

The critical angle is given by equation

$$\psi = \left[\frac{2 Z_1 Z_2 e^2}{Ed}\right] \qquad (8)$$

where $Z_1$ and $Z_2$ are the atomic numbers of the incident particle and lattice atom, respectively, $e$ is the electronic charge, $E$ is the incident particle energy, and $d$ is the distance between adjacent atoms along the chosen atomic row.

To utilize channeling, it is first necessary to orient precisely the crystal target with respect to the incident beam. Fortunately, this orientation can be done quite easily by means of the channeling effect itself (*14*), using the same elastic scattering process as in the analytical studies described above. If the crystal is mounted on a suitable goniometer allowing rotation of the crystal at a certain tilting angle to the beam, and is then rotated through 360°, a yield curve like the one shown in Figure 5 is obtained. The sharp attenuations occur as the various close-packed planes are successively aligned with the incident beam. A stereogram (Figure 6) can then be constructed by marking off on the circumference of a circle, the azimuthal angles at which these planar "dips" in yield occur. By properly connecting the pairs of points that correspond to intersections of the same plane, we readily obtain the exact location *P* of a major crystal axis—in this case the ⟨110⟩. This whole operation can be performed *in situ* prior to the analysis, and requires only 15–30 minutes of time. The beam can then be aligned exactly with the major axis by setting the goniometer at the azimuthal and tilt angles corresponding to the point P on the stereogram.

One important advantage of channeling to the analyst is that it enables the scattering from the substrate to be suppressed drastically, and thus enhances the sensitivity for detecting trace amounts of surface contaminants. This is particularly true in the case of low-mass impurities on a heavier substrate, where, as noted earlier, the scat-

# Titrisol®

**Normal solutions in no time**

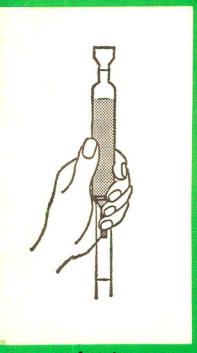

Insert




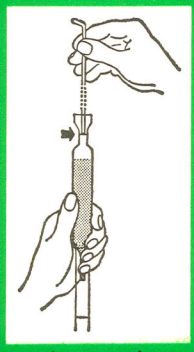

punch upper membrane

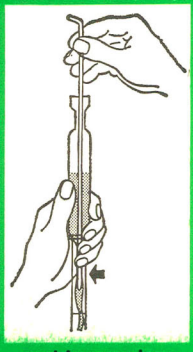

punch lower membrane

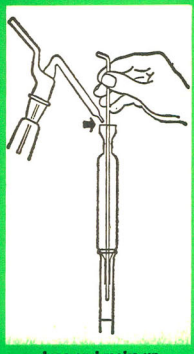

rinse and make up to volume

Titrisol ampoules — save weighing, dissolving and standardising the titre

Titrisol ampoules — due to their construction permit convenient quantitative transfer of the accurate dosage into the volumetric flask

Titrisol ampoules — save time, space and weight

Titrisol ampoules — are unbreakable, storable and always ready for use

Titrisols are absolutely reliable (titration exactness ± 0,2%)
Please ask for our special leaflet

Sole distributors in the United States:
Brinkmann Instruments, Inc., Cantiague Road, Westbury L. I., N. Y.

**E. MERCK AG · DARMSTADT · GERMANY**

Circle No. 55 on Readers' Service Card

232/I-EUS



Here's a BETTER Liquid Syringe... and it LASTS!

It's the Series "C" Pressure-Lok Liquid Syringe

- SUPERIOR ACTION
- TEFLON-TIP PLUNGER
- STARTS OUT AND STAYS LEAKTIGHT to 150 psi
- NO "FREEZE-UP"
- EXTENDED LIFE
- INTERCHANGEABLE PARTS
- OPTIONS AVAILABLE

"Teflon" is a registered Dupont Trademark

Series "C" Pressure-Lok Liquid Syringes

| Cat. No. | Size |
|---|---|
| 304101-C | 10 ul |
| 304102-C | 25 ul |
| 304103-C | 50 ul |
| 304104-C | 100 ul |

Price: $18.00

* Pat. No. 3325062

PRECISION SAMPLING CORPORATION

P. O. BOX 15119 • BATON ROUGE, LA. 70815

Yes, I want more information on why Series "C" Pressure-Lok liquid syringes are better.

NAME_____

TITLE_____

COMPANY_____

ADDRESS_____

CITY_____

STATE_____ ZIP_____

Circle No. 140 on Readers' Service Card
See ACS Laboratory Guide for All Products/Sales Office


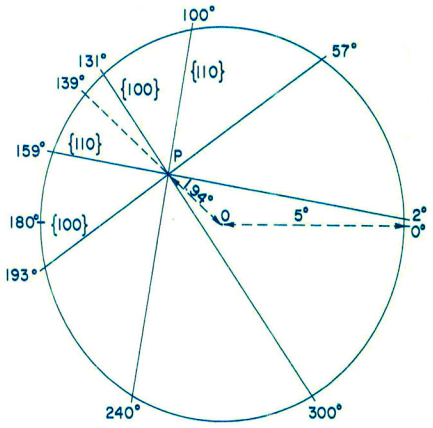


Figure 6. Stereographic representation of the rotation in Figure 5. Azimuthal angles corresponding to the planar "dips" in Figure 5 are marked off on the circumference and points corresponding to the same plane are connected by a straight line. The intersection point, P, denotes the location of the ⟨100⟩ axis. The radius of the stereogram corresponds to the tilting angle of 5.0°

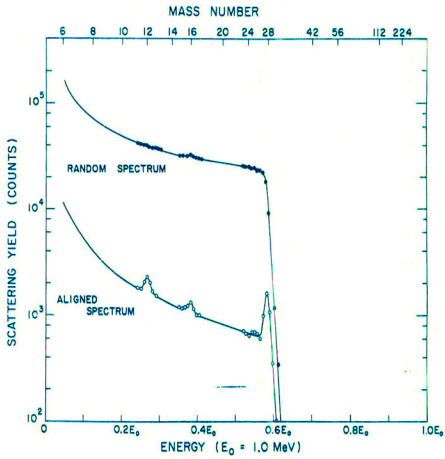


Figure 7. Aligned ⟨111⟩ and random backscattering spectra for an undoped Si crystal recorded for the same dose ($30 \times 10^{-5}$ coulomb) of 1.0-MeV He ions (7). A mass number scale (for impurities located near the crystal surface) is given. The three peaks in the aligned spectra at masses 12, 16, and 28—indicate the amount of carbon, oxygen, and disordered Si in the surface region. In order to simplify the figure, data points have been omitted except in the more-important regions of the spectra

tered particles from the surface contaminant appear superimposed on the plateau from the substrate. Figure 7 shows random and aligned spectra for 1 MeV helium ions scattered from a silicon crystal contaminated with a few atomic layers of silicon oxide and carbon (*15*). In the "random" case, the scattering from the small amount of oxygen and carbon atoms on the surface cannot be resolved because of the large background from the substrate. In the aligned case, on the other hand, the substrate background is suppressed 30–100 fold (due to channeling), and now the scattered peaks from the surface layers of carbon and oxygen are resolved quite cleanly. From the area of the oxygen peak it was calculated that the surface film contained ~0.2 $\mu g/cm^2$ of oxygen; this is equivalent to about five molecular layers of surface oxide.

The advantages of channeling in suppressing the yield from the substrate can be extended one step further by applying the so-called "double-alignment" technique. This requires simultaneous alignment of both the incident and the outgoing beam trajectories with major crystal axes. First, the incident beam is aligned with one axis—as in any channeling experiment—thereby producing a 30–100 fold reduction in the total scattered yield. Then, a well-collimated detector is aligned with another axis in order to observe only those scattered particles that also emerge along a channeling direction; under such conditions, a further 30–100 fold attenuation in yield is observed, due to the closely-related

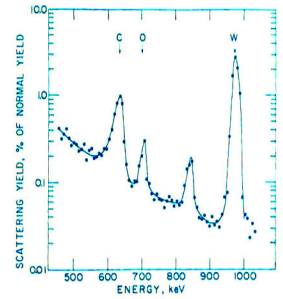


Figure 8. Energy spectrum of 1 MeV $He^+$ ions scattered 70.7° in tungsten. Incident direction = ⟨111⟩ axis. Exit direction = ⟨1$\bar{1}$1⟩ axis. Taken from Reference (16)

phenomenon of "blocking." Hence, an overall attenuation of $10^3$–$10^4$ can be achieved. The advantage of this "double alignment" procedure has been beautifully demonstrated by E. Bøgh (*16*), using tungsten crystals, and is illustrated in Figure 8. Even in this rather unfavorable (*i.e.*, high Z) target, the carbon and oxygen peaks are clearly resolved, even though they correspond to only 1.0 and 0.3 $\mu g/cm^2$ respectively—indicating that with double-alignment the sensitivity for low-mass impurities can be extended to much less than one atomic layer. The unlabelled peak at 840 keV corresponds to 0.1 $\mu g/cm^2$ of a surface contaminant around mass 40; it is probably due to potassium contamination from an aqueous KOH treatment that had been used to clean the tungsten surface before the analysis.

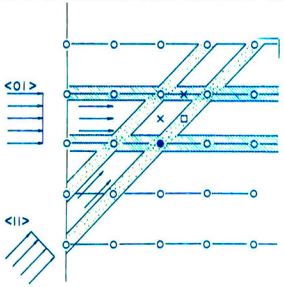


| | DIRECTIONAL EFFECT ? | | |
|---|---|---|---|
| | ● | × | □ |
| <01> | YES | 50% | NO |
| <11> | YES | NO | YES |

Figure 9. A two-dimensional model illustrating how the channeling phenomenon can be used to locate foreign atoms in a crystal (9). As shown by the table, three typical sites for a foreign atom ●, □, and X can be uniquely distinguished by studying the channeling behavior first along the 01-, and then along the 11-direction

In using channeling to suppress the background yield from the substrate, the analyst is of course making one important assumption: namely, that the scattering yield from the impurity atoms does not depend on the orientation of the underlying crystal substrate. This assumption is justified whenever the impurity atoms are contained in an amorphous or polyvrystalline surface layer. But, if they have become embedded within the host lattice (for example, by ion implantation or by diffusion), then the validity of the assumption depends critically on what type of lattice site they occupy. In fact, by studying the validity of this assumption —*i.e.*, by comparing the orientation dependence of various impurity peaks with that of the substrate, it is possible to establish the exact lattice location of specific foreign atoms within the unit cell. Such information is particularly valuable in the doping of semiconductors, and has led to the recent widespread use of the scattering technique in analyzing ion-implanted Si and Ge (Refs. *15–19*).

Let us therefore consider briefly how this orientation dependence of the scattering yield can serve as a tool for locating foreign atoms in crystals. Figure 9 shows the principles involved for a simplified two dimensional lattice, where □, X and ● represent several possible positions for an impurity atom. The interaction between a channeled beam and foreign atoms in the crystal will not show any attenuation in yield, provided the foreign atom is located in the allowed space for the channeled beam. Hence, interstitial atoms will not show any attenuation, at least along some main direction (*i.e.*, □ along the ⟨01⟩ direction and X along the ⟨11⟩ direction). On the other hand, if the foreign atom is situated along a row (*i.e.*, in the forbidden space for the channeled beam), then a large decrease in the yield of the process will be observed whenever the beam is aligned within the critical angle of that particular row. For a true substitutional position, such as (●), a large attenuation will be observed for all close-packed direc-

new
from S&S
**TLC**
Ready Plates

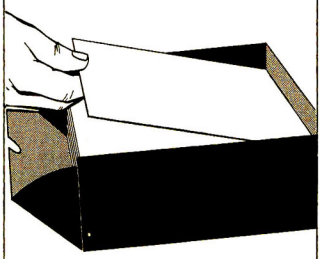

Extremely uniform coating on glass plates. 10 x 20 cm (50 per package). 20 x 20 cm (25 per package). Ready Plates individually wrapped in polyethylene bags.

Media offered as cellulose powder or silica gel with or without binder of starch or gypsum. Special polyamid, acetylated and ion exchange plates.

Working instructions available for Ready Plate separation of the following groups.*

| | |
|---|---|
| Alkaloids | Lipophylic dyes |
| Alpha amino acids | Carcinogenic hydrocarbons |
| Bleaching agents | Amines |
| Carotinoids | Insecticides |
| Cations: Ca, Mg, Al, Fe | Gasoline with test dyes |
| Monoazo dyes | Seed oils |
| Oligosaccharides | Fish oils |
| Reactive dyes | Test dyes |
| Addictive drugs | |
| Sugars | |

Chlorophylls and related natural colors

*Available with orders totaling $19.00 or more.

S&S The first name in filtration
SCHLEICHER & SCHUELL
(603) 352-3810

AC-469
Schleicher & Schuell, Inc.
Keene, New Hampshire 03431
Please send free Bulletin No. 51 on S&S Powders and Ready Plates.
Name
Address
City
State Zip

Circle No. 75 on Readers' Service Card
See ACS Laboratory Guide for All Products/Sales Office

A NEW JOURNAL

**ORGANIC MAGNETIC RESONANCE**

FIRST ISSUE FEB. 1969

This international journal is devoted to the rapid publication of original work dealing with the applications of NMR, NQR and ESR to the general problems of structural organic chemistry. In its wider context this promises papers dealing with such branches as biochemistry, medical biochemistry, pharmacology etc.

Authors who have experienced problems in getting their spectra published will welcome OMR. With the text journal is a **Spectral Supplement,** containing spectra discussed in the papers – clearly reproduced in a standard format – so that the reader can always have in front of him the spectrum under discussion.

**Organic Magnetic Resonance** together with its **Spectral Supplement** will be fully indexed and will build up to form a particularly valuable NMR data compilation.

**Editor-in-Chief**

Dr. Eric F. Mooney
University of Birmingham
P.O. Box 363, Birmingham 15, England.

**Regional Editors**

*North America*
Dr. S. L. Manatt,
Jet Propulsion Laboratory,
California Institute of Technology,
4800 Oak Drive, Pasadena, California 91103.

*Germany* Dr. G. Habermehl

*France* Prof. G. Mavel

*Australasia* Dr. T. J. Batterham

*Japan* Dr. H. Watanabe

**USA Editorial Advisory Board**

Prof. Lloyd M. Jackman, Prof. A. H. Maki
Prof. C. T. O'Konski, Dr. K. C. Ramey
Dr. C. A. Reilly, Prof. J. D. Roberts
Mr. P. Sadtler, Dr. J. Shoolery
Prof. R. W. Taft

**Annual Subscription**

With 1 copy of spectral supplement **$40**
With 2 copies of spectral supplement **$51**

*For full details and FREE specimen copy of Issue 1 use Readers Reply Service in this journal, or write to the Publisher:*

**Heyden & Son Ltd.**
**Spectrum House, Alderton Crescent,**
**London, N.W.4., England.**

Circle No. 27 on Readers' Service Card



tions. On the other hand, for the edge-interstitial position (X), only a 50% attenuation should occur, as only half of the foreign atoms are shadowed along the ⟨01⟩ direction. The other half are shadowed along the equivalent ⟨10⟩ direction. In a real (*i.e.*, three-dimensional) lattice, the situation is slightly more complex, but the same basic principles apply.

Hence, by simultaneously observing the interaction of the beam with the lattice and with specific embedded foreign atoms, one obtains a quantitative measure of the fraction of foreign atoms located along a particular row. By repeating the experiment in different crystal directions, the exact location(s) of the foreign atoms can be established. Figure 10 illustrates the three types of impurity behavior that have been observed in these lattice location studies in silicon.

(1) The Bi case: Large and essentially equal attenuations occur along both the ⟨111⟩ and ⟨110⟩ directions, indicating that Bi atoms are predominantly at the intersection of these two rows, *i.e.*, on lattice sites.

(2) The Ga case: A negligible decrease in yield is seen along either direction, indicating that the Ga atoms are *not* located within ~0.2 Å of either the ⟨111⟩ or the ⟨110⟩ atomic rows. Presumably, they are in some non-regular position in the crystal, such as at a dislocation or other lattice defect, or in a precipitate.

(3) The In case: A 60% decrease in yield occurs when the beam is aligned with the ⟨111⟩, but only a 30% decrease when aligned with the ⟨110⟩. This indicates that significant fractions of the In atoms must be located not only on the lattice sites but also in the regular interstitial holes that lie along the ⟨111⟩ (see insert in Figure 10).

Thus, we see that channeling offers to the analyst two important advantages: (i) it enhances greatly the sensitivity of the elastic scattering technique—particularly for detecting low mass surface impurities of heavier substrates; and (ii) it can be used to pinpoint accurately the type of lattice site occupied by the impurity atoms.

We should perhaps conclude on a note of warning in that channeling (like many other effects) is not always a blessing. It can also be a serious source of error if not properly taken into account. Whenever

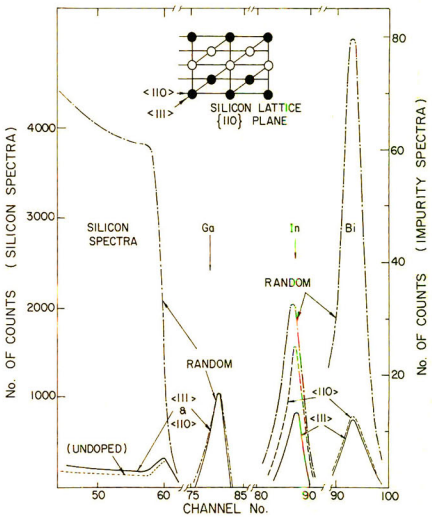


Figure 10. Composite energy spectra of helium ions backscattered from three Si crystals implanted at 450 °C with ~$10^{14}$ Ga, In, and Bi ions/cm², respectively (19). Spectra: ——— aligned ⟨111⟩; – – – aligned ⟨110⟩; —.—. random. In the silicon region (channels 45-60), the aligned spectrum for an undoped crystal is shown for comparison. The insert shows the atomic configuration in the (110) plane of the Si lattice; ● lattice sites; ○ unoccupied (interstitial) sites

an ion beam passes through a crystalline lattice, large attenuations in yield, such as those in Figures 7, 8, 10, may occur if the beam direction should inadvertently coincide with a crystal axis or plane. The resulting analytical error in extreme cases can be as large as a factor of 100 and (as we saw in Figure 10) it depends critically on where the foreign atoms are located within the lattice structure. Furthermore, it is not restricted to the elastic scattering process described here, but applies equally to all analytical methods requiring violent collisions between the incident beam and the target atoms. Hence, analytical data obtained in a single crystal by charged-particle activation or by X-ray generation are also susceptible to serious error unless channeling is carefully avoided—a fact that has not yet been universally recognized by analysts. Even in polycrystalline material, similar (but smaller) errors can arise if the crystallites exhibit any significant degree of preferred orientation, as was clearly demonstrated by the range studies of McCargo *et al.* (*20*) in polycrystalline tungsten.

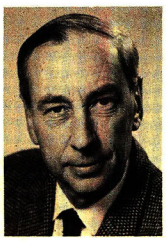

***William D. Mackintosh,*** *although born and raised in Canada, received his B.Sc. at the University of Glasgow, Scotland, in 1941. He spent the remainder of the war years flying with the R.C.A.F. in the European Theatre of Operations. The five years following the war were spent in the rubber industry. He joined Atomic Energy of Canada in 1952. His work has been in the fields of isotope production, neutron activation analysis, and reactor chemistry. His present interests are the exploitation of accelerated particles and channeling for analytical purposes.*

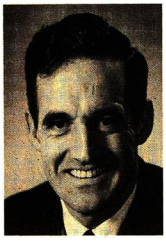

***John Davies*** *was born in Prestalyn, North Wales, in 1927, but at the age of thirteen he emigrated to Canada. He obtained his Ph.D. in physical chemistry at the University of Toronto in 1950, and since then has been working in the Research Chemistry branch at CRNL, investigating the penetration of energetic atomic particles in matter. In 1963, he was one of the first experimentalists to observe the existence of "channeling." His subsequent research interests have centered around this channeling phenomenon and particularly on its application to other fields. The success of these researches led to the Noranda award from the Chemical Institute of Canada in 1965 and the T.D. Callinan award from the Electrochemical Society in 1968.*

## Literature Cited


(1) S. Rubin, T. O. Passell, and L. E. Bailey, ANAL. CHEM., **29,** 736 (1957).
(2) R. F. Sippel, *Phys. Rev.*, **115,** 1441 (1959).
(3) R. A. Semmler, J. F. Tribby, and J. E. Brugger, **A.E.C. COO-712-89** (1964).
(4) M. Peisach and D. O. Poole, ANAL. CHEM., **38,** 1345 (1966).
(5) O. U. Anders, ANAL. CHEM., **38,** 1442 (1966).
(6) A. Turkevich, K. Knolle, R. A. Emmert, W. A. Anderson, J. H. Patterson, and E. Franzgrote, *Rev. Sci. Instrum.*, **37,** 1681 (1966).
(7) E. Bøgh and E. Uggerhøj, *Nucl. Instrum. Meth.*, **38,** 216 (1965).
(8) J. A. Davies, J. Denhartog, and J. L. Whitton, *Phys. Rev.*, **165,** 345 (1968).
(9) J. H. Patterson, A. L. Turkevich, and E. J. Franzgrote, *J. Geophys. Res.*, **70,** 1311 (1965).
(10) D. A. Thompson, H. D. Barber, and W. D. Mackintosh, *Appl. Phys. Letters*, in press.
(11) D. Powers, W. K. Chu, and P. D. Bourland, *Phys. Rev.*, **165,** 376 (1968).
(12) J. Lindhard, *Mat. Fys. Medd. Dansk. Vid Selsk*, **34** (1965).
(13) J. V. Andersen and E. Uggerhøj, *Can. J. Phys.*, **46,** 517 (1968).
(14) L. Eriksson, J. A. Davies, H. J. Denhartog, H. Matzke, and J. S. Whitton, *Can. Nucl. Technol.*, **5,** 40 (1966).
(15) J. A. Davies, J. Denhartog, L. Eriksson, and J. W. Mayer, *Can. J. Phys.*, **45,** 4053 (1967).
(16) E. Bøgh, Proceedings of the International Conference of Solid State Physics Research with Accelerators, **BNL. 50083 (C-52),** 76 (1967).
(17) W. M. Gibson, F. W. Martin, R. Stensgaard, F. Palmgren Jensen, N. T. Meyer, G. Galster, A. Johansen, and I. Solsen, *Can. J. Phys.*, **46,** 675 (1968).
(18) L. Eriksson, J. A. Davies, N. G. E. Johansson, and J. W. Mayer, *J. Appl. Phys.*, in press.
(19) J. W. Mayer, J. A. Davies, and L. Eriksson, *Appl. Phys. Letters*, **11,** 365 (1967).
(20) M. McCargo, J. A. Davis, and F. Brown, *Can. J. Phys.*, **41,** 1231 (1963).



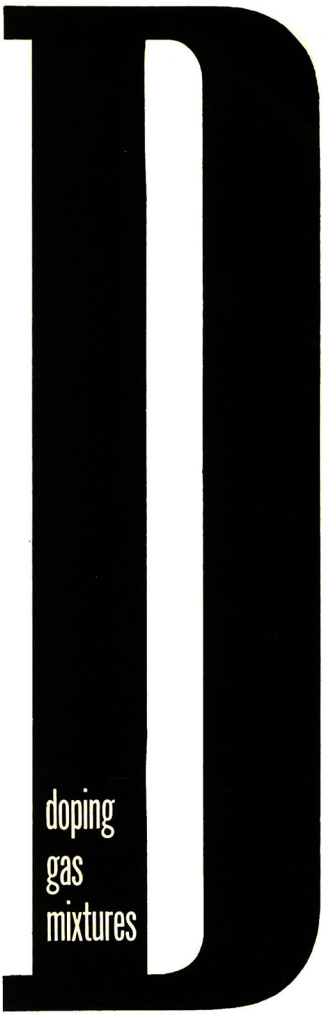


**Doping Gas Mixtures. Arsine, Phosphine, Silane, Diborane in Argon, Helium, Hydrogen, Nitrogen. In various amounts and concentrations.**

**For this year's catalog, write: Rare and Specialty Gases Dept., Airco Industrial Gases, 150 East 42nd Street, New York, N.Y. 10017.**

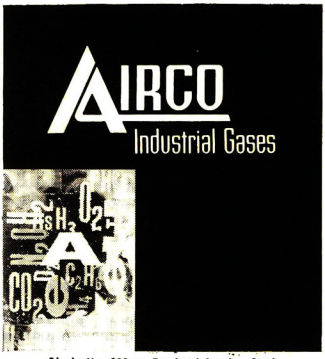


Circle No. 200 on Readers' Service Card

## THIS IS A LIST OF OPTIONS YOU WON'T NEED (THEY'RE BUILT-IN)

*Dual channel — double beam
Digital concentration readout (2)
True mathematical integrator
Recorder and computer outputs
*Push-button automatic zero control
*Servo-automatic recalibration
*Reads 2 elements simultaneously, or
Read one element w/internal standard
Push-button fail-safe flame ignition
Gas control system (3 gases)
*Push-button fail-safe $N_2O$ conversion
*Gas and flame safety monitor
*Simplified hollow cathode zone balance (2)
Six tube hollow cathode turret
*Preset independent hollow cathode current
Curved slits on monochromator
Constant head drain system
Flame emission capability
*All solid-state modular electronics
Stabilized voltage regulation
*External electronic test circuit
Single, integrated package — 18″ x 40″ x 20″

*Exclusive features

## THIS IS A LIST OF OPTIONS YOU CAN ORDER SEPARATELY

Nitrous oxide burner
Total consumption burner
UV-Vis spectrophotometer attachment
Recorder (if needed)

**Check all these features**

**See the Model 153 demonstrated—**

**Booth 339–342, Pittsburgh Conference**

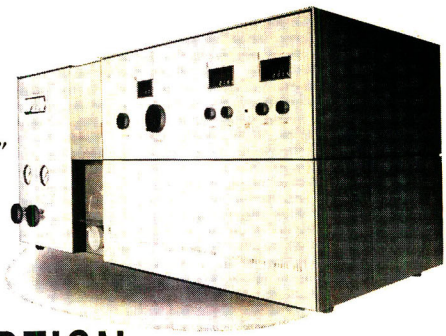

# ATOMIC ABSORPTION WITH THE OPTIONAL EXTRAS LEFT IN!

Add up the "optional extras" that are really necessary for safe, easy, dependable and precise analysis by atomic absorption. Then write for further information about the Model 153. Instrument Leasing Program details upon request.

INSTRUMENTATION LABORATORY INC. 113 HARTWELL AVE. LEXINGTON, MASS. 02173

**OFFICES IN: ATLANTA • BALTIMORE • BOSTON • CHICAGO • CLEVELAND • DALLAS • DENVER • DETROIT • HOUSTON • LOS ANGELES NEWARK • NEW YORK • PHILADELPHIA • SAN FRANCISCO • ST. LOUIS • WASHINGTON • TORONTO • MONTREAL • VANCOUVER • ZURICH**

Circle No. 126 on Readers' Service Card

See ACS Laboratory Guide for All Products/Sales Office

# 1 Part per Trillion Sensitivity...

# 0.5 mμ Resolution (with standard gratings)

# All at basic cost of $4,900.00

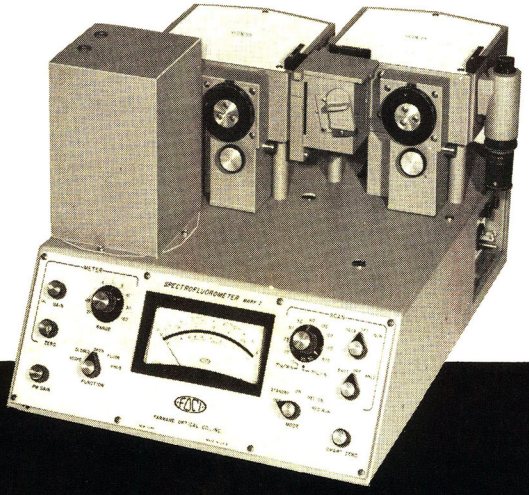

## Farrand MK-1 SPECTROFLUOROMETER

An ellipsoidal mirror which collects radiation from a high pressure xenon arc lamp is the key to the outstanding sensitivity displayed by this instrument. Two f/3.5 Monochromators accent the speed and response of the system while interchangeable detectors, varying in spectral response, encourage the instrument's wide range of analytical capabilities.

Sample chamber isolation results in less than 1°C temperature change from ambient due to lamp temperature. In addition, the instrument's standard, built-in, solid-state electronics readily accepts field retrofit of major accessories. The basic unit also features outputs for strip chart and X-Y recorders and oscilloscopes.

Phosphorescence and Cryogenic, T.L.C., Polarization, Ratio Recording and a 16-position Indexed, Enzyme Kinetics monitoring attachment are available as optional accessories.

Direct inquiries to:

Farrand OPTICAL CO., INC. COMMERCIAL PRODUCTS DIVISION
535-A South 5th Avenue, Mount Vernon, New York 10550
(914) 668-9393/Cable Address: FOCIUS NY

FOCI
A product of Farrand Optical Co., Inc. New York, N. Y.

Circle No. 182 on Readers' Service Card

See ACS Laboratory Guide for All Products/Sales Office

# Here's a new instrument that makes Far Infrared routine and push-button easy.

Up until now, working with Far IR was a time-consuming task that meant working with non-standard equipment.

But Perkin-Elmer has changed that with the FIS-3, a new double-beam instrument designed specifically for the Far IR spectral region—one that will provide results on a routine, non-complicated basis.

For one thing there's no need to stand around and adjust knobs and dials constantly. The FIS-3 is made for the research scientist who wants to push the button and walk away to more important tasks while the instrument scans the entire FIR range from 400 to 30 $cm^{-1}$ (25-333$\mu$) automatically and unattended.

To insure that maximum system energy is available, the entire optical path is evacuated—water vapor can be efficiently and quickly removed from the entire instrument in just twelve minutes. This, of course, means that you get into operation faster and run more samples per unit operating time. If desired, the sample compartment can be purged with dry air, and the remainder of the instrument evacuated.

Spectra are conveniently presented on a preprinted chart. Presentation is unbroken, continuous, and at a constant scale factor over the entire range. All the information is immediately available, easy to read directly from the chart.

Another Far IR problem has been minimized—that of sampling other than ambient temperatures. The FIS-3's unique switch-selectable double chopping mode of operation ignores these sampling effects, provides undistorted band depths.

As part of our system-oriented approach we offer a complete line of liquid, solid and gas sampling accessories, many of them specially made for use in a vacuum environment. Several of them hold multiple samples, so you can make successive sample runs without disturbing the instrument's equilibrium.

It all adds up to a new standard instrument for the Far IR. Both routine and research grade spectra are now available from one instrument.

Write for the new and detailed brochure about this newest instrument from the leader in IR. Instrument Division, Perkin-Elmer Corporation, 702 Main Avenue, Norwalk, Connecticut 06852.

**PERKIN-ELMER**

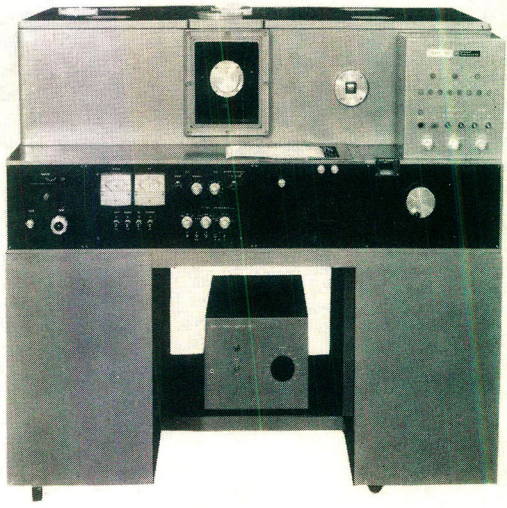

Circle No. 175 on Readers' Service Card

See ACS Laboratory Guide for All Products/Sales Office

# It's no bigger than your thumb

but you get a wide variety of porting arrangements with a Hamilton valve. You can build your own miniature piping system for corrosive fluids and gases for flow through two, three, or four ports. Valves are individually tested to 100 psi. Wetted parts are precision machined of Teflon* and Kel-F†, and encased in an outer metal body. Fittings of standard male and female luer designs allow leak-tight connection by fingertip adjustment without wrenches or lab grease.

Let us send you our new Catalog on syringes and related equipment.

Write to: Hamilton Company, P.O. Box 307B, Whittier, Calif. 90608.

*Dupont registered trademark.
†3M registered trademark.

**Repeatable Precision: Hamilton's 2, 3, and 4 port inert valves**

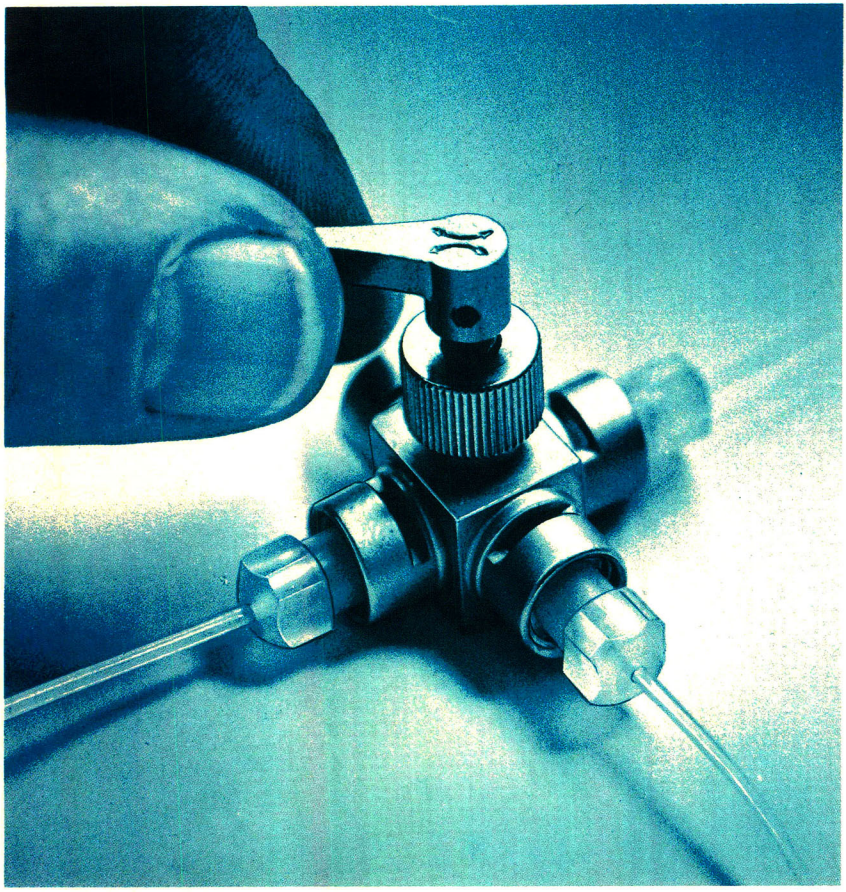

HAMILTON

Circle No. 8 on Readers' Service Card

See ACS Laboratory Guide for All Products/Sales Office

Old Egyptian weight made of black basalt with a finely polished surface. The hieroglyphics tell the weight of the stone (270 debens = 26.880 kg).



# About the weight of time.

In the good old days, time could be wasted in the laboratory.

No one found anything wrong with someone working for a few minutes with the good old two-pan balance in order to weigh out a teaspoon of potassium cyanide to the accuracy of ± 1/10,000 g.

Since 1946, things can be weighed 10 to 20 times faster with greater accuracy. It was in 1946 that the good new days began in the laboratory: Mettler introduced the one-pan substitution balance.

Since time becomes even more expensive as years go by, we have continued to improve our balances and to simplify operation. We have increased the balance sensitivity to one ten-millionth of a gram and increased the reproducibility. Success has not evaded us. Mettler produces more precision and analytical balances today than all other manufacturers in the world together.

With time, it became clear to us that the cost of lab time for thermal and volumetric measurements was as important as lab time for weighing. Our 120 researchers thus developed other new automated measurement devices which measure more quickly and more accurately.

The Thermoanalyzer is an automatic device which carries out TGA/DTG/DTA measurements simultaneously and records all defining magnitudes and measurement results graphically.

The Mettler FP1, FP2, and FP3 measurement devices determine melting points, boiling points, and dropping points practically automatically.

We have other, very novel thermal and volumetric measurement devices in the development and testing stage.

In 1990, lab time will cost even more. And we then have to be so advanced that we can smile about the good old days of the 1960s.

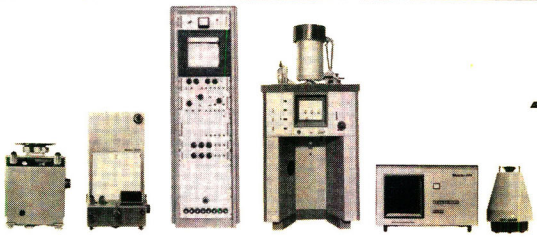

Mettler

Princeton, New Jersey
Zurich, Switzerland
Giessen, West Germany

Circle No. 181 on Readers' Service Card

See ACS Laboratory Guide for All Products/Sales Office

# Assay your way smoothly through the enzyme maze. With radiochemicals.

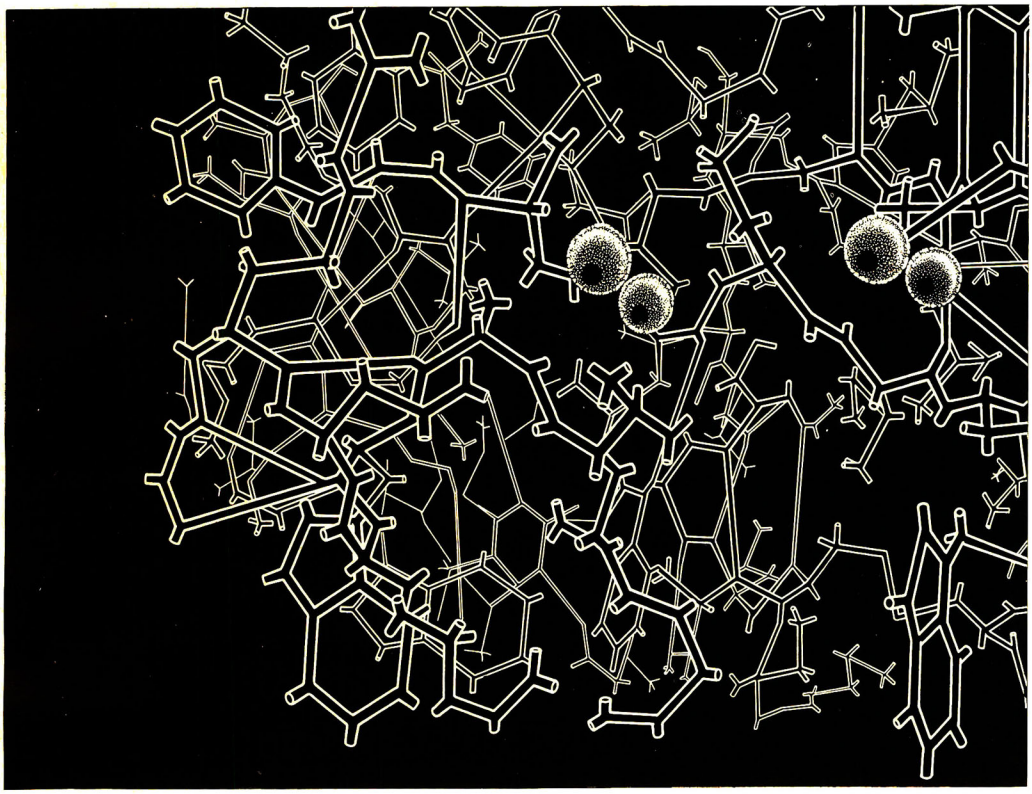

First—to those of you already performing enzyme assays—a summary of the advantages of the *radiochemical* methods of assay.

**Speed.** Sampling and separation techniques are rapid, simple, easily performed.

**Specificity.** With the proper substrate, interference reactions can be avoided. The radiochemical method of assay is thus eminently suitable for enzymes in crude extracts, and for studying effects of inhibitors, activators, and pH.

**Sensitivity.** Which permits radiochemical assays of crude-tissue extracts at high dilution, of low levels of enzyme activity, of microgram quantities of tissue, of enzymes in the presence of inhibitors such as drugs.

Secondly — if you are now using the radiochemical method of enzyme assay—a word or two about the Amersham/Searle labelled substrates especially prepared for enzyme assay.

**Accurately measured specific activities.** A critical, documented characteristic of the labelled substrates from Amersham/Searle.

**Low specific activity.** Insuring high chemical and radiochemical purity. Further, low specific activity gives Amersham/Searle labelled substrates long shelf-life.

**Low cost.** A large number of enzyme assays can be performed with a small amount of labelled substrate.

**Detailed technical information.** Ranging from the precise analytical results accompanying each Amersham/Searle compound to the objective discussion contained in the publication "Radiochemical Methods of Enzyme Assay," copies of which are furnished on request.

Call or write for specific information on labelled substrates for enzyme assay. (Do you have your copy of our 69/70 Radiochemical Catalog?) 9-211

2000 NUCLEAR DRIVE DES PLAINES, ILLINOIS 60018 TELEPHONE: (312) 296-1055

Amersham/Searle

AMERSHAM/SEARLE CORPORATION:
AN ACTIVITY OF G. D. SEARLE & CO. AND THE RADIOCHEMICAL CENTRE

**Circle No. 91 on Readers' Service Card**

# 30 seconds

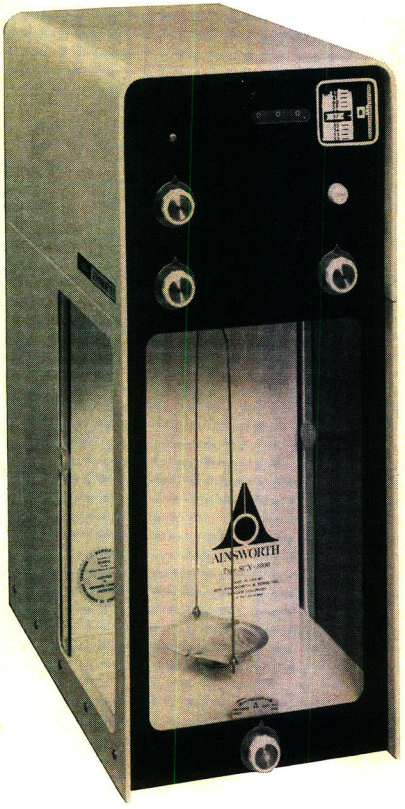

## from check-zero to readout with an accuracy of 80 micrograms

Type SCN 1000 ANALYTICAL BALANCE . . . is completely self-contained. Weights 1. to 999 g. are built-in, knob-operated, never touched. All controls on front panel are plainly marked. There is no arm-length error. Load and sensitivity are constant.

Wm. Ainsworth, Inc. 2151 Lawrence, Denver, Colorado 80205. (303) 222-0565.

| | |
|---|---|
| **CAPACITY** | 1000 g |
| **SENSITIVITY** | 1 scale division, 10 mg;<br>1 Micrometer division, .1 mg |
| **REPRODUCIBILITY** | S = ± .08 mg |
| **READOUT** | 7-digit in-line |
| **OPTIONS** | SCNB Weigh Below;<br>SCNA Explosion-proof |

AINSWORTH

*Keeping America in Balance since 1880*

D-879

Circle No. 20 on Readers' Service Card

# Now . . . Analysis As Never Before On Chromatographic Media



WITH THE Farrand

# VIS-UV CHROMATOGRAM ANALYZER

*for* UV and VISIBLE FLUORESCENCE SCANNING
FLUORESCENCE QUENCHING
UV and VISIBLE DENSITOMETRY

CHECK THESE FEATURES:

- ✓ **Unique 3 slit scanning system** averages non-uniform background for optimum sensitivity
- ✓ **Double beam ratio recording** for highest precision and accuracy
- ✓ **Double and single beam** facilities are standard
- ✓ **Two grating monochromators** provide highly efficient selection of wavelength
- ✓ **Interchangeable quartz/glass optics** provide maximum transmission throughout UV/visible range
- ✓ **Automatic digital** readout integration
- ✓ **21 speed strip chart recorder** standard in system
- ✓ **Sensitivity** to nanogram quantities on TLC plates

FOCI®
A product of
Farrand Optical Co., Inc.
New York, N.Y.

Direct inquiries to:

**Farrand OPTICAL CO., INC.** Commercial Products Division

535-A South 5th Avenue, Mount Vernon, New York 10550 (914) 668-9393 / Cable Address: FOCIUS NY

Circle No. 183 on Readers' Service Card

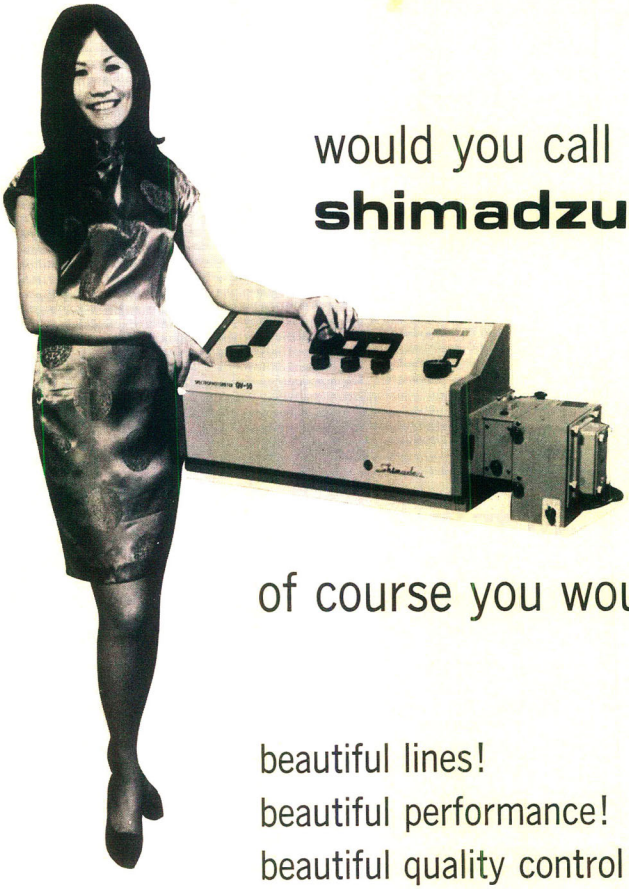

# would you call **shimadzu** beautiful?

## of course you would...

beautiful lines!
beautiful performance!
beautiful quality control!
a beautiful spectrophotomer!

Let's talk about beauty... in a spectrophotometer. And that brings us to the **shimadzu** QV-50.

Rarely does a piece of equipment perform completely as per manufacturer's specifications, and the QV-50 practically never needs servicing.

The expectations of all our users in the field were far exceeded. Range and accuracy are real. The QV-50 can expand either end of its readout from 0 to 10% and from 90% to 100% over the full scale.

**shimadzu** has internal beauty too. The enclosed monochromoter is a sealed unit (dirt and dust can't get in to affect optics and create stray light). As standard equipment, a set of thermospacers is supplied. We take this for granted, but no other instrument of its type has this as a standard feature. It also supplies a cell holder which will take from micro to 20mm. cuvettes.

The QV-50 power supply does not generate heat like its competition because of its partially transistorized construction. It will take a much greater range of accessory equipment than does any other single beam spectrophotometer of its type.

**shimadzu** 's a pioneer in the introduction of optical rotatory dispersion and circular and flow dichroism in single beam spectrophotometric instruments.

**AND THE BEAUTY OF IT ALL?** These important standards are now brought into your price range—$3500.

## COSMOS SCIENTIFIC CO.

921 BERGEN AVE., JERSEY CITY, N.J. 07306 · (201) 925-1101

*Distributed by:* **Ace Scientific Supply Co.** Linden, New Jersey; **American Instrument Co., Inc.** Silver Spring, Maryland; **Preiser Scientific Co.** Charleston, West Virginia

Circle No. 34 on Readers' Service Card

See ACS Laboratory Guide for All Products/Sales Office

# Modern Instrumental Techniques for Elemental Analysis

The 22nd Annual Summer Symposium on Analytical Chemistry is sponsored by ANALYTICAL CHEMISTRY and the ACS Division of Analytical Chemistry

University of Georgia, Athens, Georgia
June 11 to 13, 1969

**Chemistry Building, University of Georgia**

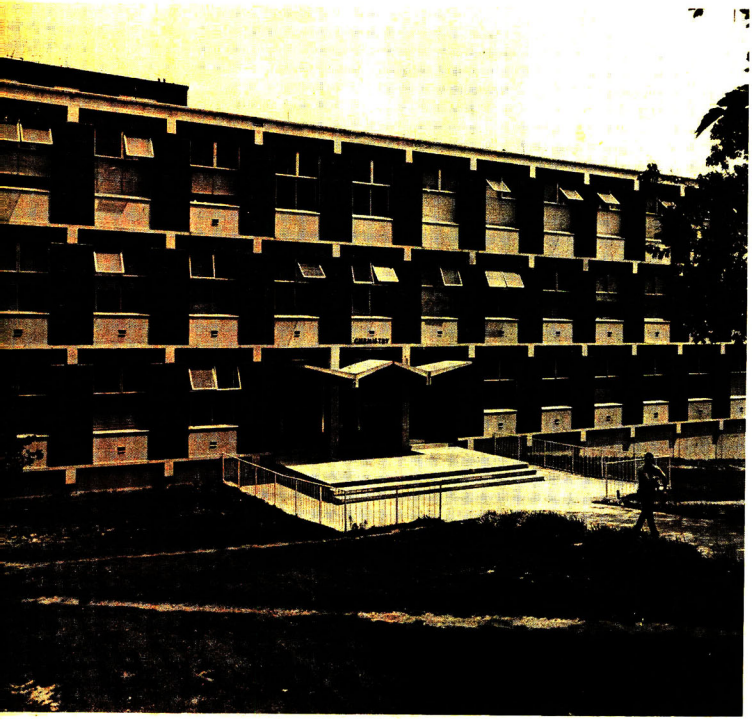

MODERN INSTRUMENTAL TECHNIQUES for Elemental Analysis is the topic of the 22nd Summer Symposium on Analytical Chemistry to be held in Athens, Georgia, June 11 to 13, 1969. Technical sessions will be held in the Chemistry Building, University of Georgia. Housing and dining facilities will be located at the James E. Oglethorpe, a private residence hall.

The program consists of twelve technical papers. The opening paper will deal with the fundamentals of quantitation. The remaining papers will cover a broad range of techniques including spectroscopy, gas chromatography, and electrochemical methods. Each speaker has been allotted a full hour and he has been encouraged to leave ample time for audience participation in discussions. Seminar rooms will be available in the Chemistry Building and the residence hall for further discussions.

Special events include a mixer to be held at Oglethorpe House Tuesday evening, and on Wednesday evening a barbecue located at a local lodge. Thursday afternoon is scheduled for free time. There is an outdoor pool at Oglethorpe House for those who care to swim. The University and other local golf courses are available by auto or cab and there are tennis courts available. The Chemistry Building will be open to visitors at this time and other open house visits will be arranged depending upon demand. The University of Georgia is the oldest chartered state university in the country and there are many interesting buildings on campus. Some may wish to visit the research facilities of the Southeast Water Laboratory.

Special activities are planned for ladies. One will include a tour of the campus and some of the outstanding ante-bellum houses in the city and will end with a tea at the recently restored ante-bellum home of the President of the University of Georgia. (A lifeguard on duty at this time will permit older children to spend the afternoon at the Oglethorpe House pool.) A second tour will include a shopping trip to Lennox Square, Atlanta, for the ladies.

Athens, Georgia, lies in the foothills of the Appalachian Mountains in northeast Georgia about 65 miles east

of Atlanta. Some of the regional attractions are the many historical sites and exhibits in Atlanta, such as Stone Mountain Park and the Cyclorama, the Great Smoky Mountain National Park, and the off-shore islands of southern Georgia. Athens can be reached by air via Southern Airways or Athens Aviation Air Taxi service connecting with Atlanta. Train service to Athens is available on Southern Railways from the eastern cities. Hertz rentals are available at the Athens Airport.

Room and board is available both for participants and their families in the James E. Oglethorpe House. Facilities include double rooms with semi-private bath, recreation rooms, conference rooms, and an outdoor swimming pool. All facilities used for the conference are air conditioned. Rooms will be available on Tuesday afternoon, June 10. Total charge for room, Tuesday through Thursday nights, and breakfast and lunch, Wednesday through Friday, will be $18.60 per person in a double room, $22.10 per person in a single room. The rate for children under 11 is half of the adult charge. The room only is $15.30 per person in a double room and $18.75 per person in a single room. Meals only may be obtained on a cash basis. Rooms are available Friday night following the symposium for $5.50 per person in a double room and $7.00 per person in a single room. Information concerning the residence facility or local motels and tourist attractions may be obtained by writing the Chairman for Local Arrangements.

Please fill out the registration form and return it along with a $10 registration deposit before May 21, 1969, to reserve accommodations and to receive appropriate information.

The Program Chairman for the Symposium is Dr. George H. Morrison, Department of Chemistry, Cornell University, Ithaca, N. Y. 14850. The Chairman for Local Arrangements is Dr. Donald E. Leyden, Department of Chemistry, University of Georgia, Athens, Georgia 30601.



James E. Oglethorpe House, Athens, Georgia

## PROGRAM

### Wednesday Morning, June 11

G. H. Morrison, Presiding

**9:00 Introductory Remarks and Announcements**

**9:15 Quantitation in Elemental Analysis.** H. Kaiser, Institüt für Spectrochemie und Angewante Chemie, Dortmund, Germany

**10:45 Atomic Absorption and Emission Spectroscopy.** V. Fassel, Iowa State University, Ames, Iowa

### Wednesday Afternoon, June 11

D. M. Hercules, Presiding

**2:30 Chemical Absorption and Fluorescence Spectrophotometry.** D. F. Boltz, Wayne State University, Detroit, Michigan

**3:30 Metal Analysis by Gas Chromatography.** R. E. Sievers, Aerospace Research Laboratories, Wright-Patterson A.F.B., Ohio, and Chemisches Institut der Universität, Tübingen, Deutschland; W. R. Wolf, K. J. Eisentraut, Wright-Patterson A.F.B.; W. G. Scribner, W. D. Ross, Monsanto Research Corp., Dayton, Ohio

### Thursday Morning, June 12

F. D. Leipziger, Presiding

**9:00 Laser Microprobe–Emission Spectroscopic Technique for Biological Research.** David Glick, Stanford University Medical School, Palo Alto, Calif.

**10:00 Electron Probe Microanalysis.** Kurt F. J. Heinrich, National Bureau of Standards, Washington, D.C.

**11:30 Ion Microprobe Analysis.** C. A. Andersen, Applied Research Labs., Goleta, Calif.

### Thursday Evening, June 12

J. C. White, Presiding

**7:30 Electrochemical Methods of Analysis.** J. K. Taylor, National Bureau of Standards, Washington, D. C.

**8:30 Ion-Selective Electrodes.** G. A. Rechnitz, State University of New York at Buffalo, Buffalo, N. Y.

### Friday Morning, June 13

V. P. Guinn, Presiding

**9:00 Electron Spectroscopic Methods.** L. A. Harris, General Electric Res. and Dev. Center, Schenectady, N. Y.

**10:00 Spark Source Mass Spectrometry.** E. B. Owens, M.I.T.–Lincoln Laboratory, Lexington, Mass.

**11:00 Activation Analysis Using High Resolution Detectors.** W. Lyon, Oak Ridge National Laboratory, Oak Ridge, Tenn.

## Registration Form, 22nd Annual Summer Symposium

### Division of Analytical Chemistry and ANALYTICAL CHEMISTRY

### University of Georgia, Athens, Georgia 30601

Date _____

Name (please print) Dr. Mr. Mrs. Miss _____

Professional Affiliation _____

Mailing Address _____

Registration Fee: $10.00

Accommodations in James E. Oglethorpe House: Room Tuesday, Wednesday and Thursday nights; breakfast and lunch Wednesday, Thursday and Friday. Total Charge, double room $18.60 per person; single room $22.10 per person, Room only: double room $15.30 per person, single room $18.75 per person. Meals only on a cash basis. Room only Friday night: double room $5.50 per person, single room $7.00 per person. Children 11 years and under half charge.

Please check appropriate items:

_____ I prefer a single room (if available)

_____ I would like to share a double room with _____ (give name)

_____ I will share a double room with someone you will assign

_____ I would like accommodations for myself and wife (or husband) and the following members of my family (give names and, if children, their ages). Adjoining rooms with bath will be assigned to families.

_____

_____

_____ I will arrange my own accommodations. (A list of motels will be supplied upon request).

_____ I expect to attend the barbecue, Wednesday, June 11. ($2.25 per person, please indicate number if more than one)

_____ I expect to attend the mixer Tuesday evening 8:30-11:00 pm. ($1.75 per person)

Please make _____ reservations for the ladies' tour of Historic Athens and Tea at Home of the President of the University of Georgia.

Please make _____ reservations for the ladies' shopping tour to Lennox Square, Atlanta, Thursday afternoon.

I plan to travel by plane ____, train ____, or auto ____.

I plan to arrive on June ____ at _____ (approximate time) and depart June _____.

This form should be returned before May 21, 1969, together with a $10.00 registration deposit to 22nd Annual Summer Symposium on Analytical Chemistry, Georgia Center for Continuing Education, University of Georgia, Athens, Georgia 30601. Please make checks or money orders payable to ACS Analytical Summer Symposium.


"Tygon -like"

"Almost Tygon"

"Tygon -type"

"Simulates Tygon"

Hogwash!

There's only one Tygon

For over a quarter of a century, the name TYGON—a registered trademark of Norton Company—has symbolized unsurpassed quality. **There is only one TYGON Tubing, a product of Norton.** Identification of genuine TYGON Tubing is quick, easy and positive—the name "TYGON" and the formulation number appear on every foot. Always insist on genuine TYGON Tubing, available at Laboratory Supply Houses everywhere.

32-156

NORTON

PLASTICS & SYNTHETICS DIV.

FORMERLY U.S. STONEWARE INC.

AKRON, OHIO 44309

Circle No. 62 on Readers' Service Card

A CORCO
FIRST

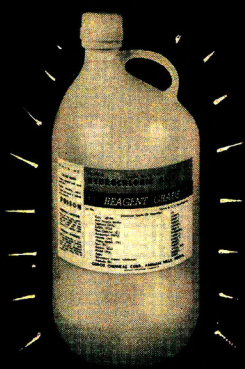

SAFER
MORE per BOTTLE
SAVES FREIGHT

CORCO
REAGENT HCl
in
NEW GALLON
PLASTIC BOTTLE

- Safer—no breakage.
- Holds 8 pints of acid.
- Less freight—20% less shipping weight for same weight of acid.
- Easier and safer disposal of empties.

Corco reagent grade ammonium hydroxide is also available in plastic 1-gallon bottles.

CORCO
CHEMICAL CORPORATION
Manufacturers of
Reagent and Electronic Chemicals
Tyburn Road & Cedar Lane,
Fairless Hills, Pa. 19030
Phone: (215) 295-5006

Circle No. 109 on Readers' Service Card
See ACS Laboratory Guide for All Products/Sales Office



# 20th Mid-America Symposium on Spectroscopy

## Chicago, Ill., May 12 to 15, 1969

THE CHICAGO SECTION in cooperation with other Mid-America Sections of the Society of Applied Spectroscopy and the Chicago Gas Chromatography Discussion Group will sponsor the 20th Mid-America Symposium on Spectroscopy. All of the program, including the exhibits, will be held in the Sheraton-Chicago Hotel in Chicago, Ill., May 12 through 15, 1969.

The technical program presently includes 180 papers from various fields of spectroscopy and gas chromatography. These include arc–spark–flame emission, atomic absorption, X-ray, NMR–EPR, Raman, infrared absorption, and nuclear particle spectroscopy. Sessions on air–water pollution, computer, and biochemical–toxicological applications are included. New for this year are sessions in Mössbauer and electron spectroscopy for chemical analyses. Symposia on trace element analyses, silicate analyses, and spectroscopy of materials under high pressure are included in the program.

An exhibit of scientific instruments, laboratory supplies, and books is part of the program. The detailed technical program given below is a tentative program. Papers, authors, and authors' addresses are given under the general subject title and not by date of presentation. The condensed program summarizes the technical program.

For further information on the meeting write to W. A. Loseke, IIT Research Institute, 10 W. 35th St., Chicago, Ill. 60616.

### CONDENSED PROGRAM

**Monday, May 12, 1969**

Emission Spectroscopy
Gas Chromatography–Mass Spectrometry
Nuclear Particle Spectroscopy
Mössbauer
Spectroscopy of Materials at High Pressure

**Tuesday, May 13, 1969**

Emission Spectroscopy
Trace Analysis
Gas Chromatography
Air–Water Pollution Studies
Mössbauer
Raman
Instrumentation and Techniques

**Wednesday, May 14, 1969**

Flame–Atomic Absorption
Biochemical–Toxicological Applications
Electron Spectroscopy for Chemical Analysis
Computer Applications
Study of Molecular Spectra

**Thursday, May 15, 1969**

X-Ray Spectroscopy
Biochemical–Toxicological Applications
Symposium on Silicate Analyses
Computer Applications
Matrix Isolation
NMR–EPR

### PROGRAM

### EMISSION SPECTROSCOPY

**Carbon and Graphite Spectroscopic Electrodes.** J. Weinard, Union Carbide Corp., Parma, Ohio

**Arc Stabilization with Cored Graphite Electrodes.** J. W. Mellichamp, U.S. Army Electronics Command, Fort Monmouth, N. J.

**Silica in Xylene by Direct Reading Emission Spectroscopy Using a Plasma Jet.** W. T. Engelskirchen, F. E. Lichte, Sinclair Research, Inc., Harvey, Ill.

**Alternate Methods for the Determination of Boron in Silicates.** John A. Schleicher, David B. Heck, Illinois State Geological Survey, Urbana, Ill.

**Spectroscopy Measurements on a High-Pressure Uranium Arc.** Richard R. Schneider, George R. Shipman, Arthur G. Randol II, University of Florida, Gainesville, Fla.

**Time-Resolved Radial Intensity Distributions in a High Voltage Spark Discharge.** R. D. Sacks, J. P. Walters, University of Wisconsin, Madison, Wis.

**The Effects of Source Parameters on Excitation in a High Voltage Spark Discharge.** J. P. Walters, University of Wisconsin, Madison, Wis.

**Studies of Phenomena Associated with Electrode Sampling in High Voltage, Oscillating Spark Discharge.** Stephen W. Brewer, Jr., John P. Walters, University of Wisconsin, Madison, Wis.

**An Electronically-Ignited Current Injection Spark Source.** J. P. Walters, Thomas V. Bruhns, University of Wisconsin, Madison, Wis.

**A Review of Recent Achievements in Analytical Emission Spectroscopy.** Anna M. Yoakum, Oak Ridge National Laboratory, Oak Ridge, Tenn.

**Spectral Response for Hollow Cathode Excitation of Some Binary and Ternary Gas Mixtures.** E. L. Grove, W. A. Loseke, IIT Research Institute, Chi-

# A time for decision in Atomic Absorption

Now you can choose from Beckman's broader line of highly sensitive instruments and accessories...and get greater precision, convenience and reliability.



# Beckman now provides a choice of Atomic Absorption instruments and accessories to fit the application–and the budget–of virtually every laboratory.

**These new models represent a three-way choice of Atomic Absorption Instrument Systems and significant Mind Free-ing advances in accuracy, precision and additional conveniences for you.**

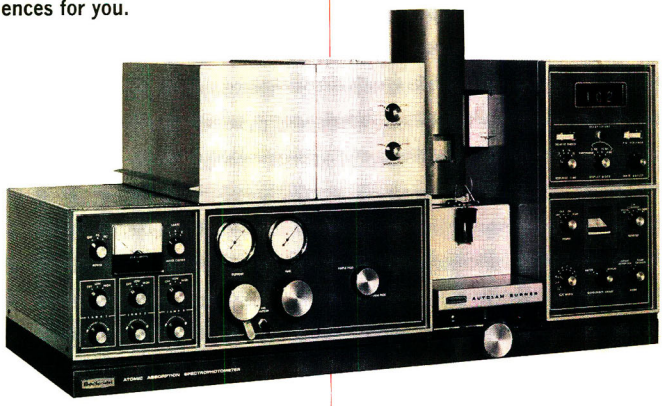

## MODEL 440

Outstanding features include–digital presentation of data, time constant selection, fine wavelength adjustment control, recorder output, coated optics for high reflectivity and long life, and single or triple pass optics. A wavelength scan drive is provided for recording lamp output. Measurement precision is further enhanced by an electronic circuit which holds and displays the photometric value at the optimum time.

## MODEL 444

Represents all the advances of the Model 440 *plus* "double beam" optics.

## MODEL 448

Is a moderately priced system planned for routine laboratory operation. This model has been specifically designed to fit limited budgets without sacrificing performance. Concentration is presented directly on the meter. Optics are coated.

## BURNERS

**Model 405 Burner:** offers maximum sensitivity. Operation may be in the hot or cold mode. Surfaces are coated for resistance to corrosion. Cleaning is facilitated because the burner dismantles easily and quickly. A wide variety of fuel and support gases may be utilized.

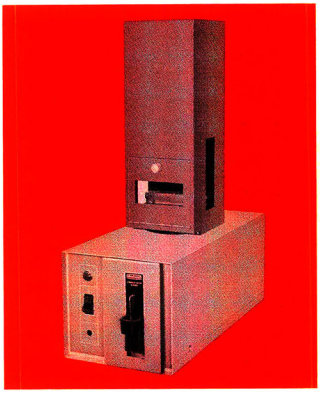

**Autolam Burner:** is a highly sensitive, yet simply designed burner, especially useful in solutions with a high concentration of solids. Surfaces are coated for corrosion resistance. Burner heads are easily interchanged. The unit is very easily cleaned.

**Autolam-S Burner:** is an economical version of the Autolam emphasizing a utilitarian design. Excellent performance is now available at a price to suit virtually any budget.

## FLAME EMISSION STUDIES

This mode of operation may be added with an accessory specially designed for optimum emission performance.

## CONCENTRATION CONVERTER

A direct presentation of concentration or absorbance is permitted with the addition of this unit. Easy to operate calibration controls eliminate manual calculation and graphing. Data is conveniently and precisely obtained. A curvature correction circuit is an integral part of this unit.

## PRINTER

Paper tape print-out of sample identification number, concentration or absorbance. Three digits of sample ID and 4 digits of sample data.

## AUTOMATIC SAMPLING SYSTEMS

**Autolam Sample Changer:** specifically designed for use with the Autolam Burner, this changer handles up to 20 samples, automatically.



**186555W Sample Changer:** automatically feeds up to 24 samples while accurately timing aspiration periods.

**200 Sample System:** permits programmed operation. Up to 200 samples may be analyzed unattended.

For complete details on any of these instruments and accessories and Beckman's complete line of Atomic Absorption supplies, contact your Beckman Sales Representative...or write for Data File No. 503.

Beckman®

INSTRUMENTS, INC.

**SCIENTIFIC INSTRUMENTS DIVISION**

FULLERTON, CALIFORNIA • 92634

INTERNATIONAL SUBSIDIARIES: AMSTERDAM; CAPE TOWN; GENEVA; GLENROTHES, SCOTLAND; LONDON; MEXICO CITY; MUNICH; PARIS; STOCKHOLM; TOKYO; VIENNA

PRINTED IN U.S.A.

cago, Ill.; I. Kaleps, Wright-Patterson Air Force Base

**Study of the Hollow Cathode Sources for Gas Monitoring in the 25 km to 65 km Altitude Region.** G. L. Johnson, J. Reich, E. L. Grove, IIT Research Institute, Chicago, Ill.

**Recent Advances in Glow-Discharge Emission for Spectrochemical Analysis.** J. Loeb, Dr. H. Ritzl, RSV Spectroscopy Division of Carl Zeiss, Hechendorf, West Germany

**Simplified Computer Operations in Spectrochemical Analyses.** Harry Dryer, Applied Research Laboratories, Detroit, Mich.

**Analytical Usage of the New Small Crater Laser Microprobe.** Fredrick Breck, Fisher Research Laboratories, Waltham, Mass.

## GAS CHROMATOGRAPHY–MASS SPECTROMETRY

**Study of Carbohydrates by Silylation.** Charles R. Sweeley, Dept. of Biochemistry, Michigan State University, Lansing, Mich.
**(Awards Address:** Chicago Gas Chromatography Discussion Group Award for outstanding work in gas chromatography)

**Quantitative Aspects of the Flame Ionization Detector in Flow Programmed Gas Chromatography.** Ram Levy, John Q. Walker, Clarence J. Wolf, Research Division, McDonnell Douglas Corp., St. Louis, Mo.

**Determination of Components in Cough Syrups.** Joseph Martin, Abbott Labs, North Chicago, Ill.

**Analysis of Polymers by Gas–Liquid Chromatography.** Michael Kulisz, V. Vincent Watson, Richardson Co., Melrose Park, Ill.

**The Use of Gas–Liquid Chromatography in the Printing Industry.** J. B. Himes, E. S. Derzko, Richardson Co., Melrose Park, Ill.

**Isolation of Gas–Liquid Chromatographic Determination of Trace Amounts of Amines in Related Compounds.** L. L. Metcalfe, Armour Industrial Chemicals, McCook, Ill.

**Capillary Gas Chromatography Analysis of Isomeric Amines in Related Compounds.** D. Martin, Armour Industrial Chemicals, McCook, Ill.

**Gas Chromatography Analysis of Perfume Compounds.** A. Modestas, Armour Dial, Inc.

**Molecular Characterization of Silicones by Gel Permeation Chromatography.** Fred Larson, Bendix Corp., Kansas City, Mo.

**Gas Chromatographic Analysis of Vaporous Contaminants in Living Spaces.** J. P. Hoeppesch, E. Lanterman, Borg-Warner, Des Plaines, Ill.

**Limiting Factors Involving Analysis by Gel Permeation Chromatography.** J. Armstrong, Arro Laboratories, Joliet, Ill.

**Functional Analysis by Combination Reaction Gas Chromatography–Mass Spectroscopy.** F. E. Regnier, J. Huang, Purdue University, Lafayette, Ind.

**Gel Permeation Chromatography Calibration of Normal Paraffins by Carbon Number.** R. E. Thompson, D. C. Ford, E. G. Sweeney, Sinclair Research, Harvey, Ill.

**VPC Analysis of Water in Chlorophyll.** T. M. Cotton, K. Ballschmiter, J. J.

← Circle No. 17 on Readers' Service Card


# ASK MATHESON...

## ...about a new flowmeter that was made for laboratories on a budget

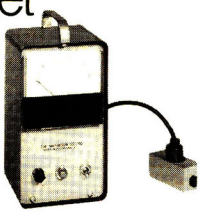

Flo-Tronic by Matheson costs little more than a rotometer. But a new thermal technique results in accuracy of 3% of full scale with changes in pressure and temperature having minimal effect on readings. Features: Fast response—2 sec. (0 to full scale)... Reproducibility—2% of full scale...Four flow ranges—0-300 to 0-10,000 std. cc./min.

## ...to explain why it pays to leave the mixing to us

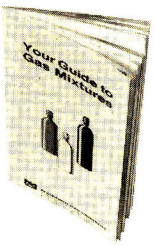


It pays because Matheson has the high load, high sensitivity analytical balances necessary to make gas mixtures gravimetrically (the gas is actually weighed). We call our gravimetric mixtures Primary Standards. They have accuracies equal to or exceeding 1% of the component value. At concentrations above 2%, accuracies are ±0.02% *absolute*. Costs a little more but these accuracies pay off for you in minimized errors and reduced overall costs. A final reason—our experience in making gas mixtures is unequalled in the industry.

## ...why the two stages in our Model 8 Regulator result in maximum control and longer life

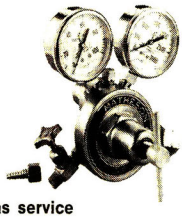

Two-stage design—high inlet pressure is reduced automatically to a pre-set intermediate pressure in the first stage which feeds gas at a relatively stable pressure to the second stage. Two stages result in a degree of control that permits an unvarying delivery pressure until the cylinder is almost empty. Because the second stage is protected from high-pressure surges, long, trouble-free service is assured.

**Ask Matheson *now*—Matheson offers the most complete gas service**

MATHESON
P. O. Box 85, East Rutherford, N. J. 07073

NAME _____

FIRM _____

ADDRESS _____

CITY _____ STATE _____ ZIP _____

Please send me "in depth" answers

☐ Flo-Tronic Flowmeter (Engineering Report)
☐ Matheson Primary Standards (Brochure)
☐ Model 8 Regulator (Catalog 26—over 100 pages devoted to gases, mixtures, and other gas handling equipment in addition to regulators)

**MATHESON GAS PRODUCTS**

**A Division of Will Ross, Inc.,** East Rutherford, N.J.; Cucamonga, Calif.; Gloucester, Mass.; Joliet, Ill.; LaPorte, Texas; Morrow, Ga.; Newark, Calif.; Whitby, Ont.

2-69G

Circle No. 23 on Readers' Service Card

# Determine surface area easily and economically.

With the Perkin-Elmer-Shell Model 212D Sorptometer, it's easy and inexpensive to determine surface areas.

It's fast—several times faster than conventional surface area measurement. This latest model handles three samples simultaneously, tripling the speed over past models. (The 212D is a third-generation instrument, so it's thoroughly proven.)

It's accurate. Even hard-to-measure samples of low surface area can be analyzed.

It's sturdy. Construction is of metal with a minimum of glass, so there's no breakage problem.

Sample requirements are modest. Measurements can be made with as little as 0.02 grams — certainly no more than 5 grams. Results are obtainable over a very broad range of surface areas.

And the cost is low—well below that of conventional techniques.

We'd like to send you a brochure and reprints of articles which describe the Sorptometer and its applications. Write to Instrument Group, Perkin-Elmer Corporation, 702 Main Avenue, Norwalk, Conn. 06852.

PERKIN-ELMER



Circle No. 173 on Readers' Service Card
See ACS Laboratory Guide for All Products/Sales Office




Katz, Argonne National Laboratory, 1043 S. LaGrange Rd., LaGrange, Ill. 60525

**Solubility Studies of Testosterone in Organic Solvents Using Gas–Liquid Chromatography.** Maryon W. Ruchelman, Jon T. Watson, The University of Texas; M. D. Anderson, Anderson Hospital and Tumor Institute at Houston, 6723 Bertner Ave., Houston, Texas 77025

**Mass Spectral Analysis of Mandelic Acid Esters.** Kenneth E. Daugherty, Technical Center, American Cement Corp., 1229 Monte Vista Drive, Riverside, Calif. 92507; John I. Stevens, Walter H. Neville, Dept. of the Army, Weapons Development and Engineering Laboratories, Chemical Process Laboratory, Edgewood Arsenal, Md.

## NUCLEAR PARTICLE SPECTROSCOPY

**Gamma Ray Spectrometer–Computer System.** J. R. Vogt, Research Reactor Facility, University of Missouri, Columbia, Mo.

**Neutron Activation Analysis of Rare Earth Impurities in Scandium Metal.** J. J. Hines, M. A. Wahlgren, Argonne National Labs, Argonne, Ill.; C. A. Edwards, Western College for Women, Oxford, Ohio

**Radiochemical Separation of Gallium by Amalgam Exchange.** R. R. Ruch, Illinois State Geological Survey, 1821 Maynard Dr., Champaign, Ill. 61820

**A Key-Lock System Based on Nuclear Radiation Spectrometry.** James Wing, Argonne National Laboratory, 9700 S. Cass Ave., Argonne, Ill. 60439

**The Effect of Channeling on the Charge-Changing Collisions of Energetic $^{3}He^{+}$ Ions Penetrating through Au(100) Monocrystals.** Manfred Kaminsky, Argonne National Laboratory, 9700 S. Cass Ave., Argonne, Ill. 60439

**General Aspects of Nuclear Gamma-Ray Resonance (NGR).** Stanley Ruby, Argonne National Laboratory, Argonne, Ill.

**Multiple Linear Regression Analysis of Scintillation Gamma-Ray Spectra: Automatic Candidate Selection.** M. A. Hogan, Hogan Associates; S. Yamamoto, D. F. Covell, Naval Radiological Defense Laboratory, San Francisco, Calif.

**A New Combustion Method for Collecting Tritiated Water from Organic Samples for Liquid Scintillation Counting.** Niilo Kaartinen, University of Turku, Finland

**A Commercial Version of Kaartinen Sample Preparation Apparatus.** D. W. Sher, A. G. Schrodt, Packard Instrument Co., Downers Grove, Ill.; Niilo Kaartinen, University of Turku, Finland

## MÖSSBAUER SPECTROSCOPY

**Application of Mössbauer Spectroscopy to Coordination and Biological Chemistry.** Leopold May, The Catholic University of America, Washington, D.C.

**On the Distinction Between Mass-Change Shift and Second-Order Doppler Shift in the Mössbauer Effect.** J. T. Dehn, U.S.A. Ballistic Research Laboratories, Md.

**The Point Charge Model for Quadrupole Splitting in $^{119}Sn$ in Mössbauer Spec-**


# ONLY ONE PART IMPURITIES IN 25,000,000 PARTS WATER



Better still, water that pure (15 megohms) is on TAP, fresh from IWT's Duplex De-Ionizer. Resin color change accurately tells you *remaining capacity* as well as *when* to change cartridges. (Conductivity meters tell water quality, when to change but not remaining capacity. IWT offers meters at extra cost.) Changing is simple and inexpensive. Further, the Duplex idea where water goes through *both* cartridges lets you exhaust a cartridge fully — you get better water at less cost. IWT IonXchangers are ideal for labs.



Let us send you a copy of Bul. DX-268 — 4-page, 4-color description of purity, cartridge options, mounting fixtures and costs.

**ILLINOIS WATER TREATMENT COMPANY**
**840 CEDAR ST., ROCKFORD, ILL. 61105**

iwt ionXchange

Circle No. 48 on Readers' Service Card

# New from Du Pont: first liquid chromatograph "with GC efficiency"

In performance, it gives gas chromatography a run for its money.

The Du Pont Liquid Chromatograph gets its resolving power in great part from a unique support material which has controlled surface porosity. The instrument was specially designed for high-pressure operation up to 3000 psi without the problems normally associated with high-pressure chromatography.

The combination of unique packing and high pressure makes possible 30-35 theoretical plates per second at carrier velocities of one to three centimeters per second for rapidly eluting compounds. Ultra sensitive detectors complement the separating power of the column.

And it's easy to operate. The Du Pont Liquid Chromatograph is a complete system. It contains a unit for solvent degassing and has a nitrogen purge for the reservoir head space. A nitrogen oven purge is also provided as an added safety feature.

It's versatile. The columns can be operated isothermally above ambient temperatures with precise control. The solvents can be changed easily and rapidly. Anion exchange, cation exchange, liquid/liquid, or adsorption techniques can be utilized on the Du Pont Liquid Chromatograph.

A complete descriptive brochure on the Du Pont Liquid Chromatograph is available; call (302) 774-7745 or write, Du Pont, Room 7249-A, Wilmington, Delaware 19898

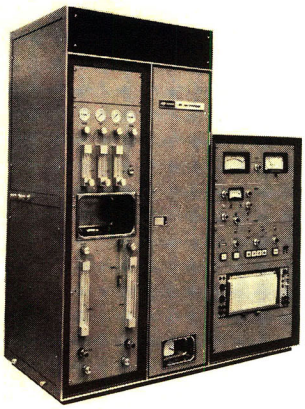

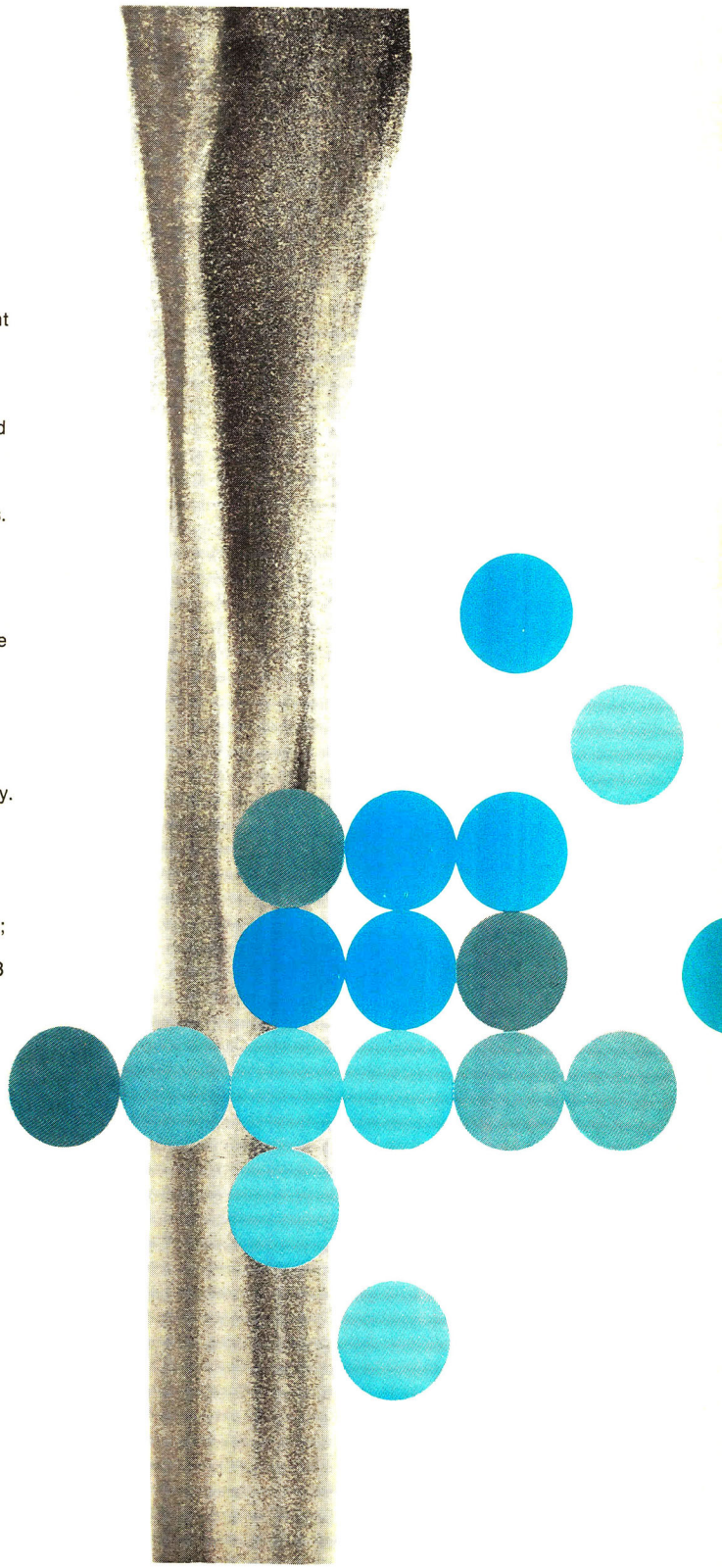

DU PONT Instruments

REG. U.S. PAT. OFF.

Circle No. 40 on Readers' Service Card

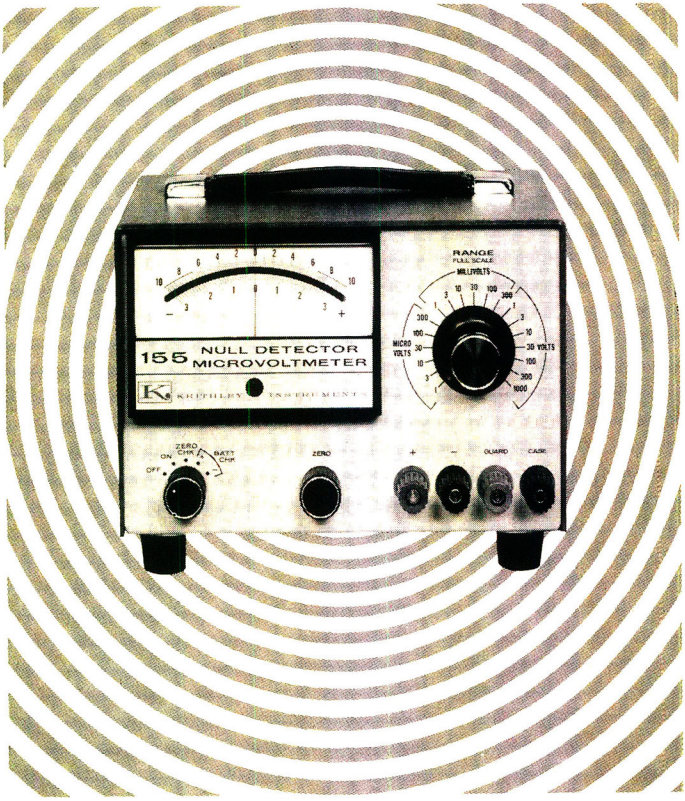


# Look what $325 buys in a 1 μV Full Scale DC Null Detector/Microvoltmeter

It buys you a portable performer with 0.15 microvolt resolution. It's handy and convenient to use. It's rugged, too—works more than 1000 continuous hours on four carbon-zinc batteries. It's the Keithley Model 155—the lowest-priced electronic null detector on the market today.

The 0.03 μv rms input noise is quieter than any other in its price class. Coupled with better than ½ μv per day stability and 1 megohm input resistance at 1 μv full scale, the 155 is ideal as a null detector for potentiometers, bridges, ratio devices and comparator circuits.

When the Model 155 isn't working as a null detector, it doubles as a 1 μv to 1000 volt microvoltmeter with 19 zero center ranges. Use it for measuring thermocouple and thermopile potentials, contact resistance, making Hall Effect studies, or whatever.

See this little giant perform. Call your Keithley Sales Engineer for your demonstration. Or contact Keithley Instruments, Inc. for complete details—28775 Aurora Road, Cleveland, Ohio 44139. In Europe: 14, Ave. Villardin, 1009 Pully, Suisse. Prices slightly higher outside the U.S.A. and Canada.

KEITHLEY

Circle No. 51 on Readers' Service Card

See ACS Laboratory Guide for All Products/Sales Office



troscopy. N. W. G. Debye, J. J. Zuckerman, State University of New York, Albany, N. Y.

**Mössbauer Spectroscopic Studies of Iron Diffusion in Rutile ($TiO_2$).** Paul P. Stampfl, John C. Travis, NASA/Goddard Space Flight Center, Greenbelt, Md.

**The Use of Mössbauer Spectroscopy on the Lanthanide Elements and Their Compounds.** Alan F. Clifford, Virginia Polytechnic Institute, Blacksburg, Va.

**Sample Preparation Methods for Overcoming Resolution Limitations in $^{57}Fe$ Mössbauer Patterns Obtained on Steels.** B. W. Christ, National Bureau of Standards, Washington, D.C.

**Mössbauer Studies of Tin Compounds with Quadrupole Splittings in Externally Applied Magnetic Fields.** N. E. Erickson, Brookhaven National Laboratory.

**Mössbauer Spectra of Some Tellurium Compounds.** Columba Curran, Thomas G. Krivak, University of Notre Dame, Notre Dame, Ind.

**Magnetic Ordering in Dilute Alloys of Iron in Gold.** C. E. Violett, University of California, Livermore, Calif.

**The Study of Retained Austenite by Means of Mössbauer Scattering Spectroscopy.** H. K. Chow, R. L. Bogner, International Chemical and Nuclear Corp., Pittsburgh, Pa. 15236

**Standard Reference Materials for Spectrometer Calibration and Correlation of Chemical Shifts of Iron and Tin Compounds.** James R. DeVoe, J. J. Spijkerman, National Bureau of Standards, Washington, D.C. 20234

## SPECTROSCOPY OF MATERIALS UNDER HIGH PRESSURE

**Raman Spectra of Solids Under Pressure.** S. S. Mitra, University of Rhode Island, Kingston, R. I.

**Pressure Dependencies of the Infrared Active Optical Phonons in Mixed Crystals $ZnS_xSe_{1-x}$.** J. R. Ferraro, C. Postmus, Argonne National Laboratory, Argonne, Ill.; S. S. Mitra, University of Rhode Island, Kingston, R. I.; C. J. Hoskins, University of Kentucky, Lexington, Ky.

**Pressure Dependencies of the Infrared Active Optical Phonons in Mixed Crystals $KCl_xBr_{1-x}$.** C. Postmus, J. R. Ferraro, Argonne National Laboratory, Argonne, Ill.; S. S. Mitra, University of Rhode Island, Kingston, R. I.; C. J. Hoskins, University of Kentucky, Lexington, Ky.

**Interferometric Measurement of Materials Under High Pressure.** J. Hiraishi, W. Fateley, Carnegie-Mellon University, Pittsburgh, Pa.

**The Effect of Pressure Upon the Optical Absorption Spectra of Silver Chloride and Silver Bromide.** Richard B. Aust, Eastman Kodak Co., Rochester, N. Y.

**Putting the Squeeze on at Maryland.** J. W. Brasch, A. J. Melveger, E. R. Lippincott, Center of Materials Research, University of Maryland, College Park, Md. 20742

**High Pressure Studies of Hydrogen Bonding.** R. Jakobsen, Y. Mikawa, Battelle Memorial Institute, Columbus, Ohio

**Panel Discussion**

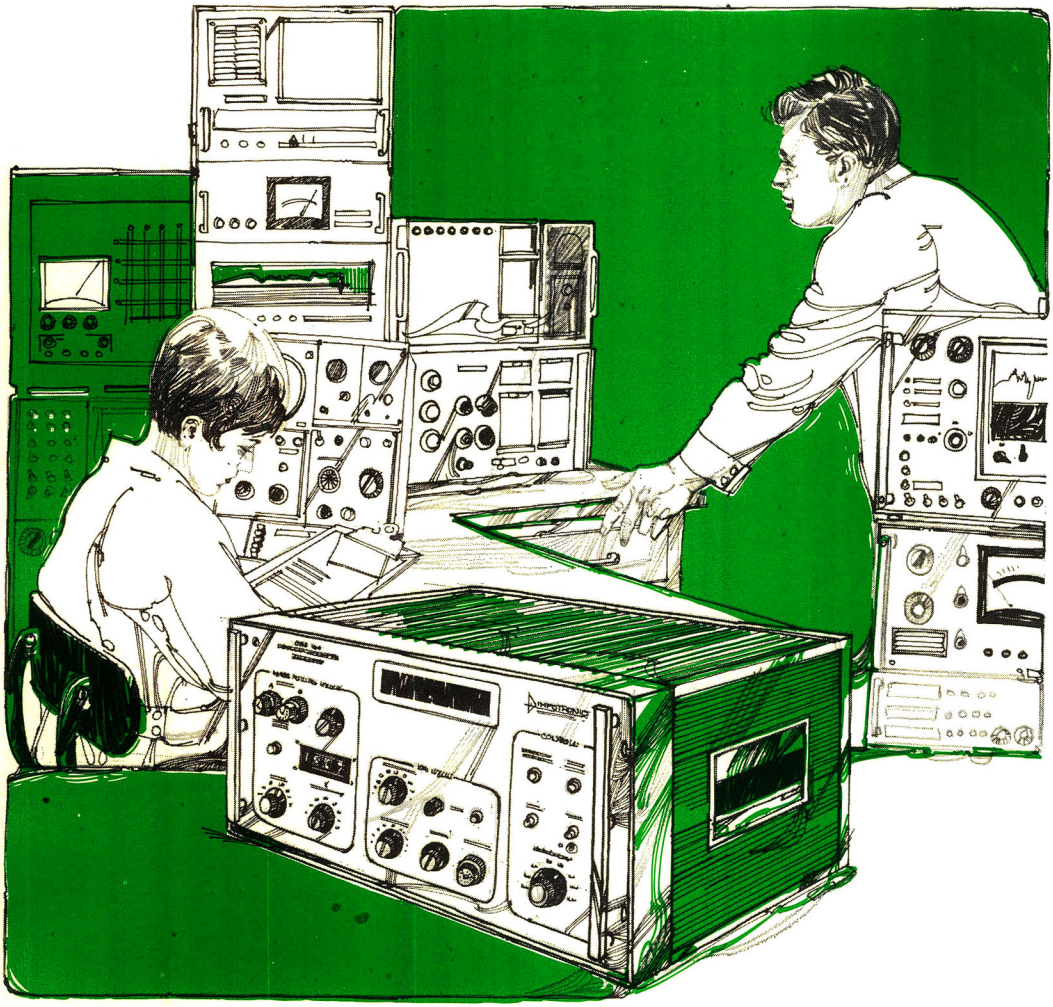

# NOW! $16.04 A DAY

## For the Newest Mass-Spec Digital Readout.

The new CRS-160 from Infotronics can calculate mass numbers when used with any mass spectrometer . . . with accelleration-voltage scanning or magnetic-flux scanning, with quadrapole or time-of-flight spectrometers. Still another mode provides peak time.

In any of the modes, the mass number or time data is printed out with 6 data digits of peak-height ion intensity.

So, what's new about its price?

The new Infotronics lease plan. It puts the CRS-160 to work in your lab without the need for capital investment. You can have the finest mass-spec readout on the market for just $16.04 a day . . . $481.25 a month including all charges for a 36-month period. And at any time, you can elect to purchase the CRS-160 outright for a special low price.

If both money and performance are important at your lab nowadays, you need to know more about the new CRS-160 and Infotronics lease plan. Call today. Area Code 713, SU 2-9770. And make it collect.

**CRS** DIGITAL SYSTEMS

INFOTRONICS CORP.

7800 WESTGLEN • HOUSTON, TEXAS 77042
BAARERSTRASSE 57 • 6300 ZUG, SWITZERLAND

401

Circle No. 125 on Readers' Service Card

# BURRELL "WRIST-ACTION"® LABORATORY SHAKERS



The same complete mixing swirl you get with your own hand and wrist has been copied mechanically in Burrell shakers. Then, superior to human wrist-action, the shaking motion operates at a constant speed—for as long as is required.

You control procedures from gentle agitation to violent swirling and repeat any operation at another time. The degree of shaking is controlled mechanically with an adjustable knob. The full torque of the constant speed motor is always applied to the oscillating mechanism. Loads need not be equalized or balanced. Shaking degrees are set, and repeated exactly at another time, to a scale graduated from 0 to 10. A built-in timer will automatically stop the shaker at any desired time up to 55 minutes or may be set to operate continuously.

## BUILD-UP® DESIGN

You Build-Up to suit your requirements. Starting with a standard shaker base unit, consisting of motor, oscillator and controls; you add a platform that accommodates Separatory Funnel Clamps or 8 Erlenmeyer flasks; and side-arms for 8, 12 or 16 flasks or bottles. Users may start with any Build-Up size and add or modify later, as all parts are interchangeable.

## Burrell Shaker BUILD-UP SIZE BT

Offered as the most versatile arrangement for general laboratory use. Includes standard shaker base unit, platform for up to 8 Erlenmeyer flasks and side arms for up to 8 flasks or bottles.

Cat. No. 75-765BT — Price complete $313.50
Separatory Funnel Clamps — $6.75 each

For more information see your Burrell representative or write for Bulletin No. 307.

BURRELL

**BURRELL** CORPORATION
SCIENTIFIC INSTRUMENTS AND LABORATORY SUPPLIES
2223 FIFTH AVENUE, PITTSBURGH, PA. 15219

Circle No. 102 on Readers' Service Card




## TRACE ELEMENT SYMPOSIUM

**Determination of Traces of Light Elements in Inorganic and Organic Materials by X-Ray Fluorescence Spectroscopy.** C. L. Luke, Bell Telephone Laboratories, Murray Hill, N. J.

**Direct Spectrographic Determination of Trace Impurities in High Purity Silver Nitrate Crystals.** A. J. Kincoln, V. LeRoy, Engelhard Industries, Inc., Newark, N. J.

**Sampling and Preparation Errors in Trace Analyses.** C. L. Grant, University of New Hampshire, Durham, N. H.

**Use of Sampling Boat Techniques for Trace Analysis of Lead.** D. C. Hildesbrand, E. E. Pickett, S. R. Koirtyohann, University of Missouri, Columbia, Mo.

**Electrodes for Trace Impurity Analysis and Determination of Traces in Gallium Metal.** M. S. Wang, Monsanto Co., St. Louis, Mo.

**Ultratrace Quantitative Metal Analysis by Mass Spectrometry of β-Diketonates.** T. L. Isenhour, University of Washington, Seattle, Wash.; B. R. Kowalski, R. E. Sievers, Wright-Patterson Air Force Base, Ohio

## AIR POLLUTION STUDIES

**Industrial Pollution Control Equipment.** Charles Skinner, Consulting Engineer, Skinner Engineering, 1301 W. 22 St., Oakbrook, Ill.

**Air Pollution and Analytical Chemist.** George Morgan, Acting Director, Division of Air Quality and Emission Data, National Air Pollution Control Administration, Cincinnati, Ohio

## WATER POLLUTION STUDIES

**Gas Chromatographic Analysis of Toxaphene in Natural Waters, Fish and Lake Sediments.** Robert A. Hughes, Gilman Veith, G. Fred Lee, Water Chemistry Laboratory, University of Wisconsin, Madison, Wis.

**Investigation of Solid Surfaces and Optically Opaque Systems by Internal Reflection Spectroscopy: Experimental Considerations.** James S. Mattson, Harry B. Mark, Jr., Walter J. Weber, Jr., Water Resources Science, University of Michigan, Ann Arbor, Mich.

**Status of Instrumentation in Pollution Analysis.** Alfred M. Tenny, Tenco Hydro/Aerosciences

**Pesticide Analyses by Gas Chromatography at Lake Michigan Basin Office.** W. DeWitt Johnson, Frederic D. Fuller, LeRoy E. Scarce, U.S. Department of the Interior, Federal Water Pollution Control Administration, Great Lakes Region, Lake Michigan Basin Office

## FLAME–ATOMIC ABSORPTION SPECTROSCOPY

**A Silicon Specific Detector Based on Interfacing a Gas Chromatograph and a Flame Emission or an Atomic Absorption Spectrometer.** J. A. Dean, Roy W. Morrow, W. D. Shultz, University of Tennessee, Knoxville, Tenn.

**An Evaluation of the Hydrogen–Argon Entrained Air Flame in Atomic Ab-**

Hewlett-Packard's respected track record of top performance, flexibility and reliability in the strip-chart recorder field is now available to OEM buyers. And while we're pretty sure you won't require rally stripes, we can offer you almost any option.

Here's a comprehensive source of *user*-specified precision strip-chart recorders offering a multiplicity of options, a variety of 5" and 10" rugged recorders, and a wide choice of recording speeds. Fast delivery of standard recorders or "specials." Maintenance, repair, parts available to you and your customer, nation-wide on a fast, local basis. And Hewlett-Packard has had years of experience in matching recorders to systems needs. We'll paint them any color you want, too.

You could say we're offering the OEM market classic models at fleet prices.

Talk to your HP field engineer. He sells lab and research recorders . . . and he sells recorders as systems components. He'll look at your problem and come up with the right answer. . . a recorder that's made . . . and priced . . . to order in quantity. Or write Hewlett-Packard, Palo Alto, California 94304; Europe: 54 Route des Acacias, Geneva.

11807

HEWLETT hp PACKARD

GRAPHIC RECORDERS

# Front Runner




Circle No. 121 on Readers' Service Card
See ACS Laboratory Guide for All Products/Sales Office

## ALCHEMY 1969...

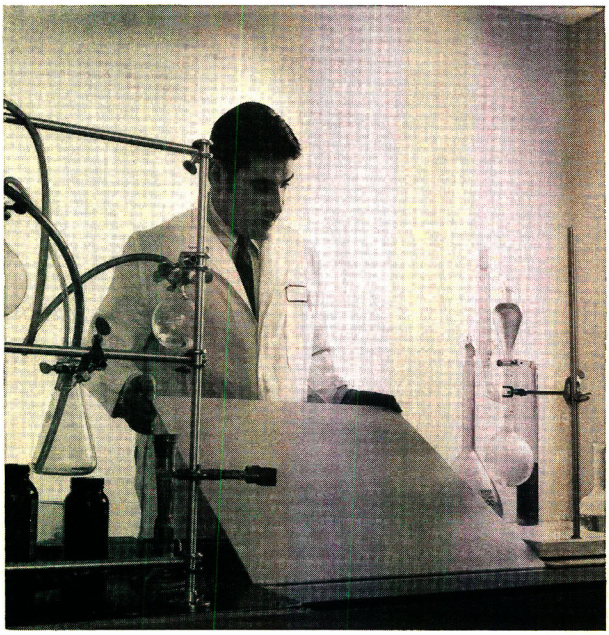

**CORNING Labtop from Fisher transmutes old workbench surfaces into brand-new supertops.**

Just cement CORNING™ Labtop to any benchtop material. At once, that worn, scarred, burned or gouged surface is covered with a Space Age glass-ceramic in handsome matte gray. *Permanently.*

Labtop is tough as case-hardened steel (it can't dent), has a mechanical strength about 20 times greater than conventional stone tops. It's extremely resistant to acids, alkalies and solvents, abrasion, and thermal shock (it's recommended for fume hoods). High in stain resistance too, and it wipes clean for a crisp new look, year in, year out.

Corning Labtop comes in 20 stock sizes for benchtops, three additional ones for reagent shelves (special sizes on request). Bulletin? Write Fisher Scientific Company, 1003 Fisher Building, Pittsburgh, Pennsylvania 15219. Or phone your Fisher representative—he can give you the details, plus a free Labtop sample that you can put through the paces for yourself. J-745

FISHER SCIENTIFIC CO.

Circle No. 43 on Readers' Service Card

See ACS Laboratory Guide for All Products/Sales Office




**sorption Spectroscopy.** Keith E. Burke, C. H. Albright, International Nickel Co., Inc., Suffern, N. Y.

**Some Improved Turbulent Flames and Their Use in Atomic Fluorescence Spectroscopy.** R. M. Dagnall, M. P. Bratzel, J. D. Winefordner, University of Florida, Gainesville, Fla.

**Digital Data Handling for Atomic Absorption Spectrophotometry.** J. E. Schallis, H. L. Kahn, Perkin-Elmer Corp., Norwalk, Conn.

**Measurement of the Degree of Atomization of Elements in an Air–Acetylene Flame.** W. P. Townsend, P. T. Zeegers, J. D. Winefordner, University of Florida, Gainesville, Fla.

**Recent Developments in Flame Emission, Absorption, and Fluorescence Methods.** R. N. Kniseley, Iowa State University, Ames, Iowa

**Determination of Calcium in Atmospheric Particulate Samples by Atomic Absorption Spectroscopy Utilizing an Internal Standard.** Jae Y. Hwang, Frederic Feldman, Instrumental Laboratory, Inc., Lexington, Mass.

**The Analysis of Electric Furnace Slags by Atomic Absorption Spectrophotometry.** W. H. Scheub, C. J. Stromsky, Timken Roller Bearing Co., Canton, Ohio

**Performance Features and Application of New Atomic Absorption Instrumentation.** N. Shifrin, J. Ramirez-Munoz, D. Barber, Beckman Instruments, Inc., Fullerton, Calif.

**Sprayer and Burner Units for Flame Emission and Atomic Absorption Measurements.** R. Mavrodineanu, Philips Laboratories, Briarcliff Manor, N. Y.

**Internal Standardization Philosophy in Flame Spectroscopy.** Frederic J. Feldman, Stanley B. Smith, Jr., Instrumentation Laboratory, Inc., Lexington, Mass.

**Determination, by Atomic Absorption Spectroscopy, of Lead and Copper Contents of Particulate Samples Collected from Air over Morton Grove, Illinois.** C. D. Burnham, C. E. Moore, T. Kowalski, J. Krasniewski, Loyola University, Chicago, Ill.

### BIOMEDICAL–TOXICOLOGICAL APPLICATIONS

**Optimization of a Spectrophotometer for the Measurements of Enzyme Reaction Rates.** Robert J. Manning, Beckman Instruments, Inc., Fullerton, Calif.

**Rat Liver Subcellular Trace Metal Alterations Resulting from Exposure to Low Concentrations (50 ppm) of Carbon Monoxide.** Stanely C. Mazaleski, Washington University School of Internal Medicine, St. Louis, Mo.; Carl A. Nau, Robert C. Duncan, Ronald L. Coleman, Oklahoma University School of Medicine

**Uses of the Laser Microprobe in Biomedicine.** I. Harding-Barlow, NASA, Palo Alto, Calif.

**New Methods for the Analysis of Human Skin and Perspiration by Infrared Spectroscopy.** B. M. Allison, Biology Department, Michigan Technological University; W. T. M. Johnson, R. P. Harroff, A. M. Collings, W. W. Johnson, Chemistry Dept., Lincoln University, Pa.

**Determination of Metals in Biological Samples with an Induction-Coupled Radio-Frequency Plasma Torch.** C. L. Grant, Donald Macnaughtan, Jr., Engineering Experiment Station, University of New Hampshire, Durham, N. H., Merle Thorpe, Humphreys Corp., Concord, N. H.

**Long Term Studies of Elemental Intake and Excretion of Three Adult Male Subjects.** Isabel H. Tipton, University of Tennessee, Knoxville, Tenn.; Peggy L. Stewart, University of Tennessee and Stewart Laboratories, Inc.

**Atmospheric Monitoring for Vapors of 1, 1-Dimethylhydrazine with a Portable Automatic Colorimetric Instrument.** Alfred M. Grosso, Manfred J. Prager, Joseph L. Kalinsky, Naval Applied Science Laboratory, Brooklyn, N. Y.

**ATR Infrared Spectroscopy of Biochemical Substances at Liquid-Nitrogen Temperature.** Frank S. Parker, New York Medical College, New York City, N. Y.

**Odor Threshold and Gas Chromatographic Assays of Vaginal Odors during Nitrofurazone Treatment.** Louis Keith, Irving Bush, Cook County Hospital, Chicago, Ill.; Andrew Dravnieks, B. K. Krotoszynski, IIT Research Institute, Chicago, Ill.

**Patterns of Urinary Copper Excretion in Patients with and without Urinary Tract Disease.** Jose A. Berrios, Frances Alexander, Al Dubin, George C. Baumgartner, Irving Bush, Hektoen Institute of Medical Research of Cook County Hospital and Chicago Medical School, Chicago, Ill.

**Dietary Zinc Intake in Man.** Dace Osis, Emily Wiatrowski, Joseph Samachson, Herta Spencer, Veterans Administration Hospital, Hines, Ill.

**Instrumentation in a Hospital Laboratory.** Alvin Dubin, Hektoen Institute for Medical Research, Chicago, Ill.

**Isolation and Identification of Morphine in Biological Material by Spectrometry and Gas Chromatography.** George Christopoulos, Cook County Coroner's Laboratory, Chicago, Ill.

**Applications of Instrumentation in Clinical Toxicology.** Eleanor Berman, Hektoen Institute for Medical Research, Chicago, Ill.

**Fluorometric Analysis of Serum and Tissue Lipids on TLC Scanner.** Donald Silverman, Hektoen Institute, Chicago, Ill.

**Fractional Vacuum Sublimation and Mass Spectrometry. Part I. Application in Toxicological Studies.** Paritosh K. De, Charles J. Umberger, Department of Forensic Medicine, New York University Medical Center and Department of Toxicology, Office of Chief Medical Examiner, New York

**Analysis of Corneal Tissue with an Electron Microprobe.** Mary Jo Ingram, Department of Physiology and Biophysics, Donald R. Doughman, M.D., Department of Ophthalmology, University of Iowa, 240 Medical Labs., Iowa City, Iowa 52240

**Quantification of Tricarboxylic Acid Cycle and Related Acids in Human Urine by Gas–Liquid Chromatography.** Diane S. Zaura, Jack Metcoff, Michael Reese Hospital and Medical Center, 2901 S. Ellis Ave., Chicago, Ill. 60616

**Data Acquisition and Data Processing**


Separate amines easily, efficiently with

# New Chromosorb* 103

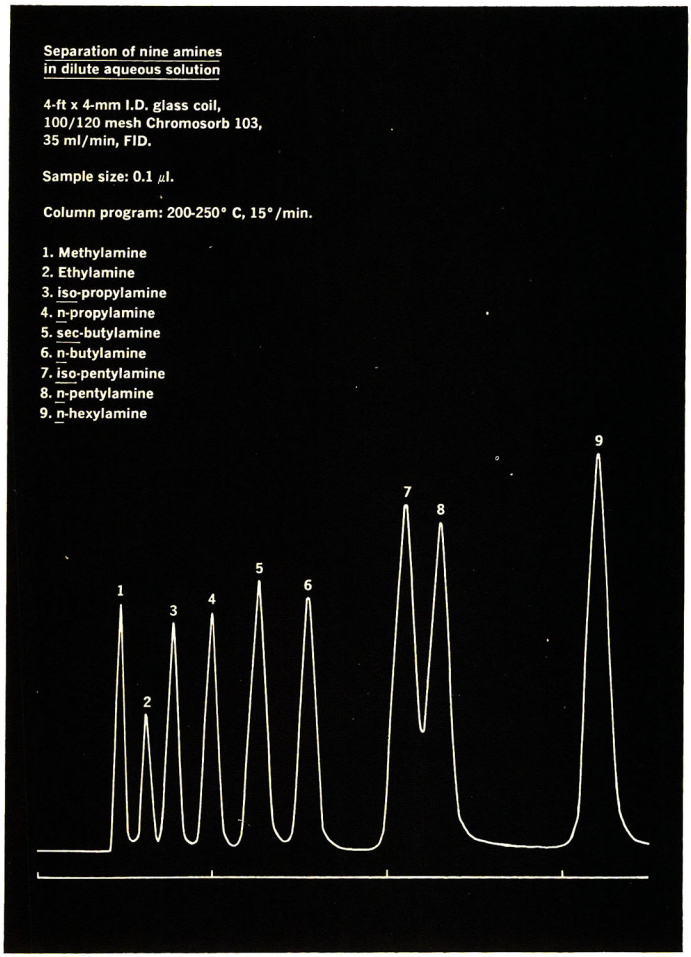


Chromosorb 103 is a polyaromatic porous resin developed by Johns-Manville as a solid-type support for the separation of amines and basic compounds.

Until now, amine separation has been both laborious and difficult. With new highly selective Chromosorb 103, it's fast and easy.

For more specific information, write for our bulletin FF-181. Johns-Manville, Box 290-C, Trenton, New Jersey.

**Johns-Manville**

*Chromosorb is a Johns-Manville registered trademark for its brand of products developed for use as support material or adsorbents for gas chromotography.

Circle No. 50 on Readers' Service Card

See ACS Laboratory Guide for All Products/Sales Office

**in Automatic Clinical Chemistry.** R. L. Faley and W. Slavin, Perkin-Elmer Corp., Norwalk, Conn.

**Evaluation of Succinyl Choline by Chemical and Instrumental Means.** Frank Fiorese, John MacDonald, Bureau of Toxicology, Illinois Department of Public Health, Chicago, Ill. 60612

## ELECTRON SPECTROSCOPY FOR CHEMICAL ANALYSIS

**Introduction to ESCA.** Royal Albridge, Vanderbilt University, Nashville, Tenn.

**Applications of ESCA.** Ragnar Nordberg, University of Uppsala, Sweden

**Use of Electron Spectroscopy in Determination of Electronic Structure in Molecules.** T. A. Carlson, ORNL, Oak Ridge, Tenn.

**Fundamentals of Electron Spectrometer Design.** C. E. Kuyatt, National Bureau of Standards, Gaithersburg, Md.

**Inelastic Electronic Scattering by Molecular Gases.** Edwin M. Lassettre, Mellon Institute, Pittsburgh, Pa.

**Design and Performance of the NBS Electron Impact Spectrometer.** J. Arol Simpson, NBS, Gaithersburg, Md.

**Auger Spectroscopy for Surface Chemical Analysis.** R. E. Weber, University of Minnesota, Minneapolis, Minn.

## COMPUTER APPLICATIONS

**The Use of a Small Computer for On-Line Processing of Mass Spectrometry Data.** A. L. Harkness, W. A. Svec, Argonne National Labs, Argonne, Ill.

**Computerized Spectrometry Analysis.** Chester D. Kylstra, Richard T. Schneider, Dept. of Nuclear Engineering Sciences, University of Florida, Gainesville, Fla.

**SpectroPlan—A Modular Approach to Computerized-Aided Spectroscopy Systems.** Richard Rabin, Varian Associates, San Carlos, Calif.

**The Impact of the Computer on Access to Chemical Information.** R. E. O'Dette, F. A. Tape, Chemical Abstracts Service, Columbus, Ohio

**A Computer Automated Diffraction System.** Larry Amiot, Argonne National Laboratory, Argonne, Ill.

**Analytical Laboratory Instrumentation and a Shared Time Computer.** Karl F. Weihman, Elwin N. Davis, Richard Wertzler, Sinclair Oil Corp., Research Division, 308 E. 148th Pl., Harvey, Ill. 60426

**Laboratory Data Acquisition and Computation.** Abraham Savitzky, Perkin-Elmer Corp., 188 Perry Ave., Norwalk, Conn. 06850

**On-Line Computer Analysis of Gas Chromatograph Data.** W. R. Olson, Control Data Corp., 6467 Lake Athabaska, San Diego, Calif. 92119; S. E. Sunderland, Goodyear Tire and Rubber, Akron, Ohio

**A Computer System for the Automation of Spectrometers.** C. H. Sederholm, IBM Scientific Center, 2670 Hanover St., Palo Alto, Calif. 94304

**The Collection of Crystallographic Structural Data Using Automated Diffractometers.** J. Benson, R. A. Jacobson, Ames Laboratory, A.E.C., 1105 Garfield, Ames, Iowa 50010

**On-Line Experiments in Spectroscopy.** William D. Gwinn, University of California, Berkeley, Calif. 94720

**Preliminary Attempts in Computer Simulation of Chemical Reactions.** Enrico Clementi, IBM Research Labs

**Conversational Time Sharing Computer Calculations of Purity from Differential Scan Calorimetry Data.** J. G. Karohl, A. P. Gray, L. R. Scott, Perkin-Elmer Corp., Norwalk, Conn.

**Computer Application to an Automated Direct Reading Emission Spectrometer.** J. J. Lowe, R. J. Martin, Gulf Research and Development Co., P.O. Drawer 2038, Pittsburgh, Pa. 15230

## MOLECULAR SPECTROSCOPY

### I. RAMAN SPECTROSCOPY

**Tensorial Properties of the Vibrational Raman Effect.** J. A. Koningstein, Carleton University, Ottawa, Canada

**Theory of Raman and Infrared Processes in Crystals: Selection Rules in Cuprite.** Joseph S. Ziomek, IIT Research Institute, Chicago, Ill. 60616

**Laser-Excited Raman Scattering in Gases.** J. J. Barrett, Perkin-Elmer Corp., Norwalk, Conn. 06852

**Remote Raman Spectroscopy.** Tomas Hirschfeld, Stanley M. Klainer, Block Engineering, Inc., 19 Blackstone St., Cambridge, Mass. 02139

**Design Considerations for Routine Raman Spectrophotometers.** Frank M. Dunnington, Hans Neumann, Spectra-Physics, Inc., 1250 W. Middlefield Rd., Mountain View, Calif. 94040

**Raman Study of Selenium Oxychloride.** J. E. Griffiths, Bell Telephone Labs, Murray Hill, N. J. 07974

**Raman Spectra of Organic Molecules in the Vapor Phase.** Donald O. Landon, J. R. Allkins, Spex Industries, Inc., 3880 Park Ave., Metuchen, N. J. 08840

## MOLECULAR SPECTROSCOPY

### II. TECHNIQUES

**Breakthroughs in Fourier Transform Spectroscopy.** P. R. Griffiths, J. O. Lephardt, University of Maryland, College Park, Md.; S. T. Dunn, Dunn Associates, Inc., Silver Spring, Md.

**Electrical Ratio Recording IR Spectrophotometer, 2.5 to 25 Microns with Ge:Cu Photodetector.** L. W. Herscher, F. J. Karle, Dow Chemical Co., 4001 Oak Court, Midland, Mich. 48640

**Environmental Particle Identification by Means of Monochromatic Radiative Scattering.** Firouz Shahrokhi, Fred M. Shofner, University of Tennessee Space Institute, Tullahoma, Tenn. 37388

**Degradation of Laser Optics.** Ted L. Barber, U.S. Army White Sands Missile Range

## MOLECULAR SPECTROSCOPY

### III. STUDY OF SPECTRA AND CHARACTERIZATION

**Infrared Spectra of Group VI Metal Carbonyls Containing Heterocyclic Diamines.** Bennett Hutchinson, Kasuo





Chromerge makes old, cumbersome methods of cleaning labware obsolete... eliminates danger and time-wasting of previous methods of preparation...long, unsatisfactory job of boiling sulphuric acid with potassium dichromate.

Chromerge does a *better* cleaning job, because its more powerful cleaning solution removes stubborn deposits which resist other cleaners, yet it protects glass surfaces, is chemically and bacteriologically clean...preserves the capacity of volumetric wear, gives a perfect miniscus for precise volumetric work!

MANOSTAT Corporation
Dept. 521
20-22 N. Moore St. N.Y., N.Y. 10013
Available through your laboratory supply dealers

Circle No. 119 on Readers' Service Card




# jeol's 5AH amino acid analyzer

## highest sensitivity...greatest versatility...lowest price

### compare the specifications:

| Specification | JEOL 5AH | Competitor–B |
|---|---|---|
| Guaranteed Sensitivity | $1x10^{-9}$mol | $1x10^{-8}$mol |
| Scale Expander | X3, X10, built-in | X5 optional extra * |
| Detection System | dual beam with preamplifiers | single beam with no preamplifiers |
| Automatic Multi-sampler | built-in | optional extra * |
| Fractionation System | built-in | optional extra * |
| Automatic Buffer Exchanger | 8-step, built-in | 4-step, optional extra * |
| Programmer (punched tape) | built-in multi-program | optional extra * single-program |
| U. V. Detector | extra | not available |
| Price | $17,300.00 (delivered) | $25,000.00 (FOB factory) |

* Included in total price.

jeol

JAPAN ELECTRON OPTICS LABORATORY CO., LTD. • NEW TOKYO BUILDING., TOKYO, 100
JEOLCO (U.S.A.) INC., 477 RIVERSIDE AVENUE, MEDFORD, MASS. 02155, U.S.A. • JEOLCO (EUROPE) SA., 16 AVENUE DE COLMAR 92 RUEIL-MALMAISON (PARIS) FRANCE • JEOLCO (AUSTRALASIA) PTY. LTD., 1 HELP STREET, CHATSWOOD, N.S.W., AUSTRALIA

Circle No. 49 on Readers' Service Card

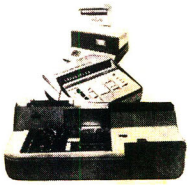

# Generation Gap



## The Wang 700 Calculator is a whole lot smarter than its predecessors.

It's the first of a new breed, a third generation programmable calculator. The difference is more revolutionary than evolutionary. It's ten times faster and more powerful than the best of the 2nd generation machines. It handles far longer programs (learns on a built-in 8192-bit core and stores permanently up to 10 blocks of 960 steps each on snap-in magnetic tape cassettes), has many more data storage registers (up to 120), and provides more hardware operations (like logs to base e and base 10, $\pi$, $e^x$, $10^x$, etc.), than any existing calculator or so-called desk-top computer.

Execution speeds for various functions range from 300 $\mu$sec for + and − to 250 msec for trig functions. A dual Nixie-type display produces 12 digit answers plus 2-digit (−98 to +99) exponents each register.

The Wang 700 has commands for loops, branches and subroutines, unmatched power for matrix and array operations. Exclusive integrated circuit design concentrates all these capabilities into a self-contained, convenient desk-top package. It's the logical heir to Wang leadership in high performance problem-solving.

WANG LABORATORIES, INC.

Dept. 4Y, 836 North St., Tewksbury, Massachusetts 01876 • Tel. 617 851-7311

**Call today for immediate trial:**

| | | | | | |
|---|---|---|---|---|---|
| (201) 241-0250 | (216) 333-6611 | (313) 278-4744 | (502) 426-1116 | (608) 244-9261 | (714) 234-5651 |
| (203) 223-7588 | (301) 588-3711 | (314) 727-0256 | (504) 729-6858 | (612) 881-5324 | (716) 381-5440 |
| (203) 288-8481 | (301) 821-8212 | (315) 463-9770 | (505) 255-9042 | (615) 588-5731 | (717) 397-3212 |
| (205) 881-5360 | (303) 364-7361 | (317) 631-0909 | (512) 454-4324 | (616) 454-4212 | (801) 487-2551 |
| (206) 622-2466 | (304) 344-9431 | (402) 341-6042 | (513) 531-2729 | (617) 542-7160 | (805) 962-6112 |
| (212) 682-5921 | (305) 563-8458 | (404) 633-6327 | (517) 835-7300 | (617) 851-7311 | (816) 444-8388 |
| (213) 278-3232 | (305) 841-3691 | (405) 842-7882 | (518) 463-8877 | (702) 322-4692 | (817) 834-1433 |
| (214) 361-7156 | (309) 674-8931 | (412) 366-1906 | (601) 234-7631 | (703) 595-6777 | (901) 272-7488 |
| (215) 642-4321 | (312) 297-4323 | (414) 442-0160 | (601) 982-1721 | (713) 668-0275 | (916) 489-7326 |
| | | (415) 692-0584 | (602) 265-8747 | (713) 668-3753 | (919) 288-1695 |

Circle No. 164 on Readers' Service Card

See ACS Laboratory Guide for All Products/Sales Office




Nakamoto, Illinois Institute of Technology, Chicago, Ill. 60616

**Infrared and Raman Spectra of Cyclopentadienyltrichlorotitanium (IV), Dicyclopentadienyldichlorotitanium (IV), and Related Compounds.** Edward Maslowsky, Jr., Kazuo Nakamoto, Illinois Institute of Technology, Chicago, Ill. 60616

**Raman and Infrared Spectra and Assignment of $BF_3NCCH_3$.** D. F. Shriver, Basil Swanson, Northwestern University, 2145 Sheridan Rd., Evanston, Ill. 60201

**Substitutional Effects on the IR Absorption Spectra of Apatites.** R. Z. LeGeros, O. R. Trautz, J. P. LeGeros, E. Klein, A. Thein, New York University, 339 East 25th St., New York, N. Y. 10010

**Low Frequency Vibrational Spectra of Several Potassium Para-Substituted Tetraarylborate Compounds.** John T. Vandeberg, Carl E. Moore, Frank P. Cassaretto, Loyola University, 2406 Kennicott Dr., Arlington Heights, Ill. 60004.

**Characterization of Carbonate Minerals in Oil Shales and Coals by Infrared Spectroscopy.** Patricia A. Estep, John J. Kovach, Arthur L. Hiser, Clarence Karr, Jr., U.S. Department of the Interior, Bureau of Mines, Morgantown Coal Research Center, Morgantown, W. Va. 26505

**Material Identification by a Nondestructive Infrared Technique—External ATR.** Jesse M. Howard III, General Electric Co., Appliance Park, Louisville, Ky. 40225

**Spectroscopic Properties of Some Metal Complexes of Gossypol.** H. N. Ramaswamy, R. T. O'Connor, Southern Utilization Research and Development Division, A.R.S., U.S.D.A., 1100 Robert E. Lee Boulevard, P. O. Box 19687, New Orleans, La. 70119

**Optically Active Crystal Vibrations of the Alkali Metal Nitrates.** Rev. J. L. Walter, University of Notre Dame, Notre Dame, Ind.

**Site Preference for Manganese in Flame-Fusion Spinel.** Carl A. Pitha, Joseph A. Adamski, Air Force Cambridge Research Laboratories, Hanscom Field, Bedford, Mass. 01730; Charles S. Naiman, MITHRAS Division of Sanders Assoc., Inc.

## X-RAY SPECTROSCOPY

**The Aging of Solder Standards.** H. R. Post, International Business Machines, Essex Junction, Vt.

**X-Ray Methods for the Analysis of Solutions.** Thomas J. Cullen, Sel-Rex Corp., Nutley, N. J.

**Applications of the Cold Cathode Discharge X-Ray Source.** William L. Baun, Materials Physics Division (MAYA) Air Force Materials Laboratory, Wright-Patterson Air Force Base, Ohio; James S. Solomon, University of Cincinnati, Ohio

**The Low Energy Absorption Maximum in X-Ray K-Absorption Spectra of Transition Metal Complexes.** G. L. Glen, Owens-Illinois, Inc., Toledo, Ohio

**A Study on the Change of Water of Crystallization by X-Ray Diffraction Data Stored in ASTM Magnetic Tape.** Frank L. Chan, Aerospace Research Laboratories, Wright-Patterson Air

# Enter the laser era $295!




## With this new, high-performance Laser, everyone can take advantage of advancing electro-optical technology

Coleman Instruments bring you the perfect working laser for coherent light applications in research and engineering. For optical testing. For surveying and alignment. For systems development. For a thousand-and-one practical and experimental uses. Its full name: The Perkin-Elmer Helium-Neon Gas Laser, Coleman Model 75.

This new laser emits a continuous, $TEM_{oo}$ single mode, red (6328 Å) beam in the visible spectrum. Nominal 1.5 milliwatt output (minimum 1.0 mW) ideally combines safety and effectiveness. Maintaining actual divergence of less than 0.4 milliradians half-angle, the Model 75 beam throws an intensely bright, small spot hundreds of feet.

Here's the ideal tool for lowering costs in the construction industry, in alignment of mechanical components, centering, determining levels, grades, straightness, flatness. It's an ideal laboratory instrument, too. The laser head is detachable from the solid-state power supply for investigations in optics. A separate tripod may be used, but is not required.

Behind this instrument is the vast laser research experience of The Perkin-Elmer Corporation. Highly skilled Delmar Scientific glassblowers shape the long-lasting laser tube, sealing on pure quartz resonator reflectors. Anticipated tube life is 4,000 hours; warranty covers one full year. There are no external optics, no complex adjustments, no maintenance. Just flip the switch, press the start button, and you've entered the laser era.

All of this utility is available to you at only $295 for the Coleman Model 75. For full information, send for Coleman Bulletin A-317.

*Write to Coleman Instruments Division,*
*The Perkin-Elmer Corporation,*
*42 Madison St., Maywood, Illinois 60153*

**Visit Our Booth At The FASEB Meeting**

**PERKIN-ELMER**

**Circle No. 167 on Readers' Service Card**

**See ACS Laboratory Guide for All Products/Sales Office**

Force Base, Ohio; G. G. Johnson, Jr., Pennsylvania State University, University Park, Pa.

**Multielement Analysis With an Improved X-Ray Quantometer.** Fred W. Johannsen, Applied Research Laboratories, Sunland, Calif.

**Application of a Computer Controlled Automatic X-Ray Spectrometer.** John Croke, Rus Westberg, Philips Electronics, Mount Vernon, N. Y.

**X-Ray Analysis of Stainless Steel and Low Alloy Steel.** Harry Dryer, Applied Research Laboratories, Detroit, Mich.

**Applications of X-Ray Emission to Coatings Analyses.** Richard W. Scott, James D. McGinness, Sherwin-Williams Research Center, Chicago, Ill.

**A Chemical Concentration X-Ray Determination of Cerium in Iron and Steels.** C. H. Albright, Michael M. Yanak, International Nickel Co., Inc., Sterling Forest, Suffern, N. Y. 10901

**A Novel Technique for the Preparation of Solid Spectrographic Standards Used in the XRF Calibration for Catalyst.** John R. Polky, Catalyst Division, Nalco Chemical Co., Chicago, Ill.

## SILICATE ANALYSES SYMPOSIUM

**Silicate Analysis—A Glance Backward and a Look Forward.** Irving May, U.S.G.S., Washington, D.C.

**Rapid Rock Analysis Today.** Leonard Shapiro, U.S.G.S., Washington, D.C.

**Electron Microprobe Analysis of Silicates.** A. A. Chodos, California Institute of Technology, Pasadena, Calif.

**Laser Microprobe of Minerals—Acro Measurements on Micro Samples.** Fred Ward, U.S.G.S., Denver, Col.

**Semiquant X-Ray Spectrographic Analysis of Silicate Materials.** Merlin Salmon, Fluo-X-Spec Analytical Laboratory, Denver, Col.

**Reference Standards in the Use of Geologic Materials.** A. T. Myers, R. G. Havens, U.S.G.S., Denver, Col.

**Silicate Analysis as Viewed by the Geological Surveys.** Neil Shimp, Illinois State Geological Survey, Urbana, Ill.

**An Evaluation of the Problem of Chemical Analysis of Trace Coloring Oxides in Optical Glasses.** D. E. Campbell, P. B. Adams, Corning Glass Works, Corning, N. Y.

**A Method for Analyzing Geologic Material by a New Mobile Direct Reading Spectrometer.** K. J. Curry, D. J. Grimes, U.S.G.S., Denver, Col.

**Computer Analysis of Optical Emission Spectra.** Armand W. Helz, F. G. Walthall, S. Berman, U.S.G.S., Washington, D. C.

**Neutron Activation Analysis: The Value of the Technique to Geochemical Studies.** Hugh Millard, Jr., P. J. Aruscavage, U.S.G.S., Denver, Col.

## MATRIX ISOLATION

**The Evolution of Matrix Isolation.** M. M. Rochkind, Bell Telephone Laboratories, Mountain Ave., Murray Hill, N. J. 07974

**A Simple Radical Source for Matrix Isolation Studies.** Alan Snelson, IIT Research Institute, 10 W. 35th St., Chicago, Ill. 60616




This product bears 10 successive coatings.

If they are not put down with utmost precision, the product doesn't work.

How well it does work is one of the great success stories of business history.

On hand at
any camera shop.




*Permit use of two decades of paper chromatography work, yet give same speed and higher resolution than other cellulose-coated TLC media. Credit the purity of the cellulose with which we start and the way we purify it further and redistribute the particle size.*

Same plant has to put only one layer on each of these.

Ought to be pretty dependable sheet for your thin-layer chromatography.

On hand at

B&A / CURTIN / FISHER / HOWE & FRENCH / NORTH-STRONG / SARGENT-WELCH / SHANDON / VAN WATERS & ROGERS / WILL

along with

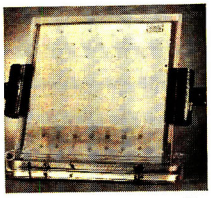

EASTMAN CHROMAGRAM Developing Apparatus, an easily assembled, fast-equilibrating chamber that saturates reproducibly with solvent vapor.

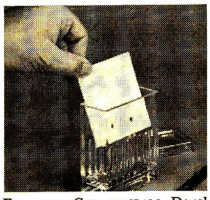

EASTMAN CHROMAGRAM Developing Jar, small and inexpensive, right for pre-testing and for the shorter migrations.

While thinking of TLC, send off a request for the detailed recipe book "EASTMAN TLC Visualization Reagents" to Eastman Kodak Company, Eastman Organic Chemicals, Rochester, N.Y. 14650.

Kodak

**Fluorescence and Absorption Spectra of Matrix Isolated Cobalt Dichloride Molecules.** J. R. Clifton, D. M. Gruen, Argonne National Laboratory, 9700 S. Cass Ave., Argonne, Ill. 60439

**Optical and EPR Spectroscopy of High-Temperature Molecules at 4°K.** W. Weltner, Jr., University of Florida, Gainesville, Fla.

**Laser Excited Fluorescence.** Arnold Bass, National Bureau of Standards, Washington, D. C.

**Generation and Study of ESR of Charged Species in Matrices at 4°K.** Paul Kasai, D. McLeod, Union Carbide Research Institute, Tarrytown, N. Y.

**Study of Copper Atoms in Rare Gas Matrices at 4°K.** Paul Kasai, Union Carbide Research Institute, Tarrytown, N. Y.

**ESR Study of Reaction Products of Discharge Gases.** Paul Kasai, Union Carbide Research Institute, Tarrytown, N. Y.

**Environmental Effects on Intersystems Crossing in Matrix Isolated Molecules.** J. J. Smith, B. Meyer, University of Washington, Seattle, Wash.

**Effects of Temperature on the Spectra of Matrix Isolated Molecules.** J. J. Smith B. Meyer, University of Washington, Seattle, Wash.

## NMR–EPR

**Whole-Body NMR Spectrometer.** Jasper A. Jackson, Wright H. Langham, Los Alamos Scientific Laboratory, Los Alamos, N. M.

**Hydration Numbers of Strong Electrolytes from Temperature Dependence of Proton Shifts.** Edmund R. Malinowski, Stevens Institute of Technology, Hoboken, N. J.

**Correlations of Chemical Shifts of Substituted Norbornenes with Taft's Sigma Function.** Martha C. Thorpe, W. C. Coburn, Jr., Southern Research Institute, Birmingham, Ala.

**$^{14}$N Chemical Shifts of Aqueous Alkyl Ammonium Chlorides.** Bruce E. Wenzel, American Oil Co., Whiting, Ind., Max T. Rogers, Michigan State University, Lansing, Mich.

**Nuclear Magnetic Resonance in Crystalline Choline Chloride.** Ralph H. Hannon, John D. Graham, Northern Illinois University, DeKalb, Ill.

**Electron Spin Resonance Studies of the Reactions of Tris (1-Naphthyl) Phosphine and its Oxide, Sulfide and Selenide with Alkali Metals in Tetrahydrofuran and 1, 2-Dimethoxyethane.** Mahdy H. Hnoosh, Ashland Chemical Co., Houston, Texas; Ralph A. Zingaro, Department of Chemistry, Texas A and M University, College Station, Texas

**Experimental Nuclear Magnetic Multiple Resonance.** M. I. Levenberg, Richard S. Eagan, Abbott Laboratories, North Chicago, Ill.

**NMR and Gel Permeation Chromatography Characterization of Etherified Melamine-Formaldehyde Resins.** Daniel A. Netzel, Dennis G. Anderson, DeSoto Inc., Des Plaines, Ill. 60018

**EPR in Irradiated Zinc Orthotitanate.** N. A. Ashford, IIT Research Institute, Chicago, Ill. 60616

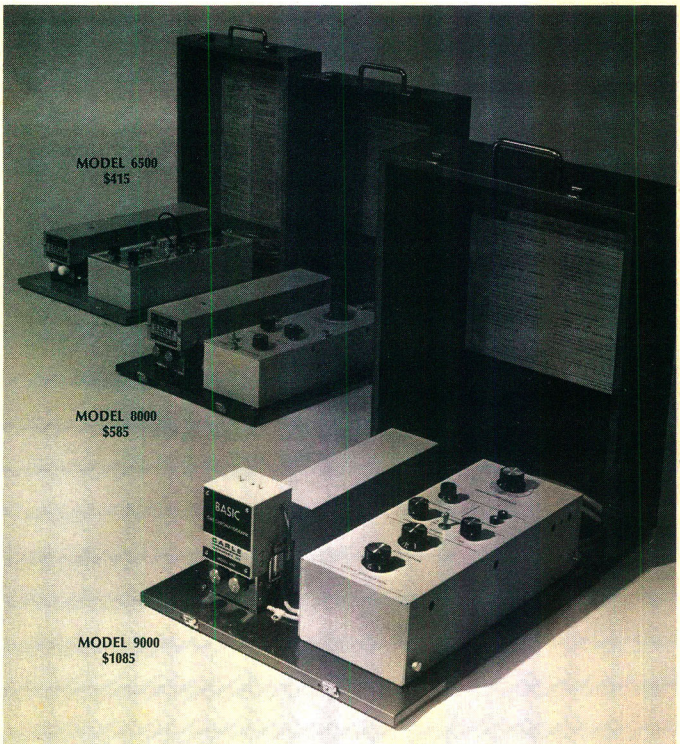


# flame ionization sensitivity– a new basic solution

FID instrumentation is not new to gas chromatography. But the Carle Model 9000 Basic™ GC with Flame Ionization Detector is . . . in concept . . . in low cost design . . . and in rugged, reliable, and simplified performance.

Start with these key features:

- Advanced design differential hydrogen flame detector.
- 1 x $10^{-11}$ MOSFET solid state electrometer.
- Proven dual column, on column inlet system.

At $1085, this is an outstanding new instrument for high sensitivity gas chromatographic applications of organic and biochemical analysis, environmental pollution, or any area where hydrogen flame sensitivity is paramount.

The Model 9000 is the latest in the Carle family of widely accepted Basic™ Gas Chromatographs. Other models include:

**MODEL 6500** – More than 750 of these units are in use throughout the world particularly in colleges and universities as an ideal instructional device.

**MODEL 8000** – A unique solution to repetitive routine analysis, the Model 8000 frees high-cost research chromatographs for more difficult problems.

Write today for Data File 123 containing complete information on all three of these instruments.

CARLE
INSTRUMENTS, INC.
1141 East Ash Avenue, Fullerton, California 92631 (714) 879-9900

Circle No. 105 on Readers' Service Card

See ACS Laboratory Guide for All Products/Sales Office



## Robert L. Stone Wins Mettler Award

**Robert L. Stone**, a leader in the development of thermal analysis measurement methods, was presented with the 1969 Mettler Award in Thermal Analysis at the Inn on the Park, Toronto, Canada, during the Third Toronto Symposium on Thermal Analysis, Feb. 25 to 26. Dr. Stone, who is now Vice President and Technical Director for Analytical Instruments, Tracor, Inc., was founder in 1959 of the Robert L. Stone Co., manufacturer of equipment for differential thermal analysis and thermogravimetric analysis. This company was acquired by Tracor, Inc., in 1966. The award, sponsored by the Mettler Instrument Corporation of Princeton, N.J., consists of a citation and $1000. Dr. Stone is an expert in ceramic engineering, differential thermal analysis, and analytical chemistry.

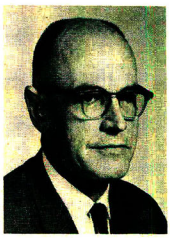

## Conference on Applications of X-Ray Analysis

The 18th Annual Denver Conference on Applications of X-Ray Analysis will be held August 6 to 8, 1969, at the Albany Hotel in Denver, Colo. Co-chairmen of the meeting are Burton Henke of the University of Hawaii and J. B. Newkirk of the Denver Research Institute, University of Denver. Papers dealing with any aspect of X-ray analysis are being solicited. A panel of invited speakers will present review papers on various aspects of very long wavelength X-ray analysis. Subjects to be included in this panel discussion include chemical bonding and valence states, light element fluorescence analysis, absorption and emission of long wavelength X-ray, X-ray astronomy, plasma spectrum analysis, and diffraction and detection of long wavelength X-rays. Contributed papers in these areas are especially welcome. Abstracts, limited to 300 words, should be sent by April 10, 1969, to Dr. J. B. Newkirk, Metallurgy Division, Denver Research Institute, University of Denver, Denver, Colo. 80210. The proceedings of this meeting will be published as Volume 13, "Advances in X-ray Analysis."

## 3. WRITING FOR TECHNICAL AND PROFESSIONAL JOURNALS

*By JOHN H. MITCHELL, University of Massachusetts*

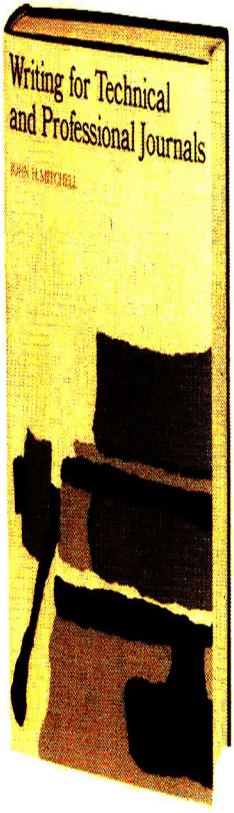


If you write for professional journals, or plan to, you'll refer again and again to this unique book. Collating style guides and instruction manuals into a single source, it defines and illustrates characteristics of professional articles ...shows how data is collected, correlated, and selected...points out the standard elements in a journal article...and illustrates conflicting sections of style guides by reprinting and reviewing representative articles.

*1968 405 pages $7.50*

**To order, circle number 3 on order card.**

**Use this card to order any of the books listed in the Wiley-Interscience ad**

### 10-DAY APPROVAL OFFER

Please send me the books whose code-numbers I have circled below, on 10 days' approval (USA and Canada only) under the following terms:

1 2 3 4 5 6 7 8 9 10 11 12 13 14 15 16
17 18 19 20 21 22 23 24 25 26 27 28 29

☐ Total Payment Enclosed (Wiley pays regular delivery charges)

☐ Bill me (for price of book plus delivery charges)

☐ Purchase order attached

Name_____

Address_____

City_____ State_____ Zip_____

*Save Money! Send full payment with order and Wiley pays regular delivery charges. Same return privilege guaranteed.*

ACA

# 4. TECHNICAL CORRESPONDENCE

## A Handbook and Reference Source for the Technical Professional

*By HERMAN M. WEISMAN, Natl. Bureau of Stand.*

This book offers an understanding of the principles and mastery of the techniques you need to communicate by letter or memo with maximum clarity and effect. You'll find specific instructions for writing each type of correspondence you normally encounter in the course of the day. The book includes letters of inquiry and request...sales and proposal letters . . . special purpose letters, such as letters to professional journals commenting on articles . . . employment letters . . . personal and non-technical correspondence . . . and professional letters and memoranda.

*1968 218 pages $6.95*



**To order, circle number 4 on order card.**

Postage Will be Paid by Addressee

**Business Reply Card**

FIRST CLASS PERMIT NO. 32664, SEC. 510, P.L.&R., NEW YORK, N. Y.

No Postage Stamp Necessary If Mailed in the United States

**John Wiley & Sons, Inc.**
605 Third Avenue,
New York, New York 10016

Dept. 80

# Outstanding Chemical Analysis books from Wiley-Interscience

## 5. Modern Separation Methods of Macromolecules and Particles

*Edited by THEODORE GERRITSEN, University of Wisconsin Medical Center.*

**CONTENTS:** Large Pore "Disc" Electrophoresis. The Application of Free-Flow Electrophoresis to the Separation of Macromolecules and Particles of Biological Importance. The Use of Gradients of Colloidal Silica for the Separation of Cells and Subcellular Particles. The Separation of Lymphocyte Populations on Glass Bead Columns. Factors in the Partition of Blood Cells in Aqueous Dextran-Polyethylene Glycol Two-Phase Systems. Partition of Macromolecules in the Polyethylene Glycol-Dextran System. Separation Based on Size and Conformation. Gel Filtration on Agarose Gels. Equilibrium Density Gradient Separation and Analysis of Lymphocyte Populations. On the Theoretical Aspects of Gel Chromatography. Differential Elution of Trapped Macromolecules. Partition in Polymer Two-Phase Systems.

**CONTRIBUTORS:** P.-Å. Albertsson. H.-C. Chen. L. C. Craig. M. H. Edgell. K. Hannig. E. J. Harfenist. K. Hellsing. C. A. Hutchison III. M. K. Joustra. T. C. Laurent. B. Obrink. H. Pertoft. D. E. Pettijohn. K. Shortman. R. L. Sinsheimer. O. Smithies. M. Sung. H. Walter. A. Wasteson.

*Volume 2 in the INTERSCIENCE series Progress in Separation and Purification.* **1969 In press**

## 6. Chromatographic and Electrophoretic Techniques

**Volume I: Chromatography**
**Third Edition**

*Edited by IVOR SMITH, Courtauld Institute, Middlesex Hospital, London, England.*

**PARTIAL CONTENTS:** Desalting and Related Techniques. Dinitro-phenyl Aminoacids. Iodoaminoacids and Related Compounds. Imidazoles. Organic Acids of the Citric Acid Cycle and Related Acids. Plant Phenols and Tannins. Phospholipids and Their Derivatives. Barbiturates. Alkaloids. Steroids. Chromatography of Radioactive Substances. Chromatography of Labeled Cell Extracts. The Spark Chamber Technique for Radio-Chromatograms. Ion-exchange Celluloses in Chromatography. Amino Sugars. Inorganic Ions. Sephadex Thin-Layer Gel Filtration. The Investigation of New Compounds.

**1969 Prob. $24.00 In press**

## 7. Topics in Organic Mass Spectrometry

*Edited by A. L. BURLINGAME, University of California, Berkeley.*

**CONTENTS:** Introduction. Techniques of Molecular Ionization. Mass Discrimination Caused by Electron-Multiplier Detectors. Correlations of Fragment Ion Structure with Energetics of Formation. Gas-Liquid Chromatography-Mass Spectrometry Combination. The Acquisition, Processing and Presentation of High Resolution Mass Spectra. High Resolution Mass Spectrometry. Mechanisms of Ion Decomposition Reactions. Mass Spectrometry of Complex Natural Compounds. Applications of Mass Spectrometry in Flavor and Aroma Chemistry. Application of Mass Spectrometry in Organic Geochemistry.

*Volume 8 in the INTERSCIENCE series Advances in Analytical Chemistry and Instrumentation.*

**1969 In press**

## 8. The Practice of Absorption Spectrophotometry

*By E. I. STEARNS, American Cyanamid Company.*

**CONTENTS:** General Principles. Analysis by Transmitted Light. Analysis by Reflected Light. Appendix A: Mounting Textile Samples for Reflectance Measurements. Appendix B: Calculating Adam's Chromatic Value Color Difference. Appendix C: Author Index. Subject Index.

**1969 353 pages $17.50**

## 9. Gas Chromatography

*By ORION EDWIN SCHUPP III, Eastman Kodak Company.*

**CONTENTS:** Introduction. Theory of Gas Chromatography. Operation, Design, and Performance of Equipment. Columns. Special Chromatographic Techniques. Qualitative Analysis. Quantitative Analysis. References. Author Index. Subject Index.

*Volume 13 in the INTERSCIENCE series Techniques of Organic Chemistry.* **1968 437 pages $16.50**

## 10. Kinetics in Analytical Chemistry

*By HARRY B. MARK, JR., The University of Michigan; and G. A. RECHNITZ, State University of New York, Buffalo; with the assistance of RONALD A. GREINKE, The University of Michigan.*

**CONTENTS:** Preface. Introduction. Measurement of Reaction Rates. Kinetic Methods for Catalyzed Reactions. Kinetic Methods for Uncatalyzed Reactions. Kinetic Methods for the In-Situ Simultaneous Determination of Closely Related Mixtures. Considerations for the Determination of Organic Mixtures Based on Differential Reaction Rates. Evaluation and Comparison of Differential Rate Methods Employed for the Simultaneous Determination of Closely Related Compounds (with the assistance of Louis J. Papa). Analytical Reactions from the Kinetic Viewpoint. Author Index. Subject Index.

**1968 339 pages $16.95**

## 11. Advances in Analytical Chemistry and Instrumentation

**Volume 7**

*Edited by CHARLES N. REILLEY, University of North Carolina; and FRED W. McLAFFERTY, Cornell University.*

**CONTENTS:** Ultramicroanalysis with the Microscope. Recent Advances in Raman Spectroscopy. The Production and Radioassay of Tritium Labeled Compounds. Application of Kinetics to Automated Quantitative Analysis. Author Index. Subject Index. Cumulative Index, Volumes 1-7.

**1969 229 pages $11.50**

■ *To order any of these books, circle appropriate number on Wiley order card.*

**WILEY-INTERSCIENCE**
a division of JOHN WILEY & SONS, Inc., 605 Third Avenue, New York, N.Y. 10016
In Canada: John Wiley & Sons Canada Ltd., 22 Worcester Road, Rexdale, Ontario

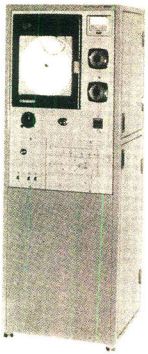

## NUMEC-Carlo Erba Sorptomatic

**An automatic BET instrument for the determination of complete adsorption and desorption isotherms for surface area and pore distribution analysis.**

- measures surface area from 1 $m^2/g$ to 2,000 $m^2/g$
- measures pore distribution from 5—300 Å radii
- reproducibility 1—5%, as related to surface area measurement
- dual range pressure recorder 0-200/0-800 mm Hg

**Price $9,500**

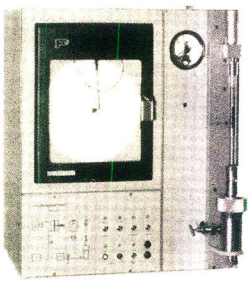

## NUMEC-Carlo Erba Porosimeter

**This automatic instrument uses the mercury intrusion method to determine pore radius from 37.5 to 75,000 Å.**

- Records on dual pressure ranges from 0-2,850 psi and from 0-28,500 psi

**Price $7,300**

**NUMEC®**

Instruments Department

NUMEC® is a subsidiary of Atlantic Richfield Co.

155 Washington Ave., Vandergrift, Pa. 15690
Phone: 412 • 567-6736

Circle No. 189 on Readers' Service Card



## Scheduled Courses in Analytical Techniques

Information is given in the following order: date, name of course, location of course, professional person(s) in charge of course, and/or sponsoring organizations and Contact (numbers in parentheses refer to addresses and telephone numbers given at the bottom of the list of scheduled courses).

**Apr. 1—Internal Reflection Techniques. Apr. 2—Gas Chromatography/Infrared Techniques.** Holiday Inn, Darien, Conn. CONTACT: Wilks Scientific Corp., South Norwalk, Conn. 06856. Tel: (203) 838-4537

**Apr. 7 to 11—Two Separate Courses: Infrared Interpretation, Part I; Gas Chromatography.** Philadelphia, Pa. Sadtler Research. CONTACT (1)

**Apr. 7 to 11—21-490/491 Mass Spectrometers.** Monrovia, Calif. CEC/Analytical Instruments Div. CONTACT (2)

**Apr. 12 to 13—Atomic Absorption Spectroscopy.** Minneapolis, Minn. Donald A. Keyworth, T. C. Rains, S. M. Pier. ACS. CONTACT (3)

**Apr. 12 to 13—Computer Programs in Chemical Research.** Minneapolis, Minn. DeLos F. DeTar, C. E. DeTar. ACS. CONTACT (3)

**Apr. 14 to 16—Seventh Annual Vacuum Technology Seminar.** Rickey's Hyatt House. Palo Alto, Calif. CONTACT: Seminar Registrar, Varian Vacuum Div., 611 Hansen Way, Palo Alto, Calif. 94303

**Apr. 14 to 18—Industrial Use of the Polarizing Microscope.** Chicago, Ill. McCrone Research Institute. CONTACT (4)

**Apr. 14 to 18—Two Separate Courses: Thermoanalysis Workshop; Electronics and Analytical Instrumentation.** Philadelphia, Pa. Sadtler Research. CONTACT (1)

**Apr. 18 to 19—Gas Chromatography.** Minneapolis, Minn. Harold M. McNair, W. E. Baitinger. ACS. CONTACT (3)

**Apr. 21—Methodology and Practical Applications in Radioactive Scanning.** New York City and Boston, Mass. Martin Wentzel. Varian Aerograph. CONTACT (5)

**Apr. 21 to 25—Photomicrography.** Chicago, Ill. McCrone Research Institute. CONTACT (4)

**Apr. 21 to 25—Infrared Interpretation, Part II.** Los Angeles, Calif. Sadtler Research. CONTACT (1)

**Apr. 22—Methodology and Practical Applications in Radioactive Scanning.** Toronto, Canada. Martin Wentzel. Varian Aerograph. CONTACT (5)

**Apr. 22 to 23—Materials Characterization Symposium.** DuPont Country Club, Wilmington, Del. CONTACT: Materials Characterization Symposium, Instrument Products Division, E.I. du Pont de Nemours & Co., Wilmington, Del. 19898

**Apr. 23—Methodology and Practical Applications in Radioactive Scanning.** Chicago, Ill. Martin Wentzel. Varian Aerograph. CONTACT (5)

**Apr. 23 to 25—Basic Gas Chromatography.** Houston, Texas. Varian Aerograph. CONTACT: Bernie Jagielski, Varian Aerograph, 3939 Hillcroft Ave., Suite 180, Houston, Texas 77027

**Apr. 25—Methodology and Practical Applications in Radioactive Scanning.** San Francisco, Calif. Martin Wentzel. Varian Aerograph. CONTACT (5)

**Apr. 25 to 26—Gel Permeation Chromatography.** Washington University. John C. Moore. CONTACT: G. L. Esterson, Box 1048, Washington University, St. Louis, Mo. 63130

**Apr. 30 to May 2—Introduction to Vacuum.** Monrovia, Calif. CEC/Analytical Instruments Div. CONTACT (2)

**May 2 to 5—Molecular Characterization of Polymers.** Washington, D.C. F. W. Billmeyer, J. B. Kinsinger, J. P. Kratohvil. ACS. CONTACT (3)

**May 5 to 7—Colorimetry and Spectrophotometry.** Gaithersburg, Md. NBS. CONTACT: I. Nimeroff, NBS Metrology Div., Washington, D. C. 20234

**May 5 to 9—Leak Detection.** Monrovia, Calif. CEC/Analytical Instruments Div. CONTACT (2)

**May 5 to 9—Identification of Small Particles.** Chicago, Ill. McCrone Research Institute. CONTACT (4)

**May 5 to 9—Two Separate Courses: Infrared Intepretation, Part I; Gas Chromatography.** Philadelphia, Pa. Sadtler Research. CONTACT (1)

**May 12 to 15—Photometry.** Gaithersburg, Md. NBS. CONTACT: C. A. Douglas, NBS Metrology Div., Washington, D. C. 20234

**May 12 to 16—Two Separate Courses: Techniques of Infrared Spectroscopy; Nuclear Magnetic Resonance.** Philadelphia, Pa. Sadtler Research. CONTACT (1)

**May 19 to 23—Two Separate Courses: Ultraviolet Spectroscopy; Fragrance and Flavors (IR, NMR, and GC).** Philadelphia, Pa. Sadtler Research. CONTACT (1)

**May 19 to 23—Infrared Interpretation, Part II.** Chicago, Ill. Sadtler Research. CONTACT (1)

**June 1 to 6—Third Course on Process Analytical Instrumentation.** Marriott Motor Hotel, Philadelphia, Pa. Curtis E. Borchers. CONTACT: T. E. Tremellen, Manager, Education & Research Services, Instrument Society of America, 530 William Penn Place, Pittsburgh, Pa. 15219

**June 4 to 6—Vacuum Instrumentation and Technology.** Cleveland Engineering & Scientific Center, Cleveland, Ohio. CONTACT: O. G. Tex Hudson, Clark Goodman Supply, 1161 Brook Pk. Rd., Cleveland, Ohio 44109

**June 8 to 27—Digital Computers in Chemical Instrumentation.** Purdue University. CONTACT: S. P. Perone, Chemistry Dept., Purdue University, Lafayette, Ind. 47907

**June 9 to 11—Use of Operational Amplifiers in Instrumentation.** Oakland, Calif. McKee-Pedersen. CONTACT: Richard G. McKee, McKee-Pedersen Instruments, P.O. Box 322, Danville, Calif. 94526

**June 9 to 13—Two Separate Courses: Infrared Interpretation, Part I; Gas Chromatography.** Philadelphia, Pa. Sadtler Research. CONTACT (1)

**June 9 to 13—Laser Raman Institute and Workshop.** University of Maryland. CONTACT: Ellis R. Lippincott, Center of Materials Research, University of Maryland, College Park, Md. 20742

**June 9 to 13—Fifth Annual X-Ray Spectrometry Clinic.** State University of New York at Albany. CONTACT: Henry Chessin, State University of New York at Albany (SUNYA), Dept. of Physics, 1400 Washington Ave., Albany, N. Y. 12203

**June 16 to 17—Chromatography Seminar.** Sharon, Pa. Penn State. CONTACT: Penn State Continuing Education, Shenago Valley Campus, South Water Ave., Sharon, Pa. 16146

**June 16 to 20—21–110 Mass Spectrometer.** Monrovia, Calif. CEC/Analytical Instruments Div. CONTACT (2)

**June 16 to 20—Summer Institute in Advanced NMR and Advanced Mass Spectroscopy.** Stevens Institute of Technology. CONTACT E. R. Malinowski, Stevens Institute of Technology, Hoboken, N.J. 07030

**June 16 to 20—Theory and Interpretation in Mössbauer Spectroscopy.** Catholic University, Washington, D. C. CONTACT: Leopold May, Dept. of Chemistry, Catholic University, Washington, D. C. 20017

**June 16 to 21—Automation Analysis in Chemistry.** Washington, University. CONTACT: Institute for Continuing Education in Engineering and Applied Science, Washington University, St. Louis, Mo. 63130

**June 17 to 27—Two Intensive Courses in Infrared Spectroscopy: June 17 to 21, Technique; June 23 to 27, Applications.** MIT. Richard C. Lord, Dana W. Mayo. CONTACT (6)

**July 7 to 11—X-Ray Techniques in the Industrial Laboratory.** London, England. McCrone Research Institute. CONTACT (4)

**July 7 to 11—Infrared and Raman Spectroscopy: Techniques, Theory, and Interpretation.** UCLA. W. J. Lehman, H. J. Sloane. CONTACT (7)

**July 14 to 18—Industrial Use of the Polarizing Microscope.** London, England. McCrone Research Institute. CONTACT (4)

**July 14 to 18—Reflection Spectroscopy: Theory and Applications.** UCLA. W. N. Hansen, T. B. Hirschfeld. CONTACT (7)

**July 19 to Aug. 9—Research Instrumentation.** Brooklyn Campus, Polytechnic Institute of Brooklyn. (Partially supported by NSF grants under its College Teacher Program; also open to industrial and academic scientists). CONTACT: Kenneth Jolls, Office of Special Programs, Polytechnic Institute of Brooklyn, 333 Jay St., Brooklyn, N. Y. 11201. Tel: (212) 643-4442 or 643-2266

**July 22 to 26—Techniques of Infrared Spectroscopy.** University of Minnesota. CONTACT: Dept. of Conferences and Institutes, Nolte Center for Continuing Education, University of Minnesota, Minneapolis, Minn. 55455

**July 28 to Aug. 1—Chemical Interpretation of Infrared Spectra.** University of Minnesota. CONTACT: Dept. of Conferences and Institutes, Nolte Center for Continuing Education, University of Minnesota, Minneapolis, Minn. 55455

**Aug. 4 to 8—Ninth Annual Program in Infrared and Ultraviolet Absorption Spectroscopy.** Arizona State University. CONTACT (8)

**Aug. 11 to 15—Workshop on the Measurement of the Appearance of Properties of Materials.** Marriott Twin Bridges Motor Hotel, Washington, D. C. CONTACT: Hunterlab, 9529 Lee Highway, Fairfax, Va. 22030

**Aug. 18 to 20—Residual Gas Analyzer Spectra Interpretation.** Monrovia, Calif. CEC/Analytical Instruments Div. CONTACT (2)

**Aug. 18 to 29—Modern Industrial Spectroscopy.** Arizona State University. CONTACT (8)

**Aug. 18 to 29—Physical Measurement and Analysis.** MIT. CONTACT (6)

[1] Sadtler Educational Division, Sadtler Research Laboratories, Inc., 3316 Spring Garden St., Philadelphia, Pa. 19104. Tel: (215) 382-7800

[2] Coordinator of Training and Technical Publications, Bell & Howell, 1500 S. Shamrock Ave., Monrovia, Calif. 91106

[3] Education Office, American Chemical Society, 1155 16th St., N. W., Washington, D. C. 20036. Tel: (202) 737-3337

[4] Mrs. Miriam L. Fallert, McCrone Research Institute, 451 East 31st St., Chicago, Ill. 60616. Tel: (312) 842-7105

[5] Paul Batchelder, Varian Aerograph, 2700 Mitchell Dr., Walnut Creek, Calif. 94598. Tel: (415) 939-2400

[6] Director of the Summer Session, Room E19-356, Massachusetts Institute of Technology, Cambridge, Mass. 02139

[7] University Extension, UCLA, 10851 Le Conte Ave., Los Angeles, Calif. 90024

[8] Jacob Fuchs, Dept. of Chemistry, Arizona State University, Tempe, Ariz. 85281

## Microfiche Edition of Laboratory Guide

A microfiche edition of the "1968–69 ACS Laboratory Guide to Instruments, Equipment and Chemicals" is available in limited quantities at no cost to interested people who have microfiche readers or printer readers and would like to have the film. The entire guide is included on 8 cards. Interested persons should write to Microform Division, American Chemical Society Publications, 1155 Sixteenth St., N.W., Washington, D.C. 20036.


How do you get the highest resolution **consistently** in ion exchange chromatography?

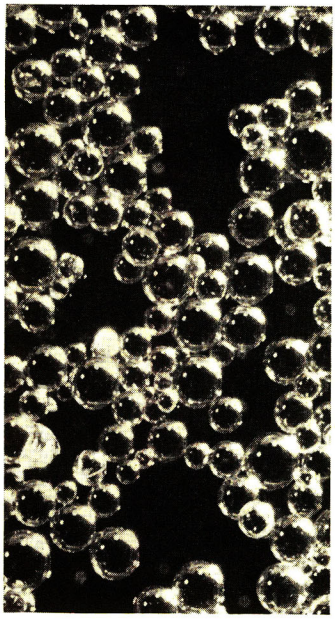

# Only by using Bio-Rad AG® resins!

BIO-RAD AG resins represent the highest level of purity available for ion exchange chromatography.

AG resins are exhaustively purified and sized to specific ranges to assure sharp resolution and highest reproducibility. For example, the maximum iron content in AG-1 anion resin is 0.00005%.

For the full story on BIO-RAD and its role in ion exchange technology—including valuable data on Bio-Rex resins, specialty resins, resin selection, regeneration and applications—send for our general catalog, Price List T.

BIO-RAD Laboratories

**Dept. A-4 • 32nd and Griffin Ave.**
**Richmond, California 94804**

Circle No. 18 on Readers' Service Card
See ACS Laboratory Guide for All Products/Sales Office

**Looking for a fraction collector?**



**How about the most compact one made?**

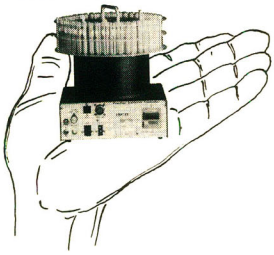

**The least expensive?**

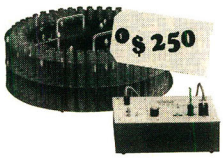


**Or a fancy rectangular one?**

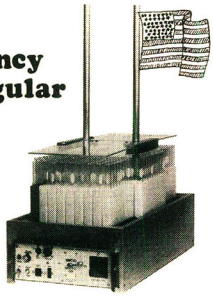

**ISCO has all kinds.**

**Write for our 1969 catalog.**

INSTRUMENTATION SPECIALTIES CO., INC.
4700 SUPERIOR LINCOLN, NEBRASKA 68504
PHONE (402) 434-0231 CABLE ISCOLAB LINCOLN

Circle No. 3 on Readers' Service Card
See ACS Laboratory Guide for All Products/Sales Office

# CALENDAR OF EVENTS

| | |
|---|---|
| March 31 to April 3 | **National Atomic and Molecular Physics Congress.** University of Manchester. Sponsor: Atomic and Molecular Physics Subcommittee of The Institute of Physics and The Physical Society. CONTACT: F. H. Read, Atomic and Molecular Physics Group, Dept. of Physics, The Schuster Laboratory, University of Manchester, Manchester, 13, England |
| April 1 | **25th Annual Quality Control Conference.** University of Rochester. Sponsor: Rochester Section of American Society for Quality Control. CONTACT: Industrial Management Council, 12 Mortimer St., Rochester, N. Y. 14604. Page 47 A, Jan. |
| April 13 to 18 | **157th National ACS Meeting.** Minneapolis, Minn. Includes Analytical Chemistry Division Sessions. CONTACT: Fred McLafferty, Cornell Univ., Ithaca, N. Y. 14850. Page 41 A, Mar. |
| April 14 to 15 | **Conference on Dynamic Experiments in Electron Optical Instruments.** Imperial College, London. CONTACT: The Institute of Physics and The Physical Society, 47 Belgrave Square, London, S.W. 1, England |
| April 14 to 16 | **Fourth National ISA Instrument Maintenance Management Symposium.** Statler-Hilton Hotel, Detroit, Mich. CONTACT: A. T. Upfold, Polymer Corp., Ltd., Sarnia, Ontario, Canada |
| April 17 | **American Microchemical Society Meeting.** Wagon Wheel Inn, Conshohocken, Pa. (Norristown, Conshohocken Turnpike Exit, West of Philadelphia). Subject: The Periphery of Microchemistry. William J. Porter, U.S. Dept. of Agriculture. CONTACT: L. M. Brancone, Lederle Laboratories Div., American Cyanamid Co., Pearl River, N.Y. 10965 |
| April 17 to 18 | **Gulf Coast Spectroscopic Group Spring Meeting.** Holiday Inn, Bossier City, La. CONTACT: Tom Pewitt, Shell Oil Co., Norco, La. |
| April 21 to 26 | **EUCHEM Conference of Metalproteins.** Heligoland, Germany. Includes Sessions on Physical Methods for the Study of Proteins (ESR, NMR, ORD, CD). CONTACT: W. Fritsche, Gesellschaft Deutscher Chemiker, 6000 Frankfurt (M), Postfach 119075, Germany |
| April 27 to 30 | **Third Conference on Isotopes Applications.** Gatlinburg, Tenn. CONTACT: J. H. Gillette, Oak Ridge National Laboratory, P.O. Box X, Oak Ridge, Tenn. 37830 |
| April 27 to May 1 | **Scientific Apparatus Makers Association Annual Meeting.** The Greenbrier, White Sulphur Springs, W. Va. CONTACT: Scientific Apparatus Makers Assoc., 1140 Connecticut Ave., N.W., Washington, D. C. 20036 |
| April 29 to May 1 | **Second Annual Scanning Electron Microscope Symposium.** IIT Research Institute, Chicago, Ill. CONTACT: E. P. Fahy, IIT Research Institute, 10 W. 35th St., Chicago, Ill. 60616. Page 47 A, Jan. |

## Coming Events

**May 1 to 2—Metrochem '69.** Hilton Hotel, New York City. Sponsors: New York and North Jersey Sections, ACS. CONTACT: George Heinze, Johnson and Johnson Research Center, New Brunswick, N. J. 08903

**May 4 to 9—Spring Meeting Electrochemical Society.** Commodore Hotel, New York City. CONTACT: The Electrochemical Society, 30 East 42nd St., New York, N. Y. 10017

**May 5 to 7—15th ISA Analysis Instrumentation Symposium.** Jung Hotel, New Orleans, La. CONTACT: G. Byers, The Boeing Co., 1326 Seville Dr., New Orleans, La. 70122

**May 5 to 7—American Society for Quality Control 23rd Annual Technical Conference and Exhibit.** Biltmore Hotel, Los Angeles, Calif. CONTACT: American Society for Quality Control, 161 West Wisconsin Ave., Milwaukee, Wis. 53203

**May 12 to 15—20th Annual Mid-America Symposium on Spectroscopy.** Sheraton-Chicago Hotel, Chicago, Ill. CONTACT: Richard L. Terry, Sinclair Research, Inc., 400 East Sibley Blvd., Harvey, Ill. 60426. Tel: (312) 468-9300, Ext. 503. Page 48 A, Apr.

**May 17 to 25—International Chemistry Exhibition; XX International Congress—Chemistry Days 1969.** Milan, Italy. Sponsor: Federation of Scientific and Technical Associations. CONTACT: Federazione Delle Associazioni Scientifiche e Tecniche, 20121 Milan, Via Marcona 49, Italy

**May 18 to 23—17th Annual Conference on Mass Spectrometry and Allied Topics.** Sheraton-Dallas Hotel, Dal-

las, Texas. Sponsor: ASTM Committee E-14. CONTACT: J. M. McCrea, Applied Research Laboratory (73), U. S. Steel Corp., Monroeville, Pa. 15146. Page 47 A, Dec.

**May 20 to 21—Fourth Annual Seminar on Pesticide Residue Analysis.** University of Manitoba, Winnipeg, Manitoba, Canada. Sponsors: Canada Dept. of National Health and Welfare and Manitoba Dept. of Health. CONTACT: Ben Berck, Canada Dept. of Agriculture Research Station, Winnipeg, Canada

**May 21 to 23—10th Symposium on Electron, Ion, and Laser Beam Technology.** NBS, Gaithersburg, Md. CONTACT: L. Marton, National Bureau of Standards, Washington, D.C. 20234

**May 25 to 28—52nd Canadian Chemical Conference and Exhibition.** Queen Elizabeth Hotel, Montreal, Que. CONTACT: Chemical Institute of Canada, 151 Slater St., Ottawa 4, Ontario, Canada

**May 26 to 30—XV Colloquium Spectroscopicum Internationale.** Madrid, Spain. CONTACT: E. Arsensi Alvarez-Arenas, Serrano, 119, Madrid-6, Espana

**June 4 to 6—International Congress on Automated Analysis.** Conrad Hilton Hotel, Chicago, Ill. CONTACT: Jerome E. Golin, Technicon Corp., Ardsley, N. Y. 10502

**June 5 to 6—Third Great Lakes Regional ACS Meeting.** DeKalb, Ill. Includes Analytical Chemistry Sessions, CONTACT: Richard C. Bowers, Northern Illinois University, DeKalb, Ill. 60115

**June 5 to 11—Fifth International Meeting of Forensic Sciences.** Toronto, Canada. CONTACT: Frank L. Wilson, Dept. of the Attorney General, Parliament Bldg., Toronto 2, Canada

**June 9 to 13—Gordon Research Conference on Magnetic Resonance.** New Hampton School, New Hampton, N.H. CONTACT: W. George Parks, University of Rhode Island, Kingston, R.I.

**June 11 to 13—ACS Analytical Chemistry Summer Symposium.** University of Georgia, Athens, Ga. Sponsors: Analytical Chemistry Division and ANALYTICAL CHEMISTRY. Subject: Modern Instrumental Techniques for Elemental Analysis. CONTACT: G. H. Morrison, Dept. of Chemistry, Cornell University, Ithaca, N. Y. 14850. Page 45 A, Apr.

**June 12 to 13—Vacuum Microbalance Techniques, Eighth Conference.** Wakefield (near Boston), Mass. CONTACT: W. W. Czanderna, Dept. of Physics, Clarkson College of Technology, Potsdam, N.Y. 13676

**June 12 to 13—24th Annual Northwest Regional ACS Meeting.** University of Utah, Salt Lake City, Utah. Includes Analytical Chemistry Sessions. CONTACT: Edward M. Eyring, Dept. of Chemistry, University of Utah, Salt Lake City, Utah 84112

**June 22 to 27—ASTM 72nd Annual Meeting.** Chalfonte-Haddon Hall, Atlantic City, N. J. CONTACT: American Society for Testing and Materials, 1916 Race St., Philadelphia, Pa. 19103

**June 23 to 25—4th IMEKO—Photon Detectors Symposium.** Hotel International, Prag. CONTACT: IMEKO Secretariat, Budapest, 5, P. O. B. 457


# Let's Reflect...

## What's Best In Today's Infrared?

Wilks Scientific Internal Reflection Spectrophotometers and ATR Accessories can solve all of your routine, and most non-routine, infrared sample-handling problems. We design them that way — with you in mind! Here is just a sampling of Wilks "better ideas in infrared."

WILKS SCIENTIFIC CORPORATION
SOUTH NORWALK • CONNECTICUT 06856
TELEPHONE • (203) 838-4537

**Model 8 Internal Reflection Infrared Spectrophotometer**

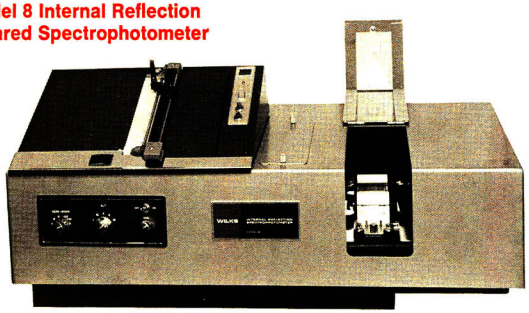

A compact, high-performance unit with a versatile optical system that provides both internal reflection and transmission capability. The Model 8 can be supplied as a complete instrument, or as a field modification. Other custom modifications available.

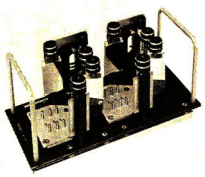

**Model 12 Double-Beam Attachment**

Quality and analytical versatility are offered in the Model 12. Dual-optical system has self-contained beam attenuator, and the reference and sample beam assemblies are track-mounted for rigidity and adjustment for different beam separations. Differential analysis is possible. Fits most IR spectrophotometers.

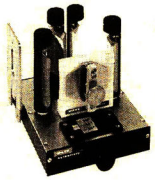

**Model 50 Variable-Angle Internal Reflection Attachment**

This is the A.T.R. attachment for "the analyst who has everything". It has the most advanced design of any A.T.R. infrared attachment available. Continuously variable adjustment from 30° to 60°. Particularly useful in studying changes and effects of surface treatments on films, elastomers, and other materials.

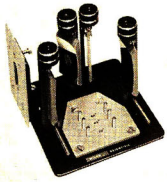

**Model 9 Single-Beam Attachment**

Of such high-performance, the Model 9 has frequently been copied — but never equalled. You have the versatility of 30°, 45°, and 60° angles of incidence. Reflector plates in all materials may be utilized. Fits all Perkin-Elmer and Beckman Spectrophotometer sampling compartments.

Circle No. 187 on Reader's Service Card

See ACS Laboratory Guide for All Products/Sales Office

**July 13 to 19—VII International Congess of Clinical Pathology.** Montreal, Canada. CONTACT: VII International Congress of Clinical Pathology, P. O. Box 8, Station "G," Montreal 18, Canada

**July 14 to 16—Conference on Nonconventional Electron Microscopy.** St. Catherine's College, Oxford, England. CONTACT: The Institute of Physics and The Physical Society, 47 Belgrave Square, London, S.W.1, England

**July 14 to 18—International Conference on Atomic Absorption Spectroscopy.** Sheffield, England. CONTACT: A.A.S. Conference Secretary, Society for Analytical Chemistry, 9/10 Savile Row, London, W.1, England. Page 49 A, July

**July 15 to 18—Meeting on NMR Spectroscopy.** Birmingham, England. CONTACT: The Chemical Society, Burlington House, London, W.1, England

**July 16 to 18—Symposium on Surface Area Determination.** University of Bristol. Sponsors: IUPAC, Society of Chemical Industry, School of Chemistry, University of Bristol. CONTACT: D.H. Everett, University of Bristol, Bristol BS8, 1TS, England

**July 16 to 18—Fourth National Conference on Electron Microprobe Analysis.** Huntington-Sheraton Hotel, Pasadena, Calif. CONTACT: A. A. Chodos, Geology Dept., California Institute of Technology, Pasadena, Calif. 91109

**July 21 to 25—International Symposium on Analytical Chemistry.** Birmingham, England. Sponsors: SAC and IUPAC. CONTACT: D. M. Peake, 61 Lodge Rd., Walsall, Staffordshire, England. Page 57 A, Aug.

**July 28 to Aug. 1—28th ISA Research Conference on Instrumentation Science.** Hobart & Wm. Smith College, Geneva, N.Y. CONTACT: N.E. Huston, University of Wisconsin, 1815 University Ave., Madison, Wis. 53706

**Aug. 4 to 5—Eleventh Annual Rocky Mountain Spectroscopy Conference.** Denver, Colo. CONTACT: H. N. Barton, Dow Chemical Co., P.O. Box 888, Golden, Colo. 80402

**Aug. 4 to 7—International Conference on Raman Spectroscopy.** Carleton University, Ottawa, Canada. CONTACT: J. A. Koningstein, Chemistry Dept., Carleton University, Ottawa, Canada

**Aug. 6 to 8—Denver Conference on Applications of X-Ray Analysis.** Albany Hotel, Denver, Colo. CONTACT: J. B. Newkirk, Denver Research Institute, University of Denver, Denver, Colo. 80210. Page 66 A, Apr.

**Aug. 11 to 15—Gordon Research Conference on Analytical Chemistry.** New Hampton School, New Hampton, N.H. CONTACT: W. George Parks, University of Rhode Island, Kingston, R.I.

**Aug. 13 to 27—8th International Congress and General Assembly of the International Union of Crystallography.** State University of New York at Stony Brook. CONTACT: David Shoemaker, Dept. of Chemistry, Massachusetts Institute of Technology, Cambridge, Mass. Page 89 A, Feb.

**Aug. 17 to 22—Annual Meeting American Association of Clinical Chemists.** Denver, Colo. CONTACT: David A. Roethel, 1155 16th St., N. W., Washington, D. C. 20036

**Aug. 17 to 24—3rd NMR Symposium.** University of Toronto, Toronto, Ont. Sponsor: Physical Chemical Division (CIC) and University of Toronto. CONTACT: Chemical Institute of Canada, 151 Slater St., Ottawa 4, Ontario, Canada

**Aug. 18 to 22—Gordon Research Conference on Separation and Purification.** Colby Junior College, New London, N.H. CONTACT: W. George Parks, University of Rhode Island, Kingston, R.I.

**Aug. 18 to 22—Gordon Research Conference on Ion Exchange.** Kimball Union Academy, Meriden, N.H. CONTACT: W. George Parks, University of Rhode Island, Kingston, R.I.

**Aug. 25 to 29—International Conference on Luminescence.** University of Delaware. Sponsors: IUPAC and American Physical Society. CONTACT: R. B. Murray, Dept. of Physics, University of Delaware, Newark, Del. 19711

**Aug. 31 to Sept. 4—International Conference on Calorimetry and Thermodynamics.** Warsaw, Poland. CONTACT: H. Kehiaian, Secretary, Organizing Committee, Institute of Physical Chemistry, Polish Academy of Sciences, P. O. Box 49, Warsaw 42, Poland

**Sept. 16 to 18—17th Detroit Anachem Conference and Instrument Exhibit.** Statler Hilton Hotel, Detroit, Mich. CONTACT: James A. Burns, Jr., Ethyl Corp., 1600 W. Eight Mile Rd., Ferndale, Mich. 48220

**Oct. 20 to 23—16th Spectroscopy Symposium of Canada.** Holiday Inn Hotel (downtown) Montreal, Canada. Sponsor: Spectroscopy Society of Canada. CONTACT: R. A. Burley, Noranda Research Centre, 240 Hymus Blvd., Pointe Claire, Quebec, Canada

**Other conferences scheduled for September, October, and November were listed in the March issue, pages 50 A and 51 A.**

## New Journal on Organic Magnetic Resonance

Heyden & Son Limited of London has announced the publication of a new journal, *Organic Magnetic Resonance*. The journal will include original work dealing with the applications of NMR, NQR, and ESR to the general problems of structural organic chemistry, book reviews, and review articles. In addition, a major feature of the journal is the provision in a special supplement to each issue, for the reproduction in standard format of full original spectra of compounds together with experimental details.

Editor-in-Chief is Eric F. Mooney, University of Birmingham, P.O. Box 363, Birmingham 15, England. There are regional editors in North America (S. L. Manatt, Jet Propulsion Laboratory, California Institute of Technology, 4800 Oak Grove Dr., Pasadena, Calif. 91103), Germany, France, Australia, and Japan and an editorial advisory board representing a wide geographical distribution. Papers in the journal may be published in English, French, or German.

The first issue of this journal appeared in January 1969. Issues will appear bimonthly. Annual subscriptions (including postage) for libraries, universities, and other multiple-reader institutions are £16.10s.0d. (U.S.A., $40) with one copy of spectral supplement and £20.10s.0d. (U.S.A., $51) with two copies of the spectral supplement. Private subscribers ordering directly from the publisher for personal-use copies may subscribe for £5.0s.0d. (U.S.A. $15 per annum). Publishing offices are: Heyden & Son Ltd., Spectrum House, Alderton Crescent, London, NW4, England.

## Industry Items

**Baird-Atomic, Inc.,** Cambridge, Mass., has announced the purchase of the manufacturing and distribution rights to three instruments formerly distributed by **Bausch and Lomb, Inc.,** Rochester, N. Y. The instruments are the 2-meter dual grating spectrograph, research dual grating spectrograph, and the 1.5-meter concave grating spectrograph. Baird-Atomic, Inc., a scientific instrument firm, has a Spectrochemical Equipment Division which makes direct reading spectrometers and accessory equipment.

**IMASS, Inc. (Instrumentation for the Materials and Structural Sciences),** P. O. Box 134, Accord, Mass. 02018, is a new independent scientific instrument and equipment marketing company. The firm will sell the Rheovibron, an instrument for evaluating the viscoelastic properties of materials under dynamic testing conditions at controlled frequencies and temperatures, and other instruments for evaluating thermal and chemical properties, particle size, molecular and structural configuration, and stress-strain properties.

**Leeds & Northrup Co.** has purchased a 20,000 square-foot building in North Wales, Pa., for expansion of its Process Analytical and Environmental Instrumentation Division.

Murray E. Volk and Associates announce the acquisition of **Isolab Supply Co.,** 665 W. Bowery St., Akron, Ohio. Isolab will henceforth be known as **Isolab Incorporated** with headquarters in Elkhart, Ind. Isolab makes and distributes products for scientific and clinical laboratories.

# EG&G Picoammeters were the first with ~~pereision~~ precision digital readout

The original Picoammeters designed expressively for digital readout of low-level current measurement. EG&G Automatic Digital Picoammeters eliminated the need to rely on the expertise of a skilled scientist to interpret analog presentations. Or, the pseudo-accuracy of competitive digitized versions of analog instruments. EG&G Digital Picoammeters facilitate the routine measurement of low-level currents, where greater amounts of higher-accuracy data are required.

Since the introduction of the first Digital Picoammeter several years ago, we, at EG&G, have been hard at work refining and improving the basic concept. Now, with the second generation we've significantly reduced those "second order effects" so characteristic of meter movement instruments. The new generation of EG&G Automatic Digital Picoammeters also includes accurate range correlation, negligible zero drift on all ranges, and a high normal mode noise rejection. The speed of the automatic range changing, which must be commensurate with speed of response is accomplished by transient-free switching of high resistance feedback elements.

The new generation of EG&G Picoammeters which embody these new techniques includes the Model ME-930A Digital Picoammeter for general lab work and automatic digital data acquisition systems. Its current measuring range is $10^{-11}$ amps through $10^{-2}$ amps full scale in ten decade steps. A full Digital Picoammeter with automatic range changing capability and automatic polarity selection. All solid state design with MOS FET input, remote function control and optional printer drive (for use with the new EG&G Teletypewriter coupler), digital readout of level, range, and polarity. Of course, an analog output is also available.

For the precision work needed in Standard and Calibration Labs there's the Model ME-1035 Precision Picoammeter with digital readout. It has a current measuring range of $10^{-5}$ amps to $10^{-12}$ amps with $10^{-15}$ amps resolution. Accuracy is ±.5% on the $10^{-12}$ amps range. All solid state design with low level MOS FET input, temperature controlled feedback resistors for added stability, pushbutton range control, adjustable summing point voltage and current offset monitor, and pushbutton controls for rapid internal calibration requiring no external standards or sources.

For further details on how EG&G Digital Picoammeters can help you, contact your local EG&G Lab Products Division representative. Or, write EG&G, Inc., Laboratory Products Division, P.O. Box 755, Goleta, California, 93017.

EG&G
LABORATORY PRODUCTS DIVISION







Circle No. 41 on Readers' Service Card

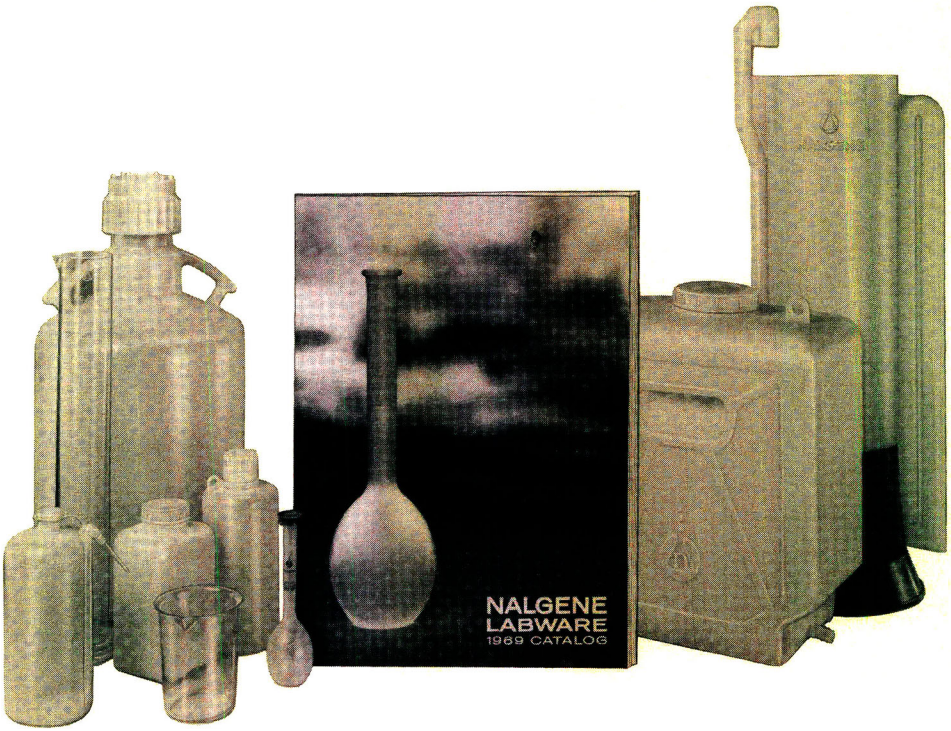


# Read any good books lately?

Here's one. The 1969 Nalgene Laboratory Catalog–56 pages of descriptions, specifications, and prices on the complete Nalgene® Labware line. Plus, laboratory equipment from other divisions of Sybron Corporation.

This is the most complete line of plastic products manufactured specifically for the laboratory. Every item is precision molded of the proper material, and in the most efficient design for specific laboratory functions. Every year, more and more laboratories *specify* Nalgene Labware to make sure they get all the safety and economy benefits of the finest plastic labware.

Here are some items of special interest from our 1969 Catalog:

**NALGENE PIPET WASHER-RINSERS.** Exclusive one-piece design eliminates all washer-rinser problems. Back siphoning is impossible. Wide range of cycling speeds. Repeats automatically. Also available–unbreakable Nalgene Pipet Jars and Baskets.

**NALGENE LABORATORY BOTTLES.** Widest range of unbreakables available anywhere. Variety of materials, designs and sizes to handle any laboratory application. Safer and easier to use because they're designed specifically for the laboratory. New linerless polypropylene closures make them leakproof without danger of contamination. Our Teflon® bottles have fluorocarbon closures.

**NALGENE ASPIRATOR CARBOYS.** Rectangular and conventional designs–with spigot or tubulation. Tough, rigid, no-leak construction. Sizes from 1 to 13 gal. Larger sizes have molded-in handgrips for greater safety.

**NALGENE WASH BOTTLE.** One-piece construction of bottle and tube eliminates any possibility of leakage. Entire contents can be dispensed without tipping or shaking. Hundreds of thousands in use all over the world. Sizes from 30-1000 ml.

**NALGENE GRADUATES AND BEAKERS IN TPX.** Crystal clear, shatter-proof, autoclavable, chemically resistant. Graduates from 10-1000 ml; beakers from 30-1000 ml. TPX is a trademark of Imperial Chemical Industries Limited for their brand of methylpentene polymer.

**NEW! NALGENE VOLUMETRIC FLASKS.** First plastic volumetric flasks. All the accuracy of standard glass flasks–plus the unbreakability of plastic. Precision molded and individually calibrated, handle any procedure now done with glassware. Won't etch or contaminate. Can be autoclaved repeatedly without affecting accuracy. Sizes from 100-1000 ml.

**NEW! NALGENE AUTOCLAVABLE CARBOY.** Use to prepare, store, *and autoclave* 5-gallon batches of culture media, distilled water, and other solutions. Withstands repeated autoclaving, has screw closure and two carrying handles for maximum safety and convenience.

**NEW! NALGENE DESICCATOR AND PLATE.** Unbreakable desiccator with tubulation on lower part for easy handling. Will hold 24-inch vacuum for more than 24 hours, implosion-safe at full vacuum. Cover is transparent polycarbonate; lower part is chemically-resistant polypropylene. Accepts Nalgene Nucerite® Plate (230 mm) or standard glass plate.

Most Nalgene Labware can be assorted for maximum discount–another good reason to specify Nalgene Labware from your lab supply dealer. Ask him for our 1969 Catalog or write Dept. 6704, Nalgene Labware Division, Rochester, New York 14602.

NALGENE LABWARE DIVISION

NALGE
SYBRON CORPORATION

**Visit Our Booth At The Federation Show**

# RADIOMETER's pHM 26




. . . with unique calibrated ISO pH and electrode sensitivity controls

## *Advanced Capabilities for the Most Demanding* **pH** *Measurements*

### *Capabilities to . . .*

- **expand** scale reading 10-fold from any integral pH value in the range of 0-14 pH.
- **reproduce** results within ± 0.002 pH and ± 0.1 mv.
- **grow** into an automatic titrator by addition of other Radiometer modular components.
- **accomplish** accurate dead-stop end-point titrations, with special scale for this purpose.
- **measure** oxidation-reduction potentials ranging from −2800 to +2800 mv.

### *Unique Capabilities to . . .*

- **determine,** by separate control, electrode sensitivity and match it to pH meter response.
- **perform** rapid two-buffer method calibrations using ISO pH control.
- **allow** pH measurements at two pre-selected temperatures without re-calibration.

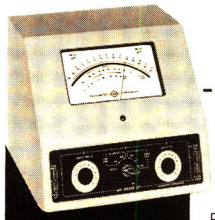

pHM 27
Specifically for blood pH work.

**THE LONDON COMPANY**
811 SHARON DRIVE
CLEVELAND, OHIO 44145

RADIOMETER COPENHAGEN

In Canada: Bach-Simpson Limited Box 2484. London

Please send me the facts on Radiometer pH meters.

Name_____ Title_____

Company_____ Dept._____

Address _____

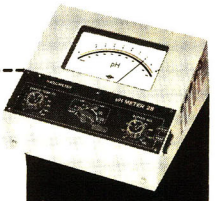

pHM 28
For general purpose laboratory work.

Circle No. 129 on Readers' Service Card

See ACS Laboratory Guide for All Products/Sales Office

# NEW DATA PRINTER

## from Coleman prints concentration directly on your record form

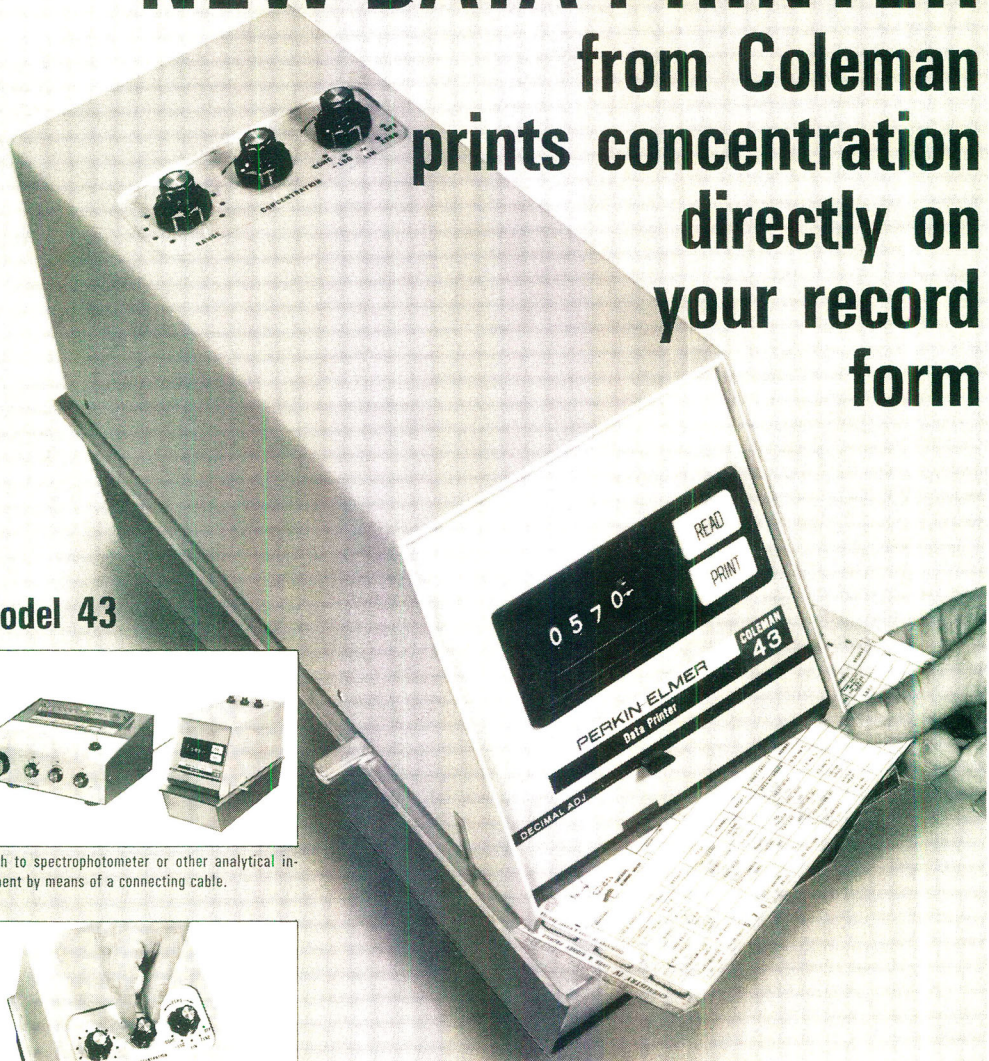


## Model 43



Attach to spectrophotometer or other analytical instrument by means of a connecting cable.



Operation is simple. Adjustments are minimal. Insert known sample, turn Printer to concentration mode, and adjust for digital reading of known concentration.

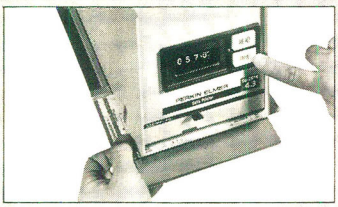

Printout is quick and easy. Simply insert card or record form into printing area and push PRINT button. Readout is recorded anywhere you want it on form and carbons. Print same results on several cards if you wish.

Only the new COLEMAN Data Printer gives you direct concentration printout on your medical records. And it's priced below $1900. Can be connected to spectrophotometers, pH meters, or flame photometers in seconds. Saves time, increases accuracy. Eliminates 3 major sources of error: 1. Reading; 2. Converting the reading to concentration; 3. Recording concentration on your record.

Provides precise, permanent, clearly printed records. Prints results of transmittance or pH, absorbance or concentration determinations.

***Send for Bulletin A-332***
***Write to Coleman Instruments Division, The Perkin-Elmer Corporation, 42 Madison Street, Maywood, Illinois 60153***

**PERKIN-ELMER**

Circle No. 30 on Readers' Service Card

VISIT OUR BOOTH—FASEB MEETING

Circle No. 1 on Readers' Service Card →

# The only time you have to stop the new Brinkmann Fraction Collector is when you run out of fractions.

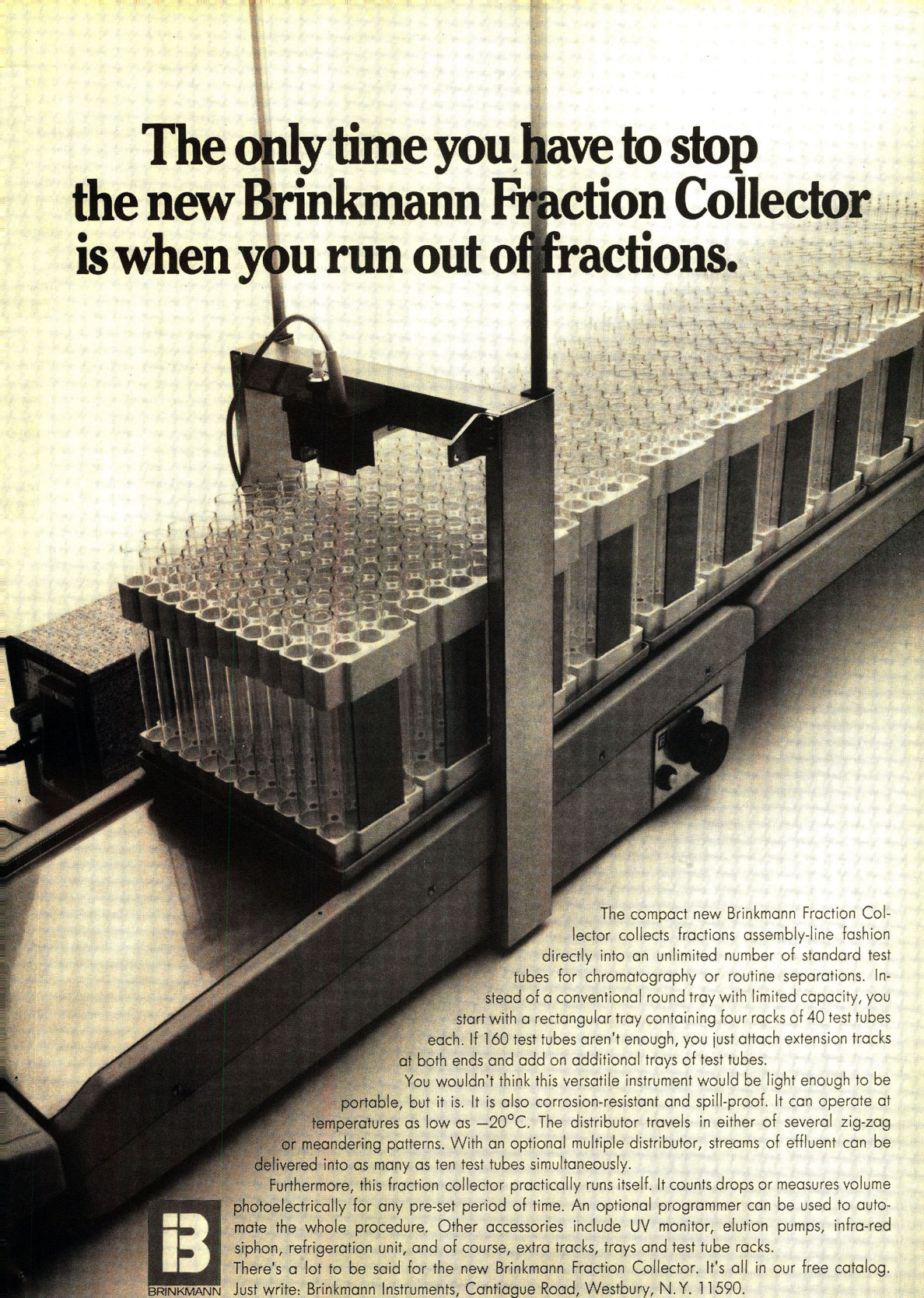

The compact new Brinkmann Fraction Collector collects fractions assembly-line fashion directly into an unlimited number of standard test tubes for chromatography or routine separations. Instead of a conventional round tray with limited capacity, you start with a rectangular tray containing four racks of 40 test tubes each. If 160 test tubes aren't enough, you just attach extension tracks at both ends and add on additional trays of test tubes.

You wouldn't think this versatile instrument would be light enough to be portable, but it is. It is also corrosion-resistant and spill-proof. It can operate at temperatures as low as −20°C. The distributor travels in either of several zig-zag or meandering patterns. With an optional multiple distributor, streams of effluent can be delivered into as many as ten test tubes simultaneously.

Furthermore, this fraction collector practically runs itself. It counts drops or measures volume photoelectrically for any pre-set period of time. An optional programmer can be used to automate the whole procedure. Other accessories include UV monitor, elution pumps, infra-red siphon, refrigeration unit, and of course, extra tracks, trays and test tube racks.

There's a lot to be said for the new Brinkmann Fraction Collector. It's all in our free catalog. Just write: Brinkmann Instruments, Cantiague Road, Westbury, N.Y. 11590.

BRINKMANN

**Double element heating tapes... waterproof**

Only 1/16" thick, can be wrapped on tubes as small as 1/8" diameter. Operable to 480° F (temperature limit of Silicone rubber coverings). Ribbon type heating element.

- 1/4" Wide, 9.082 ohms per ft., 95¢ per ft.
- 1/2" Wide, 3.768 ohms per ft., $1.40 per ft.
- 1" Wide, 1.88 ohms per ft., $2.00 per ft.
- Add $5.00 each unit for finishing ends and fitting with plug and supply cord.

**Cal-Cord heating cords withstand *high* temperatures**

Cal-Cords are only 3/16" in diameter, can be wrapped on tubes as small as 1/2" diameter.

- 400° C Medium Cal-Cord—glass fabric insulation, lengths 2 to 16 ft., 80 to 640 watts, $6.50 to $35.00.
- 600° C Super Cal-Cord—quartz fabric insulation, lengths 2 to 8 ft., 200 to 800 watts, $8.00 to $25.50.

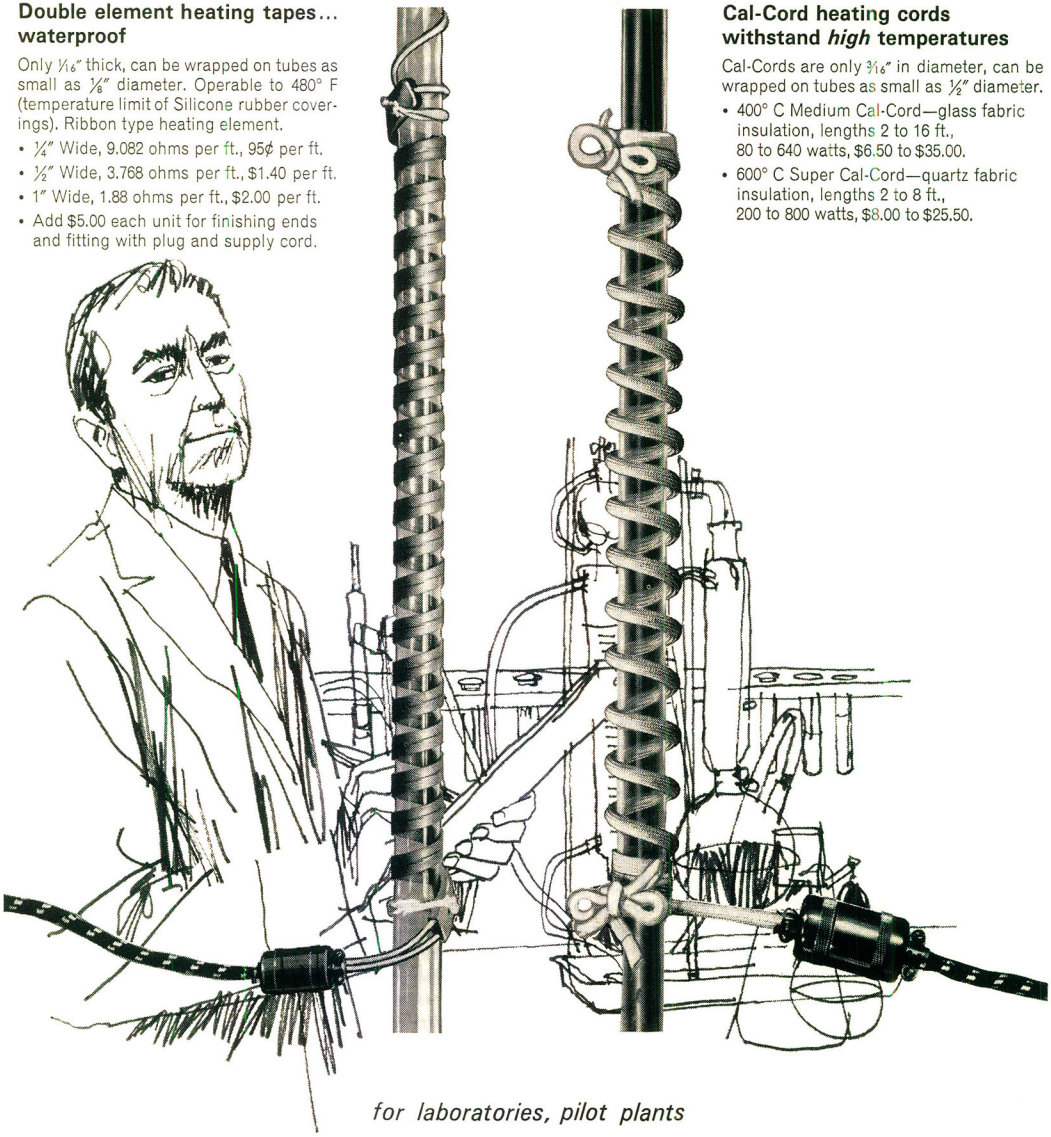

*for laboratories, pilot plants*

# rugged...flexible... safe heating tapes; cords—by Glas-Col

Glas-Col heating cords and tapes can be loaded right up to insulation limits without burning out. They can be flexed, twisted and coiled again and again, on small diameter equipment, without damage. They're built to withstand rough service and last for years.

Heating elements terminate at one end into a single twistlock connection for joining to supply cord (included with each unit). No loose terminals at ends. More information on request.

**GLAS-COL®**
**HEATING TAPES**
**Glas-Col Apparatus Company**
Dept. AC, 711 Hulman St., Terre Haute, Ind.
*U.S. Patents 2,952,001; 2,982,932; 2,989,613

**Circle No. 16 on Readers' Service Card**

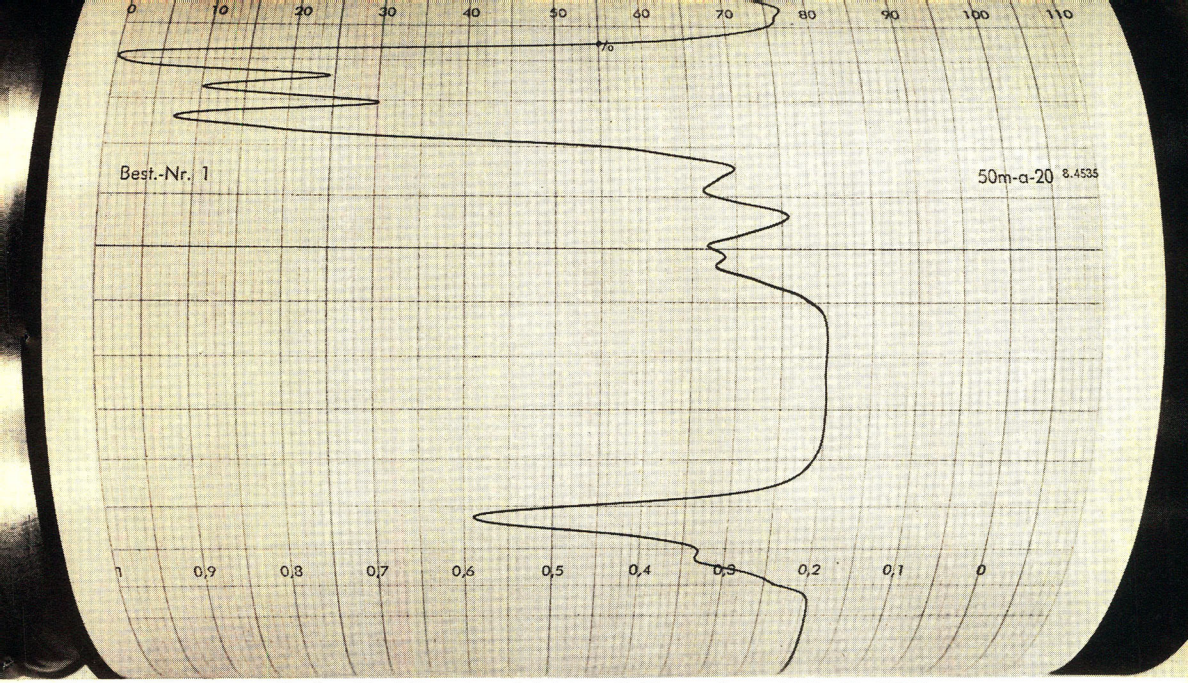


*Three* successive scans, *one over the other,* of the visible spectrum of a holmium oxide filter prove the repeatability of the DMR 21.

# One thing about the accuracy of our DMR 21 Recording Spectrophotometer:

# It bears repeating

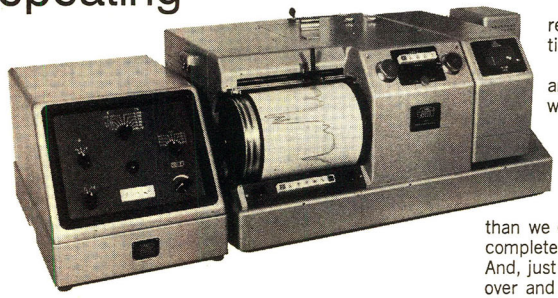

For dependable accuracy and long-term stability, the double-beam DMR-21 is unmatched. Over a 185-2500 nm range, it gives you wavelength accuracies of 0.05 at 200 nm. and 0.3 at 400 nm., with a repeatability of 0.01 and 0.1 respectively. That's because the prism and scale are mounted on one unit with no movable connection. But that's only *one* thing.

There are a number of other features that make the DMR 21 unique in its field. Here are a few:

A specially-designed drum recorder with a 500 mm recording length, repetitive scanning with unsurpassed repeatability and easy operation.

A three-point control that varies pen response down to one-half second. Half the time of other instruments.

Fully thermostated cell compartment and cell holders, standard equipment only with Zeiss. Widest variety of cells.

Maximum versatility for analytical or life science procedures, including pushbutton selection of 10 chart speeds and 8 wavelength presentations.

In fact, the DMR 21 has more features than we can detail here. Features that make it a complete system that will do a lot of things for you. And, just as important, will keep on doing them—over and over and over again. For more details, write: Carl Zeiss Inc., 444 Fifth Avenue, New York, N.Y. 10018.

Nationwide service.

ZEISS

THE GREAT NAME IN OPTICS

CARL ZEISS WEST GERMANY

ATLANTA, BOSTON, CHICAGO, COLUMBUS, DENVER, HOUSTON, LOS ANGELES, PHILADELPHIA, ST. LOUIS, SAN FRANCISCO, SEATTLE, WASHINGTON, D.C.

Circle No. 170 on Readers' Service Card

See ACS Laboratory Guide for All Products/Sales Office

# We make the world's broadest line of mass spectrometers. But that's not why most people buy from us.

As the world's largest supplier of Mass Spectrometers, Perkin-Elmer is in a position to give you the best back-up in the industry. We give you full applications support. Our monthly three-day training courses instruct your technical staff as to the proper and most efficient methods for accurate results. Our highly skilled specialists are readily available for prompt local service.

You can have the Mass Spectrometer best tailored to your specific requirements at Perkin-Elmer. You can choose from nine instruments. You can lease or buy.

Perkin-Elmer Mass Spectrometers are available from $22,500 to $130,000. For further information, write: Instrument Division, The Perkin-Elmer Corporation, 702 Main Ave., Norwalk, Conn. 06852

PERKIN-ELMER

MODEL RMU-6:
Versatility and reliability have made this medium resolution instrument the world's most popular Mass Spectrometer.

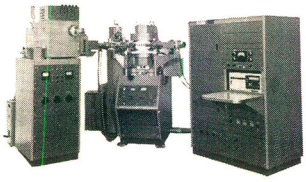



MODEL RM-6K:
For the high temperature chemist, the 2500°C Knudsen cell Mass Spectrometer.

MODEL 270:
A high performance double focusing Mass Spectrometer with integral Gas Chromatograph inlet system.

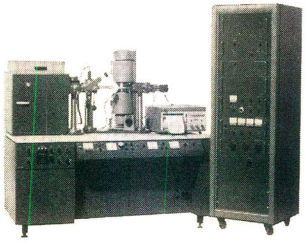

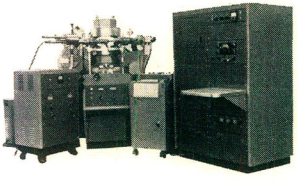

MODEL RM-6S:
For accurate isotope ratio work and analysis of inorganics via surface ionization. The RM-6R is available for precise isotope ratio determination of gases. Features a dual inlet system and a double collector.

MODEL RMU-7:
The double focusing high resolution version of the RMU-6, for precise mass measurements and molecular structure elucidation.





MODEL RMS-4:
A low-cost medium resolution Mass Spectrometer designed for a wide range of applications.

MODEL RMH-2:
The world's highest resolution Mass Spectrometer commercially available. Unsurpassed mass measurement accuracy throughout the entire mass range.

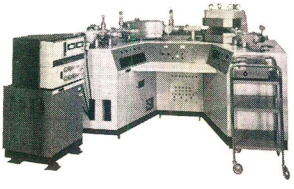



COMPUTER CAPABILITY:
On-line and time-sharing digital computer systems are available for all our Mass Spectrometers.

Circle No. 176 on Readers' Service Card

Circle No. 70 on Readers' Service Card →

See ACS Laboratory Guide for All Products/Sales Office

# Precision Vacuum Pumps are causing a quiet revolution!

Not too many people appreciate the irritating clatter and rapping noise commonly associated with vacuum pumps. That's one of the big reasons why Precision pumps enjoy such wide acceptance today, just a little more than a year since their introduction. Virtually noiseless and vibrationless, they offer an advantage that is welcome in any environment.

And they do a better pumping job! Compare published performance curves and you'll find Precision pumps are more efficient at actual working pressures—up to a remarkable 79% at one micron. Guaranteed ultimate vacuum runs to 0.1 micron of mercury—$1 \times 10^{-4}$ Torr.

You can select the pump that's performance matched to your job—7 two-stage models, in capacities ranging from 25 to 1500 liters/minute, at prices ranging from $150 to $1600. They're quieter, more compact, more efficient, yet less expensive than anything on the market today—easy to service too—right on the spot.

Write for Bulletin 650-B, a 24-page catalog of complete pump data, or ask your favorite laboratory supply salesman. He can tell you all the other reasons for specifying a Precision Vacuum Pump. Precision Scientific Company, 3737 West Cortland Street, Chicago, Illinois 60647.

PRECISION PS SCIENTIFIC

SUBSIDIARY OF GCA CORPORATION



# If you don't know why Florisil is the right adsorbent for chromatography

## write!




Send for your copy of this 32 page book. It's full of reasons why highly-selective Florisil and Florisil TLC are preferred for column and thin layer chromatography. Gives you chemical composition, physical properties, adsorptivity data and a bibliography that indicates studies and applications in 12 areas: general; vitamins, alkaloids-nitrogen compounds-drugs; steroids-hormones; pesticide residues; antibiotics; petroleum and shale oil; enzymes; terpenes; lipids, carcinogens, miscellaneous studies. Write for your copy now.

**Floridin**

**FULLER'S EARTH • ATTAPULGITE CLAY • ACTIVATED BAUXITE**

Shipping Points: Quincy, Fla. & Ochlocknee, Ga.
Sales Offices: 3 Penn Center, Pittsburgh, Pa.
580 Sylvan Ave., Englewood Cliffs, N.J.
3400 Peachtree Road, Atlanta, Georgia
8000 Bonhomme Avenue, St. Louis, Missouri
10601 W. Crestridge Drive, Minnetonka, Minn.
5645 Milton Street, Dallas, Texas

**Circle No. 4 on Readers' Service Card**

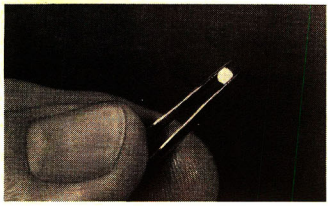

Micro-sampling is just one capability of two new spectrophotometers, the Beckman IR-18 and IR-20. Both are equipped with mind-freeing conveniences that gain you think-time.

Until now, you could find the versatile capability of the IR-18 and IR-20 only in a research-priced instrument. Now in addition to precise micro-sampling performance, you gain a combination of work-saving benefits. Operation is simple. Standout features include coded controls for routine (0), fast (△), and high resolution (□) scans... automatic scan and reset...75 precalibrated charts/roll...7 slit programs...scale expansion...9 speeds, from 6 minutes to 50 hours...abscissa expansions of 4X and 10X without an external recorder...a large, easily accessible sample compartment...built-in circuit tests. Data is presented on a flatbed, strip chart recorder. Accuracy and reliability are unexcelled in any other moderately priced IR instrument. IR-20's wave number range is 4000-250 $cm^{-1}$; IR-18's is 4000-600 $cm^{-1}$. For complete details, contact your Beckman representative or write for Data File #202.

Ask about our leasing program.

# In IR... Beckman introduces the Mind Free-ers

Beckman®

INSTRUMENTS, INC.

**SCIENTIFIC INSTRUMENTS DIVISION**

FULLERTON, CALIFORNIA • 92634

INTERNATIONAL SUBSIDIARIES: GENEVA; MUNICH; GLENROTHES, SCOTLAND; TOKYO; PARIS; CAPETOWN; LONDON; MEXICO CITY; STOCKHOLM; VIENNA

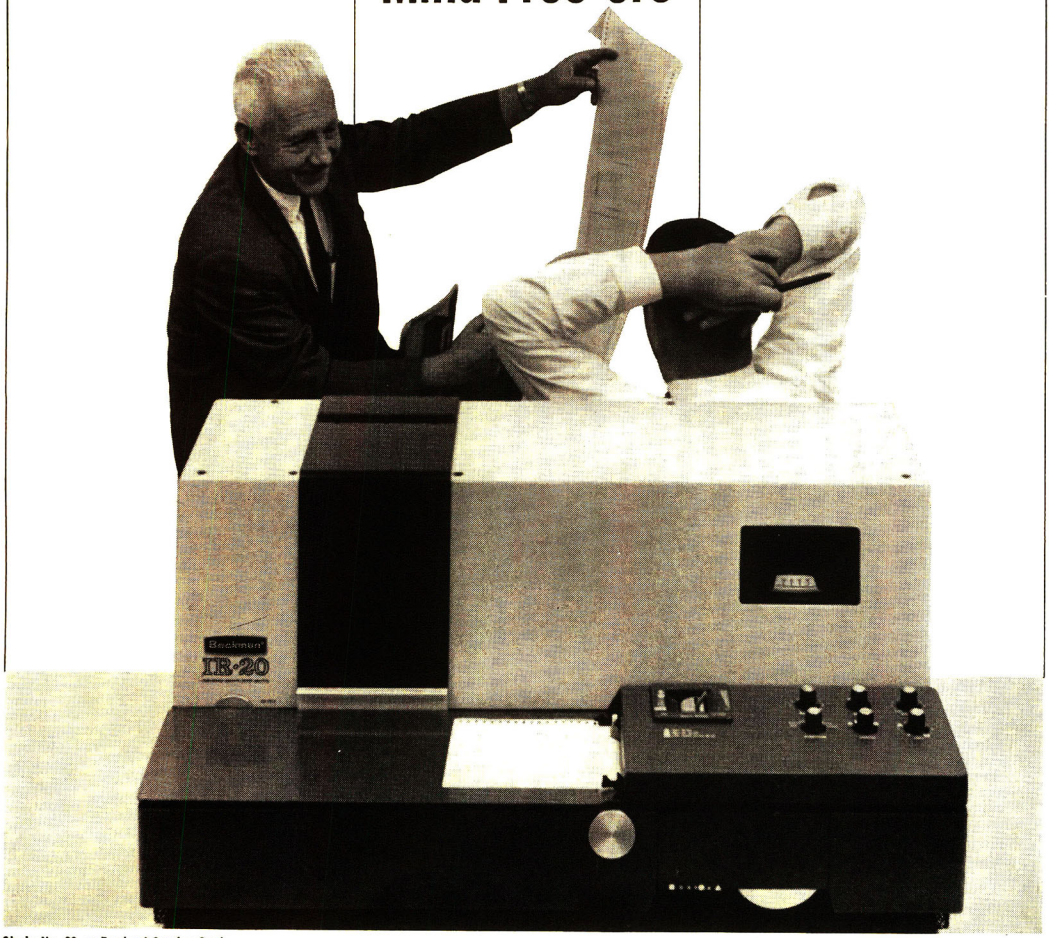


Circle No. 90 on Readers' Service Card

# Wouldn't it be great if someone designed a 160 g top-loader with 1 mg accuracy and all-digital readout?

## Someone has. Sartorius.

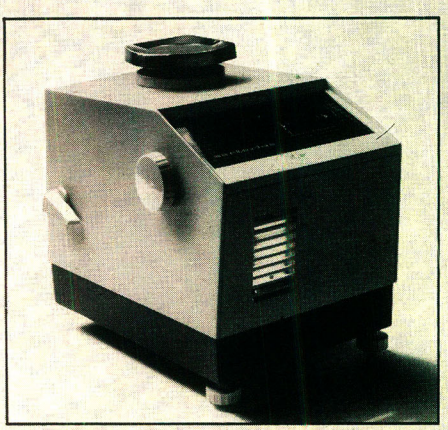

There are other top-loading balances with 160 g capacity, but none is as accurate and easy to read as the new Sartorius 2255... and none is as stable.

To eliminate interpolation error with 'between the line' results, the Model 2255 provides all-digital readout to 1 mg. To further insure accuracy, there is absolutely no discernible swing—this balance stays at the indicated weight. There's no need to squint, either. Its huge new optical scale is a pleasure to read, even under the most adverse lighting conditions.

At only $725, the above features alone would make the 2255 a great buy, but there are more. The Taramatic® single knob taring system and below-balance weighing accessories are included at no extra cost.

For research, quality control, student use, or any other application requiring 1 mg weighing accuracy at loads up to 160 g, this is the simplest, yet most advanced top-loading balance available.

Sartorius all-digital top-loaders also come with higher capacities. Our 40-page catalog describes them all. For your copy, just write: Sartorius Division, Brinkmann Instruments, Cantiague Road, Westbury, N.Y. 11590.

**sartorius balances**



# BOOK REVIEWS

**Theories Moleculaires de la Resonance Magnetique Nucleaire: Applications a la Chimie Structurale.** G. Mavel. x + 325 pages. Gordon & Breach Scientific Publishers, Inc., 150 Fifth Ave., New York, N. Y. 10011. 1966. $19.50

Reviewed by J. P. Laurent, Ecole Nationale Superieure de Chimie, 38, Rue de trente-six-points, Toulouse, France

As mentioned in the preface, this book has been written to be a bridge between people who are interested in the theoretical aspects of NMR spectrometry and those who are especially concerned with experimental problems. As a second purpose, the author—considering NMR as a part of molecular spectroscopy—attempts to survey the background of all important applications of NMR to the determination of molecular structure rather than to provide a full coverage of the whole subject.

Chapters 1 and 2 are brief outlines of basic phenomena and concepts. After a short description from the physical point of view—that is to say "the nuclear aspects of magnetic resonance" —the author, dealing in the molecular aspects of NMR, presents the $\delta$ and $J$ effects to which two important chapters (3 and 4) are then devoted. From semi-empirical interpretations, such as correlations between spectral and structural parameters, to more elaborate theoretical treatments, nearly all the features of the screening and coupling effects are reviewed. The main spectral systems are analyzed and described in the 5th section. The last three chapters (6, 7, 8) are concerned with topics of more particular interest: multiple-quantum transitions, multiple resonance spectra, effects of chemical exchange upon spectral appearance.

This book presents a wide spread of experimental data and includes summaries of nearly all of the most important theoretical methods in the field of analyzing spectra and relating spectral parameters to the electronic structure of molecules, but the subject seems too vast to be encompassed within 300 pages. To some extent this limitation of space is prejudicial to the clarity of the book. However, compensation is afforded by the extensive tabulation of published data (about 2,000 references), the literature being surveyed up to 1965.

Finally, this book provides a valuable tool for those who want a comprehensive review and a ready source of references in the field of applications of NMR spectrometry to structural problems.

**Practical Polarography: An Introduction for Chemistry Students.** J. Heyrovský and P. Zuman. vii + 237 pages. Academic Press, Inc. 111 Fifth Ave., New York, N. Y. 10003. 50s ($6)

Reviewed by James J. Lingane, Department of Chemistry, Harvard University, Cambridge, Mass. 02138

This little book (237 pages) is intended to be solely a laboratory manual. Although edited by Dr. Zuman a year after Heyrovský's death, it still adheres faithfully to the pattern set by the previous Czech, Polish, and German editions over the past 20 years. A cardinal characteristic of Professor Heyrovský's teaching philosophy was that theory should be completely excluded from a laboratory manual, and, although the junior author indicates in the Preface that he is not fully in accord, nonetheless this present edition achieves this dubious aim fully as well as its predecessors did.

An introductory 28-page chapter contains a qualitative description of polarographic principles, the dropping electrode, polarographic cells, and some basic techniques. This is a very good account of polarographic technique as it was in the beginning.

The second chapter briefly reviews the various types of limiting currents and polarographic waves. It is surprising to note (page 31) the use of the ferric–ferrous couple, written in terms of the simple ions, as an example of a system which produces a reversible cathodic–anodic wave, when in fact the polarogram of this couple is not accessible to the dropping electrode because of the direct reduction of ferric ion by mercury.

The treatment of instrumentation in the third chapter does not represent the true state of the art today. It over-emphasizes photographically recording polarographs, and only hints, cursorily and incompletely, at more modern instrumentation.

The remaining three chapters, which constitute the major part of the text, provide many examples of the polarographic characteristics and determination of a variety of substances. Detailed procedural directions are supplied. The examples are well chosen from both the organic and inorganic fields to illustrate many facets of classical polarography, including kinetic and catalytic waves. Examples of the applications of polarography in such diverse fields as metallurgy, biochemistry, pharmacy, medicine, and the food industry are presented. There is also a section on amperometric titrations.

The text is illustrated copiously with more than 70 actual polarograms for each of the cases cited, which breathes life and reality into the treatment. It would be hard to think of any aspect of *classical* polarography which is not included. The book concludes with extensive tables (33 pages) of half-wave potentials of organic and inorganic substances and a bibliography.

In my opinion this laboratory manual has some obvious shortcomings, but what book does not? Those of us who have spent the better part of our scientific lives trying to eradicate the myth that analytical chemistry is no more than a technical art cannot help being annoyed by a textbook which not only deliberately excludes theory, but even avoids treating basic principles in an adequately quantitative manner. It is less than up-to-date with respect to modern instrumentation, and ignores such techniques as a.c. polarography, pulse and square-wave polarography, etc. On the other hand, Chapters IV, V, and VI constitute such a good phenomenological review of so many aspects of classical polarography that the book can be of real value to newcomers in the field.

**Reagent Chemicals. American Chemical Society Specifications.** 4th ed. xviii + 651 pages. American Chemical Society Publications, 1155 16th St., N. W., Washington, D. C. 20036. 1968. $14

Reviewed by David H. Freeman, Analytical Chemistry Division, National Bureau of Standards, Washington, D. C. 20234

This is a compilation of specifications, procedures, and standards that is intended to serve for the characterization of reagents as needed for precise

← Circle No. 160 on Readers' Service Card

With a Mettler Preventive Maintenance Agreement, one of our 40 full-time service specialists will help you prevent inaccurate weighings. You may not know it, but your balance could be yielding incorrect results because of misuse or poor operating conditions. To guard against these weighing inaccuracies and to prevent future problems, a Mettler service specialist will check and adjust your balance in your lab once a year under a Mettler Preventive Maintenance Agreement.

This factory-trained specialist will diagnostic-test, clean, lubricate, adjust and final-test your Mettler balance to maintain its accuracy, reliability and precision of performance.

The time and money you could save by eliminating incorrect weighings could more than pay for the Mettler Preventive Maintenance Agreement. As a bonus, you'll receive many extra years of useful service from your Mettler.

For further information, write to Mettler Instrument Corporation, Box 71, Hightstown, N.J. 08520.

IT'S ALMOST AS IF HE CAME WITH THE **BALANCE**

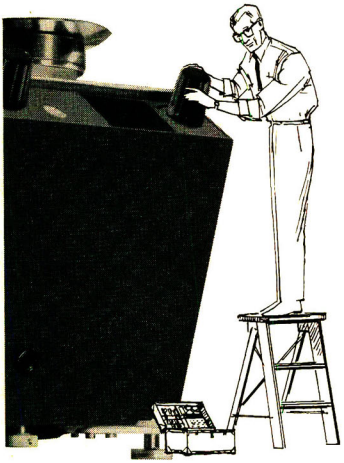

Mettler®

See ACS Laboratory Guide for All Products/Sales Office

Circle No. 134 on Readers' Service Card



analytical work. Approximately 300 chemicals are covered of which 200 are inorganic and 100 are organic. Traditional test procedures are clearly presented and in most cases they can be carried out by a chemical technician with a minimum experience of approximately two years of college-level chemistry.

The purpose of this book is well known. It is intended to provide a base that defines minimum adequate criteria for the composition of a chemical reagent to determine if it "meets ACS specifications." The book is copyrighted, but it is not a proprietary document and any chemist may apply its test procedures and, if he so chooses, state in print that his reagent meets the given requirements. This compilation inescapably exerts a two-fold influence for setting a minimum reagent standard, and for defining a competent approach to reagent characterization.

The test procedures are classical and seldom require instrumental methods. A few procedures call for the use of absorption spectrophotometry or of flame photometry. There is an isolated infrared technique that tests for organic contamination. There are a few apparent errors. For example, the procedure for the mild desiccant, anhydrous calcium chloride, does not include a test for its possible contamination by water. In the test procedure for ethyl ether to which water and ethanol are added in small quantities to inhibit the formation of explosive peroxides, no test for stabilizing additives is given. The use of analytical gas–liquid chromatography is restricted to a test for hydrochloric acid for extractable organic substances. It is unfortunate that this important method is not applied to the evaluation of any of the organic solvents.

The most discouraging feature is that the compilation is thoroughly unmodern. The work is intended to support analytical chemists, but it ignores the power of today's analytical measurements capabilities. The editors note that the procedures may not be adequate for all purposes, but they fail to see a substantial decline in terms of the significance of the procedures to the needs of chemistry. It may be argued that instrumental methods require too elaborate apparatus and highly experienced workers. However, it is a mistake to decide that these should be largely ignored.

Those who are concerned with reagent analysis should give heed to the errors of omission in this revised edition of ACS reagent specifications. The procedures dealing with organic analysis are quite weak. Well established methods, including NMR, infrared, visible, ultraviolet, and mass spectrometry, and gas–liquid and thin-layer chromatography, are too useful and too important to deny their application to organic reagents. Preconcentration techniques are involved only sporadically in testing for trace contaminants. The presence of particulate matter is of growing and widespread importance, quantitative tests are easily made, and they should have been included. Other methods such as emission spectrometry, polarography, and activation analysis have all achieved durable recognition in trace chemical analysis, but they have been omitted. Finally, the use of suitable container materials and recommended storage conditions is critically related to reagent quality and these subjects should have been treated.

In this day of significant analytical problems in areas as diverse as semiconducting materials, air pollutants, meteorites and lunar samples, and clinical specimens, an enlightened concept of reagent evaluation is essential. The philosophy behind this document needs extensive re-evaluation and study.

**Annual Review of NMR Spectroscopy, Vol. 1.** E. F. Mooney, Editor. x + 353 pages. Academic Press, Inc., 111 Fifth Ave., New York, N. Y. 10003. 1968. $14

Reviewed by James L. Sudmeier, Department of Chemistry, University of California, Los Angeles, Calif. 90024

"Annual Reviews of NMR Spectroscopy" now takes its place among "Advances in . . .", "Progress in . . .", and chapters in "Annual Review of Physical Chemistry" and in the biennial "Annual Reviews" appearing in *Analytical Chemistry*. The plan is to offer one chapter each year which is a general review of proton NMR, reviews on fluorine NMR, and conformational analysis every two or three years, and the remaining chapters on special topics. Volume 1 contains chapters on proton and fluorine NMR, and chapters on conformational analysis, spectral interpretation, heteronuclear double resonance, NMR of polymers, and signal-to-noise enhancement.

Did we really need another NMR review? My own feeling is that with the explosive growth of NMR literature, we can only applaud the efforts of reviewers to keep us abreast. Volume 1 of "Annual Reviews" is slanted toward physical organic chemistry, though it will be of interest to most workers in the NMR field. It is well illustrated, well written, and practical rather than

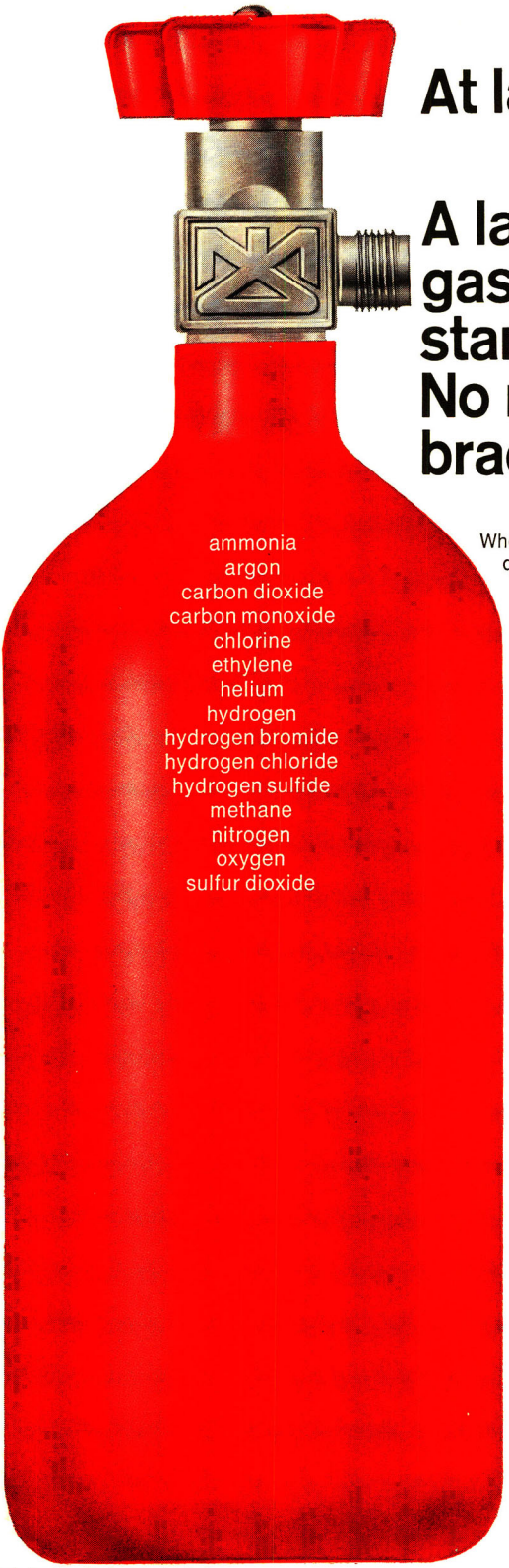


# At last.

# A laboratory reagent gas cylinder that stands alone. No racks, ring stands, brackets, or clamps.

When you buy Merck Laboratory Reagent Gases you get a quality product with three extras: Extra safety. Extra convenience. Extra bench space.

**Extra safety** because the cylinder is self-supporting, compact in size, and color-coded.

**Extra convenience** because it handles like a standard reagent bottle but delivers twice the volume of a lecture bottle. Reduces order and handling frequency 50%.

**Extra bench space** because it's shorter than a lecture bottle, narrower than a sphere, and has no ring stand to take up room.

With all these extras in the cylinder, you could say we've introduced a new standard cylinder to the industry.

Besides ample stocks, your local Merck distributor also has something extra for you. A colorful, ready reference file containing 15 technical data sheets with actual-size reproductions of the cylinders. It's all free. Call him. He's expecting you.

MERCK

**We think you should expect something extra**

Circle No. 14 on Readers' Service Card

See ACS Laboratory Guide for All Products/Sales Office

CARVER LABORATORY PRESS

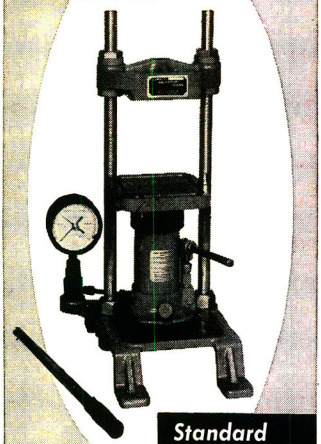

Standard For Research

*. . . solves the pressing problem of forming KBr Pellets*

Many insoluble materials, mixed with Potassium Bromide, can be formed in a die **under pressure** into pellets or wafers for quantitative and qualitative analysis.

**The CLP supplies the pressure** – up to 40,000 lbs., if needed.

This specific use is only one of the ways this versatile laboratory assistant meets the challenge of research and development.

***Some of the many uses are:***

- Dehydrating
- Pressing out various oils, stearines and waxes
- Pressure filtering of thick fluids
- Compression tests
- Fatty acid determinations
- Plastic molding, forming and blocking
- Embossing and forcing
- Pressing mother liquors from crystals
- Extracting Vaccines and Viruses

**(The NEW Carver Laboratory Press (Model C-12 ton) complete with Gauge..... $430.00**

20 Ton Models also available – additional Standard Accessories for other applications can be supplied.

***Send for latest bulletin.***

FRED S. CARVER INC.
HYDRAULIC EQUIPMENT
54 RIVER ROAD, SUMMIT, N. J.

Circle No. 28 on Readers' Service Card
See ACS Laboratory Guide for All Products/Sales Office



theoretical in its approach. The chapter on NMR of polymers is quite comprehensive and should be of great value to polymer chemists. The use of nuclear Overhauser effects in structural determination was omitted, unfortunately, and the chapter on signal-to-noise enhancement does not add greatly to what has been said in other recent chapters on this subject.

The series shows promise of being the most comprehensive and most useful *annual* review of proton NMR, and as such will be an invaluable addition to the collections of many NMR users.

**Methods in Microanalysis, Vol 3: The Determination of Carbon and Hydrogen and the Use of New Combustion Catalysis.** J. A. Kuck, Editor. xxi + 580 pages. Gordon & Breach Scientific Publishers, Inc., 150 Fifth Ave., New York, N. Y. 10011. 1968. $36

Reviewed by E. W. D. Huffman, Huffman Laboratories, Inc., 3830 High Court, P. O. Box 350, Wheatridge, Colo. 80033

This is the third volume of the series "Methods in Microanalysis." It contains excellent translations of original papers from the less familiar languages —such as Russian, Czech, and Chinese —from journals not readily available. The papers of Miroslav Večeřa and Jirí Horáček and their associates are featured. In addition, there are a few translations of papers from German and readily available journals which complement the others. There are 53 papers in all.

The experimental work and the reporting of it are impressive. Dr. Kuck's selection has been made in favor of the practicing microanalyst. The papers for the most part have to do with practical problems. There are some improved old methods and some new suggestions.

The papers cover a wide range of facets and include: a statistical evaluation of some of the methods of elemental analysis (C, H, N, S, Cl) which questions the usually cited ±3% (absolute), claiming the true range is much wider; the use of copper, antimony, and bismuth for the removal of halogen from the combustion gas stream and simultaneous determination of halogen; a study of the pyrolysis products of organic compounds under analytical conditions; the measurement of carbon dioxide by changes in the electrical conductivity of barium and sodium hydroxide solutions; the coulometric measurement of hydrogen by the electrolysis of water; the simultaneous determination of carbon and halogen and carbon and phosphorus by wet combustion methods; an iodometric determination of hydrogen which has an accuracy of ±0.05%; a number of papers on the evaluation of the *new* combustion catalysts—cobalt sesquioxide, thermally decomposed silver permanganate, and a mixture of silver tungstate, magnesium oxide, and zirconium oxide. The more rapid combustion possible in the presence of these catalysts is taken advantage of in some automatic combustion equipment described. Two papers are devoted to the determination of hydrogen on an ultramicro scale based on the diffusion of hydrogen through silica at elevated temperatures. And, in spite of the title of the book, there are papers on the determination of active hydrogen and on hydrogenation.

This book is recommended for all who are interested in organic elemental analysis.

## New Books

**Analytical Methods for Atomic Absorption Spectrophotometry.** The Perkin-Elmer Corporation, Norwalk, Conn. 06852. 1968. Looseleaf Noteboook. $25

At the beginning of this book is found a general information section related to the operation of atomic absorption spectrophotometers. Various analytical methods that can be applied to atomic absorption analyses, burner operating notes, and descriptions of possible interferences are given. Following the general information section is an atomic absorption bibliography, and the final portion of the book gives specific information for the determination of individual elements as well as the determination of those elements in a variety of matrices. The authors are the staff of the Perkin-Elmer Atomic Absorption Department. This revision replaces the original version (January 1964) and all subsequent supplements through November 1966. The book can be purchased as Perkin-Elmer Part No. 303-0152.

**Bibliography for Atomic Absorption Spectroscopy.** Fisher Scientific Co., J308 Fisher Building, Pittsburgh, Pa. 15219. Looseleaf Notebook. $25

The Jarrell-Ash Division of Fisher Scientific Co. has published a 461-page bibliography to aid analysts engaged in atomic absorption and, more re-

cently, atomic fluorescence spectroscopy. The volume organizes its several thousand entries by element (76, from aluminum to zirconium), and these, in turn, are cross-referenced as to argricultural, biological, geochemical, metallurgical, petrochemical, instrumental, etc. The bibliography will be kept up to date as additional material becomes available.

**Solid-Liquid Separation: A Review and a Bibliography.** J. B. Poole and D. Doyle, Editors. xiii + 1003 pages. The Chemical Publishing Co., Inc., 212 Fifth Ave., New York, N. Y. 10010. 1968. $19.50

This book is the first attempt to survey the voluminous literature of solid–liquid separation. Over 5000 references have been abstracted and classified by subject matter and date. The bibliographic section is preceded by 25 review articles dealing with the theoretical aspects of solid–liquid separation methods and with the application of the methods in a wide variety of industries. The authors of these articles have tried to show where research is currently needed.

**Chem Sources.** 10th ed. 525 pages. Directories Publishing Co., P. O. Box 422, Flemington, N. J. 08822. 1969. $35

This 10th edition provides information for chemical buyers who require source information for both general and rare organic and inorganic compounds. Chemicals are listed alphabetically by chemical name only. Asterisks identify basic producers.

**Encyclopedia of Industrial Chemical Analysis, Vol. 7: Benzene to Brewery Products.** Foster Dee Snell, Editor-in-Chief. xi + 712 pages. John Wiley & Sons, Inc., 605 Third Ave., New York, N. Y. 10016. 1968. $35 subscription, $45 single copy

This encyclopedia provides proven classical and instrumental methods, techniques, and procedures for the analysis and evaluation of raw materials, intermediates, and finished products—a critical selection for the Development, Plant, and Purchase Department for all users of chemicals and chemical products. Topics covered are: benzene, benzoic acid, benzyl and phenylethyl alcohols, beryllium, bile acids and salts, bioassay, bismuth, bleaching agents, bonded abrasives, boron, brake fluids, brake linings, and brewery products. The main body of

Circle No. 96 on Readers' Service Card →
See ACS Laboratory Guide for All Products/Sales Office →

BAUSCH & LOMB
ANALYTICAL SYSTEMS DIVISION

atomic absorption

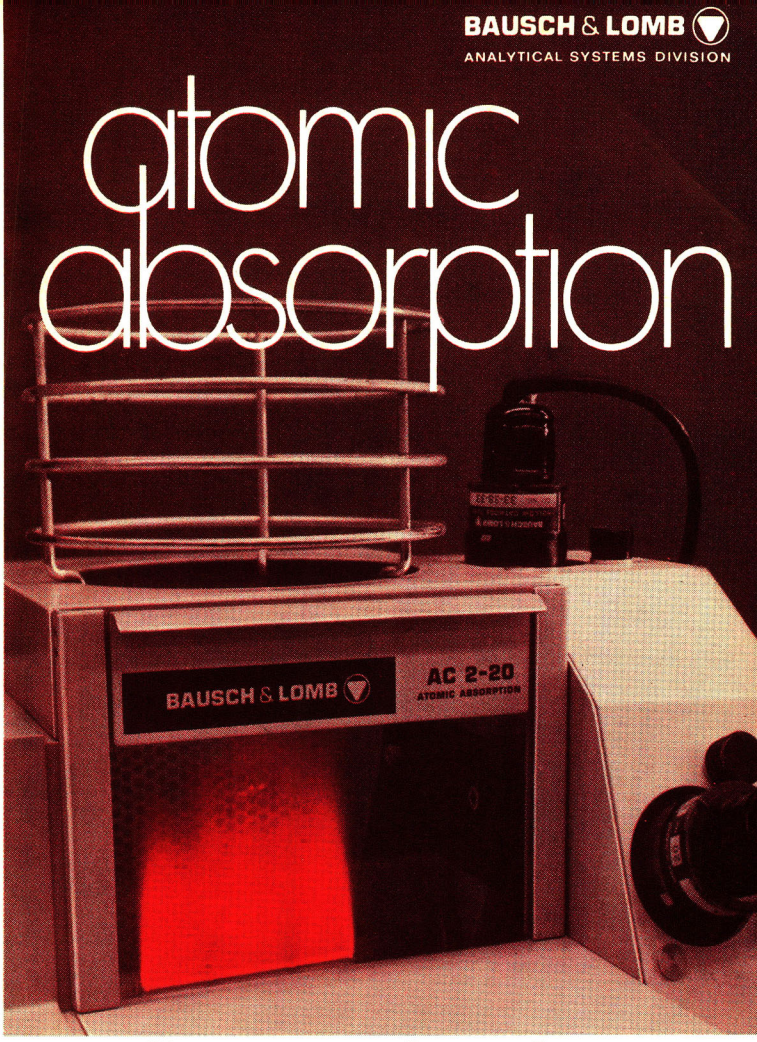


flame under glass

Flame is enclosed behind a special, tempered glass to eliminate effects of outside air currents and contaminants . . . just one feature in a long list that make the AC2-20 today's most advanced atomic absorption system. It combines safety, versatility, operational convenience and reliability with superior sensitivity and exceptional performance.

**Reliability you can count on**

- Finest, high dispersion monochromator (two 1200 lines/mm "Certified-Precision" gratings) assures superior linear dispersion, eliminates adjacent interference lines.
- Wavelength Range—190-800nm

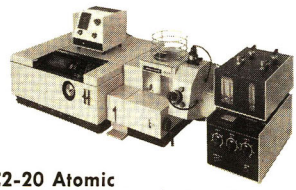

AC2-20 Atomic Absorption Spectrophotometer

- Single pass system utilizes region of highest free atom density; higher signal-to-noise ratio, too.

**Unmatched Operator Convenience**

- Three-lamp system with indicator pilot lights, lamp identification, remote switching, *easy centering, focusing* and *interchange*. Lamps on standby—no wait for warm-up.
- Flowmeters for both fuel and support gas indicate over entire range, simplify repeatability.
- No flashback in routine operation . . . remote piezoelectric burner ignition.

**Outstanding Versatility and Flexibility**

- 3-in-1 capability: flame-emission, UV—visible and atomic absorption.

We'll be happy to send you Catalog 33-2225 which has the full story. Analytical Systems Division, Bausch & Lomb, 60916 Bausch Street, Rochester, New York 14602.

Visit our Booths L20-23 at the FASEB Convention

**The best digital integrator now interfaces with any analytical lab instrument.**

## LOG LINEAR ADAPTER

This adapter converts the output signal from amino acid analyzers, automatic colorimetric analyzers and spectrometers to a concentration-linear signal which is then automatically integrated.

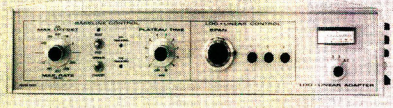

## ATOMIC ABSORPTION ADAPTER

The output from either manual or automatic sampling atomic absorption spectrometers are converted by this adapter to a numerical value which is a function of concentration.

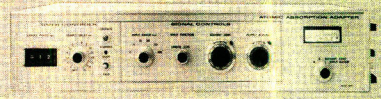



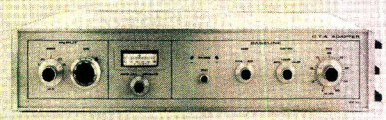

## DTA ADAPTER

Exothermic and endothermic transitions that produce positive and negative going signals are converted by this Differential Thermal Analysis Adapter to all positive going signals for quantitation and printout.

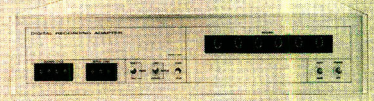

## DIGITAL RECORDING ADAPTER

This adapter converts the 1504 integrator to a printing analog to digital converter. The combination automatically samples any electrical signal on a pre-selected time base and prints out integrated values which represent data points as a function of time.

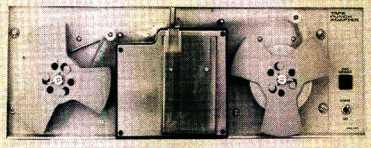

## TAPE PUNCH ADAPTER

The adapter codes each integral and retention time generated by the 1504 and punches this coded number onto paper tape suitable for computer entry. An optional alpha-numeric keyboard permits sample identification and instructions to be entered on the tape.

Model 1504 Digital Integrator is a third generation instrument that interfaces with all lab voltage analogs, and provides not only digital equivalents of peak areas from both linear and non-linear outputs, but also data points on the curve or time dependent integrals. Plug-in adapters allow precise integration of colorimeter signals, computer logic, metal ion concentration or quantitation of both endothermic and exothermic thermal transitions. When you add a baseline compensator and time printout device, it's easy to understand why Nester/Faust's 1504 solves almost every analytical situation. Nester/Faust Mfg. Corp., 2401 Ogletown Rd., Newark, Del. 19711, (302) 737-6330. In Europe: Spalentorweg 20, 4055 Basel, Switz. Ph. (061) 24 46 14.

*See for yourself,*

*ask for literature or a free demonstration*

NESTER/FAUST

Circle No. 184 on Readers' Service Card

See ACS Laboratory Guide for All Products/Sales Office

the work presents in alphabetical arrangement chemical and physical characteristics . . . types of analysis available for the material itself and in mixtures . . . commercial and analytical standards . . . and a substantial bibliography.

**Perspectives in Structural Chemistry. Vol. 2.** J. D. Dunitz and J. A. Ibers, Editors. ix + 178 pages. John Wiley & Sons, Inc., 605 Third Ave., New York, N. Y. 10016. 1968. $10.95

This second volume in a series of review books on structural chemistry—that branch of the science that deals with the metrical aspects of molecular structure—is intended to answer the needs of active structural chemists, both theoretical chemists and nonspecialists. The contributors to the series have been asked to provide constructive, critical, chemically-oriented reviews of a given area in structural chemistry. Contributions to this volume are Conformations of Medium Rings by J. D. Dunitz (70 pages) and Stereochemistry of Metal Cluster Compounds by Bruce R. Penfold (80 pages). A complete author and subject index is provided at the end of the book.

**Automation in Industrial Pharmaceutical Process and Quality Control.** Truman L. Hall, Editor. 282 pages. The New York Academy of Sciences. 2 East 63rd St., New York, N. Y. 10021. 1968. Paperbound. $10

This series of papers is the result of a conference held in March 1967. It is intended to update the technological advances that have occurred in automated testing in the pharmaceutical industry and to point out present practices that can be applied to pharmaceutical and biological quality control and in-process control, as well as applications in analyses conducted as part of research. Data reduction and processing systems are dealt with, and innovations and new breakthroughs in the laboratory and in production are considered.

**Starch and Its Derivatives, 4th edition.** J. A. Radley. viii + 558 pages. Barnes & Noble, Inc., 105 Fifth Ave., New York, N. Y. 10003. 1968. $22.50

This 4th edition of Starch and Its Derivatives, coming 15 years after the last (3rd edition), constitutes an up-to-date review of the present state of knowledge of starch chemistry and technology. A number of prominent


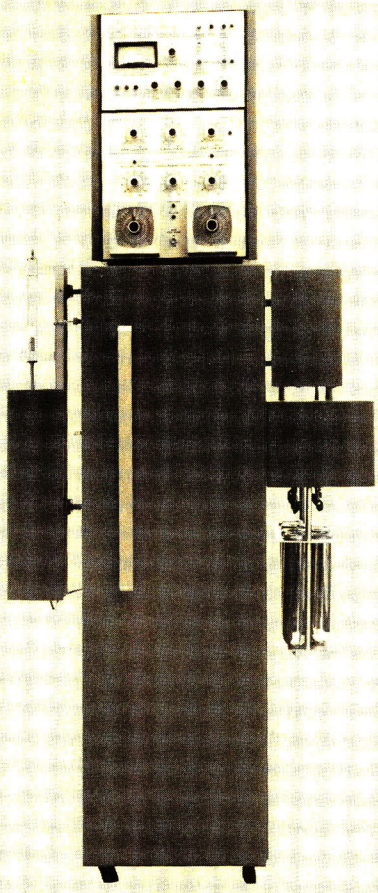

PREPKROMATIC 750
NEWEST
PREPARATIVE CHROMATOGRAPH

Model 750 is the latest Nester/Faust development in low cost preparative scale separating with high resolution and unattended operation! The column oven holds 75 feet of ¾" Bi-Wall columns and is air-cooled; SCR controls temperature up to 500°C. An automatic injector provides reproducible, trouble-free operation from 200 microliters to 2 ml in 200 microliter increments with accuracy to ±0.5%. Efficient and trouble-free exit for collection of all types of samples—including those which aerosol—is provided by our unique system; six glass traps are accommodated. Temperature programming is easy to use and fully reproducible through SCR control and two precision adjustable timing devices —and the entire system is protected by fail-safe circuitry. Get all the facts, write today for complete literature. NESTER/FAUST Mfg. Corp., 2401 Ogletown Rd., Newark, Del. 19711, (302) 737-6330. In Europe: Spalentorweg 20, 4055 Basel, Switz.

NESTER/FAUST

Circle No. 185 on Readers' Service Card

See ACS Laboratory Guide for All Products/Sales Office

BEL-ART

for PLASTIC

safety products




POLYETHYLENE
EYE WASH BOTTLE

DIRECTIONS IN 4 LANGUAGES

Eye injuries treated on the spot... fast and effective. Just apply pressure on flexible bottle. Can be used in standing or supine position.

A captive snap-on cap keeps cup clean and ready for use. Side air-vent, below the cup, acts as a valve for air re-fill of free space in bottle. This prevents draw-back of contaminated wash into bottle. In two sizes... 16 oz. and 32 oz.

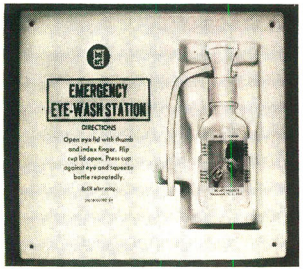


EYE WASH SAFETY STATION

• COLORFUL • ATTRACTIVE
• DISTINCTIVE

Molded of high-impact plastic, station is readily identifiable and convenient to use. Socket holds eye wash bottle securely and keeps discharge tube in place. Bottle is easily released for quick emergency use.

At your local supply house.

*Send for NEW 80 page catalog 469*
*For your FREE copy write Dept. A-4*

BEL-ART PRODUCTS
PEQUANNOCK, N. J. 07440

Circle No. 24 on Readers' Service Card
See ACS Laboratory Guide for All Products/Sales Office



workers have contributed chapters on their specialized field of work. The literature references have been vigorously pruned to those which are pertinent to the actual presentation of the facts and arguments presented, while those of historical or ephemeral value have been relegated to the "Additional Bibliography," which also contains some references to useful papers which appeared while this volume was at press. The book is divided into two sections, The Structure and Reactions of Starch (12 chapters) and Amylases and Their Action on Starch (5 chapters) plus an author and subject index.

**Die Analyse der Luft und ihrer Verunreinigungen in der freien Atmosphare und am Arbeitsplatz.** Wolfgang Leithe. xiii + 228 pages. Wissenschaftliche. Verlagsgesellschaft mbH, 7000 Stuttgart 1, Postfach 40, Germany. 1968. DM 58

## U. S. Government Publications

The following publications can be ordered from the Superintendent of Documents, U. S. Government Printing Office, Washington, D. C. 20402; the Clearinghouse for Federal Scientific and Technical Information, Springfield, Va. 22151; or from local U. S. Department of Commerce Field Offices. **(Note:** Foreign remittances must be in U. S. exchange and should include an additional one fourth of the publication price to cover mailing costs)

**Microwave Spectral Tables, Vol. 4: Polyatomic Molecules without Internal Rotation.** Marian S. Cord, Jean D. Petersen, Matthew S. Lojko, and Rudolph H. Haas. xii + 418 pages. 1968. $5.50

This 4th in a 5-volume NBS Monograph contains data on the microwave spectra of 166 polyatomic molecules incapable of exhibiting internal rotation. Measured frequencies, assigned molecular species, and assigned quantum numbers are given for about 14,000 spectral lines observed by coherent radiation techniques. Molecular data such as rotational constants, dipole moments, and various coupling constants, determined by such techniques, are also tabulated. References are given for all included data, and the contents are indexed according to empirical formula and according to chemical name.

**Theoretical Mean Activity Coefficients of Strong Electrolytes in Aqueous Solutions from 0 to 100°C.** Walter J. Hamer. NBS Publication NSRDS-NBS 24. v + 271 pages. $4.25

Values of the mean activity coefficient, a basic physical-chemical parameter that measures the departure of a real solution from ideality, are here tabulated for strong electrolytes in water, as calculated from 7 theoretical equations widely referred to in the literature. They are those of (1) Debye–Hückel, frequently referred to as the limiting law of Debye and Hückel, (2) Güntelberg, (3) Davies, (4) Scatchard, (5) Bjerrum, (6) what may be called a modified or extended Güntelberg expression, and (7) a modified or extended Scatchard expression.

**Separation and Purification Section: Summary of Activities July 1967 to June 1968.** David H. Freeman, Editor. NBS Technical Note 459. xi + 45 pages. Paperbound. 60 cents

**Spectrochemical Analysis Section: Summary of Activities July 1967 to June 1968.** Bourdon F. Scribner, Editor. NBS Technical Note 452. xii + 80 pages. Paperbound. $1

## Clearinghouse Offers New Document Service

A new subscription service for obtaining microfiche (sheet microfilm) copies of scientific and technical documents grouped by field of interest will soon be available from the Commerce Department's Clearinghouse for Federal Scientific and Technical Information. Beginning March 1, 1969, Clearinghouse customers will be able to order, from any of several hundred basic categories, unclassified reports and translations of foreign technical literature sponsored by over 100 Federal agencies and other organizations. Orders can be placed by subject category, by originating agency (DoD, NASA, AEC, etc.) or by subject category within an agency collection. The new service, Selective Dissemination of Microfiche (SDM), will be a faster and more economical method of obtaining copies of the latest scientific and technical documents in selected fields of interest. Detailed information on the categories, cost, and method of ordering SDM are available upon request from the Clearinghouse (152.15), U.S. Department of Commerce, Springfield, Va. 22151.

Have you ever wished that you could buy *one* densitometer so versatile it could serve you from the most humdrum test to the most exciting frontiers of biochemical research? This is it.

The Joyce, Loebl Chromoscan is a double-beam, recording/integrating densitometer that can take on virtually *any* densitometry job of interest to the biochemist... as *purchased.* And it is not a warmed-over conversion of instruments designed for other work, nor a limited-use unit beefed up with accessory afterthoughts. It was designed as an instrument for biochemistry... from the start.

Look what you get in our Chromoscan, either built-in or with economically matched accessories:

Capabilities for studies involving reflection and transmission densitometry / fluorescence / colorimetry / U.V. absorption / gel and disk electrophoresis / paper, starch, agar, cellulose-acetate media / thin-layer chromatography / enzymes / kinetic reactions / ultra-centrifuge patterns / iodine assays / continuous flow.

Record magnification? Digital readout? High and low speed recording? Specimen viewing? Variable slits? Specimen holders for all media? Filters? They're yours with the Joyce, Loebl Chromoscan.

Flexibility puts this instrument out front in research. (For instance, it figures prominently in recent RNA work.)

Accuracy makes it equally useful for repetitive clinical tests. A dual-beam, null-balance system utilizing optical reference wedges delivers base-line stability you simply won't find in electronic systems. Yet it costs less than you may think.

**Better than ever through Tech/Ops national sales and service organization.**

Find out what our Chromoscan can do for you. Write to Joyce, Loebl & Co., Inc., an affiliate of Technical Operations, Incorporated, Department D-4, 111 Terrace Hall Avenue, Burlington, Mass. 01803.

tech/ops®

Circle No. 179 on Readers' Service Card

# Discover The Joyce, Loebl Chromoscan

...the biochemist's densitometer that can run clinical tests or analyze R.N.A.



# our point of view!

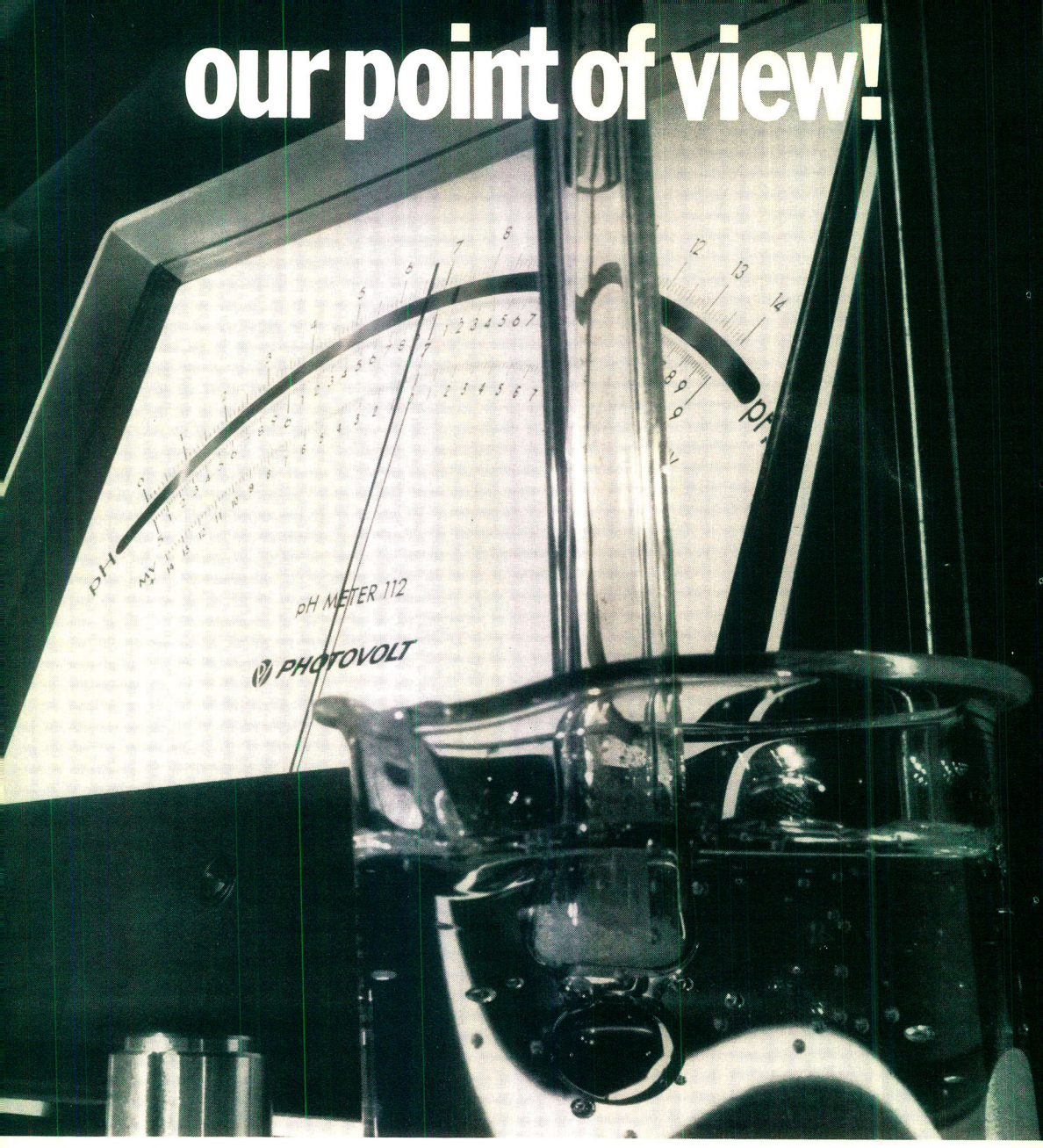


## No need to be without an expanded scale pH meter–it's only $40 more.

Photovolt's *Expander IV*, pH meter 112, is $395.00–only $40 more than most laboratory models.

Any range of four pH units can be expanded over the entire scale. This solid state unit is readable and reproducible to within 0.005 pH and accurate to within 0.01 pH. An expanded millivolt range, ± 140 mv, readable to 0.5 mv extends *Expander IV's* ability to all ion selective electrodes.



*Expander IV* is supplied with a single, fast, high-sensitivity electrode, but it also accepts all others, including ion selective and redox electrodes.

An output is available for Karl Fischer titrations, as well as a 10 mv recorder output.

Our point of view is that there is no longer any reason to be without an expanded scale pH meter. What's your point of view?

**PHOTOVOLT CORPORATION** *1115 Broadway, New York, N.Y. 10010 · (212) 989-2900*

Circle No. 138 on Readers' Service Card

See ACS Laboratory Guide for All Products/Sales Office

## EDITORS' COLUMN

ANALYTICAL SCIENTISTS have a genuine need for marshalling available resources into useful packages. A few years ago it became apparent that several existing files of infrared spectroscopy data were in existence that were not being fully utilized; these collections were in general the property of government agencies or industrial organizations. The gathering of these data into a single, available body of material became one of the first concerns of the National Standard Reference Data System when the group was organized in the National Bureau of Standards in 1963. With the aid of NBS and some interested professional groups, such as the Coblentz Society and ASTM, a special task force was created to deal with the problem of collecting, evaluating, and publishing spectra available from diverse sources.

Thus far, this task force, called the Joint Committee on Atomic and Molecular Physical Data, has been mostly involved with infrared data, but active programs are planned or have been initiated for Raman spectra, NMR spectra, and others. Representation on the Joint Committee now includes members from the Coblentz Society, ASTM, American Petroleum Institute, Manufacturing Chemists Association, the Society for Applied Spectroscopy, the American Chemical Society, and the Spectroscopy Society of Canada.

Primary concern has been given to *evaluation* of available spectra, especially in terms of classes defined in ANAL. CHEM., **38**, 27A (August 1966).

The first set of 1000 evaluated infrared spectra, collected by the Joint Committee, contains about 500 pharmaceuticals, 100 organosilicon compounds, and miscellaneous other organic compounds. Most of these spectra are Class III (compounds have verified structures); the set of 1000 is available at a


# The Unspoiler.




Too bad. Set up a gas chromatography system, develop a proper technique and then spoil it with a leaky system. For as little as $310.00 the GOW-MAC Gas Leak Detector will find the leaks in your system and make your chromatography more accurate. Cordless, portable and equipped with a self-contained rechargeable battery and charger, or line operated, the GOW-MAC pin points leaks of inert, combustible, light or heavy gases in hot or cold pressurized systems and in hard to reach test points through use of a stabilized thermal conductivity cell and a self-contained solid-state amplifier. Signals audibly or visually. Single knob for null balance makes operation simple. Sensitivity is $10^{-3}$cc at atmosphere/second of Helium. For Helium or Hydrogen it sees 10ppm of gas in static systems. Selected by the United States Navy for testing underwater equipment, the GOW-MAC Gas Leak Detector can help you stop spoiling your accuracy and eliminate costly and dangerous gas leaks in your lab. For catalog and prices, write or call collect.

GOW MAC GOW-MAC INSTRUMENT CO.

*Gas Analysis since 1935* • 100 Kings Road, Madison, New Jersey 07940 • Tel: (201) 377-3450

Circle No. 118 on Readers' Service Card

See ACS Laboratory Guide for All Products/Sales Office

*A point of view on*

# OPTIMIZED SAMPLE COUNTING

*Run the standards. And re-run the standards. And re-set the controls. Or—turn to our Mark II™ Liquid Scintillation System. With automatic self-calibration for reproducible counting of all samples.*

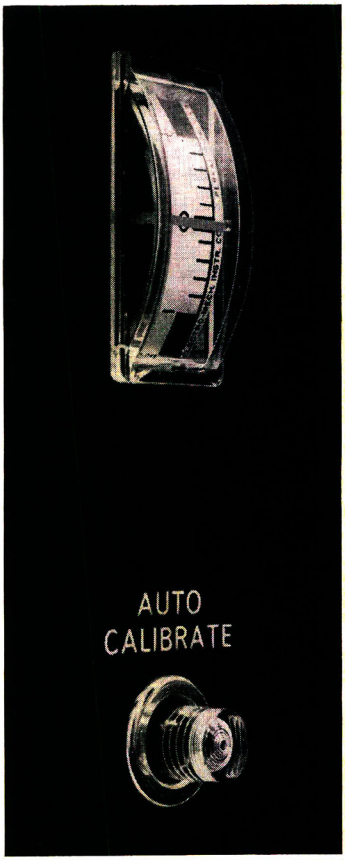


MARK II



Almost any liquid scintillation system you can name requires frequent re-running of standards for calibration curves. A lot of control setting and re-setting.

But with our 300-sample, cooled Mark II there's *automatic* self-calibration. The sample counted today yields the same results when counted again—tomorrow or next month.

And since the Mark II also has automatic program selection, it can accommodate up to 12 different counting programs. Which means you can count 12 *different* sample types (or batches) each with discrete quench, isotope, and counting conditions. All counted *automatically*. All counted *optimally*.

Window settings? Again, *automatically* selected. With pre-set push-button controls. (Of course, if you'd like to set them yourself, you can—there's a full range of manual adjustments.)

So far, you've heard only part of the story on the Mark II's top-of-the-line performance. Performance that means (among other things) a figure of merit which allows the counting of samples at activities *lower* than any other system.

Performance with no sacrifice in simplicity. The complete A-to-Z Mark II story. From your Nuclear-Chicago sales engineer. Call him. Or write to us.

9-214

**NUCLEAR-CHICAGO**

A SUBSIDIARY OF G. D. SEARLE & CO.

2000 Nuclear Drive, Des Plaines, Illinois 60018, U.S.A.
Donker Curtiusstraat 7, Amsterdam W. The Netherlands

ALS-264

Circle No. 127 on Readers' Service Card

cost of $265.00 (including binders) from the printer, Sadtler Research Laboratories, 3316 Spring Garden Street, Philadelphia, Pa. 19104. For further information, contact Dr. A. Lee Smith, Spectroscopy Laboratory, Dow Corning Corp., Midland, Michigan 48641.

### Editor in Absentia

"As this is being written, I am beginning a six-months stay in Europe on a sabbatical leave of absence from the University of Illinois. There may be some questions as to the changes in procedure and responsibility brought about by this circumstance.

During the past few years, we have worked toward increasing the degree of responsibility of the Washington staff, particularly its senior members. The promotions of Dr. John K. Crum to Managing Editor and of Mrs. Virginia Stewart and Mrs. Josephine Pechan to Associate Editors became effective on January 1, 1969 (see *Chem. Eng. News*, **47**, (*1*), 64 (January 6, 1969)). With the aid of the Advisory Board, the file of reviewers in each specialty has been revised and enlarged. Accordingly, it has become possible to handle the majority of manuscripts, namely those receiving favorable reviews and requiring only moderate revision, with only an occasional suggestion by the Editor.

For the next several months, a procedure has been worked out to avoid delays and yet to keep me posted on reviewer's comments, and to permit me to exercise my final responsibility for the contents of each issue. It is hoped thereby that the service to our readers will not be adversely affected by my absence. In return, it is my hope to gain fresh insights into the status of analytical chemistry in other countries, and to pass some of these along."

*Herbert A. Laitinen*
*Albufeira, Portugal*
*February 8, 1969*


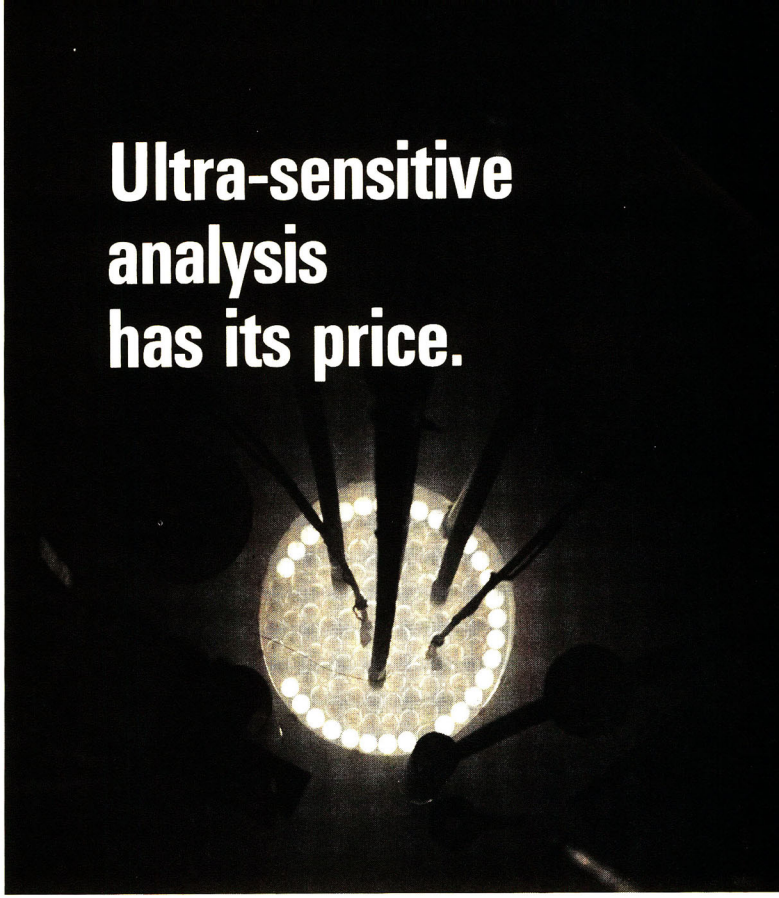


**$20**

Here's the fast, low-cost way to get an ultra-sensitive analysis for the elements present in a sample. It's Gulf General Atomic's **ACTIVATION ANALYSIS SERVICE.** Take a look.

**COST:** A typical one-element, non-destructive analysis costs $20 per sample, in quantity. Some are as little as $6 per sample.
**METHOD:** Samples are irradiated in one of Gulf General Atomic's TRIGA® reactors (reactor core shown above). The induced radioactivities are then identified and measured quantitatively, and the data are processed in GGA's computer center.
**SENSITIVITY:** Limits of detection for over 70 elements range from 10$\mu$g to $10^{-6}$ $\mu$g. Median sensitivity is approximately $10^{-3}$ $\mu$g (0.001 ppm in a one gram sample).
**PRECISION & ACCURACY:** Typical accuracy in a routine analysis is ±2-4% of the value, with a precision in the range of ±1-3% of the value.
**SAMPLES:** The technique is applicable to the analysis of virtually every conceivable solid or liquid material, including ores, semiconductors, petroleum, water, polymers, solvents, biological tissues, and agricultural products. Most analyses can be performed without destroying the sample.
**CAPABILITIES:** GGA's Activation Analysis Service is the largest, most comprehensive service of its type in the world. Analyses have been performed for over 600 organizations in the past eight years. Major facilities include three TRIGA reactors, several electron linear accelerators and neutron generators, and a UNIVAC 1108 computer.
**GET SPECIFIC DETAILS** in terms of your analytical problem. Write to Activation Analysis Service, Dept. 302, Gulf General Atomic, P.O. Box 608, San Diego, California 92112. Or phone 714/453-1000, Ext. 327.

Circle No. 45 on Readers' Service Card

Gulf General Atomic

# Here's our new Model 402 ultraviolet-visible spectrophotometer. It's your best buy anywhere!

Our new Model 402 is designed for a high level of automation where many samples must be accurately measured during the day with minimum operator attention. You'll find it equally versatile for scanning spectra quickly when monitoring a reaction, a titration, a liquid chromatography separation (often using a flow cell), or for tracing a kinetic reaction on one wavelength with time.

The 402 has a unique Flowchart recording system (Pat. Nos. 3363259, 3396403) using preprinted roll charts for precise, simplified data handling. Any 0.3 absorbance units can be expanded 5X to cover the full ordinate scale with a precision of 0.002 absorbance units.

You can do single, repetitive, or superimposed scans of one to four samples sequentially or at chosen time intervals over the range of 190-850 mμ. You can select any 40 millimicron wavelength interval (or multiples of 40 mμ). You can stop or start scans in any of these wavelength regions at three selected scanning rates.

For time rate analysis (enzyme assays) you can automatically follow a kinetic reaction in each of four sample cells at controlled temperatures and print out a chart of reaction rates for each sample.

You get all this automation, speed, and convenience at moderate cost. It will pay you to come to Perkin-Elmer for your spectrophotometer needs. We offer the broadest line of ultraviolet and fluorescence instruments in the world. For example, our economical Model 202 gives you a range of 190 to 390 and 350 to 750 mμ recorded on notebook size (8½x11) chart paper, the same high photometric accuracy as the Model 402, 1 to 10X ordinate scale expansion with an external recorder and a wide range of accessories including multiple sampling units. For further information on the new Model 402 or the Model 202 write Instrument Division, Perkin-Elmer Corporation, 402 Main Avenue, Norwalk, Connecticut 06852.




Circle No. 177 on Readers' Service Card

See ACS Laboratory Guide for All Products/Sales Office

# If lasers alone produced good Raman spectra, there'd be no need for the Cary 81.



*Howard Cary—Chairman of the Board, Cary Instruments, a Varian Subsidiary.*

For meaningful Raman spectroscopy, highly efficient optics are just as essential as a strong excitation source. We know because, years ago, we built an instrument that had only one of these requirements. We were stuck with the weak sources then available, so we put extra effort into the optical design. The result was the Model 81, which gave useful Raman spectra using mercury arc excitation. Then, with the advent of lasers, we realized our dream of a Raman spectrometer with the speed, breadth of application, and sample volume capacity of infrared equipment.

OUR OPTICAL SYSTEM

Lasers, with their small beam diameters, generally excite small round spots on Raman samples. The key to maximum light-gathering power is to fill the tall entrance slits of the monochromator. Only the Model 81, through its unique image slicer, takes energy from this round spot and converts it into tall thin images that match the entrance slits exactly. We say slits (plural) because another unique feature of the 81 is the Shurcliff double slit system, which essentially superimposes two complete double monochromators in the same space. So the entrance "slit" of the Cary 81 is really two 100 mm slits side-by-side, giving an effective slit height of 200 mm—all filled with Raman energy generated by a spot source.

Working together, the advanced optical design features of the Cary 81 provide at least 7 times more light-gathering power than any other Raman instrument.

Therefore, the 81 analyzes smaller samples, handles more dilute samples and records weaker Raman bands.

SAMPLING VERSATILITY

You choose between front and right-angle illumination. The benefit of our coaxial front illumination (only Cary has it) is twofold. For transparent liquids, Raman energy generated along capillary sample cells is collected through total internal reflection. While, for opaque samples, maximum Raman energy is always collected regardless of the opacity or thickness of the sample.

EASE OF OPERATION

No Raman spectrometer is as convenient to use as the Cary 81. A unique coupled scan and chart drive automatically maintains the same wavenumber scale on the chart as you change scan speeds or even reverse the scan. What's more, you can go back and record several spectra on the same section of chart at different sensitivities or scan speeds, an especially useful ability for polarization studies.

A WORD ABOUT RAMAN VERSUS INFRARED

Raman spectroscopy is now a useful, meaningful complement to IR. Sample handling in Raman is actually simpler than in infrared. Symmetrical vibrations of molecules are easily and conveniently observed; and depolarization measurements aid in band assignments. Further, one Raman instrument complements two IR units (at a considerably lower price), since one Raman spectrometer covers a wider wavenumber range than that covered by a standard and a far IR spectrometer combined.



For data and spectra about the 81, write Cary Instruments, 2724 South Peck Road, Monrovia, California 91016. Ask for data file A810-49.

*At Cary Instruments, we are continually looking at new applications and new high-intensity sources to use in Raman spectroscopy. For example, the Cary 81 pictured on the left is equipped with both helium-neon and argon-ion laser sources.*

CARY instruments · a varian subsidiary

See ACS Laboratory Guide for All Products/Sales Office

Circle No. 106 on Readers' Service Card

# WEIGHT WATCHERS:
# These Mettler balances can help reduce your weighing problems

If you have weight problems, chances are they can be solved with one of these three Mettler balances. Two are top-loaders, one an analytical. Collectively, they solve virtually any weighing problem in the laboratory. Individually, they perform their special jobs with unique speed, ease and precision.

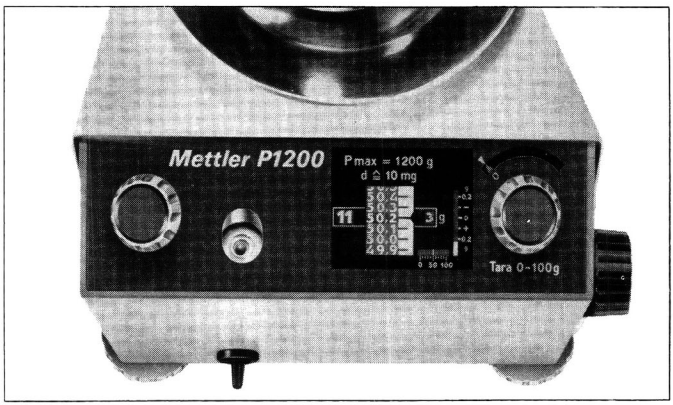


### Weight Watching Has Never Been Easier

The Mettler P1200, a well established and versatile top-loading balance, now has digital readout. This feature permits even relatively unskilled operators to obtain accurate results without misinterpretation or reading errors.

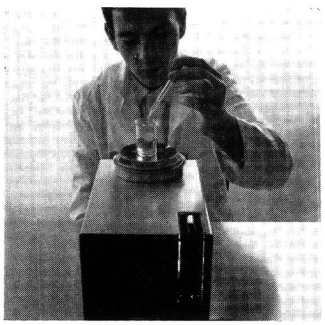

The P1200 will tackle weighings to 1200 grams (plus 100-gram tare), and give you a precision of ±5 mg. That's better than one part in 250,000. But despite its capabilities for handling the bigger weighing jobs, the P1200 will also complete a weighing in just three seconds. It will also checkweigh to plus or minus values as fast as you can place an object on the scale, and without referring to scale readout. Powdery, granular or liquid substances can be filled rapidly by the use of a filling guide which shows the approximate weight on the pan throughout the entire weighing operation. This eliminates time-consuming interruptions for reading the balance.

### Remove Grams — Positively

The P160, another top-loader, weighs unknowns to 160 grams with a precision of ±1 mg. In addition to having all the features of the P1200, it is ideally suited for weight loss studies. It has a reverse scale which gives a positive reading as weight decreases in drying, evaporation and residue determination studies. This feature eliminates time-consuming calculations and the possibility of arithmetical errors. It also simplifies gravimetric titrations (for more information on the advantages of gravimetric titrimetry, write for Bulletin M-1014A).

### A Well-Balanced Balance

Slight changes in the balance level of the P1200 and the P160 (as in all Mettler top-loaders) are automatically compensated for by a zero point restoration feature. We call it Mettler Levelmatic. If your balance is out of plumb beyond its compensation range, you won't be able to make a weight reading because the readout is automatically obscured. Because Levelmatic automatically compensates for most shifts in zero position, it is rarely necessary to re-zero the balance before weighing.

### Have Your Cake and Eat It

If you need an analytical balance to watch your weight, consider the Mettler H20 . . . it's really two balances in one. It gives you the 160.1-gram capacity of a macro-analytical balance, and the ±0.01 mg precision of a semi-micro instrument. The H20 readout, like the P1200 and P160, is digital. It also has a high-speed filling guide, and an optional accessory will let you weigh objects below the balance; for example, to make specific gravity measurements by weighing objects submerged in liquids.

Because of the unrestricted optical taring feature of the H20, you can tare off the weight of your container in seconds, and begin weighing-in with readout at zero. You can't make a weighing mistake. If you're adding several components, you can dial back to zero for each one.

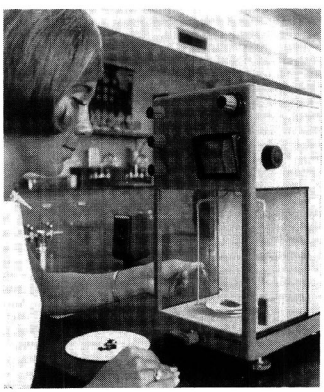

### Some Food For Thought

In case you have a weighing requirement that can't be solved by one of these three balances, Mettler has 35 more models ranging from top-loaders that weigh to 13 kilos all the way through analyticals to ultra micro instruments with precision of ±0.1 μg. We'll bet a gram-cracker that one of these will fill the bill. To arrange for a free demonstration or trial, or for further particulars, write to Mettler Instrument Corporation, 20 Nassau Street, Princeton, New Jersey 08540.

Circle No. 180 on Readers' Service Card
See ACS Laboratory Guide for All Products/Sales Office

Mettler®

# *Spectrochemical data processing

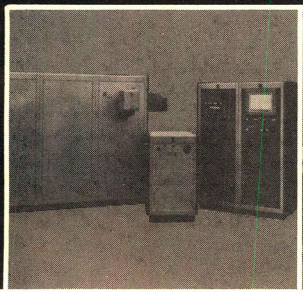

**UVAQ OPTICAL EMISSION QUANTOMETERS**
Air and/or vacuum analysis. Purchase this direct reader with a limited number of spectral channels — then expand later to as many as 56 line detectors. Choose from four different sample stands, many source units — practically any readout format. Detects trace concentrations down to 0.0001%. Stable, reliable, accurate, UVAQ is the UNIVERSAL VACUUM/AIR QUANTOMETER.

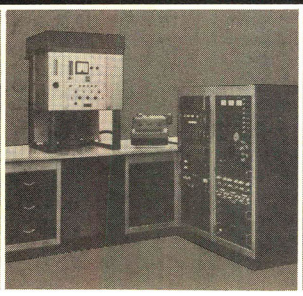

**X-RAY FLUORESCENCE QUANTOMETERS**
Unique combinations of fixed and scanning spectrometers for the simultaneous analysis of up to 22 elements. High power or conventional X-ray tubes, and appropriate fully focusing crystals and detectors provide sensitivity and speed in the analysis of all elements heavier than oxygen — solids, liquids or powders. Various readout consoles.

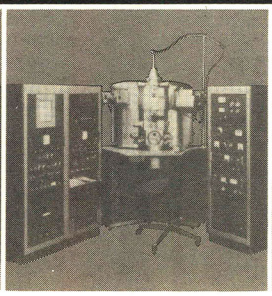

**EMX-SM ELECTRON MICROPROBE**
High sensitivity X-ray microanalysis with integrated scanning electron microscope for dispersive microprobe analysis of five elements simultaneously from 1Å to 94Å with 4X to 10,000 magnifications. Electron beam less than 0.2 micron. Modular design. Choice of readouts. Send for detailed technical booklet.

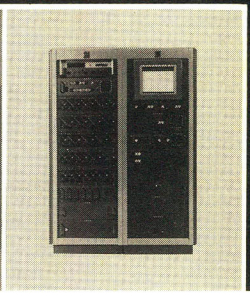

*** SPECTROCHEMICAL DATA PROCESSING**
All of these instruments can be supplied with computer readout. A full digital computer can be supplied, or interface equipment can be supplied to match your computer. An integral analog or digital computer can be included in a UVAQ system to automatically linearize or solve equations.

Quantometer is a trade name which stands for spectrochemical analysis instrumentation produced and developed exclusively by ARL . . . and ARL stands for industry leadership in design innovation and volume production for over three decades of specialization in the field of spectrochemistry. ARL introduced the first commercial air spectrometer and the first commercial vacuum spectrometer. ARL pioneered in electron microprobes, and is the world's largest manufacturer of them. ARL continually advances the state of the spectrochemical art. All ARL instruments are completely modular in design, concept and construction, ready to grow and change as your requirements change.

ARL
**APPLIED RESEARCH LABORATORIES**
Subsidiary of BAUSCH & LOMB
P. O. Box 129, Sunland, California 91040
Telephone 213-352-6011
Sales and Service Offices Worldwide

Circle No. 93 on Readers' Service Card

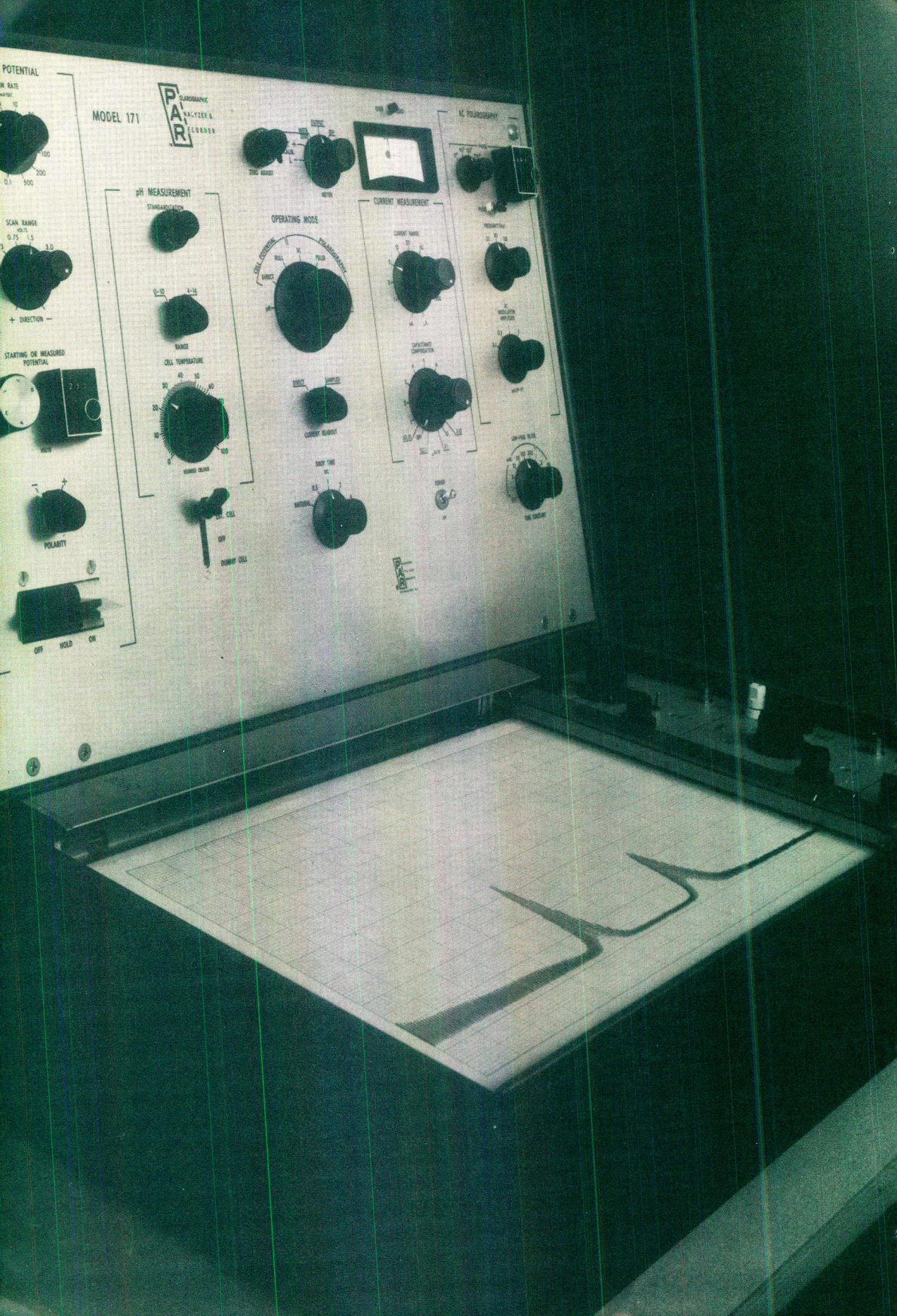
POTENTIAL
MODEL 171
PAR
pH MEASUREMENT
OPERATING MODE
CURRENT MEASUREMENT
AC POLAROGRAPHY
SCAN RANGE
+ DIRECTION −
STARTING OR MEASURED POTENTIAL
POLARITY
OFF
HOLD
ON

# Now, with one instrument, you can perform

# SIX MAJOR MODES OF POLAROGRAPHIC ANALYSIS

- **DC Polarography**
- **Peak Current DC Polarography**
- **Pulse Polarography**
- **Derivative Pulse Polarography**
- **Phase Sensitive AC Polarography**
- **Peak Current Phase Sensitive AC Polarography**

The PAR™ Model 171 Polarographic Analyzer and Recorder is the only available instrument which can perform ac, dc, and pulse polarography. It features:

**Current sensitivities** ranging from 1 nanoampere to 500 microamperes Full Scale.

**Scan rate, scan range and starting potential** independently selectable: Twelve scan rates from 0.1 to 500 mV/S; scan ranges from 300 mV to 4.5 volts are available with starting potential selectable anywhere within ±5 volts.

**Built-in three electrode capability** with ±100 volts of compliance.

**AC polarography frequencies** internally selectable: 20, 80, 135 Hz; modulation amplitudes 0.1, 0.5, 1.0, 5, 10 mV; phase readability to 0.1 degree; low-pass filter time constants to 100 seconds.

**Normal and derivative pulse polarography** with 40 mS potential pulse and 5 mS current readout.

**Mercury drop timer** allows precisely calibrated drop times of 5, 2, 1, and 0.5 seconds with no distortion of current wave-forms for pulse polarography and peak current measurements.

**Internal Zener-diode regulated power supplies** which can be calibrated against built-in standard cell.

**11 x 17 X-Y recorder** with calibrated scale expansion and zero-offset controls.

Additional applications such as anodic stripping analysis, pH measurement, specific ion measurement, direct potentiometry and controlled potential electrolysis can easily be performed.

The Polarographic Analyzer and Recorder, complete with mercury drop timer, X-Y recorder and connecting cables, is priced at $6,500. For more information or a demonstration write Princeton Applied Research Corporation, Box 565, Princeton, New Jersey 08540 or call (609) 924-6835.

Also ask about the Model 170 Electrochemical System, capable of performing virtually any electrochemical experiment.

PAR **PRINCETON APPLIED RESEARCH CORPORATION**

Typical Curves Produced by Model 171
Solution: $10^{-3}$ M Benzophenone, $10^{-1}$ M Tetraethylammonium Bromide in Dimethylformamide.

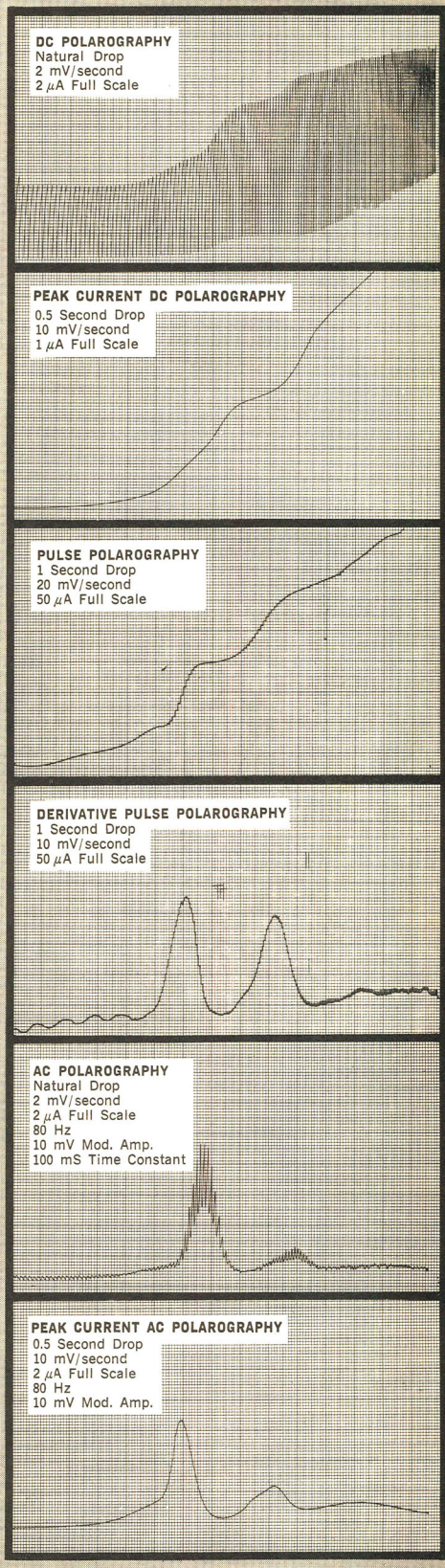


Circle No. 72 on Readers' Service Card

# Aha, the old computer-in-the-rumble-seat trick.




Sometimes, computers can be completely ignored.

Like when it's a Computerpack from DIGITAL. Computerpacks are complete laboratory systems for special purpose jobs. Like pulse-height analysis. Or signal averaging. Or gas chromatography. Each Computerpack comes with everything needed for the job. The hardware. The software. The interfaces. The works. You plug in the problem, and out comes the answer.

However.

Inside lurks an honest-to-goodness computer. A PDP-8/I. 1.5 $\mu$sec fast. 4096-word core memory. FORTRAN, FOCAL, BASIC-speaking. And software that runs over 4,000 installations around the world. All right there, ready and willing.

Computerpacks are made for specific laboratory tasks. But with that computer along, who knows what might happen when the sun goes down.

DIGITAL EQUIPMENT CORPORATION, Maynard, Massachusetts 01754, Telephone: (617) 897-5111 — Cambridge, Mass. • New Haven, Conn. • Rochester, N.Y. • New York City • Long Island, N.Y. • Princeton, Parsippany, N.J. • Washington, D.C. • Cocoa, Fla. • Atlanta • Knoxville, Tenn. • Huntsville • Philadelphia • Pittsburgh • Cleveland • Dayton • Chicago • Minneapolis • Ann Arbor • Houston • Dallas • Salt Lake City • Denver • Albuquerque • Los Angeles • San Francisco • Seattle. INTERNATIONAL, Ottawa • Toronto • Montreal • Edmonton • Reading • Manchester • Paris • Munich • Cologne • The Hague • Stockholm • Milan • Sydney • West Perth • Melbourne • Tokyo.

digital
COMPUTERS · MODULES

Circle No. 37 on Readers' Service Card
See ACS Laboratory Guide for All Products/Sales Office

Advisory Panel

Jonathan W. Amy Jack W. Frazer
Glenn L. Booman Howard V. Malmstadt
Robert L. Bowman William F. Ulrich



# Liquid Chromatography Detectors

By Ralph D. Conlon

THE TECHNIQUES grouped under the general term liquid chromatography are enjoying a comeback in the analytical arsenal. Liquid chromatography has long taken a place behind the more glamorous and sophisticated gas chromatography, and instrument manufacturers were willing to leave it there because of the limited market and because the area is so large that only a few specific techniques which gained prominence were defined well enough to instrument. Examples are amino acid and polymer separations. This very diversity combined with generally higher resolving power has finally forced interest and effort into liquid chromatography. The major reason for this Renaissance is that the compounds which are too high in molecular weight or too heat labile for gas chromatography now represent a formidable percentage of the chemical families of interest.

Whenever analytical effort is channeled into a new or renewed area, it soon follows that instrumentation must be developed and used to carry a part of the work load. Thus the rare separation, which required use of liquid chromatography and which could be developed and applied by taking numerous portions of the effluent and subjecting them to further chemical or physical tests, has now become a flood of work and the old methods cannot be economically tolerated.

The use of an appropriate detector to aid in developing and performing liquid chromatography separations is an obvious first thought in making the technique as useful and painless as possible. In methods development, the idea is to select the best column and solvent system based on the sample functional groups. It is generally necessary to evaluate several alternative systems until the optimum method is developed. If a suitable effluent stream monitor is available, the chemist need only study the recorded elution pattern to evaluate the system under test and make appropriate changes to column or solvent and try again until a satisfactory result is obtained.

Another valuable application for stream monitors is in checking the activity of commercial or prepared column material. The elution volumes and resolution of a simple test mixture are easily determined as a check on each batch of adsorbent. A similar use is the determination of elution volumes of individual components with a given column–solvent system. This is one of the simplest methods for determining if a given system will separate two or more materials where the materials are available in pure form. A stream monitor provides precise information as to time and milliliters required to elute and the degree of band broadening. If the elution volumes are sufficiently different to give a practical separation, the column and solvent are usable. Additionally this technique provides the order of removal from the column.

The advantages of efficient stream monitoring as an aid to methods development, and later application of the method, over collecting and testing or drying and weighing small portions of the effluent need not be belabored. As in gas chromatography, however, the detectors bring certain requirements of their own which must be accommodated to achieve satisfactory results. Flow rate, stream temperature, and detector environment, for example, are important parameters and must be controlled. For this reason the best use is made of detectors in the context of a total system whether commercial or homemade.

The purpose and scope of this article is to suggest several approaches to liquid chromatography stream monitoring; briefly how they work, and what criteria to use in testing the chemical system to determine which are likely candidates. Since there is no true "universal" detector for liquid chromatography, it is necessary to select one on the basis of the problem at hand and in doing a variety of separations it is expected that additional detectors will be needed. The minimum practical sample sizes suggested are not the best values reported but should be obtainable without extreme precautions. Where possible the sample size should be increased to the practical limit of resolution to take advantage of signal-to-noise ratio. Five of the techniques discussed have been incorporated into instruments and are commercially available. A brief look at four systems which show promise as future monitors is also presented.

### Refractive Index

Refractive index comes closest to being the universal detector for liquid chromatography. It has been compared to the thermal conductivity detector in gas chromatography because like thermal conductivity the refractive index changes whenever the carrier is contaminated by a solute. The trivial exception to this is the case where solvent and solute have the same refractive index. Refractive index has many features recommending it, level of sensitivity is good, measurement is nondestructive to the sample, and operation is simple.

Refractive index detectors for liquid chromatography are based primarily on two different measurement principles. The angle of deviation technique utilizes the actual bending of a ray of monochromatic light as it passes through the flowing effluent stream contained in a suitable optical cell. The bending angle changes as a function of sample concentration and is monitored by an electromechanical arrangement which moves either the source or a photodetector to maintain optical alignment. The movement is converted into an electrical signal by means of a retransmitting slide wire or balance potentiometer. Such devices are sensitive, stable, and expensive. The

# For the basic tools of liquid transport...

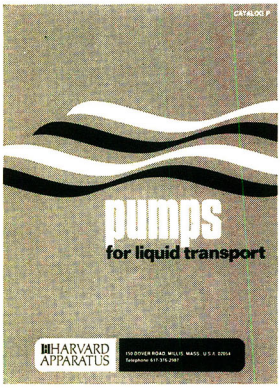


# this is the place!

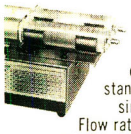

**SYRINGE PUMPS**

Over 66 models, offering constant, linear flow from standard syringes mounted in single or multiple channels. Flow rates from 0.00075 ml./hour to 720 ml./min. Accuracies to ±0.5%

**TUBING PUMPS**

Multi-channel, contamination-free pumping in closed systems. Reversible flows from 0.126 ml./hour to 2.28 liters/min. Nine different models. Accuracies to ±0.5%.





**PISTON PUMPS**

Precise flow rates from 0.01 to 0.999 ml./stroke on intermittent or timed bases. Single and multi-channel models and complete systems available.

**Send today for your free catalog of all Harvard laboratory volume liquid pumps.**

HARVARD APPARATUS
**Dept. B-19, P.O. Box 24**
**Millis, Mass. 02054**
Please send free Catalog P.

NAME
DEPARTMENT
INSTITUTION
CITY
STATE ZIP

**Circle No. 193 on Reader's Service Card**
**See ACS Laboratory Guide for All Products/Sales Office**


second approach makes use of the reflection principle first elucidated by Fresnel in which the intensity of the reflected component of a beam of light impinging on the surface of the effluent stream changes inversely with the refractive index.

The reflectance technique has certain advantages such as a smaller permissible flow, cell volume, and lower cost. Although there is no theoretical limit to the sensitivity obtainable with the reflectance technique, the commercial units available presently are less sensitive by a factor of about 50 to 100 based on manufacturers' specifications.

The application decision is based simply on the difference in refractive index between the solvent carrier and the sample. The refractive index of most of the common solvents can be found in handbooks of chemistry. If the sample material is not listed, this value can be measured with a laboratory refractometer of the Abbe type. Assuming that the sample will become diluted about 100 to 1 by the solvent carrier in the column (a general rule of thumb for all liquid chromatographic separations) and assuming that a $10^{-5}$ change in refractive index is readily detected, then the sample size in milligrams is roughly the reciprocal of the difference in refractive index between solvent and sample.

Temperature control of the column effluent and detector is critical in refractive index monitoring. Many solvents used in liquid chromatography have a temperature coefficient of about $3 \times 10^{-4}$ R.I. units per degree centigrade so control of better than a thousandth of a degree is necessary to achieve the higher sensitivity settings of commercial refractometers. Flow rate should be held constant for long term separations as an aid to maintaining thermal equilibrium. This mode of monitoring is usable with gradient elution but at a lower sensitivity since it is not possible to compensate the gradient completely even with differential type monitors. A reduction in sensitivity of 10 or more will be necessary which may be partially made up by increasing the sample size.

### Electrolytic Conductivity

In electrolytic conductivity monitoring the specific conductivity of the effluent stream is continuously detected and entrained sample is indicated by a change in conductivity. This is one of the simplest and most dependable of the current monitoring techniques and its use is expanding rapidly as cell parameters and measuring circuitry are improved to permit use with both aqueous and nonaqueous effluents.

The use of conductivity measurement to determine water and reagent purity is a well known laboratory procedure. The standard apparatus consists of a pair of carefully spaced platinum electrodes contained in a probe assembly which is immersed in the sample. Alternating voltage in the range 60 to 1000 hertz at 14 volts is applied to the cell which forms one leg of a Wheatstone bridge. The bridge is brought to balance, as indicated by a phase detector, with variable resistors in opposing legs of the bridge. Conductivity or resistance parameters are then read out directly with proper correction made for the cell constant which is a geometric parameter based on electrode size and spacing.

To utilize this technique for stream monitoring, the immersion cell is replaced by a low volume flow-through cell and variations in conductivity of the carrier liquid due to eluted sample are continuously recorded. Response is linear with concentration over a wide range so quantitation of the output signal is possible with suitable preliminary calibration. Best use is made of this monitor in single solvent chromatography since solvent gradients will cause a proportional shift in baseline. Detection sensitivity is a function of the difference in conductivity between eluting solvent and sample and so can be estimated from handbook values or determined experimentally by measuring a dilution series of sample in solvent with the monitoring cell. Sample sizes as low as 10 micrograms are detectable under conditions of constant flow rate and controlled temperature.

Gel filtration chromatography provides many applications for the electrolytic conductivity detector. The separation of proteins on gel columns using buffered aqueous eluting solvent has been successfully monitored in the lab as well as on a production scale in a pilot plant environment. The simplicity of operation, ease of cleaning, and freedom from maintenance and recalibration are important advantages of electrolytic conductivity monitoring.

### Heat of Adsorption

The heat of adsorption detector is an excellent choice for the researcher doing a variety of liquid chromatographic separations which require different column media because it is also a "universal" detector within certain limitations.

The principle of this monitor involves detection of the minute temperature changes which accompany the interaction of sample and solvent with the separation medium in the column. As solvent molecules are displaced by sample molecules at the adsorbent surface a local temperature change reflects

the exchange. A thermistor is used to detect the temperature change of the adsorbent and second thermistor imbedded in a nonadsorbing granular material is provided to aid in compensating for changes in steam or ambient temperature. Many approaches have been used in measuring these thermal reactions, including imbedding thermistors in the column, temperature monitoring at the point of emergence of the effluent from the column bed, and directing the effluent through a cell containing a small portion of the column bed material and the measuring thermistor. The latter approach is favored because of the flexibility offered. By repacking the cell or substituting a second pre-packed cell, the unit can be moved from column to column for a variety of studies.

All four major areas of separation: ion exchange, adsorption, partition, and molecular filtration provide a measurable change in temperature at the sample–column material interface. The real value of the heat of adsorption detector is in qualitatively visualizing the elution pattern and is therefore an excellent choice in methods development and in survey methods in which the presence or absence of a constituent is the important information, and not necessarily the amount.

The peak height is, in fact, a function of concentration, but frequent calibration is necessary in order to achieve what would be considered acceptable analytical accuracy. Unavoidable changes in the activity of the separation medium in the cell which occur from run to run and even during a run are primarily responsible for the lack of precision.

An apparent disadvantage could be considered to be the unconventional peak shape which has the general appearance of the first derivative of a Gaussian curve because the detector responds with a positive and negative going peak for each material eluted. This actually does not present any real problem because it is simply a matter of familiarity. Even the interpretation of two unresolved peaks or a peak with a shoulder is not difficult, and can in fact be facilitated by the first derivative presentation.

Two environmental considerations are essential to successful operation. The detector, and preferably the electronics should be maintained at an absolutely constant temperature with regard to short term variation. Since the detector is capable of measuring a change of about $10^{-5}$ degree Centigrade, it is not practical to control the temperature by adding increments of heat or cold. Most manufacturers instead provide a thermal ballast – thermal barrier environment usually consisting of a noncontrolled water bath which is well isolated from laboratory environment. This provides the best short term constancy of temperature but changes of 4 or 5 degrees in room temperature will result in excessive drift in long term studies.

The second requirement is that the flow rate be constant and surge-free. Flow rate rather than pressure must be constant, since only constant flow will guarantee that the stream velocity at the thermistor surface will be constant. Surging in the stream results in intolerable baseline noise. Positive displacement syringe pumps offer the best solution.

The heat of adsorption detector can be used in gradient elution chromatography but a shift in baseline will occur reflecting the change in solvent composition. As in the case of the refractive index detector the unit cannot be operated at maximum sensitivity for gradient elution applications but still can be useful.

The practical minimum sample size depends on the adsorption-desorption characteristics of the column material, solvent, and sample with ion exchange separations generally giving more signal. An average minimum sample injection is about one microgram per component for ion exchange separations and about 0.1 to 1.0 milligram for adsorption on silica gel.

The zero dead volume construction of the heat of adsorption detector makes it a valuable aid in studying band broadening in the column and extra-column peak effects. With proper calibration relative heats of adsorption can be measured for any liquid–solid system.

### Ultraviolet and Visible Absorption

The application of ultraviolet or visible light absorption to stream monitoring is a natural extension of the use of spectrophotometers to examine individual portions of the effluent. In contrast to refractive index and heat of adsorption, UV or visible absorption is a specific parameter in that the sample material must exhibit a suitable extinction at some region of the UV spectrum or, in the case of visible absorption, combine with a complexing reagent to form a color derivative. This monitoring approach is among the simplest to evaluate since the UV absorption characteristics are either known from prior work on the system or can be easily obtained by running an absorption spectrum on a manual or recording

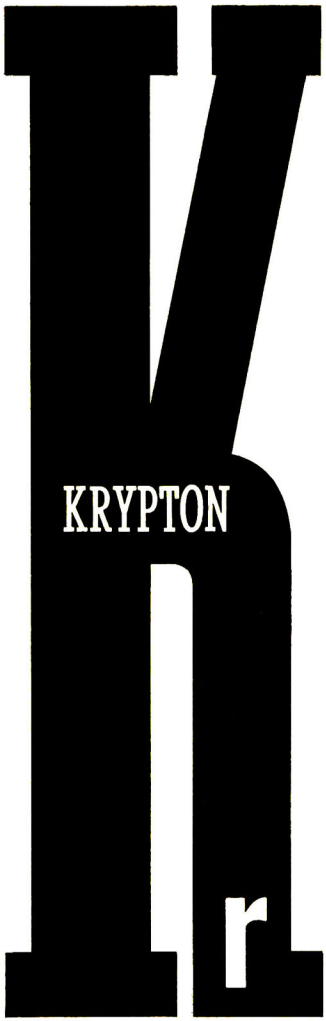


**Krypton. We have it for you pure or ultra pure or radioactive. In all kinds and sizes of containers.**

**For this year's catalog, write: Rare and Specialty Gases Dept., Airco Industrial Gases, 150 East 42nd Street, New York, N.Y. 10017.**

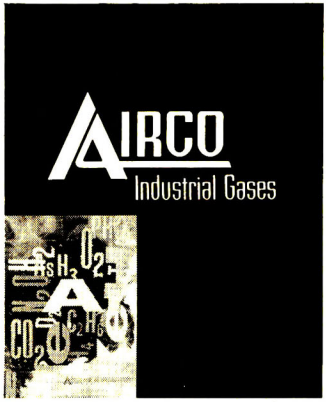


Circle No. 201 on Readers' Service Card




**because our cell is guaranteed to withstand ultrasonic cleaning.**

With new all-glass seal construction, our premium Double Dot™ Cell can be cleaned by ultrasonic methods. Absolutely cleaned without damage or breakage to the cell structure—without hours of soaking in solvents. The new Double Dot Cells feature distortion-free and ultra parallel optical surfaces for greatest accuracy. All this in a rugged design that is guaranteed to withstand ultrasonic cleaning—a Beckman exclusive. And versatile because it fits all manufacturers' spectrophotometers which use standard 10mm rectangular cells.

For complete details, write for Data File 1317 or contact your Beckman Field Sales Representative. He'll also tell you about the Double Dot Cell's one-year guarantee.

Beckman®
INSTRUMENTS, INC.
SCIENTIFIC INSTRUMENTS DIVISION
FULLERTON, CALIFORNIA • 92634

INTERNATIONAL SUBSIDIARIES: AMSTERDAM, CAPE TOWN, GENEVA, GLENROTHES, SCOTLAND; LONDON; MEXICO CITY; MUNICH; PARIS; STOCKHOLM; TOKYO; VIENNA

Circle No. 10 on Readers' Service Card
See ACS Laboratory Guide for All Products/Sales Office

spectrometer. The discovery of a suitable color developing reagent for visible absorption requires more chemistry but the evaluation procedure is the same.

After the proper wavelength has been established, it is desirable to substitute a single wavelength device for continuous monitoring. In this way an expensive versatile spectrometer is not committed for long periods. Optical filters with sufficient monochromaticity are available in any required wavelength from 2000 Angstroms in the ultraviolet up through the visible region.

The solvent system must be selected so that it is transparent at the analytical wavelength. This then allows the UV or visible monitor to be used with gradient elution techniques. Other features of this monitoring technique are: no additional temperature control is normally required in the usual laboratory environment, the technique is sufficiently insensitive to flow rate that a simple pump or even gravity feed can be employed in less demanding situations, and the specificity allows a degree of qualitative information to be obtained.

Sample size requirement is dependent upon the absorption characteristic of the sample used but an acceptable minimum sample size under average conditions is 10 to 100 milligrams. An additional pump-to-meter color developing reagent into the column effluent stream must be supplied for continuous monitoring of colorless effluents in the visible region.

### Flame Ionization Detector

The flame ionization detector combines high sensitivity, wide dynamic range, quantitative response, and the added advantage of being usable with gradient elution techniques. The singular limitation is that the sample must be relatively nonvolatile at normal laboratory temperatures. For this reason most applications to date have been made on lipids, proteinaceous materials, polymers, and other high boiling samples.

The flame ionization detector has long served gas chromatography, and the mechanics of thermal ionization and ion current monitoring are well known and demonstrated. The effluent stream sampling problem however is made more complex in liquid chromatography because the carrier must be separated from the sample material before combustion can take place, and this in turn creates difficulties in introducing the sample into the flame. The manufacturers of commercial flame ionization detectors for liquid chromatography solve these problems by applying all or a portion of the column effluent onto a moving flexible metal sample transport such as a small chain or wire. The carrier solvent is driven off by gentle heating in a stream of inert gas and the sample residue is then carried into the flame where volatilization and ionization occur. An increase in ion current is detected and a typical peak-shaped signal form is produced on a strip chart recorder. At least three mechanisms are presently being used to get the sample into the flame cone including:

a. burning residue directly on the wire,
b. using the flame heat to volatilize the sample before ignition, and
c. providing a heated chamber between the wire and the burner where the sample is removed from the wire by pyrolysis and the gaseous pyrolysis products directed into the flame.

Based on published data there appears to be an improvement in signal-to-noise ratio when the latter two techniques are employed.

As stated earlier, the selection of flame ionization is dictated primarily by the volatility of the sample. Since the metal carrier wire moves at a constant speed the loss of sample from the wire due to volatilization is also constant from run to run so sufficient precision is maintained so long as such losses are small. The technique of making a suitable dilution of sample in the solvent and applying it directly to the metal carrier with a syringe is very useful in evaluating this detector for both volatility losses and minimum detectable limit.

Commercial flame ionization detectors for liquid chromatography are equipped with temperature controls for the critical areas so additional protection from environmental variations is not required. Variations in flow rate will affect elution times as in gas chromatography but the detector noise level is not seriously affected by minor variations.

The flame ionization detector requires approximately 10 nanograms per second to shift the baseline a detectable amount above the noise level. A practical minimum sample size based on a 100 to 1 dilution in the column is about one milligram for a peak which elutes in ten minutes. Since a rate function is involved longer elutions require more sample.

### New Detectors

The detectors described here are new only in that they are not now commercially available. The principles involved are familiar and promise to be very useful to liquid effluent monitoring.

*Radioactivity.* Separation and detection of radioactive compounds, although not widely used by analytical chemists is worthy of mention because of certain advantages accruing from this technique and because of recent major improvements in the scintillation medium.

The advantages of radioactivity in liquid chromatography where commercial tagged species, or suitable activation service is available, are good quantitation, wide dynamic range, usable with gradient elution, and low minimum detectable sample size.

The availability of calcium fluoride scintillators promises to extend this monitoring technique to many solvent systems which previously were impractical because of the solubility properties of the presently used anthracene scintillator. The solubility properties of calcium fluoride approach those of glass for most solvents commonly used in liquid chromatography.

Radioactivity monitors employing the scintillation technique normally consist of a tube or cell packed with a scintillator which has a suitable efficiency for $C^{14}$ betas. The column effluent passes through the packed cell placing the isotope in direct contact with the scintillator. The light pulses generated are detected with a photomultiplier and counted or converted to a voltage level with a ratemeter. Work to date with the calcium fluoride scintillator (primarily by the manufacturer, Harshaw Chemical) indicates a high efficiency for $C^{14}$ betas and even some success with tritium-labeled compounds.

*Fluorescence.* The number of important chemical families which absorb ultraviolet radiation and re-radiate at longer, often visible, wavelengths is growing to such an extent that this highly specific measurement will probably be instrumented and packaged in a form intended for use in liquid chromatography. Workers are now using ultraviolet spectrophotometers and other general purpose instruments in utilizing fluorescence just as UV, visible, and infrared spectrometers can be used to monitor electromagnetic absorption at analytical wavelengths when equipped with flow-through type cells. In general however it is an inconvenience to commit expensive general purpose equipment to long-term duty as a monitor.

The major advantages of fluorescence monitoring are the very low minimum detectable sample size of about $10^{-9}$ gram and specificity. Used in conjunction with a second detector such as heat of adsorption the resulting chromatograms can yield valuable qualitative information.

It is essential that the solvents used in performing the separation be transparent to both the exciting ultraviolet energy and the fluorescence wavelength. With suitable solvents the fluorescence monitor is also usable with gradient elution chromatography. The minimum detectable limit is dependent upon the efficiency with which the wavelength conversion occurs with the individual sample but $10^{-8}$ to $10^{-9}$ gram is detectable with several fluorescent materials.

*Polarography.* One of the most efficient techniques for the determination of metal ion concentration is the simple two electrode polarograph in which a linearly increasing voltage ramp is applied to a suitable electrode pair which traditionally are a calomel reference and a dropping mercury electrode. The plot of current *versus* voltage indicates the amount of each metal ion present at the corresponding applied potential.

This technique has been applied to liquid chromatography monitoring by applying a fixed potential, chosen to be high enough to reduce the metal ions present, to a platinum electrode pair. Platinum electrodes are chosen because the calomel-DME pair introduce excessive dead volume to the system. Frequent regeneration of the platinum pair is necessary as the electrode surface becomes contaminated with the ions in solution. Sensitivities of $10^{-12}$ to $10^{-14}$ gram per second or $10^{-7}$ molar ion concentration are obtainable with polarographic detection. It is sometimes necessary to introduce a suitable electrolyte into the column effluent stream by means of a constant flow metering pump before the effluent passes into the measuring cell in order to reduce the voltage drop across the cell. With suitable cell design the three electrode polarographic cell could be employed for use with organic solvent systems in which the low concentration of electrolyte required may be included in the eluting solvent mixture as it is prepared before introduction on column.

*Dielectric Constant.* Physical property monitors are always attractive because they are nondestructive to the sample, provide instantaneous response, and, particularly in the case of electrical measurements, contribute very little to extra-column band broadening.

Dielectric constant or capacitance monitors respond to the polarity or, better, the polarizability of the mate-

first aid kit




**Ultra Carbon's Ultra-Pure Preformed Graphite Electrodes cure many problems for spectroscopists. For a chance at self-diagnosis write for a sample!**

Ultra Carbon offers the most complete selection of basically different electrode shapes available today. Over 120 shapes distilled from the experience gained in supplying over 2,000 different types. Formed from the finest materials using unique procedures that assure uniform graphitization at known energy levels, the electrodes are purified after machining by the famed "F"® purification process. Each box carries an individual certificate of analysis and provides maximum contamination protection. For a free sample matched to your method of analysis write: Ultra Carbon Corporation, P.O. Box 747, Bay City, Michigan 48709.

® Registered Trade Mark.

ULTRA CARBON®

See ACS Laboratory Guide for All Products/Sales Office
Circle No. 15 on Readers' Service Card

**For Soft X-ray-VUV-UV Spectroscopy**

# Here's a versatile 2-meter Grazing Incidence Monochromator/Spectrograph that closes the wavelength gap ...precisely

This exclusive McPherson grazing incidence scanning monochromator and spectrograph gives you a unique capability. Now, you can scan photoelectrically, or photograph, from the soft X-ray (10Å) through the UV (2500Å). And achieve first order resolution of better than 0.3Å with the standard 300 L/mm grating. Proportionately improved resolutions can also be achieved with the optional 600 L/mm and 1200 L/mm gratings. Its versatility is further enhanced by an adjustable angle of incidence which may be set from 82° to 88° and the rapid interchangeability of the kinematically mounted gratings. This means that you can literally choose the exact wavelength coverage and resolution you need.

The basic modular design of the Model 247 allows quick, simple conversion from monochromator mode to spectrographic mode. As a monochromator, the Model 247 is an excellent source of radiation for studies such as ionization and dissociation where photon energies from 5 to above 1240 electron volts are required. As a spectrograph, a camera attachment replaces the monochromator scanning slit and a vacuum chamber encompasses the 30-inch focal curve. The Model 247 is especially appropriate for aerospace researchers and scientists, plasma and nuclear physicists.

McPherson offers a complete line of precision instruments for accurate analysis of the spectral range from soft X-ray to near IR. For complete information on the versatile Model 247 grazing incidence combination Monochromator/Spectrograph, write or call.

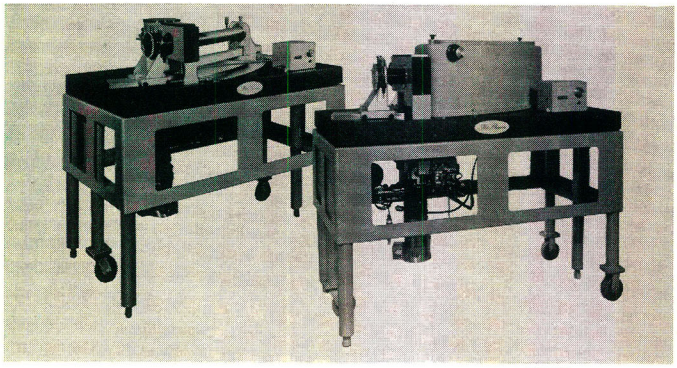

**Agent for U.S.A., McPherson offers the book ESCA by Kai Siegbahn et al, an important new work on electron spectroscopy for chemical analysis. $25.20 per copy.**



McPherson

SUBSIDIARY OF GCA CORPORATION

McPHERSON INSTRUMENT CORPORATION
530C Main Street, Acton, Massachusetts 01720 • 617-263-7733

Circle No. 131 on Readers' Service Card

rial between the plates. The best use is made of this technique, therefore, when the polarity of sample and solvent are widely different.

The detector portion consists of a pair of parallel plates or concentric cylinders in close proximity through which the effluent is directed. An alternating potential in the range of 10 to 100 megahertz is applied to the cell connected in a standard capacitance bridge circuit.

Dielectric constant is the electrical analog of refractive index and so exhibits much the same advantages and disadvantages. As would be expected, use is not recommended with gradient elution techniques particularly if the gradient is a function of solvent polarity. The practical minimum sample size is in the one to ten milligram range. Response is linear with concentration over several decades so direct quantitation with area analysis is possible. To date the best use for this technique has been made with gel filtration chromatography.

### Summary and Discussion

The use of a suitable detector to monitor liquid effluent is an important first step in reducing the time and effort required to develop and utilize liquid chromatographic procedures. In the absence of a true universal detector, however, certain tests must be performed on typical dilutions of sample in carrier so that a proper decision can be made on the choice of detector. Monitors such as refractive index, ultraviolet absorption, and electrolytic conductivity are readily evaluated for application on their laboratory counterparts. Heat of adsorption requires some experimentation to establish detection limits but is an excellent choice for general use where absolute quantitation is not essential. Flame ionization offers sensitivity, quantitative response, and freedom from baseline drift with gradient elution. This detector should be a first choice when working with low volatility samples. Special purpose detectors such as visible absorption, radioactivity, and fluorescence are used where the chemical system dictates.

Research in detectors is proceeding along predictable lines utilizing classical instrumental principles such as polarography, fluorescence, and dielectric constant. For the most part they are special purpose devices in that they utilize a specific chemical property or functional group. It is reasonable to assume that certain individual detectors will demonstrate a particular utility for a given area of liquid chromatography such as electrolytic conductivity and refractive index have

shown in molecular weight separations. The need at present appears to be for a widely applicable detector which is not affected by solvent gradients. The ability to manipulate separation by varying the ionic strength or polarity of the eluting solvent during analysis is a powerful aid and adds a unique and indispensable dimension to liquid chromatography. More and better detectors will have to be built which can accommodate the gradient in a convenient and efficient manner without excessive loss in sensitivity.

Sensitivity will continue to be a paramount consideration as more classical methods and new procedures are adapted to narrow bore high speed columns which require as much as 50 to 100 times reduction in sample size.

Use of liquid chromatography as a preparative separation technique will continue to grow in importance in the preparation of pure fractions for use as reagents or for study and identification. The availability of equipment to carry out separations unattended will require that stream monitoring be employed. The wide dynamic range detectors such as refractive index and electrolytic conductivity are good choices.

The use of series multiple detectors to monitor the column effluent promises to yield a new dimension of utility to liquid chromatography by achieving quantitative and qualitative information from a single analysis.

**Acknowledgment**

The author thanks Dr. D. P. Raval for his helpful comments and for his suggestions regarding practical minimum sample sizes for several of the detectors discussed.

---

For information on manufacturers of detectors, see the "1968–69 ACS Laboratory Guide to Instruments, Equipment and Chemicals."

***Ralph D. Conlon is Vice President and Director of Research at Nester/Faust Manufacturing Corporation, 2401 Ogletown Rd., Newark, Del. 19711.***

## COMMENTARY

by Ralph H. Müller



Mr. Conlon has given cogent reasons for the revived interest in liquid chromatography and has indicated that new and improved detectors can contribute heavily to further improvements. We are inclined to believe that a breakthrough can be achieved in a variety of approaches, particularly if the immediate application to liquid chromatography is temporarily ignored. To be sure, one must keep in mind that very small samples must be used and all operating conditions must be compatible with the ultimate application. One impediment to progress has been the tendency to automate classical physical chemical techniques, largely because they are so well understood and generally accepted.

Let us consider the case of refractometry. The two main methods, that of angular deviation and the other involving the critical angle at a boundary, have been exploited in many ways and have been successfully automated. However, there are many other approaches which have not been accorded the attention which they deserve. It should be quite easy to automate the "schlieren," a striae effect, as a measure of refraction gradients. In this technique, a point source of light, after passing through the system, is brought to focus on a tiny stop which completely obscures the light. If any density gradient arises in the system, refraction will occur and some of the light will escape the stop. This method will detect refraction effects in gases of the order of $\pm 1$ unit in the seventh decimal place. It is widely used in delineating shock waves in gases in ballistic and aerodynamic studies. The same can be done with much higher light economy by using a set of Ronchi plates. Another method which we have described involves the change in light scattering which occurs when a liquid or solution is in contact with a translucent matrix such as a small disc of filter paper or fiber glass or a ground glass surface [R. H. Müller, *Analyst*, **77**, 557 (1952)]. In general, as the refractive index of the liquid increases and approaches that of the matrix, more light is transmitted along the optic axis and less is scattered laterally. This is related to the ancient Bunsen grease spot photometer. A similar phenomenon is the Christiansen Filter in which a tube is filled with tiny glass beads. The latter are completely immersed in a liquid of almost the same refractive index, such as ethyl cinnamate. If the whole assembly is heated or cooled, the system becomes a monochromator because, with an initial beam of white light at a certain temperature, the liquid will have a refractive index exactly identical with that of the glass beads and will be transmitted freely with no scattering. This condition holds only for a given wavelength and we thus have a temperature controlled monochromator.

A great advance in instrumentation was made when it was discovered that delicate galvanometers and bulky thermostats are difficult to operate in fighter planes or bombers. Unless one wishes to study a chemical system over a wide range of temperatures such as reaction velocities, we believe it is fair to say that temperature control in an instrument should be avoided if it is at all possible to provide automatic compensation for temperature changes. Thermistor networks are easy to design for electrolytic conductance measurements even though the temperature coefficient is quite high. The same is true for refractive index measurements. The cell first described by Harry Svenson for differential refractometry utilizes a tiny rectangular chamber with a diagonal glass partition. The unknown solution circulates through one portion of the chamber and the other holds a reference liquid or solution. The double refraction, in opposite directions, leads to a lateral shift in the light beam parallel to the optic axis. Because the cells are in intimate contact, they have essentially the same temperature and disturbance from this source as second or third order effects.

Some new thinking on conductance measurements is badly needed. Physical chemists still think of the Wheatstone bridge as it was used by Kohlrausch; two resistors in the ratio arms and a variable resistor in the arm adjacent to the conductance cell. At balance, the reciprocal of this resistor is calculated in order to get the desired conductance. They rarely think of using the resistor in the arm diag-

# Heath pH/Electrometer with New Recorder Features!

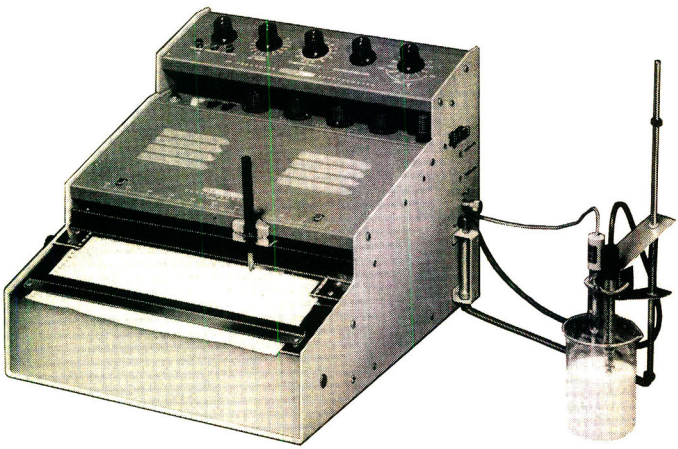

New features have been added to the Heath/Malmstadt - Enke EU - 301 pH/Electrometer, increasing the efficiency and reliability of the recorder:

- New circuit board construction
- New 3-terminal floating ground input
- New drive geometry assures uniform pen response with low friction
- New, more convenient operating controls

**plus . . .**

The EU-301 pH Recording electrometer can measure and record a span of 1 pH Unit on a full 10" scale. It performs also as an electrometer, accepting source impedance as high as 1000 Megohms.

- Multi-pH ranges: full scale pH spans of 1, 2, 5, 10 and 14. Any 1 (or 2, 5 . . .) pH unit over entire region of interest can be switched for full scale on 10" scale or recorder chart
- Multi-mV ranges: full scale mV spans of 50, 100, 200, 500, 1000 and 1400. 14 calibrated 50 mV increments of zero suppression can be switched in on all mV spans
- Direct reading: pH is read directly from the 10" scale; expanded ranges are made direct reading by interchangeable scales (e.g. 6.000-8.000 pH)
- Scale readability: 0.1% of full scale span, up to 0.001 pH and 50 uV on lowest spans
- High Accuracy: better than 0.5% of any full 0.005 pH on span of 1
- Accepts glass and calomel electrodes: Beckman, Corning, Leeds and Northrup, Thomas . . . without adapters and accomodates electrodes of different diameters
- Temperature compensated: manual adjust from 0 to 100°C or automatic control by accessory probe
- Versatile Recording Speeds: Standard chart speed is 2"/min., other interchangeable chart drives ranging from 1/2"/hr. to 12"/min. are available
- Modular design: adapts to plug-ins or modules. Recorder may be separated for other applications.
- Fully factory assembled, adjusted and calibrated. A unique design with unequalled versatility and excellent performance make this unit a highly valuable instrument in any laboratory.

**EU-301A,** with Single-Speed Interchangeable Chart Drive Motor .....**$315***
**EU-301N,** with 21-Speed Chart Drive .....**$399***

**Free Catalog**
**For more information on Heath pH/Electrometers and other test instruments send for the Heath Scientific Instrumentation Catalog.**

HEATH

**HEATH COMPANY, Dept. 520-01**
**Benton Harbor, Michigan 49022**

☐ Please send FREE Scientific Instrumentation Catalog.

Name _____

Address _____

City _____ State _____ Zip _____

Prices & specifications subject to change without notice. EK-272
*Mail order prices; F.O.B. factory.

Circle No. 122 on Readers' Service Card

See ACS Laboratory Guide for All Products/Sales Office




onally across from the conductance, the value of which at balance gives the conductance directly. Of course, the scale is not linear, but that is the nature of the beast. Under appropriate conditions of measurement, the use of d.c. can furnish conductance measurements in no wise inferior to a.c. measurements. It would be profitable to study brief pulses of d.c., possibly with periodic reversal of polarity, to minimize small polarization effects.

It is conceivable that direct automatic weighing of effluent droplets could be worked out. They would certainly be of general applicability. The Cahn Electrobalance could be used or a light cantilever beam with strain gauge or photoelectric readout. At least we are aware of the pitfalls to be encountered. For freely falling drops, the density as well as surface tension effects have to be considered. The latter are small for solutions of electrolytes but can be high for many organic systems. Most likely, it would be desirable to eject small, precisely defined volumes of effluent into a tiny, nonwettable weighing pan. After a second or two for recording the weight, the contents of the pan would be dumped into a receiver and become ready for the next sample.

There is also the question of whether it would be practical to receive effluent droplets in a light liquid immiscible with the sample droplet and measure its rate of fall through the liquid photoelectrically. In some systems, the sample could be recoverable, but there are obvious cases in which it would not. One may also ask if the famous Kelvin Electric Pail effect holds any promise. As he showed, droplets emerging from an orifice are electrostatically charged and by collecting them in a Faraday cup relatively enormous potentials can be built up. Presumably, such drops could be electrostatically deflected and preferentially so.

Mr. Conlon has done our readers a great service in outlining the reasons for renewed interest in liquid chromatography and in discussing the many possible means, many of them already commercially available, for detecting the various fractions. Our few observations and hunches may contribute little to the main problem but we think it must be realized that in a sense we have run out of phenomena awaiting automation. With present day instrumental techniques, some unusual and obscure effects may be worthy of study.

# What's the world's highest performance single-focusing mass spectrometer?

It's the Varian-MAT CH-5. No other single focusing instrument can match these CH-5 capabilities: • Resolution: greater than 10,000 (10% valley) • Sensitivity: $10^{-12}$ grams per second of cholesterol produces a good spectrum • Mass Range: up to m/e 3,600.

But buying a mass spectrometer for your laboratory is more than a numbers game with specifications. The proof is sitting down at the controls yourself and getting specified performance *or better* in your own laboratory.

Also, the best performance in the world means little if your mass spectrometer doesn't have the versatility to solve your kinds of problems. That's why the CH-5 comes with a full range of accessories such as: • Direct Sample Introduction Probe • GC Inlet • Peak Matcher • Field Ionization/Electron Impact Source • Thermal Ionization Source • Isotope Ratio Detection Systems • Knudsen Cell System • Data Acquisition Systems, plus many more.

And beyond that, there are Varian Application specialists to assist you; Regional Service Centers; and "Start Now," a Rent-Purchase-Lease Program for those short of cash.

When you get a CH-5 Mass Spectrometer System, you get more than the world's highest performance single-focusing mass spectrometer. You get Varian performance plus!

Write for details. Datafile M-3.

**varian**
analytical instrument division

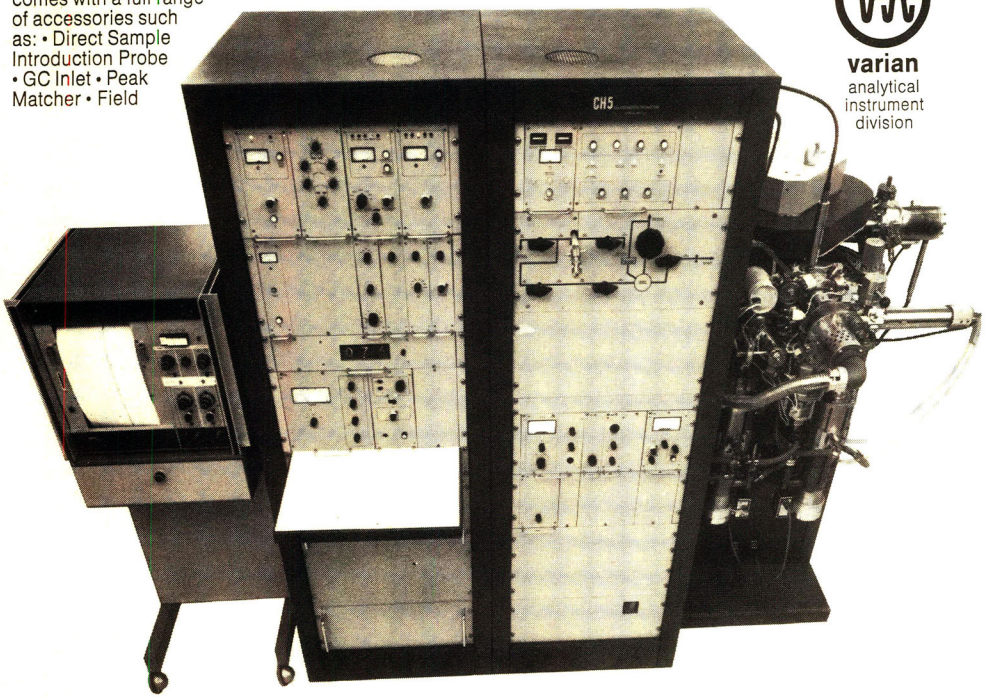


Circle No. 195 on Readers' Service Card

See ACS Laboratory Guide for All Products/Sales Office

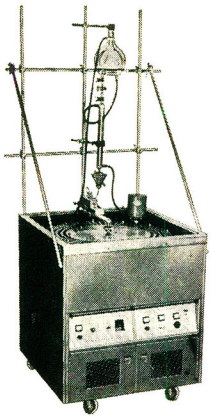

**FRACTION COLLECTORS**

Choice of 25 circular models for SHORT-RUN, SECTIONAL, MICRO, PREPARATIVE AND REFRIGERATED collections. Refrigeration provided from reservoir to test tubes. **Bulletin AC 3-4000B.**

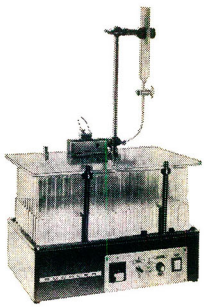

**FRACTOMETTE 200**

Smallest available linear fraction collector using 200 18mm O.D. tubes. Only 11½" wide. Provides drop, time and volume methods of collection directly into tubes. Operates at normal, cold room or refrigerated temperatures. **Bulletin AC 3-4300.**

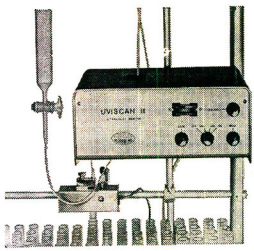


**UVISCAN III**

U.V. Monitor for column chromatography. Double beam, all solid state. Amplifier and search unit in a single housing. Filters for 240-260 or 280 millimicron operation. **Bulletin AC 3-5060.**

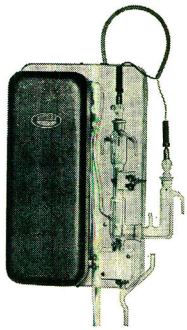

**FRACTOPHORATOR**

Continuously eluting gel electrophoresis apparatus usable with all makes of Fraction Collectors. Suitable with refrigerated columns. **Bulletin AC 3-1800.**

# Specify Buchler Instruments

## For Column Chromatography
## . . . for Electrophoresis
## . . . for Evaporation

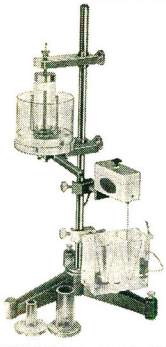

**UNIVERSAL DENSITY GRADIENT SYSTEM**

Permits formation of linear gradients from 5 ml. to 50 ml. in the same unit. Universal Piercer will process any size centrifuge tube. **Bulletin AC 2-5100.**



**FLASH EVAPORATORS**

Glass-Teflon connection prevents contaminating backdrip. Spiral or Dewar condenser assures high evaporation rate. Portable, Universal, Special models. Shown with temperature controlled water bath. **Bulletin AC-FE-1000B.**

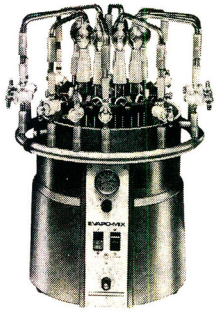


**ROTARY EVAPO-MIX**

Rapid and simultaneous evaporation of fractions directly from 10 test tubes or other vessels under vacuum and temperature controlled conditions. **Bulletin AC 3-2100A.**

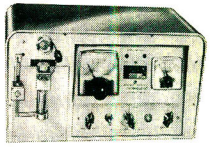

**CHLORIDOMETER**

Automatic titration of serum chloride in 40 seconds. Direct readout in mEq/l, push-button reset. Also applicable for enzyme, peptide and bromide determinations. Only 10 lambda sample required. **Bulletin AC 4-2000.**

BUCHLER INSTRUMENTS

LABORATORY APPARATUS • PRECISION INSTRUMENTS

**BUCHLER INSTRUMENTS, INC.**

1327 16TH STREET, FORT LEE, NEW JERSEY 07024

Circle No. 168 on Readers' Service Card

See us at the Federation Booth #WI-3

See ACS Laboratory Guide for All Products/Sales Office

# Keep ahead in Atomic Absorption. Our new Model 403 computes, types reports.

Perkin-Elmer's new Model 403 Atomic Absorption Spectrophotometer does a lot more for you than any previous AA instrument. It gives you a typewritten analytical report in any format you choose the instant you run your last sample —and produces a computer tape at the same time.

You set zero absorbance automatically. Just push a button.

You read concentration directly on four illuminated digits (part of a built-in, special-purpose, digital computer) and, on a recorder or teletypewriter.

Each sample read-out is the automatically computed average of 10 individual readings or, if you wish, of 100 individual readings.

The 403 has a working curve corrector which really corrects nonlinearity simply, accurately.

To go to flame emission, flip two switches and read your answer directly in digits. For scanning, you have four-speed wavelength drive.

We can just mention the automatic ignition, automatic gas flow regulation, new flashback-proof pre-mix burner, and pre-set lamps which are exchanged in five seconds. If you are Pittsburgh (Cleveland) bound, plan to see the Model 403 operating there. For full details on this new double-beam instrument, write for our new brochure. Write: Instrument Division, Perkin-Elmer Corporation, 402 Main Avenue, Norwalk, Conn. 06852.

PERKIN-ELMER



Circle No. 178 on Readers' Service Card
See ACS Laboratory Guide for All Products/Sales Office

# Turner Model 330 Spectrophotometer



■ *210-1000 millimicron capability*

■ *10 millimicron bandwidth*

■ *takes Thomas Roto-Cell for rapid 2-cell scanning*

■ *takes Thomas 10 mm Flow Cell Adapter and Flow-Through Probe for semi-automated procedures**

**SPECTROPHOTOMETER, Turner Model 330.** Diffraction grating monochromator provides fixed 10 mμ bandwidth. Solid-state a.c. power supply and amplifier. Meter reads in absorbance and transmittance. Photometric accuracy ±1% T; repeatability ±0.25%. Visible Range model covers 335-710 mμ range.

Stray light is held to less than 0.5%. Narrow bandwidth and low stray light result in resolution superior to that provided by instruments of comparable price. Useful for clinical and other routine testing. Sturdiness and simplicity of operation make the instrument suitable for industrial and educational use.

Setting of 100% T is accomplished by adjusting voltage input to tungsten lamp; feedback regulator circuit ensures stable performance. Output signal of 1 volt is provided for recorder or external readout. Wavelength range can be extended to 1000 mμ by substitution of plug-in, near-IR photodiode, offered as accessory. Ultraviolet lamp is available to extend range to 210 mμ; *information on request.*

Sample holder takes cuvette 13 mm o.d. x 100 mm long. Holder for cuvettes 19 mm x 105 or 150 mm, is offered separately. *Cuvettes not supplied.*

**Thomas Accessories for Model 330**

**Roto-Cell®.** The Model 330 can be adapted for rapid scanning by means of the Thomas 9085-C51 Roto-Cell, a 2-place water-jacketed cell carrier. Sample and blank are interchanged instantly within the instrument by turning a knob.

**Flow Cell.** Thomas 9085-F50 Flow Cell Adapter adapts Model 330 to semi-automated procedures. Takes 0.25 ml cell with 10 mm light path.

**9090-B10. Spectrophotometer, Visible Range Model 330,** as described. Range 335 to 710 mμ. With 3-wire cord and plug for 100 to 130 volts, 48 to 65 cycles, a.c.; 50 watts. . .**595.00**

***Save time and increase accuracy by adapting the Model 330 to semi-automated procedures with Thomas Flow Cell Adapter, Flow-Through Probes, Digital Readout or Printout. See pages 974, 976, 983-987 of Thomas 1968 Catalog.***

***Detailed bulletin sent upon request.***

Thomas **ARTHUR H. THOMAS COMPANY**

*Scientific Apparatus and Reagents*

**VINE STREET AT 3RD • P.O. BOX 779 • PHILADELPHIA, PA. 19105, U.S.A.**

Circle No. 81 on Readers' Service Card

See ACS Laboratory Guide for All Products/Sales Office

ANALYTICAL CHEMISTRY

April 1969, Vol. 41, No. 4



*Editor:* HERBERT A. LAITINEN

EDITORIAL HEADQUARTERS
Washington, D. C. 20036
1155 Sixteenth St., N.W.
Phone: 202-737-3337 Teletype WA 23

*Managing Editor:* John K. Crum

*Associate Editors:* Josephine Pechan, Virginia E. Stewart

*Editorial Assistants:* Eugenie C. Callaghan, Ana Sol de Gutiérrez

*Contributing Editor:* R. H. Müller

*Production Staff—Washington:*

*Director of Design:* Joseph Jacobs

*Production Manager:* Bacil Guiley

*Art and Layout:* Norman W. Favin

*Production Staff—Easton, Pa.:*

*Associate Editor:* Charlotte C. Sayre

*Assistant Editor:* Elizabeth R. Rufe

*Advisory Board:* Klaus Biemann, A. E. Cameron, Lyman Craig, Henry Freiser, John Funkhouser, Marcel Golay, D. R. Johnson, Joseph Jordan, D. W. Margerum, W. Wayne Meinke, R. A. Osteryoung, R. L. Pecsok, C. N. Reilley, A. Lee Smith, James D. Winefordner

AMERICAN CHEMICAL SOCIETY PUBLICATIONS

*Director of Publications,* Richard L. Kenyon

*Director of Business Operations,* Joseph H. Kuney

*Publication Manager, Journals,* David E. Gushee

*Executive Assistant to the Director of Publications,* Rodney N. Hader

*Circulation Development Manager,* Herbert C. Spencer

*Assistant to the Director of Publications,* William Q. Hull

REGIONAL EDITORIAL BUREAUS

NEW YORK, N. Y. 10017
733 Third Ave.

PHILADELPHIA, Pa. 19107
Philadelphia National Bank Building
Broad & Chestnut Streets

PITTSBURGH, Pa. 15219
530 William Penn Place

CHICAGO, Ill. 60603
36 South Wabash Ave.

CLEVELAND, Ohio 44114
1367 East Sixth St.

SAN FRANCISCO, Calif. 94104
57 Post St.

LOS ANGELES, Calif. 90005
422 South Western Ave.

HOUSTON, Texas 77002
514 Main Bldg.
1212 Main St.

FRANKFURT/MAIN, West Germany
32 Grosse Bockenheimerstrasse

LONDON, W. C. 2, England
27 John Adam St.

TOKYO, Japan
Iikura Central Building, 4th Floor
12 Iikura Kata-machi, Azabu
Minato-ku, Tokyo

WASHINGTON, D. C. 20036
1155 Sixteenth St., N. W.

*Advertising Management*

REINHOLD PUBLISHING CORP.
(for Branch Offices, see page 152 A)

*For submission of manuscripts, see page 2 A.*

# Five-Year Collective Index

Fifteen-year collective indexes covering Volumes 1–15 and 16–30 of ANALYTICAL CHEMISTRY and its predecessor, the Analytical Edition of INDUSTRIAL AND ENGINEERING CHEMISTRY proved to be so well received as to establish a tradition. To avoid an inordinately long period between collective indexes, and to keep the size of the project within reasonable bounds, it was decided in 1964 to change to a five-year period, covering Volumes 31–35. Under the able leadership of Dr. Lawrence T. Hallett, the fourth collective index, covering Volumes 36–40 has been prepared for publication in 1969 (see announcement, p. 46A of the March issue).

Of special interest to members of the Analytical Chemistry Division of the American Chemical Society is the special discount price of $6 for Division members, for orders received prior to September 1, 1969, as compared with the $10 price for nonmembers. The discount should serve as an additional incentive for divisional membership for those who have a professional commitment to analytical chemistry as a science but who have neglected to join the division. Membership information is available from Dr. J. C. White, Analytical Chemistry Division, Oak Ridge National Laboratories, Oak Ridge, Tenn. 37830.



# Interfacially Active Acids in a California Crude Oil.

## Isolation of Carboxylic Acids and Phenols

Wolfgang K. Seifert and W. Glenn Howells[1]

*Chevron Oil Field Research Co., P.O. Box 1627, Richmond, Calif. 94802*

**This report is part of a general study of the naturally occurring anionic surfactants in a Midway Sunset (California) crude oil. Quantitative extraction was effected with alcoholic base. The crude oil contains 2.5 wt% carboxylic acids which, in the presence of aqueous alkali, are interfacially active. The acids were separated from phenols by a sequence of exhaustive back extractions with petroleum ether, two-stage ion exchange, and repeated silica gel chromatography. Pure phenolic material is interfacially inactive. Carboxyphenols appear to be present. During isolation, about one third of the interfacially active acids was generated from the original crude oil by hydrolysis. Spectroscopic and chemical evidence is given for the presence of phenols and carboxylic acids. Number average molecular weights determined on the methyl esters and acids by three different methods indicate a range of 300–400. A quantitative infrared technique for acid value determination is described. Heteroatoms appear to be incorporated in some of the active acids.**

CARBOXYLIC ACIDS have been recognized as constituents of certain crude oils for many years. Since the first publication by Hell and Medinger (*1*) 94 years ago, an enormous amount of time and effort has been expended in attempts to determine the structures of these materials. The extensive research on carboxylic acids in petroleum conducted prior to 1955 has been excellently described in detail by Lochte and Littmann (*2*). Except for straight chain fatty acids, it is interesting to note that prior to 1955 only two acids with as many as ten carbon atoms had been identified. Since then, Bock and Behrends (*3*) have identified $C_{11}$ and $C_{12}$ branched carboxylic acids in commercial Austrian naphthenic acid mixtures. More recently, Cason and his collaborators, working with California refinery-processed commercial naphthenic acids, have succeeded in extending this upper limit in carbon number to $C_{14}$, $C_{15}$, $C_{19}$, and $C_{20}$ isoprenoid acids (*4*), to a monocyclic $C_{11}$ isoprenoid acid (*5*), and to a $C_{11}$ isoprenoid acid as well as a $C_{10}$ nonisoprenoid acid (*6, 7*).

Other studies pertinent to the work being described here have been reported by Reisberg and Doscher (*8*) and also by Neumann (*9*). These workers have described the isolation of interfacially active materials from various crude oils. Reisberg and Doscher showed that the interfacially active components present in Ventura (California) crude oil are acidic in nature, while Neumann, working with Eichlingen-Niedersachsen (West Germany) crude, reported the identification of phenols as the main interfacially active components. Perhaps the first study of interfacially active components of crude oil, however, was that of Bartell and Niederhauser (*10*). From their study on Rio Bravo (California) crude, they concluded that the interfacially active material was closely related to the resins and asphaltenes of crude oil. Investigators at the U. S. Bureau of Mines examining Wilcox (Oklahoma) crude oil (*11*) concluded that porphyrins and related substances are the major contributors to the interfacial activity of crude oils.

The purpose of the present studies was to quantitatively extract an entire virgin crude oil to obtain all components substituted by anionic functional groups and then to locate and identify in this extract the components which, at alkaline pH, have maximum interfacial activity. The ultimate objective is to determine the chemical structure of the compounds in these particular fractions. This paper will deal with that portion of the work leading to the isolation, separation, and preliminary identification of the most active fractions.

### EXPERIMENTAL

A sample of the production fluid from Midway-Sunset 31E, Well 5-3A, was collected at the well head from a previously flushed delivery line using a 5-gal glass carboy washed beforehand with distilled water and purged with nitrogen. On standing, the production fluid settled into two phases consisting of crude oil containing 1 wt% water and a lower aqueous connate water phase.

**Extraction of Crude Oil.** See Figures 1 and 2. Two duplicate extractions were carried out as follows. The crude oil (900 grams) was dissolved in 1350 grams of isopentane and the solution extracted ten times with 800-ml portions of 1% sodium hydroxide in 70% ethanol, followed by two extractions with 800 ml of 70% ethanol. The asphaltenes which precipitated during this procedure were dissolved in residue-free xylene, extracted with ethanolic sodium hydroxide, and the extract combined with the main batch of extract (Figure 2). Intermediate emulsified phases were broken by addition of a large excess of residue-free xylene. All of the combined basic extracts were divided into six batches and each extracted ten times with 600 ml of petroleum ether. These petroleum ether extracts were reduced in volume to about 15 liters at 400 mm/35 °C and then back extracted with ethanolic sodium hydroxide (Figure 2). This back extract was also combined with the main batch of alkaline extract and concentrated to 8 liters which after acidification with HCl at 0 °C was extracted with diethyl ether until the extracts were colorless. The combined diethyl ether extracts were washed with water to neutrality, concentrated to 200 ml at 400 mm/35 °C, dried with 2 grams of

[1] Present address, Forest Chemicals Division, MacMillan Bloedel Research Ltd., Vancouver 12, B.C., Canada.

(1) C. Hell and E. Medinger, *Ber.*, **7**, 1216 (1874).
(2) H. L. Lochte and E. R. Littmann, "Petroleum Acids and Bases," Chemical Publishing, New York, 1955.
(3) R. Bock and K. Behrends, *Z. Anal. Chem.*, **208** (5), 338 (1965).
(4) J. Cason and D. W. Graham, *Tetrahedron*, **21**, 471 (1965).
(5) J. Cason and K-L. Liauw, *J. Org. Chem.*, **30**, 1763 (1965).
(6) J. Cason and A. I. A. Khodair, *J. Org. Chem.*, **31**, 3618 (1966).
(7) *Ibid.*, **32**, 3430 (1967).
(8) J. Reisberg and T. M. Doscher, *Producers Monthly*, **20**, 46 (1956).
(9) H. J. Neumann, *Erdöl und Kohle*, **17**, 346 (1964).
(10) F. E. Bartell and D. O. Niederhauser, "Fundamental Research on Occurrence and Recovery of Petroleum," American Petroleum Institute, New York, N. Y., 1946–7, p 57.
(11) H. N. Dunning, J. W. Moore, and M. O. Denekas, *Ind. Eng. Chem.*, **45**, 1759 (1953).

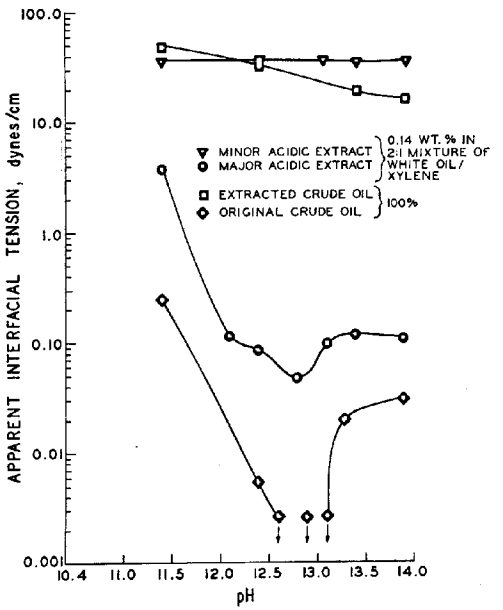


**Figure 1. Interfacial activities of original and extracted crude oil and extracts**

magnesium sulfate, and filtered. The solvent was removed at 200 mm/50 °C. The last traces of water were removed by azeotropic distillation with benzene. Stripping to constant weight at 0.3 mm/50 °C gave 64.0 grams (3.5 wt% yield of crude oil) of major acidic extract (I) from both duplicate extractions. The petroleum ether extract was acidified, washed with water, filtered, and solvent stripped to give 76.4 grams (3.6 wt% yield of crude oil) of minor acidic extract (II).

An aliquot of the extracted oil (to which the extracted asphaltenes had been added, Figure 2) was washed with connate water, and emulsions which formed during this process were broken by addition of ethanol. The acid number of this washed extracted oil was 0.25 mg KOH/gram.

**Generation of Acids.** To crude oil (10 grams) diluted with 15 ml of isopentane was added 100 ml of 1% sodium hydroxide in 70% aqueous ethanol. The mixture was shaken overnight and then a predetermined amount of 1.8*N* sulfuric acid added for neutralization of the 100 ml of aqueous ethanolic sodium hydroxide. The acid number of the product was 1.65 mg KOH/gram. In a parallel blank experiment, 10 grams of crude oil, 15 ml of isopentane, and 100 ml of aqueous ethanolic sodium hydroxide already neutralized with 1.8*N* sulfuric acid prior to mixing with the crude oil were shaken overnight. The acid number of this material was 1.49 mg KOH/gram. The difference in acidity between the two runs of 0.16 mg KOH/gram is a measure of the generation of acids during contact of the crude oil with base.

**Reagents for Chromatography.** Benzene (Baker and Adamson and Mallinckrodt Chemical) and methanol (Baker and Adamson) used for the ion exchange and silica gel chromatographic separations were distilled prior to use through a 60 by 2.5 cm i.d. glass column containing Penn State packing. Similarly, acetic acid (Baker and Adamson), acetone (Baker and Adamson), 100% ethanol (Commercial Solvents Corporation), and *n*-heptane (Phillips Pure Grade)

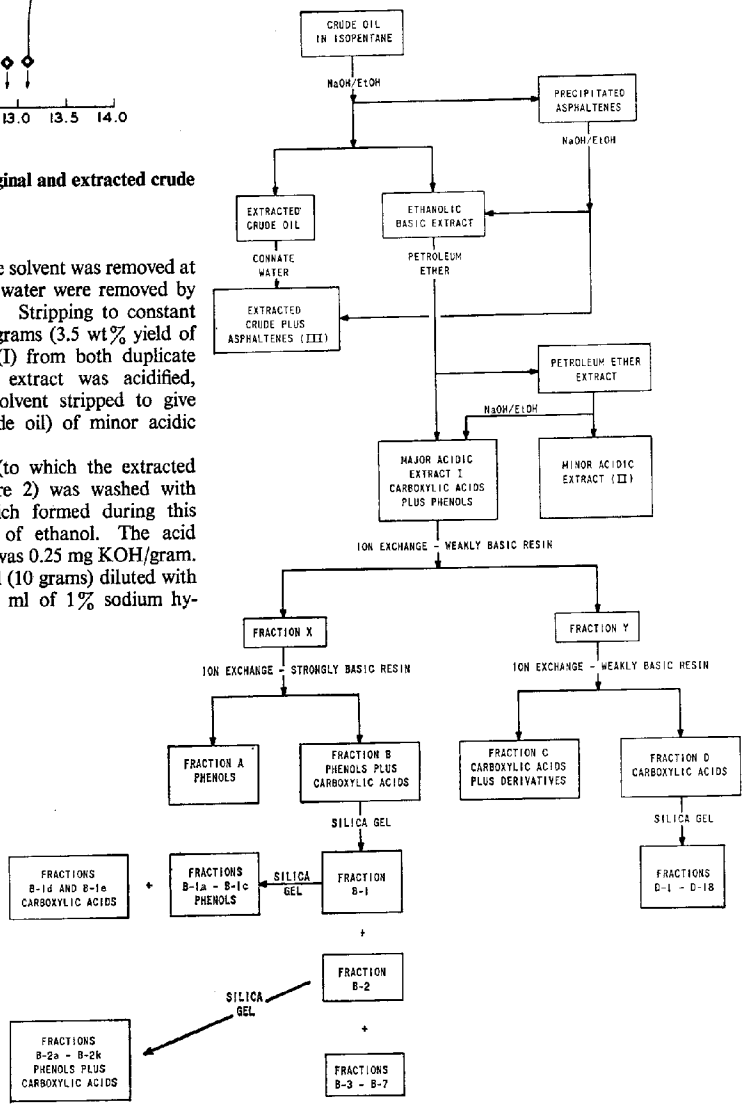


**Figure 2. Extraction and separation scheme**

were distilled through a 30 by 2-cm i.d. Vigreaux column, while ether (J. T. Baker Co.) was passed through a 50 by 7-cm i.d. column of Merck Reagent Grade alumina. The weakly basic ion exchange resin used was Duolite A-6 of Diamond Alkali Co., and the strongly basic resin was IRA-401 of Mallinckrodt. For silica gel chromatography, Grade 923, silica gel mesh 100–200 of Grace/Davison Co. was used.

**Ion Exchange Chromatography.** Major Acidic Extract (I): A glass column 65 by 7-cm i.d. filled with distilled water was packed with Duolite A-6 resin to a height of 20 cm and successively washed with 10 liters of distilled water, 8 liters of 2% aqueous sodium hydroxide, and again with distilled water until neutral. Absolute ethanol, 7 liters, was then passed through the column followed by 6 liters of a 2:1 mixture of benzene:absolute ethanol. To this column was added 36.50 grams of I dissolved in 80 ml of benzene and 50 ml of ethanol. Initial elution of the column was carried out with 13.5 liters of a 2:1 mixture of benzene:absolute ethanol until the eluate became colorless. After solvent removal, 24.10 grams of Fraction X (66% yield) was obtained. The column was then eluted with a 2:2:1 mixture of absolute ethanol:benzene:acetic acid until the eluate became colorless. The solvent mixture, 13 liters, was removed using *n*-heptane to azeotrope out the acetic acid and 13.08 grams of Fraction Y (35.8% yield) was obtained.

In each instance, solvent was removed using a rotary evaporator. Final pumping of fractions to constant weight was conducted at 0.4 mm/50 °C.

FRACTION X. A column 86 by 2. 4-cm i.d. of Amberlite IRA-401 resin was prepared in the manner described above. A solution of 22.98 grams of Fraction X in 50 ml of benzene and 25 ml of absolute ethanol was placed on the column and elution carried out initially with a 2:1 mixture of benzene:absolute ethanol. After removal of the 19 liters of solvent, 6.85 grams (29.7% yield) of Fraction A was obtained. Further elution with 13 liters of a 2:2:1 mixture of absolute ethanol:benzene:acetic acid gave, after solvent stripping and use of *n*-heptane for azeotropic removal of acetic acid, 16.06 grams of Fraction B (69.9% yield).

FRACTION Y. A 110 by 2.9-cm i.d. column of Duolite A-6 ion exchange resin was prepared. To this resin was added 12.68 grams of Fraction Y dissolved in 30 ml of benzene and 15 ml of absolute ethanol. Elution of the column with 9 liters of a 2:1 mixture of benzene:absolute ethanol afforded, after solvent stripping, 1.87 grams of Fraction C (14.8% yield). A further 10.68 grams of Fraction D (84.2% yield) was eluted with 15 liters of a 2:2:1 mixture of ethanol:benzene:acetic acid.

**Silica Gel Chromatography.** FRACTION B. A solution of 7.99 grams of Fraction B in 10 ml of benzene was placed on a silica gel column (170 by 6.4-cm i.d.). The solvent mixtures employed for eluting the individual fractions (B-1 to B-7) are shown in Table II. Total recovery was 103.8 wt%. Fractions B-1 and B-2 were then chromatographed on 117 by 2.8-cm i.d. silica gel columns. The various fractions (B-1a to B-1e, 99.0 wt% recovery, and B-2a to B-2k, 99.7 wt% recovery) obtained from these separations are also included in Table II.

FRACTION D. To a 170 by 6.3-cm i.d. column was added 7.01 grams of Fraction D dissolved in 35 ml of benzene. Following elution, Fractions D-1 to D-18 were isolated (Table III) in 96.6% yield.

Analysis for oxygen, sulfur, and nitrogen were carried out by neutron activation, X-ray fluorescence, and by the Kjeldahl method, respectively. Acid numbers were determined by potentiometric titration in xylene/isopropanol as solvent.

**Instrumental Methods.** Infrared spectra were obtained in 0.05-mm microcells on a Perkin Elmer Model 337 grating infrared spectrophotometer fitted with a beam condenser and using $CCl_4$ as solvent for the range 4000–1200 $cm^{-1}$ and $CS_2$ for 1333–650 $cm^{-1}$. The exact frequency of 3610 ± 2 $cm^{-1}$ for phenols was determined by calibration with a Beckman IR-10 spectrophotometer and an auxiliary recorder for scale expansion using water vapor bands as points of reference. Interfacial tension measurements were made against sodium hydroxide using a pendent drop apparatus described previously (*12*). The data obtained represent apparent interfacial tensions at a drop life of 10–12 sec. Nuclear magnetic resonance and high resolution mass spectra were obtained using Varian Model A-60 and AEI MS-9 instruments, respectively.

**Diazomethane Reactions.** CARBOXYLIC ACIDS. Methyl esters for molecular weight determinations were prepared by allowing selected fractions listed in Tables II and III to react with diazomethane, prepared by the method of De Boer and Backer (*13*), in ether solution for one day at room temperature (40 mmole $CH_2N_2$ per 100 ml ether; 1 wt% sample in ether; mole ratio of $CH_2N_2$ to RCOOH equaled 15–25). After quenching with acetic acid and azeotroping with heptane and benzene to constant weight, the infrared spectra of the products showed quantitative removal of carboxylic acids (1710 $cm^{-1}$) and formation of esters (1740 $cm^{-1}$). Fraction B-2c was methylated at −78 °C for 72 hours using a 10-fold molar excess of diazomethane in ether and worked up as above.

PHENOLMETHYLETHERS. *Ortho*-(2-decyl) phenol, Fraction B-1a, and β-naphthol were each allowed to react at room temperature with 4-fold or higher molar proportions of diazomethane in ether solution. The diazomethane was replenished daily. After a total reaction time of six days, the products were worked up as described above. Methylation as determined by infrared had proceeded to a very small extent for *ortho*-(2-decyl) phenol, to approximately one-half for Fraction B-1a and completely for β-naphthol.

Methylation of Fraction B-1a (14 mg) with dimethyl sulfate was conducted at room temperature for 94 hrs using 169 mg (4.2 mmole) of sodium hydroxide and 534 mg (4.2 mmole) of dimethyl sulfate. The reaction mixture was acidified with HCl, extracted with ether, washed with water, dried and solvent stripped. Infrared showed that approximately one third of the hydroxyl groups in Fraction B-1a had been methylated.

## RESULTS AND DISCUSSION

Crude oil from a particular section of the Midway Sunset (California) field was chosen for this fundamental study because of its high degree of interfacial activity at alkaline pH (Figure 1) and its high acidity (Table I). Additionally, this crude oil has a low viscosity (95 centistokes at 100 ° F) which was important for the following reason. To efficiently extract the crude oil with sodium hydroxide, it was necessary to reduce the viscosity further by addition of a low boiling solvent which could readily be distilled off later. Addition of a higher proportion of isopentane, which would be necessary to reduce the viscosity of a more viscous oil, would bring about precipitation of all of the asphaltenes. It was found that Midway Sunset asphaltenes, when quantitatively isolated in a separate experiment and dissolved in xylene (0.14 wt% concentration), showed moderate interfacial activity (>1 dyne/cm) at alkaline pH. However, at a concentration (4.7 wt%) equal to that at which the asphaltenes occur in the crude oil, an immeasurably low value (<0.003 dynes/cm) was found at pH 12.1. Because of this and in view of the claims of Bartell and Niederhauser (*10*) and since a complete study was to be made of the interfacial activity of all of the crude oil components substituted by anionic functional groups, isopentane addition

(12) H. Y. Jennings, *Rev. Sci. Instr.*, **28**, 774 (1957).
(13) T. J. De Boer and H. J. Backer, *Rec. Trav. Chim.*, **73**, 229 (1954).

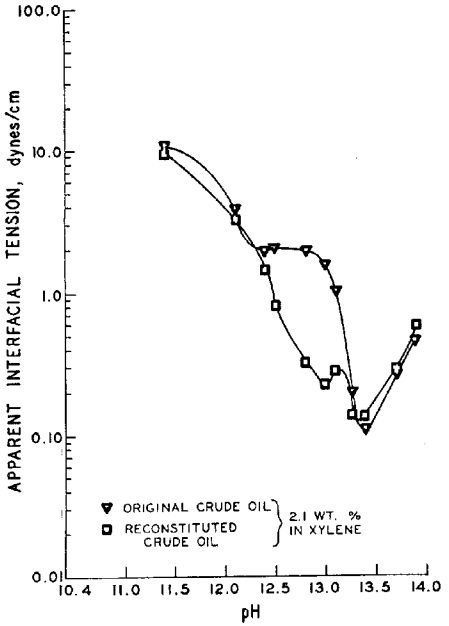


**Figure 3. Interfacial activity of original crude oil and oil reconstituted from extracted oil and extracts**

was minimized and the small amount of precipitated asphaltenes was worked up separately.

As shown in Figure 2, the crude oil was extracted using aqueous ethanolic sodium hydroxide. Use of aqueous sodium hydroxide did not completely remove the acidity and interfacial activity from the oil. The ethanolic basic extract was separated by back extraction with petroleum ether (Figure 2) into a major acidic extract (I) and a minor acidic extract (II) which, as shown in Figure 1, were interfacially very active and slightly active, respectively. The extracted crude oil (III), containing nonextractable asphaltenes, was devoid of activity (Figure 1), showing that the interfacially active material had been removed quantitatively from the crude oil.

However, the total amount of isolated acids, as measured by potentiometric titration of the extracted oil (III) and of the major (I) and minor (II) acidic extracts was 40–50% higher than that corresponding to the acidity of the original crude oil. Separate experiments showed that 10% of this acidic material was formed during extraction and the remainder during the workup outlined in Figure 2. This Midway Sunset crude oil has a saponification number of 4.4 mg KOH/gram and the hydrolysis of compounds, such as carboxylic esters (*14*) which are known to occur in some crude oils, could be responsible for the increase in acidity.

However, the important consideration was whether the interfacially active components had been augmented during extraction and workup. The increase in interfacial activity produced during the isolation procedure is shown in Figure 3. The reconstituted oil prepared by combination of appropriate amounts of extracts (I and II) and extracted oil (III) showed greater activity between pH 12.4 and pH 13.4 than the starting crude.

Back extraction with petroleum ether did not quantitatively separate the nonpolar interfacially inactive material from the

(14) G. I. Jenkins, *J. Inst. Pet.*, **51**, 313 (1965).

**Table I. Analysis of Original Crude Oil, Acidic Extracts, and Ion Exchange Fractions**

| | Wt % of crude oil | Acid number, mg KOH/g | Wt % oxygen | Wt % sulfur | Wt % nitrogen |
|---|---|---|---|---|---|
| Crude oil | ... | 2.6 | ... | 1.05 | 0.67 |
| Major acidic extract | 3.54 | 92.9 | 8.6 | 1.36 | 1.32 |
| Minor acidic extract | 3.63 | 2.5 | 1.9 | 1.11 | 0.14 |
| Fraction A | 0.69 | 4.1 | 6.5 | 1.87 | 2.60 |
| Fraction B | 1.62 | 76 | 8.7 | 1.33 | 0.89 |
| Fraction C | 0.19 | 22 | 18.0 | 2.17 | 0.72 |
| Fraction D | 1.06 | 155 | 12.1 | 1.30 | 1.39 |

polar interfacially active material. Therefore, the major acidic extract (I) was separated further by a two-stage ion exchange process involving initial use of a weakly basic resin to give the less polar Fraction X and the very polar Fraction Y. Subsequent separation of Fraction X using a strongly basic resin then afforded the nonpolar Fraction A, which was interfacially inactive, and the polar Fraction B, which was very active as shown in Figure 4. Fraction Y was similarly separated into two fractions, C and D, by use of a weakly basic resin. Fraction C was slightly active, while Fraction D was very active, as may also be seen in Figure 4.

Infrared examination of these four ion-exchange fractions showed that inactive Fraction A possessed hydroxyl absorption at 3610 $cm^{-1}$ and no carbonyl absorption while Fractions B, C, and D, which are all active, did have carbonyl absorption at 1710 $cm^{-1}$ (*15*). As described later in this paper, ab-

(15) K. Nakanishi, "Infrared Absorption Spectroscopy—Practical," Holden-Day, San Francisco, and Nankodo Co., Ltd., Tokyo, 1962, pp 30–44.

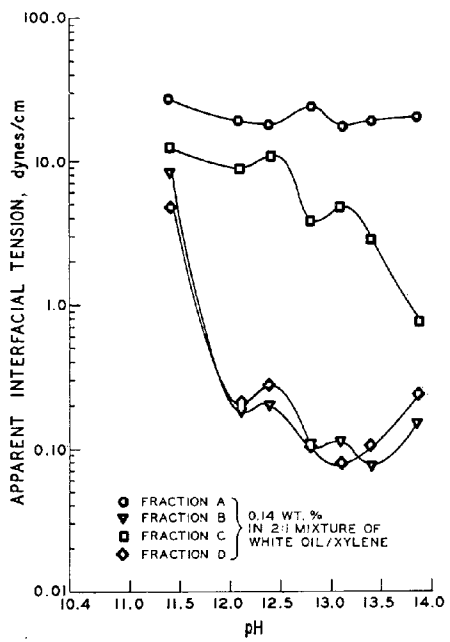


**Figure 4. Interfacial activity of fractions derived by ion exchange chromatography**

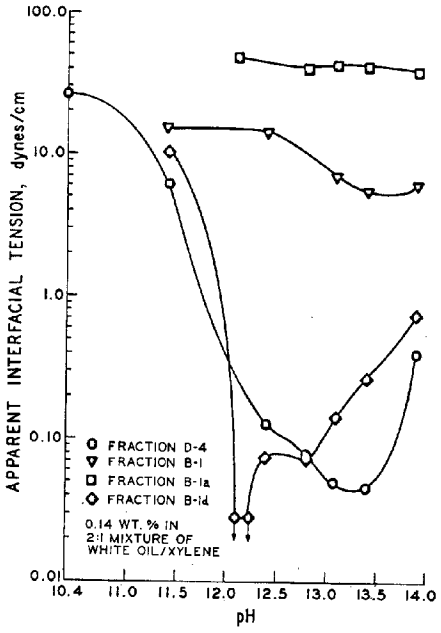


**Figure 5. Interfacial activity of selected fractions obtained by silica gel chromatography**

sorption at 3610 $cm^{-1}$ proved to be due to phenols and that at 1710 $cm^{-1}$ to carboxylic acids. Analytical data obtained on Fractions A, B, C, and D are shown in Table I, together with data on the major (I) and minor (II) acidic extracts. Comparison of the acid numbers of the various fractions and the interfacial tension profiles showed that interfacial activity and acidity parallel one another. Furthermore, Fractions B and D, which are the most interfacially active fractions, account for most of the major acidic extract (Table I). Since they both possess some phenolic absorption, together with carboxylic acid absorption, they were subjected to silica gel chromatography (Figure 2). This method of separation, which gave poor results when applied directly to the major acidic extract (I), succeeded in producing pure group types in many cases.

Chromatography of Fraction B gave Fractions B-1 and B-2 in major yield (Table II). Fraction B-1, when chromatographed on silica gel, gave fractions that possessed phenolic absorption and no carboxylic absorption, for example B-1a. This fraction was interfacially inactive (Figure 5). Also obtained from B-1 were fractions, for example B-1d, that contained only carboxylic acid absorption. This fraction possessed extreme interfacial activity (Figure 5).

Fraction B-2, in contrast to B-1 when chromatographed on silica gel, did not furnish phenols free of carboxylic acids (Table II). Furthermore, fractions which exhibited both phenolic and carboxylic absorption, for example B-2c, were found to be interfacially very active. The question arose whether these were difunctional compounds or mixtures of carboxylic acids and phenols. Therefore, Fraction B-2c was treated with diazomethane under conditions that almost completely methylated (90–95%) the acids but left the phenols unaffected. Chromatography of the methylated material on silica gel again failed to produce pure phenolic compounds but instead gave esters and phenols together in all fractions. The final fraction possessed phenolic, carbomethoxy, and some carboxylic acid absorption. This indicated the possibility that molecules were present which were substituted by both phenolic and carboxylic groups. Additionally, the resistance to esterification of some of the acids in B-2c may be ascribed to steric hindrance, a factor which has previously been suggested for parallel observations of this sort (*16*).

The fraction of intermediate polarity, Fraction C (Figure 2), was also separated by silica gel chromatography into ten fractions, each of which showed one or more carbonyl absorptions at 1710, 1730, 1740, and 1760 $cm^{-1}$, indicative of carboxylic acids and derivatives. A variety of carbonyl containing compounds such as carboxylic esters (*14*), lactones (*17*), quinolones (*18*), aliphatic ketones (*2*), and fluorenones (*19*) have all previously been identified in crude oil-derived materials. Since this fraction showed only moderate interfacial activity (Figure 4) and amounted to only 0.2 wt% of the crude oil, it was not investigated further.

As might be expected, Fraction D, the most acidic fraction, as measured by its retention on a weakly basic ion exchange resin and its acid number, possessed far less phenolic absorption than Fraction B. Interfacial tension profiles of fractions derived from Fraction D (Table III) showed that D-3, D-4, and D-5 were the most active in this series. The complete profile of Fraction D-4 is shown in Figure 5.

The minor acidic extract (II) (Figure 2), which was slightly active, was also separated by a two-step ion exchange procedure using a Duolite A-30B column to give a less polar fraction which was inactive and a more polar fraction which showed slight interfacial activity. Subsequent silica gel chromatography of the active fraction gave a small amount of material with an interfacial tension minimum of 0.1 dynes/cm at pH 12.1. Infrared examination led to the conclusion that less than 0.1 wt% (based on crude oil) of carboxylic acids was present in the minor acidic extract (II) compared with a total of about 2.5 wt% (Tables I–III) in Fractions B, C, and D derived from the major acidic extract (I). No further studies were made on any of these fractions derived from the minor acidic extract (II) because of the low proportions in which they were produced.

As shown in Tables II and III, the number average molecular weights of the interfacially active acids range from 300 to 400. Of special interest are the data obtained on Fractions D-4, D-5, and D-6 (Table III). Since association of the carboxylic acids in these fractions was found to occur even in dilutions of 0.05% in chloroform, molecular weights were determined by vapor phase osmometry of the methyl esters prepared with diazomethane (Tables II and III). Polymethylene formation (*20*) from diazomethane occurred to a negligible extent. Comparison of the molecular weights of the esters with those of the carboxylic acids, obtained both by freezing point depression in camphor (Rast) and titration (Table III), indicates that either more than one mole of diazomethane has reacted per mole of carboxylic acid or a small amount of association is occurring during the molecular weight measurement

(16) K. Hancock and H. L. Lochte, *J. Am. Chem. Soc.*, **61**, 2448 (1939); W. Shive, J. Horeczy, G. Wash, and H. L. Lochte, *ibid.*, **64**, 385 (1942); W. O. Ney, W. W. Crouch, C. E. Rannefeld, and H. L. Lochte, *ibid.*, **65**, 770 (1943).
(17) D. H. R. Barton, W. Carruthers, and K. H. Overton, *J. Chem. Soc.*, **788** (1956).
(18) E. C. Copelin, ANAL. CHEM., **36**, 2274 (1964).
(19) D. R. Latham, C. R. Ferrin, and J. S. Ball, *ibid.*, **34**, 311 (1962).
(20) R. A. V. Raff and K. W. Doak, "High Polymers," Vol. XX, Part I, "Crystalline Olefin Polymers," Interscience, New York, 1965, p 1.

**Table II. Silica Gel Chromatographic Separation of Fraction B**

| Fraction | Eluent | Liters | Wt. % of Fraction B | Apparent Interfacial Tension[1] | | Infrared Spectral Data | | Molecular Weight of Methyl Esters[4] | Wt. % Oxygen | Wt. % Sulfur | Wt. % Nitrogen |
|---|---|---|---|---|---|---|---|---|---|---|---|
| | | | | Dynes/cm | pH | $\epsilon COOH^2$ / $\epsilon CH_2$ | $OH^3$ | | | | |
| B-1 | Benzene | 9 | 21.5 | 5.2 | 13.6 | 0.13 | xxx | - | - | - | - |
| | 5/95 Ether/ Benzene | 18 | | | | | | | | | |
| B-1a | Benzene | 2 | 9.2 | 40 | 13.9 | 0 | xxx | | 4.7 | 0.71 | 0.6 |
| B-1b | Benzene | 1 | 4.9 | 29 | 13.9 | 0 | xxx | | - | - | - |
| B-1c | Benzene | 5 | 4.9 | 24 | 13.9 | 0 | xxx | | - | - | - |
| B-1d | 3/97 Ether/ Benzene | 5.5 | 1.1 | <0.003 | 12.1 | 0.61 | 0 | 485 | - | - | - |
| B-1e | Ether | 5 | 1.2 | <0.003 | 13.1-13.4 | 0.71 | 0 | | - | - | - |
| B-2 | 10/90 Ether/ Benzene | 4 | 38.9 | 0.03 | 12.7 | 0.77 | x | - | - | - | - |
| B-2a | Benzene | 2 | 0.5 | 11 | 13.9 | 0.06 | xxx | | - | - | - |
| B-2b | Benzene | 4 | 8.0 | 1.4 | 13.6 | 0.27 | xx | | - | - | - |
| B-2c | Benzene | 2 | 3.6 | 0.01 | 12.2 | 0.59 | x | | - | - | - |
| B-2d | Benzene | 4 | 4.9 | <0.003 | 12.8-13.4 | 0.79 | x | 385 | - | - | - |
| B-2e | Benzene | 2 | 2.0 | <0.003 | 12.8-13.1 | 0.81 | x | 375 | - | - | - |
| B-2f | Benzene | 4 | 2.7 | 0.07 | 12.7 | 0.95 | 0 | 365 | - | - | - |
| B-2g | Benzene | 2 | 1.1 | 0.04 | 13.1 | 0.93 | 0 | 375 | - | - | - |
| B-2h | Benzene | 4 | 1.8 | 0.03 | 13.4 | 1.04 | 0 | 395 | - | - | - |
| B-2i | Benzene | 3 | 2.3 | 0.09 | 12.4 | 0.76 | 0 | 355 | - | - | - |
| B-2j | 5/95 Ether/ Benzene | 6 | 9.4 | 0.05 | 13.0 | 0.95 | 0 | 405 | 10.0 | 1.15 | 0.6 |
| B-2k | Ether | 3 | 2.5 | 0.17 | 12.1 | 0.75 | 0 | | - | - | - |
| B-3 | 20/80 Ether/ Benzene | 17 | 13.5 | 0.07 | 13.1 | 0.95 | 0 | 460 | 9.5 | 1.87 | 0.8 |
| B-4 | 35/65 Ether/ Benzene | 16 | 13.5 | 0.10 | 12.7 | 0.71 | 0 | 445 | 10.5 | 1.11 | 1.6 |
| | 75/25 Ether/ Benzene | 12 | | | | | | | | | |
| | 50/50 Ether/ Benzene | 8 | | | | | | | | | |
| | Ether | 4 | | | | | | | | | |
| B-5 | 10/90 Methanol/ Ether | 9 | 10.9 | 0.11 | 13.4 | 0.50 | 0 | 445 | 11.1 | 2.39 | 2.5 |
| B-6 | 25/75 Methanol/ Ether | 10 | 3.0 | 0.27 | 13.9 | 0.38 | 0 | Insol[5] | 14.0 | Insol[5] | 3.1 |
| B-7 | Methanol | 6 | 2.5 | - | - | 0.49 | 0 | Insol[5] | 24.4 | Insol[5] | >4.7 |

[1] Determined on 0.14 wt. % solutions of isolated fraction in a 2:1 mixture of white oil:xylene.

[2] Extinction coefficient ratio (infrared) of $\epsilon_{1710}$ $cm^{-1}/\epsilon_{2934}$ $cm^{-1}$.

[3] Hydroxyl absorption at 3610 $cm^{-1}$: xxx = strong
xx = medium
x = weak
0 = absent

[4] Number average molecular weight determined by vapor phase osmometry (Thermonam) as methyl esters in 0.3 wt. % solution in $CHCl_3$.

[5] Fraction insoluble in appropriate solvent.

of the esters due to the presence of other functional groups. Methyl stearate itself shows the theoretical molecular weight under identical conditions. However, there is good agreement between the molecular weights determined on the acids by the two methods [Table III, columns (a) and (c)].

Particularly noteworthy is the directional agreement between quantitative infrared values of Fractions D-4, D-5, and D-6 ($\epsilon$1710 $cm^{-1}/\epsilon$2934 $cm^{-1}$, Table III) based on the carbonyl absorption of the carboxylic acid and the molecular weight measurements by all three methods. For example, Fraction D-5 possesses the lowest molecular weight and the highest $\epsilon$1710 $cm^{-1}/\epsilon$2934 ratio. The reference wave length of 2934 $cm^{-1}$ was chosen as an internal standard for these quantitative infrared measurements (*21*, *22*) since this crude oil is predominantly aliphatic, rather than aromatic. Therefore, the

(21) H. H. Willard, L. L. Merritt, and J. A. Dean, "Instrumental Methods of Analysis," 3rd ed., D. Van Nostrand, Princeton, N. J., 1958, p 147.
(22) S. J. Cristol, W. K. Seifert, and S. B. Soloway, *J. Am. Chem. Soc.*, **82**, 2351 (1960).

**Table III. Silica Gel Chromatographic Separation of Fraction D**

| Fraction | Eluent | Liters | Wt. % of Fraction D | Apparent Interfacial Tension[1] Dynes/cm | pH | εCOOH[2] / εCH₂ | Molecular Weight[3] a | b | c | Wt. % Oxygen | Wt. % Sulfur | Wt. % Nitrogen |
|---|---|---|---|---|---|---|---|---|---|---|---|---|
| D-1 | Benzene | 1 | 0.5 | - | - | - | - | - | - | - | - | - |
| D-2 | 10/90 Ether/ Benzene | 1 | 0.2 | - | - | - | - | - | - | - | - | - |
| D-3 | 10/90 Ether/ Benzene | 2 | 0.9 | 0.035 | 13.4 | 1.14 | - | - | - | - | - | - |
| D-4 | 10/90 Ether/ Benzene | 8 | 15.3 | 0.046 | 13.4 | 1.15 | 330 | 395 | 332 | 10.8 | 0.82 | 0.2 |
| D-5 | 10/90 Ether/ Benzene | 8 | 22.2 | 0.080 | 13.0 | 1.42 | 295 | 345 | 294 | 16.4 | 1.43 | 0.5 |
| D-6 | 30/70 Ether/ Benzene | 5 | 15.3 | 0.18 | 13.9 | 1.27 | 360 | 395 | 331 | - | - | - |
| D-7 | 50/50 Ether/ Benzene<br>75/25 Ether/ Benzene | 6<br>6 | 6.8 | 0.17 | 13.4 | 0.99 | - | - | - | 12.2 | 1.39 | 1.5 |
| D-8 | Ether | 17 | 3.4 | 0.23 | 13.4 | 0.84 | - | - | - | - | - | - |
| D-9 | 5/95 Methanol/ Ether | 7 | 2.0 | 0.17 | 13.1 | 0.85 | - | - | - | 12.9 | 1.38 | 1.2 |
| D-10 | 5/95 Methanol/ Ether | 7 | 1.6 | 0.32 | 13.7 | 0.98 | - | - | - | - | - | - |
| D-11 | 5/95 Methanol/ Ether | 7 | 8.6 | 0.22 | 13.9 | 0.90 | - | - | - | 15.3 | 1.87 | 1.9 |
| D-12 | 20/80 Methanol/ Ether | 5 | 0.4 | 0.64 | 13.9 | - | - | - | - | - | - | - |
| D-13 | 20/80 Methanol/ Ether | 6 | 3.3 | 2.9 | 13.9 | 0.44 | Insol[4] | | | 17.7 | Insol[4] | 2.0 |
| D-14 | 50/50 Methanol/ Ether | 4 | 0.7 | - | - | - | Insol | | | - | Insol | - |
| D-15 | 50/50 Methanol/ Ether | 2 | 3.9 | 3.2 | 13.9 | - | Insol | | | 26.2 | Insol | 2.8 |
| D-16 | Methanol | 4 | 0.4 | - | - | Insol[4] | Insol | | | - | Insol | - |
| D-17 | 5/5/90 Acetone/ Water/Methanol | 12 | 2.7 | - | - | Insol | Insol | | | - | Insol | - |
| D-18 | 5/5/20/70 Water/ Acetone/Acetic Acid/Methanol | 6 | 8.4 | - | - | Insol | Insol | | | 27.5 | Insol | 2.2 |

[1] Determined on 0.14 wt. % solutions of isolated fraction in a 2:1 mixture of white oil:xylene.

[2] Extinction coefficient ratio (infrared) of $\epsilon_{1710}$ cm$^{-1}$/$\epsilon_{2934}$ cm$^{-1}$.

[3] Number average molecular weight determined by: (a) titration, assuming one carboxyl group per molecule. (b) vapor phase osmometry of methyl esters in 0.3 wt. % solution in $CHCl_3$. (c) freezing point depression in camphor.

[4] Fraction insoluble in appropriate solvent.

2934 cm$^{-1}$ band representing the sum of paraffinic and naphthenic $CH_2$ symmetric stretching vibrations is essentially independent of the composition. This correlation of infrared with molecular weight measurements indicates a high degree of purity of these carboxylic acids and permits the calculation of acid equivalent weights from infrared data which, in contrast to titrimetric determinations, can be obtained conveniently on a microscale. The application of this method to a variety of crude oils has been reported (*14*). Testing this technique for various fractions of Midway-Sunset crude oil led to the empirical correlation that a value of unity for the $\epsilon$1710 cm$^{-1}$/$\epsilon$2934 cm$^{-1}$ ratio corresponds to an acid number of 129 mg KOH/gram (equivalent weight 435). Furthermore, this correlation is evidence that the 1710 cm$^{-1}$ absorption stems exclusively from carboxylic acids. Additional evidence was obtained by observing a quantitative shift from 1710 cm$^{-1}$ to 1740 cm$^{-1}$ (*15*) after methylation and a shift from 1710 cm$^{-1}$ to 1560 cm$^{-1}$ when the acids were converted to triethylammonium salts. Octanoic acid showed identical behavior. In dilute solution the 1710 cm$^{-1}$ carbonyl absorption of carboxylic acid dimers was displaced to 1760 cm$^{-1}$ typical of monomeric carboxylic acids (*15*) and the free hydroxyl of carboxylic acids (*15*) at 3533 cm$^{-1}$ was also observed.

As noted above, Fraction B-1a (Table II) possessed no interfacial activity, had no carboxylic acid absorption, but did exhibit hydroxyl absorption. In view of the claims of Neumann (*9*) and because of the presence of such significant amounts of hydroxyl-containing material in Midway-Sunset crude oil, these materials were examined.

It was further found that Fraction B-1a in dilute carbon tetrachloride solution had a free hydroxyl stretching band at 3610 cm$^{-1}$. Although in general free O—H stretching frequencies for phenols, tertiary, secondary, and primary alcohols occur at 3610 cm$^{-1}$, 3620 cm$^{-1}$, 3630 cm$^{-1}$, and 3640

$cm^{-1}$, respectively (*15*), variations in structure are known to influence these frequencies (*23*). Therefore, the totally unknown molecular environment of these hydroxyl groups ruled out the possibility of making structural assignments solely on the basis of infrared spectra.

Lower alkylated phenols have been found in various types of petroleum fractions from many different fields, but the structures of these phenols have been determined in only a few cases (2). Unfortunately, the structure determination of most of the phenols has been carried out on refinery products (2); and, in view of the known increase in phenol content that takes place during cracking processes (*24*), a direct correlation between phenols isolated from refinery caustic washes and those in virgin crude is not possible.

Various standard phenol reactions such as the azo coupling reaction, the ferric chloride color test, and the Liebermann and Reimer-Tiemann reactions were applied to the hydroxylic Fraction B-1a, but results were inconclusive. Acetylation with acetyl chloride gave a product whose NMR spectrum showed signals at $\delta$2.19 and $\delta$2.25 corresponding to acetyl methyl hydrogens in positions meta (or para) and ortho, respectively, to substituents on aromatic rings (*25*). No signal at $\delta$2.00 characteristic for *n*-amylacetate was observed indicating absence of alcohols. Methylation of approximately one-half of the hydroxyl groups (as determined by infrared) in Fraction B-1a was achieved by frequent replenishment of diazomethane over a 6-day period at room temperature. This extent of methylation was intermediate to the total methylation of $\beta$-naphthol and the small amount of methylation which occurred with ortho (2-decyl) phenol under similar conditions. As it has been reported previously (*26*) that alcohols do not undergo methylation by diazomethane, these methylation studies confirmed the NMR results that the hydroxyl groups are principally phenolic. Furthermore, substantial methylation of the sodium salt of Fraction B-1a was achieved using dimethyl sulfate, a method that is reported (*27*) to be very difficult for the methylation alcohols.

The most conclusive evidence for phenols, however, was obtained by high resolution mass spectrometry. When a sample of Fraction B-1a was vaporized directly into the ion source of the mass spectrometer, a molecular weight range of 290–450 was observed with the largest individual peaks at *m/e* 328, 330, 342, 344, 356, and 358. A very prominent peak at *m/e* 135 proved to be $C_9H_{11}O^+$ when its exact mass was measured at high resolution. This is consistent with the presence of I or II as parts of larger molecules and would be formed by

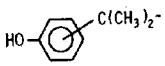


I

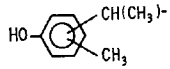


II

benzylic cleavage of a longer side chain. The structure of this fragment is probably that of a substituted hydroxytropylium ion (*28*). It is the oxygenated analogue of the *m/e* 119 peak seen in the spectra of alkyl benzenes (*29*) and is a common fragment of alkylphenols.

A small portion of Fraction B-1a was converted to trimethylsilyl (TMS) ethers (*30*) by treatment with Sil-Prep (a mixture of hexamethyldisilazane and chlorotrimethylsilane in pyridine, Applied Science Laboratories, State College, Pa.). Three peaks were examined at high resolution.

| | |
|---|---|
| *m/e* 193 | $C_{11}H_{17}OSi$ ($C_8H_8OH$) |
| *m/e* 414 | 21% $C_{28}H_{34}OSi$ ($C_{25}H_{25}OH$) |
| | 79% $C_{27}H_{46}OSi$ ($C_{24}H_{37}OH$) |
| *m/e* 416 | 30% $C_{28}H_{36}OSi$ ($C_{25}H_{27}OH$) |
| | 70% $C_{27}H_{48}OSi$ ($C_{24}H_{39}OH$) |

The peak at *m/e* 193 is the TMS derivative of the *m/e* 121 fragment which is very common in the spectra of alkylphenols. Without evidence derived from model compounds, its structure cannot be specified; but it is probably either III or IV,

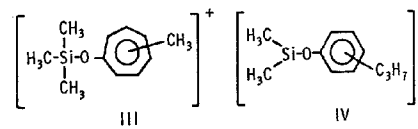


III IV

both of which result from rearrangements of higher mass ions.

The other four species, two each at *m/e* 414 and *m/e* 416, are probably molecular ions of the TMS ethers of the phenolic compounds listed above in parentheses and which appeared at 342 and 344 in the spectra of the unsilylated fraction. These compositions correspond to hydroxylated polynuclear hydrocarbons, and the following structures are possible.

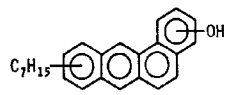


m/e 342: $C_{25}H_{25}OH$

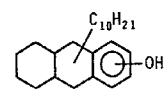


m/e 342: $C_{24}H_{37}OH$

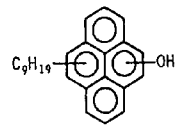


m/e 344: $C_{25}H_{27}OH$

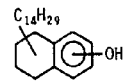


m/e 344: $C_{24}H_{39}OH$

It must be emphasized that these structures are merely possibilities. If the basic ring systems depicted above are, in fact, present, it should be noted that the alkyl carbon atoms are not necessarily present as single chains. The phenolic compounds with peaks at 328 and 330 and at 356 and 358 are the lower and higher homologues, respectively, of the compounds shown above.

For every fraction listed in Tables I–III, including those free of phenolic compounds, the amount of oxygen when determined was found to be higher than that expected for carboxylic acids alone on the basis of their molecular weights. This indicates that at least in the phenol-free fractions, other oxy-

(23) L. J. Bellamy, "Infrared Spectra of Complex Molecules," 2nd ed., Methuen, London, 1958, Chap. 6.
(24) E. Field, F. H. Dempster, and G. E. Tilson, *Ind. Eng. Chem.*, **32**, 489 (1940).
(25) L. P. Lindeman and S. W. Nicksic, ANAL. CHEM., **36**, 2414 (1964).
(26) H. Meerwein and G. Hinz, *Ann.*, **484**, 1 (1931).
(27) L. Gattermann, "Die Praxis des Organischem Chemikers," Walter de Gruyter, Berlin, 1959, p 213.
(28) T. Aczel and H. E. Lumpkin, ANAL. CHEM., **32**, 1819 (1960).
(29) H. M. Grubb and S. Meyerson, "Mass Spectrometry of Organic Ions," F. W. McLafferty, Editor, Academic Press, 1963, Chap. 10.
(30) S. Friedman, M. L. Kaufman, W. A. Steiner, and I. Wender, *Fuel*, **40**, 33 (1961).

genated structures, for example heterocyclics, are incorporated in the interfacially active carboxylic acids. Most of the nitrogen appears in the interfacially active major acidic extract (I) and not in the inactive minor extract (II) (Table I). Nitrogen contents of the active acid fractions of 0.2-2% (Tables II and III) indicate that on an average basis 5–50% of the interfacially active carboxylic acids contain one nitrogen atom per molecule. Similarly, 10–30% of all acids on an average contain one sulfur atom per molecule. The functional group types including these hetero atoms and their contributions to the interfacial activity are being investigated.

## CONCLUSIONS

This paper presents the first part of a study of the material which renders a particular crude oil interfacially active at alkaline pH. Techniques of quantitative isolation, separation, and partial group-type identification are described. During the course of extraction with ethanolic base and workup, 40–50% more interfacially active acidic material than originally present in the crude oil is generated by hydrolysis. The nonpolar and interfacially inactive components of the extract are shown to be separable from the polar and very active material by a sequence of back extraction with nonpolar solvent, two ion exchange chromatographies in series using resins of different basicity, and repeated silica gel chromatography with solvent mixtures ranging in polarity from benzene to methanol.

Pure carboxylic acid fractions isolated in this fashion show high interfacial activity at strongly alkaline pH as determined by the pendent drop method. In some instances, interfacial tensions of less than 0.003 dynes/cm are observed at 0.14 wt% concentration. The carboxylic nature of the acids is demonstrated by infrared studies before and after esterification and salt formation and by a correlation of quantitative infrared determination with potentiometric titration which serves to determine acid values by infrared spectroscopy. The number average molecular weights as determined by vapor pressure osmometry of the methyl esters and titration of the acids, as well as by freezing point depression in camphor, range from 300 to 400. Sulfur and nitrogen appear to be incorporated in some of these acids.

Hydroxylic fractions obtained free of carboxylic acids are shown to be mainly phenolic in nature by means of infrared, nuclear magnetic resonance and mass spectroscopy, and conversion to phenol methyl ethers using either diazomethane or dimethyl sulfate. Although the presence of alcohols cannot be ruled out entirely, high resolution mass spectrometry indicates that the backbone of these hydroxylic compounds are partially or totally aromatic polynuclear hydrocarbons. In contrast to a previous study on a German crude oil, these phenolic compounds are interfacially inactive at alkaline pH.

Mixtures of phenolic and carboxylic group types appear to be carboxyphenols; and since they possess high interfacial activity, they will be the subject of future studies.


## ACKNOWLEDGMENT

The authors wish to express their appreciation to C. E. Johnson, H. Y. Jennings, Jr., and G. H. Newman for helpful discussions and for the determination of interfacial tension profiles, to the staff of the Analytical and Physical Measurements Section of Chevron Research Co., especially to R. M. Teeter for high resolution mass measurements of phenols, and also to A. D. Alderman and J. P. S. Dhillon for their technical assistance.

RECEIVED for review August 5, 1968. Accepted October 23, 1968. This paper was presented in part at the Gordon Research Conference on Geochemistry, N. H., August 1968, and in full at the 157th ACS Meeting, Division of Petroleum Chemistry, Minneapolis, Minn., April 1969.


# Effect of Phenols on the Interfacial Activity of Crude Oil (California) Carboxylic Acids and the Identification of Carbazoles and Indoles


**Wolfgang K. Seifert**

*Chevron Oil Field Research Co., P.O. Box 1627, Richmond, Calif. 94802*



**Progressive esterification of carboxylic acids, naturally occurring in a California crude oil, with diazomethane under conditions that leave phenols unmethylated is shown to result in an analogous progressive decrease of interfacial activity at alkaline pH. A quantitative correlation between carboxylic acid content and degree of interfacial activity is demonstrated. The effect of phenols on the interfacial activity of carboxylic acids is investigated by exhaustive methylation of both phenols and carboxylic acids followed by selective hydrolysis of the carbomethoxy groups. Accurate measurements of apparent interfacial activities of the hydrolysis products and functional group analysis by different quantitative infrared techniques show that phenols have a diminishing effect on the interfacial activity of the carboxylic acids. The absence of significant quantities of porphyrins, primary and secondary amides, and thiols in the interfacially active material is demonstrated. Indoles substituted on the pyrrole ring and/or carbazoles were identified as integral parts of the interfacially active carboxylic acids. Identification was achieved by comparison of the free —NH— frequencies of active fractions with those of model compounds in the fundamental and in the near infrared regions.**


A PREVIOUS PAPER (*1*) describes the isolation and separation of interfacially active carboxylic acids from a California crude oil. Purely phenolic fractions which occur abundantly in the alkaline extract were found to be interfacially inactive; however, mixtures of phenols and carboxylic acids possessed high

(1) W. K. Seifert and W. G. Howells, ANAL. CHEM., **41**, 554 (1969).

interfacial activity and in some instances the active species appeared to be carboxyphenols.

This paper deals with the synergistic effect of phenols and other weakly acidic anionic functional materials on the apparent interfacial activity of the carboxylic acids in this crude oil. The possibility of a quantitative relation between carboxylic acid content and interfacial activity was explored. An investigation of the presence of thiols (*2, 3*), amides (*4*), and porphyrins (*5, 6*) was carried out because they have been reported in crude oils and they are expected to be alkali soluble (*7–9*) under our extraction conditions. In the course of searching for amides, infrared spectrometric information was developed for some aromatic secondary amine type structures, which are most likely incorporated in the interfacially active carboxylic acids.

## EXPERIMENTAL

**Methylation.** Diazomethane was prepared by the method of De Boer and Backer (*10*). The products described in Figure 1 were obtained by allowing 235 mg of major acidic extract (*1*) dissolved in 10 ml of anhydrous ether to react with 160 mg of diazomethane dissolved in 15 ml of ether at −50 °C. Aliquots of 5 ml were removed after 1 min, 10 min, and 110 min, quenched with 10-ml portions of 10 vol% of acetic acid in ether and azeotroped to constant weight with heptane and benzene using a vacuum rotary evaporator. Phenols were not methylated even after 110 min reaction time. The remainder of the reaction mixture was allowed to react for 5 days at room temperature and the solvent evaporated at reduced pressure.

For maximum possible etherification of phenols (products of Figures 4–6), 400 mg of major acidic extract (*1*) were dissolved in a solution of 880 mg of diazomethane in 45 ml of ether. The flask was capped with a capillary and kept at room temperature. Everyday for the first 10 days the solvent was evaporated in the hood, and a freshly prepared solution of 10 mmole of diazomethane in 20 ml of ether was added. The solution was then kept at room temperature with excess diazomethane for one month. After evaporation of the solvent, the methylated product was dissolved in benzene. The polymethylene (*11*) which had formed was removed by filtration and washed with benzene. The benzene solutions were combined. The methylated product which was isolated in quantitative yield after vacuum evaporation of the solvent showed complete absence of infrared absorption at 1710 $cm^{-1}$ (carboxylic acids) and presence of a sharp band at 1740 $cm^{-1}$ (esters). The phenolic hydroxyl absorption at 3610 $cm^{-1}$ had decreased to one third of its original value (Table I).

**Hydrolysis in Ethanol.** See Figure 4. A solution of 31 mg of the 6-week methylated major acidic extract in 10 ml of *N*/2 ethanolic KOH sealed with reflux condenser and calcium chloride tube was heated in a constant temperature bath to 95 °C. A parallel blank experiment, namely, 184 mg of the unmethylated extract dissolved in 25 ml of *N*/2 ethanolic KOH, was conducted in the same bath. Quantitative infrared measurements on an aliquot removed from the methylated product after three hours of hydrolysis and worked up as described below indicated incomplete hydrolysis. After 27 hr of reaction, both products were worked up in identical fashion as follows: The solutions were quenched with excess 1*N* HCl at 0 °C and each was extracted 6 times with 5 ml of ether. Each combined ether extract was washed with water, solvent stripped in vacuo, and the products were dried by repeated azeotropic distillation with benzene at 5 mm/50 °C until constant weight was attained.

The yield of the methylated and saponified product ($D_1$, Table I) was 33.1 mg (107% of theory). The blank sample yielded 173.4 mg of product $C_1$ (100% of theory).

**Hydrolysis in Isopropanol/Xylene.** See Figures 5 and 6. A solution of 209.5 mg of the major acidic extract dissolved in a mixture of 25 ml *N*/2 isopropanolic KOH and 50 ml xylene sealed with reflux condenser and calcium chloride tube were heated simultaneously in a bath of 90 °C for three days with a solution of 10 mg of 6-weeks methylated major acidic extract in 6 ml of xylene and 3 ml of *N*/2 isopropanolic KOH. These solutions were acidified with 25 ml and 3 ml of 1*N* HCl at 0 °C, respectively, and worked up as described above. Yields were 200.9 mg (98% of theory) and 8 mg (80% of theory).

**Analysis of Porphyrins.** The sample was dissolved in a mixture of heptyl alcohol, toluene, and hexane; and the extinctions at 570 mμ (V-type) and 550 mμ (Ni-type) were determined. Calculations were based on the extinction coefficients of Mesoporphyrin IX (V: $2.6 \times 10^4$, Ni: $3.5 \times 10^4$ $l \cdot mole^{-1} \cdot cm^{-1}$).

**Instrumental Analyses.** Interfacial tension measurements were carried out by the pendent drop method (*12*). Since extreme precision is significant for the conclusions made in this paper, previously unreported details of the experimental technique (*12*) are given as follows: To ensure that the drop size is controlled by the inside diameter of the needle tip and that aging of the surfactant solution is prevented, the needle is filled with excess surfactant solution prior to submersion into the base solution. This prevents the base from wetting the inner walls of the needle tip. Control of the drop size by the inside tip diameter requires careful cleaning of the needle tip with a pipe cleaner. The average drop life was 11–13 sec except for products $C_2$ (6–14 sec) and $D_2$ (2–3 sec). For reasons of high activity and droplet instability at the smallest applicable needle diameter (o.d. 0.013 cm), all values given are the average of three measurements.

Infrared spectra in the fundamental region were obtained in carbon tetrachloride using a Perkin Elmer Model 337 infrared spectrophotometer. When 0.05-mm microcells were used, the instrument was fitted with a beam condenser. The frequencies of aromatic amine absorptions (Table II) were determined with a Beckman IR-10 spectrophotometer equipped with an auxiliary recorder for scale expansion using ammonia vapor bands as points of reference, affording an accuracy of ±2 $cm^{-1}$. Studies in the near infrared region were carried out with a Cary Model 14 M recording spectrophotometer.

Microcoulometric thiol determinations were made with the Dohrmann cell (*13*) using *n*-dodecyl mercaptan as a standard.


(2) American Petroleum Institute Research Project 48, Report No. 22, 7/1/62–7/1/63.
(3) H. J. Coleman, C. J. Thompson, R. L. Hopkins, and H. T. Rall, *J. Chem. Eng. Data*, **10**, 80 (1965).
(4) E. C. Copelin, ANAL. CHEM., **36**, 2274 (1964).
(5) A. Treibs, *Angew. Chem.*, **49**, 682 (1936).
(6) H. N. Dunning, J. W. Moore, and M. O. Denekas, *Ind. Eng. Chem.*, **45**, 1759 (1953).
(7) D. L. Yarbroff, *ibid.*, **32**, 257 (1940).
(8) B. Nagy and U. Colombo, "Fundamental Aspects of Petroleum Geochemistry," Elsevier Publ. Co., Amsterdam, 1967, pp 206, 209, and 214.
(9) R. L. Shriner and R. C. Fuson, "The Systematic Identification of Organic Compounds," 3rd ed., Wiley, New York, 1948, p 60.
(10) T. H. J. De Boer and H. J. Backer, *Rec. Trav. Chim.*, **73**, 229 (1954).
(11) R. A. V. Raff and K. W. Doak, "High Polymers," Vol. XX, Part I, "Crystalline Olefin Polymers," Interscience, New York, 1965, p 1.
(12) H. Y. Jennings, *Rev. Sci. Instrum.*, **28**, 774 (1957).
(13) J. A. Challacombe and J. A. McNulty, "Applications of the Microcoulometric Titrating System as Detector in Gas Chromatography of Pesticide Residues," 144th National Meeting, ACS Div. Agr. Food Chem., Los Angeles, Calif., April 1963.

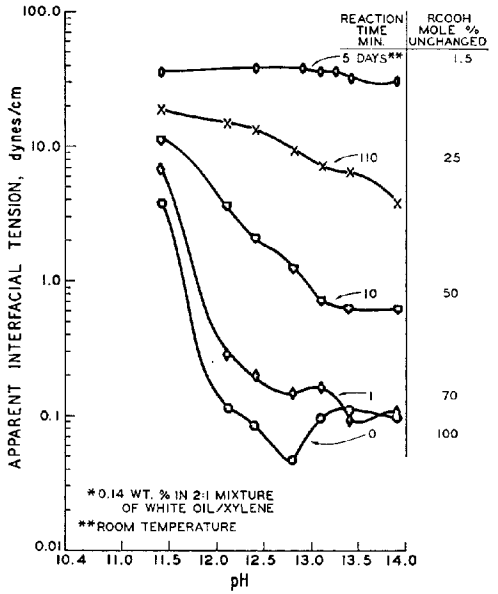


**Figure 1. Interfacial activity of major acidic extract produced by reaction with diazomethane at −50 °C**

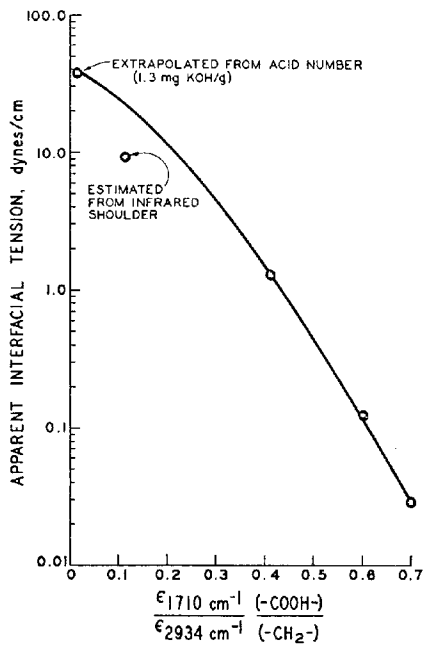


**Figure 2. Correlation between interfacial activity at pH 12.8 and carboxylic acid content after stepwise esterification**

## RESULTS AND DISCUSSION

The major acidic extract, whose isolation from crude oil with alkali has been described previously (*1*), contains 98 wt% of all carboxylic acids and almost all of the interfacial activity present in the California crude oil on which this study is being performed. All interfacial tensions reported are apparent data obtained by the pendent drop method (*12*) using short drop lives without attempting to attain thermodynamic equilibrium.

Figure 1 shows the effect of gradual esterification of the carboxylic acids with diazomethane on the interfacial activity of this extract. Examination of successive aliquots withdrawn from the reaction mixture (Figure 1) indicated a decrease in interfacial activity which paralleled the progressive esterification of carboxylic acids. The direct dependence of interfacial activity on carboxylic acid content after esterification is illustrated in Figure 2. Measurements were made at pH 12.8, the point of minimum interfacial tension. The acid content was determined by quantitative infrared analysis (*1*). The carboxylic acids of highest interfacial activity are esterified at the fastest rate as shown by comparison of the interfacial tension profile for the half-esterified extract at 10 min (Figure 1) with the profile for the untreated extract (Figure 3). The latter figure shows that twofold dilution reduces the interfacial activity of the extract far less than does 50% esterification of the carboxylic acids.

The progressive esterification was carried out under previously described conditions (*1*) that did not allow methylation of the phenols. Therefore, indirect elimination of mercaptans as contributors to the interfacial activity was possible as follows: Since mercaptans are weaker acids than phenols and the rate of methylation with diazomethane decreases with decreasing acidity of the acidic hydrogen, mercaptans would also have survived the diazomethane treatment. The interfacial inactivity of the esterification product, therefore, proves

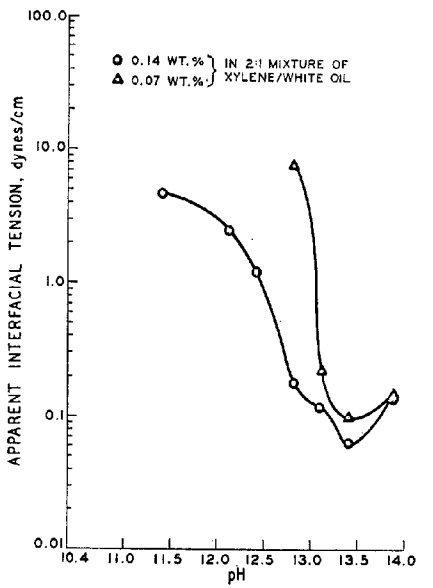


**Figure 3. Interfacial activity of major acidic extract before hydrolysis at different concentrations**

that phenols, mercaptans (if present), and any other anionic functional groups of equal or weaker acidity are in themselves not contributors to the interfacial activity of the extract. However, the more acidic thiophenols may have formed thioethers with diazomethane. Therefore, a further direct micro-

**Table I. Synergism between Phenols and Carboxylic Acids**

| Reactant[a] | Product | Hydrolysis: Time, hr | Hydrolysis: Solvent | Quantitative infrared analysis: $\epsilon OH^b/\epsilon CH_2$ | % $OH^c$ remaining | $AOH^d$ | % $OH^c$ remaining | $\epsilon COOH^e/\epsilon CH_2$ | % $COOH^e$ remaining | Apparent interfacial tension at pH 13.4, dynes/cm: Concentration, % 0.135 | 0.0675 |
|---|---|---|---|---|---|---|---|---|---|---|---|
| A | .. | 0 | ... | 0.067 | 100 | 0.22 | 100 | 0.65 | 100 | 0.060 | 0.096 |
| B | .. | 0 | ... | 0.023 | 34 | 0.05 | 23 | 0 | 0 | 35.22 | 46.57 |
| A | $C_1$ | 27 | Ethanol | 0.067 | 100 | 0.22 | 100 | 0.70 | 108 | ... | 0.125 |
| B | $D_1$ | 27 | Ethanol | 0.025 | 37 | 0.06 | 27 | 0.67 | 103 | ... | 0.073 |
| A | $C_2$ | 72 | Isopropanol/xylene | 0.066 | 99 | 0.21 | 95 | 0.67 | 103 | 0.097 | 0.106 |
| B | $D_2$ | 72 | Isopropanol/xylene | ... | ... | ... | ... | 0.75 | 115 | 0.008 | 0.071 |

[a] Compare reaction scheme.
[b] Extinction coefficient ratio of $\epsilon 3610\ cm^{-1}/\epsilon 2934\ cm^{-1}$, 8.86-cm cells, carbon tetrachloride.
[c] Based on major acidic extract prior to methylation or hydrolysis.
[d] Absorbance of 3610 $cm^{-1}$, 8.86-cm cells, carbon disulfide.
[e] Extinction coefficient ratio of $\epsilon 1710\ cm^{-1}/\epsilon 2934\ cm^{-1}$, 0.05-mm microcells, carbon tetrachloride.

coulometric method (*13–15*) of thiol determination was applied. Assuming a number average molecular weight of 350, the major acidic extract showed the negligible amount of 0.07% thiols, and some 10 selected fractions of high interfacial activity displayed a range of 0.003% to 0.15%. These values all are insignificant compared with the 70% or more carboxylic acid content.

Because in many active fractions the interfacially inactive (*1*) phenols were the most abundant alkali-soluble compounds in addition to carboxylic acids and because some evidence pointed toward carboxyphenols (*1*), it was of interest to study possible synergistic effects between the two types. The synergism of long chain alcohols on the surface tension of soap is known (*16*). The following scheme outlines the approach employed in examining synergism in the major acidic extract.

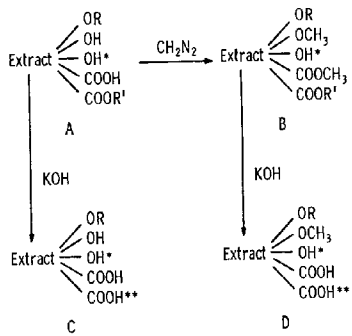


**Reaction scheme**

-OH* - Unreactive
-COOH** - Generated by Hydrolysis

After methylation of all carboxyl and the maximum possible amount of phenolic hydroxyl groups in the major acidic extract A, the carbomethoxy groups and other saponifiable derivatives in Product B were selectively hydrolyzed. The interfacial activity of Product D was compared with that of the unmethylated extract which had been hydrolyzed under identical conditions (Product C). The main difference between Products D and C is the higher phenolic hydroxyl content of the latter.

Determination of hydroxyl groups was carried out by two different methods of quantitative infrared analysis (Table I). For the internal ratio method (*17, 18*) in carbon tetrachloride (Column 1, Table I), the free hydroxyl absorption at 3610 $cm^{-1}$ served as an analytical peak; in order to avoid hydrogen bonding, spectra were obtained at a concentration of about 1 mmole/l in long path length cells. The reference peak, namely the methylene absorption at 2934 $cm^{-1}$, was determined after a further 10-fold dilution. In this fashion, all absorbances were determined in the accurately measurable range of 0.2–0.8 absorbance units. Traces of water which could not be avoided in carbon tetrachloride showed a doublet at 3710 $cm^{-1}$ and 3615 $cm^{-1}$ with a relative extinction coefficient ratio of 2:1. The phenol values at 3610 $cm^{-1}$ were, therefore, corrected for contribution of absorption by water, based on the intensity of the 3710 $cm^{-1}$ absorption. An alternative, but less accurate, phenolic hydroxyl determination was performed in carbon disulfide (Column 2, Table I) again at a concentration of 1 mmole/l. The carboxylic acid content was determined by the ratio method described previously (*1*) (Column 3, Table I). These analyses showed that repeated addition of excess diazomethane to the major acidic extract A at room temperature during a period of 6 weeks resulted in quantitative esterification of carboxylic acids and 66–77% etherification of phenols and complete loss of interfacial activity of product A (Table I). Some polymethylene formed from diazomethane itself (*11*) was easily separated by precipitation with benzene.

Hydrolysis of products A and B with *N*/2 ethanolic potassium hydroxide for 27 hours resulted in carboxyl contents slightly higher than those of the starting materials. No change in phenolic hydroxyl content could be detected within the experimental error of both methods of analysis (products $C_1$ and $D_1$, Table I). The formation of some carboxylic acids from saponifiable derivatives present in the extract is not surprising and has been reported previously for extended ambient temperature hydrolysis in ethanolic sodium hydroxide (*1*). Interfacial activities of this pair of products are shown in Figure 4 and values of apparent interfacial tension at pH

(14) R. L. Martin and J. A. Grant, ANAL. CHEM., **37**, 644 (1965).
(15) W. K. Seifert, "Novel Methods of Isolation and Identification of Odoriferous Compounds in Polypropylenebenzene Sulfonate," IVth International Congress on Surface Active Substances, Gordon and Breach, New York, 1967, Vol. 1, p 471.
(16) H. Schulman, W. Stoeckenius, and L. M. Prince, *J. Phys. Chem.*, **63**, 1677 (1959).
(17) H. H. Willard, L. L. Merritt, and J. A. Dean, "Instrumental Methods of Analysis," 3rd ed., D. Van Nostrand, Princeton, N. J., 1958, p 147.
(18) S. J. Cristol, W. K. Seifert, and S. B. Soloway, *J. Amer. Chem. Soc.*, **82**, 2351 (1960).

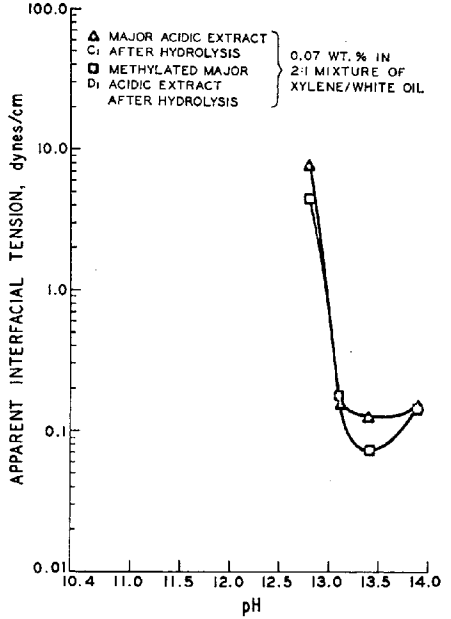


**Figure 4. Effect of 27-hour hydrolysis with *N*/2 ethanolic KOH on interfacial activity of major acidic extract and its methyl ester**

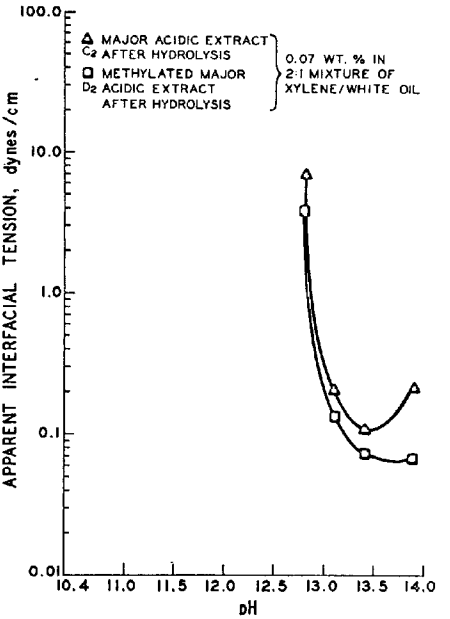


**Figure 5. Effect of 72-hour hydrolysis with *N*/2 KOH in isopropanol/xylene on interfacial activity of major acidic extract and its methyl ester (0.07%)**

13.4, the point of maximum activity, are listed in Table I. All interfacial tension measurements related to the problem of synergism between phenols and carboxylic acids were carried out in 2:1 xylene/white oil solvent to prevent the small amount of precipitation which was observed to occur with the previously described 1:2 xylene/white oil solvent. This latter solvent ratio was satisfactorily used for obtaining the data in Figure 1. Figure 4 indicates that product $D_1$ with the much smaller phenolic hydroxyl content (Table I) possesses greater interfacial activity than product $C_1$. As this conclusion depends mainly on the different values at the point of maximum interfacial activity, another pair of products ($C_2$ and $D_2$) was prepared using different conditions (solvent, reaction time) of hydrolysis (Table I).

In analogy to the first hydrolysis experiments, a small increase in carboxyl content was observed in both products while the phenolic hydroxyl content of the hydrolyzed product $C_2$ remained the same as that of the starting material A. Product $D_2$ possessed less phenolic hydroxyl content than product $D_1$. However, it could not be analyzed quantitatively owing to lack of sample (see Experimental). Figures 5 and 6 show the interfacial tension profiles of the product pair $C_2$ and $D_2$ at two concentrations. The very low apparent values of interfacial tension obtained for product $D_2$ at 0.14% concentration (Figure 6) may in part be due to the shorter drop life (see Experimental). In analogy to the previous hydrolysis experiments (Figure 4), however, now clearly outside any experimental error, these measurements illustrate the negative synergistic influence of phenols on the interfacial activity of carboxylic acids. The increase of carboxyl content of 15% after hydrolysis in the methylated extract $D_2$, in comparison with an increase of only 3% in the unmethylated product $C_2$, may be a contributing factor. However, it cannot solely be responsible for the higher interfacial activity of product $D_2$ since Figure 3 shows a smaller or equal change of interfacial activity at pH 13.4 by 50% dilution than that observed after methylation and hydrolysis (Figures 5 and 6). Nearly quantitative yields were obtained in all reactions (see Experimental), and therefore the possibility of fractionation during workup may also be excluded.

The conclusion is that phenolic hydroxyl groups present in this crude oil synergistically diminish the interfacial activity of the carboxylic acids.

Further support to these findings was obtained by observing greater interfacial activity in a mixture of isomers of phenyl stearic acid than in their hydroxylated analogs (*19*). A possible explanation for the greater activity of the crude oil extract after hydroxyl capping is that an increase in hydrophobic character and oil solubility has occurred causing a shift of the hydrophile lipophile balance (HLB) (*20*) toward the optimum for this system.

Previous work has shown (*12*) that it takes about 5 min to reach constant interfacial tensions between crude oil and surfactant solutions. The high activity of the materials described here results in much smaller drop lives, even at the smallest applicable needle sizes (see Experimental). Since the system, therefore, is not in thermodynamic equilibrium, theoretical explanations are difficult to make. However, one may speculate that hydrogen bonding of phenols to carboxylic acids or their anions in the oil phase or possibly the oil/water interface plays a role in this phenomenon. Thus, hydroxyl capping and decrease of association may in part be responsible for the observed increase of interfacial activity of the acids.

After these conclusions, the presence of potentially alkali-soluble, weakly acidic components other than phenols and

(19) C. E. Johnson, Chevron Oil Field Research Co., personal communication, 1967.
(20) L. I. Osipow, "Surface Chemistry, Theory and Industrial Applications," Reinhold, New York, 1962, p 311.

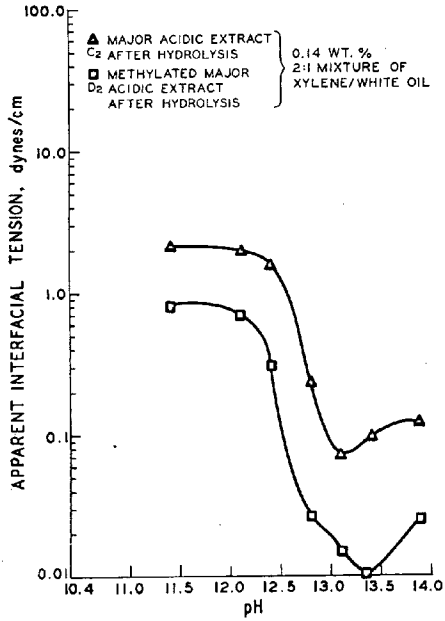


**Figure 6. Effect of 72-hour hydrolysis with *N*/2 KOH in isopropanol/xylene on interfacial activity of major acidic extract and its methyl ester (0.14%)**

thiols became of interest. The interfacially active major acidic extract (Figure 3) contained 1.3% nitrogen, which is 10 times the concentration present in the alkali-soluble inactive extract (*1*) and twice the concentration present in the crude oil. Nitrogen, in amounts ranging from 0.2% to 2%, was also found in fractions of highest interfacial activity isolated by separation of the major acidic extract (Figure 3). Since these fractions had previously been subjected to separations by various methods selective for carboxylic acids, it is assumed that at least part of the nitrogen is structurally incorporated in the interfacially active carboxylic acids. More specifically, an infrared absorption at 3483 $cm^{-1}$, which was prominent in the interfacially active major acidic extract, was investigated. This absorption falls in the —NH— stretching region. The active extract was, therefore, tested for porphyrins, primary and secondary amides, and amines.

Since some porphyrins isolated from petroleum possessed propionic acid side chains (*5*) and in view of the correlation of carboxylic acid content and interfacial activity shown in Figure 1, a contribution was conceivable provided this type of porphyrin was present in sufficient quantities. An analysis indicated the presence of 100 ppm V-type and 200 ppm Ni-type porphyrins in the crude oil. The interfacially active major acidic extract (Figure 3) possessed 80 ppm Ni-type and a trace of V-type porphyrins. When this is compared with 2.5 wt% of carboxylic acids, any contribution of porphyrins to the interfacial activity of this California crude oil has to be ruled out. Besides, Etioporphyrin II was found to absorb at a different wavelength (3310 $cm^{-1}$) from the interfacially active extract, and this absorption would not even be visible at the low concentration of porphyrins present. There are crude oils which contain much larger amounts of porphyrins (*21*).

(21) R. L. Fisher and H. N. Dunning, "Chromatography Resolution of Petroleum Aggregates," U. S. Bureau of Mines Rept. Invest., 5844, 1961, p 4.

However, studies on Boscan crude oil and United States oils have revealed (*8*) "that carboxylated porphyrins made up less than 5% of porphyrin material present in young oils with an even smaller proportion in older oils." Recently, specific porphyrins free of carboxylic acid groups were identified in Boscan crude by high resolution mass spectrometry (*22*). In view of this information and data reported in Figure 1 of this paper, the previous conclusion by H. N. Dunning and coworkers (*6*) obtained on a North Belridge Kern County, Calif., crude that "the metal porphyrin complex constituents of petroleum are major contributors to the interfacial activity exhibited by the petroleum sample" is questionable. It does not appear that their conclusion can have any general validity for the interfacial activity in crude oils.

Other alternatives for —NH— type compounds in crude oil are primary and secondary amides. Bezinger (*23*) determined the presence of amides in Russian crude oils; and cyclic amides, namely, 2-quinolones, have been reported (*4*) in a California crude oil. Imides are strongly acidic enough to be alkali soluble (*9*) and amides may also be soluble under the exhaustive extraction conditions applied here (*1*). A primary acid amide such as that of tetradecanoic acid shows a free —NH— doublet at 3400 $cm^{-1}$ and 3520 $cm^{-1}$ in dilute solution and a combination band (*24*) at 5100 $cm^{-1}$, all of which are absent in the active extract. Secondary amides, such as *N*-methyl hexadecanoic acid amide, have combination bands (*24*) at 5000–4975 $cm^{-1}$. The intensities are about one half of that of the —NH— overtone at 6802 $cm^{-1}$. The active extract lacks absorption at 5000 $cm^{-1}$. Absorption near 1650 $cm^{-1}$, characteristic for amide carbonyl (*4*), is very small and could also be due to tertiary amides (*25*). It is, therefore, concluded that significant amounts of primary and secondary amides are absent in the active extract.

The 3483 $cm^{-1}$ infrared band was identified as generally being due to secondary aromatic amine functional groups (*26*) as follows. Treatment of a 0.001 molar solution of the major acidic extract in carbon tetrachloride with excess HCl gas resulted in almost complete disappearance of this free —NH— band and simultaneous precipitation of the ammonium salt. More specifically, the fundamental —NH— frequencies of carbazole, indole, and pyrrole are reported (*27*) to occur as shown in Table II. A good review of the presence of these three compound types in petroleum is available (*28*), and various techniques of separation and identification for low molecular weight homologs in light catalytic cycle oil have been published more recently (*29*, *30*). These techniques involve

(22) E. J. Gallegos, 7th World Petroleum Congress, Mexico City, April 2, 1967, I.P. No. 30.
(23) N. N. Bezinger, M. A. Abdurakhamanov, and G. D. Gal'pern, "The Nitrogen Compounds in Petroleum. I. The Nature of the Neutral Nitrogen Compounds in Petroleum," Petroleum Chemistry, U.S.S.R., Vol. 1, 1962, pp 13–19; (Neftekhimiya, Vol. 1, 1961, pp 23–8).
(24) R. M. Bly, Chevron Oil Field Research Co., personal communication, 1967.
(25) L. J. Bellamy, "The Infrared Spectra of Complex Molecules," John Wiley, New York, 1954, p 182.
(26) K. Nakanishi, "Infrared Absorption Spectroscopy," Holden-Day, San Francisco, Calif., 1962, p 38.
(27) N. Fuson, M. L. Josien, R. L. Powell, and E. Utterback, *J. Chem. Phys.*, **20**, 145 (1952).
(28) D. R. Latham, I. Okuno, and W. E. Haines, "Nonbasic Nitrogen Compounds in Petroleum," ASTM Symposium on Hydrocarbon Analysis, Houston, Texas, Jan. 22, 1965, Publication No. 389, p 385.
(29) H. V. Drushel and H. L. Sommers, ANAL. CHEM., **38**, 19, (1966).
(30) D. K. Albert, ANAL. CHEM., **39**, 1113 (1967).

Table II. Free —NH— Infrared Data[a]

| | —NH— fundamental | | —NH— overtone (found) | | |
|---|---|---|---|---|---|
| | Reported (27) frequency, $cm^{-1}$ | Found frequency, $cm^{-1}$ | Frequency, $cm^{-1}$ | $\epsilon$[b] $l \cdot mole^{-1} \cdot cm^{-1}$ | $\epsilon$6135–6096 $cm^{-1}$[c] / $\epsilon$6849–6803 $cm^{-1}$ |
| Carbazole | 3483 | 3483 | 6816 | 1.58 | 0.07 |
| 2-Methyl carbazole | ... | ... | 6816 | 1.31 | 0.05 |
| Pyrrole | 3497 | 3495 | 6840 | 1.50 | 0.43 |
| Indole | 3491 | 3492 | 6835 | 1.98 | 0.25 |
| 2-Methyl 3-propyl indole | ... | 3481 | 6812 | 1.52 | 0.05 |
| 2,5-Dimethyl pyrrole | ... | 3479 | 6803 | 0.96 | 0.23 |
| Major acidic extract | ... | 3481–3 | 6812 | ... | 0.12 |

[a] In carbon tetrachloride solutions.
[b] Based on peak heights.
[c] Ratio of extinction coefficient of aromatic —CH— overtone to that of —NH— overtone.

gas chromatography which is not applicable to the higher molecular weight carboxylic acid type materials investigated here. Therefore, a brief study of the free —NH— bands in the fundamental and the near infrared region was conducted at concentrations of less than 0.05 mole/l to avoid intermolecular hydrogen bonding (*27*). The position of the fundamental —NH— frequency of the interfacially active (Figure 3) major acidic extract points to carbazoles and/or indoles substituted on the pyrrole ring and perhaps substituted pyrroles (Table II). The same conclusions are obtained from the —NH— overtone frequencies (Table II). However, ratios of extinction coefficients of —CH— overtones at 6135–6096 $cm^{-1}$ to those of —NH— overtones at 6849–6803 $cm^{-1}$ are sufficiently different for the model compounds listed in Table II to conclude that —NH— type components in the interfacially active major acidic extract are mainly indoles disubstituted on the pyrrole ring and/or carbazoles. Amounts of 5–6 mole % are calculated using the extinction coefficients of —NH— overtones and fundamental absorptions of carbazole and 2-methyl 3-propyl indole as standards and a number average molecular weight of 350 for the interfacially active extract.

The —NH— groups resist methylation with diazomethane under conditions of phenol methyl ether formation. Therefore, information on the effect of carbazoles and indoles on the interfacial activity of the naturally occurring crude oil carboxylic acids, as has been described for phenols in this paper, could not be obtained. However, model compound studies conducted elsewhere (*19*) indicated synergistic enhancement of interfacial activity of carboxylic acids by addition of indole.

Further elucidation of this problem appears possible by alkylation of the —NH— functions of the methylation products listed in Figures 4 and 5—e.g., by preparing the Grignard derivatives, —N—MgX, and reacting with dimethylsulfate—and subsequent interfacial tension and functional group studies analogous to the scheme described for phenols in this paper.


## ACKNOWLEDGMENT

The author wishes to express his appreciation to R. M. Bly for infrared measurements and stimulating consultation, to F. Baumann for microcoulometric thiol determinations, to W. D. Redfield for porphyrin determinations, and to R. House for helpful discussions. Technical assistance by L. T. Shoji for very accurate interfacial tension measurements and many pertinent observations and also by A. D. Alderman and J. P. S. Dhillon is acknowledged.

Received for review August 5, 1968. Accepted October 23, 1968. This paper presented in part at the Gordon Research Conference on Geochemistry, New Hampshire, August 1968, and in full at the 157th ACS Meeting, Division of Petroleum Chemistry, Minneapolis, Minn., April 1969.

# Sulfur Compound Type Distributions in Petroleum Using an In-Line Reactor or Pyrolysis Combined with Gas Chromatography and a Microcoulometric Sulfur Detector

**Harry V. Drushel**

*Esso Research Laboratories, Humble Oil and Refining Company, P.O. Box 2226, Baton Rouge, La. 70821*

**A rapid method for determination of sulfur compound types in petroleum was developed which involves dealkylation of the condensed thiophenes using an in-line catalytic reactor or noncatalytic pyrolysis. The resulting reaction products were separated by gas chromatography and the compounds containing sulfur were quantitatively detected with a Dohrmann microcoulometric sulfur detector. Nonthiophenic compounds, primarily aliphatic sulfides, were converted to $H_2S$ and detected in the same manner. Precision was 2 to 3% and analysis time was 1 hour. Data agreed very well with high resolution mass spectrometric analysis. Results from use of the method on hydrodesulfurized vacuum gas oils showed that the ease of desulfurization followed the order: benzothiophenes≫dibenzothiophenes>benzonaphthothiophenes.**

INCREASED EMPHASIS on clean air will require a reduction in the sulfur content of residual fuels for power plants and of fuel oil for home heating use. The petroleum industry has been active in developing desulfurization processes to meet these needs. A knowledge of the types of sulfur-containing compounds present and their fate during hydrodesulfurization would aid in understanding mechanisms and kinetics during process development.

The analysis of residual fuels and heavy vacuum gas oils is difficult and time-consuming. Drushel and Sommers (*1*) isolated and characterized sulfur compounds in a vacuum gas oil. The separation procedure, which required several steps involving chemical reaction and liquid–solid chromatography, resulted in the recovery of only about 60% of the sulfur compounds present. Such an approach would be unsuccessful on residua because of decreased reactivity, increased side reactions, and poor selectivity during chromatographic separation.

Martin and Grant (*2*) developed an excellent rapid method for sulfur compound types based on combination of a microcoulometric sulfur detector with gas chromatography. They circumvented the problems of high boiling point and complexity associated with gas oils and residua by subjecting the samples to catalytic dealkylation in a small laboratory-scale reactor. This step provided a quantitative measure of aliphatic sulfides which decompose to $H_2S$ and made the remaining condensed thiophenes amenable to separation by gas chromatography. Drushel and Sommers (*1*) compared data from this technique with data from isolation and characterization of sulfur compounds and found the results to be comparable for a vacuum gas oil.

This paper describes the use of pyrolysis and in-line reactors combined with gas chromatography and microcoulometry to obtain essentially complete sulfur compound type analysis. The method is rapid, requiring only the time necessary to complete the temperature program cycle on the gas chromatograph of about 1 hour. Precision for each of the sulfur types was within 2 or 3% based on the total sulfur content. The method has been applied to vacuum gas oils and their hydrodesulfurized products. Results from the use of this method have provided insight into the mechanism of hydrodesulfurization.

(1) H. V. Drushel and A. L. Sommers, ANAL. CHEM., **39**, 1819 (1967).
(2) R. L. Martin and J. A. Grant, *ibid.*, **37**, 649 (1965).

## EXPERIMENTAL

A simple block diagram of the combined apparatus is shown in Figure 1. A more detailed description of each component of the system is given below.

**Gas Chromatograph.** A Micro-Tek model 2500-R gas chromatograph (GC) was used throughout this study.

For the earlier portion of the study, involving use of the in-line, $Al_2O_3$-filled, dealkylation reactor, ¼-inch aluminum columns were used. A metal transfer line carried the effluent from the GC to the combustion unit of the Dohrmann microcoulometer. For this study the combustion tube and special GC inlet system as supplied by Dohrmann Instruments was used. The carrier gas was helium; the flow rate was 50 cc/min.

For the latter portion of this study, in which a pyrolyzer and glass columns were used, a special modification was made in order to use the temperature programming feature and oven of the GC. The ordinary inlet and outlet blocks were bypassed. All of the glass components of the system were mounted in a transite housing which was inserted between the main housing of the GC and the removable oven cover. This permitted operation of the all-glass system and use of the temperature programming feature of the GC without having to dismantle any portion of the inlet or outlet block section of the chromatograph. The carrier gas was nitrogen; the flow rate was 50 cc/min.

**In-Line Alumina Dealkylation Reactor.** The reactor consisted of a 6-inch length of stainless steel tube of about ¼-inch i.d. which was packed with a 3-inch length of F-20 chromatographic grade alumina. The temperature was maintained at 600 °C by means of electrical resistance wire wound around the reactor insulated with a layer of asbestos. The temperature necessary to carry out dealkylation using $Al_2O_3$ was previously established by Martin and Grant (*2*). The inlet end of the reactor was machined to retain a Silicone rubber septum through which samples were injected. Samples were introduced directly onto the alumina packing. The helium carrier gas, which entered the reactor near the septum, swept the cracked products through a heated ⅛-inch stainless steel transfer line to the GC column. A ¼-inch x 10-foot column packed with 10% Carbowax 20M on Chromosorb W was used to obtain the necessary separation between the aromatic sulfur compound types. The temperature was programmed from room temperature to a maximum of 275 or 300 °C in order to achieve elution of the condensed thiophenes. Such high temperatures accelerated deterioration of the column requiring its replacement after three or four weeks.

**Pyrolyzer.** The pyrolyzer was constructed from Vycor glass tubing using several loops representing an overall length of about 12 inches (see Figure 2). At carrier gas flow rates near 50 cc per minute, this length of tubing provided several seconds residence time for pyrolysis. A Silicone rubber septum, through which the sample was injected, was mounted where the carrier gas entered the pyrolyzer. The exit end of the pyrolyzer made

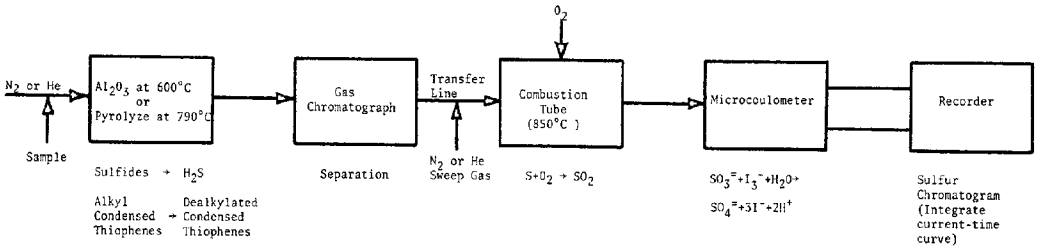


**Figure 1. Schematic diagram of combined apparatus for sulfur compound type determination**

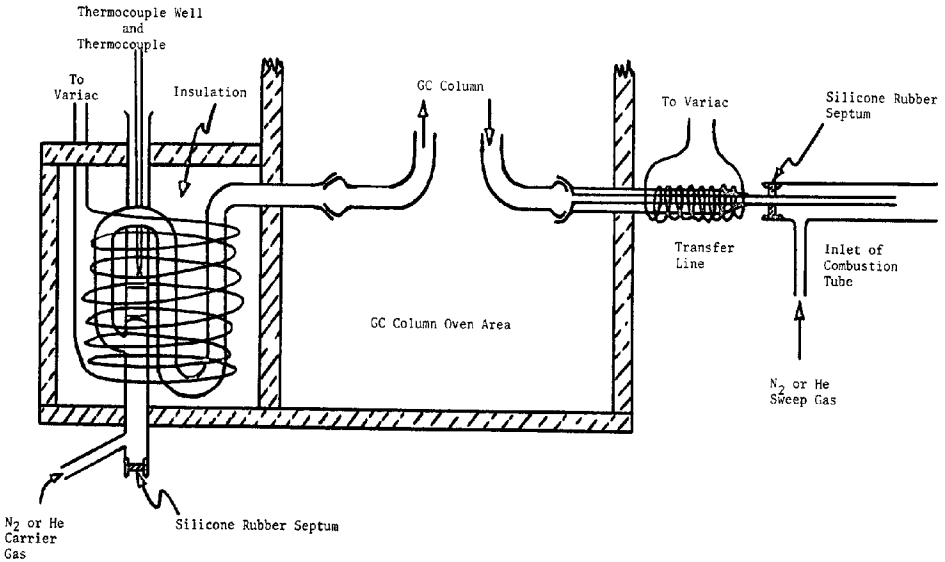


**Figure 2. Schematic diagram of all-glass pyrolysis–GC–transfer line system**

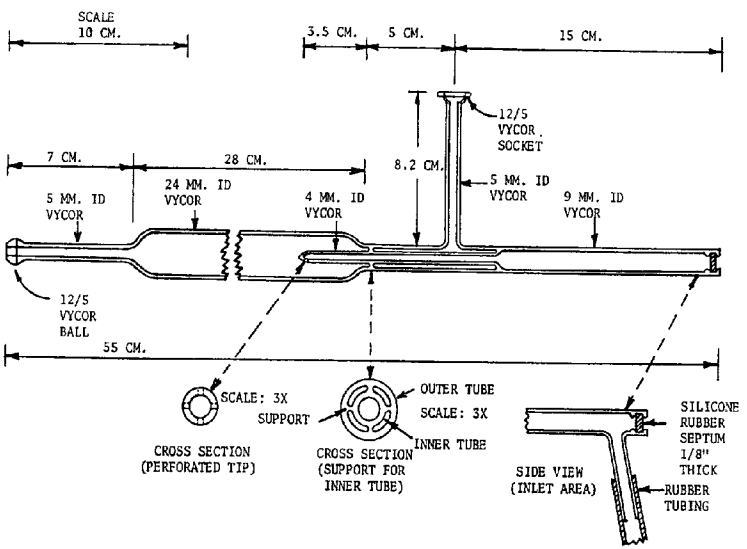


**Figure 3. Combustion tube for determination of sulfur by microcoulometry**

connection with the glass GC column by means of a ball joint. The joint was well greased with Silicone grease and held in place by means of a screw-tightened clamp.

**Glass Column and Transfer Line.** The U-shaped GC columns were made from ¼-inch glass tubing with ball joints at each end. Components separated by the column were transferred to the combustion tube by means of a ⅛-inch i.d. glass transfer line. The transfer line was heated to a temperature of about 350 °C using electrical resistance wire insulated with asbestos. The capillary tip of the transfer line made connection to the inlet of the combustion tube by means of a Silicone rubber septum as shown in Figure 2.

**Combustion Tube.** The combustion tube was constructed from Vycor glass as shown in Figure 3. Essentially, it was an open, unpacked combustion tube of large internal diameter into which the sample was swept by means of an inert carrier gas ($N_2$ or He). The combustion zone, through which oxygen flowed, was maintained at a temperature of 850 °C. The inlet area was maintained at 550 °C. This tube permitted the direct injection of up to 5 μl of sample without carbon formation or incomplete combustion. The $SO_2$ produced by the combustion of sulfur compounds was titrated by means of the Dohrmann T-300-P titration cell.

The combustion tube shown in Figure 3 was used successfully for the determination of total sulfur by combustion using the Dohrmann microcoulometer. Samples containing as little as 1 ppm sulfur were analyzed in less than 2 minutes by direct injection with a syringe. Precision ($2\sigma$) was of the order of 3 ppm at the 100-ppm sulfur level. The use of this combustion tube for determination of total sulfur will be the subject of a future publication.

**Microcoulometer.** The Dohrmann microcoulometer was used throughout this study. In most cases, the bias voltage was 100-120 mV, the gain was set at 20, and the range (resistance in ohms) varied according to the amount of sample and sulfur content for each analysis. In addition, the signal from the microcoulometer to the recorder was filtered by means of a simple resistance-capacitance network to reduce short term noise. The current was recorded on a 1-mV recorder with Disc integrater.

**Reference Compounds.** All reference compounds used for calibration purposes were Eastman, white-label, organic chemicals. Solutions of the pure compounds were made up in spectro-grade toluene. Petroleum samples containing more than 0.2 to 0.4% sulfur were diluted with toluene.

## DISCUSSION OF RESULTS

**Method Using an In-Line Alumina Dealkylation Reactor.** A typical sulfur chromatogram of a vacuum gas oil (VGO) fraction (425–455 °C) using the alumina in-line reactor at 600 °C

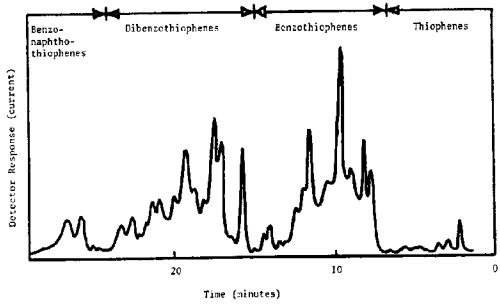


**Figure 4. Sulfur chromatogram of a VGO fraction (425–455 °C) using the in-line alumina dealkylation reactor at 600 °C**

**(10-ft Carbowax 20M Column)**

is shown in Figure 4. The alumina reactor serves to decompose the aliphatic sulfides (designated as nonthiophenic sulfur, NTS) to $H_2S$ and thiols and at the same time dealkylates the condensed thiophenes sufficiently so that they may be separated on the GC column. Figure 4 shows that sufficient dealkylation has taken place for adequate separation of the sulfur compounds by type. A serious difficulty was encountered, however, because of the fact that the system was constructed of metal components. The $H_2S$ produced during the reaction was completely lost as a result of reaction with the exposed metal surfaces of the reactor, inlet block, column, outlet block, or transfer line. Even though the $H_2S$ was lost, it was possible to calculate the distribution of the various condensed thiophenes. The distribution was calculated on the basis of the relative area for each of the groups of peaks representing the various thiophene types. The area, being proportional to the amount of sulfur detected, provided data in terms of the relative weight per cent of the total thiophenic sulfur present. Also, the results were normalized to 100% rather than calculated on the basis of the amount of sulfur injected into the reactor-GC system.

Table I lists some of the data obtained on a typical 425–455 °C vacuum gas oil fraction as well as a corresponding hydrodesulfurized product. These data are also compared with results obtained using the small laboratory alumina cracking reactor as proposed by Martin and Grant (*2*). The results from the in-line reactor agree quite well with those using the small laboratory reactor. There is also agreement, as shown in Table I, with our earlier study (*1*) in which we isolated the

**Table I. Sulfur Compound Type Distribution Using the In-Line Alumina Reactor Combined with Gas Chromatography and a Microcoulometric Sulfur Detector (Comparison with Other Methods)**

| | Total S (wt %) | Relative wt % of thiophene sulfur | | | |
|---|---|---|---|---|---|
| | | Thiophene (T) | Benzothiophene (BT) | Dibenzothiophene (DBT) | Benzonaphtho-thiophene (BNT) |
| VGO[a] fraction (425–455 °C) | 2.76 | | | | |
| In-line alumina reactor | | 3.6 | 30.3 | 52.7 | 13.4 |
| | | 2.5 | 30.7 | 55.3 | 11.6 |
| | | 1.6 | 33.8 | 52.1 | 12.6 |
| Separate laboratory alumina dealkylation reactor | | 1.5 | 30.4 | 52.4 | 15.6 |
| | | 2.0 | 33.6 | 51.2 | 13.1 |
| High resolution MS analysis of isolated sulfur compounds | | 2 | 37 | 46 | 15 |
| Hydrodesulfurized product of above | 0.29 | | | | |
| In-line alumina reactor | | 4.1 | 6.4 | 68.3 | 21.2 |
| Separate laboratory reactor | | 4.6 | 10.7 | 63.0 | 21.7 |

[a] Vacuum gas oil.

sulfur compounds and characterized them by means of high resolution mass spectrometry.

**Method Using Pyrolysis.** BEHAVIOR OF SOME REFERENCE COMPOUNDS. The distribution of sulfur-containing products from the pyrolysis of reference compounds is tabulated in Table II. These data show that thiophene, benzothiophene (BT), and dibenzothiophene (DBT) survive pyrolysis at 790 °C with little change. Only a very small amount of $H_2S$ is produced from these compounds. However, hexyl sulfide undergoes decomposition to produce essentially $H_2S$. If the pyrolysis temperature is raised to 900 °C even the thiophenic compounds decompose to produce measurable amounts of $H_2S$. In addition, at the higher temperature a significant amount of sulfur is not recovered as compared to pyrolysis at 790 °C. The loss of sulfur at the higher temperature is attributed to incorporation of sulfur into carbon which tends to form more readily at the higher temperature.

EFFECT OF TEMPERATURE. Figure 5 shows the effect which pyrolysis temperature has on the per cent of total sulfur which is not recovered during the analysis. As the pyrolysis temperature is increased, more of the sulfur becomes fixed as an integral part of the carbon deposited on the surface of the pyrolyzer. Concurrently, the higher temperature probably promotes the formation of more highly condensed aromatic sulfur compounds (not necessarily present in the sample originally) which cannot be eluted from the gas chromatograph because of their high boiling point.

The distribution of sulfur compound types as a function of pyrolysis temperature is presented in Table III. Near 650 °C the temperature is too low to achieve sufficient dealkylation of the thiophenic nuclei and they are not resolved during the gas chromatographic separation. Increasing the pyrolysis temperature increases the relative percentage of $H_2S$, but, conversely, decreases the relative percentage of the condensed thiophenes as well as the overall recovery of sulfur.

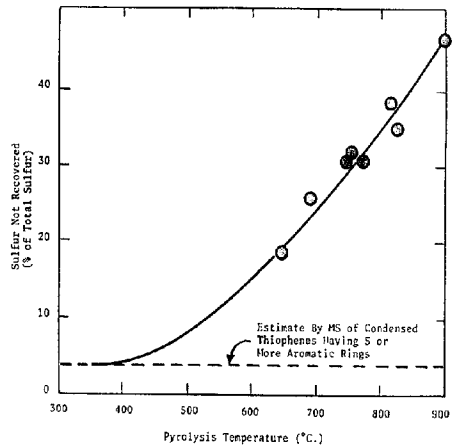


**Figure 5. Effect of pyrolysis temperature on sulfur recovery**

**(VGO, 425-455 °C, 2.91% S)**

Figure 6 depicts the conversion of normal hexyl sulfide to $H_2S$ (or thiols) as a function of pyrolysis temperature. From this figure it is seen that the decomposition of the normal hexyl sulfide begins at 475–525 °C. The conversion to $H_2S$ is essen-

**Table II. Pyrolysis Behavior of Some Reference Sulfur Compounds**

| | % of Total sulfur injected | | | | |
|---|---|---|---|---|---|
| Pyrolysis at 790 °C | $H_2S$[a] | Prepeaks | Original compound | Postpeaks[b] | Not recovered |
| *n*-Hexyl sulfide | 98.5 | 0 | 0 | 0 | 1.5 |
| Thiophene | 0 | 0 | 95.6 | 3.5 | 0.9 |
| Benzothiophene | 0.2 | 0 | 88.7 | 11.1 | 0 |
| Dibenzothiophene | 2.3 | 0 | 86.6 | 11.4 | 0 |
| Pyrolysis at 900 °C | | | | | |
| *n*-Hexyl sulfide | 72.6 | 12.5 | 0 | 0 | 14.9 |
| Thiophene | 6.9 | 0 | 82.2 | 2.9 | 8.0 |
| | 6.1 | 0 | 81.2 | 1.3 | 11.4 |
| | 7.9 | 0 | 84.2 | 1.5 | 6.4 |
| Benzothiophene | 5.1 | 3.1 | 67.0 | 18.7 | 6.1 |
| Dibenzothiophene | 1.3 | 0.8 | 70.0 | 27.9 | 0 |
| Phenyl sulfide | 58.8 | 0 | 0 | 21.2 | 20.0 |

[a] Includes unresolved thiol.
[b] Only slightly greater retention time and would be included in a typical analysis.

**Table III. Effect of Pyrolysis Temperature on the Distribution of Sulfur Compound Types and the Sulfur Not Recovered**
**(2 μl VGO, 425-455 °C, 2.91% S, 1/10 dilution in toluene)**

| | % of Total sulfur injected | | | | | |
|---|---|---|---|---|---|---|
| Pyrolysis temperature (°C) | Aliphatic sulfides, AS ($H_2S$) | BT | DBT | BNT | Sulfur not recovered SNR | BNT + SNR |
| 565 | 2.0 | | (Sulfur types not dealkylated and resolved) | | | |
| 635 | 6.5 | | (Sulfur types not dealkylated and resolved) | | | |
| 690 | 15.4 | 21.0 | 27.1 | 10.7 | 25.8 | 36.5 |
| 746 | 17.4 | 17.0 | 22.1 | 12.5 | 31.0 | 43.5 |
| 755 | 16.8 | 17.4 | 22.0 | 11.9 | 31.9 | 43.8 |
| 774 | 17.3 | 17.5 | 22.2 | 12.1 | 30.9 | 43.0 |
| 815 | 22.8 | 12.5 | 16.0 | 10.3 | 38.4 | 48.7 |
| 900 | 28.0 | 9.5 | 15.8 | 6.7 | 40.0 | 46.7 |

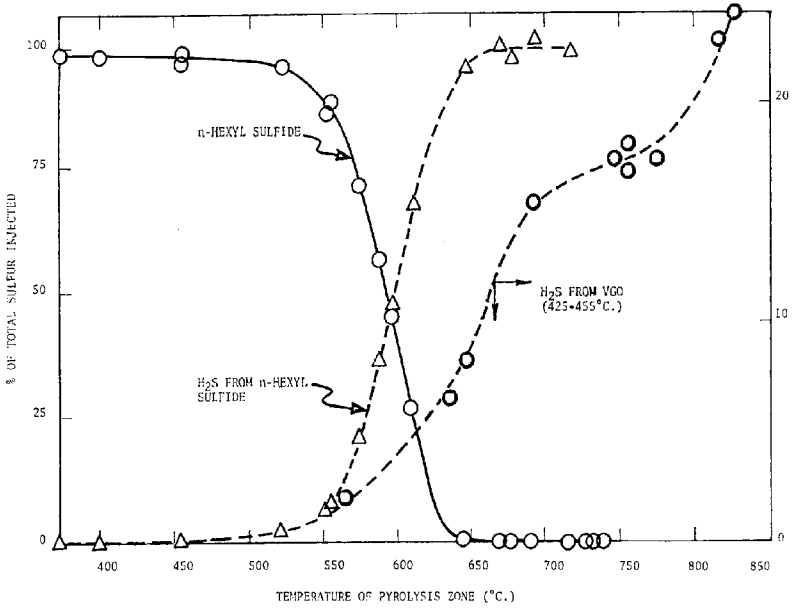


**Figure 6. Effect of temperature on decomposition of aliphatic sulfides to $H_2S$**

tially complete once temperatures near 650 °C are reached. In this same figure, a plot of the relative percentage of $H_2S$ produced from a vacuum gas oil fraction (425–455 °C) is shown as a function of pyrolysis temperature. In this case, the temperature required to decompose the aliphatic sulfides in the sample appears to be about 50° or so above that of the pure reference compound. In fact, there seems to be a plateau in the curve around 700–800 °C. Above 790 °C the relative percentage of $H_2S$ increases still more. It is felt that this increase above 790 °C can be attributed to the decomposition of sulfur-containing molecules which are more complex than simple aliphatic sulfides. The presence of diaryl or alkyl aryl sulfides is indicated. Thiaindanes may be responsible for such behavior. Some data obtained with pure compounds indicate that about half of the thiaindane yields $H_2S$ while the remainder dehydrogenates to form benzothiophenes.

INFLUENCE OF SAMPLE BOILING RANGE ON THE RECOVERY OF SULFUR. Figure 7 shows that the sulfur in thiophenic structures with 4 aromatic rings or more plus the sulfur which is not recovered increases as a function of the boiling range of the sample being analyzed. Such a trend is due undoubtedly to a combination of a real increase in the percentage of highly condensed thiophenes as well as an increase in the amount of sulfur which remains bound to the carbon produced during pyrolysis. As the boiling point increases, the aromatic structures which are usually present tend to form carbon more readily.

CHOICE OF GLC COLUMN. An SE-30 column was tried as a typical nonpolar column for separation according to boiling point. The column functioned well but because of the high temperatures needed the substrate tended to bleed excessively. This caused the formation of deposits of finely divided silica in the combustion tube.

A column prepared from de-ashed (to remove metal catalyst residues) ethylene–propylene copolymer on Chromasorb W provided good resolution with separation by boiling point (see Figure 8). A similar column prepared from amorphous poly-

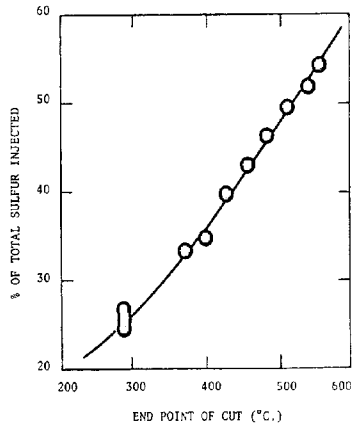


**Figure 7. Effect of boiling point of fraction on sulfur in benzonaphthothiophenes plus sulfur not recovered (BNT + SNR)**

propylene supported on Chromasorb W treated with excess potassium carbonate behaved in a similar manner except that the $H_2S$ peak was missing (see Figure 8). This permits the more accurate measurement of thiophene which is not always resolved from the $H_2S$. If the $H_2S$ peak is large, the thiophene peak may be completely engulfed. Fortunately, the thiophene content of the VGO fractions is rather low and the simple thiophenic species are easy to remove by hydrodesulfurization.

A polar column should separate the condensed thiophene types better than a nonpolar column, as pointed out by Martin and Grant (2). For this reason we selected a Carbowax 20M column. Typical sulfur chromatograms are shown in Figure 9. Note that the resolution between contiguous members of an homologous series is less but the separation by type is better than with the nonpolar columns. One disadvantage of the

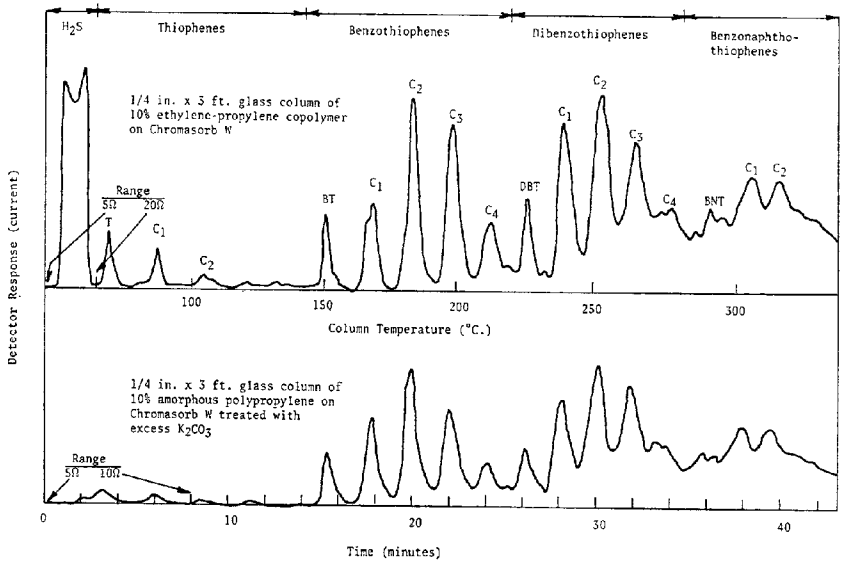


**Figure 8. Behavior of nonpolar columns in separating sulfur compounds from pyrolysis of VGO**

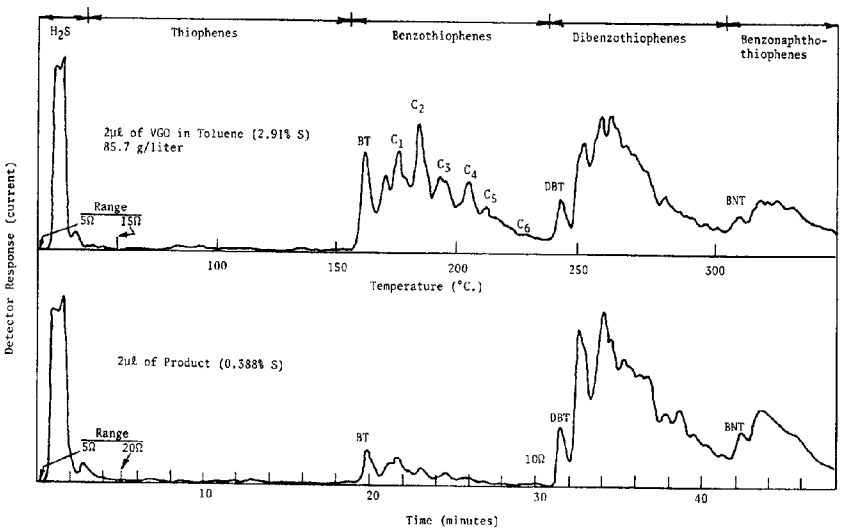


**Figure 9. Comparison of sulfur chromatograms of pyrolyzed VGO and hydrodesulfurized product (399–425 °C fraction)**

Carbowax 20M column is its temperature limit which permits elution of the condensed thiophenes with up to only four aromatic rings, the benzonaphthothiophenes (BNT).

ANALYSIS OF VGO AND HYDRODESULFURIZED PRODUCT FRACTIONS. Figure 9 compares the sulfur chromatograms of a typical VGO fraction with a hydrodesulfurized product fraction of the same boiling range. Note that a very striking decrease in the relative percentage of benzothiophenes (BT) has occurred as a result of hydrodesulfurization. On the other hand, dibenzothiophenes (DBT) and benzonaphthothiophenes (BNT) appear to be more difficult to remove by hydrodesulfurization. The relative area of the $H_2S$ peak is about the same after hydrodesulfurization as it is before. It is possible that hydrogenated intermediate products are formed which are not catalytically cracked (carbon–sulfur bond scission). For example, benzothiophenes may become hydrogenated to form thiaindanes, which, if not catalytically cracked, would fall in the category of nonthiophenic sulfur (NTS) by this method. The concentration of intermediate thiaindanes might even be higher than the NTS value because pyrolysis of such compounds would yield some $H_2S$ (or NTS) and some benzothiophenes (BT). This explanation is logical because aliphatic sulfides (the major compound type in the NTS category) originally present in the VGO should have been essentially removed by hydrodesulfurization.

Table IV lists results obtained on the distillate fractions of the VGO and its product. The data include the weight percentage of each fraction, the total sulfur content, the ali-

Table IV. Sulfur Compound Type Distributions Using the Pyrolysis–GC–Microcoulometric Method
(Pyrolysis Temperature 790 °C)

| VGO[b] fraction | Fraction wt % | Total sulfur (wt %) | Aliphatic sulfide sulfur[a] Wt % | Aliphatic sulfide sulfur[a] % of total S | Relative wt % of total sulfur: Non-thiophenic sulfur (NTS) | Benzo-thiophene (BT) | Dibenzo-thiophene (DBT) | Benzo-naphtho-thiophene (BNT) | Sulfur not recovered (SNR) |
|---|---|---|---|---|---|---|---|---|---|
| Total VGO | — | 2.86 | 0.62 | 21.7 | — | — | — | — | — |
| Init–371 | 1.5 | 2.94 | 0.62 | 21.1 | 14.1 | 25.4 | 27.2 | 11.5 | 21.8 |
| 371–399 | 3.8 | 2.93 | 0.57 | 19.5 | 15.7 | 22.0 | 27.5 | 9.4 | 25.4 |
| 399–425 | 19.0 | 2.91 | 0.54 | 18.6 | 16.4 | 20.0 | 23.7 | 9.7 | 30.2 |
| 425–455 | 22.6 | 2.81 | 0.53 | 18.9 | 15.9 | 19.0 | 22.2 | 12.1 | 30.9 |
| 455–482 | 16.3 | 2.79 | 0.54 | 19.4 | 18.8 | 18.1 | 16.6 | 13.4 | 33.0 |
| 482–510 | 18.6 | 2.83 | 0.56 | 19.8 | 21.1 | 16.1 | 13.2 | 11.1 | 38.5 |
| 510–538 | 13.4 | 3.03 | 0.57 | 18.8 | 22.2 | 14.4 | 11.7 | 9.7 | 42.0 |
| 538–552 | 3.6 | 3.24 | 0.62 | 19.1 | 22.8 | 12.8 | 10.1 | 8.4 | 45.9 |
| Bottoms | 1.2 | 3.43 | 0.60 | 17.5 | 22.6 | 10.8 | 7.7 | 4.9 | 54.0 |
| Hydrodesulfurized product fraction | | | | | | | | | |
| Total product | — | 0.406 | 0.045 | — | — | — | — | — | — |
| Init–371 | 7.9 | 0.242 | — | — | 14.1 | 4.7 | 39.2 | 8.5 | 33.5 |
| 371–399 | 6.5 | 0.338 | — | — | 13.5 | 5.7 | 42.9 | 13.2 | 24.7 |
| 399–425 | 23.6 | 0.388 | — | — | 14.1 | 4.4 | 32.3 | 12.5 | 36.7 |
| 425–455 | 15.6 | 0.393 | — | — | 14.0 | 4.2 | 26.0 | 15.6 | 40.2 |
| 455–482 | 20.8 | 0.425 | — | — | 18.8 | 3.7 | 16.9 | 12.9 | 47.7 |
| 482–510 | 18.6 | 0.453 | — | — | 20.4 | 3.9 | 15.1 | 10.6 | 49.9 |
| 510–538 | 2.8 | 0.477 | — | — | 26.6 | 5.2 | 13.0 | 9.7 | 45.6 |
| 538–552 | 3.6 | 0.508 | — | — | 28.1 | 4.4 | 11.4 | 8.6 | 47.5 |
| Bottoms | 0.8 | 0.565 | — | — | 29.1 | 10.2 | 17.9 | 10.5 | 32.3 |

[a] By direct determination using the iodine complex method (*3*).
[b] Vacuum gas oil..

phatic sulfide sulfur (*3*), and the sulfur compound type distribution. It is interesting that the aliphatic sulfides and NTS agree in fractions near the middle of the VGO boiling range. The iodine complex method indicates a rather constant relative percentage of aliphatic sulfide sulfur throughout the VGO boiling range. The NTS, however, shows a gradual increase with boiling point. This may imply an increase with boiling point of alkyl aryl sulfides or thiaindanes which are only partially detected by the iodine complex method.

(3) H. V. Drushel and J. F. Miller, ANAL. CHEM., **27**, 495 (1955).

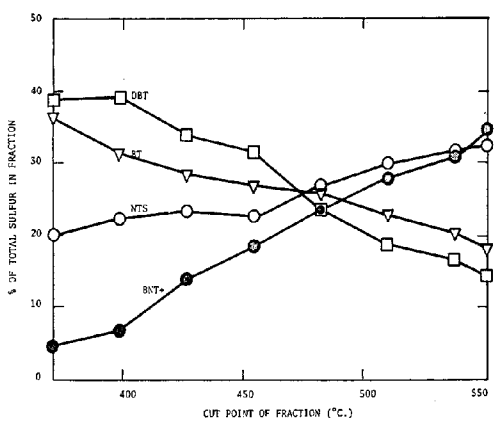


**Figure 10. Sulfur compound type distribution in VGO fractions**

**NTS —nonthiophenic sulfur**
**BT —benzothiophenes**
**DBT —dibenzothiophenes**
**BNT+—condensed thiophenes with four (benzonaphthothiophenes) or more aromatic rings**

A very striking decrease in benzothiophenes is produced by hydrodesulfurization. As a result, DBT and BNT tend to be the major thiophenic species in the product. The ease of sulfur removal, in general, follows the order: BT >> DBT > BNT+.

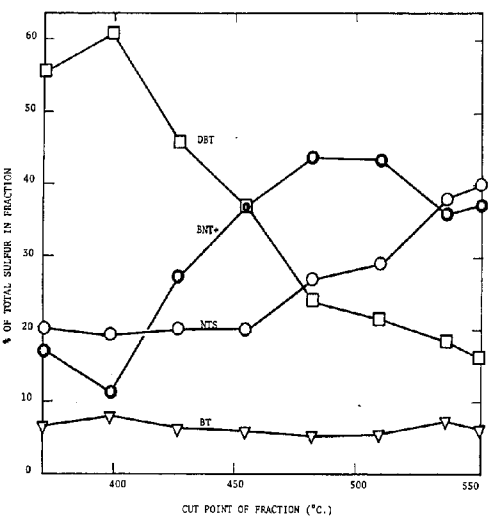


**Figure 11. Sulfur compound type distribution in hydrodesulfurized product fractions**

**NTS —nonthiophenic sulfur**
**BT —benzothiophenes**
**DBT —dibenzothiophenes**
**BNT+—condensed thiophenes with four (benzonaphthothiophenes) or more aromatic rings**

It was assumed that the amount of sulfur remaining with the carbon at 790 °C was about 30% of the total sulfur in the case of the VGO fractions as shown in Figure 5. Therefore, the values for BNT and SNR were combined and reduced by 30 to yield a value for a category of thiophenes with four or more aromatic rings (BNT+). After making this correction, the values were normalized to 100%. Corrected results were plotted for the VGO fractions (see Figure 10) and corresponding product fractions (see Figure 11) as a function of the cut point of the fractions. The decrease in the relative percentage of benzothiophenes and the increase in the relative percentage of dibenzothiophenes can be seen by comparison of Figures 10 and 11.


ACKNOWLEDGMENT

The author thanks J. S. Ellerbe for assistance in performing the experimental work and J. R. Wagner for constructing the all-glass pyrolyzer, GC column, transfer line, and combustion tube.

RECEIVED for review June 13, 1968. Accepted January 17, 1969.


# Composition of Asphalt Based on Generic Fractionation, Using Solvent Deasphaltening, Elution-Adsorption Chromatography, and Densimetric Characterization


L. W. Corbett

*Esso Research and Engineering Co., P.O. Box 51, Linden, N.J. 07036*



**This paper describes a convenient method for determining asphalt composition based on fractionation into four generic components. The method involves solvent deasphaltening for recovery of asphaltenes, followed by elution-adsorption chromatography to yield saturates, naphthene-aromatics, and polar-aromatics. The densimetric method was then applied to define the average chemical structures present. Examples are presented to show the effect of distillation and crude source, noting that molecular weight as well as chemical structure varies appreciably. This suggests that these two characteristics should be considered along with the proportion of each component when making asphalt composition analyses.**


THE COMPOSITION OF ASPHALT has been the subject of much study in the past because such data can provide help in the handling of problems related to the usage of asphalt. As evidence of this, there are over eighty publications dealing with the separation and/or characterization of asphalt components. A few of the more commonly cited literature references are indicated here (*1-5*).

Considering the variables of both molecular size and the types of hydrocarbons present in an asphalt, one is immediately impressed with the complexity of composition. This consideration also suggests that no one method can handle all of these variables without involving a lengthy procedure. Taking a compromise approach, a simplified method was worked out whereby the separation into hydrocarbon types was emphasized. As a result it was found that a separation could be made which yielded four classes or types of components, and that each of these represented a reasonably distinct generic hydrocarbon class. This paper describes the technique used in making such a separation, together with examples showing the effect of vacuum distillation and crude source on the proportioning of the four components. In addition, the densimetric method (*6*) was applied in order to chemically characterize each of the components and to support the logic of the generic classification.

## EXPERIMENTAL

**Apparatus.** All work reported was performed with standard laboratory equipment except for the chromatographic column. The column was prepared from a piece of 3.1 × 100-cm borosilicate tubing to which was attached a 2-mm stop-cock made of Teflon (Du Pont) with vernier adjustment and with 35/25 ball joint fittings at both top and bottom.

**Procedure.** The procedure used is based upon solvent precipitation of asphaltenes followed by elution-adsorption chromatography of the petrolene fraction, illustrated by the scheme shown in Figure 1. As common to most methods, asphaltenes are precipitated first with a paraffin solvent at a high dilution ratio, by the principle of disparity of molecular size and type between solvent and asphaltenes. Normal heptane is preferred for this step because of its purity and other properties that permit filtration steps without precipitation of wax components. It is also used in one standardized test (*7*) for asphaltene content of bitumen. The chromatographic step which follows involves the use of active alumina and elution solvents of increasing polarity. This step permits the separation of components of different polarity as illustrated in Figure 2 which shows the relationship between the eluate and the per cent of petrolene fraction recovered. It will be noted that three distinct concentrations can be separated depending upon the eluant and the volume of the eluate. In previous publications (*8, 9*), it was shown that nonpolar solvents of the type used here will elute saturated hydrocarbons under these conditions with less than 0.5% carry through of aromatics (*10*) or other polar compounds. A fraction of intermediate polarity can then be removed with benzene as eluant without release of the highly polar components. This intermediate fraction has been designated as naphthene-aromatics because of the predominance of these two hydrocarbon types.


(1) J. Marcusson, *Z. Agnew Chem.*, **29**, 21 (1916).
(2) F. R. Grant and A. J. Hoiberg, *Proc. AAPT*, **12**, 87 (1940).
(3) F. S. Rostler and H. W. Sternberg, *Ind. Eng. Chem.*, **41**, 598 (1949).
(4) R. N. Traxler and H. E. Schweyer, *Oil Gas J.*, **52** (19) 158 (1953).
(5) L. R. Kleinschmidt, Jr. *Res. NBS* **54**, 163 (1955).
(6) L. W. Corbett, ANAL CHEM., **36**, 1967 (1964).
(7) Inst. of Pet. Standards for Petroleum and its Products 143/67, Part 1, Sec. 2, 25th Ed. (1966).
(8) L. R. Snyder, ANAL. CHEM., **33**, 1538 (1961).
(9) L. R. Snyder and W. F. Roth, *ibid.*, **36**, 128 (1964).
(10) L. W. Corbett, ACS, Petroleum Division, April 1967.

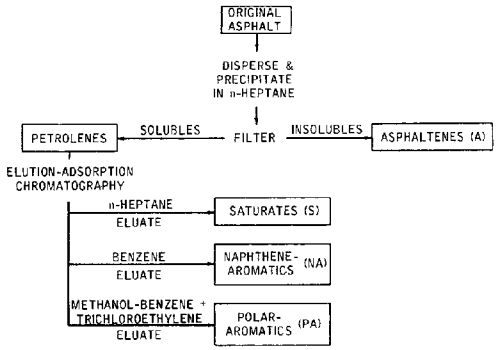


**Figure 1. Scheme for separation into four generic components**

The justification of this becomes apparent later as the result of characterization analyses. In order to release and partially solubilize the most polar components, a highly polar solvent such as a 50% mixture of methanol and benzene (*11*) was found to work well at this point. Trichloroethylene was then used to more completely solubilize and chase out the highly polar components. As shown in Figure 2, the eluant solvent is added about 100–200 ml in advance of the fraction cut point in order to provide for the lag between addition of the solvent at the top and the separation made at the bottom of the column. Thus three distinct hydrocarbon types can be separated and recovered by the chromatographic scheme described. Table I lists the stepwise details involved and Table II, an example of repeat analyses on the same asphalt.

**Component Characterization.** It has previously been reported that asphalt or heavy petroleum fractions may be characterized by use of the densimetric method (*6*). This involves a calculation based upon the relationship between molar volume and atomic H/C ratio. It requires only the measurement of per cent hydrogen, per cent carbon, and molecular weight followed by a calculation step. For this molecular weights were determined in benzene using a Mechrolab Vapor Pressure Osmometer at 37 °C, standardized with benzil. The analysis is then summarized in terms of molecular weight, fraction of carbon atoms in aromatic rings, average number of carbon atoms per molecule, the number of aromatic and naphthene rings per molecule. The number average molecular weight and the number of carbon atoms pertain to the relative molecular size. The fraction of carbon in aromatic rings and the number of rings per molecule are indicative of the degree of aromaticity, while the number of

(11) H. E. Schweyer and E. L. Chipley, *Proc. HRB Record*, No. 178, 30 (1967).

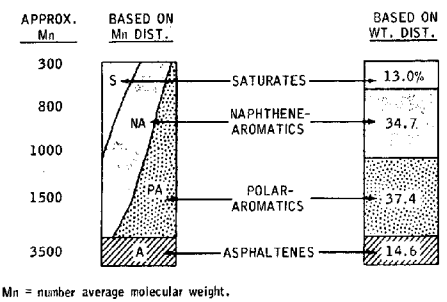


**Figure 3. Typical distribution of generic components in asphaltic residue (89 Pen)**

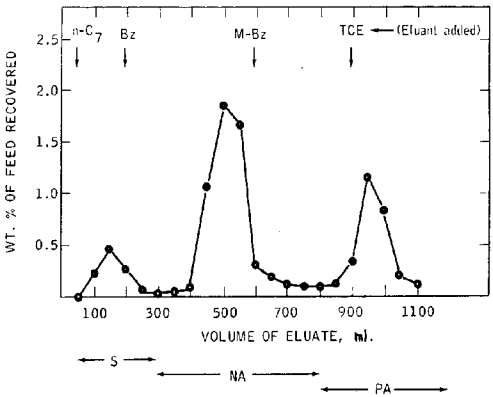


**Figure 2. Elution-adsorption chromatogram of petrolenes**

naphthene rings is a relative measure of naphthenicity. This permits a cross comparison of chemical characteristics, bringing in the concept of molecular size and the relative amount of aromaticity and naphthenicity. Table III exemplifies the

**Table I. Procedure for Asphalt Separation**

1. Place 10–15 gram [100/(100-% Asphaltenes)] in 2-l Erhlenmeyer and add 100-ml of *n*-heptane (99+ mol %) per gram of asphalt
2. Heat on steam bath while stirring, then let stand overnight
3. Filter slowly through Whatman No. 1 paper in 12-cm Buchner and wash thoroughly with warm *n*-heptane until clear
4. Transfer insolubles to fresh heptane, warm to 100 °F, filter, and wash again. Under a nitrogen atmosphere, dry insolubles and weigh as asphaltenes
5. Concentrate petrolene–heptane solution on steam bath to a volume of 50 ml
6. Prepare F-20 alumina by drying at 750 °F for 16 hours and store in tight glass containers
7. Add about 450 grams of alumina to 3- × 100-cm chromatographic column with gentle tapping and immediately prewet with 50 ml of *n*-heptane
8. Follow prewet solvent in step 7 with the 50 ml of petrolene solution and *n*-heptane eluant. Add more eluant and recover eluate according to following schedule:

| Eluant feed | Eluate vol., ml. | Fraction recovered |
|---|---|---|
| *n*-Heptane | 200 | Saturates |
| Benzene | 100 | Saturates |
| Benzene | 300 | Naphthene–aromatics |
| Methanol-benzene | 300[a] | Naphthene–aromatics |
| Trichloroethylene | 300 | Polar–aromatics |
| Trichloroethylene | 300 | Polar–aromatics |
| Trichloroethylene | Hold-up | Polar–aromatics |

9. Combine eluates into tared 400-ml beakers and evaporate to dryness and constant weight using a steam bath and nitrogen sparge
10. Weigh fractions to the nearest 0.01 g and calculate weight per cent

[a] This fraction may be cut short or enlarged depending upon the descent of the black ring (polar–aromatics) during elution.

**Table II. Repeat Composition Analyses of a Venezuelan 90 Penetration Asphalt Binder**

| Generic fraction | | |
|---|---|---|
| Saturates | 13.9% | 14.1% |
| Naphthene–aromatics | 34.2 | 34.8 |
| Polar–aromatics | 36.7 | 35.9 |
| Asphaltenes | 14.0 | 14.3 |
| | 98.8 | 99.1 |

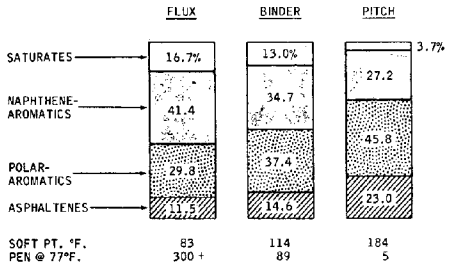


**Figure 4. Effect of vacuum reduction on composition**

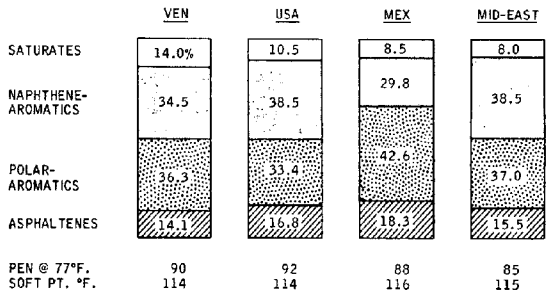


**Figure 5. Effect of crude source on composition**

repeatability of these characteristics when applied to the three chromatographic fractions reported in Table II. The characterization of asphaltenes was not made because of inherent difficulties in obtaining reliable tests for molecular weight and per cent carbon and hydrogen. The divergent results found in molecular weight measurement of asphaltenes is explained (*12*) as caused by compositions of individual sheets which associate into larger micelles.

## RESULTS AND DISCUSSION

In order to study the distribution of generic components in an asphalt residuum, a separation by vacuum distillation was made first in order to yield a series of contiguous boiling point cuts. After deasphaltening of the vacuum distillation residuum, solvent separation was applied to obtain fractions in the higher boiling regions which could not be handled by conventional distillation. Analysis of each of these fractions gave the composite picture on the left in Figure 3, with number average molecular weights shown to indicate the approximate range of molecular sizes involved. Thus it became apparent that the distribution of the generic types is quite dependent upon the degree to which a residuum is reduced. The same analysis, shown in the block diagram on the right of this figure, is based strictly on weight proportion as measured by the analysis. This figure does not tell as much as the previous one, but it is easier to arrive at and satisfies the practical needs for composition analysis.

The effect of vacuum reduction on composition is shown by the block illustrations in Figure 4. It will be noted here that both saturates and naphthene–aromatics decrease as distillation progresses, whereas the polar–aromatics and asphaltenes tend to increase by concentration. This points out the advisability of making composition comparisons on the same level

(12) J. D. Dickie and T. F. Yen, ANAL. CHEM., **14**, 1847 (1967).

**Table III. Repeat Characterization Analyses of a Venezuelan 90 Pen Asphalt Binder**

| | | |
|---|---|---|
| Generic fractions | | |
| Saturates | | |
| Molecular weight | 570 | 543 |
| Density, 20/4 ° | 0.873 | 0.889 |
| No. C atoms/mole | 40 | 39 |
| No. naphthene rings/mole | 3.0 | 2.9 |
| Naphthene–aromatics | | |
| Molecular weight | 660 | 671 |
| Density, 20/4 ° | 0.993 | 0.991 |
| Fraction carbon, aromatic | 0.26 | 0.26 |
| No. C atoms/mole | 47 | 48 |
| No. aromatic rings/mole | 2.6 | 2.6 |
| No. naphthene rings/mole | 3.3 | 3.4 |
| Polar–aromatics | | |
| Molecular weight | 1158 | 1081 |
| Density, 20/4 ° | 1.076 | 1.072 |
| Fraction carbon, aromatic | 0.44 | 0.44 |
| No. C atoms/mole | 81 | 76 |
| No. aromatic rings/mole | 8.4 | 7.9 |
| No. naphthene rings/mole | 3.5 | 3.4 |

**Table IV. Comparison of Fraction Characteristics of Asphalt Residua Prepared by Vacuum Distillation**

| Designation: | Flux | Binder | Pitch |
|---|---|---|---|
| Soft pt., °F | 83 | 114 | 184 |
| Pen at 77 °F | 300+ | 89 | 5 |
| Generic fraction | | | |
| Saturates | | | |
| Molecular weight | 520 | 626 | 883 |
| Density, 20/4 ° | 0.864 | 0.870 | 0.871 |
| No. C atoms/mole | 37 | 45 | 63 |
| No. naphthene rings/mole | 2.9 | 3.1 | 3.7 |
| Naphthene–aromatics | | | |
| Molecular weight | 603 | 720 | 918 |
| Density, 20/4 ° | 0.984 | 0.989 | 0.992 |
| Fraction carbon, aromatic | 0.25 | 0.26 | 0.22 |
| No. C atoms/mole | 42 | 51 | 65 |
| No. aromatic rings/mole | 2.1 | 2.8 | 3.1 |
| No. naphthene rings/mole | 3.1 | 3.6 | 4.1 |
| Polar–aromatics | | | |
| Molecular weight | 1004 | 1045 | 1309 |
| Density, 20/4 ° | 1.062 | 1.069 | 1.081 |
| Fraction carbon, aromatic | 0.38 | 0.39 | 0.42 |
| No. C atoms/mole | 68 | 73 | 89 |
| No. aromatic rings/mole | 4.7 | 6.6 | 8.9 |
| No. naphthene rings/mole | 3.3 | 3.7 | 3.9 |

**Table V. Comparison of Fraction Characteristics of Asphalt from Different Crude Sources**

| Source | Ven. | USA | Mex. |
|---|---|---|---|
| Pen. at 77 °F | 90 | 92 | 88 |
| Generic fractions | | | |
| Saturates | | | |
| Molecular weight | 557 | 630 | 476 |
| Density, 20/4 | 0.877 | 0.869 | 0.866 |
| No. C atoms/mole | 40 | 45 | 34 |
| No. naphthene rings/mole | 3.0 | 3.1 | 2.2 |
| Naphthene–aromatics | | | |
| Molecular weight | 666 | 800 | 578 |
| Density, 20/4 | 0.992 | 0.991 | 1.001 |
| Fraction carbon, aromatic | 0.26 | 0.24 | 0.27 |
| No. C atoms/mole | 48 | 56 | 41 |
| No. aromatic rings/mole | 2.6 | 2.9 | 2.3 |
| No. naphthene rings/mole | 3.4 | 3.7 | 3.0 |
| Polar–aromatics | | | |
| Molecular weight | 1120 | 1330 | 1115 |
| Density, 20/4 | 1.074 | 1.084 | 1.067 |
| Fraction carbon, aromatic | 0.44 | 0.43 | 0.38 |
| No. C atoms/mole | 79 | 90 | 75 |
| No. aromatic rings/mole | 8.2 | 9.2 | 6.6 |
| No. naphthene rings/mole | 3.5 | 4.0 | 3.4 |

**Table VI. Summary of Composition and Characterization as Found in Typical 85/100 Straight Reduced Asphalt**

| Component | Wt % range | Physical nature | Density 20/4° (Av) | Mole Wt, (Av) | Fraction Arom (fa) | Av No. rings/mole Nap | Av No. rings/mole Arom | Chemical structure |
|---|---|---|---|---|---|---|---|---|
| Saturates | 5–15 | Colorless liquid | 0.87 | 650 | 0.00 | 3.0 | 0.0 | Pure paraffins + pure naphthenes + mixed paraffin–naphthenes |
| Naphthene–aromatics | 30–45 | Yellow to red liquid | 0.99 | 725 | 0.25 | 3.5 | 2.6 | Mixed paraffin–naphthene–aromatics + sulfur-containing compounds |
| Polar–aromatics | 30–45 | Black solid | 1.07 | 1150 | 0.42 | 3.6 | 7.4 | Mixed paraffin–naphthene–aromatics in multi-ring structures + sulfur, oxygen, nitrogen-containing compounds. |
| Asphaltenes | 5–20 | Brown to black solid | 1.15 | 3500 | 0.50 | — | — | Mixed paraffin–naphthene–aromatics in polycyclic structures + sulfur, oxygen nitrogen-containing compounds. |

of consistency or on asphalts submitted to some common level of treatment. Table IV lists the fraction characteristics of these same asphalts. One notable effect of distillation is the increase in molecular weight from flux to the highly reduced pitch, also the gradual increase in number of rings per molecule. Thus, both the proportion of generic fractions and their chemical nature are dependent upon the amount of reduction by distillation.

Crude source is also a factor in composition analysis as illustrated in Figure 5. In this case all four asphalts have about the same penetration and softening point, while each inherently contains different amounts of the four generic fractions. Table V illustrates how both the molecular size and relative amount of aromatic and naphthene rings can vary according to crude source. Based on a limited number of analyses, it can safely be stated that greater variations than this will be found among asphalts used in paving.

Table VI is included in order to summarize the general range of composition found in most straight run asphalts. Every asphalt contains some of each of these components, and it is believed (*13*) that each contributes different qualities to the total asphalt. A brief description of the physical nature is also added in which it will be noted that saturates and naphthene–aromatics are liquid in nature whereas the polar–aromatics and asphaltenes are solids. This has prompted the added description that saturates and naphthene–aromatics are soft or plasticizing type components whereas the polar–aromatics and asphaltenes are hard components. Shown also in this table is a general description of the chemical structures involved in each component as judged by the densimetric method of characterization.

In general we have found that differences in molecular size and ring characteristics, as dependent upon distillation and crude source, is quite pronounced. This suggests that both the molecular size and the chemical characteristics of each component should be considered along with the compositional proportion of each component. The separation technique used here will provide a basis for determining these parameters, and this will aid in a better understanding of the fundamentals involved and their relationship to the overall asphalt.

RECEIVED for review October 30, 1968. Accepted January 7, 1969. This paper was presented in part at the 156th National Meeting of the ACS, Division of Petroleum Chemistry, Atlantic City, N.J., September 1968.

(13) J. Knotnerus, *Ind. Eng. Chem., Prod. Res. Develop.*, **6**, 43 (1967).

# Relative Oxygen Absorption and Volatility Properties of Submicron Films of Asphalt Using the Quartz Crystal Microbalance

W. H. King, Jr., and L. W. Corbett

*Esso Research and Engineering Co., Linden, N.J. 07036*

**The use of the quartz crystal microbalance for measuring relative oxygen uptake or absorption in submicron films of asphalt has proved to be a sensitive and reliable tool. It has shown that polar-aromatics absorb oxygen very quickly while asphaltenes absorb at a slow but prolonged rate. Saturates and naphthene-aromatics show virtually no absorption of oxygen but are relatively much more volatile. This is consistent with previous findings that relate the chemical and physical character of these components with their general resistance to oxidative type conditions. Significant differences between total asphalts can be shown, and it appears that they can be rated according to their oxygen absorption properties.**

IT IS GENERALLY AGREED that oxygen plays an important role in most asphalt hardening reactions, and that this hardening is brought about by oxygen uptake through absorption or oxidative type reactions. The primary effect is an increase in asphalt viscosity or stiffness with subsequent loss of ductility and flexibility. This in turn influences the cohesive and flexibility properties of asphalt-aggregate mixtures, which then is reflected in pavement service qualities. References (*1*) through (*7*) provide helpful background on the specific effect of temperature, film thickness, oxygen rate, and hydrocarbon character on asphalt hardening. In addition, over 70 other general literature references have been noted that report on hardening in service, indicating considerable interest in this field.

This report describes the use of the quartz crystal microbalance for measuring the absorption and/or volatility of various asphalt paving binders and the generic fractions from one of these binders. The method is an adaption of that developed by Fischer and King (*8*) for the measurement of oxygen stability of elastomers. It is based on the use of a piezoelectric quartz crystal on which is deposited a 0.3-micron film of the material to be tested. When electrically excited, the crystal vibrates at a high frequency in direct proportion to the mass of the film. Changes in the mass of the film, caused by the uptake of oxygen or by its volatilization, are then detected and recorded by measuring the change in oscillation frequency.

## EXPERIMENTAL

**Apparatus.** Piezoelectric quartz crystals function as very sensitive microbalances. The use of these for microweighing was proposed by Sauerbrey (*9*), while King (*10*) showed that they can be used for measuring absorption of moisture and other gases on films of polymers and other coating materials. Devices using the vibrating crystal owe their high degree of sensitivity to the high stability and small size of the crystal vibrator and also for the ability to measure frequency changes at a high level of accuracy. The crystal used here gives a 230-cycle-per-second (cps) signal per microgram of coating in which the following Equation (*8*) relates frequency change to mass change:

$$\Delta F = 2.3 \times 10^6 \times F^2 \times \frac{\Delta W}{A} \qquad (1)$$

where $\Delta F$ is the frequency change in cps caused by mass change $\Delta W$, $F$ is the frequency of vibration in megahertz, $A$ is the area ($cm^2$) of the coated electrode, $W$ is the mass (grams) of the sample film.

Frequency is measured during the test, and the per cent change in weight of the sample calculated as follows:

$$\% \text{ Wt Change} = \frac{\text{Change in Frequency in cps} \times 100}{\text{Frequency in cps due to coating}} \qquad (2)$$

As pictured in Figure 1, the crystal plate is a 10-megacycle AT cut 0.5 × 0.5-inch square by 0.007-inch thick, with gold electrodes on each side of the crystal, each covered with nickel by electrodeposition. The crystal cover shown is a temporary one used to protect the crystal and its coating before being installed in the test cell. The detector and test reference crystals are mounted in a 2- × 4-inch brass cell as shown in the flow control and electrical scheme Figures 2 and 3. The cell is mounted on oscillator circuits (TRO-2, modified Pierce Oscillator), which are connected to a mixer that feeds the frequency meter and thence a recorder. The specimen cell is closely regulated in temperature to 150 ± 0.15 °C with a proportional controller and is equipped to receive either nitrogen or oxygen at 150 psig. The rate of exit gas is regulated to 500 ml per minute at room conditions, using a soap film meter.

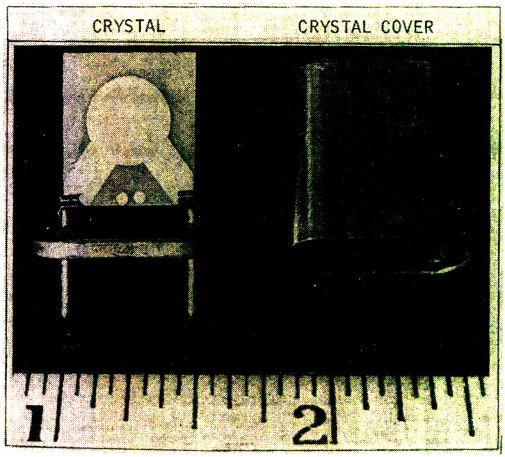


**Figure 1. Crystal electrode with crystal cover**

(1) J. Ph. Pfeiffer, "The Properties of Asphaltic Bitumen," Elsevier Publ. Co., New York, 1950.
(2) J. W. A. Labout and W. P. Van Oort, ACS Petroleum Division, Sept. 1954.
(3) W. P. Van Oort, *Ind. Eng. Chem.*, **48**, 1196 (1956).
(4) Blokker and Van Hoorn, 5th World Pet. Congr., June (1959).
(5) J. Knotnerus, Jr., *Inst. Pet.*, **42**, 355 (1956).
(6) R. G. Larsen, R. E. Thorpe, F. A. Amfield, *Ind. Eng. Chem.*, **34**, 183 (1942).
(7) E. R. Booser and M. R. Fenske, *ibid.*, **44**, 1850 (1952).
(8) W. F. Fischer and W. H. King, Jr., ANAL. CHEM., **39**, 1265 (1967).
(9) G. Z. Sauerbrey, *Physik*, **155**, 206 (1959).
(10) W. H. King, Jr., ANAL. CHEM., **36**, 1735 (1964), U.S.P. 3,164,004.

**Procedure.** The crystal electrode is first coated with the asphalt or asphalt fraction to be tested by spraying as 2% solution (in benzene) until a coating equivalent to 5000 ± 20 cycles is obtained. An artist's spray gun (Pasche) operating at 10 psig was found ideal for this work, spraying an equal amount on each side of the crystal. The coated crystal and an uncoated reference crystal, regulated to the same frequency, are then placed in the cell, pressurized with nitrogen to 150 psig and brought to 150 °C with a gas purge of 440 standard cc per minute. Earlier work had shown that at lower pressures and lower temperatures, the oxygen uptake is quite slow, thus making the test undesirably long. Time is important because the more volatile components are continually evaporating during the test. The use of 150 °C permitted some comparison with the elastomer work cited above; also, it is the approximate temperature at which most asphalt–aggregate hot mixes are made.

As soon as the test conditions above stabilized, frequency measurements were taken and frequency change (loss or gain) *vs.* time was recorded. Figures 4 and 5 have been reproduced from the operating charts on a percentage weight change per minute basis. The average weight loss was calculated as the average of the loss lines under nitrogen before and after the introduction of oxygen. The weight gain or oxygen uptake was then measured as the average tendency to show gain plus the volatile loss that had to be overcome. This assumes that the same amount of volatile loss will take place under oxygen as under nitrogen. Although this may not be strictly true, the conditions of time, pressure, and gas rate were closely duplicated in order to maintain the relative nature of the test.

## RESULTS AND DISCUSSION

Drawing upon the experience with elastomers when using this method, it was believed that the relative oxygen stability of asphalts or asphalt fractions could be determined. It was soon found, however, that some modification of the procedure was necessary because of the inherent differences between elastomers and asphalt, particularly the spray application of the coating and the regulation of the gas pressure and flow rate

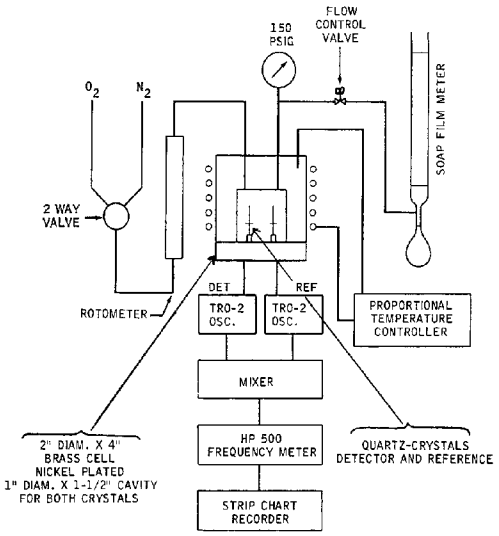


**Figure 2. Flow control scheme for the quartz crystal microbalance**

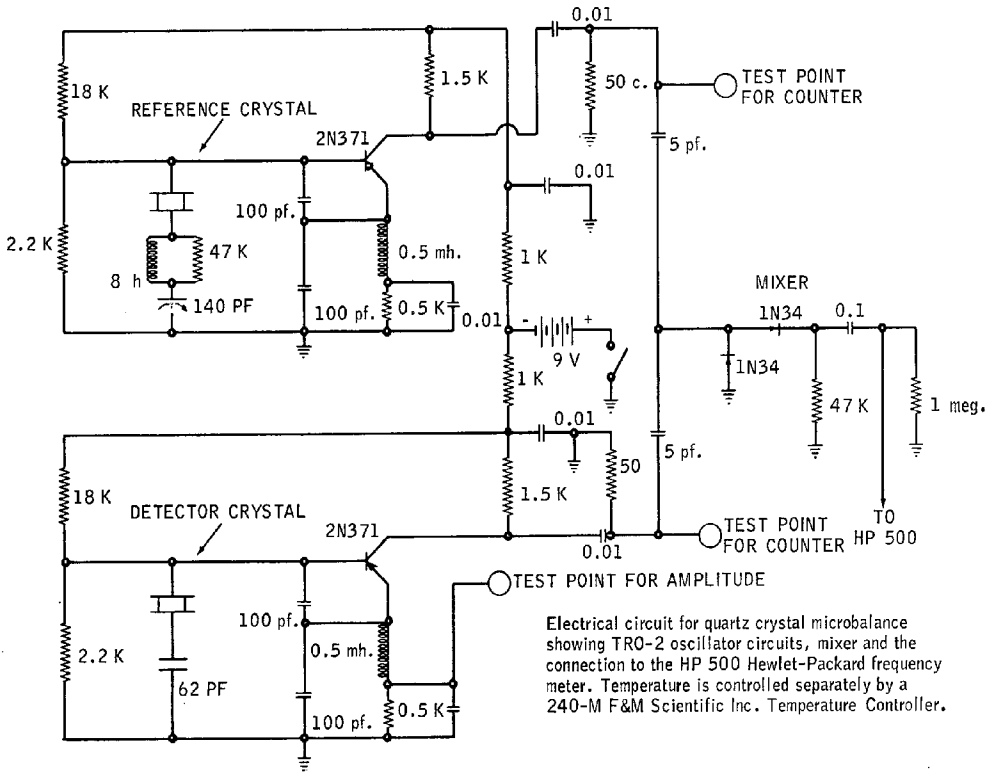


Electrical circuit for quartz crystal microbalance showing TRO-2 oscillator circuits, mixer and the connection to the HP 500 Hewlet-Packard frequency meter. Temperature is controlled separately by a 240-M F&M Scientific Inc. Temperature Controller.

**Figure 3. Crystal oscillator drawing**

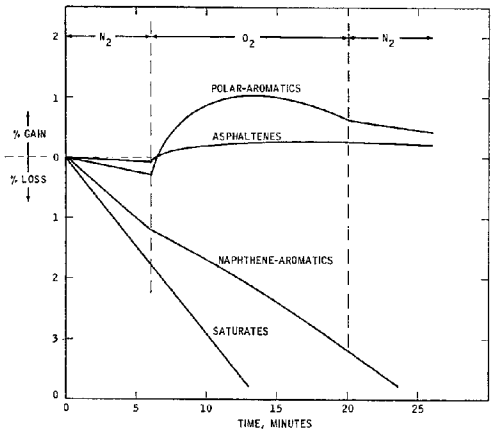


**Figure 4. Gain–loss relationship of asphalt fractions measured by quartz crystal microbalance**

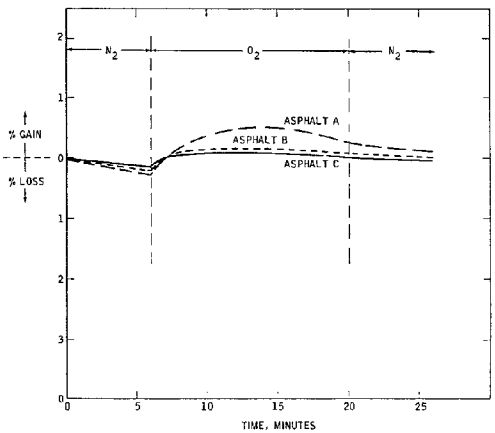


**Figure 5. Gain–loss relationship of asphalts measured by quartz crystal microbalance**

during the measurements. A higher pressure was found necessary in order to reduce volatility effects, and increased flow rates was used to speed up oxygen uptake. The test was then applied to each of the four generic fractions (*11*) of asphalt which are known to be distinctly different in their average chemical structure. After differences between them were found, the test was then applied to total paving binders of approximately the same consistency but from different crude sources. This provided us with background on the susceptibility to oxygen of each hydrocarbon type found in asphalt as well as a means for comparing asphalts from different crude sources.

Referring to Figure 4 we find that each of the asphalt fractions respond differently under the same conditions of exposure to nitrogen and oxygen. All materials show an initial evaporative weight loss under nitrogen (downward slope) which tends to diminish as the run progresses. Upon introduction of oxygen, all materials (except the saturates) showed some measure of weight or oxygen uptake (upward slope), tending to reverse the loss trend. The saturates display relatively high weight loss rates under nitrogen, whereas asphaltenes are relatively low, with the other fractions intermediate. Because there was a consistent directional loss under both nitrogen and oxygen in the case of the saturates, it was assumed that they did not absorb oxygen. Naphthene–aromatics showed only a minor oxygen uptake, and the polar–aromatics showed a great deal of uptake rather quickly followed by an early reversal toward the weight loss direction. Asphaltenes showed a relatively slow oxygen uptake with a delayed tendency for reversal. Tests on asphaltenes were discontinued after an extended exposure without much indication of a return to the loss direction, as experienced with the other fractions. A careful study of repeat asphaltenes curves showed a consistent tendency under oxygen to gain weight for a prolonged period. This is oxygen uptake but at a relatively slow rate. The data in Table I reflect average weight change per minute over the

(11) L. W. Corbett, ANAL. CHEM., **41**, 576 (1969).

**Table I. Quartz Crystal Microbalance Measurements on Asphalt and Asphalt Generic Fractions Made at 150 °C in Submicron Films under Nitrogen and Oxygen at 500 ml/min and 150 psig**

| Run No. | Fraction | % Wt change per min | | Total % gain | Average % wt change per min | |
|---|---|---|---|---|---|---|
| | | Loss | Gain | | Loss | Gain |
| 17 | Saturates | 0.275 | 0 | 0 | 0.305 | 0 |
| 21 | Saturates | 0.335 | 0 | 0 | | |
| 22 | *N*-Aromatics | 0.197 | 0.032 | 0.229 | 0.182 | 0.031 |
| 23 | *N*-Aromatics | 0.167 | 0.030 | 0.197 | | |
| 19 | *P*-Aromatics | 0.037 | 0.052 | 0.089 | | |
| 26 | *P*-Aromatics | 0.049 | 0.016 | 0.065 | 0.044 | 0.079 |
| 27 | *P*-Aromatics | 0.045 | 0.039 | 0.084 | | |
| 38 | Asphaltenes | 0.0035 | 0.0128 | 0.016 | 0.003 | 0.016 |
| 39 | Asphaltenes | 0.0032 | 0.0130 | 0.016 | | |
| 19 | Asphalt A | 0.042 | 0.051 | 0.093 | 0.042 | 0.102 |
| 20 | Asphalt A | 0.041 | 0.071 | 0.112 | | |
| 29 | Asphalt B | 0.023 | 0.022 | 0.045 | | |
| 30 | Asphalt B | 0.029 | 0.012 | 0.041 | | |
| 32 | Asphalt B | 0.021 | 0.024 | 0.045 | 0.029 | 0.043 |
| 34 | Asphalt B | 0.034 | 0.008 | 0.042 | | |
| 36 | Asphalt B | 0.030 | 0.012 | 0.042 | | |
| 37 | Asphalt B | 0.036 | 0.009 | 0.045 | | |
| 40 | Asphalt C | 0.028 | 0.004 | 0.034 | 0.033 | 0.039 |
| 41 | Asphalt C | 0.037 | 0.008 | 0.035 | | |

arbitrary 14-minute exposure period used for comparing the four fractions. Thus, it appears that asphaltenes will take up more oxygen in the long run although its initial rate of uptake is less. This does not invalidate findings of others that asphaltenes are highly susceptible to oxygen absorption; it only indicates that the polar aromatics in these thin films will absorb relatively more initially, but less over a longer period. In general, this seems to correlate well with the chemistry of these components summed up as follows:

Saturates are the most volatile with naphthene–aromatics next and asphaltenes by far the least. Directionally this is consistent with average molecular weight measurements on these fractions and also with gel-permeation analyses which related the molecular sizes in the same order.

Polar–aromatics are the quickest to absorb oxygen with asphaltenes probably absorbing more but at a much slower rate. Saturates appear to be unaffected by oxygen under these conditions and naphthene–aromatics only slightly so. This is consistent with earlier observations (*12*) that polar–aromatics are the first to convert to asphaltenes under air-blowing conditions, while the saturates are virtually unaffected.

Figure 5 is a comparison of total asphalts from three different Near East crude sources. Asphalt A in this case showed the greatest loss under nitrogen as well as the greatest degree of oxygen uptake. In comparison with this, Asphalt C showed the least volatility and least oxygen uptake. Asphalt B was repeat tested six times giving a coefficient of variation of 21% on loss and 5% on total gain under oxygen. This is based on all of the data as reported in Table I. The well-known Student "t" test was applied to loss and gain data on the three total bitumen from which it was found that there is no significant difference between the gain for Asphalts B and C. However, there is a significant difference at the 95% probability level between the total gain data on Asphalt A *vs.* either Asphalt B or C. From this work we conclude that:

The method shows excellent repeatability and sensitivity as a means for measuring the relative oxygen absorption at 150 °C in very thin films.

Asphalt A absorbs oxygen at a significantly higher rate than either Asphalt B or C under the conditions of this test.

Based on the work reported here, we recommend this method and technique for use as a means of detecting relative differences in the oxygen absorption properties of paving binders or their modified compositions.

RECEIVED for review October 30, 1968. Accepted January 7, 1969.

(12) L. W. Corbett and R. E. Swarbrick, AAPT, **29**, 104 (1960).

# Mechanism of Trace Counterion Transport through Ion-Exchange Membranes

**W. J. Blaedel, T. J. Haupert,[1] and M. A. Evenson[2]**

*Chemistry Department, University of Wisconsin, Madison, Wis. 53706*

**An equation for the flux of a trace counterion between two solutions separated by an ion-exchange membrane is derived and experimentally verified. The flux equation is based on a mechanism that considers the heterogeneous surface exchange reactions in addition to the diffusional processes occurring within the membrane and within the stationary liquid films adjacent to the membrane surfaces. The equation is tested using both synthetic anion- and cation-exchange membranes for systems containing singly and multiply charged trace and bulk ions. Experimental evidence is also presented to indicate the influence of the surface exchange reaction on the overall rate of ion transport.**

INCREASED APPLICATIONS of ion-exchange membranes to analytical problems have led to an increased interest in their fundamental properties and mode of operation. Of special interest is the transport rate of a trace counterion across an ion-exchange membrane separating two solutions that also contain another electrolyte at much greater concentrations. The analytical promise of such systems in the separation and concentration of trace ions has been shown (*1*, *2*). However, the efficiency of such applications depends greatly upon the rate of ionic transport between the two solutions. The present study was undertaken to obtain a quantitative understanding of the factors that influence the rate of such transport.

Three general approaches have been used previously to investigate ion-exchange kinetics. These include application of the Nernst-Planck flux equation, the theory of irreversible thermodynamics, and the transition theory. These have been recently reviewed (*3*, *4*). The present approach applies the steady-state principle to a system of simultaneous rate processes to give a set of flux equations, one for each step in the transport mechanism. The set of flux equations is then solved for the overall counterion flux.

Previous studies of ion-exchange kinetics consider the ion transport process to be diffusion controlled either within the membrane or within the external liquid phase (*5*, *6*). In this paper, the influence of the heterogeneous ion-exchange reactions that occur at each solution–membrane interface is also considered. Although the possibility of rate control in ion-exchange processes by the surface exchange reaction has

[1]Present address, Chemistry Department, University of Arizona, Tucson, Ariz. 85721

[2]Present address, University Hospitals, University of Wisconsin, Madison, Wis. 53706

(1) W. J. Blaedel and T. J. Haupert, ANAL. CHEM., **38**, 1305 (1966).
(2) W. J. Blaedel and E. L. Christensen, *ibid.*, **39**, 1262 (1967).
(3) N. Lakshminarayanaiah, *Chem. Rev.*, **65**, 491 (1965).
(4) G. Eisenman, J. P. Sandblom, and J. L. Walker, Jr., *Science*, **155**, 965 (1967).
(5) M. A. Peterson and H. P. Gregor, *J. Electrochem. Soc.*, **106**, 1051 (1959).
(6) F. Helfferich, "Ion Exchange," McGraw-Hill, New York, N.Y., 1962, pp 345–53.

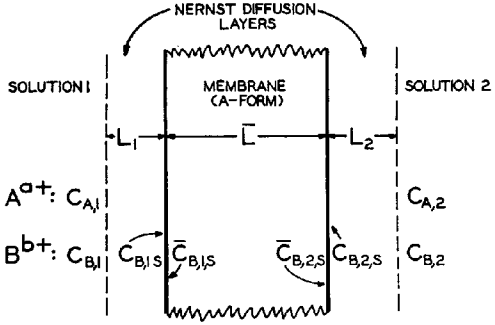


**Figure 1. Membrane–solution system**

been suggested, the existence of such control has not yet been experimentally shown, and it has been ignored in most studies (7).

The following treatment of ion-exchange kinetics describes the influence of the heterogeneous ion-exchange reaction on the overall rate of ion transport. By proper selection of experimental conditions, the rates of the diffusional processes were maximized in order to enhance the possibility of observing the rate of the chemical process. The influence of the diffusional processes was reduced by the use of thin, highly permselective membranes and by very efficient stirring. Furthermore, the employment of steady-state flow techniques and the restriction of measurements to the transport of a trace species permitted the attainment of a nonequilibrium, time-independent system in which the concentrations of all bulk species and the activity coefficients of all species were virtually constant in each phase. These techniques simplified both the theoretical relationships and the experimental methods needed to confirm them.

## THEORY

The mechanism of transport of a trace counterion across an ion-exchange membrane separating two solutions is postulated to consist of three rate processes: diffusion through the two liquid films adjacent to the membrane surface, the heterogeneous exchange reaction occurring at the two membrane–solution interfaces, and diffusion through the membrane. Transport occurs through the five regions shown in Figure 1, which represents a cross section of a cation exchange membrane that separates two solutions of different composition. Each solution contains a bulk electrolyte $[A(ClO_4)_a$ at $C_A F]$ and a trace electrolyte $[B(ClO_4)_b$ at $C_B F]$. Diffusion layers in the solution are of thickness L and the thickness of the membrane is $\bar{L}$. Subscripts 1 and 2 refer to the values of the quantities in the two solutions and the subscript S designates values of surface concentrations at the membrane–solution interface. Accordingly, the five steps in the overall transport of counterion B from solution 1 to solution 2 are: (1) Diffusion of B through the liquid film from the bulk of solution 1 to the membrane surface. (2) Exchange at the solution 1–membrane interface of aqueous B with resin-bound A, fixing B into the membrane and releasing A into solution. (3) Diffusion of B through the membrane. (4) Exchange at the membrane–solution 2 interface of resin-bound B for aqueous A, liberating B into solution and fixing A into the membrane. (5) Diffusion of the liberated B through the liquid film into the bulk of solution 2.

(7) F. Helfferich in "Ion Exchange," Vol. 1, J. A. Marinsky, Ed., Marcel Dekker, New York, N.Y., 1966, p 68.

The following flux equations can be written for each of the five elementary steps in the overall transport mechanism. In expressing the flux for steps 1, 3, and 5, it is assumed that they are simple diffusional processes that occur through linear concentration gradients of the tracer-ion $B$ and that there are no significant concentration gradients of the bulk counterion $A$ throughout the aqueous or membrane phases. In expressing the flux for steps 2 and 4, it is assumed that the forward and reverse heterogeneous exchange reactions are simple one-step processes that occur according to Equation 6, which is first order with respect to tracer-ion $B$, and of $b/a$ order with respect to the bulk counterion $A$. At this point in the derivation, this assumption is a trial and error assumption which seems to have no fundamental justification, and whose acceptance must await presentation of the experimental results.

$$\text{Flux through liquid film in solution 1} = \frac{D_1}{L_1}(C_{B,1} - C_{B,1,S}) \tag{1}$$

$$\text{Exchange flux at membrane–solution 1 interface} = k_f(C_{B,1,S})(\bar{C}_{A,1,S})^{b/a} - k_b(\bar{C}_{B,1,S})(C_{A,1,S})^{b/a} \tag{2}$$

$$\text{Flux through membrane} = \frac{\bar{D}}{\bar{L}}(\bar{C}_{B,1,S} - \bar{C}_{B,2,S}) \tag{3}$$

$$\text{Exchange flux at membrane–solution 2 interface} = k_b(\bar{C}_{B,2,S})(C_{A,2,S})^{b/a} - k_f(C_{B,2,S})(\bar{C}_{A,2,S})^{b/a} \tag{4}$$

$$\text{Flux through liquid film in solution 2} = \frac{D_2}{L_2}(C_{B,2,S} - C_{B,2}) \tag{5}$$

In Equations 1–5, the barred quantities refer to the membrane phase. $D$ represents the diffusion coefficient of the transported species (Ref 6, p 269), whereas $k_f$ and $k_b$ are the rate constants for the heterogeneous reaction:

$$B^b(\text{aq}) + \frac{b}{a}A^a(\text{memb}) \underset{k_b}{\overset{k_f}{\rightleftharpoons}} B^b(\text{memb}) + \frac{b}{a}A^a(\text{aq}) \tag{6}$$

Activities do not appear in the above rate equations. In Equations 2 and 4, activities are approximated by molar concentrations whereas Equations 1, 3, and 5 are the simplified forms of the general flux equation:

$$J_i = D_i C_i\left(\frac{d \ln C_i}{dx} + \frac{d \ln \gamma_i}{dx}\right) \tag{7}$$

For systems containing a single bulk electrolyte and a trace electrolyte, the activity coefficients are constant throughout each phase and the general flux equation approaches Fick's first law of diffusion upon which Equations 1, 3, and 5 are based.

If the two solutions are flowing past the membrane at constant rates, the system will attain a steady state. At steady state, any one of the diffusional processes or the exchange reaction may predominate in determining the overall rate of ion transport but the fluxes through each of the five regions will all be equal. Equations 1 through 5 can be solved for $J_B$, the steady-state flux of species $B$, by eliminating the four unmeasurable surface concentrations of the trace ion:

$$J_B = \frac{\dfrac{(\bar{C}_{A,1,S})^z}{(C_{A,1,S})^z}C_{B,1} - \dfrac{(\bar{C}_{A,2,S})^z}{(C_{A,2,S})^z}C_{B,2}}{\dfrac{\bar{L}}{\bar{K}\bar{D}} + \dfrac{1}{k_f(C_{A,1,S})^z} + \dfrac{1}{k_f(C_{A,2,S})^z} + \dfrac{L_1(\bar{C}_{A,1,S})^z}{D_1(C_{A,1,S})^z} + \dfrac{L_2(\bar{C}_{A,2,S})^z}{D_2(C_{A,2,S})^z}} \tag{8}$$

In Equation 8, $K = k_f/k_b$, and $z = b/a$.

Equation 8 can be simplified by the following considerations. Because the concentration of the bulk electrolyte is

much greater than that of the trace, concentration gradients of the bulk counterion in both the membrane and aqueous phases can be considered negligible, and the surface concentrations are equal to the bulk concentrations:

$$C_{A,1,S} = C_{A,1}, \quad C_{A,2,S} = C_{A,2} \tag{9}$$

$$\bar{C}_{A,1,S} = \bar{C}_{A,1}, \quad \bar{C}_{A,2,S} = \bar{C}_{A,2} \tag{10}$$

Further, because the membrane phase is predominantly in the $A$-form,

$$\bar{C}_{A,1} = \bar{C}_{A,2} = Q/a \tag{11}$$

$Q$ is the ion-exchange capacity of the membrane expressed in milliequivalents per milliliter. Using Equations 9–11 to eliminate all surface concentrations, Equation 8 becomes:

$$J_B = \frac{\dfrac{C_{B,1}}{(C_{A,1})^z} - \dfrac{C_{B,2}}{(C_{A,2})^z}}{\dfrac{\bar{L}}{K\bar{D}(Q/a)^z} + \dfrac{D_2L_1(C_{A,2})^z + D_1L_2(C_{A,1})^z}{D_1D_2(C_{A,1})^z(C_{A,2})^z} + \dfrac{(C_{A,1})^z + (C_{A,2})^z}{k_f(Q/a)^z(C_{A,1})^z(C_{A,2})^z}} \tag{12}$$

Equation 12 has the same form as Ohm's law: the flux or ion current is directly proportional to a chemical potential difference and inversely proportional to a resistance. The difference in chemical potential is determined by the ratios of the two counterion concentrations in the two solutions. The resistance may be considered to be the equivalent of three resistances in series: diffusional resistance through the membrane (first term in the denominator of Equation 12), diffusional resistance in the liquid films (second term in the denominator), and the resistance due to the heterogeneous exchange reaction at the interfaces (last term in the denominator).

Equation 12 is in accord with previously reported properties of ion exchange membranes. Thus the chemical potential that causes transport of $B$ is dependent upon the concentration of $A$ as well as that of $B$, and it is therefore possible for transport of $B$ to occur from a region of low concentration to a region of high concentration, as has been observed (*1,2*). Also the displacement of these concentrations from their equilibrium values determines the tracer-ion flux. When the net flux is zero, the system is at ion-exchange equilibrium and Equation 12 describes the equilibrium distribution of the two counterions:

$$\frac{C_{B,1}}{(C_{A,1})^z} = \frac{C_{B,2}}{(C_{A,2})^z} \tag{13}$$

This distribution is derivable from equilibrium principles, and its analytical significance has been shown (*1,2*).

Qualitative consideration of the factors that affect the flux of species $B$ indicates that these factors are correctly represented in Equations 8 and 12. Thus, a large difference in the concentrations of species $B$ between the two solutions, large diffusion coefficients, and a large forward rate constant for the heterogeneous exchange reaction will all result in a large flux of species $B$. However, thick liquid films, a thick membrane, and a large rate constant for the reverse exchange reaction will all favor a low flux of the trace ion.

Partial experimental verification of Equation 12 may be obtained with a simplified system in which the bulk electrolyte concentrations and the hydrodynamic regimes are the same in both solutions. Then,

$$C_{A,1} = C_{A,2} = C_A \tag{14}$$

$$D_1 = D_2 = D \tag{15}$$

$$L_1 = L_2 = L \tag{16}$$

Equation 12 then simplifies to give a linear relationship between the reciprocal flux function (RFF, or $(C_{B,1} - C_{B,2})/J_B$) and the $z$th power of the bulk electrolyte concentration:

$$\text{RFF} = \frac{C_{B,1} - C_{B,2}}{J_B} = \frac{\bar{L}}{K\bar{D}(Q/a)^z}C_A{}^z + \frac{2L}{D} + \frac{2}{k_f(Q/a)^z} \tag{17}$$

The reciprocal flux function can be measured rather simply. If the influent acceptor solution is tracer-free, the tracer flux can be found from a mass balance:

$$J_B = \frac{C_{B,2}F_2}{60A} \tag{18}$$

This equation relates the tracer counterion flux (mmoles $cm^{-2}$ $sec^{-1}$) to the flow rate $F_2$ of the acceptor solution ($cm^3$ $min^{-1}$), the effective surface area of the membrane ($cm^2$), and the steady-state molar concentration of the trace ion in the acceptor solution. With Equation 18, the reciprocal flux function can be written:

$$\text{RFF} = \frac{60A}{F_2}\left(\frac{C_{B,1}}{C_{B,2}} - 1\right) \tag{19}$$

Equation 19 permits easy measurement of the reciprocal flux function by measuring the flow rate of solution 2, the surface area of the membrane, and the steady-state concentration ratio of the tracer. The absolute tracer concentrations need not be known.

It is necessary to point out that deviations from Equation 17 may be expected because activities were not used in its derivation. Thus, $K$, the selectivity coefficient, is not independent of concentration but is related to the thermodynamic equilibrium constant, K:

$$K = \mathrm{K}\frac{\gamma_B\,\bar{\gamma}_A{}^z}{\bar{\gamma}_B\,\gamma_A{}^z} \tag{20}$$

Also the forward rate constant, $k_f$, is concentration dependent, being related to the thermodynamic rate constant (*8*), $k_f^*$:

$$k_f = k_f^*\frac{\bar{\gamma}_A{}^z\,\gamma_B}{\gamma_{AB}{}^{\ddagger}} \tag{21}$$

The activity coefficients are for the species denoted by the subscripts. The activity coefficient $\gamma^{\ddagger}_{AB}$ is for the activated complex. The effects of these concentration dependencies will be considered in the discussion of experimental results.

## EXPERIMENTAL

The objective of the experimental work was threefold: to support the proposed transport mechanism by verifying Equation 17; to support the inclusion of the heterogeneous exchange reaction in the proposed mechanism as a contributing rate process; and to support the postulated diffusional nature of the transport process through the membrane phase.

**Materials.** All reagents were analytical grade and were used without further purification. Radioisotopes $^{24}Na$ and $^{42}K$ were prepared at the University of Wisconsin reactor. All other radioisotopes were obtained from commercial sources and were used as received. Four different ion-exchange membranes were used. These included a sulfonated polyethylene cation-exchange membrane (C-103, American Machine and Foundry, Springdale, Conn.), a quaternary ammonium anion-exchange membrane (A-104, American Machine

(8) M. Boudart, "Kinetics of Chemical Processes," Prentice-Hall, Englewood Cliffs, N.J., 1968, p 54.

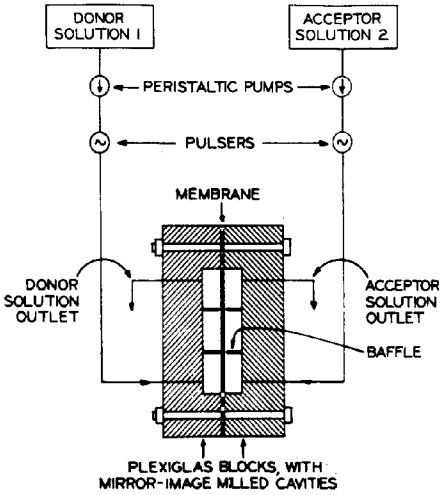


**Figure 2. Apparatus for measurement of counterion transport**

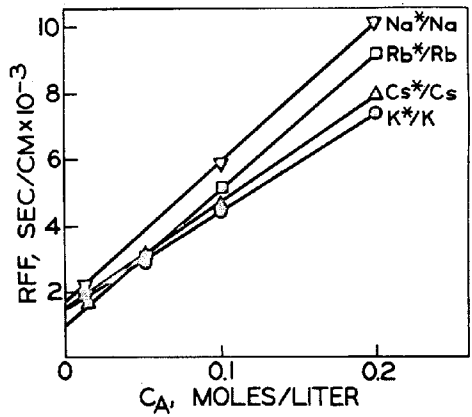


**Figure 3. RFF for isotopic systems**

**AMF C-103 cation-exchange membrane. Alkali chlorides, $a = b = 1$**

and Foundry), an acrylic acid cation-exchange membrane (P-116, RAI Research Corp., Old Greenwich, Conn.), and a sulfonated Teflon (Du Pont) cation-exchange membrane (P-1010, RAI Research Corp.). Prior to use, the cation-exchange membranes were rinsed several times with ethanol and converted to the sodium form by placing them in $1F$ $NaClO_4$ for several days. The $NaClO_4$ solutions were replaced daily. The anion-exchange membrane was pretreated similarly, being converted to the chloride form with $1F$ NaCl. The P-116 and P-1010 membranes were about 0.001″ thick, several-fold thinner than the C-103 and A-104 membranes.

**Verification of Equation 17.** Both isotopic and nonisotopic systems were investigated to verify Equation 17. For the isotopic cases, a radioisotope of the bulk counterion was used as the tracer species whereas for the nonisotopic cases, the bulk and trace counterions were different elements.

The apparatus used to measure the ion flux for the isotopic systems is shown schematically in Figure 2. The cell consisted of two mirror-image Plexiglas blocks (Rohm and Haas Co., Philadelphia, Pa.) between which a C-103 cation-exchange membrane was sandwiched. Each block had a milled channel, 4.96 cm long, 0.76 cm wide, and 0.16 cm deep, through which a solution flowed. Each channel contained two baffles, 0.1 cm high and made of 0.003″ platinum foil, that were used to increase turbulence. Tygon tubes were cemented to the ports of the cell with cyclohexanone. The solution in each channel was pumped with a peristaltic pump. A constant speed pump (New Brunswick Scientific Co., New Brunswick, N.J.) was used for the donor solution (Solution 1, Figure 1) and a variable speed pump (Harvard Apparatus Co., Dover, Mass.) was used for the acceptor solution (Solution 2, Figure 1). All transport measurements were made with the cell immersed in a thermostat at 25 ± 0.1 °C.

Pulsers were used in the inlet streams to produce mixing by periodic reversals in the direction of solution flow. Each pulser consisted of a roller-bearing mounted off-center on a 300 rpm motor shaft. The rim of the bearing compressed a section of Tygon tubing (1 inch long, 0.25 inch i.d.) through which the solution flowed. The pulsers were held on adjustable platforms that permitted variation of the pulsing amplitude. All transport data were obtained at pulsing amplitudes sufficiently large so that the rate of transport was independent of the pulsing amplitude. This assured that the stirring was at maximum efficiency. Under such conditions, about one third of the volume of each chamber was displaced 5 times per second. This high degree of pulsing was imposed to reduce the thicknesses of the liquid diffusion layers and thus minimize their influence on the observed transport rate.

Solution 1, designated as the donor, was pumped through one channel and contained the bulk electrolyte plus a radiotracer. Solution 2, designated as the acceptor, was pumped through the other channel and contained only the bulk electrolyte always at the same concentration as that of the donor.

The transport of four tracers, $^{24}Na$, $^{42}K$, $^{86}Rb$, and $^{137}Cs$ was studied, each in a bulk electrolyte of the corresponding chloride salt. The reciprocal flux function was determined at usually four bulk electrolyte concentrations between 0.01 and $0.2F$ with each concentration run at three different acceptor solution flow rates. These flow rates were about 0.5, 0.9, and 1.4 ml/min and were obtained accurately in each case by measuring with a stopwatch the time required to collect ten milliliters of the effluent solution. All transport measurements were made at steady state. This was assured by taking several samples at increasing times and accepting the value that became independent of the time of sampling. In these experiments, steady state was achieved within 30 minutes. Radioactivities were measured on 5-ml samples of each solution with a scintillation counter (Model 810c, Baird-Atomic, Cambridge, Mass.) in conjunction with a spectrometer (University II Series, Model 530, Baird-Atomic). Counting intervals were selected to register approximately $10^4$ counts. Results are given in Figure 3.

**Nonisotopic Systems.** For systems containing unlike tracer and bulk electrolytes, an apparatus similar to that described in the preceding section was used but with a cell of somewhat different dimensions. Each solution channel was 5.1 cm long, 0.64 cm wide, and 0.15 cm deep. The baffles were of Teflon instead of platinum. This cell had a slightly higher ratio of membrane surface area to solution volume than the cell used for the isotopic systems and was consequently more efficient. Also, the solutions were pumped at constant rates using peristaltic pumps (New Brunswick Scientific Co.). Flow rates were about 3 ml/min.

In these experiments, $^{110m}Ag$, $^{133}Ba$, $^{137}Cs$, $^{140}La$, $^{85}Sr$, and $^{65}Zn$ were added to the donor solution, each with sufficient carrier to make the solution initially $10^{-5}F$ in the corresponding trace ion. The reciprocal flux function was determined for each tracer in bulk electrolytes of $HClO_4$ and of $NaClO_4$, following the same procedure as above but at usually four concentrations of each bulk electrolyte. Bulk electrolyte concentrations ranged between 0.005 and $0.2F$. The results of these experiments are shown in Figures 4 and 5.

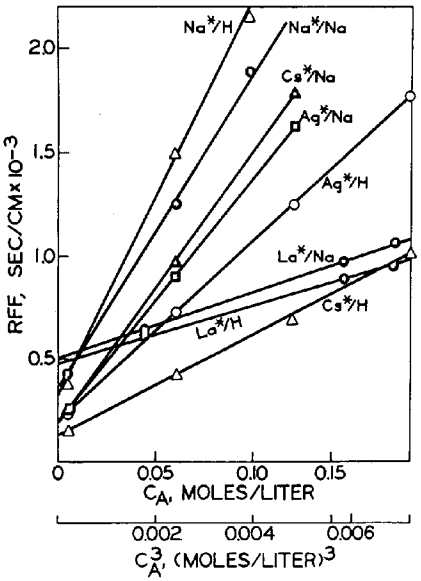


**Figure 4. RFF for nonisotopic systems**

AMF C-103 cation-exchange membrane. Metal perchlorates. Designation: trace ion*/bulk ion. $C_A^3$ scale applies to La plots

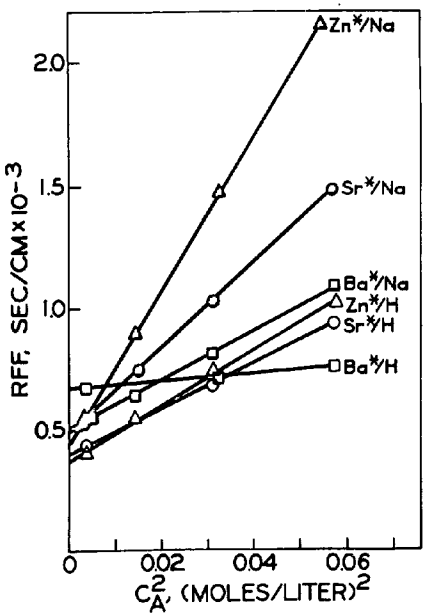


**Figure 5. RFF for nonisotopic systems**

AMF C-103 cation-exchange membrane. Metal perchlorates. Designation: trace ion*/bulk ion

**Additional Verification of Equation 17.** Using the same apparatus and experimental procedure as for the nonisotopic systems, Equation 17 was verified for a system employing a divalent bulk counterion. Figure 6 shows the transport behavior of tracer-$^{22}$Na in a bulk electrolyte of $CaCl_2$. The transport of an anionic counterion was studied using an AMF A-104 anion exchange membrane and tracer-$^{125}$I in a bulk electrolyte of NaCl. The results of these experiments are shown in Figure 7. Also shown in Figure 7 are the results of transport measurements on $^{133}$Ba in a bulk electrolyte of $NaClO_4$ through the P-116 and P-1010 cation-exchange membranes.

**Temperature Dependence of RFF.** The temperature dependence of the reciprocal flux function was investigated using an AMF C-103 membrane in a system containing tracer-$^{133}$Ba and $NaClO_4$ as the bulk electrolyte with the same apparatus and sampling procedure as described for the nonisotopic systems. For each of four temperatures (10, 25, 40, and 60 °C), the reciprocal flux function was determined at three bulk electrolyte concentrations. Temperature control was achieved

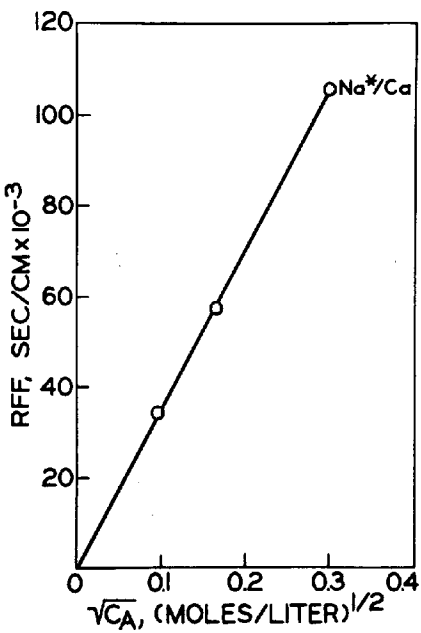


**Figure 6. RFF for $Ca(ClO_4)_2$ bulk electrolyte**

AMF C-103 cation-exchange membrane

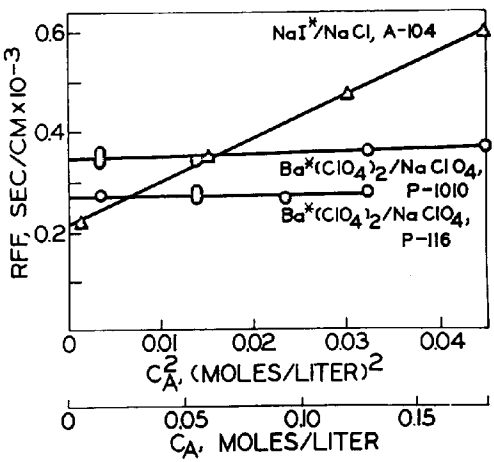


**Figure 7. RFF for transport through various membranes**

Designation: trace ion*/bulk ion, membrane

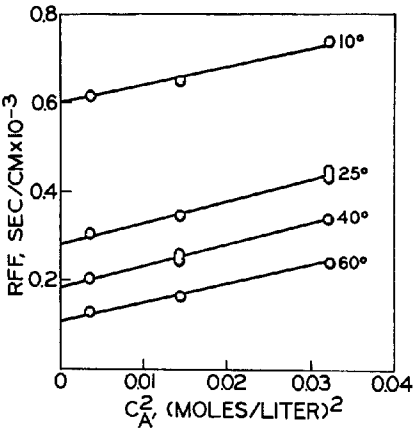


**Figure 8. Temperature dependence of RFF**

**AMF C-103 cation-exchange membrane. $Ba^{+2}Cl_2/NaClO_4$**

with a thermostated water bath. The results of these measurements are shown in Figure 8.

## RESULTS AND DISCUSSION

**Validity of the Flux Equation 17.** The linear dependence of RFF upon $C_A^z$, as described by Equation 17, is well demonstrated for uni-, di-, and tri-valent counterions over substantial ranges of concentration by the plots in Figures 3–8.

The isotopic systems in Figure 3 represent the most precise test of Equation 17 because the selectivity coefficient ($K$) is unity and independent of concentration. Each point in Figure 3 represents an average of four determinations of RFF taken over three different flow rates for the acceptor solutions. The relative standard deviation of a single determination of RFF for the isotopic cases was found to be 4.6%. A least-squares analysis of the plots of Figure 3 shows mean probable errors of 0.96% in the slopes and 3.3% in the intercepts. The probable error is the deviation that is exceeded in half of the observations.

Theoretically, curvature should be introduced into these plots by the concentration dependence of the forward rate constant ($k_f$ in Equation 17). But the low probable error in the slopes shows that there is little deviation from linearity in the plots. Two alternative explanations may be advanced for the good linearity of the isotopic plots: 1) The $k_f$-containing term that represents the influence of the ion-exchange reaction in Equation 17 may be unimportant for the isotopic cases at 25 °C. 2) The activity coefficient ratio of Equation 21 for the isotopic case may not vary greatly with concentration below 0.2$F$. The data of this paper do not permit a choice between these alternatives.

On the other hand, the twelve nonisotopic cases of Figures 4 and 5 show a mean probable error of 4.3% in the slopes and 3.2% in the intercepts. Because the errors of method and equipment are virtually identical for the isotopic and nonisotopic cases, the significantly greater deviation from linearity for the nonisotopic cases may be ascribed to the greater concentration dependences of $K$ and perhaps $k_f$. In all cases, however, these dependences are slight because the deviations from linearity are not large at concentrations below 0.2$F$, and Equation 17 adequately describes the transport of trace counterions.

It should be pointed out that the data in Figures 3, 4, and 5 were gathered over a period of about a year. The transport rates measured for each tracer in the two bulk electrolytes ($HClO_4$ and $NaClO_4$) were determined around the same time and are comparable. But the rates for different tracers are not precisely comparable: different membrane specimens and/or slightly different equipment (pulsers, etc.) may have been used.

The systems of Figures 3, 4, and 5 all contained the same type of membrane (AMF C-103) and only univalent bulk counterions. Further work was done to show the applicability of Equation 17 to other kinds of systems. Figure 6 is a plot of RFF *vs.* $C_A^{1/2}$ for a system containing Na-tracer and Ca-bulk counterions. A least-squares analysis shows a probable error of 2.0% in the slope, indicating good linearity and agreement with Equation 17. Of particular notice is the greatly reduced tracer transport rate of a univalent ion in a divalent bulk counterion matrix. The large slope of Figure 6 is indicative of the low values of the selectivity coefficient and/or membrane diffusion coefficient for this type of system and suggests that interactions in the membrane phase limit the observed transport rate.

Figure 7 presents data for three other types of membranes, one of which is anionic. The linearity of these plots again supports the validity of Equation 17. The very low slopes for the P-1010 and P-116 membrane systems indicate the insignificance of the concentration dependent term in Equation 17 which represents diffusion through the membrane phase. This is in accord with the thinness of these membranes.

The preceding transport data amply establish the linear dependence of RFF upon $C_A^z$, as called for by Equation 17, and prove the sufficiency of Equation 17 and the transport mechanism from which it is derived. However, it does not prove that all steps of the mechanism are necessary. In particular, the straight-line dependence of RFF upon $C_A^z$ may also be explained by a mechanism that involves only the diffusional steps and not the rate of the heterogeneous ion-exchange reaction. To establish the latter, further work is needed. Most obviously, a study of the dependence of RFF upon the ion-exchange capacity ($Q$) of the membrane might indicate the importance of the ion-exchange reaction in limiting the counter-ion transport rate. For such a study, membranes with closely specified properties and selectable capacities would be needed, but are not presently available. There are other considerations, however, that indicate the importance of the ion-exchange reaction, as described in the following sections.

**Range of Applicability of Equation 17.** It should be noted that the concentration ranges over which the data of Figures 3–7 were taken were around 0.005–0.2$F$. Deviations from the mechanism upon which Equation 17 is based occur outside this range. Above 0.2$F$, the Donnan exclusion of the co-ion begins to break down and counterions can enter the membrane phase by a nonexchange process.

At very low concentrations, the high transport rate (low RFF) called for by Equation 17 was not attained. This was shown experimentally for both an isotopic system ($^{22}Na$ tracer, $NaClO_4$ bulk electrolyte) and a nonisotopic one ($^{133}Ba$ tracer, $NaClO_4$ bulk electrolyte). At $10^{-4}M$ $NaClO_4$, the RFF for the tracer $^{22}Na$ is about 80% greater than the intercept determined by extrapolation of RFF values measured at $NaClO_4$ concentrations above 0.005$M$. For the $^{133}Ba$ tracer, the discrepancy is even larger, amounting to about a 3-fold increase. Similar effects were noted for lower $NaClO_4$ concentrations, and for P-1010 and P-116 membranes. No further work was done to determine whether or not another transport mechanism applies in the low concentration domain.

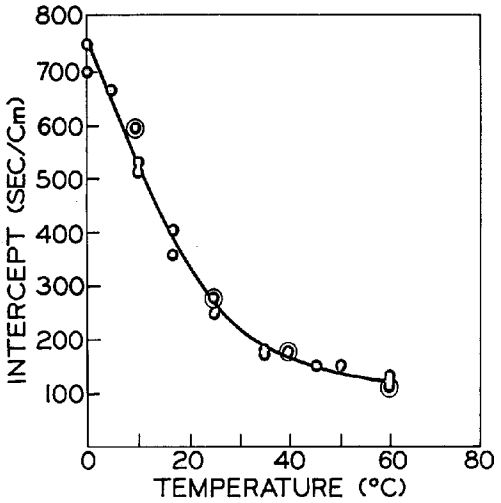


**Figure 9. Temperature dependence of intercepts**

**AMF C-103 cation-exchange membrane. $Ba^*Cl_2/NaClO_4$. The four large circles represent intercepts taken from Figure 7. Small circles represent single values of RFF taken in 0.06$M$ $NaClO_4$, so dilute that the RFF is virtually equal to the intercept**

**Indirect Evidence for the Influence of the Heterogeneous Exchange Reaction.** For any given system, it is possible to assess the relative importances of the three types of rate processes (*viz.* diffusion through the membrane, diffusion through the liquid films, and the heterogeneous exchange reaction) by examining plots of RFF *vs.* $C_A^{\ z}$. According to Equation 17, the slope of such plots determines the contribution of membrane phase diffusion to the RFF and this contribution is concentration dependent. On the other hand, the contributions to the RFF by liquid film diffusion and by the heterogeneous exchange reaction are concentration independent, and they are represented by the value of the intercept. Accurate measurement of the slope and intercept together with membrane and liquid film characteristics ($\bar{L}$, $K$, $Q$, $L$, and $D$) might permit good estimates of $\bar{D}$ and $k_f$, which in turn might give insight to the nature of the diffusion through the membrane and to the nature of the ion-exchange reaction. Such measurements are presently under investigation.

However, in the absence of extensive and accurate data on membrane and liquid film characteristics, examination of the intercepts of the systems in Figures 4 and 5 indicate strongly that some factor other than the rate of diffusion through the liquid film exerts an influence on the overall rate of counterion transport in some of the systems. The intercept is equal to

$$\frac{2L}{D} + \frac{2}{k_f (Q/a)^z}$$

where $D$ and $k_f$ actually represent values at infinite dilution. If the heterogeneous ion-exchange reaction is too fast to have any influence on the intercept [$2/k_f(Q/a)^z$ small], then the magnitude of the intercept should be dependent only upon $2L/D$. For such cases, the intercept for a particular trace ion should be the same in systems with different bulk electrolytes because $D$ for that trace ion at infinite dilution should be independent of the nature of the bulk electrolyte, providing that there is no interaction. Departure from such behavior may be taken as evidence that some factor other than liquid film diffusion is exerting an influence on the magnitude of the intercept.

**Table I. Analysis of Intercepts**

| Trace ion, $B$ | Bulk ion, $A$ | Intercept, sec/cm | Difference sec/cm | Difference relative, % |
|---|---|---|---|---|
| $Ag^+$ | $H^+$ | 195 | 8 | 4 |
| | $Na^+$ | 203 | | |
| $Na^+$ | $H^+$ | 323 | 39 | 11 |
| | $Na^+$ | 362 | | |
| $Cs^+$ | $H^+$ | 135 | 46 | 29 |
| | $Na^+$ | 181 | | |
| $Ba^{2+}$ | $H^+$ | 667 | 160 | 27 |
| | $Na^+$ | 507 | | |
| $Sr^{2+}$ | $H^+$ | 391 | 101 | 23 |
| | $Na^+$ | 492 | | |
| $Zn^{2+}$ | $H^+$ | 367 | 75 | 19 |
| | $Na^+$ | 442 | | |
| $La^{3+}$ | $H^+$ | 480 | 28 | 6 |
| | $Na^+$ | 508 | | |

Table I contains an analysis of the intercept data from Figures 4 and 5. The last column gives, for each trace counterion, the relative difference between the intercepts in systems containing bulk counterions of hydrogen and of sodium. For all tracers except $^{110m}Ag$ and perhaps $^{140}La$, the differences are much greater than would be expected from the precision with which the intercepts were measured (about 3%), indicating that some factor other than liquid film diffusion and membrane diffusion is affecting the overall rate of counterion transport.

The hypothesis may be made that this factor is the surface exchange reaction. This hypothesis may be tested by observing the effect of temperature on the transport rate.

**Temperature Dependence of RFF.** Figure 8 shows RFF plots for $^{133}Ba$ tracer in $NaClO_4$ bulk electrolyte at several temperatures. It is notable that the slopes are negligibly temperature dependent, indicating that the product $K\bar{D}$ in the slope expression of Equation 17 is practically independent of temperature. Experimentally, $K$ for the exchange of sodium by barium was observed to decrease by about 20% between 25 and 60 °C, so the temperature dependence of $\bar{D}$ should be positive and small. This behavior reflects the low activation energy of the counterion transport process through the membrane phase and supports the assumption of a simple diffusional process occurring within the membrane.

On the other hand, the intercepts of Figure 8 are markedly temperature dependent, particularly at low temperature. Figure 9 shows the relationship more clearly, being a plot *vs.* temperature of the intercepts of Figure 8, together with additional values measured at other temperatures. At high temperatures, the temperature coefficient of the intercept approaches a limiting value of a few per cent per degree, about the same as that for a diffusional process. At low temperatures, the temperature coefficient of the intercept is much greater, indicating that a chemical process with a significant activation energy is influencing the value of the intercept and the rate of counter ion transport. As the only nondiffusional step in the transport mechanism, the heterogeneous ion exchange reaction might be such a chemical process.

Heretofore, ion exchange processes in aqueous media have been considered to be fast and to have no significant activation energies. Yet some interfacial processes, like chemisorption and crystallization do have high activation energies and low rates. It is conceivable that a counterion passing from a dilute aqueous phase into the polymer matrix with its high ionic strength and partially nonaqueous character might

undergo a change in state that has a significant activation energy associated with it.

By observing the temperature dependence of the reciprocal flux function, it may be possible to correct the value of the intercept for diffusion in the liquid phase and thereby to obtain the forward rate constant ($k_f$) for the chemical process. This information would open a new path to the quantitative study of the thermodynamics of heterogeneous ion exchange reactions. A number of systems are currently being examined in this laboratory and the results of these investigations will be presented in a forthcoming publication.

ACKNOWLEDGMENT

For samples of membranes donated in the early stages of this work, thanks are extended to both the American Machine and Foundry Company and the RAI Research Corporation.

RECEIVED for review November 4, 1968. Accepted January 15, 1969. This work was supported in part by the United States Atomic Energy Commission Grant No. AT(11-1)-1082. The material was presented in part at the 153rd National Meeting, ACS, Miami Beach, Fla., April 1967.

# On Rapid Laboratory Dialysis

**Lyman C. Craig and Hao-Chia Chen**

*The Rockefeller University, New York, N.Y. 10021*

**Attempts to devise a practical, rapid, and highly efficient laboratory dialyzer have resulted in the construction of an improved countercurrent "thin film" dialysis column which will clear the tritium count in tritiated water, on a single pass requiring 6–8 min, to the extent of at least six orders of magnitude. Bacitracin, mol wt 1422, can be cleared to the extent of 99+%. Data are presented to show that the column in its present form is useful for desalting peptide, protein, and nucleotide solutions, for proton exchange studies, for various binding studies, and certain bio-assays. It can be used as an ultrafiltration device by using a polymer to provide a higher osmotic pressure in the diffusate than is in the retentate stream.**

IT HAS LONG BEEN RECOGNIZED in chemical engineering and in physiology that a basic problem connected with the selective separation of mixtures of solutes by membrane diffusion is that of the rate of transport of a given solute across the membrane. At the present time, this is emphasized by extensive efforts to improve and reduce the size of the various types of dialysis devices employed in hemodialysis. The problem is being studied from many different viewpoints which involve mainly an attempt to prepare more efficient membranes by making them thinner and stronger and by incorporating them in a more efficient dialysis device. Ultrafiltration, a closely related procedure, is also being widely investigated. Thus far the major effort has been directed toward the removal of small solutes (urea) from large ones (the plasma proteins) and, therefore, little attention has been given to differential dialysis and the problems of selectivity.

In previous papers from this laboratory (*1*, *2*) it has been shown that the most important basic parameter for the achievement of higher selectivity in dialysis is "restricted diffusion" (*2*, *3*). Solutes are separated on the basis of their relative Stokes radii. It has also been postulated (*4*) with good evidence that this is the most important parameter in gel filtration, presently one of the most effective and widely used separation techniques in biochemistry. In dialysis, which can be an effective supplementary technique to gel filtration, the highest selectivity is reached by an arrangement which provides the highest possible rate of transport of diffusable solute across the membrane. This has been shown in a static dialysis device (*2*) and in a countercurrent dialyzer (*5*) of preliminary design. This paper will describe further experiments which serve to define the problem and the parameters somewhat more clearly for the continuous dialyzer.

Experiments bearing on the problem actually are rather simple in concept but necessarily must depend on many different parameters. In spite of this, relatively minor changes in the design of the dialyzer, previously described (*5*), permit the overall process to be evaluated in a rather simple manner which coincides with the way it can be used effectively in a variety of biochemical experiments. In this arrangement both the retentate and diffusate effluent streams can be collected in a fraction collector. A pulse of a solution containing 1*N* sodium chloride and 0.1% dextran blue run into the entering retentate stream will then give two effluent patterns such as those shown in Figure 1 when both effluent streams in the fraction collector are analyzed for sodium chloride and for the blue dye. The performance of the blue dye which does not pass through the membrane can be observed visually as it passes up the column in a more or less discrete thin band. All the sodium chloride should and does appear in the diffusate effluent. Attempts to improve the dialyzer were monitored by experiments of the type shown in Figure 1 in which the objective was the reproducible achievement of the narrowest bands possible from both streams.

With the foregoing approach to improvement the thin film dialyzer has now been brought to the point where it becomes a useful and discriminating tool for many uses in biochemistry. Some of them are the following: desalting; comparison of molecular (diffusional) size, Stokes radii; ultrafiltration (accelerated by using a nondiffusable solute in the diffusate stream to cause osmotic flow); tritium–hydrogen exchange; as a substitute for trichloroacetic acid (TCA) precipitation in such bioassays as that of the specific t-RNA estimation; a wide variety of binding studies; and experiments with partial enzymatic degradation of large molecules.

The value of the rapid dialyzer in some of these applications will be discussed briefly in this paper in connection with actual experiments. Full treatment for the remainder of the above points will be given in future papers.

(1) L. C. Craig, T. P. King, and A. Stracher, *J. Amer. Chem. Soc.*, **79**, 3729 (1957).
(2) L. C. Craig, *Science*, **144**, 1093 (1964).
(3) E. M. Renken, *J. Gen. Physiol.*, **38**, 225 (1954).
(4) G. K. Ackers, *Biochemistry*, **3**, 723 (1964).
(5) L. C. Craig and K. Stewart, *ibid.*, **4**, 2712 (1965).

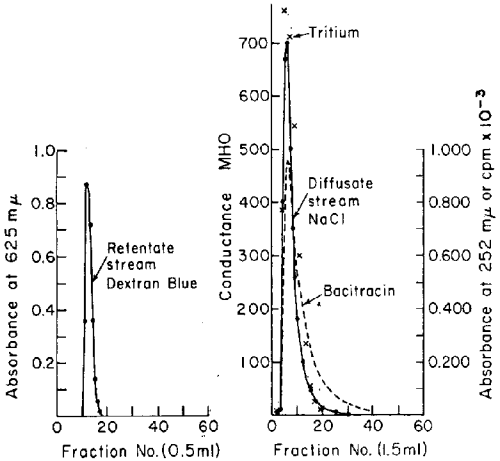


**Figure 1. Effluent patterns from the thin film dialyzer**

## EXPERIMENTAL

The modified thin film dialyzer which best permits the type of performance demonstrated in Figure 1 is shown in Figure 2. A modification required for this type of evaluation is one which permits the retentate effluent to be transported to the fraction collector with the minimum of holdup after it reaches the top of the dialysis membrane. This is accomplished with size 24 Kel-F tubing, one end of which reaches to the membrane inside the glass collar which holds the upper end of the dialysis tubing. The other end leads to a pump and from there to the fraction collector. The diffusate effluent stream flows out the lower end of the column through the hypodermic needle which serves as a bearing and into the fraction collector. Its rate of flow can be regulated by gravity or by passage through a pump.

The upper end of the inside glass tube is of different design than in the previous model (*5*). It is of smaller outside diameter at the point where it leaves the membrane and extends upward through the glass collar about 5 cm to provide sufficient length for the support clamp. The capillary tube (0.70 mm i.d.) extending through this tube to the bottom of the dialysis membrane has a Becton-Dickinson syringe glass joint sealed to it at the top.

The pumps used in this study were Holter Bilateral Roller pumps, Model RD 044 (The Holter Co., Bridgeport, Pa.) which use silastic pumping tubes. These tubes were also convenient for making connections to the Kel-F tubing.

The outer glass tube of the dialysis column was made to rotate by two small round rubber belts operating in balanced opposition to each other as shown in the insert in Figure 2. They were driven by two pulleys which were driven by two longer belts in turn driven by a single pulley on the shaft of an electric motor. The tension on the belts could be adjusted so that any increased friction due to maladjustment of the membrane would cause the belts to slide rather than tear the membrane. The overall design provides minimal friction or pressure on the membrane. The bearing at the bottom is a No. 18 Becton-Dickinson syringe needle 8 cm in length with the sharp tip ground off and passed into a Teflon (Du Pont) tube which fits it rather snugly. This provides a flexible bearing when the Teflon tube is held by a rubber stopper in a support clamp. The inside glass tube supporting the membrane is held only at the top by passing through a rubber bushing held in a clamp. Thus very little pressure or friction is transmitted to the membrane. A single membrane can often be used continuously for weeks or even months without replacement and thus many runs can be made on a single calibrated membrane.

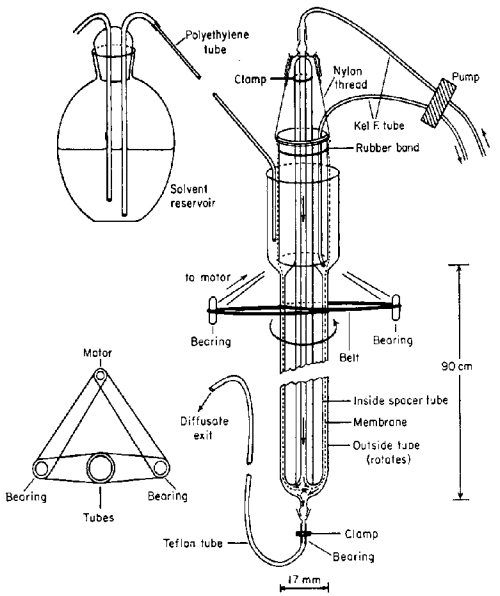


**Figure 2. Schematic drawing of thin film countercurrent dialyzer**

It was found that the efficiency of the dialyzer was considerably improved when an inside tube larger than the diameter of the casing was used. Visking dialysis casing No. 20 or seamless cellulose casing No. 18 both have a wet inflated diameter of approximately 15 cm. An inside tube 17 mm in outside diameter proved about optimum after a method was developed for drawing the wet casing over the glass inside tube so that it was not stretched beyond the elastic limit and thus caused to exhibit regions of nonuniform tension. With this arrangement, the membrane when in place has been stretched approximately 13% in the circular direction. The method most satisfactory for stretching it over the inside tube is the following:

A length of tubing approximately 100 cm long is wetted and the diameter of one end enlarged by pushing it over a tapered glass tube (*6*). This end is then pushed over the wet (with frequent dipping) surface of the glass collar (18 mm i.d.) nearly to the top. It is temporarily held on the glass collar by wrapping a stretched rubber band around the upper edge.

The inside main tube is inverted and held by a clamp at a point just above the small tapered joint. The surface of the inside glass tube is smeared with glycerol and 10 or 15 ml of glycerol placed inside the dialysis tubing attached to the glass collar. The glass collar and tubing are then carefully and gently drawn over the glass tubing at a smooth even rate. While the tubing is being drawn over the glass tube, a constant stream of water from a wash bottle is directed at the tubing at the point where it passes onto the glass tube. The rapid osmotic flow of water through the membrane into the glycerol seems to provide a lubricating film and thus even stretching of the membrane. If the membrane does not slip over the inside glass tube smoothly, it will have regions stretched beyond the elastic limit and will tend to balloon at these points in the dialyzer during operation.

After the casing has been pulled over the glass tube, it is kept wet and can be moved easily up or down on the glass tube. Its position is adjusted so that the glass collar is approxi-

(6) L. C. Craig, "Advances in Analytical Chemistry and Instrumentation," Vol. 4, C. N. Reilley, Ed., Interscience Publishers, New York, 1965, p 56.

mately 6 or 7 cm below its final position and the bottom then tied off with a silk thread. The membrane is flushed again with water to ensure its easy movement on the glass tube and the glass collar moved up to its final position. It is secured there by tying two nylon threads, previously tied around the glass collar to two hooks attached to the capillary tube extending from the top as shown in Figure 2. The dialysis casing is thus under tension longitudinally as well as circularly for it has been stretched approximately 5 cm.

The assembly is then carefully inserted into the outer tube as shown in Figure 2 keeping all surfaces wet. Its position is adjusted by the clamp at the top so that it hangs evenly in the outer tube which is filled with water. The outer tube must be kept always full of water or a buffer solution.

The two streams are now started with the retentate stream rate set at about 0.5 to 0.8 ml/min. Rotation of the outer main tube is also started. The first test of a satisfactory membrane is met when water passes steadily through the retentate effluent tube at a rate slightly less than that injected. The diffusate effluent stream should pass by gravity at a rate up to 5 or 10 ml/min without causing the membrane to balloon. If this is accomplished, the assembly is ready for solute testing by passing approximately 0.5 ml of a solution of dextran blue in 1.0*N* NaCl into the retentate stream and by chasing it through with water.

Because, as shown in Figure 1, all the measurable sodium chloride is removed from the retentate stream on a single pass, a more rigorous test is required. For this purpose tritiated water (0.1 to 1.0 mCi.) is ideal for it has been found to pass these cellophane membranes at a rate not too different from sodium chloride and can be measured at very high dilution with a Bray scintillation solution and a counter. It was found that a good membrane was capable of reducing the tritium count of a pulse of $10^8$ cpm in the retentate stream to less than $10^2$ cpm on a single pass when the diffusate flow rate approximated 3 to 10 times that of the retentate. This clearance could be accomplished at 0 °C as well as at room temperature.

Another type of test of the efficiency involved the relative rates for the clearance of larger molecules such as bacitracin, mol wt 1420 (*2*) and subtilin, mol wt 3500. At room temperature a pulse of bacitracin was cleared to the extent of over 99% and on a continuous feed-in basis (steady state) to the extent of 97%. This compares to the 67% reported with the earlier dialyzer (*5*) at the same rate. Subtilin was cleared to the extent of approximately 70%. Although lysozyme (mol wt 14,000) and insulin at pH 3 (mol wt 12,000 partially dissociated to 6000) pass slowly through Visking 20 in the static thin film dialysis unit (*2*), in the continuous unit only a negligible amount diffuses into the diffusate stream on a single pass.

## RESULTS AND DISCUSSION

From a theoretical as well as a practical standpoint, it is of considerable importance to learn as much as possible about the various parameters which determine the rate of transfer of a given solute through a semipermeable membrane when the only driving force involved is a concentration gradient across the membrane. Previous papers have dealt with this problem for a static type of dialyzer (*1*, *6*, *7*) and have shown the advantage of a maximum membrane area to retentate volume —*e.g.*, a "thin film" dialysis cell—in studying the various parameters. The same should hold for a continuous type of dialyzer but here there is a complication. Because of viscosity a certain pressure is needed to cause a very thin film of solution to flow evenly over a considerable length of a membrane in a controlled way. Pressure, however, distorts the effective pore size and the membranes tend to become plugged due to ultrafiltration. The design of dialyzer given in Figure 2 minimizes this problem by rotating the outside tube continuously. This motion causes the diffusate stream to flow in a spiral movement down the tube in a uniform thin film and thereby avoids channelling. Moreover, it was found to keep the membrane in micro oscillation or fluctuation as well and even to cause the retentate stream to spiral, albeit much more slowly than with the diffusate stream. The movement of the membrane can be observed clearly by introducing a small air bubble in the retentate stream. The movement of the retentate solution also can be observed with the dextran blue dye. If the bore of the outer tube should be perfectly round, the rotation of the outer tube would not be expected to cause the membrane to fluctuate as efficiently as if the bore of the tube was slightly off from round. In support of this idea was the finding that an apparatus made from selected commercial tubes seemed to give a dialysis result of higher efficiency than those made from precision bore tubing.

Obviously, the highest transport rate across the total membrane area would be reached by having the thinnest possible membrane and the thinnest possible flowing retentate solution film. In the apparatus of Figure 2, the thin film results mainly from two pressures. One is from the tension of the membrane. It is stretched over the inside tube. The other comes from a measure of support provided by the moving diffusate solution film. The latter is deduced from the fact that the annular space between the inner and outer tube (with the membrane between) is rather critical and about 0.3 mm in depth. A slightly larger annular space always has given a less satisfactory result. It was found necessary to make the inside tube from tubing precision ground and polished on the outside. The outer tube was selected from a supply of ordinary 20-mm o.d. commercial tubing in the following way: a single thickness of masking tape was wrapped around the inside precision tube at several points along its length. A satisfactory outer tube was one that would barely allow the taped inner tube to be inserted without sticking but not when two layers of the tape were put around the inner precision tube.

Even when the two tubes were mated in this way, a dialysis column of maximum efficiency was not always reached. It could be that the roundness of the inside of the outer tube in these cases was too nearly perfect or conversely deviated too much. Experiments are in progress to make a controlled slightly eccentric outer tube. All attempts to reduce the annular space to less than approximately 0.3 mm have given columns that would not permit the diffusate stream to flow properly.

The thinness of the membrane and its strength would be expected to be very important parameters. Unquestionably a thinner membrane providing the critical degree of tension would be superior. Our few experiments with a thinner membrane, however, have failed apparently because of lack of sufficient strength. Visking 20 dialysis tubing and 18 seamless cellulose casing (about 0.02 mm in thickness) have both given good membranes although a number of the sections tested failed apparently because of nonuniformity.

Attempts to alter the pore size by acetylation (reduction) or $ZnCl_2$ treatment (*7*) (enlarging) were successful in the first case but not in the second. The $ZnCl_2$ treatment reduces the strength of the membrane and causes it to balloon in the countercurrent process. However, such membranes gave a considerably increased rate of transport (*8*) when the column was operated in the cocurrent manner (see later). In the

(7) L. C. Craig and William Konigsberg, *J. Phys. Chem.*, **65**, 166 (1961).

(8) S. Simon and L. C. Craig, to be published.

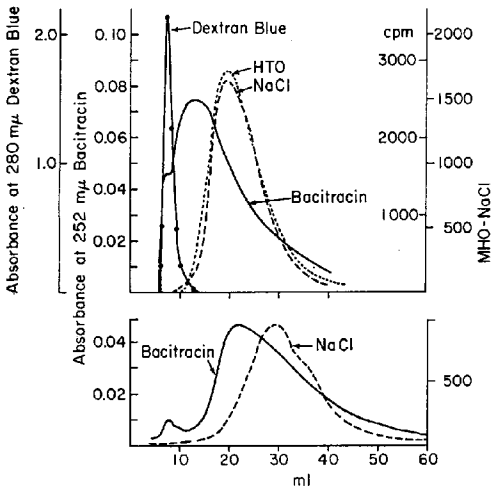


**Figure 3. Retentate effluent patterns with diffusate stream immobilized**

**Upper patterns = single pass; lower patterns = two passes**

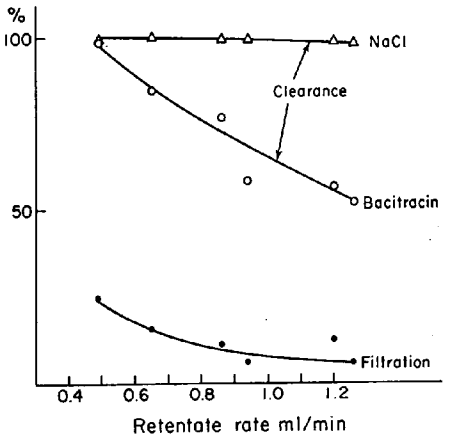


**Figure 4. Effect of rate of flow on differential clearance**

cocurrent system, the pressure on the membrane is equalized in contrast to the countercurrent procedure. The latter requires a slightly higher retentate pressure at the bottom of the column than at the top in order to cause the solution to move. The diffusate film stream is not as thin as that of the retentate by a factor of two or three. Acetylation strengthens the membrane.

In certain respects a dialysis procedure with the apparatus of Figure 2 operated to give the result of Figure 1, resembles the idealized concept of gel filtration (*4*, *9–13*). It, of course, can be made to correspond more closely by reducing the flow of the diffusate stream to 0. In this case, with the test mixture used in Figure 1, both solutes would emerge in the retentate stream as shown in Figure 3. The dextran blue band corresponds to the band in gel filtration which is unable to penetrate the gel. The band of sodium chloride which penetrates the membrane is retarded as would be expected but it is relatively broad, a result which could be caused by greater instability of the concentration gradients as compared to gel filtration. There is also the possibility that gel filtration is a more complicated process than that of the idealized view and is dependent on parameters other than simple diffusion.

It is obvious with this procedure from Figure 3 that a solute larger than sodium chloride such as bacitracin (mol wt 1422) would be expected to be retarded somewhat more than dextran blue but not as much as sodium chloride. However, it would also be expected that a wider effluent band would result because of a lower diffusion rate and greater disequilibrium in the column sense. The latter would cause the band to extend beyond the sodium chloride band and thus confuse the separation. Figure 3 confirms this. The difficulty is analogous to the type of behavior found in countercurrent distribution (CCD) when transfers are made well before equilibrium is reached on each transfer, except for the possible case when the partition isotherms are not linear. If the isotherms are not linear, a striking band sharpening can result or at least this is an explanation for the not uncommon phenomenon in the countercurrent distribution of large molecules (*14*).

The experiment of Figure 3 seems sufficient to show conclusively that this type of countercurrent dialysis, no matter how efficient, will not provide a clear banding out of mixtures of different sized solutes in the way that gel filtration does. The basic difficulty is that "restricted diffusion" operates just as efficiently in the transport of solute from the diffusate stream back into the retentate stream as in the opposite direction. The solvent environment of a solute in both is identical.

How then does the postulated theory of partition and "restricted diffusion" operate in gel filtration? One obvious difference between "thin film countercurrent dialysis" and gel filtration is that in the latter the solute is always in a "restricted" environment in the gel phase and in almost microscopic contact with the moving phase. With the concept of "restricted diffusion," there would be a considerably greater probability for a smaller solute to enter the gel phase from the interstitial moving phase than for a larger one. On the other hand there would not be this difference in the transport from the gel phase to the moving phase. Both small and large molecules would be in the "restricted" openings and could have more nearly the same probability of escaping into the moving phase. Such a state of affairs would, if it could be made to operate, cause the front of the band of bacitracin in Figure 3 to be advanced more rapidly than that of sodium chloride but not cause the trailing rear to be retarded over that of sodium chloride. Both bands would thereby be sharpened and a discrete banding out of solutes could result which would be selective on the basis of Stokes radii.

In the case of the thin film dialyzer, the separation particularly of the nondialyzable solute from the dialyzable solute is greatly improved by the countercurrent flow of the diffusate stream as can be seen from a comparison of Figure 1 with Figure 3. The advantage is further emphasized by the fact that sodium chloride can be separated readily from bacitracin with Visking 18 casing lightly acetylated. It can even be separated from bacitracin in the more porous Visking 20 and,

(9) P. Flodin, in "Dextran Gels and Their Applications in Gel Filtration," Pharmacia; Uppsala, (1962).
(10) J. Porath, *Pure Appl. Chem.*, **6**, 233 (1963).
(11) P. G. Squire, *Arch. Biochem. Biophys.*, **107**, 471 (1964).
(12) T. C. Laurent and J. Killander, *J. Chromatog.* **5**, 103 (1961).
(13) H. Determann, "Gel Chromatography," p 63, Springer-Verlag, Inc., New York, 1968.
(14) L. C. Craig, in "Analytical Methods of Protein Chemistry," P. Alexander and R. Block, Eds., Pergamon Press, New York, (1960), p 136.

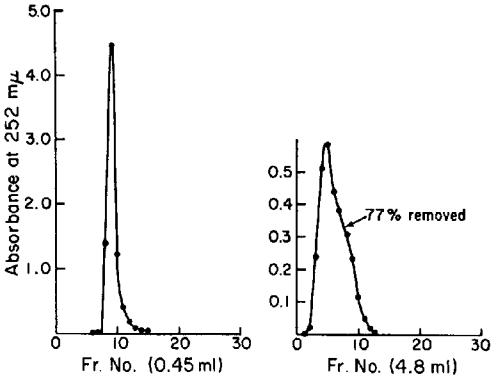


**Figure 5. Shapes of patterns with partial clearance**

**Visking 18 casing. Solute = bacitracin**

therefore, less selective membrane by selecting the most suitable rate of flow of the retentate stream. In this case, the retentate has passed through the dialyzer before all the larger solute can pass into the diffusate stream. The effect of rate on the clearance of NaCl and bacitracin is shown in Figure 4. At a rate of 1.2 ml/min in the retentate stream, nearly 50% of the bacitracin could be recovered essentially free of salt. Although a membrane with smaller pores would be much more effective, Figure 4 demonstrates that rate adjustment can add greatly to selectivity.

In the countercurrent procedure, the shape, position, and width of the emerging bands are of some interest and not entirely those expected. From Figure 1, the diffusate bands for tritiated water, sodium chloride, and bacitracin occur at nearly the same position and that in spite of the fact that bacitracin is more than tenfold larger than the others, it gives a band with the trailing edge only a little displaced from those of the smaller solutes.

When the membrane is of such a porosity that only part of the solute escapes into the diffusate stream on a single pass, the shape of the retentate curve and its position remain nearly the same, Figure 5. It appears to occur a little later and to be sharpened a little. The diffusate band also occurs a little later and is somewhat broader.

After consideration of band widths, positions, and shapes, it would appear that the most important parameter as regards selectivity is "pore size." Differential rates of diffusion in free solution offer little separation. The concept of "restricted diffusion" must be brought into play to explain the observations. A "pore size" which will give a balance of per cent solute in the retentate stream to that in the diffusate stream similar to that in Figure 5 provides a very sensitive way to compare the relative "diffusional" sizes of two solutes. It complements the result obtainable with the static thin film dialysis cell (*7*), and may give quite a different result where the effective size is an average of several conformational forms in dynamic equilibrium. If this is true, the technique should be of interest in binding studies. For a number of reasons the cyclic antibiotic polypeptides are excellent models to investigate this possibility.

Actinomycin D (mol wt 1258) has been shown by spectroscopic methods (*15*) to bind strongly to the deoxyguanidine

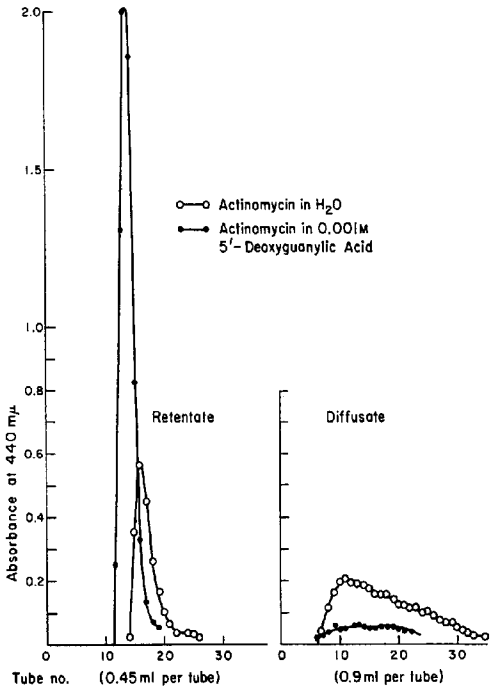


**Figure 6. Binding studies with Actinomycin**

residue in DNA and to the free nucleotide as well. A 2-mg sample of the antibiotic in 0.5 ml of water gave the retentate and diffusate patterns shown in Figure 6. When this experiment was repeated with water containing 0.001*M* 5′-deoxyguanylic acid (mol wt 345) a striking difference was noted. The relative per cent found in the retentate and diffusate, 24 and 76%, respectively, was changed to 89 and 11%. A similar result was obtained when a molar equivalent of the free nucleotide was added to the antibiotic and pure water used as the solvent. Dr. W. I. Taylor was able to show the binding clearly by the static thin film dialysis technique also but failed to show any binding when the amino group was removed from the actinomycin. However, a repeat of the experiment of Figure 6 with this derivative clearly showed an effect although the binding obviously was much weaker. It is likely, therefore, that the continuous thin film dialyzer will be a sensitive tool for studying weak binding effects. This will be further demonstrated (*16*) by studies with lysozyme.

The technique should be of interest also in studying association phenomena with solutes of intermediate size. The tyrocidines are particularly good models for these studies since their association behavior has been thoroughly studied (*17*). In aqueous solution they are extensively associated to a wide range of molecular sizes. The association is apparently largely due to hydrophobic bonding and is inhibited by organic solvents such as acetic acid, methanol, and dimethylformamide. On the other hand, it is increased by addition of salt. The effect of these additives is clearly shown by Figure 7. Addition of

(15) I. H. Goldberg, M. Rabinowitz, and E. Reich, *Proc. Natl. Acad. Sci.*, **48**, 2094 (1962).

(16) L. C. Craig, H. C. Chen, and E. J. Harfenist, "Modern Separation Methods of Macromolecules and Particles" in Progress in Separation and Purification, C. van Oss, Ed. John Wiley and Sons, New York, in press.

(17) M. A. Ruttenberg, T. P. King, and L. C. Craig, *Biochemistry*, **5**, 2857 (1966).

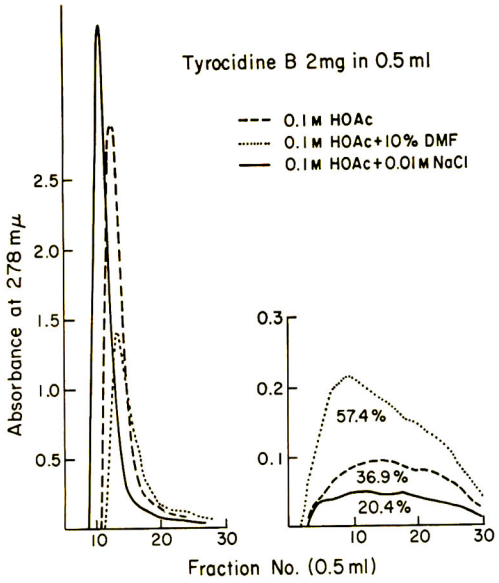


**Figure 7. Study of association-dissociation with tyrocidine B**

dimethylformamide causes a higher per cent of tyrocidine B to pass through the membrane into the diffusate stream. Sodium chloride even at 0.001*M* has the opposite effect. A higher concentration would prevent diffusion through this membrane almost completely.

These experiments serve to emphasize the importance of critical "pore size" for selective separations based on solute size. An equally important problem as far as practical separations are concerned deals with the optimum physical arrangement to take advantage of "pore size." One approach to this problem would be to lengthen the column. Experiments with shorter columns indicated a rough correlation between the length of the column and its efficiency in removal studies. However, for a number of reasons it does not appear practical to build a column much longer than 90 cm. A more practical approach involves mounting a number of such columns on a single stand. In Figure 8 this has been done with four dialysis tubes. All four are driven by a single motor. The effluent streams from each unit in this arrangement can, with an adequate number of pumps, be directed into the adjoining unit or into a fraction collector as desired. If the four are operated in series, this would be the equivalent of a column 360 cm in length.

Other advantages stem from this arrangement. The optimum rate of flow of the entering retentate stream is about 30 ml per hour. Four such dialyzers operating in parallel would afford 120 ml per hour, which makes the rapid desalting of substantial volumes of solution quite practical.

Another advantage is the possibility of a true countercurrent separation potential with constant feed in a central unit when the units are connected in series. This possibility will be explored in the future after the maximum efficiency for each unit has been reached. This could reduce the concentration requirement of previous designs (*18*, *19*).

For the problem of desalting large volumes of solution, the

(18) R. H. Signer, W. Hanni, W. Noestler, W. Rottenberg, and P. von Tavel, *Helv. Chim. Acta*, **29**, 1984 (1946); **30**, 334 (1947).
(19) H. Vink, *Arkiv Kemi*, **19**, 531 (1962).

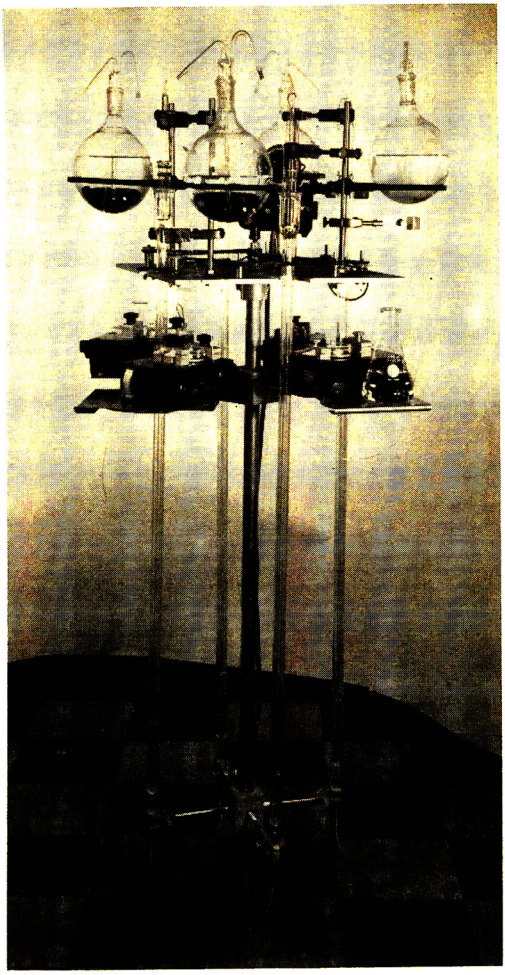

**Figure 8. Four dialysis tubes mounted on a single stand**

column can be operated in a cocurrent manner by reversing the direction of flow of the diffusate stream. This requires a second pump to force the diffusate solvent in at the bottom of the column and remove it, as in the case of the retentate stream, from the top. Tests with salt solutions showed that a practical rate of flow would be 10/1 for the diffusate and retentate streams, respectively. At this rate, approximately 90% of the salt was removed in a single unit on a single pass. A second pass would increase the removal to 99%.

The rapid and complete clearance of tritium logically suggests the use of this procedure in proton exchange work (*20*) much as Englander (*21*) has done with sephadex. It has the advantage over sephadex of being applicable to small peptides as is evident from the studies of Laiken, Printz, and Craig (*22*) with gramicidin S-A.

A dialysis technique for rapid removal has many possible applications in biochemistry. For instance, it can replace trichloroacetic acid precipitations in radioactive tracer incorporation experiments in large molecules. In the bio-assay of a

(20) L. C. Craig, H. C. Chen, and W. I. Taylor, *J. Macromol. Sci., Part A*, in press.
(21) S. W. Englander, *Biochemistry*, **2**, 798 (1963).
(22) S. Laiken, M. Printz, and L. C. Craig, *ibid.*, **8**, 519 (1969).

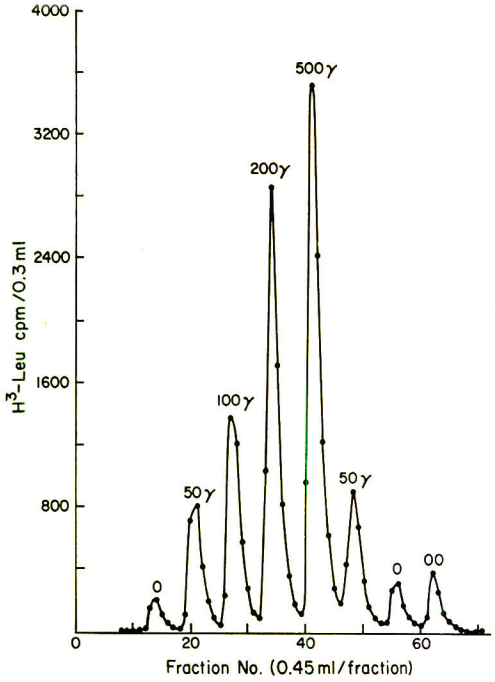


**Figure 9. Amino acid clearance study for t-RNA assay**

specific t-RNA, a sample of the t-RNA was incubated with the desired radioactive amino acid and enzyme preparation in the usual way (*23*). The mixture was passed through the dialyzer in a few minutes to remove the unincorporated amino acid. A direct count in the scintillation counter then showed the amount incorporated and permitted calculation of the amount of the specific amino acid t-RNA. Figure 9 shows the result when different weights of crude t-RNA from *E. coli* were incubated with $H^3$ leucine and successively passed through the dialyzer. The dose response curve from this chart is shown in Figure 10. This use of the dialyzer, suggested by Dr. Charles O'Neal of this University, requires only a fraction of the t-RNA needed in the standard TCA precipitation procedure.

In normal operation of the dialyzer when the retentate and diffusate streams do not differ significantly in osmotic pressure, there is a reduction in volume of the retentate stream of 10–15% on a single pass which apparently is due to ultrafiltration. This can be increased to various degrees by adding a polymeric solute such as polyethylene glycol 4000 or 1540 to the diffusate stream in order to provide a higher osmotic pressure. The effect is clearly shown in Figure 11 in which the per cent ultrafiltration observed by comparison of retentate influent and effluent rate is plotted against the polymer concentration. The values given are for a single pass at 25 °C and are quite sensitive to the rate of flow of the retentate stream.

The effect on the rate of clearance of a solute of a combination of ultrafiltration and dialysis is also shown in Figure 11. For this purpose ATP was chosen because it is known from studies with the static thin film dialysis (*24*) that it has a surprisingly large diffusional size for its molecular weight and would show only partial clearance on a single pass through

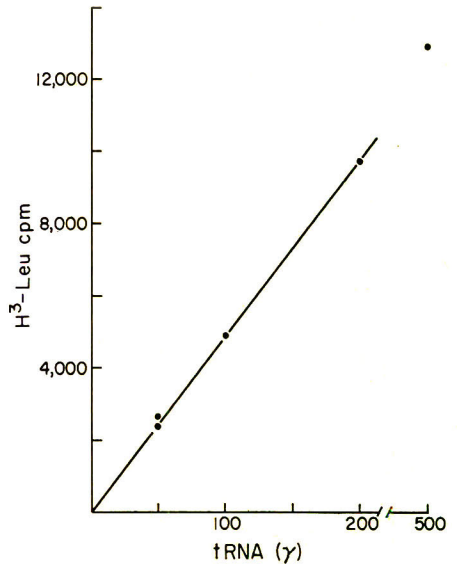


**Figure 10. Dose response curve for t-RNA assay**

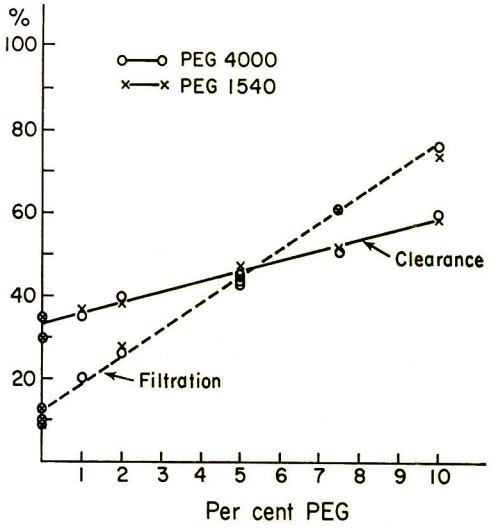


**Figure 11. Effect of osmotic flow on clearance rate**

the continuous dialyzer with Visking 20 casing. The 60% clearance for ATP could be further improved by adding $MgCl_2$ in a small amount to the solution. This reduces the diffusional size of ATP (*24*). From these data it is obvious that the thin film dialyzer can be used so that the desired reduction in volume of a solution can be achieved at the same time that rapid dialysis is accomplished and thus improve the clearance of any solute to be removed for analytical purposes.


## ACKNOWLEDGMENT

Tubing obtained from Mr. Al Pyne, Wilmad Glass Company, Buena, N.J.

RECEIVED for review October 4, 1968. Accepted January 7, 1969. Investigation supported in part by a grant from the National Institutes of Health No. AM 02493.



(23) J. Goldstein, T. P. Bennett, and L. C. Craig, *Proc. Natl. Acad. Sci.*, **51**, 119 (1964).
(24) W. I. Taylor and L. C. Craig, The Rockefeller University, 1968, unpublished data.

# A Spectrophotometric Reaction Rate Method for Determination of Bismuth Using a Dimeric Heteropolymolybdate

L. G. Hargis

*Department of Chemistry, Louisiana State University in New Orleans, New Orleans, La. 70122*

**A new method for the determination of bismuth(III) is described based on the initial rate of formation of the reduced dimeric heteropolymolybdate, 18-molybdobismuthophosphoric acid, from the reaction between phosphate, bismuth, molybdate, and ascorbic acid. The relative precision for the analysis of 4 ppm bismuth was better than 0.5% and of 0.04 ppm bismuth, the lower concentration limit, better than 10%. The formation of the reduced 18-molybdobismuthophosphoric acid is accomplished under conditions where 12-molybdophosphoric acid does not reduce. The method is simple and rapid, requiring only 20–60 seconds of reaction time. A study of diverse ions is presented and advantages of the rate method are discussed.**

SPECTROPHOTOMETRIC determinations of bismuth using molybdate (*1*) and 12-molybdophosphoric acid (*2*) are established methods, but both suffer the disadvantage of having to deal with unstable solutions and thus careful control of the time of measurement is required. The method by Guyon and Cline (*1*) is based on the catalytic effect of bismuth(III) on the reduction of acidic molybdate to molybdenum blue. The method by Campbell and Mellon (*2*) using 12-molybdophosphoric acid is based on an enhancement of the blue color formed when 12-molybdophosphoric acid is reduced in the presence of bismuth. Their study of the bismuth–phosphate–molybdate reaction raised some interesting questions concerning the nature of the bismuth participation in the reaction.

Recently it has been shown that bismuth can react with 12-molybdophosphoric acid to produce a mixed, dimeric heteropolymolybdate presumably containing both phosphate and bismuth as central groups (*3*). A kinetic and spectrophotometric study of the formation and reduction of this dimeric heteropolymolybdate (*4*) has led to the development of this reaction rate method. The rate method takes advantage of the fact that the dimeric, bismuth complex can be reduced much more rapidly than ordinary 12-molybdophosphoric acid. Thus, under controlled conditions, the initial rate of formation of the reduced dimeric complex from bismuth, phosphate, molybdate, and ascorbic acid was directly proportional to the bismuth concentration.

Under conditions suitable for bismuth analysis it is not possible to prepare reduced 18-molybdobismuthophosphoric acid completely without concomitant formation of some reduced 12-molybdophosphoric acid. Thus, conventional spectrophotometric methods have involved measurements at a carefully selected time after the start of the reaction. The proposed rate method takes full advantage of the difference in reactivity of the two complexes and measurement of initial rate of formation of the reduced 18-molybdobismuthophosphoric acid is accomplished before any reduced 12-molybdophosphoric acid is produced.

(1) J. C. Guyon and L. J. Cline, ANAL. CHEM., **37**, 1778 (1965).
(2) R. H. Campbell and M. G. Mellon, *ibid.*, **32**, 54 (1960).
(3) L. G. Hargis, *Anal. Lttrs.*, **1**, 799 (1968).
(4) H. D. Goldman and L. G. Hargis, ANAL. CHEM., **41**, 490 1969).

## PRELIMINARY CONSIDERATIONS

**Rate Equation.** The formation and reduction of 18-molybdobismuthophosphoric acid can be written as:

$$H_3PO_4 + Bi^{3+} + 9Mo(VI)_t \underset{k_{-1}}{\overset{k_1}{\rightleftharpoons}} \text{18-MBiPA} + 9H^+$$

and

$$\text{18-MBiPA} + \text{Red} \xrightarrow{k_2} \text{Blue} + \text{Ox}$$

Where $Mo(VI)_t$ refers to the total concentration of Mo(VI), 18-MBiPA to 18-molybdobismuthophosphoric acid, Red to the reductant, ascorbic acid, Ox to the oxidation product of ascorbic acid, and Blue to the reduced heteropolymolybdate. The reduced heteropoly complex exhibits strong absorption in the visible and near-infrared spectral regions and absorbance measurements at 725 nm conform to the Beer-Lambert law (*4*). The equation for the rate of formation of the heteropoly blue has been developed previously (*4*) and is given by

$$\frac{dA}{dt} = \frac{k_1 [H_3PO_4] [Bi^{3+}] [Mo(VI)_t]^9}{\left(\frac{k_{-1} [H^+]^9}{k_2 [\text{Ascorbic Acid}]}\right) + 1} \qquad (1)$$

When the initial concentrations of phosphate, molybdate, perchloric acid, and ascorbic acid are the same for a series of samples, the initial rate of change of absorbance is directly proportional to the bismuth concentration,

$$\left(\frac{dA}{dt}\right)_i = K[Bi^{3+}] \qquad (2)$$

**Optimum Solution Parameters.** If the ratio of $[H^+]$ to [Ascorbic Acid] could be kept small, the first term of the denominator in Equation 1 would be much less than one and Equation 1 would be greatly simplified:

$$\frac{dA}{dt} = k_1 [H_3PO_4] [Bi^{3+}] [Mo(VI)_t]^9 \qquad (3)$$

Unfortunately, this limiting condition could not be reached. The extent to which the $[H^+]$ can be lowered is controlled by the formation of reduced 12-molybdophosphoric acid (12-MPA) in the blanks. It is desirable to have a low acidity in order that the reaction rate be fast, but it cannot be so low that 12-MPA is reduced or that the initial reaction period is passed too quickly for easy measurement. In any event, control of the reactant concentrations is not difficult and the rate can be made directly proportional to bismuth concentration.

In setting up an analysis procedure, certain priorities must be observed with regard to selection of the proper reagent concentrations. The best precision and sensitivity is obtained by observing three factors: the rate of change of absorbance should be large, 12-molybdophosphoric acid should not be reduced during the initial reaction period, and the initial reaction period (less than 5% of the entire reaction) should prevail for at least 20 seconds to allow a satisfactory measurement.

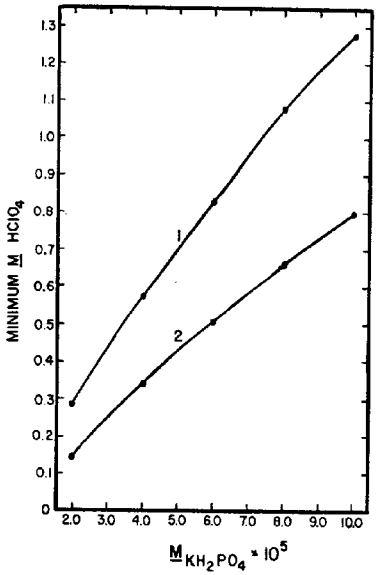


Figure 1. Minimum $HClO_4$ concentration which gives negligible reduction of 12-MPA

*1.* $[Na_2MoO_4]/[KH_2PO_4] = 100/1$
*2.* $[Na_2MoO_4]/[KH_2PO_4] = 50/1$

**Induction Period.** At all the conditions studied, an induction period preceded the linear rate period. The induction period depended, in part, on both the molybdate and the acid concentration, tending to increase as these concentrations increased. Because continuous absorbance *vs.* time curves were recorded, it was easy to determine when the induction period had passed.

**Temperature Control.** Temperature variations had a significant effect on the reaction rate, and therefore all solutions and the spectrophotometer cell compartment were thermostated at 26.00 ± 0.05 °C.

## EXPERIMENTAL

**Kinetic Measurements.** Spectrophotometric kinetic measurements were made on a Cary 15 recording spectrophotometer at 725 nm. This wavelength does not correspond to the absorbance maximum which is at 815 nm (*3*) but some compromise was necessary as the Cary instrument was not equipped to measure beyond 800 nm. For most experiments, the 0.0–0.1 absorbance slidewire was used allowing estimates of $10^{-4}$ absorbance units to be made from the graph paper.

**Reagents.** All solutions were prepared from reagent grade chemicals using distilled water and stored in polyethylene bottles to avoid silicon contamination. Because molybdate will polymerize somewhat in solution, all Mo(VI) solutions were prepared at least 24 hours prior to their first use in order to ensure that the molybdate aggregates had reached a stable equilibrium (*5*).

The stock phosphate–molybdate–perchloric acid solution referred to in the general procedure section was prepared by dissolving $KH_2PO_4$ and $Na_2MoO_4 \cdot 2H_2O$ in perchloric acid and diluting such that $[KH_2PO_4] = 6.0 \times 10^{-4}M$, $[Na_2MoO_4] = 6.0 \times 10^{-2}M$, and $[HClO_4] = 8.00M$.

Stock bismuth solutions were prepared by dissolving a weighed amount of $Bi(NO_3)_3 \cdot 5H_2O$ in the required amount of perchloric acid and diluting with distilled water. The stock solutions were standardized volumetrically using a standard EDTA procedure.

Ascorbic acid solutions are not stable for long periods of time at room temperature and were prepared fresh every few days. All stock ascorbic acid solutions used in this study were 0.210*M*. The concentrations of ascorbic acid in the final solutions were always much larger than the concentrations of bismuth or phosphate.

**General Procedure.** In order to obtain the best possible results, it was necessary to employ a certain set of solution conditions that depended somewhat on the range and level of the bismuth concentrations to be analyzed. The procedure described here is acceptable for the stated bismuth concentration range.

Transfer the dissolved sample containing 0.02 to 0.30 mg of bismuth(III) to a small beaker and neutralize with dilute sodium hydroxide to a pH of 3.5–9 using a pH meter. Exact neutralization is unnecessary for a large amount of acid will later be added to the sample. Do not be concerned if some turbidity is observed as it will disappear when the phosphate–molybdate–perchloric acid solution is added. Transfer the neutralized sample to a 50-ml volumetric flask and add exactly 5 ml of the phosphate–molybdate–perchloric acid solution, mix, and allow the solution to stand 5 minutes to ensure that all the bismuth redissolves before diluting to volume with distilled water. Transfer exactly 2 ml of this solution to a dry 1-cm absorption cell. Rapidly add 0.100 ml of the ascorbic acid solution using a microliter syringe, mix, and place the cell in the spectrophotometer. Record the absorbance at 725 nm *vs.* time until the rate is no longer linear with time (less than 2 minutes).

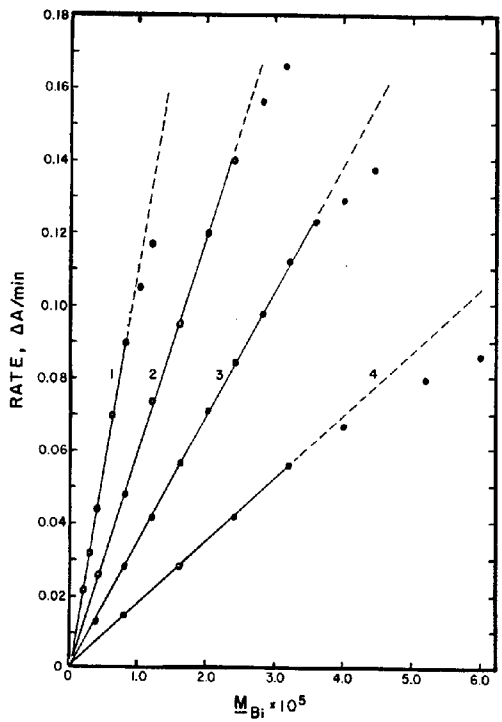


Figure 2. Working curves for various phosphate–molybdate concentrations at the minimum acidity

*1.* $KH_2PO_4 = 20.0\mu M$, $Na_2MoO_4 = 2.00mM$, $HClO_4 = 0.280M$
*2.* $KH_2PO_4 = 40.0\mu M$, $Na_2MoO_4 = 4.00mM$, $HClO_4 = 0.560M$
*3.* $KH_2PO_4 = 60.0\mu M$, $Na_2MoO_4 = 6.00mM$, $HClO_4 = 0.800M$
*4.* $KH_2PO_4 = 80.0\mu M$, $Na_2MoO_4 = 8.00mM$, $HClO_4 = 1.08M$

(*5*) S. R. Crouch and H. V. Malmstadt, *ibid.*, **39**, 1084 (1967).

**Calculations.** A calibration graph is prepared by plotting initial reaction rate *vs.* bismuth concentration for a series of known samples. The concentration of unknowns can be read directly from this calibration graph. Initial reaction rates were obtained graphically from the initial slopes of the absorbance *vs.* time curves. The conditions described in the above procedure are suitable for final concentrations of 0.4 to 6.0 ppm of bismuth. Both lower and higher concentrations can be determined by the same procedure using different reagent concentrations.

## RESULTS AND DISCUSSION

**Preliminary Experiments.** In order to obtain the largest rate of formation of reduced 18-MBiPA without concomitant formation of reduced 12-MPA, it was necessary to determine the minimum acidity at which formation of reduced 12-MPA was negligible (rate of formation of less than 0.0010 absorbance unit per minute). The particular acidity at which this is achieved depends on both the phosphate and the molybdate concentrations. Two series of molybdate–phosphate solutions at concentration ratios of 100/1 and 50/1 were prepared at several different acidities and reduced with ascorbic acid. The minimum acidity at which the rate of formation of reduced 12-MPA was less than 0.0010 absorbance unit per minute was plotted against the phosphate concentration as shown in Figure 1. Once the phosphate and molybdate concentrations to be used in an analysis are selected, the minimum acidity to be used is found readily from the graph.

**Standard Calibration Graph.** In order to show the importance of this acidity effect, calibration graphs were prepared from known amounts of bismuth using several different molybdate–phosphate concentrations at the minimum acidity. These graphs, shown in Figure 2, were linear only as long as the phosphate concentration was at least twice that of the bismuth concentration. Hence, if lower bismuth concentrations are treated with lower phosphate concentrations (thus lower acidities) to take advantage of the greater slopes of the working curves, linear plots are obtained for only small concentration ranges of bismuth. The final selection of the solution conditions to be used will depend, in part, on prior knowledge of the approximate bismuth concentration or range of concentrations.

An attempt was made to prepare a suitable calibration graph for concentrations less than 0.05 mg of bismuth (1 ppm Bi final concentration) by decreasing the ratio of molybdate to phosphate concentration from its previous value of 100/1 to a value of 50/1. Much lower acidities were now possible (see Figure 1) and calibration graphs similar to those shown in Figure 2 were obtained, differing only in that they remained linear over an even smaller range of bismuth concentrations. As expected the slopes of the calibration plots were considerably steeper. Using the molybdate–phosphate reagent at a 50/1 concentration ratio and the corresponding minimum acidity, a 0.04 ppm bismuth solution gave an initial reaction rate of 0.0050 absorbance unit per minute. At these low concentrations, reaction rates for the blanks were determined and subtracted from the bismuth reaction rates.

**Effect of Ionic Strength.** No ionic strength effects were noted at the usual solution conditions. Ordinarily the acidity is greater than 0.5*M* which minimizes any ionic strength effect. At the lower acidities used for very small amounts of bismuth, it may be advisable to add a large amount of inert electrolyte such as sodium perchlorate to all samples to avoid possible discrepancies.

**Precision and Accuracy.** An indication of the accuracy obtainable is shown in Table I. The calibration graph used was prepared from seven solutions of known concentration. These data show that an accuracy of better than 1.5% can be expected for simple aqueous systems. An estimate of the precision of the analysis was obtained from the results of replicate samples at two different concentration levels. The results are shown in Table II. Other experiments indicated that the lower concentration limit was about 0.04 ppm bismuth and samples of this concentration could be measured with approximately 10% relative error.

The rate measurements described here, made by manually determining the initial slopes of recorded absorbance *vs.* time curves, are ordinarily subject to some operator bias. The method should be quite applicable to automatic procedures (*6*, *7*) which are somewhat less time consuming and less subject to operator bias.

**Table I. Accuracy of Results**

| Measured reaction rate, ΔA/min. | Bismuth concentration, ppm | | |
|---|---|---|---|
| | Taken | Found | % Error |
| 0.0137 | 0.82 | 0.81 | − 1.2 |
| 0.0282 | 1.63 | 1.64 | + 0.6 |
| 0.0569 | 3.26 | 3.29 | + 0.9 |
| 0.0697 | 4.08 | 4.08 | 0.0 |
| 0.0954 | 5.71 | 5.65 | − 1.1 |

**Table II. Precision of Results**

| 4.18 ppm Bismuth | 0.42 ppm Bismuth |
|---|---|
| Measured rate, ΔA/min × $10^4$ | Measured rate, ΔA/min × $10^4$ |
| 713 | 294 |
| 710 | 301 |
| 710 | 292 |
| 714 | 306 |
| 709 | 297 |
| 707 | 316 |
| 704 | 315 |
| | 316 |
| | 308 |
| Av. 708 | 305 |
| Rel std dev 0.5% | 3.2% |

**Table III. Effect of Diverse Ions**

| Ion | Added as | Tolerance, ppm |
|---|---|---|
| $Na^+$ | $NaClO_4$ | > 1,000 |
| $K^+$ | $KNO_3$ | > 1,000 |
| $NH_4^+$ | $NH_4NO_3$ | > 1,000 |
| $Ag^+$ | $AgNO_3$ | > 1,000 |
| $Tl^+$ | $TlNO_3$ | 950 |
| $Cu^{2+}$ | $Cu(NO_3)_2$ | 750 |
| $Fe^{2+}$ | $FeSO_4$ | 50 |
| $Hg^{2+}$ | $Hg(NO_3)_2$ | 40 |
| $Co^{2+}$ | $Co(NO_3)_2$ | > 1,000 |
| $Ni^{2+}$ | $Ni(NO_3)_2$ | > 1,000 |
| $Zn^{2+}$ | $Zn(NO_3)_2$ | > 1,000 |
| $Pb^{2+}$ | $Pb(NO_3)_2$ | > 1,000 |
| $Cr^{3+}$ | $Cr(ClO_4)_3$ | > 1,000 |
| $Fe^{3+}$ | $Fe(NO_3)_3$ | 40 |
| $AsO_3^{3-}$ | $NaAsO_2$ | 850 |
| $SbO^+$ | $KSbC_4H_4O_7$ | > 1,000 |
| $ClO_4^-$ | $NaClO_4$ | > 1,000 |
| $NO_3^-$ | $KNO_3$ | > 1,000 |
| $C_2H_3O_2^-$ | $NaC_2H_3O_2$ | 900 |
| $F^-$ | NaF | 20 |
| $Cl^-$ | KCl | 100 |
| $SO_4^{2-}$ | $Na_2SO_4$ | > 1,000 |

(6) H. V. Malmstadt and G. P. Hicks, *ibid.*, **32**, 394 (1960).
(7) W. J. Blaedel and G. P. Hicks, in "Advances in Analytical Chemistry and Instrumentation," Vol. 3, C. N. Reilley, Ed., Wiley, New York, N.Y., 1964, pp 130–3.

**Diverse Ions.** The effect of many diverse ions was studied using the procedure described in the experimental section for the analysis of 4 ppm of bismuth. An error of less than 2.5% was considered negligible. The results of this study are summarized in Table III.

Iron(III) and mercury(II) are reduced by the ascorbic acid and can be tolerated only in small amounts. Iron(II) slowly reduces the heteropoly acid to heteropoly blue, but if the samples are measured very soon after preparation, small amounts of iron(II) can be tolerated. Apparently the reduction by iron is considerably slower than that by ascorbic acid and has only a small effect on the rate. Fluoride interferes seriously, probably by complexing with the Mo(VI). Chloride is the only other important anion interference but no explanation for its interference can presently be offered.

**Advantages of the Rate Method.** The reaction rate method has many advantages over conventional spectrophotometric methods using similar chemical systems. In the rate method it is not necessary to make absorbance measurements at a very carefully selected time in order to avoid or compensate for blank absorption. The presence of other materials that absorb at the measurement wavelength or that impart a turbidity to the solution will not normally interfere in the reaction rate method. These advantages coupled with the excellent precision and good sensitivity obtainable should make this a very useful method.

RECEIVED for review December 23, 1968. Accepted January 30, 1969.

# Use of Ion Selective Electrodes in Enzymic Analysis.

## Cation Electrodes for Deaminase Enzyme Systems

**G. G. Guilbault, R. K. Smith, and J. G. Montalvo, Jr.**

*Chemistry Department, Louisiana State University in New Orleans, New Orleans, La. 70122*

**The response, selectivity, and use of the 39047 and 39137 Beckman cationic electrodes for the determination of $NH_4^+$ activity are reported. Both electrodes were found to respond to $NH_4^+$ in the concentration range $10^{-1}$ to $10^{-5}M$ with a deviation of ± 0.5 mV in the $10^{-1}$ to $10^{-4}M$ region and ± 20 mV at $10^{-4}$ to $10^{-5}M$ region. The response characteristics of the micro 39047 electrode were found to be $Ag^+ > H^+ > K^+ > NH_4^+ > Na^+ > Li^+ \gg Mg^{2+}$, $Ca^{2+}$. Those of the 39137 electrode were $Ag^+ > K^+ > H^+ > NH_4^+ > Na^+ > Li^+ > Mg^{2+}$, $Ca^{2+}$. At a pH of 7 the only serious interferences in the assay of $[NH_4^+]$ are $Ag^+$ and $K^+$. Both electrodes were used for the assay of deaminase enzyme systems: urea-urease, glutamine-glutaminase, asparagine-asparaginase, D- and L-amino acids-amino acid oxidases. All substrates and enzymes could be assayed with a precision and accuracy of about 2.5%.**

CATION-SENSITIVE glass electrodes (*1*, *2*) are finding widespread use in analytical chemistry. Excellent reviews on ion selective electrodes and their applications have been prepared by Rechnitz (*3*, *4*).

Beckman (*5*) markets a cationic electrode (39137, formerly designated 78137) that has a reported selectivity $H^+ > Ag^+ > K^+$, $NH_4^+ > Na^+ > Li^+ \gg Mg^{2+}$, $Ca^{2+}$. This electrode has been used for the determination of sodium ions in acidic silica sol systems (*6*), for estimating exchangeable potassium in soils (*7*), to study the weak complex formed by sodium ion and malic acid (*8*), and for the direct determination of alkali metal ions by a tetraphenylboron titration (*9*, *10*). Rechnitz (*11*) has studied the response of the cation-sensitive electrode to alkali metal ions in nonaqueous solution, and Jacobson (*12*) has developed a method for the continuous assay of potassium in the presence of ammonia with the Beckman cation electrode.

Katz and Rechnitz have used the cation-sensitive glass electrode (39137) for the determination of urea (*13*) and urease (*14*) via complete conversion of urea to $NH_4^+$ by enzyme-catalyzed hydrolysis. The potential of the solution after hydrolysis is proportional to the amount of $NH_4^+$ produced and hence to the concentration of urea or urease. Katz (*15*) applied this method to study the effect of various ions on the urease catalyzed hydrolysis or urea.

Although considerable attention has been paid to use of the Beckman cation selective electrode for determination of various cations, a complete study of the selectivity of the electrode towards $NH_4^+$ has not been made (*16–18*). In this paper the results of a thorough investigation of the response, selectivity and use of the cation electrode for determination of $NH_4^+$ activity are reported. The application of this electrode to a study of the kinetics of deaminase enzyme systems (urease, asparaginase, glutaminase, amino acid oxidase and amine oxidases) is likewise reported.

### EXPERIMENTAL

**Apparatus.** All potentiometric measurements were made with a Beckman research model pH meter. EMF *vs.* time curves for the dynamic response measurements and enzyme

(1) G. Eisenman, D. O. Rudin, and J. U. Casby, *Science*, **126**, 831 (1957).
(2) G. Eisenman, *Biophys. J.*, **2**, 259 (1962).
(3) G. A. Rechnitz, *Chem. Eng. News*, June 12, 1967, p 146.
(4) G. A. Rechnitz, in "Glass Electrodes for Hydrogen and Other Cations," G. Eisenman, Ed., Marcel Dekker, Inc., New York, 1967.
(5) Beckman Instrument Co., Bulletin 7017-a, Beckman Instrument Co., Fullerton, Calif.
(6) T. A. Taulli, ANAL. CHEM., **32**, 186 (1960).
(7) M. M. Mortland, Quarterly Bulletin, Michigan Agricultural Sta., **43**, (3), 491 (1961).
(8) G. A. Rechnitz, *Talanta*, **11**, 617 (1964).
(9) G. A. Rechnitz, S. B. Zamochnick, and S. A. Katz, ANAL. CHEM., **35**, 1322 (1963).
(10) J. E. McClure and G. A. Rechnitz, *ibid.*, **38**, 136 (1966).
(11) G. A. Rechnitz and S. B. Zamochnick, *Talanta*, **11**, 979 (1964).
(12) H. Jacobson, ANAL. CHEM., **38**, 1951 (1966).
(13) S. A. Katz and G. A. Rechnitz, *Z. Anal. Chem.*, **196**, 248 (1963).
(14) S. A. Katz, *Anal. Chem.*, **36**, 2500 (1964).
(15) S. A. Katz and J. A. Cowans, *Biochem. Biophys. Acta*, **107**, 605 (1965).
(16) L. Budd, *J. Electroanal. Chem.*, **5**, 35 (1963).
(17) K. Cammann, *Z. Anal. Chem.*, **216**, 287 (1966).
(18) G. A. Rechnitz and G. Kugler, *ibid.*, **210**, 174 (1965).

reactions were obtained by displaying the output signal of the pH meter on a Brown potentiometric recorder. The cation electrodes used in this study were the 39047 micro glass electrode and two 39137 large glass electrodes, one obtained in May of 1968, the second in May, 1967. All electrodes were from Beckman Instrument Co. A conventional Beckman saturated calomel electrode was used in all studies. In those studies involving $Ag^+$ ion a salt bridge filled with tris-$HNO_3$ buffer was used to prevent contamination of the SCE. All measurements were carried out in a thermostated cell at 25 ± 0.1 °C.

**Chemicals.** Stock solutions of all ions were prepared by dissolving the reagent grade chemicals (Fisher) in tris (hydroxymethyl amino-methane) buffer, 0.1*M*, pH 7.0. The tris was used both to maintain a constant pH and a constant ionic strength. A series of standard solutions were prepared by suitable dilution of the stock solutions, keeping the ionic strength constant at 0.1*M* by the addition of appropriate volumes of tris.

**Enzymes.** Stock 1 mg/ml solutions of all enzymes were prepared in triply distilled water. The activity of all enzymes was assayed by standard procedures and was found to be: urease (jack bean, Sigma, Type IV, 2.50 unit per mg), glutaminase (E. Coli, Sigma, 0.5 unit per mg—one unit is that amount which effects the deamination of 1 μmole of glutamine per minute at pH 4.9 and 37 °C), asparaginase (E. Coli, Sigma, 20 units per mg—1 unit will liberate 1 μmole of ammonium nitrogen per minute at pH 8.6 and 37 °C), L-amino acid oxidase (Crotolus Adamanteus venom, Sigma, Type I, activity 0.3 units/mg), D-amino acid oxidase (hog kidney, Sigma, activity 0.059 units/mg).

**Substrates.** Stock 0.1*M* solutions of all substrates: urea, asparagine, glutamine, D- and L-tyrosine, proline, and leucine (Sigma) were prepared in 0.1*M* tris buffer, pH 7.0. Dilutions were made to the optimum substrate concentrations as described below.

**Procedure.** POTENTIOMETRIC METHODS. Potentiometric measurements for the construction of calibration curves and the study of the effect of interfering ions were carried out in the conventional manner. Into the electrochemical cell (50 ml capacity) were placed 25 ml of solution, a cation electrode, and a reference electrode. All solutions were magnetically stirred [bar made of Teflon (Dupont)]. All electrode potentials were rapidly attained, and generally the equilibrium potentials were read within 2.5 minutes after immersion of the electrodes into the test solution. The cation electrode was soaked in triply distilled water between measurements.

Electrode response curves were obtained by addition of concentrated solutions of the ions to either triply distilled water or to some concentration of ion tested. The resulting emf *vs.* time curves were smooth and reproducible after an initial mixing period at constant pH and ion strength.

**Determination of Urease, Glutaminase, Asparaginase, D- and L-Amino Acid Oxidase.** To 24 ml of tris buffer, pH 7.0, is added 1 ml of a solution of the enzyme to be analyzed (urease, glutaminase, asparaginase, D- or L-amino acid oxidase). The 39137 cation selective electrode and calomel electrode are immersed in the solution and the potential is automatically recorded. The potential of the system should correspond to a low level of $NH_4^+$, as determined from a calibration curve. A large positive potential indicates the presence of extraneous alkali metals ($K^+$, $Na^+$, etc.) which will interfere. If such a potential is observed, add 1 gram of a cation exchange resin (Dowex 50 or equivalent) and rapidly stir the solution for 5 min. Filter off the resulting solution and add 1 ml of the appropriate substrate solution (urea, glutamine, asparagine, D-proline or L-tyrosine) such that the overall substrate concentration is $10^{-2}M$. The change in potential with time, due to production of $NH_4^+$, is automatically recorded. The enzyme present can be calculated from a plot of $\Delta E$/min *vs.* enzyme concentration.

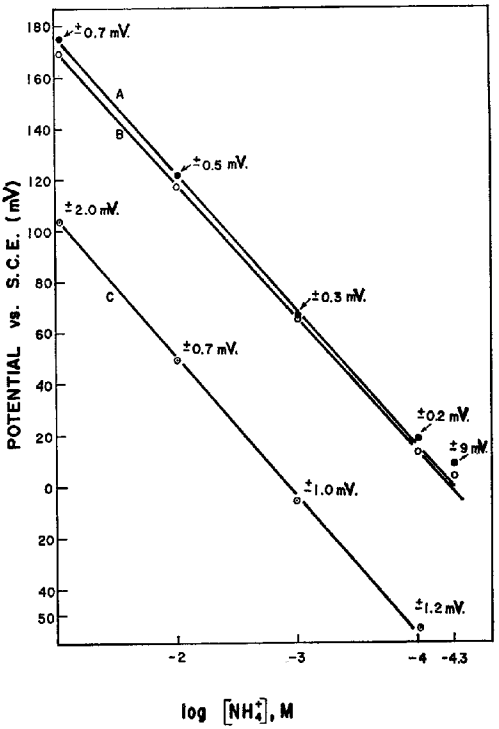


**Figure 1. Calibration plots of potential (*vs.* SCE) *vs.* log $NH_4^+$ for three cationic specific electrodes**

$\mu = 0.1M$
A — Beckman 39137 electrode (1968)
Slope = 52.5 ± 1.5 mV
B — Beckman 39137 electrode (1967)
Slope = 53.0 ± 1.5 mV
C — Beckman 39047 electrode
Slope = 53.5 ± 1.0 mV

**Determination of Urea, Glutamine, Asparagine, D- or L-Amino Acid.** The procedure as described above is followed, except that a 1-mg/ml solution of the appropriate enzyme (40-mg/ml solution of D-amino acid oxidase) is added. At zero time 1 ml of a solution of the substrate to be analyzed (urea, glutamine, asparagine, D- or L-amino acid) is added. Again the change in potential with time, $\Delta E$/min, is recorded, and the concentration of substrate present is calculated from a calibration plot of $\Delta E$/min *vs.* concentration.

## RESULTS AND DISCUSSION

**Response of Electrodes to Ammonium Ion.** The Beckma 39047 and 39137 cation electrodes have sensing tips comprised of specially formulated glass (the 39137 electrode is identified with the composition 27% $Na_2O$, 4% $Al_2O_3$ and 69% $SiO_2$) which measures the activity of monovalent cations in a manner analogous to pH determination with a glass electrode. The glass electrode tip is a membrane which is sensitive to ionic activity differences. A standard solution within the electrode has a fixed ionic activity, and the unknown solution with which the tip of the electrode comes in contact has an activity, with respect to the ion sensed, which may be either the same or different from that of the internal solution. This activity difference between the internal standard solution and the test solution is indicated as a voltage. The voltage change due to

**Table I. Selectivity Ratios for Various Cations Relative to $NH_4^+$**

T = 25 ± 0.10 °C. All potentials were determined in 0.1*M* tris buffer, pH 7.0, except $H^+$ which was determined in triply distilled water

| Cation | $K_{M^+/NH_4^+}$ 39137 (1967) | 39137 (1968) | 39047 |
|---|---|---|---|
| $Ag^+$ [a] | — | 0.402 | 0.246 |
| $H^+$ | 0.40 | 0.468 | 0.404 |
| $K^+$ | 0.43 | 0.416 | 0.427 |
| $Na^+$ | 3.16 | 4.03 | 3.94 |
| $Li^+$ | 56.5 | 83.5 | 95.6 |
| $Mg^{2+}$ | $3.1 \times 10^4$ | $2.6 \times 10^4$ | 1,230 |

[a] Tris-$HNO_3$ salt bridge used to prevent fouling of SCE Tris-$HNO_3$ buffer used as supporting electrolyte and solvent

activity differences in test solutions should obey the Nernst equation:

$$E_{obs} = E^{\circ\prime} + \frac{0.0591}{n} \log a_{(C^+)} \text{ (at 25 °C)} \quad (1)$$

Because the cationic electrodes (39047 and 39137) respond to $NH_4^+$, a plot of *E vs.* log of $NH_4^+$ concentration should be a straight line with a slope of 59.1 mV at 25 °C. A plot for three such electrodes is shown in Figure 1. Lines A and B are the responses of two 39137 electrodes, one recently purchased (line A) and one a year old (line B). Line C is for the 39047 micro cationic electrode. All electrodes respond to ($NH_4^+$) over the concentration range $10^{-1}$ to $10^{-5}M$. The voltages of the two 39137 electrodes are close to one another, whereas the potential of the 39047 micro electrode is considerably less positive. Evidently, the filling solution of the micro electrode (yellow for the 39047 and colorless for the 39137) and/or the internal reference differs appreciably from that of the macro electrode. Otherwise, Curve C in Figure 1 should agree with Curves A and B. Another 39047 electrode recently obtained from Beckman had a colorless filling solution and give voltages for line C very close to A and B. Both of the 39137 electrodes give excellent reproducible voltages from day to day at concentrations of $10^{-4}M$ and above (± 0.5 mV average). At a concentration of $10^{-5}$ to $10^{-4}M$ higher deviations result (± 20 mV). Slightly higher deviations are observed with the 39047 electrode. None of the electrodes give a completely Nernstian response to [$NH_4^+$], having slopes of about 53 mV/decade change in concentration.

The hydrolysis of $NH_4^+$ ion in solution was considered in calculations of the ($NH_4^+$) activity reported in Figure 1:

$$NH_4^+ + H_2O \rightleftharpoons NH_3 + H_3O^+ \quad K_h = 5.5 \times 10^{-10}. \quad (2)$$

At a pH of 7 the ratio of ($NH_4^+$)/($NH_3$) is about 180; hence almost all of the $NH_4^+$ is in the cationic form.

**Dynamic Response Characteristics.** The response characteristics of the ammonium-ion sensitive electrode (39137) were evaluated by exposing the electrode to a rapid change in ammonium ion concentration and recording the resulting emf *vs.* time function. Some typical response curves obtained ($\mu = 0.1M$) are reproduced in Figure 2. The electrode was soaked in distilled water, then exposed to $10^{-1}$ (A), $10^{-2}$ (B), $10^{-3}$ (C), $10^{-4}$ (D), and $5 \times 10^{-5}M$ (E) concentrations of $NH_4^+$. Essentially identical curves were obtained upon going from more concentrated to less concentrated solutions.

All curves are smooth and of identical shape. The expected emf values were obtained in all cases. The response rates are all very fast, the response half-time, $t_{\frac{1}{2}}$, obtained being less than 1 second. The high response rate of this electrode indicates that continuous monitoring of ammonium ion activity in aqueous solutions is possible.

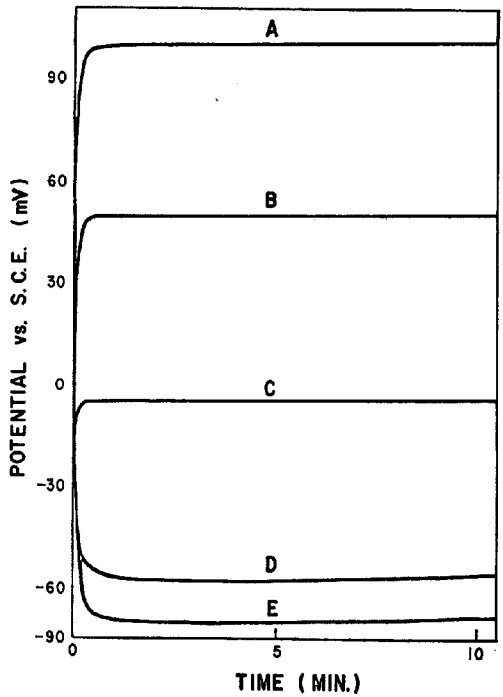


**Figure 2. Dynamic response curves of the 39137 cationic electrode to various concentrations of $NH_4^+$**

$\mu = 0.1M$
A — 0 to $10^{-1}M$
B — 0 to $10^{-2}M$
C — 0 to $10^{-3}M$
D — 0 to $10^{-4}M$
E — 0 to $5 \times 10^{-5}M$

The pretreatment of the electrode had a pronounced effect on the electrode response. The electrode exhibited a faster, better response if soaked for several days before use in triply distilled water. More drift was observed if the electrode is soaked in ($NH_4^+$) solutions before use, rather than in water.

The best potential readings were obtained after about 2.5 minutes, although readings can be taken after about 30 seconds.

**Effect of Cations on Electrode Response.** The response of the Beckman 39137 electrode is reported to be $H^+ > Ag^+ > K^+$, $NH_4^+ > Na^+ > Li^+$. In order to establish the selectivity of the cationic electrodes, the selectivity ratios, *K*, defined by Eisenman's simplified Equation 1:

$$E\begin{pmatrix} M_2^+ = 0.1M \\ M_1^+ = 0 \end{pmatrix} - E\begin{pmatrix} M_2^+ = 0 \\ M_1^+ = 0.1M \end{pmatrix} = \frac{RT}{F} \ln K_{M_1^+/M_2^+}. \quad (3)$$

were determined for 3 electrodes with respect to $NH_4^+$. These ratios are reported in Table I. These results indicate that the selectivity of the cationic electrode varies from electrode to electrode, and may be different from that claimed by the manufacturer. The selectivity ratios of the large cationic electrode, recently obtained [39137 (1968)] are vastly different from those of the small (39047) electrode and even from the large cationic electrode obtained a year ago [39137 (1967)]. The order of selectivity of the small electrode found agrees with that claimed except that the electrode responds better to $NH_4^+$ than to $Na^+$: $Ag^+ > H^+ > K^+ > NH_4^+ >$

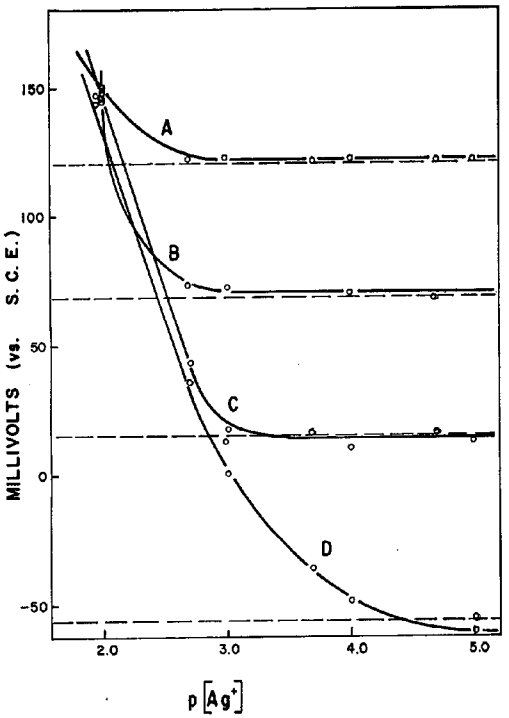


Figure 3. Calibration plot of potential (*vs.* SCE) *vs.* $p$ [$Ag^+$] at various $NH_4^+$ concentrations

$\mu = 0.1M$
A — $10^{-2}M$ $NH_4^+$
B — $10^{-3}M$ $NH_4^+$
C — $10^{-4}M$ $NH_4^+$
D — $10^{-5}M$ $NH_4^+$

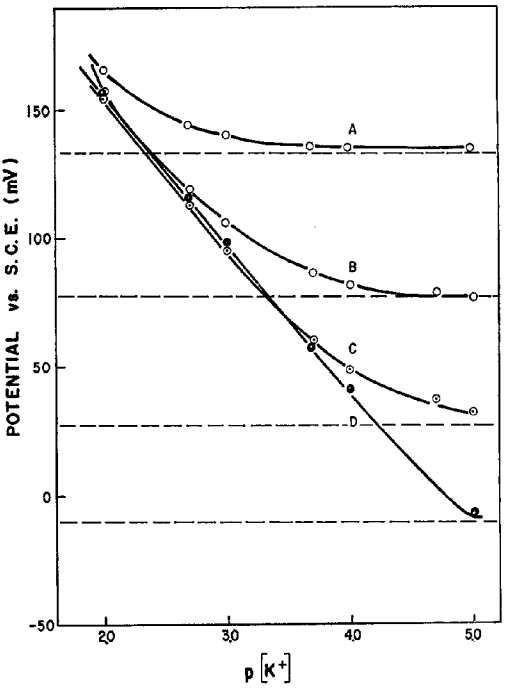


Figure 4. Calibration plot of potential (*vs.* SCE) *vs.* $p$ [$K^+$] at various $NH_4^+$ concentrations

$\mu = 0.1M$
A — $10^{-2}M$ $NH_4^+$
B — $10^{-3}M$ $NH_4^+$
C — $10^{-4}M$ $NH_4^+$
D — $10^{-5}M$ $NH_4^+$

$Na^+ > Li^+ \gg Mg^{2+}$. The order of the large electrode is different from that claimed: $Ag^+ > K^+ > H^+ > NH_4^+ > Na^+ > Li^+ \gg Mg^{2+}$. These observations are consistent with the finding by Eisenman (*19*, *20*) that two different batches of Beckman 78137 electrodes were found to differ both in respect to their electrode properties and the characteristics of ionic diffusion. This indicated that the two batches, although supposed to be identical, must have differed slightly in actual composition ($Na_2O/Al_2O_3$ ratio) and degree of hydration. It should be pointed out that these selectivity ratio differences obtained here with the various electrodes would include the effects of cesium and rubidium ions.

Tests of the effect of these cations ($Ag^+$, $K^+$, $Na^+$ and $Li^+$) on the cationic electrode were made over the concentration range of $NH_4^+$ ion of $10^{-2}M$ to $10^{-5}M$. The concentration range of the cations was varied from $10^{-2}$ to $10^{-5}M$. The ionic strength was kept constant at $0.1M$ and the pH at 7 with tris buffer. Some typical response curves describing the results of this study are given in Figures 3–6 for $Ag^+$, $K^+$, $Na^+$ and $Li^+$–$NH_4^+$ solutions. The potential response of the electrode is plotted *vs.* $p$ ($M^+$) at various ($NH_4^+$) concentrations. The horizontal dashed lines indicate the response expected if ($M^+$) had no effect on the electrode response. Thus in an analysis of ($NH_4^+$) in concentrations above $10^{-4}$ either by direct potentiometry or in an enzymic analysis, $Li^+$ would not be a serious interference at concentrations below $5 \times 10^{-3}M$ and sodium below $5 \times 10^{-4}M$. Experimental findings showed that $H^+$ does not interfere below $10^{-4}M$ (pH 4); above $10^{-8}M$ (pH 8) interference due to conversion of $NH_4^+$ to $NH_3$ is important. $K^+$ and $Ag^+$ are serious interferences and must be removed. $Mg^{2+}$, $Ca^{2+}$, and other divalent ions have very little effect. Plots for $Mg^{2+}$ similar to those in Figures 3–6 yielded calibration plots that agreed with the calibration plot due to $NH_4^+$ given above within experimental error.

**Assay of Deaminase Enzymes.** Because of its rapid response to ($NH_4^+$), its approximately Nernstian response and good selectivity, the cationic electrode (39137 and 39047) should be an ideal tool for following the activity of deaminase enzymes:

$$\text{Substrate} \xrightarrow{\text{Deaminase}} > NH_4^+$$

Katz and Rechnitz (*13*, *14*) have studied the use of the 39137 electrode for assay of urea and urease. The potentials recorded after enzymic hydrolysis were proportional to the concentration of urea and urease.

In this study we attempted to develop continuous automatic assay procedures for the urease, glutaminase, asparaginase, amino acid oxidase, glutamate dehydrogenase and amine oxidase enzyme systems, for the specific assay of both enzyme and substrate.

(19) G. E. Eisenman, in "The Electrochemistry of Cation-Sensitive Glass Electrodes," from *Advances in Analytical Chemistry and Instrumentation*, C. N. Reilley, Ed., Vol. 4, 1965, p 213.
(20) "Glass Electrodes for Hydrogen and Other Cations," G. Eisenman, Ed., Marcel Dekker, Inc., New York, 1967, p 137.

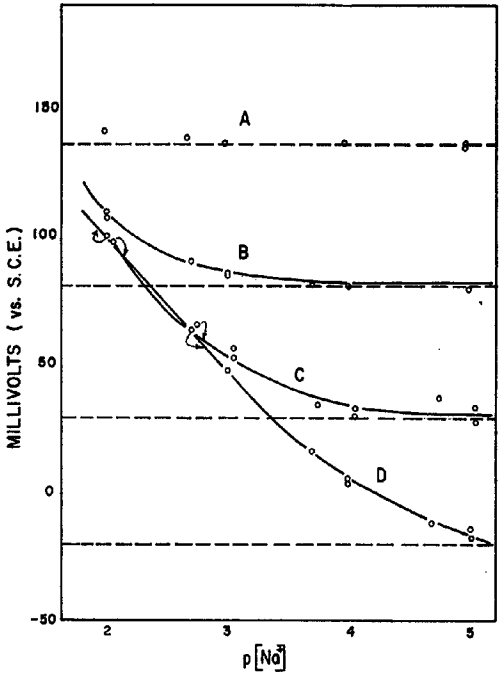


Figure 5. Calibration plot of potential (*vs.* SCE) *vs. p* [$Na^+$] at various $NH_4^+$ concentrations

$\mu = 0.1M$
A — $10^{-2}M$ $NH_4^+$
B — $10^{-3}M$ $NH_4^+$
C — $10^{-4}M$ $NH_4^+$
D — $10^{-5}M$ $NH_4^+$

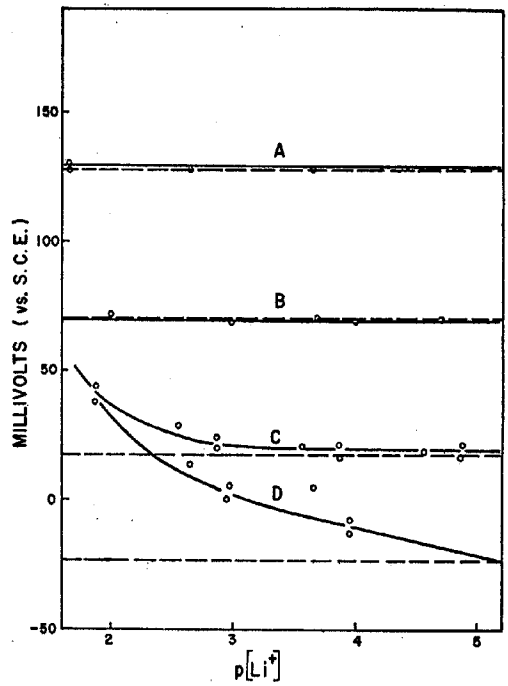


Figure 6. Calibration plot of potential (*vs.* SCE) *vs. p* [$Li^+$] at various $NH_4^+$ concentrations

$\mu = 0.1M$
A — $10^{-2}M$ $NH_4^+$
B — $10^{-3}M$ $NH_4^+$
C — $10^{-4}M$ $NH_4^+$
D — $10^{-5}M$ $NH_4^+$

**Table II. Substrates and Enzymes Determined Electrochemically with the ($NH_4^+$) Sensitive Electrode**

| Substance | Range | Rel error % |
|---|---|---|
| Urea | 0.5–100 μg/ml | 2.0 |
| Urease | 0.0010–0.04 units | 2.5 |
| Glutamine | 0.5–10 μg/ml | 5.0 |
| Glutaminase | 0.0010–0.40 units | 5.0 |
| Asparagine | 0.5–10.0 μg/ml | 3.0 |
| Asparaginase | 0.0010–0.40 units | 3.0 |
| L-Tyrosine | 1–40 μg/ml | 2.0 |
| L-Leucine | 1–40 μg/ml | 2.5 |
| D-Tyrosine | 10–100 μg/ml | 3.5 |
| D-Methionine | 10–100 μg/ml | 4.0 |
| L-Amino acid oxidase | 0.010–0.2 units | 2.5 |
| D-Amino acid oxidase | 0.05–1.0 units | 3.5 |

**Table III. Effect of Various Ions on the Urea–Urease Reaction**

Urea = 0.01*M* Urease = 0.04 μg/ml

| Ion | Conc., *M* | % Inhibition |
|---|---|---|
| $Ag^+$ | $10^{-3}$ | 100 |
| | $10^{-4}$ | 93.5 |
| | $10^{-5}$ | 63.9 |
| | $10^{-6}$ | 17.5 |
| $Hg^{2+}$ | $10^{-5}$ | 75 |
| | $10^{-6}$ | 43 |
| $K^+$ | $10^{-2}$ | 82.5 |
| | $10^{-3}$ | 43 |

| | | |
|---|---|---|
| Urea | $\xrightarrow{\text{Urease}}$ | $NH_4^+$ |
| Glutamine | $\xrightarrow{\text{Glutaminase}}$ | $NH_4^+$ |
| Asparagine | $\xrightarrow{\text{Asparaginase}}$ | $NH_4^+$ |
| Amino acid | $\xrightarrow{\text{Oxidase}}$ | $NH_4^+$ |
| Amine | $\xrightarrow{\text{Oxidase}}$ | $NH_4^+$ |
| Glutamic acid | $\xrightarrow{\text{Dehydrogenase}}$ | $NH_4^+$ |

Initially, before initiation of the enzymic reaction, a zero potential should be recorded, because the enzyme and substrate are molecular, and not ionic. Then upon enzymic reaction a potential would be observed due to production of $NH_4^+$:

$$E = E^{\circ\prime} + 0.0591 \log (NH_4^+) \quad (4)$$

Differentiation of this equation with respect to time yields:

$$\frac{dE}{dt} = 0.0591 \frac{1}{(NH_4^+)} \frac{d(NH_4^+)}{dt} \quad (5)$$

Assuming that $1/(NH_4^+)$ is changing relatively more slowly with time than the time differential of $(NH_4^+)$ in the initial stage of reaction, the rate of change in the potential, $dE/dt$, is then directly proportional to the rate of change in the $(NH_4^+)$ concentration with time. Thus, instead of a point by point relation of the potential reading to the log of the $(NH_4^+)$ concentration for calculation of the progress of the enzymic

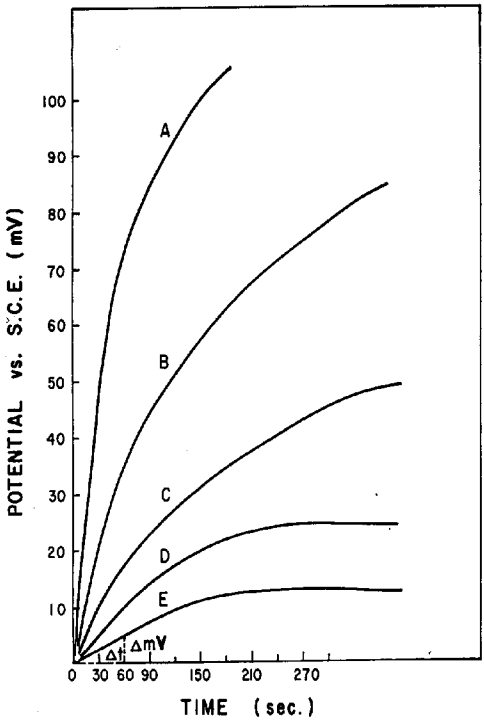


**Figure 7. Response curves of potential (*vs.* SCE) *vs.* time for the urease catalyzed hydrolysis of urea**

**Urea = 0.01*M*, pH = 7.0, Tris Buffer, 0.1*M***
**A — 0.04 units urease**
**B — 0.016 units urease**
**C — 0.008 units urease**
**D — 0.004 units urease**
**E — 0.002 units urease**

reaction, we need only take the initial rate of reaction by drawing a tangent to the $E$ *vs.* time curves (illustrated in Figure 7 for urea–urease). The validity of the above assumptions and procedure has been proved by Guilbault *et al.* for enzyme reactions using a platinum indicator electrode (*21–24*). The same reasoning should hold for the ($NH_4^+$) selective cationic electrode, and proof of the validity of this method lies in the observation that calibration plots of the change in potential with time, $\Delta E/\Delta t$, are linear with change in concentration of both enzyme and substrate in all systems studied.

Some results obtained in the use of this method for the analysis of various enzymes and substrates are indicated in Table II. The urease, glutaminase, asparaginase and D- and L-amino acid oxidase systems worked well. Attempts to get the glutamic acid dehydrogenase system to work failed, probably because of the presence of ions in the enzyme. This was indicated by the large potentials observed before initiation of the enzymic reaction and the serious drift problems encountered. All attempts to remove the ionic interferences failed. Similar problems were sometimes encountered in assay of the other enzyme systems, but such problems were generally eliminated by pretreatment of the enzyme and/or substrate with an ion exchange resin. A potential problem can be easily spotted by a pretesting of the potential of the enzyme and substrate with the cationic electrode. If the potential is not indicative of a low level of $NH_4^+$, the presence of ionic contaminants is indicated. The only serious interferences at pH 7 are $K^+$ and $Ag^+$ which exhibit a better response to the cationic electrode than $NH_4^+$. This effect is demonstrated in Table III which shows the effect of these two ions on the urea-urease system as the apparent per cent inhibition. In the case of $Ag^+$ the effect is evidently not only a response of the electrode to $Ag^+$ but also an inhibition of the enzyme. $Hg^{2+}$, $Pb^{2+}$, and $Cu^{2+}$ are inhibitors of urease.

**Table IV. Effect of pH on the Rate of Hydrolysis of Urea by Urease**

| (Urease) = 0.04 μg/ml | Urea = 0.01*M* |
|---|---|
| pH | ΔmV/min |
| 7.0 | 500 |
| 7.5 | 500 |
| 8.0 | 450 |
| 8.5 | 400 |
| 9.0 | 375 |
| 9.5 | 350 |

The effect of pH on the assay of the urea–urease system is shown in Table IV. A maximum rate of change in potential with time was observed at a pH of 7–7.5. This same pH optimum was observed for all the enzyme systems studied. At higher pH's (> 7.5) increasing amounts of $NH_4^+$ are present in the form of $NH_3$ to which the electrode is not responsive.

Methods for the assay of the monoamine and diamine oxidase systems were not initially successful, due primarily to too low an activity of the enzyme (producing too little $NH_4^+$ to be measured). Slight rates were observed. Both these enzymes are currently being purified, and will be retested at a later date.

A comparison of the sensitivity of the electrochemical procedure described herein to fluorescence methods (*25*) indicates the electrochemical methods to be about two orders of magnitude less sensitive for the assay of the amino acids and the amino acid oxidases (*25*). The methods should be quite useful for the assay of the other enzyme systems that liberate $NH_4^+$, where sensitive fluorometric methods are not available.

RECEIVED for review October 24, 1968. Accepted December 22, 1968.

(21) G. G. Guilbault, D. N. Kramer, and P. Cannon, ANAL. CHEM., **34,** 842 (1962).
(22) *Ibid.*, **36,** 606 (1964).
(23) G. G. Guilbault, D. N. Kramer, and P. Cannon, *Anal. Biochem.*, **5,** 208 (1963).
(24) G. G. Guilbault, D. N. Kramer, and P. Goldberg, *J. Phys. Chem.*, **67,** 1747 (1963).
(25) G. G. Guilbault and J. Hieserman, *Anal. Biochem.*, **26,** 1 (1968).

# An Automatic, Multiple-Column Gas Chromatographic Analysis of Methanol Synthesis Reaction Mixtures

**Robert L. Burnett**

*Chevron Research Co., Richmond, Calif. 94802*

**A multiple-column automatic process chromatographic analysis is described for handling the diverse products encountered during the synthesis of methanol by CO hydrogenation. The required separations present a rather complex analytical problem, because the reaction mix samples may contain CO, $CO_2$, light paraffins, light olefins, alcohols, water, aldehydes, ketones, ethers, and esters in major or minor amounts. The technique of column switching and sample fractionation described results in a very satisfactory onstream, one-sample analysis of effluent product.**

IN THE SYNTHESIS OF METHANOL by hydrogenation of carbon monoxide, a large variety of products is encountered in addition to methanol, $H_2$, and CO. Depending upon the selectivity of the synthesis catalyst employed and the conditions under which it is operated, greater or lesser amounts of the following are produced: water, $CO_2$, light paraffins, light olefins, alcohols heavier than methanol, aldehydes, ketones, ethers, and esters. Gas chromatography offers the opportunity for a rapid, onstream quantitative analysis of most or all of these components; but because of the great diversity in compound type, rather unique combinations of columns are required.

An automatic process chromatograph equipped with sample valve, column bypass valves, program reset, and automatic base line zeroing offers the opportunity to construct an analytical separation scheme based upon the use of several columns specific to the critical separations required. The operation of chromatographs, sample valves, and column switching techniques of this type has been discussed by Villalobos and Turner (*1–3*) and by Nuss (*4*).

## EXPERIMENTAL

**Apparatus.** The chromatographic equipment employed consists of a Beckman Model D Process Analyzer, a Beckman Model 520 Programmer, an Aerograph Model 471 Electronic Digital Integrator, and a Leeds and Northrup Speedomax G 1-millivolt recorder.

The Model D analyzer houses the chromatographic columns and is equipped with three Beckman six-port Teflon (Du Pont) slider valves. A fourth Teflon slider valve is located in the pilot plant exit gas stream and serves as the sample inject valve. Samples may also be introduced by syringe through a septum for calibration purposes. Nupro Type-S needle valves serve as variable restrictors for matching column pressure drops. The needle valve bodies are located inside the analyzer oven, but extension handles extending through the oven wall make them adjustable from outside.

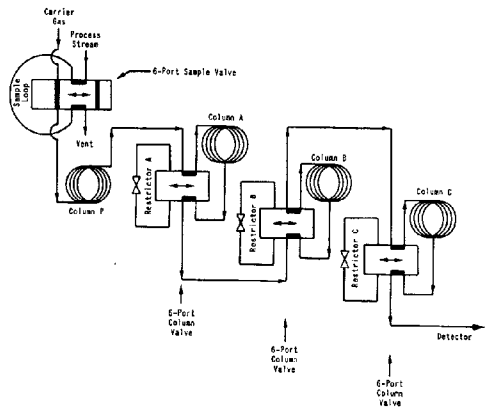


**Figure 1. Schematic diagram of chromatographic sample stream**

The Model 520 programmer uses a program of operations which are recorded on a continuous loop magnetic tape. Signals from the tape then allow repetitive analyses to be made, complete with sample injection, for as long as the programmer remains in the automatic mode. Automatic integration is carried out by the digital integrator which receives the chromatographic signal directly. Programmer and integrator reset work together so that integrator peak retention time printout will be reproducible from sample to sample.

A recorder with the present chromatograph–integrator combination is not necessary for quantitative purposes. However, the recorder is indispensable for monitoring, calibration, and trouble shooting. Elimination of the recorder would eliminate also the use of the automatic base line zeroing feature of the chromatograph.

**Columns.** Figure 1 is a schematic diagram indicating the sample flow pattern and the location of each column employed. The four columns are listed below, along with the purpose of each. The columns are maintained at a temperature of 155 °C, and the hydrogen carrier gas flow rate is 50 ml per minute. Hydrogen was employed in order to eliminate the hydrogen peak which would otherwise be present due to the large $H_2$ concentration in the process stream.

COLUMN P. P is a 10-foot by 3/16-inch o.d. (316 stainless steel tubing) column containing 10% Carbowax 6000 on 35/60 mesh Teflon-6. Its purpose is to retard water and alcohols beyond the permanent gases and lighter hydrocarbons. Teflon is used as support for the polar Carbowax in order to minimize the tailing of water. All components in the sample pass through this column as there is no bypass provided.

COLUMN A. A is a 5-foot by 3/16 inch o.d. copper tubing column containing 10% tetracyanoethylated pentaerythritol on 60/80 mesh Porapak T. Its purpose is to spread the portion

(1) R. Villalobos and G. S. Turner, *ISA (Instr. Soc. Amer.) J.*, **10**, 67 (1963).
(2) R. Villalobos and G. S. Turner, in "Gas Chromatography," Instrument Society of America Symposium June 1962, L. Fowler, Ed., Academic Press, New York, N.Y., 1963, p 105.
(3) G. S. Turner and R. Villalobos, in "Gas Chromatography," Instrument Society of America Symposium, June 1961, N. Brenner, J. E. Callen, and M. D. Weiss, Eds., Academic Press, New York, N.Y., 1962, p 363.
(4) G. R. Nuss, in "Gas Chromatography," Instrument Society of America Symposium, June 1962, L. Fowler, Ed., Academic Press, New York, N.Y., 1963, p 119.

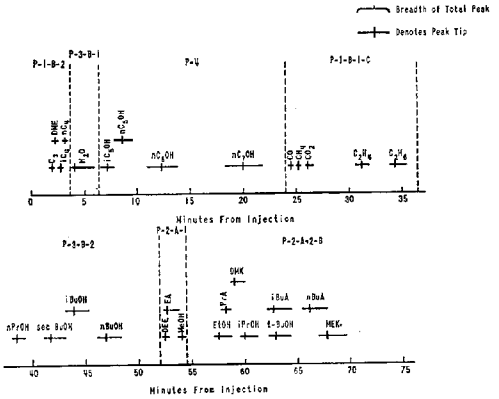


**Figure 2. Retention times in finished analysis**

of the total sample which passes through it so that several subsequent cuts may be made.

COLUMN B. B is a 4-foot by 3/16-inch o.d. (copper tubing) 60/80 mesh Porapak Q column whose purpose is twofold: It brings about the separation of water and alcohols, and separates the lightest materials sufficiently so that a cut may be made between ethane and propane.

COLUMN C. C is a 12-foot by 3/16-inch o.d. copper column containing 60/80 mesh activated carbon. Its purpose is to bring about the separation of CO, $CO_2$, methane, ethane, and ethylene.

**Analysis Plan.** Putting together the retention time data for each of the four columns, the following plan of analysis was devised. The nomenclature employed to identify sample fractions denotes by letter the sequence of columns through which each portion passes. The number after a letter identifies a fractionation within that column.

Columns P + B + C are initially in the carrier gas stream when the sample is injected (Column A is bypassed).

COLUMN P FRACTIONATIONS. The sample is separated into four fractions, P-1, P-2, P-3, and P-4 in Column P.

Fraction P-1. This fraction is passed directly to Column B, where it becomes Fraction P-1-B.

Fraction P-2. After P-1 has passed into Column B, Column A is switched back into the carrier gas stream to receive Fraction P-2 (which now becomes P-2-A). C is bypassed shortly after this to store the lightest materials from P-1-B in C. This stored fraction now becomes P-1-B-1-C. The heavier materials, P-1-B-2, are allowed to pass from B to the detector when C is bypassed and are the first components to appear on the chromatogram.

Fraction P-3. When P-2 has cleared Column P, Column A is bypassed so that P-3 may pass directly to B, becoming Fraction P-3-B. Fraction P-2-A is meanwhile stored in A. C is still being bypassed at this point.

Fraction P-4. After P-3 has cleared Column P, Column B is bypassed (in addition to A and C) so that Fraction P-4 may pass directly to the detector. The system is so arranged that, at this point, water, which was least retained from Fraction P-3-B, has just passed through the detector (as Fraction P-3-B-1); but *n*-propanol from the same fraction has not yet emerged from Column B. Thus, the remainder of Fraction P-3-B, now designated P-3-B-2, is stored in B.

P-B SEQUENCE FRACTIONS. Four fractions pass in sequence from Column P to Column B.

Fraction P-1-B-1. This fraction contains CO, etc., and is stored in Column C after emerging from Column B. This stored fraction, now P-1-B-1-C, is brought out of C right after P-4 passes over the detector.

**Table I. Abbreviations Used for Component Peak Identification**

| Abbreviation | Compound |
|---|---|
| MeOH | Methyl alcohol |
| EtOH | Ethyl alcohol |
| iPrOH | Isopropyl alcohol |
| nPrOH | Normal propyl alcohol |
| secBuOH | Secondary butyl alcohol |
| iBuOH | Isobutyl alcohol |
| tBuOH | Tertiary butyl alcohol |
| nBuOH | Normal butyl alcohol |
| $iC_5OH$ | Isoamyl alcohol |
| $nC_5OH$ | Normal amyl alcohol |
| $nC_6OH$ | Normal hexyl alcohol |
| $C_3$ | Propane |
| $iC_4$ | Isobutane |
| $nC_4$ | Normal butane |
| $iC_5$ | Isopentane |
| $nC_5$ | Normal pentane |
| $nC_6$ | Normal hexane |
| $nC_7$ | Normal heptane |
| $nC_8$ | Normal octane |
| $nC_9$ | Normal nonane |
| DME | Dimethyl ether |
| DEE | Diethyl ether |
| EA | Ethylaldehyde (acetaldehyde) |
| PrA | Propylaldehyde (propionaldehyde) |
| iBuA | Isobutyraldehyde |
| nBuA | Normal butyraldehyde |
| DMK | Acetone (dimethyl ketone) |
| MEK | Methyl ethyl ketone |

**Table II. Alcohol Analysis Automatic Program**

| Switch position no. | Functions | Time from inject, minutes | Purpose |
|---|---|---|---|
| 1 | A Out | − 2.8 | Ready columns for sample injection |
| 2 | B In | − 2.7 | |
| 3 | C In | − 2.6 | |
| 4 | Input short | − 2.5 | Zero recorder base line |
| 5 | Auto zero | − 2.4 | |
| 6 | Blank | − 0.1 | |
| 7 | Sample inject | 0 | |
| 8 | Blank | 0.50 | Return sample value to fill position |
| 9 | A In | 1.30 | Cut between P-1 and P-2 |
| 10 | C Out | 1.70 | Cut between P-1-B-1 and P-1-B-2 |
| 11 | A Out | 3.25 | Cut between P-2 and P-3 |
| 12 | B Out | 6.45 | Cut between P-3 and P-4 |
| 13 | C In | 24.00 | Bring P-1-B-1-C out of C |
| 14 | C Out, B in | 36.50 | Bring P-3-B-2 out of B |
| 15 | B Out, A in | 52.00 | Bring P-2-A-1 out of A |
| 16 | B In | 55.30 | Cut between P-2-A-1 and P-2-A-2, bring latter through B |

Fraction P-1-B-2. This fraction contains $C_3$, DME, $iC_4$, and $nC_4$. It is the first portion of the sample to pass over the detector, as indicated above.

Fraction P-3-B-1. This fraction contains only water and follows P-1-B-2 out of B and over the detector.

Fraction P-3-B-2. This alcoholic fraction is brought directly from B to the detector following the elution of P-1-B-1-C.

P-A SEQUENCE FRACTIONS. Fraction P-2-A-1. This fraction, which has been stored in A for some time, is passed from A to the detector following the elution of Fraction P-3-B-2. Methanol is included in this fraction.

Fraction P-2-A-2. When methanol (from Fraction P-2-A-1) has emerged from A (and through the detector), Column B

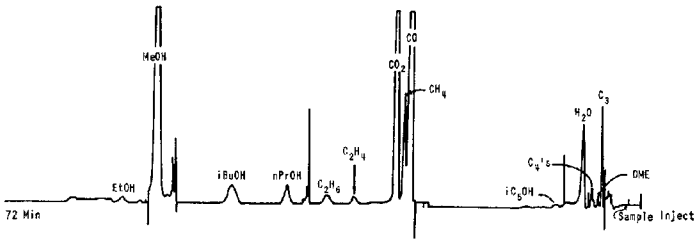


**Figure 3. Automatic reaction mix sample with integrator tape**




is switched into the carrier gas stream to accept Fraction P-2-A-2. These are the last components to appear in the chromatogram (as Fraction P-2-A-2-B).

## RESULTS AND DISCUSSION

**Finished Analysis.** Figure 2 charts the resultant analysis, giving the location with respect to time of each emerging peak. Table I lists the component abbreviations used. Location of fractions as they are listed above is also given in Figure 2. (Paraffins above $nC_4$ have not been included as they have not been observed.) Few serious overlaps are encountered. One of the worst such cases is with isobutyraldehyde and *t*-butanol. However, because the latter is not formed during methanol synthesis, this is not a problem.

Table II presents a timetable of the program functions as they occur. A stepping switch advances one position every time it is triggered by a pulse from the magnetic tape timer in the chromatographic programmer. The positions on the stepping switch are wired electrically to the various operations as listed.

Figure 3 is a reproduction of an actual chromatogram of the alcohol synthesis reactor effluent. Indicated thereon are peak identifications. The peaks with the flat tops (CO, $CO_2$, MeOH) have gone offscale, as the sample was run at a low enough attenuation to permit seeing the smaller peaks. The digital integrator receives the chromatographic signal directly and has such a wide dynamic range that no signal attenuation is necessary. The resolution between CO and $CH_4$ in Figure 3 is not as good as that indicated possible in Figure 2. The reason for this is that CO is very much larger than any other peak, as the methanol synthesis is operated at low per pass conversions. In order to keep the smaller peaks large enough to integrate accurately, it is necessary to run such large samples (in this case, 2 ml at 350 °F and atmospheric pressure) that the column tends to be overloaded with CO. Resolution with nearby peaks, therefore, suffers. Figure 3 also includes a reproduction of the digital integrator tape. Area printouts not identified are due to column switching transients and do not interfere with the proper area determination of real peaks.

**Table III. Determination of Relative Molar Area Response of Carbon Monoxide and Methanol**

**(rmr for CO = 100, hydrogen carrier gas)**

| % MeOH | $rmr_{MeOH}$[a] | $\sigma$rmr (% of value) |
|---|---|---|
| 2.81 | 77.0 | 8.3 |
| 5.46 | 68.6 | 6.0 |
| 10.5 | 70.0 | 1.3 |
| 12.8 | 72.8 | 1.7 |
| 22.6 | 75.0 | 0.7 |

[a] Weighted mean value of $rm_{MeOH} = 73.3$.
$\sigma$ of weighted mean = 1.3%.

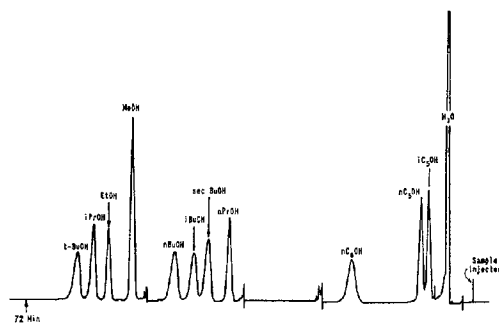


**Figure 4. Chromatogram of mixed alcohol sample, manually injected**

**Unlabeled base line deviations are switching transients and pressure pulses**

Figure 4 is a chromatogram of a qualitative liquid blend of all $C_1$ to $C_4$ alcohols plus iso- and normal pentanol, normal heptanol, and water. Not all of these are formed during methanol synthesis, but all are nicely separated by this analysis.

Figure 5 is a similar manually injected sample of a qualitative blend with some of the possible lighter components. Figure 6 is a chromatogram of some of the possible non-alcoholic products which may be formed during methanol synthesis. It will be noted that a small piece of propionaldehyde elutes earlier than the major portion of that component. This is due to the fact that the cut between Fractions P-A-1 and P-A-2 was made slightly late. This was necessary in order to include all of the methanol in one peak in the reaction mix samples because methanol was present in large amounts and tended to tail out. In our reaction mix samples, propionaldehyde is not present in detectable quantities.

The foregoing examples show that while all components are not completely resolved, the separations achieved are sufficient to allow a very good monitoring of product quality and extent of reaction. The total time of analysis is 72 minutes.

**Calibration.** In converting a set of chromatographic area data to component concentrations, the method of internal

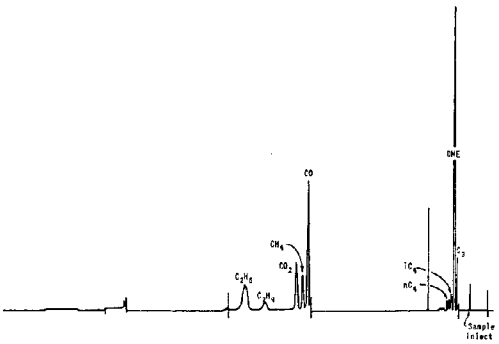


**Figure 5. Manually injected sample of mixed gases**

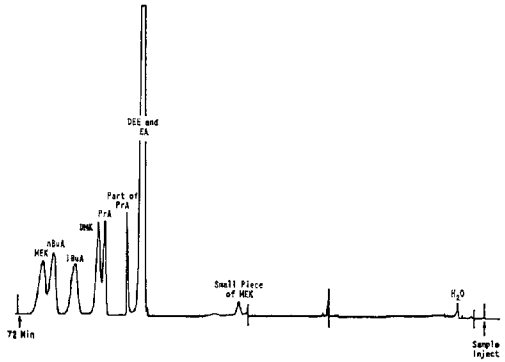


**Figure 6. Manually injected sample of some possible non-alcoholic products of alcohol synthesis process**

normalization is most conveniently employed. It is necessary, however, to have relative thermal conductivity detector response information available for each component. While such data are fairly plentiful in the literature for the case where helium is the carrier gas (*5–7*), response data are rather scarce when hydrogen is used as carrier gas (*8–10*).

(5) D. M. Rosie and R. L. Grob, ANAL. CHEM., **29,** 1263 (1957).
(6) A. E. Messner, D. M. Rosie, and P. A. Argabright, *ibid.*, **31,** 230 (1959).
(7) W. A. Dietz, *J. Gas Chromatogr.*, **5,** 68 (1967).
(8) R. Kaiser, "Gas Phase Chromatography," Vol. III, Butterworths, Washington, D.C., 1963, p 92.
(9) F. van de Craats, "Gas Chromatography, 1958," D. H. Desty, Ed., Butterworths, Washington, D.C., 1958, p 248.
(10) E. G. Hoffman, ANAL. CHEM., **34,** 1216 (1962).

Because of the sparse information available, a set of relative molar responses was determined for most of the substances to be analyzed using the specific columns to be employed. The components determined comprise two groups: those normally gaseous and those normally liquid. The gas component molar responses (relative to CO) were determined by injecting constant volume samples of each pure component with the aid of a gas sample valve. The liquid component relative molar responses were determined by syringe injection of a series of weighed mixtures, each of which included methanol as the common reference.

In order to relate the response data for one of the above groups to that of the other, one gas and one liquid component were compared. This was accomplished for CO and methanol

**Table IV. Relative Molar Area Response for Components Encountered in Alcohol Synthesis Reaction Mix**

| Component | Molecular weight | rmr: This paper, $H_2$ carrier gas | rmr: van de Craats (*9*), $H_2$ carrier gas | rmr: Messner *et al.* (*6*), He carrier gas |
|---|---|---|---|---|
| Gaseous | | | | |
| CO | 28 | 100 | 100 | 100 |
| $CO_2$ | 44 | 119 | 121 | 114 |
| $CH_4$ | 16 | 88 | 92 | 86 |
| $C_2H_4$ | 28 | 138 | 122 | 114 |
| $C_2H_6$ | 30 | 145 | 130 | 121 |
| $C_3H_8$ | 44 | 176 | 160 | 155 |
| $iC_4H_{10}$ | 58 | 204 | 181 | 195 |
| $nC_4H_{10}$ | 58 | 231 | 187 | 202 |
| DME | 46 | 178 | — | — |
| Liquid | | | | |
| $H_2O$ | 18 | 56 | — | 50 |
| MeOH | 32 | 73 | — | 131 |
| EtOH | 46 | 97 | — | 171 |
| iPrOH | 60 | 109 | — | 198 |
| nPrOH | 60 | 112 | — | 202 |
| tBuOH | 74 | 127 | — | 228 |
| secBuOH | 74 | 125 | — | 231 |
| iBuOH | 74 | 130 | — | — |
| nBuOH | 74 | 136 | — | 226 |
| $nC_5OH$ | 88 | 152 | — | — |
| $nC_6OH$ | 102 | 165 | — | 281 |
| DEE | 74 | 130[a] | — | 262 |
| Acetone | 58 | 110[a] | — | 205 |
| MEK | 72 | 120[a] | — | 233 |
| EA | 44 | 95[a] | — | — |
| PrA | 58 | 110[a] | — | — |
| BuA | 72 | 130[a] | — | — |

[a] Estimated, rather than experimentally determined.

by mixing the two substances in the vapor phase prior to sampling through the gas sample valve in the pilot plant reactor effluent. Known rates of each were metered into the reactor which served as the mixing chamber ahead of the sample valve. The reactor contained only inert alundum, and the temperature of 350 °F at 1000 psig served to vaporize the methanol (in the concentration employed) without bringing about chemical reaction. The pressure of this mixed stream was reduced to atmospheric before entering the gas sample valve. Table III summarizes the results for a series of several CO-MeOH concentrations. Standard deviations determined from 8–20 replications at each concentration are included as an estimate of precision. The lower methanol concentrations were achieved at lower methanol injection rates and resulted in somewhat greater variations in efficiency of mixing.

Table IV lists those substances whose relative molar response factors have been evaluated in the above manner. Added to this list are several additional components (which always appeared in the analysis in very small amounts) not determined in this work. Molar response factors for these latter substances were estimated from the alcohol data, based on molecular weight. Because CO is the major component in the reaction mix samples, it was assigned the value of 100 for its relative molar response. For comparison, Table IV also includes molar responses referred to CO taken from Messner, Rosie, and Argabright (*6*) and van de Craats (*9*). Values from the former cannot be compared with those of this paper in a meaningful way, as the carrier gas is not the same. The data of van de Craats, unfortunately, do not include any alcohols. Those of Hoffman (*10*) do not include CO or hydrocarbons below pentane.

In comparing one set of empirical data of this type with another, it is difficult to account for differences between them. In spite of the difference in carrier gas, the data of Messner (*6*) suggests that perhaps the alcohol values determined in the present work are low. However, Kaiser (*8*) shows for a limited quantity of data that differences in response for light compounds in hydrogen carrier gas as compared with helium are appreciable when the molecular weight of the substance is low. (For CO, the relative molar response in hydrogen is given as 1.3 times that in helium.) As the molecular weight approaches 86, the hydrogen and helium response factors become more nearly equal and are essentially the same above that level. Because CO has been chosen as the reference in this paper, the relative molar responses for the heavier alcohols might, therefore, be expected to be somewhat lower in hydrogen than in helium. On the other hand, Hoffman (*10*), also on the bais of a limited amount of data, states that the same factors may be used for $H_2$ as well as He as carrier gases without essential loss of accuracy.

Column factors may also enter into the differences between this work and Messner's. Water and the alcohols are notorious for tailing; and Porapak and Teflon-supported columns available now but not at the time of Messner's work are superior in this respect.

**Precision and Accuracy.** Because this analysis was performed on a complex reaction mixture subject to change at any time due to fluctuating process variables or to catalyst activity decline, precision and accuracy are difficult to evaluate. Consecutive samples from the process stream agreed quite well with one another, the percentage concentration of all components being within 5% or less of the amount present from one sample to the next. Methanol and CO, the two highest in concentration, reproduced within 1% of the amount present.

Checks for accuracy on a complete reaction mixture by some other analytical method were not possible. The best indication of reliability of results was a carbon balance done over all components in the product with the knowledge that all carbon originated with the CO. Such carbon balance calculations always resulted in closures within 5% or less when the set of hydrogen area-response factors determined for this work was employed. Early carbon-balance calculations employing the helium factors of Messner resulted in closures as poor as ±20% and prompted the calibration work discussed above.

RECEIVED for review November 7, 1968. Accepted January 21, 1969.

---

## Correction

## Spectrophotometric Determination of Trace Amounts of Silver(I)

The development of a spectrophotometric method for the determination of trace amounts of silver(I) was recently reported in this journal [M. T. El-Ghamry and R. W. Frei, ANAL. CHEM., **40**, 13 (1968)]. The procedure utilized the ternary complex formed by silver(I), 1,10-phenanthroline, and tetra bromo (R) fluorescein. In the meantime it has been brought to the authors' attention that the investigation of ternary complexes involving silver–1,10-phenanthroline and a number of anionic dyestuffs has been reported elsewhere (B. W. Bailey, Ph.D. Thesis, University of London, 1967). In the latter study, systems utilizing fluorescein and halogenated fluoresceins were investigated. It was determined that all halogenated fluoresceins undergo a bathochromic shift on complexing with silver–1,10-phenanthroline and the various complexes have similar chemical and physical properties. The most sensitive color reactions were observed with the use of tetra chloro (P) tetra iodo (R) fluorescein. The behavior of the complex in both aqueous and organic media and the structure were investigated. This correction acknowledges the previous contribution to the analytical uses of ternary complexes and the silver–phenanthroline–fluorescein complexes in particular.

# A Rapid and Selective Method for the Spectrophotometric Determination of Niobium

**Robert Villarreal and Spence A. Barker**

*Argonne National Laboratory, Idaho Division, Idaho Falls, Idaho 83401*

**A rapid and selective method for the separation and determination of niobium in uranium-fissium alloy has been developed. The procedure is based on the extraction into toluene of niobium with *N*-benzoyl-*N*-phenylhydroxylamine (BPHA) from 9–12*M* HCl containing stannous chloride. The Nb–BPHA complex in toluene is contacted with ammonium thiocyanate in 4*M* HCl and the color intensity of the Nb–BPHA–SCN complex in toluene is measured at 365 mμ. Of 48 elements tested, only tantalum interferes at all levels. Milligram quantities of tartrate, oxalate, citrate, fluoride, and other common anions do not interfere; hydrogen peroxide interferes but is easily destroyed. The ionic molar absorptivity of the colored complex measured under the conditions of the procedure is 32,000. Beer's law is obeyed from 0 to 50 μg Nb. At the 0.01% niobium level in uranium-fissium alloy, the relative precision of the method is ± 2%.**

METHODS FOR THE DETERMINATION of niobium are generally long and tedious, and require preliminary separations for the removal of interfering ions. Masking reagents, added to improve selectivity, greatly reduce the sensitivity of many methods. Thiocyanate methods are perhaps the most commonly used for niobium, but are subject to several chemical interferences. Hydrogen peroxide and 8-quinolinol methods lack sensitivity and are also subject to chemical interferences. Chromogenic reagents such as 4-(2-thiazolylazo) resorcinol (*1*), 4-(2-pyridylazo) resorcinol (*2*), bromopyrogallol red (*3*), and various azo-dyes (*4*) were recently introduced for the determination of niobium. Although these reagents are very sensitive for niobium, they cannot be directly used on highly colored solutions or on solutions containing large amounts of uranium. *N*-Benzoyl-*N*-phenylhydroxylamine (BPHA) has been used for the gravimetric determination of niobium (*5*, *6*) and for the separation of niobium, tantalum, and titanium from other elements (*7*). Alimarin and Petrukhin (*8*) have investigated the BPHA extraction of niobium, titanium, tantalum, vanadium, and zirconium from sulfuric acid solutions. Lyle and Shendrikar (*9*) have studied the extraction of niobium, protactinium, and tantalum from hydrochloric acid solutions. Afghan *et al.* (*10*) used BPHA for the extraction and determination of titanium. Vita *et al.* (*11*) reported a detailed study on the extraction of 52 elements with BPHA, and the subsequent determination of niobium with PAR and zirconium with Arsenazo III.

The nuclear fuel used in Experimental Breeder Reactor II (EBR-II) is a uranium-fissium alloy consisting of 95% uranium and a 5% mixture of molybdenum (2.5%), ruthenium (1.9%), rhodium (0.30%), palladium (0.19%), zirconium (0.10%), and niobium (0.01%). The routine determination of niobium in this fuel requires a method that is highly selective, sensitive, and preferably rapid. The outlined method has been successfully applied to the determination of niobium at the 0.01% level in the analysis of uranium-fissium alloy. The selectivity of the procedure should make it widely applicable for the determination of niobium. In this highly selective method, niobium is extracted with BPHA into toluene from 9–12*M* hydrochloric acid in the presence of stannous chloride, which reduces metal ions. The Nb–BPHA complex in toluene is shaken with ammonium thiocyanate in 4*M* hydrochloric acid to form a colored complex in the toluene which is measured at 365 mμ. An unsuccessful attempt was made to identify the exact composition of the Nb–BPHA–SCN complex. The ionic molar absorptivity for the colored complex measured under the conditions of the procedure is 32,000. The absorbance of the colored complex obeys Beer's law from 0 to 50 μg Nb in 10 ml of toluene.

## EXPERIMENTAL

**Apparatus.** Absorbance measurements were made with a Beckman Model B spectrophotometer in matched 1-cm silica cells against deionized water. Gamma counting of Nb-95 tracer was performed with an ND-180 512-channel analyzer.

**Conditions.** All experiments and measurements were conducted at room temperature (25 °C).

**Reagents.**

1% BPHA. Dissolve one gram of *N*-phenylbenzohydroxamic acid (Eastman Organic Chemicals, catalog No. 7297) in 100 ml of either ethanol or acetone. This solution is stable for at least one month if kept in the refrigerator.

40% $SnCl_2$. Dissolve 40 grams of stannous chloride by heating in 75 ml of 12*M* HCl. After cooling, make to 100 ml with 12*M* HCl. This solution should be made fresh every week.

25% $NH_4SCN$. Dissolve 250 grams of $NH_4SCN$ in deionized water and dilute to one liter. Extract the $NH_4SCN$ solution with 100 ml of hexone. Discard the hexone. Remove residual hexone from the solution by washing with 100 ml of chloroform. Discard the chloroform. Filter the washed solution through fast quantitative filter paper.

Thioglycolic acid. Purified (Fisher A-319).

Fluoboric acid. 48–50%.

Niobium solution (1 mg/ml). Dissolve 1.0 gram of niobium metal by prolonged heating with concentrated sulfuric acid. Cool. Add 40 ml of 18*N* sulfuric acid, 50 ml of 10% tartaric acid solution and dilute to 1 l with 6*M* HCl.

Chemicals used in interference studies were reagent grade.

**Dissolution of Uranium-Fissium Alloy.** Place a 1-gram sample in a 125-ml Erlenmeyer flask containing 15 ml deionized water. Dissolve the sample by adding 20 ml of a 4:1 HCl–$HNO_3$ mixture and heating on a hot plate. The dissolution should

(1) V. Patrovsky, *Talanta*, **12**, 971 (1965).
(2) P. Pakalns, *Anal. Chim. Acta*, **41**, 283 (1968).
(3) R. Belcher, T. V. Ramakrishna, and T. S. West, *Talanta*, **12**, 681 (1965).
(4) I. P. Alimarin and S. B. Savvin, *ibid.*, **13**, 689 (1966).
(5) A. K. Majumdar and A. K. Mukherjee, *Anal. Chim. Acta*, **19**, 23 (1958).
(6) A. K. Majumdar and A. K. Mukherjee, *ibid.*, **21**, 245 (1959).
(7) F. J. Langmyhr and T. Hongslo, *ibid.*, **22**, 301 (1960).
(8) I. P. Alimarin and O. M. Petrukhin, "Analytical Chemistry," Elsevier, New York, N.Y., 1963, p 152.
(9) S. J. Lyle and A. D. Shendrikar, *Talanta*, **12**, 573 (1965).
(10) B. K. Afghan, R. G. Marryatt and D. E. Ryan, *Anal. Chim. Acta*, **41**, 131 (1968).
(11) O. A. Vita, W. A. Levier and E. Litteral, *ibid.*, **42**, 87 (1968).

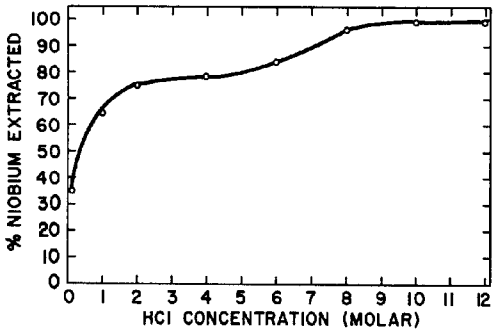


**Figure 1. Niobium extracted *vs.* HCl concentration**

**8.27 $\mu$g Nb with $^{95}$Nb tracer**
**1 ml of 1% BPHA in ethanol, 20 ml × x*M* HCl,**
**1 ml of 40% $SnCl_2$, 10 ml toluene**

proceed as rapidly as possible without spattering until the sample is dissolved. Any undissolved residue (primarily Ru) is separated by centrifugation in a 40-ml cone and dissolved in 2 ml of 6*M* NaOH and 5 ml of NaOCl heated in a hot water bath for 10 min. The alkaline solution is cooled, acidified with 12*M* HCl, added to the original solution, and this solution diluted to 50 ml volume with deionized water.

**Sample Preparation.** Samples in which niobium may have polymerized or have precipitated should be strongly fumed with concentrated sulfuric acid. Also, sample aliquots larger than 3 ml should be fumed with 2 ml concentrated sulfuric acid to a volume less than 1 ml. The residual sulfuric acid is taken up with 20 ml of 12*M* HCl and transferred directly to a separatory funnel for analysis.

**Analytical Procedure.** For samples which do not require sulfuric acid fuming, pipette an aliquot containing 2–20 $\mu$g of niobium into a 60-ml separatory funnel. Add 20 ml of 12*M* HCl, 1 ml of $SnCl_2$ solution, and mix thoroughly. From this point on, the specified times should be followed fairly closely, as large deviations may lead to erratic results. Add 1 ml of 1% BPHA, mix thoroughly, and allow to stand 1 min. Extract the Nb–BPHA complex into 10 ml of toluene by shaking for 1 min. Allow the phases to separate completely; drain off and discard the aqueous phase. Add 20 ml of 4*M* HCl and 5 ml of 25% $NH_4SCN$ solution and shake for 1 min. As soon as the toluene phase is clear, transfer a portion or drain through cotton into a 1-cm cell and measure the color intensity at 365 m$\mu$. Color measurement must be made within 1 hour after adding the $NH_4SCN$ solution (see Color Development). Run blanks and standards with sample as described above.

## EFFECTS OF VARIABLES

**Nb–BPHA Extraction.** Extraction of the Nb–BPHA complex into toluene is quantitative from 0–12*M* hydrochloric acid. Niobium carrier with niobium-95 tracer was extracted with BPHA into toluene from 0.1*M* to 12*M* HCl, the phases were separated by centrifugation, and aliquots of each phase were counted to determine the fraction of niobium extracted. The results of the tracer experiments are shown in Figure 1. The extraction of niobium-95 tracer with BPHA from 9–12*M* HCl was complete within 1 min. Extraction of metal ions other than niobium is minimized at high acid concentrations and the possibility of hydrolysis or polymerization of niobium is reduced.

Metal-thiocyanate complexes are insoluble in toluene but the Nb–BPHA–SCN complex is soluble in toluene. Selectivity of the procedure is greatly enhanced, because, under

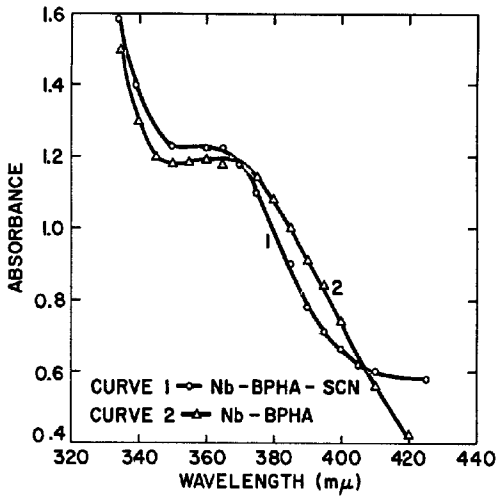


**Figure 2. Absorption spectrum**

**Curve 1. 33 $\mu$g Nb in 10 ml toluene**
**Curve 2. 99 $\mu$g Nb in 10 ml toluene**

the conditions of the method, only toluene-extractable metal–BPHA complexes can react with thiocyanate and remain in toluene.

**Effects of Other Ions.** The effect of various ions was determined by adding known quantities of test ion to a niobium standard and blank and noting the effect on the final absorbance. Ten milligrams each of Li, B, Na, Mg, K, Ca, Fe, Y, Mo, Ru, Sn, Ba, La, mixed rare earths, Th, U, and 1 mg each of Al, Si, Ti, Cr, Mn, Ni, Cu, Zn, Co, Bi, Pt, Rh, Pd, In, W, and Re gave no interference in the method. Greater quantities of most of these test elements were not investigated for interference. Titanium and Pt in amounts greater than 1 mg and Zr in amounts greater than 20 $\mu$g gave positive interference. Small quantities of fluoride in the Ti and W test solutions may have contributed to the noninterference of these elements. Vanadium in amounts greater than 0.25 mg gave negative interference. Tantalum interfered at all levels. However, the interference of V and Zr up to 1 mg may be masked with 1 ml of 85% phosphoric acid, but greater quantities of Zr will precipitate as zirconium phosphate. Ten milligrams of Zr may be masked with 0.1 ml of fluoboric acid. One milligram of Ag may be kept in solution by masking with thiourea. Ten milligrams of Bi gave positive interference but was masked by 0.5 ml of thioglycolic acid. Masking agents, if needed, should be added to the 9–12*M* HCl before addition of BPHA. Reduction by $SnCl_2$ eliminates the interference of several cations, notably Co, Mo, and Fe, that interfere in most thiocyanate procedures. Up to 0.5 g of $SnCl_2$ added to 20 ml of 12*M* HCl does not adversely affect the procedure.

One hundred milligrams of citrate, oxalate, tartrate, thiourea, thioglycolic acid, phosphate, sulfate, nitrate, perchlorate, iodide, bromide, and 10 mg of fluoride gave no interference. Greater quantities of fluoride as HF leached impurities from the borosilicate separatory funnel and gave high results. At least 100 mg of fluoride as fluoboric acid does not interfere. Hydrogen peroxide, if present, interferes seriously but may be easily destroyed by heating the 9–12*M* HCl to near boiling prior to addition of BPHA.

Tantalum is the only ion found whose interference at all levels was not eliminated by complexing agents.

**Color Development.** The greatest color and stability for the Nb–BPHA–SCN complex was achieved by shaking the Nb–BPHA complex in toluene with an acid solution of 0.65*M* $NH_4SCN$. The optimum acid concentration for color development with $NH_4SCN$ was 3–4*M* HCl. Higher acid concentrations greatly increased the blank while lower acid concentrations gave much less color.

The Nb–BPHA–SCN color formed rapidly with a 1-min shaking time and was stable for 1–2 hr if kept in the dark. Exposure to indirect sunlight in the laboratory increased the absorbance of the solution; however, the blank increased at the same rate and the net absorbance remained constant for 1–2 hr. Exposure of the colored complex in toluene to direct sunlight quickly caused formation of a yellowish turbidity. Production of turbidity by laboratory fluorescent light was very much slower than by sunlight.

One milliliter of thioglycolic acid added to the 4*M* HCl before addition of $NH_4SCN$ stabilized the colored complex for 1–2 hr in indirect sunlight and fluorescent light of the laboratory.

**Absorption Spectra.** The absorption spectra of both the Nb–BPHA–SCN complex and the Nb–BPHA complex in toluene are shown in Figure 2. The peak wavelength for both complexes is in the near ultraviolet region from 360 to 365 mμ.

The wavelength of 365 mμ was selected to provide maximum net absorbance readings together with an acceptably low blank.

**Sensitivity.** The absorptivity of the extracted Nb–BPHA–SCN complex measured under the conditions of the procedure at 365 mμ was calculated from a Beer's law plot to be 344 l/g-cm. The corresponding molar absorptivity (ionic molar absorptivity) is 32,000 and the sensitivity index for the reaction is 0.0029 μg Nb/cm². The colored species obeys Beer's law over the range studied from 1 to 50 μg niobium in 10 ml toluene.

The Nb–BPHA complex in toluene may be used for the determination of niobium, but the molar absorptivity for the Nb–BPHA complex in toluene is only 10,000 at 365 mμ, which is similar to 8-quinolinol but is much more selective. The Nb–BPHA complex in chloroform is the basis of a method described by Shigematsu *et al.* (*12*).

**Precision.** Analyses of 8 aliquots taken from a uranium-fissium solution gave 7.89 ± 0.12 μg Nb/ml. At the 95% confidence level, this represents a relative precision of ±2%.


ACKNOWLEDGMENT

The authors express their appreciation to John Young for preliminary work on the procedure and to Earl Ebersole for his technical assistance and help in preparing the report.

RECEIVED for review November 4, 1968. Accepted December 31, 1968.


(12) T. Shigematsu, Y. Nishikawa, and S. Goda, *Bull. Inst. Chem. Res., Kyoto University*, **43**, 347 (1965).

# Design of Membrane-Covered Polarographic Gas Detectors


**Daniel P. Lucero**

*Electro-Analytical Transducer Corporation, Fullerton, Calif. 92633*



**Membrane-covered polarographic gas detectors are designed by employing the relationships between their design constraints, specifications, and performance parameters. The application of the detector determines the functional dependence between specificity, sensitivity, time rate of response, and wearout time. Specificity is established by the electrochemical characteristics of the detector cell. Sensitivity is determined by the membrane material and its thickness. Time rate of response characteristics are determined by the properties of the electrolyte reservoir and the membrane and the internal geometrical design of the detector. The detector can wearout by several modes which depend upon the application. Wearout by depletion of the electrolyte solvent medium is the most common. Temperature response characteristics can be established by signal temperature compensation and active thermal control. Total gas pressure, humidity, and shock and vibration also affect the detector performance by altering its parametric relationships.**


MEMBRANE-covered polarographic gas detectors are electrochemical devices which measure the partial pressure of a particular molecular species present in gas mixtures and/or dissolved in liquids. They are commonly comprised of a sealed cartridge containing the essential elements of an electrolytic cell which is exposed to the gas molecules of the external environment through a semipermeable membrane. Their optimal operating mode is in the diffusion limited condition —*i.e.*, the mode where the electrode reaction consumes the electroactive molecular species at a greater rate than it can migrate through the membrane or diffusion barrier. Thus, the operating and performance characteristics of these detectors are primarily established by the mass transport properties of the membrane and its dimensional and geometrical configuration (*1*). Every aspect of the design is affected by the membrane characteristics. In only a few cases is the membrane of secondary importance in which consideration of its parameters may be relegated to the latter design stages. During the early phase of the design, it is mandatory that the design constraints and performance specifications be totally considered in order to characterize fully the detector elements and their parametric interdependence and to delineate and project design tradeoffs which will be required.

The basic configuration of a detector electrolytic cell is illustrated in Figure 1. All the essential elements are shown with the critical dimensional parameters of the cell. The configuration of the cell can be drastically changed to reflect the optimum design for a specific application. However, the general configuration represented by Figure 1 serves more effectively to relate the fundamental principles and techniques in the design of membrane-covered polarographic gas detectors.

(1) D. P. Lucero, ANAL. CHEM., **40**, 707 (1968).

## DESIGN AND PERFORMANCE CONSTRAINTS

All constraints and specifications which will be imposed on the detector and its performance are clearly defined at the outset of the design program. They can loosely be classified into three groups: (1) performance specifications, (2) environmental specifications, and (3) utility constraints as shown by Table I. Many of the specifications listed are closely associated and could be justifiably classified into more than one group. Further, their relative importance must be assessed to establish the order and degree by which the specifications may be degraded, if such steps become necessary, during the development. Obviously the application or intended use of the detector is of major concern at this stage. For example, the requirements of atmospheric gas analysis, blood oxygen tension measurements, analysis of gases dissolved in seawater, etc., dramatically alter the configuration of the detector to suit the particular application.

## SPECIFICITY

Polarographic detectors achieve a high degree of specificity by controlling the electrochemical parameters of the system. A unique combination of the working electrode surface material, electrode potential, supporting electrolyte, and the reference electrode ensures that the working electrode reaction sites be electrochemically active only to a single molecular species. Ideally, this condition in the development is obtained prior to initiation of the detector design. The electrochemical and chemical parameters of the cell should also be well enough defined to minimize cell failures and permit the characterization of electrochemical and chemical failure modes ascribed to cell side reactions. In any event, complete reaction specificity cannot always be attained and side reactions may occur. In many cases the electrical current arising from the side reactions is far below the current or signal level of the detector sensitivity requirements. If it remains at such a level, the interference is not serious and periodic adjustment of the zero current may be sufficient to correct the signal reading. When this background current is relatively large and reasonably stable and the concomitant reaction products do not deactivate or change the electrode surface, and it does not consume large quantities of the electrolyte, the detector signal may be compensated for this current. However, when side reactions and correspondingly large currents arise from the presence of a molecular species, such as may be present in the detector environment, whose concentration varies with time, location, and other conditions, it may be impossible to discern the origin of and/or characterize the detector background signal. It may arise from side reactions, from the molecular species under observation, and/or from a combination of both. The effects of these types of interferences may be reduced by utilizing gas separation devices employing membranes and other diffusion barriers which preferentially transport one molecular species over another (*2*).

Because membrane-covered polarographic gas detectors operate in the diffusion limited condition, and their performance characteristics are functions of the membrane transport properties, in a sense, the membrane acts as a gas separator whose geometrical configuration is compatible with the detector and is an integral part of it. The effectiveness of a membrane material in reducing the signal interference from side reactions can be assessed by utilizing the permeation ratio of

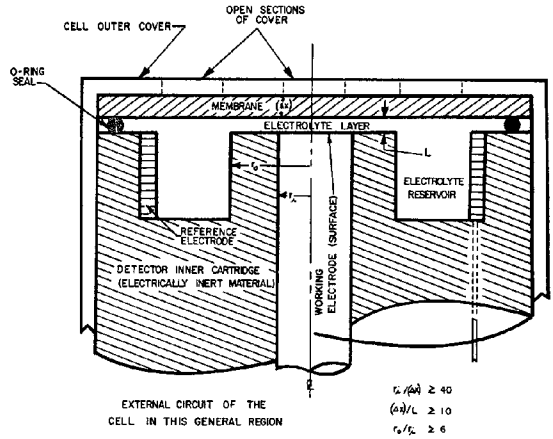


**Figure 1. Electrolytic cell of membrane-covered polarographic gas detector**

the material (*2*). It is defined as the ratio of the steady state diffusion current of the active gas to that of the interfering gas. The ratio provides a relative measure of the degree of gas separation which membranes fabricated from different materials can achieve when the electrical currents due to both gases are diffusion limited. Thus, the permeation ratio is the ratio of the diffusion conductance of the material to the active and inactive gases as given by the expression: $\alpha = P_a(\Delta X)_a/P_g(\Delta X)_g$, where $\alpha$ = permeation ratio, dimensionless, $P$ = membrane material permeability coefficient, moles/sec-cm²mmHg/cm, $(\Delta X)$ = membrane thickness, cm, $a$ and $g$ = subscripts denoting active and inactive gases, respectively. It reveals the membrane parametric relationship which yields the optimum diffusion specificity to be that with maximum and minimum material permeability coefficients to the active and inactive gases, respectively. In the case where the interfering current is not diffusion limited, the solubility coefficients of the membrane material and electrolyte solvent medium should be as small as possible to minimize the inactive gas concentration and the side reaction currents.

## SENSITIVITY AND SIGNAL LEVEL

The sensitivity limit of polarographic gas detectors is a function of the flux density ratio of the fundamental reaction to the highest level interfering side reaction or background reaction. A perfectly constant background reaction rate may be compensated by an artificially supplied opposing current of equal magnitude. Because the background reaction is rarely completely constant, the signal-to-noise ratio would be determined by the random variations of background reaction current. The magnitude and variation of this current may be characterized only with the noise information of single electrochemical cells operating under specifically defined conditions. Therefore, only the sensitivity limit and signal characteristics as determined by the detector design parameters will be considered.

The detector signal is related to the parameters of the systems by Equation 1:

$$i/p_a = nF[PA/(\Delta X)] \quad (1)$$

$i$ = detector signal level, $A$

$p_a$ = partial pressure of the electroactive molecular species in the external environment of the detector, mm Hg

(2) D. P. Lucero and F. C. Haley, *J. Gas Chromatog.*, **6**, 477, (1968).

**Table I. Classification of Detector Design Constraints**

| Performance specifications | Environmental conditions | Utility constraints |
|---|---|---|
| Specificity | Temperature response | Maintenance |
| Sensitivity | Operating temperature limits | Dimensions |
| Minimum signal level | Pressure response | Weight |
| Stability and drift | Shock and vibration | Configuration |
| Wearout time | Humidity | Power requirements |
| | Corrosion | Readout |
| | Erosion | Alarm |
| | External turbulence | |
| | Gas and liquid flow | |

$n$ = number of equivalents in each mole of the electroactive species, equivalents/mole

$A$ = diffusion cross-sectional area (projected area of the electroactive surface), cm²

F = Faraday constant, 96,500 coulombs/equivalent

Equation 1 is utilized to estimate the membrane mass conductance required to yield a predetermined signal current level per unit electroactive gas concentration in the atmosphere. The detector current is given above in amperes per mm Hg pressure of the electroactive species in the environment. If the surrounding environment is a liquid, the partial pressure of the dissolved gas is related to its concentration in the liquid by Henry's law. The gas concentration in Equation 1 is expressed on a ppm basis by taking each mm Hg partial pressure of the gas equivalent to 1315 ppm of the atmosphere. Thus, to attain a current/concentration level of $10^{-11}$ $A$/ppm when $n = 2$, a membrane with a mass conductance of 0.521 $\times 10^{-16}$ mole/sec-ppm or 3.96 $\times 10^{-12}$ mole/sec-mm Hg is required. The mass conductance of the detector membrane is defined by the expression: $K = PA/(\Delta X)$, $K$ = mass conductance, moles/sec-mm Hg. In utilizing Equation 1 for these purposes, a design contingency factor is added because the selection of membranes for a given cross-section diffusion area is limited to materials of given permeability coefficients and standard fabricated thicknesses. It is unlikely that the membrane mass conductance will match the value calculated from Equation 1.

Equation 1 is a reasonable approximation of the detector signal. Its accuracy is based on the restriction that mass transport through the membrane over the working electrode surface be one-dimensional and the diffusion impedance be composed entirely of the membrane impedance. A one-dimensional relationship is established when the lateral dimensions of the membrane are infinite relative to its thickness: a dimensional ratio of 40 to 1 is sufficient to approximate this condition. The overall diffusion impedance of the detector, however, is usually derived from the membrane impedance and the impedance of the thin layer of electrolyte over the working electrode surface in a series arrangement. In most detectors, the membrane diffusion impedance is at least 30 times larger than that of the electrolyte and Equation 1 is accurate within 5%. However, if this geometrical relationship cannot be conferred on the detector, then Equation 1 is modified to include the mass transport characteristics of the electrolyte layer as shown in Equation 2:

$$i/p_a = nF/[(\Delta X)_m/P_mA + (\Delta X)_e/P_eA] \qquad (2)$$

$m$ and $e$ = subscripts denoting membrane electrolyte layer, respectively

Presuming the membrane mass requirements do not change, a thinner membrane and/or a membrane with a larger permeability coefficient must be utilized when the electrolyte layer diffusion impedance becomes significantly large. The increase required in the membrane mass conductance is proportional to the signal attenuation due to the electrolyte layer impedance.

The detector signal and sensitivity requirements establish the characteristics of the membrane as described by Equation 1 or 2. These characteristics apply only to that region of the membrane directly over the working electrode surface. Other regions of the membrane may be altered in any fashion without seriously affecting the detector signal level and sensitivity. Other criteria determine the characteristics of the other regions of the membrane.

## TIME RATE OF RESPONSE CHARACTERISTICS

The time rate of response characteristics of polarographic detectors operating in the diffusion limited condition are established by the mass exchange processes between the detector and its surroundings and between various regions within the electrolytic cell. Mass transport through the membrane, of course, is the most important exchange process. The detector time rate of response is related to the parameters of the membrane by Equation 3:

$$t_c = (\Delta X)^2_m/D_m \qquad (3)$$

$t_c$ = detector time constant, seconds

$D_m$ = diffusion coefficient of the membrane for the electroactive species, cm²/sec

Equation 3 gives the time constant of a detector which is represented by a one-dimensional single node system—*i.e.*, the equation is totally descriptive only when certain conditions regarding diffusion and solution parameters of the gas in the detector are met. A single node detector is defined as a detector whose signal level and time rate of response characteristics are mathematically described with reasonable accuracy by lumping the mass capacitance and diffusion impedance terms into a single node. A departure from this condition will result in a slower responding device and the response curve will exhibit characteristics commonly referred to as "tailing" at the higher per cent response levels. A single node representation is, of course, only an approximation of the detector characteristics. A completely accurate model is comprised of an infinite number of nodes.

The number and arrangement of nodes depicting the detector operation to specific accuracy limits is determined by the geometry of the detector and the diffusion and solubility coefficients of the electroactive species in the membrane material and electrolyte solvent. The minimum required lattice density of mass capacitance and diffusion impedance

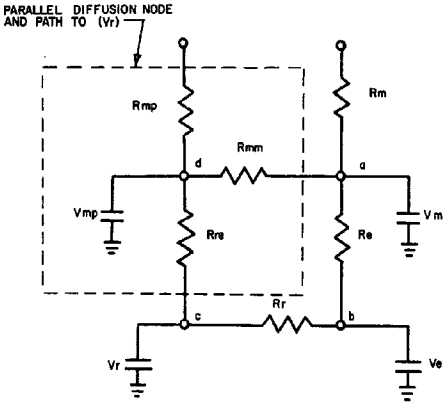


**Figure 2. Membrane electrolyte–reservoir nodal lattice of the detector**

$R_m$ = Membrane diffusion impedance over working electrode surface

$R_e$ = electrolyte layer impedance over electrode surface

$R_r$ = electrolyte impedance between electrolyte reservoir and electrolyte layer nodes

$R_{mp}$ = membrane impedance over the reservoir

$R_{re}$ = electrolyte impedance between the reservoir and the membrane over the reservoir

$R_{mm}$ = membrane impedance between the two membrane nodes

$V_m$ = membrane capacitance over electrode surface

$V_e$ = electrolyte layer capacitance over electrode surface

$V_{mp}$ = membrane capacitance over reservoir

elements is established by comparing the calculated values of the detector signal level and time constant utilizing different lattice densities. Calculations are made with an increasing lattice density for each computational cycle until the difference in the signal level and time constant of succeeding cycles is within the accuracy limits desired. Identical results can be obtained by representing the general diffusion equation with a mutually coupled finite difference operator and computing the dynamic error of the operator (*3*). This is equivalent to computing the time constant error. Equation 3 is ordinarily sufficiently accurate for most applications. However, a multinodal model can be employed to illustrate the dynamic response of the detector, to supply design information, to aid in the interpretation of experimental results, and describe the mass exchange processes. There are two fundamentally important nodes of the lattice which determine to a large extent the detector time rate of response characteristics: the nodes comprised of the membrane directly over the working electrode surface and the electrolyte reservoir illustrated in Figure 1. The electrolyte reservoir is that compartment within the detector cartridge which ordinarily contains the reference electrode and a large portion of the electrolyte. The lattice arrangement of a typical detector is shown in Figure 2. The time rate of response characteristics of the detector can be delineated by observing the mass exchange through the lattice of Figure 2. Three cases will illustrate the detector dynamic response: (1) the case where the detector is represented by node (*a*), (2) the case where the detector is represented by node (*a*) and (*b*) together, and (*3*) the case where node (*d*) is appended to the lattice.

**Single Node Representation.** All the mass entering and leaving the lattice or detector is transported through the membrane over the working electrode surface ($R_m$). It saturates the membrane mass capacitance ($V_m$). The impedance of the electrolyte layer over the working electrode surface ($R_e$) and the capacitance ($V_e$) are small compared to ($R_m$) and ($V_m$) and may be neglected in time dependent calculations. The interconnecting impedance between the electrolyte layer and reservoir ($R_r$)—*i.e.*, nodes (*b*) and (*c*)—is extremely large and the rate of mass transport through it may be assumed to be zero. Therefore, the dynamic response of the detector for this condition is established by the rate at which ($V_m$) is saturated with molecules of the electroactive species. The signal level of the detector is given by the expression: $i = i_o[1 - e^{-\alpha t}]$, $i_o$ = 100% detector response signal level, $A$, and $\alpha = D_m/(\Delta X)^2{}_m$. Figure 3 illustrates the rate of response curve.

**Binodal Representation.** All the mass entering and leaving the lattice is transported through ($R_m$) to saturate ($V_m$). The mass flows on through ($R_e$) into ($V_e$). However, in this case, the magnitude of ($R_e$) is comparable to ($R_m$) and therefore some of the mass which would have saturated ($V_e$) is diverted through ($R_r$) into the electrolyte reservoir mass capacitance ($V_r$). The time rate of response curve for this lattice arrangement is shown in Figure 3. It closely follows the single node response curve and then departs sharply and "tails" off into a slower responding curve. The point of its departure occurs when the concentration of the gas at ($V_e$) or the diffusion potential between nodes (*b*) and (*c*) is sufficient to promote the transport of a significant amount of the total mass flow to ($V_r$). Departures from the ideal single node curve are

(3) M. C. Gilliland, Annales de l'Association Internationale Pour le Calcul Analogique, No. 2, April 1962, p 78.

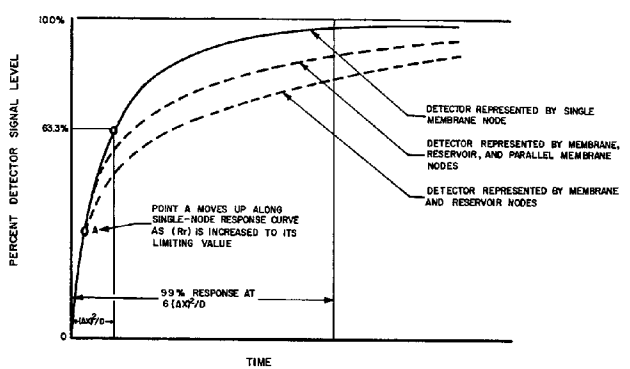


**Figure 3. Detector time rate of response characteristics**

mainly at the higher detector response levels because the diffusion potential between nodes (*a*) and (*b*) is decreased and concurrently the potential between nodes (*b*) and (*c*) is increased. In other words, as the total mass flow rate into the detector is decreased, the fraction of total flow rate to ($V_r$) is increased. Eventually the mass flowing through ($R_r$) completely saturates ($V_r$) and the diffusion potential between nodes (*b*) and (*c*) is reduced to zero. Mass exchange processes similar to that just described explain much of the characteristic "tailing" observed in many membrane-covered polarographic gas detectors. Caution must always be exercised, however, when inspecting experimental results to ensure that "tailing" is not misinterpreted as electrochemical phenomena and vice versa. There are electrochemical reactions involving the oxides of noble metal catalysts and their subsequent chemical reduction which can manifest themselves in a manner resembling the "tailing" characteristics of response curves (*4,5*). In addition, some electrolytic processes may induce similar results by temporarily changing the reaction kinetics at the electrode surfaces (*6*).

A technique for improving the detector time rate of response characteristics by minimizing the "tail" is to increase the impedance ($R_r$) and thus more closely approach a single-node type of operation by minimizing the mass flow to ($V_r$).

There is a practical limit, however, to the maximum value of ($R_r$). It is established by the total cell voltage available, the ohmic voltage drop across it, and the minimum potential energy required at the electrolyte-working electrode surface interface. This is the potential energy required to maintain a sufficiently large electrode reaction rate to ensure diffusion limited operation of the detector at all times (*7*) and to supply the voltage which provides electrochemical reaction specificity. The cell resistance is the most likely parameter to vary during storage and operation of the detector. These variations are induced by changes to either the thickness of the electrolyte layer or its electrical resistivity. The voltage drop across the electrolyte layer represents more than 99% of the total ohmic drop between the reference and working electrodes. Therefore, a periodic measurement of the cell electrical impedance is sometimes made to determine if it has exceeded a maximum value. If it has, the impedance may be reduced with increases in the electrolyte layer thickness by pulling the membrane away from the working electrode surface and its inner cartridge support. Also, in many detectors, it is possible to provide means in the design and construction of the membrane holder to ensure that the electrical impedance will vary only over a very narrow range by mechanically preventing changes in the electrolyte layer thickness. In most cases, the minimum electrolyte layer thickness as established by the cell electrical impedance and the diffusion impedance are at cross purposes —*i.e.*, electrically the thickness should be maximized and by diffusion considerations it should be minimized. It is obvious that the lower thickness limit is established by the electrical considerations.

A measurement of the cell electrical impedance and a knowledge of electrolyte resistivity can yield the layer thickness. Assuming the electrolyte layer in the detector of Figure 1 is a flat right-circular thick-walled annular cylinder in which current and mass flow radially, the electrical and diffusion impedance is given by an equation of the form: $R = \ln(r_o/r_i)/2\pi DL$, where $L$ = electrolyte layer thickness, cm, $r_o$ and $r_i$ = outside and inside radii of the cylinder, respectively, cm, and $D$ = diffusion or electrical conductivity coefficient respectively, cm²/sec or mho/cm. This equation can be utilized to preset and adjust $L$. This particular case and the effects of $L$ have been carefully considered at this point because the "tailing" of detector time rates of response curves is invariably confused as electrochemical or chemical effects, side reactions, contaminations, etc., by many workers in the field.

As ($R_r$) is increased, the detector response curve is detached from the single-node response curve at high response levels, Point *A* Figure 3. The "tailing" is less severe, and in general it more closely resembles the single node response curve. Additional and identical improvement can also be obtained by minimizing ($V_r$). The minimum value of ($V_r$), however, is established by the detector wearout time specifications.

**Detector with Parallel Membrane Node.** It is obvious from an inspection of the lattice of Figure 2 that additional improvements to the detector time response can be obtained by providing a separate parallel diffusion path to ($V_r$). The parallel node (*d*) shown in Figure 2 will not directly affect node (*a*) because the membrane diffusion impedance ($R_{mm}$) between nodes (*a*) and (*d*) can easily be made very large and may then be neglected without compromising the utility and accuracy of the detector analytical model. The membrane impedance ($R_{mp}$) and electrolyte reservoir impedance ($R_{re}$) should be minimized to saturate ($V_r$) with the mass flowing through ($R_{mp}$) and ($R_{re}$) in a minimum time to reduce the flow potential between nodes (*b*) and (*c*) as rapidly as possible. The detector rate of response curve with a parallel membrane node is shown in Figure 3. It resembles the single-node detector more closely than the detector represented by the binodal lattice. The point of detachment of the curve from the single-node response curve is approximately identical to that of the binodal lattice but not as severe. This characteristic is due primarily to the different time constants of nodes (*a*) and (*c*)—*i.e.*, node (*a*) is not seriously affected by the presence of node (*d*) until the detector is at 40% or more of total saturation.

The time rate of response curves of Figure 3 are intended to illustrate the relative changes which occur in the detector performance by variation of the mass transport parameters of the system. The actual magnitude of the response curve changes depend upon the initial parametric values and conditions. The detector time rate of response specifications are important criteria in establishing the requirements of the membrane material and its dimensions. Equation 3 is the basic relationship which is adequate in the early design stages and also after corrections are made to the response curves by a multinodal analytical model. In addition, these specifications have a design impact on the geometrical relationships between the working and reference electrodes, the size and shape of the electrolyte reservoir, the amount of detector exposure to the environment, and the overall design of the membrane and membrane holder.

## DETECTOR WEAROUT CHARACTERISTICS

The detector can cease to function correctly by either a gradual drift outside its performance specifications and/or by sudden and complete ceasing of operation. This behavior may occur for a variety of reasons which can be traced to four basic wearout modes: (1) consumption of the reference electrode, (2) depletion of the solvent medium, (3) contamination of the working electrode surface, and (4) localized concentra-

(4) J. S. Mayell and S. H. Langer, *J. Electrochem. Soc.*, **111**, 438 (1964).
(5) S. W. Feldberg, G. C. Enke, and C. E. Bricker, *ibid.*, **110**, 826 (1963).
(6) W. G. French and T. Kuwana, *J. Phys. Chem.*, **68**, 1279 (1964).
(7) S. Glasstone, K. J. Laidler, H. Eyring, "The Theory of Rate Processes," McGraw-Hill, New York, 1941, p 576.

tion changes in the electrolyte. The dominant mode which governs the detector wearout behavior is determined by a combination of factors related to the detector functional design, environmental conditions, and the particular application. Most other malfunctions are failure modes resulting from defective construction, poor design, poor workmanship, etc. Common failure modes are shorting of the electrodes in the external circuit, loss of the electrolyte solvent through leaks, gross impurities, a defective membrane, and mechanical separation at dissimilar material joints and interfaces. Failure modes are not a part of this discussion.

**Consumption of the Reference Electrode.** It is highly desirable for most detectors that their electrodes serve only to provide catalytic reaction sites and a means of introducing the external circuit to the cell. Detectors whose cell reactions involve the electrode material will eventually wear out because of consumption of its reference electrode unless it is periodically replaced as part of a preventive maintenance procedure. The electrode replacement time and/or the wearout time is related to the amount of material consumption required to reduce the electrode surface area to the condition where polarization of the electrode will cause the detector signal to drift out of specification for lack of the proper reaction potential balance. It is presumed that the electrolyte is freshly replenished on several occasions prior to this. The electrode wearout or replacement time is expressed by the relationship: $t_{wo} = nFN_{re}/i_{AVG}$, $t_{wo}$ = detector wearout time, seconds, $N_{re}$ = number of moles of the reference electrode which must be consumed to obtain wearout, moles, and $i_{AVG}$ = average detector current over the time $t_{wo}$, $A$. Many times the wearout time or the magnitude of $N_{re}$ can be significantly extended by incorporating an electrode with a geometrical configuration whose reacting surface remains relatively unchanged as the electrode material is consumed. An electrode in the form of a flat sheet or an electrode which utilizes the inside surface area of a thin wall, large diameter cylinder approximately fulfills this requirement, since the surface area actually increases as the electrode is consumed. However, if an electrode geometry is employed whereby the reacting surface area decreases as it is consumed, the detector will display a gradual signal drift. The drift is due to polarization caused by a gradual increase of the electrode current density. It is necessary to conduct experiments to establish the minimum allowable value of the ratio of the area of the reference electrode to that of the working electrode when the effects of polarization become significant.

The wearout time for the condition when the inner surface of a cylinder is utilized as the reference electrode is given by Equation 4:

$$t_{wo} = \frac{\rho \pi L_c}{M_e i_{AVG}} \left[ R_i^2 - \left( \frac{A_w y_{min}}{2\pi L_c} \right) \right] \qquad (4)$$

$y_{min}$ = minimum allowable value of the electrode surface area ratio, dimensionless

$\rho$ = density of reference electrode material, gm/cm³

$M_e$ = molecular weight of reference electrode material, g/mole

$R_i$ = inner radius of cylinder, cm

$A_w$ = working electrode surface area, cm²

The detector signal may also drift out of specifications because of shift of the cell dynamic equilibrium by changes to the concentration of the electrolyte. Concentration changes arise from the addition of the reaction products and/or depletion of the reactant. Periodic replacement of the electrolyte can prevent this from occurring by minimizing the concentration changes which are effective in causing a significant potential equilibrium shift. These concentration changes must be large enough to shift the cell equilibrium potential to the point where the rate of reaction at the working electrode surface is affected and either disturbs the diffusion limited mode of operation or promotes significant interfering side reactions or both. The diffusion limited condition can be permanently disrupted by moderate positive and negative shifts in the cell equilibrium potential (*8*) while negative potential shifts will usually promote side reactions (*9*). The wearout modes described above commonly apply to detectors employed to measure the concentration of dissolved gases in liquids.

**Depletion of Electrolyte Solvent Medium.** The most common wearout mode for detectors measuring the concentration of gases in gas mixtures is loss of the electrolyte solvent medium by diffusion through the membrane. The maximum wearout time for this mode may be ascribed to the time required for complete loss of the solvent medium as shown by Equation 5:

$$t_{wo} = V_l(\Delta X)_m(\rho_l/\rho_v) \Big/ A_s(P_m)_s(p_{vp} - p_o) \qquad (5)$$

$V_l$ = total volume of solvent contained in the detector, cm³

$\rho_l$ = liquid density of solvent, g/cm³

$\rho_v$ = vapor density of solvent, g/cm³

$(P_m)_s$ = membrane permeability coefficient to solvent vapor cc/sec-cm²-mm Hg/cm

$A_s$ = total membrane area exposed to environment, cm²

$p_{vp}$ = vapor pressure of the solvent at a given temperature mm Hg

$p_o$ = partial pressure of the solvent in the environment mm Hg

Observing the position of the electrolyte in the detector cartridge, the electrolyte reservoir, and the electrolyte layer, as illustrated in Figure 1, shows that the actual wearout time due to solvent loss can be much less than the time given by Equation 5. For example, if the solvent lost from the electrolyte layer is not replenished at a given minimum rate, the electrical conduction path between the electrodes is reduced and the cell ohmic resistance is increased because the layer thickness decreases. As the cell ohmic resistance and potential drop increase, less potential is available at the reaction sites or the working electrode surface–electrolyte interface. The detector will operate in a normal fashion until the energy is insufficient to sustain the reaction rate at the level required to maintain the diffusion limited condition. The detector can eventually cease to function entirely because of a complete break in the circuit within the cell. As the detector wears out in this mode, the signal decays very rapidly to zero.

The wearout time given by Equation 5 more closely approximates the behavior of a detector possessing means of supplying solvent to the electrolyte layer; several schemes can be employed to accomplish the solvent transfer from the electrolyte reservoir. A porous solid element can be employed within the cell, the electrolyte reservoir, and the periphery of the electrolyte layer to transport solvent by capillary pumping action (*10*). In some cases, the solvent may be accommodated

(8) S. Glasstone, "Introduction to Electrochemistry," 1st ed., Van Nostrand, New York, 1956, pp 440–1.
(9) *Ibid.*, pp 454–5.
(10) A. E. Scheidegger, "The Physics of Flow Through Porous Media," University of Toronto Press, 1960, Chap. 3.

in the form of a gel instead of a liquid. As the solvent is depleted, the gelling agent dries into a porous or skeletal structure which eventually fills the detector cell. This lattice provides the surface and porous medium required to employ capillary pumping. More sophisticated detectors incorporate devices which exert a small pressure head to transport electrolyte to all the vital regions of the detector cell. Identical problems arise in detectors which employ gravity to transport solvent within the cell. For example, reversal of the gravitational orientation of the cell can severely reduce the flow potential or introduce an opposing force to prevent the liquid transfer. The solvent transfer schemes, devices, and design arrangements previously mentioned may confer the detector with a partial immunity to these types of problems when the detector geometrical configuration and interrelationships are constrained within certain limits. Surface active agents may also be utilized in conjunction with the other schemes to aid in the solvent transfer process. However, their use should be considered early in the development to coordinate their chemical compatibility with the electrochemical system.

This wearout mode provides additional criteria to determine the properties and characteristics required and the membrane. It applies especially to detectors operating in a gaseous environment. The membrane should provide a maximum diffusion impedance to the electrolyte solvent vapor—*i.e.*, a minimal membrane exposure or a minimum membrane thickness.

**Contamination of the Working Electrode Surface.** The detector signal can drift out of specification by contamination of the electrode surface with deposits of the solid products of side reactions. Side reactions of this nature occur at low level rates. They are usually totally unanticipated during the early stages of the development. Solid deposits on the working electrode surface which inhibit its catalytic activity undoubtedly are deleterious to the operation of the detector and should be avoided. In an ideal development program, of course, all chemical and electrochemical problems are eliminated or defined and corrective measures developed and implemented at the outset of the design program. Nevertheless, some electrode contaminating reactions may occur at such slow rates that it is possible to operate a detector satisfactorily over a reasonable length of time despite their presence. In some cases, these types of reactions are completely reversible upon shutdown. In addition, a special combination of environmental conditions—*e.g.*, the presence of a chemical reducing or oxidizing agent—can start and sustain undesirable side reactions. For example, the presence of hydrogen will reduce heavy metal ions of the electrolyte (*11*, *12*). The signal drift resulting from a steady deactivation of working electrode catalytic sites such as by metal deposits is usually a slow steady process which eventually completely desensitizes the detector.

**Localized Electrolyte Concentration Changes.** A condition can arise where localized electrolyte concentration changes, generally in the region of the working electrode surface, shift the equilibrium potential of the cell. Concentration changes in the electrolyte layer cause a shift in the cell equilibrium potential and/or inhibit the rate of the fundamental reaction as defined by mass action principles. One of the most common ions associated with this problem is the hydrogen ion. An example of ($H^+$) changes near the working electrode is utilized to define the important cell parameters and their interrelationships in the illustration of this failure mode.

A quantitative estimate of ($H^+$) changes can be obtained by a mass accounting of $H^+$ in the electrolyte layer directly over the working electrode surface. The volume of the electrolyte layer is given by: $V_{ie} = \pi r^2 L$. The $H^+$ production rate at the working electrode surface is presumed to be proportional to the detector signal current $[dH^+/dt]_p = i/n\mathrm{F}$. The rate of $H^+$ loss from the electrolyte layer due to diffusion is $[dH^+/dt] = [2\pi D/L]\,[C_e - C_r]\,\ln(r_o/r_i)$ where $C_r$ = concentration of $H^+$ in the electrolyte reservoir, moles/cm³ and $C_e$ = concentration of $H^+$ in the electrolyte layer, moles/cm³. The solution to this equation is given in Equation 6:

$$C_e = C_r + (\alpha/\beta)[1 - e^{-\beta t}] \qquad (6)$$

$$\alpha = i/V_{ie}n\mathrm{F},\ \beta = 2\pi D\ln(r_o/r_i)/V_{ie}L$$

The maximum $C_e$ is obtained when $t = \infty$ in Equation 6. Thus, $(C_e)_{MAX} = C_r + \alpha/\beta$. Caution must be exercised in evaluating $\beta$ because the largest of either the osmotic diffusion coefficient or the ionic diffusion coefficient ($D^+$) (*13*) is employed. Hence, when localized concentration changes in the electrolyte are suspected as the reasons for certain malfunctions, Equation 6, or a similar expression which accounts for the specific geometrical and environmental conditions, may be utilized to help substantiate or refute these conclusions. The estimated concentration change is engaged to determine the corresponding equilibrium potential change.

## TEMPERATURE RESPONSE CHARACTERISTICS

The detector temperature response characteristics are proportional to the temperature response of the flux of the electroactive species through the membrane. When dimensional changes of the membrane with temperature are negligible, the only parameter of major importance which varies with temperature is the membrane material permeability coefficient (*14*). Its functional temperature dependence is expressed by Equation 7:

$$i = [n\mathrm{F}Ap_a(P_m)_o/(\Delta X)_m]e^{-E/RT} \qquad (7)$$

$(P_m)_o$ = reference permeability coefficient (permeability coefficient where temperature response data are extrapolated to infinite temperature), mole/sec-cm²-mm Hg/cm

$E$ = permeability activation energy (point-to-point migration potential energy barrier of nonequilibrium thermodynamics), cal/mole

$R$ = universal gas constant, 1.98 cal/mole-°K

$T$ = absolute temperature of the membrane, °K

The permeability coefficient temperature variation is the single most important temperature-dependent parameter of the detector. Its characteristics must be resolved early in the development because it is a vital criterion in selecting the membrane material. It is also equally important that the membrane not exhibit any change of phase over the operating temperature range.

Other membrane parameters which could be reviewed are coefficient of thermal expansion, heat distortion temperature, thermal conductivity, and brittleness temperature. The thermal properties of other materials utilized in the construction of the detector should also be weighed for mechanical, structural, chemical, etc., compatibility with the system.

(11) A. H. Webster and J. Halpern, *J. Phys. Chem.*, **61**, 1245 (1957).
(12) J. Halpern, *ibid.*, **63**, 398 (1959).
(13) I. M. Kolthoff and J. J. Lingane, "Polarography," Interscience, New York, 1955, Chap. 2.
(14) B. J. Zwolinski, H. Eyring, and C. E. Reese, *J. Phys. Colloid Chem.*, **53**, 1426 (1949).

The basic detector thermal design can be classified into two categories: signal temperature compensation and active thermal control.

**Temperature Compensation.** Relatively large signal changes are experienced with only small changes in membrane temperature. Detector signal coefficients are temperature dependent. They range from 1 to 6%/ °C, depending on the membrane material utilized, and can double over a 10 °C span. Temperature correction is accomplished by changing the detector signal readout by an amount proportional to the membrane temperature. In applications where the environmental temperature varies only slightly and where some thermal control is exercised—*e.g.*, a blood sample cuvette (*15*)—signal correction is not necessary or is permissible to administer at a later time following readout. However, in applications where rapid temperature changes occur and membrane thermal stabilization cannot be ensured, temperature compensation of the signal prior to readout is mandatory.

Because the detector signal is an electrical current whose magnitude is directly proportional to the gas concentration, temperature compensation will consist of adjustment of the signal by a factor corresponding to the membrane temperature (*16*, *17*). Signal temperature compensation involves two major design problems aside from those associated with the shaping characteristics of temperature sensitive electronic elements which may be utilized in the compensatory circuits: (a) measurement of membrane or detector signal temperature coefficient characteristics over a specified environmental temperature range and (b) location of the temperature transducer at a suitable site within the detector cartridge. There are other considerations which must also be included in the evaluation of the optimum design approach. However, most can be reviewed independently with only minor changes necessary as the design develops.

In the selection of the membrane material to be utilized by the detector, it is important that information regarding the permeability temperature characteristics of the material be available. Material phase changes and permeability hysteresis within the operating temperature range should be avoided unless, of course, other material properties endow the detector with desirable characteristics which offset the problems introduced by this behavior. If the membrane permeability temperature characteristics are known with a reasonable degree of certainty, then the simplest means to establish the detector signal coefficient is to measure it directly. The detector signal is measured at several stable temperature points and plotted in the form of $\log(i)$ *vs.* $1/T$. It is a linear relationship with a negative slope of magnitude $E/R$. Material phase changes are indicated by a sudden change in slope (*18*). The signal temperature coefficient in terms of per cent signal change per degree centigrade is a function of temperature and increases with temperature. This characteristic, of course, complicates the design of the temperature compensating system. Simplicity in design is gained at the expense of accuracy because, in the simplest case, the signal correction is made in proportion to the average value of the coefficient over the operating temperature range. The smaller the temperature range the more accurate will be the signal correction. All permeability temperature data, regardless to what form it is reduced or how it is utilized, should be derived, interpolated, and extrapolated from the semilogarithmic plot described above.

In some cases, deficiencies in the mechanical design, arrangement, assembly, dimensional tolerances, promote strange temperature behavior in the detector. Expansion and contraction of the electrolyte and gas bubbles trapped within the electrolyte can alter the signal characteristics at various temperature levels. Invariably workers in the field tend to attribute the anomalies which arise to changes in the diffusion properties of the membrane. This is very unlikely unless a material phase change occurs. Off-sets or jogs in the curve, without changes to its slope, are common when the membrane holder assembly fails to maintain a reasonably constant membrane tension and electrolyte layer thickness within limits over the environmental temperature range.

The location of the temperature transducer within the detector cartridge should ideally be at the center of the membrane directly over the working electrode surface because it is precisely the membrane temperature at this point which is proportional to the signal. At the present time it is physically impossible to locate a transducer at this site without seriously affecting the operation of the detector by obstructing the mass flow or changing the effective thickness of the membrane. The criterion of a suitable site is that where the site thermal time constant matches that of the ideal site as closely as possible. A poor match will make calibration of the detector very difficult and the first signal readings for rapid temperature changes will be inaccurate. Invariably the thermal time constant of the transducer will be larger than that of the membrane and thus the signal readings will not be totally correct until the transducer and membrane are thermally stabilized. The stabilization time is given by the equation: $t_s = [(t_c)_T - (t_c)_m]$, $t_s$, $(t_c)_T$, and $(t_c)_m$ are the detector stabilization time, temperature transducer thermal time constant, and the membrane time constant.

Five sites within the detector cartridge illustrated by Figure 1 are analyzed to determine their thermal characteristics. The locations are shown in Figure 4. Table II summarizes the results of the thermal analysis which was performed for a detector with a working electrode diameter of 2 mm and with the geometry of Figure 1. The detector is assumed to be immersed in quiescent air at atmospheric pressure, 760 torr. The largest part of the thermal impedance of sites 3, 4, 5 and the membrane is comprised of the detector cartridge cover impedance and the air boundary layer impedance on the membrane external surface. It is proportional to the reciprocal of the convection heat transfer coefficient at the surface and is related to properties and flow moduli (*19*) of air. The impedance of sites 1 and 2 are comprised of the boundary layer impedance and the network of conductive impedance elements within the detector. A representative time constant of a membrane element 0.003 cm thick is 3.2 seconds. The time constants of sites 3 and 4 are 27 and 14 seconds, respectively. Seemingly insignificant changes in the cartridge cover geometry alter the time constants of sites 1, 2, and 3. For example, the time constant of site 3 can be increased from 14 to 1200 seconds by closing the opening through the cover over the electrolyte reservoir. This condition arises when the detector wearout time is extended by reduction of the solvent medium vapor loss rate. Although site 1 is impractical, it is reduced from 104 to 3.2 seconds by enlargement of the cartridge cover opening

(15) J. W. Severinghaus, *J. Appl. Physiol.*, **13**, 515 (1968).
(16) E. J. Angelo, Jr., "Electronic Circuits," McGraw-Hill, New York, 1958, p 194–6.
(17) E. Koeonjian and J. S. Schaffner, *Comm. and Electronics*, **14**, 396 (1954).
(18) R. M. Barrer, "Diffusion In and Through Solids," Cambridge University Press, London, 1951, Chap. 8.
(19) W. H. McAdams, "Heat Transmission," McGraw-Hill, 3rd ed., New York, 1954, Chap. 7.

Table II. Thermal Characteristics of Transducer Location Sites in a Temperature Compensated Detector

| Site No. | Description | Capacitance (cal/°K) | Impedance [a] (sec–°K/cal) | Time constant (seconds) |
|---|---|---|---|---|
| 1 | Detector membrane adjacent to region directly over working electrode surface | $3 \times 10^{-4}$ | $3.45 \times 10^{5}$ | 104 |
| 2 | Inner cartridge adjacent to working electrode and electrolyte layer | $1.6 \times 10^{-3}$ | $5.65 \times 10^{5}$ | 905 |
| 3 | Open end of electrolyte reservoir adjacent to membrane | $4.2 \times 10^{-4}$ | $0.65 \times 10^{5}$ | 27 |
| 4 | Directly behind working electrode surface | $2.2 \times 10^{-4}$ | $0.65 \times 10^{5}$ | 14 |
| 5 | Detector cartridge cover in region adjacent to opening directly above the membrane over working electrode surface | $1 \times 10^{-2}$ | $0.75 \times 10^{5}$ | 750 |
| Membrane | Membrane over working electrode surface | $0.5 \times 10^{-4}$ | $0.65 \times 10^{5}$ | 3.2 |

[a] The detector environment at the membrane face is quiescent air. Thermal impedance and time constant of sites 3, 4, and 5 and the membrane are reduced by a factor of thirty when environment is quiescent water or whole blood. Stirred or flowing fluids will provide an additional reduction by a factor which depends upon fluid flow and properties moduli.

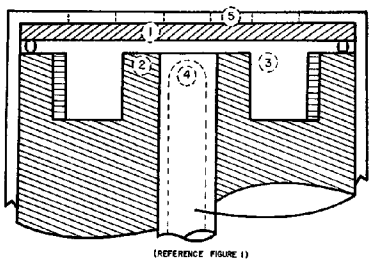


**Figure 4. Tranducer location sites in a temperature-compensated detector**

over the electrode surface. The lateral membrane conductive impedance is virtually eliminated leaving only the boundary layer impedance. This change in geometry will also reduce the time constant of site 2 from 905 to 45 seconds for the same reasons. Of course, enlargement of the opening will concurrently decrease the detector wearout time.

The convection heat transfer coefficient at the membrane external surface increases approximately by a factor of 30 when operating in a liquid such as water or whole blood. It is due primarily to the increase in fluid density and thermal conductivity. Thus, the impedance and thermal time constants of sites 3, 4, and 5 and the membrane are reduced by 30. When the fluids are stirred and/or flow past the membrane, a further reduction will occur, the magnitude of which depends on the fluid properties and flow moduli (*20*).

**Thermally Controlled Detector** Detector temperature compensation does not always extend the operating temperature range because the liquid supporting electrolyte will freeze at low temperatures, the detector signal and time rate of response are significantly reduced by the decrease in the permeability and diffusion coefficients at low temperatures, and/or the membrane material will experience a phase change over the temperature range. Thus in many applications, the detector operating environmental temperature range can only be extended by active thermal control. In this manner, lowering of the liquid electrolyte freezing point with additives beyond the lower environmental temperature limit will not always render the detector completely operational. Extension of the lower temperature limit is achieved by providing the detector with heat energy. Heated detectors are maintained at a preset level above a specified environmental temperature. When the environmental temperature is higher than the preset temperature, the detector will be at an equilibrium temperature established by the heat exchange between it and its environment.

A heated detector imposes three basic design constraints. They are related to the means employed to activate the heating elements, the temperature gradients within the detector, and the design requirements to conserve energy.

An estimate of the power requirements to maintain the detector cartridge at a given average temperature is given by: $Q = U(\Delta T)$, $U$ = overall heat transfer coefficient, cal/sec-°C and $(\Delta T)$ = temperature difference, °C, between the detector cartridge and the environment.

The overall heat transfer coefficient incorporates every mode of heat loss from the detector. It may be that the temperature difference will vary with the particular mode of heat transfer or the environment may possess temperature gradients which disallow this simplification. In this case, the heat transfer terms must be separated such as $Q = \Sigma U(T - T_s)$. Radiation heat transfer can probably be neglected in most cases, as it is doubtful that maximum temperature will ever exceed 180 °C.

A heated detector may also be employed to heat the gas upstream of the membrane. In this manner, the temperature gradient across the membrane is reduced and the temperature compensation becomes more accurate.

It is advisable to place the heating element within the detector cartridge at a point where sufficient thermal insulation is available and the heat loss path thermal conductance is controlled to a reasonable degree. The critical regions whose temperatures must be maintained above a given point are the electrolyte layer and reservoir and the membrane directly above the surface of the working electrode. It is probable that at extremely low temperatures, variations will be experienced in the signal caused solely by temperature changes of the membrane unless the heating element and control temperature transducer are imbedded in the membrane. Temperature compensation will provide sufficient accuracy over only a limited range. The most direct manner to overcome this defficiency in accuracy is to heat the external surface of the membrane and the gas/liquid mass adjacent to the membrane. An estimate of the amount of heat required is made by the heat transfer rate at the heat exchange surface.

(20) W. H. McAdams, "Heat Transmission," McGraw-Hill, 3rd ed., New York, 1954, Chap. 10.

## PRESSURE RESPONSE

The pressure response characteristics of the detector signal are given by Equation 8:

$$i = [nFA(P_m)_o/(\Delta x)_m]P_a^n e^{-E/RT} \quad (8)$$

$n$ = exponent determined experimentally

It is important to understand that the exponential pressure relationship where $n = 1$ is a result of Henry's law for the membrane material. Variations from the linear relationship are experienced at higher pressures where deviations from Henry's law occur.

Other serious high pressure effects may occur in mechanical effects on the membrane system. Increases in the total pressure of the gas to 3 atmospheres will alter the relationship of Equation 8. Mechanical forces on the detector, especially on the membrane, account for these changes. For example, an increase in total pressure may affect the electrolyte thickness to increase the signal, such as when the layer is decreased. The decrease is a result of a reduction of electrolyte layer thickness to increase its ohmic resistance and thus deprive the electrolyte–electrode interface of sufficient potential energy to operate in the diffusion limited condition. The compressibility of water is $2.32 \times 10^{-7}$ atm$^{-1}$. A two-fold change in electrolyte layer thickness is thus unlikely. However, when air pockets are present in the electrolyte reservoir such a change in electrolyte layer thickness is possible. For example, let the initial electrolyte layer thickness be $10^{-3}$ cm spread out over a 0.3 cm$^2$ area. Assuming the electrolyte layer thickness is reduced by one half, a two-fold change in pressure is required for an air pocket with a 0.06-cm diameter. Air pockets of larger diameters are usually present in the electrolyte reservoir and consequently larger changes in the electrolyte layer thickness are possible than have been outlined above. Thus, the design of the cartridge and the membrane holder should account for this possibility as a design constraint. Negative changes in pressure will experience the same effect in the reverse direction—*i.e.*, the signal will start to decrease and continue to do so because of the increase in the electrolyte layer thickness. The signal will be given by Equation 2 when the appropriate changes are made to the term which includes the electrolyte layer thickness.

Some of these effects, however, may only be temporary. For instance, as the environmental pressure is decreased, the gas pocket immediately increases in volume. It also begins to transport gas out of the detector—*i.e.*, as the gas in solution migrates through the membrane, more gas in the air pocket goes into solution until the internal and external pressure of the detector cartridge are equalized. Unequal gas pressures will exist because the membrane is elastic and a higher total gas pressure can exist internally. In this case the membrane is stretched as gas is transported by diffusion. The tension on the membrane is relieved when the pressure is equalized on both sides of the membrane. The time for equilibrium to be established will vary and depend upon the position of the air pockets. Only when there are no air pockets present and the gas is all dissolved in the electrolyte will the equilibrum time be predictable.

The method and technique of mounting and holding the membrane in place is an important aspect of the design and may greatly affect the detector pressure response characteristics. Effort should be devoted to ensuring the stability of the membrane in its position. Stretching of the membrane and the application of large amounts of tension should be avoided in order to prevent changes in its permeability properties.

## HUMIDITY

When normal design precautions are taken to avoid problems with humidity—*e.g.*, hermetic seals, sealed connectors—the signal may still be affected. If the temperature conditions are such that the front end of the detector is cooler than the atmosphere, condensation of water will occur on the cool surface. The water will not affect the detector unless condensate collects over the membrane. A film of liquid water over the membrane will add a diffusion barrier in series with the membrane and electrolyte layer. The signal or diffusion rate will be reduced and the time constant increased. A design which includes a protective covering over the membrane such as a Teflon pulp and glass-frit disks may be saturated with liquid water. The pores and voids will be filled with liquid water and will evaporate at a relatively slow rate. A film of liquid water 0.002 cm thick will reduce the detector signal level by approximately 33% when employing Teflon in an oxygen polarographic gas detector. The signal will vary as the thickness of the liquid water film changes. The detector time constant will increase approximately 18%.

The advantages of a heated detector are underscored when considering this humidity problem. At environmental temperatures below the heated temperatures of the detector, humidity is not a problem because condensate will not collect.

A problem may arise when a part of the forward end of the detector is thermally insulated by virtue of coincidence and not design such that condensate collects. It is advisable to include drainholes to avoid this condition. The particular application for the detector should also be considered to suggest a preferred orientation relative to gravity, wind, and air currents, and other conditions which may be helpful in reducing the problems introduced by a high humidity environment.

## SHOCK AND VIBRATION

The detector should be designed to withstand shock and vibration which it may experience in operation, storage, and transport. Outside the mechanical integrity of the design and its components there are certain failure modes which stand out above others. The primary failure modes are associated with the electrode system and the membrane. The shock failure mode is generally associated with the rupture of the membrane and the rupture of bonded surfaces.

Many electrode systems in polarographic detectors contain a small central working electrode and a much larger peripheral reference electrode. This configuration is somewhat standard because of the need to provide a large electrode area. The electrode area ratio should be as large as described in the previous sections. The central electrode is usually supported and surrounded by some inert material such as an insulating epoxy, delrin, or polypropylene. The electrode material may be metal such as gold, which exhibits very poor adhesive properties. Thus, slight movement of the electrode into or out of its support will have adverse effects by temporarily or permanently altering the relationships between the membrane, the electrolyte layer, and the electrolyte reservoir.

RECEIVED for review November 22, 1968. Accepted January 9, 1969.

# Electrochemical Reduction of Benzil in Alkaline Methanol-Water Solution

H. E. Stapelfeldt[1] and S. P. Perone

*Department of Chemistry, Purdue University, Lafayette, Ind. 47907*

**Conventional DME polarography, stationary electrode polarography, cyclic voltammetry, and step functional controlled-potential electrolysis techniques were employed to study the electrochemical reduction of benzil in alkaline solution. Results obtained indicate that at pH ≥ 11 the overall reduction process is a reversible, two-electron transfer involving a single proton. The reduction product, a stilbenediolate species, undergoes a subsequent first-order chemical rearrangement to give the benzoin anion. The kinetics of the rearrangement reaction were found to be pH independent at pH ≥ 11, and the rate constant obtained by cyclic voltammetry and potential step electrolysis was approximately 2 sec$^{-1}$ in this region. The observed rate constant decreases with pH decreasing below 11, consistent with kinetic studies carried out previously at pH ≤ 8, and indicative of a change in the primary product to a stilbenediol species.**

SEVERAL STUDIES have been made on the electrochemical reduction of benzil in aqueous–alcohol solvent. Although the reduction has been well characterized in the acid and neutral pH range (*1–4*), there is some question as to the exact nature of the reduction at pH's greater than 8 or 9.

Pasternak (*1*) suggests that the conventional dropping mercury electrode (DME) polarographic reduction of benzil produces stilbenediol (I) which rearranges rapidly in alkaline solution to give benzoin (II).



(I) (II)

At pH greater than 10 the reduction of benzil appears polarographically reversible, and reduction waves are observed for both benzil and benzoin. Several authors (*2, 4, 5*) report the observation of electrooxidizable species following the reduction of benzil at the mercury electrode in alkaline solution. This species has been reported as being the benzil ketyl radical (III) (*5*) or radical anion, the dianion of benzoin (IV) (*2*), or a stilbenediolate species (V) (*4*).

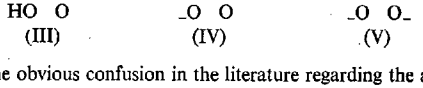

(III) (IV) (V)

The obvious confusion in the literature regarding the alkaline electrochemical reduction process prompted the work reported here. The objective of these studies was the extension of reduction studies carried out previously at low pH (*3*), in order to provide sufficient electrochemical data that electroanalytical techniques might be employed to monitor photochemical processes following the flash photolysis of benzil (*6*). This work employed DME polarography, stationary electrode polarography, and step functional controlled-potential electrolysis to provide both qualitative and quantitative characterization of the benzil reduction process in alkaline solution.

[1] Present address, Armed Forces Radiology Research Institute, Bethesda, Md.

## EXPERIMENTAL

**Instrumentation.** DME polarographic data were obtained using the Metrohm E-261 Polarecord (Metrohm AG, Herisau, Switzerland) and the Sargent Model XV Polarograph. Cyclic voltammetric and step functional controlled-potential electrolyses were employed using an operational amplifier potentiostat described previously (*7*). A Hewlett-Packard Model 202-A function generator, modified for single-cycle operation, provided the triangular and square-wave voltages for the potentiostat. Readout was obtained on either the Esterline-Angus Speed-Servo, 1 mV, 1/8-second recorder or the Model 536 Tektronix Oscilloscope, equipped with D, T, and G plug-in units and Polaroid camera. Spectrophotometric measurements were made with the Cary Model 14 recording spectrophotometer.

**Electrolysis Cells and Electrodes.** The electrolysis cell was jacketed and used in conjunction with a Sargent S-84880 constant temperature circulator to maintain the temperature at 25 ± 0.5 °C. The electrode assembly and electrodes used have been described previously (*3*).

**Reagents.** The preparation of sample solutions in 50% (by volume) methanol solvent and the deaeration procedure used have been described previously (*3*). Acetate, phosphate, glycine, carbonate, and NaOH buffer solutions were used and all pH values given (except 12 and 13) are measured values. Ionic strength was maintained at 0.1, adding KCl to solutions when required. The benzil and chemicals used in the preparation of buffer solutions were all reagent grade and were used without further purification.

## RESULTS AND DISCUSSION

**DME Polarography.** Conventional DME polarographic experiments were performed with benzil in 50% methanol–water solvent, varying the calculated pH from 8.5 to 13. The results obtained show that the benzil reduction approaches reversibility as the pH is increased beyond 8.5, in agreement with previous observations. Table I gives $E_{1/2}$ and polarographic log-plot slopes as a function of solution pH. The exact pH dependence of $E_{1/2}$ in the reversible region of pH 11 to 13 was examined in greater detail, and the data are shown in Table I, Part *B*. A plot of $E_{1/2}$ *vs.* pH in this region is linear with a least-squares slope of $-20.2 \pm 8.9$ mV/pH, at the 95% confidence level.

The results obtained in the reversible region above pH 11 suggest that, at least in very alkaline solution, the number of electrons, *n*, required for the reduction of benzil, equals 2, and that one proton is taken up in the electrode process.

(1) R. Pasternak, *Helv. Chim. Acta*, **31**, 753 (1948).
(2) A. Vincenz-Chodkawska and Z. R. Grabowski, *Electrochim. Acta*, **9**, 789 (1964).
(3) H. E. Stapelfeldt and S. P. Perone, ANAL. CHEM., **40**, 815 (1968).
(4) R. H. Philp, Jr., R. L. Flurry, and R. A. Day, Jr., *J. Electrochem. Soc.*, **111**, 328 (1964).
(5) H. Berg, *Naturwissenschaften*, **48**, 100 (1961).
(6) H. E. Stapelfeldt and S. P. Perone, ANAL. CHEM., **41**, 628 (1969).
(7) S. P. Perone and J. R. Birk, *ibid.*, **38**, 1589 (1966).

**Table I. DME Polarographic Results as a Function of pH**

A. pH dependence of $E_{1/2}$ and log-plot slope

| pH | $E_{1/2}$ (*vs.* SCE), V | Log-plot slope,[a] mV |
|---|---|---|
| 8.5 | − 0.688 | 75 |
| 9.9 | − 0.734 | 42 |
| 11 | − 0.780 | 38 |
| 12 | − 0.800 | 34 |
| 13 | − 0.815 | 32 |

[a] The log-plot is based on the reversible polarographic current–voltage relationship (*8*): $E = E_{1/2} - (0.059/n) \log [i/(i_d - i)]$

B. pH dependence of $E_{1/2}$ from pH 11 to 13

| pH | $E_{1/2}$ (V *vs.* SCE) |
|---|---|
| 11.0 | − 0.780 |
| 11.6 | − 0.788 |
| 11.8 | − 0.788 |
| 12.0 | − 0.800 |
| 12.2 | − 0.802 |
| 12.4 | − 0.808 |
| 12.6 | − 0.813 |
| 12.8 | − 0.819 |
| 13.0 | − 0.815 |

The suggestion that one proton per molecule is involved in the reduction is based on the fact that the pH dependence in the reversible region is linear, and is more nearly consistent with a one-proton involvement (−30 mV/pH) than two (−60 mV/pH). The diminished observed dependence is probably due to the fact that the true pH increases somewhat less than calculated in this region (*9*). Unfortunately no fundamental data could be found to allow the accurate calculation or measurement of the true pH of the methanol–water solutions used.

At base concentrations greater than 0.1*M* NaOH the experimentally measured value of the polarographic diffusion current, $i_d$, in the limiting region is lower than expected on the basis of the analytical concentration of benzil in solution. A corresponding decrease in the spectrophotometric absorption maximum at 262 mμ is observed under the same conditions. This may be explained by the formation of an addition compound in alkaline solution (*10*):

$$\phi C(=O)-C(=O)\phi + OH^- \rightarrow \phi C(OH)(-O^-)-C(=O)\phi \quad (1)$$

This is the first step in the well known benzilic acid rearrangement. Under the experimental conditions used here, the subsequent rearrangement of the α-hydroxyketone to give benzilic acid is quite slow (*11–13*). In order to avoid these complications, however, the pH was maintained at or below 13 for the work reported here.

**Stationary Electrode Polarography and Cyclic Voltammetry.** Cyclic voltammetry provides a means of observing both an electrochemical reduction and the product of that reduction,

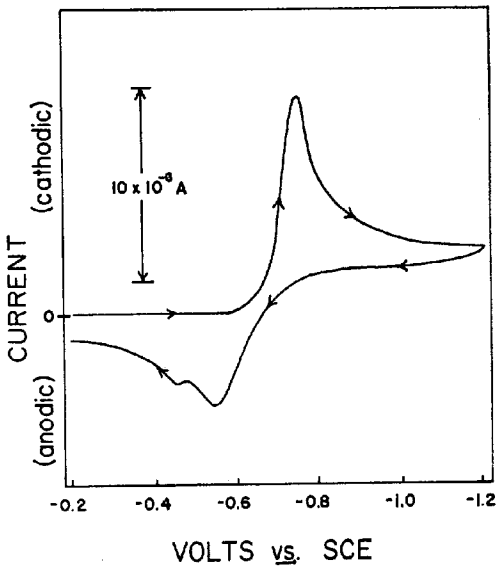


**Figure 1. Cyclic triangular-wave voltammetry in slightly alkaline solution**

**Reduction of 9.6 × 10⁻⁴*M* benzil, pH 8.5, 50% methanol, scan rate = 150 mV per second**

provided the latter is electroactive. This technique is especially useful for mechanistic studies in which a chemical reaction is coupled to the charge-transfer process (*14*). It is possible to deduce qualitatively the nature of the coupled chemical reaction and then obtain quantitative data on the kinetics of the reaction.

Figures 1 and 2 show typical cyclic voltammetric curves for benzil at pH < 11 and pH > 11. Both the anodic and cathodic voltammetric peaks were found to shift to more cathodic potentials as the pH was increased. The peak separation $\Delta E_p$ becomes smaller at higher pH, indicating that the reduction process approaches reversibility. These observations are consistent with the DME polarographic results. The anodic portion, including two distinct oxidation peaks at pH < 11 (*3*), gradually changes to a single oxidation peak reversible to the benzil reduction at pH ≧ 11.

Nicholson and Shain's theoretical treatment of stationary electrode polarography (*14*) considers several kinetic cases coupled to the electron-transfer step. For each case, the theoretical current function depends on a kinetic parameter containing the ratio of the rate constant to the voltage scan rate. This makes possible the definition of some general diagnostic criteria for the characterization of unknown systems. The most useful correlations are the variations—with changes in voltage scan rate—of the cathodic peak current $i_{pc}$, the cathodic peak potential $E_{pc}$, and the ratio of the anodic to cathodic peak currents $i_{pa}/i_{pc}$. Applying these criteria to the reduction of benzil in 0.1*M* NaOH, 50% methanol, one finds the voltammetric behavior shown in Figure 3, which is typical of a reversible electron-transfer followed by an irreversible chemical reaction,

$$O + ne^- \rightleftarrows R \xrightarrow{k} Z \quad (2)$$

(8) L. Meites, "Polarographic Technique," Interscience, New York, N.Y., 1955, Chapters 4 and 5.
(9) L. Meites, Ed., "Handbook of Analytical Chemistry," McGraw-Hill, New York, N.Y., 1963, p 11-8.
(10) S. Selman and J. F. Eastham, *Quart. Rev.* (London), **14**, 221 (1960).
(11) F. H. Westheimer, *J. Amer. Chem. Soc.*, **58**, 2209 (1936).
(12) J. Hine and H. W. Haworth, *ibid.*, **80**, 2274 (1958).
(13) W. H. Puterbaugh and W. S. Gaugh, *J. Org. Chem.*, **26**, 3513 (1961).
(14) R. S. Nicholson and I. Shain, ANAL. CHEM., **36**, 706 (1964).

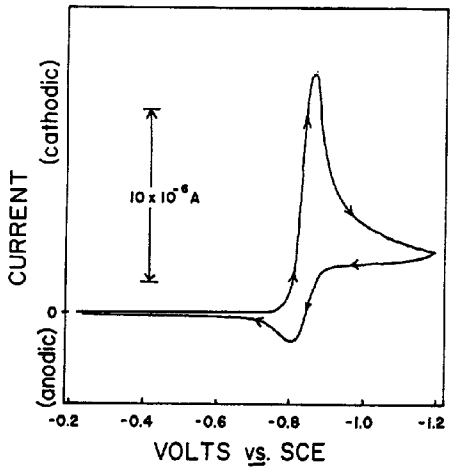


**Figure 2. Cyclic triangular-wave voltammetry in very alkaline solution**

**Reduction of $9.6 \times 10^{-4}M$ benzil, pH 13, 50% methanol, scan rate = 150 mV per second**

The shape of the cathodic portion of the experimental stationary electrode polarogram was compared to the theoretical shape of a simple reversible reduction predicted by Nicholson and Shain (*14*). This comparison, shown in Figure 4, demonstrates the best fit for $n$ equal to 2. Thus, a reversible, two-electron reduction, consistent with the DME polarographic observations, is indicated.

The ratio of the anodic to cathodic peak currents was found to be independent of the benzil concentration (using a constant scan rate) as shown in Table II. These results indicate that the succeeding chemical reaction is simple first-order. As might be expected from Equation 2, the anodic portion of the cyclic polarogram is very sensitive to the kinetics of the succeeding chemical reaction. Kinetic data may be obtained by correlating the ratio of peak currents, $i_{pa}/i_{pc}$, to the scan rate, under the appropriate conditions (*14*).

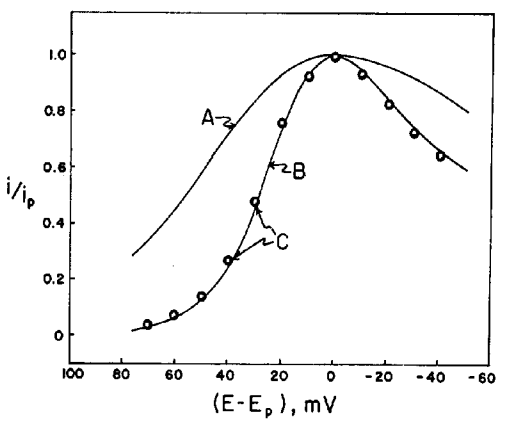


**Figure 4. Shape of the stationary electrode polarogram in very alkaline solution**

*A.* **Theoretical (*14*). Reversible case, $n = 1$**
*B.* **(Solid line) Theoretical (*14*). Reversible case, $n = 2$**
*C.* **(Points) Experimental. $1 \times 10^{-3}M$ benzil, 50% methanol, pH 13, scan rate = 50 mV per second**

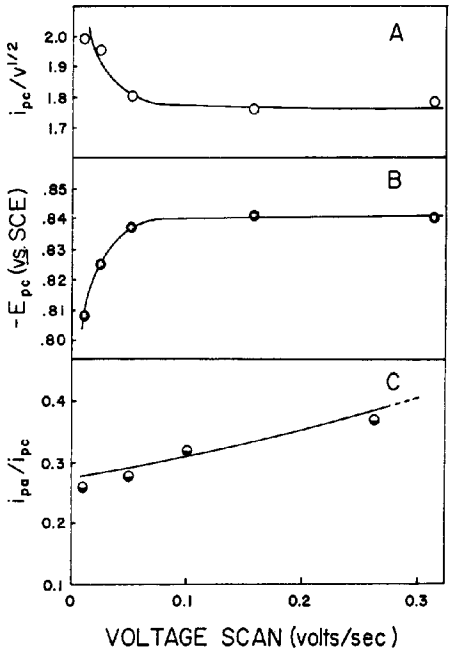


**Figure 3. Dependence of voltammetric data on scan rate**

*A.* **Variation of cathodic peak current, $i_{p_c}$, with changing scan rate**
*B.* **Variation of cathodic peak potential, $E_{p_c}$, with changing scan rate**
*C.* **Variation in the peak current ratio, $i_{p_a}/i_{p_c}$, with changing scan rate**

Experimental cyclic voltammetric data and calculated kinetic values for the benzil system at pH 12 and 13 are given in Table III. Cyclic polarograms obtained at pH 11 show a rather broad anodic peak, probably due to some contribution from the geometric *cis* and *trans* isomers of the stilbenediol reduction product as observed at lower pH (*3*). As a result, the peak ratio $i_{pa}/i_{pc}$ measured at pH 11 appears low and the experimental rate constant obtained with cyclic voltammetry is subject to question. At pH below 11 the electrode reaction can no longer be considered reversible, and consequently the theoretical treatment of Nicholson and Shain (*14*) is no longer applicable.

**Step Functional Controlled-Potential Electrolysis.** Kinetic data can also be obtained using the technique of step functional controlled-potential electrolysis (*15*). This technique does not

(15) W. M. Schwarz and I. Shain, *J. Phys. Chem.*, **69**, 30 (1965).

**Table II. The Ratio of Anodic to Cathodic Peak Currents, as a Function of Benzil Concentration in 0.1$M$ NaOH, 50% Methanol–Water Solvent, Scan Rate = 150 mV/sec**

| Benzil concentration $\times 10^4 M$ | $i_{pa}/i_{pc}$ [a] |
|---|---|
| 0.384 | 0.277 |
| 0.96 | 0.266 |
| 2.88 | 0.263 |
| 4.80 | 0.275 |
| 9.60 | 0.297 |

[a] Average of 4 or more determinations.

**Table III. Cyclic Voltammetric Data and Kinetic Results for Benzil in 50% Methanol–Water Solvent**

| pH | $\tau$ (sec)[a] | $i_{pa}/i_{pc}$[b] | k ($sec^{-1}$)[c] |
|---|---|---|---|
| 12 | 0.30 | 0.54 | 2.9 ± 0.1 |
| 12 | 0.63 | 0.45 | 2.0 ± 0.1 |
| 13 | 0.22 | 0.66 | 2.2 ± 0.1 |
| 13 | 0.33 | 0.61 | 1.8 ± 0.1 |
| 13 | 0.50 | 0.52 | 1.7 ± 0.1 |
| 13 | 0.85 | 0.43 | 1.7 ± 0.1 |
| 13 | 1.13 | 0.32 | 2.6 ± 0.1 |

[a] Time between $E_{1/2}$ and the switching potential $E_\lambda$. Scan rates used were between 15 and 250 mV/sec.
[b] Average of four or more determinations.
[c] Calculated from theoretical tabulations of Nicholson and Shain (*14*).

**Table IV. Kinetic Results Using Step Functional Controlled-potential Electrolysis for Benzil in 50% Methanol Solvent**

| pH | $\tau$ ($E_{step}$), sec | $k$ ($sec^{-1}$) |
|---|---|---|
| 8.5[a] | 2.5 | 0.12 ± 0.01 |
| 8.5[a] | 5.0 | 0.12 ± 0.01 |
| 9.9[a] | 0.25 | 1.6 ± 0.2 |
| 9.9[a] | 1.0 | 0.73 ± 0.17 |
| 9.9 | 0.50 | 0.46 ± 0.16 |
| 11 | 0.10 | 1.6 ± 0.2 |
| 11 | 0.50 | 1.9 ± 0.2 |
| 12 | 0.10 | 2.1 ± 0.2 |
| 12 | 0.50 | 2.3 ± 0.2 |
| 13 | 0.10 | 2.2 ± 0.2 |
| 13 | 0.50 | 1.8 ± 0.2 |

[a] These results reflect only the more unstable *trans* isomer of stilbenediol.

suffer from the limiting requirement of strict electrode reversibility as does cyclic voltammetry, and therefore it may be used to check or extend the kinetic results obtained by cyclic voltammetry. The potential step method requires only that there be some potential where species $R$ (Equation 2) can be converted to $O$ unimpeded by electron transfer kinetics.

In this technique, the working electrode potential is stepped from some initial value to a value where the generation of $R$ is determined only by diffusion of species $O$ to the electrode surface. At some time, $\tau$, the potential is then returned to its original value, which is sufficiently anodic that species $R$ is reoxidized to $O$ under the influence only of diffusion and chemical kinetics. From the ratio of the anodic current at some time $t$, ($\tau < t < 2\tau$), to the cathodic current at time $t - \tau$, it is possible to obtain kinetic data from theoretical working curves (*15*). Results obtained by this method as a function of solution pH are shown in Table IV.

Only the kinetic data obtained at pH 9.9 varied significantly with time within a given experiment and between experiments, indicating that at that pH there is some deviation from the simple first-order kinetics observed at pH $\leq$ 8.5 (*3*) and pH $\geq$ 11. One possible explanation for these results is a complicating acid–base equilibrium between the benzil reduction product favored at pH $\leq$ 8.5 (*3*) and the reduction product favored at pH > 10.

The experimental rate constant for pH 9.9, $\tau$ equal to 0.50 second, reflects an initial electrode potential which is sufficiently anodic to oxidize both isomeric stilbenediol species formed by the benzil reduction. Kinetic observations at pH $\leq$ 8 (*3*) indicate that the two isomers rearrange at different rates, the more easily oxidizable *trans* species reacting about three times as fast as the *cis* species. Therefore, one would expect the observed value of $k_2$ reflecting the oxidation of both isomers (Table IV, pH 9.9, $\tau$ = 0.50 second) to be lower as indicated.

The kinetic data obtained by the two different experimental techniques are in reasonably good agreement at those pH's where both were applied. In addition, except for pH 9.9, kinetic results are consistent upon varying the time scale of the experiment. Thus, the evidence is quite strong for a first-order succeeding chemical reaction, with a rate constant of about 2 $sec^{-1}$ at pH $\geq$ 11. The rate constant apparently falls off very sharply with pH decreasing below 11. This is consistent with previous work in acid solution (*3*), and suggests that the reduction product at pH > 10 is a stilbenediolate, while at lower pH the stilbenediol is favored. The observed rate constant for the rearrangement of the benzil reduction product is pH independent at pH below 6 and above 10. Thus, combining stationary electrode and DME polarographic observations, the overall alkaline reduction process can best be described by the general equation:

$$\begin{matrix} \phi C{-}C\phi \\ \| \quad \| \\ O \quad O \end{matrix} + 2e^- + H^+ \rightleftarrows R \xrightarrow{k} Z \qquad (3)$$

On the basis of the above observations it seems unlikely that the product of the electrode reaction, $R$, is a benzil ketyl radical species because $n$, the number of electrons required, should then equal unity. Moreover, other investigators (*16,17*) have shown that the ketyl radical undergoes a second-order chemical reaction. Also, in highly alkaline solution the benzil ketyl radical species should be termed a radical anion, since $pK_A$ for the radical has been reported (*16*) to be approximately 5.9. Therefore, in contrast to the observed results in Table I, one would expect no pH dependence for the benzil reduction if $R$ were the ketyl radical anion.

The ketyl radical anion can be formed by chemical reaction of benzil and benzoin in alkaline solution (*18*), and in 0.1$M$ base the equilibrium Benzil + Benzoin $\rightleftarrows$ 2(Ketyl Radical).

$$K_{eq} = \frac{[\text{Radical}]^2}{[\text{Benzil}][\text{Benzoin}]} \approx 3 \times 10^{-3} \qquad (4)$$

has been reported (*5, 19*). Berg (*20*) indicates that the ketyl radical is reversibly oxidized at the mercury electrode at the potential at which benzil is reduced. One might therefore expect to observe the equilibrium concentration of radical in the cyclic voltammetric experiments when benzil is reduced forming benzoin. However, under the experimental conditions used here, the maximum possible concentration is but a few per cent of the initial benzil concentration.

A possibility not previously considered is that species $R$ is either the benzoin anion (VI) or its enolic form (VII), a monoprotonated stilbenediolate.

$$\begin{matrix} \phi CH{-}C\phi \\ | \quad \| \\ {-}O \quad O \end{matrix} \qquad \begin{matrix} \phi C{=}C\phi \\ | \quad | \\ HO \quad O{-} \end{matrix}$$

(VI) (VII)


(16) A. Beckett, A. D. Osborne, and G. Porter, *Trans. Faraday Soc.*, **60,** 873 (1964).
(17) H. Berg, *Zh. Anal. Khim.*, **216,** 165 (1966).
(18) L. Michaelis and E. S. Fetcher, *J. Amer. Chem. Soc.*, **59,** 1246 (1937).
(19) J. L. Ihrig and R. G. Caldwell, *ibid.*, **78,** 2097 (1956).
(20) H. Berg, *Z. Chem.*, **2,** 237 (1962).

[Because there is no experimental evidence to suggest a specific structural formula for the stilbenediolate species, the structure (VII) was used in this work.] Species such as these are consistent with the general reaction scheme given in Equation 3. On the basis of previous studies on the oxidation of benzoin in alkaline solution (*21–23*), it appears that the oxidation proceeds via the transient stilbenediolate intermediate, (VII),

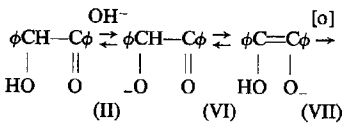


(5)

and that this intermediate actually undergoes the oxidation. Therefore, it seems most likely that species *R* is the stilbenediolate (VII).

The colored ketyl radical anion species (VIII)

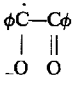


(VIII)

has been prepared by electrolysis of benzil in alkaline solution (*2*), most probably by the secondary reaction of unreduced benzil and the stilbenediolate (VII) formed by the electrode reaction. This observation coupled with the suggested mechanism for the benzoin oxidation (Equation 5) supports the idea that, in the absence of an oxidizing agent such as benzil (analogous to the situation near the electrode surface when benzil is being reduced), the stilbenediolate (VII) intermediate might rapidly rearrange (tautomerize) to the benzoin anion (VI).

Therefore, a more specific description of the overall electrode process in highly alkaline solution seems to be:

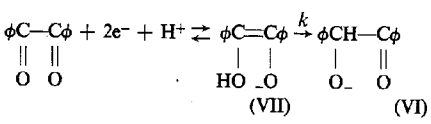


(6)

in which the stilbenediolate (VII) can be reversibly reoxidized with respect to the benzil reduction. In addition, considering previous studies in acid and neutral solution (*3*) along with those reported here, the overall process at pH 8.5 and below appears to be:

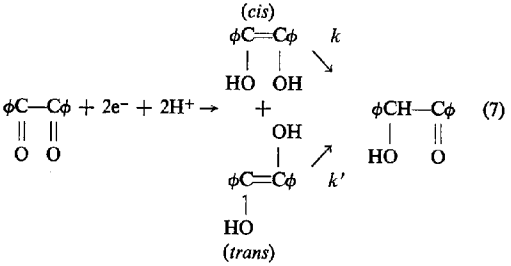


(7)

where the stilbenediol is not reversibly coupled. Moreover, at these low pH's both geometric *cis* and *trans* isomers are formed giving rise to the two anodic peaks shown in Figure 2.

## SUMMARY

In alkaline solution (pH > 11) benzil is reduced reversibly to a stilbenediolate intermediate which rearranges (tautomerizes) to the benzoin anion. The stilbenediolate species can be oxidized to the benzil ketyl radical by unreduced benzil in the electrolysis cell. Thus, any ketyl radical formed is not a direct product of the electron transfer reaction at the electrode, but rather of a secondary chemical reaction of benzil and the stilbenediolate.

The observations made here, combined with electrochemical results reported previously for benzil at pH ≦ 8 (*3*), indicate that in the pH region 9–10 the acid–base equilibrium process for the stilbenediolate

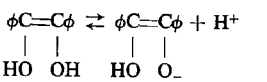


(8)

complicates the kinetics of the rearrangement reaction. In the region of pH below about 8, the diprotonated stilbenediol (I) (*cis* and *trans*) appears to be the product of the benzil reduction, and undergoes a much slower rearrangement to benzoin.

## ACKNOWLEDGMENT

The authors wish to thank Mr. C. Kaminski for performing some of the polarographic experiments.

RECEIVED for review September 5, 1968. Accepted January 15, 1969. Work supported by Public Health Service, Grant No. CA-07773 from the National Cancer Institute.

(21) A. Weissberger, *Ann. Chem.*, **502**, 74 (1933).
(22) B. A. Marshall and W. A. Waters, *J. Chem. Soc., A*, **1961**, 1579.
(23) S. Patai and I. Shenfeld, *ibid., B*, **1966**, 366.

# Photo-Electrochemical Behavior of Benzil

## Potentiostatic Monitoring Following Flash-Photolysis

H. E. Stapelfeldt[1] and S. P. Perone

*Department of Chemistry, Purdue University, Lafayette, Ind. 47907*

**Electrochemical monitoring techniques have been applied to the study of rapid secondary photolytic processes following flash-irradiation of benzil solutions. The photoreduction of benzil was qualitatively characterized using potentiostatic electrolysis to obtain a current-voltage profile of photolytic intermediates. Quantitative data for the rapid second-order disproportionation of the photo-produced, ketyl radical anion were obtained by potentiostatic electrolysis and time-delayed potentiostatic electrolysis in 0.1*M* NaOH, 50% methanol. Kinetic data were obtained as a function of pH using continuous potentiostatic monitoring following flash irradiation. The results suggest that at pH < 10, the predominant reaction is between the ketyl radical and ketyl radical anion. In addition, it appears that the photoreduction mechanism differs considerably from the electroreduction mechanism for benzil.**

Several workers have applied electroanalytical techniques to the study of photolytic processes following flash-irradiation of solutions (*1*, *2*). Most recently, Birk and Perone (*3*) have demonstrated the use of potentiostatic measurement techniques at stationary hanging mercury drop electrodes, utilizing individual current–time curves following the flash to obtain rapid kinetic data. They developed a theoretical current–time relationship which accounts for the second-order reaction of the electroactive photo-product. To test the validity of their approach they studied the kinetics of dimerization of the ketyl radical formed in the flash-photolysis of benzophenone, a chemical system well characterized both photochemically and electrochemically.

It was the purpose of this work to demonstrate further the general applicability of potentiostatic analysis in photolytic studies by applying the technique to a chemical system which had not been well characterized previously. A system which appeared amenable to study was benzil (diphenyldiketone) in aqueous–alcohol solution, for which few results have been reported (*1*, *4*, *5*). Of necessity, application of an electrochemical monitoring technique to any photolysis system requires some prior knowledge of that system's electrochemical behavior. Therefore, preliminary electrochemical studies were carried out by these authors (*6*, *7*), and the results of that work will be referred to in the interpretation of photo-electrochemical results reported here.

## EXPERIMENTAL

**Apparatus and Procedure.** The cell, electrodes, electrode assemblies, monitoring instrumentation, flash instrumentation, and general experimental procedure have been described previously (*2*). The working electrode was a hanging mercury drop electrode (HMDE) of the microburet type (*7*). A Luggin capillary probe was used for all potential-step work.

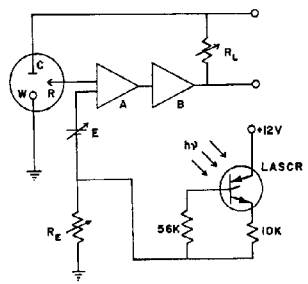


**Figure 1. Potential-step circuitry**

| | |
|---|---|
| *A* | Philbrick SK2-V operational amplifier |
| *B* | Philbrick SK2-B booster amplifier |
| *C* | Counter electrode |
| *R* | Reference electrode |
| *W* | Working electrode (HMDE) |
| $R_L$ | Load resistor, for current measurement |
| *E* | Low-voltage power supply, to adjust initial electrode potential |
| $R_E$ | Variable resistor, (0-1.5K), to adjust magnitude of potential-step |
| *LASCR* | Light Activated Silicon Control Rectifier (General Electric, L8F) |

Flash irradiation was provided by an FX-47-A flash-tube (Edgerton, Germeshausen & Grier, Inc., Boston, Mass.) modified to have a three-inch arc length. Voltages of 4 kV to 5 kV applied to a 4 μf or 8 μf capacitor provided energy inputs to the flash-tube varying between 32J and 100J. Flash times were the order of several microseconds.

To obtain potentiostatic data in the region where benzil is reduced, electrode potentials had to be applied at the same time as the flash irradiation so that the benzil concentration around the electrode was not depleted before the flash. This was accomplished by using a light-activated silicon control rectifier (LASCR, General Electric L8F) in the configuration shown in Figure 1. The LASCR is switched to the conducting state by the flash, thereby applying a known additional potential to the input of the controlling amplifier-potentiostat. This results in a cathodic step of the working electrode potential simultaneous with the flash. The rise time of the potential step was about 20 microseconds.

Time-delayed potentiostatic studies (*2*) were carried out, requiring in each experiment that no electrode reaction take place during some known time interval after the flash. This was made possible by the use of the LASCR, a time-delay circuit, and two miniature Hg-wetted reed relays (Magnecraft W131-PCX-9) combined as shown in Figure 2. The flash discharge switches the LASCR on, initiating the time-delay. After the predetermined time-delay has elapsed both relays

[1]Present address, Armed Forces Radiobiology Research Institute, Bethesda, Md.

(1) H. Berg, *Z. Anal. Chem.*, **216**, 165 (1966).
(2) S. P. Perone and J. R. Birk, Anal. Chem., **38**, 1589 (1966).
(3) J. R. Birk and S. P. Perone, *ibid.*, **40**, 496 (1968).
(4) A. Beckett, A. D. Osborne, and G. Porter, *Trans. Faraday Soc.*, **60**, 873 (1964).
(5) H. Berg, *Naturwissenschaften*, **49**, 11 (1962).
(6) H. E. Stapelfeldt and S. P. Perone, Anal. Chem., **41**, 623 (1969).
(7) H. E. Stapelfeldt and S. P. Perone, *ibid.*, **40**, 815 (1968).

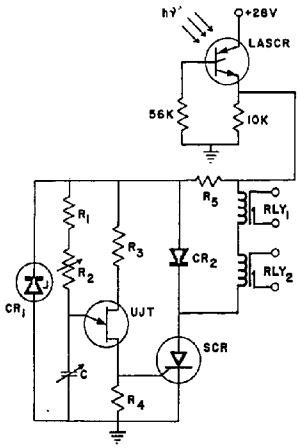


Figure 2. Time-delay potential step circuitry

*LASCR* Light Activated Silicon Control Rectifier (General Electric L8F)
*UJT* Unijunction transistor (GE 2N1671)
*SCR* Silicon control rectifier (Motorola 2N4170)
$CR_1$ Zener diode, Motorola IN4746
$CR_2$ Rectifier, IR-IN2071
$C$ Capacitor, variable, (1 to 20 $\mu$f)
$R_1$ 2.2 Kohms
$R_2$ 100 Kohms, 10-turn Helipot
$R_3$ 100 ohms
$R_4$ 47 ohms
$R_5$ 560 ohms
$RLY_1$ Relay (Magnecraft W131-PCX-9), faster closing, triggers scope sweep
$RLY_2$ Relay (Magnecraft W131-PCX-9), slower closing, grounds working electrode

close, the faster-closing (by about 20 microseconds) triggering the oscilloscope sweep, the slower-closing relay connecting the working electrode to ground allowing electrolysis to take place. In this manner the delay current–time curve is recorded. Because the current could not be accurately measured at times much less than 1 millisecond after the delay, the shortest time-delay period which could be used was about 20 milliseconds in order that the measurement time would not contribute significantly to the delay. The current measurement was made 2 milliseconds after the working electrode was grounded for all time-delays used here. For the chemical processes studied here, one could assume negligible chemical reaction during the 2-milliseconds measurement time.

**Reagents.** Benzil (Baker, reagent grade) was used without further purification. Preparation of sample solutions in 50% (by volume) methanol and the solution deaeration procedures have been described previously (*7*). All chemicals used in the preparation of buffers were reagent grade and were used without further purification.

## RESULTS AND DISCUSSION

**Qualitative Study, 0.1*M* NaOH.** Flash-photolysis studies were carried out using a $5 \times 10^{-4}M$ benzil solution, 0.1*M* NaOH, in 50% methanol. Qualitative characterization was achieved by obtaining a current–voltage profile (*2*). That is, the potential of the working electrode was held constant for a given flash experiment, but was varied in a series of identical

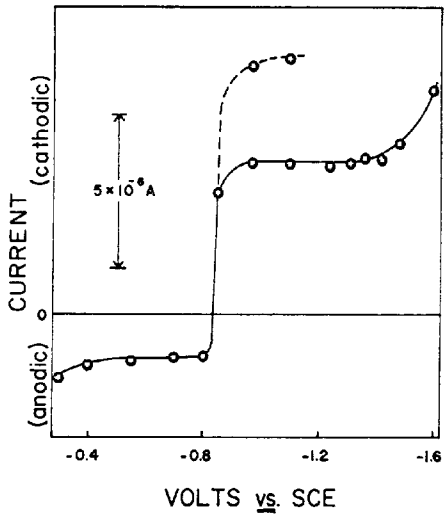


Figure 3. Current–voltage profile from continuous potentiostatic analysis

Currents measured 0.1 sec after flash irradiation. $4.8 \times 10^{-4}M$ benzil, 0.1*M* NaOH, in 50% methanol. Dashed line represents current measured without flash, using potential step technique

runs. Data were obtained in the form of current–time curves as a function of electrode potential. To obtain data in the region where benzil is reduced, the working electrode potential initially was set anodic of the benzil reduction wave, and then stepped cathodic simultaneous with the flash. The potential jump circuitry described in Figure 1 was used.

Electrolysis currents were measured at a fixed time after each flash (0.1-second), corrected for the blank current (current measured under the same conditions, but in blank buffer solution), and plotted as a function of working electrode potential to provide the current–voltage profile (Figure 3). This qualitative picture of reactants, products, and intermediates shows three distinct regions of interest: an oxidation process at potentials anodic of −0.83 V *vs.* SCE, a reduction process at potentials cathodic of −0.83 V *vs.* SCE, and a second reduction process at potentials more cathodic than −1.5 V *vs.* SCE. The oxidation current at potentials anodic of −0.83 volt is attributed to the benzil ketyl radical on the basis of the second-order kinetic observations discussed below. The reduction process cathodic of −0.83 V corresponds to the reduction of benzil to a stilbenediolate, while at potentials cathodic of −1.5 V benzil and/or the stilbenediolate may be reduced directly to deoxybenzoin. These assignments are consistent with previous electrochemical observations of these authors (*6*) as well as Pasternak (*8*), Philp (*9*), and Sobieski (*10*), and the photochemical studies of Beckett (*4*) and Berg (*1*, *5*).

The current–voltage profile (Figure 3) suggests that oxidation of the ketyl radical is reversible with the benzil reduction. If this were true, one would expect the height of the anodic step to be half of the difference in the cathodic step heights

(8) R. Pasternak, *Helv. Chim. Acta*, **31**, 753 (1948).
(9) R. H. Philp, Jr., R. L. Flurry, and R. A. Day, Jr., *J. Electrochem. Soc.*, **111**, 328 (1964).
(10) J. F. Sobieski, Ph.D. thesis, The Institute of Paper Chemistry, Appleton, Wis., 1967.

(with flash and without flash), because the anodic process involves a single electron while the cathodic requires two electrons, and negligible chemical reaction has occurred in 0.1 second. Figure 3 shows this to be approximately true. However, because of the limited conversion of benzil (20%–30%) to the radical and the experimental uncertainty in measured currents, a definite assignment of $E_{1/2}$ for the radical oxidation cannot be made.

By analogy to other photoreactive ketones (*2,4*) and on the basis of observed experimental data, the most probable photochemical process for benzil can be described by:

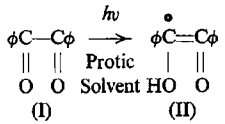


(1)

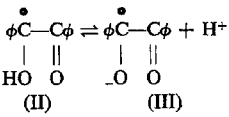


(2)

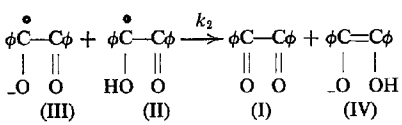


(3)

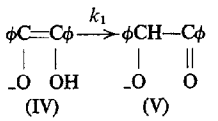


(4)

where: (I) is benzil, (II) is the ketyl radical, (III) is the ketyl radical anion, (IV) is the stilbenediolate (monoprotonated), (V) is the benzoin anion, $k_2$ is a second-order rate constant, and $k_1$ is a first-order rate constant. Beckett, Osborne, and Porter (*4*) have measured the $pK_A$ for the ketyl radical (Equation 2) and found it to equal approximately 5.9. Their work, along with that of Metzger (*11*), indicates that the subsequent radical reaction (Equations 3 and 4) is a disproportionation reaction rather than a dimerization, for ultimately benzoin is formed. There is additional evidence of this in equilibrium studies (*12, 13*) between benzil, benzoin, and the ketyl radical in alkaline solution.

When speaking of the second-order reaction of the ketyl radical following photolysis, one must bear in mind that there exist three possible reactions: (1) reaction between two radical anions, (2) reaction between radical and radical anion, and (3) reaction between two radicals. Only the kinetics of the reaction can reveal which of the three predominates. The electrochemical oxidation process does not distinguish between the radical or radical anion, but will reflect the predominant reaction at all pH's. In the interest of simplicity the following discussions will refer to radical reactions with the understanding that any one of the three specified above may be involved. The pH study below outlines the predominant reactions involved at each pH.

**Quantitative Study, 0.1*M* NaOH.** Kinetic measurements for the ketyl radical disproportionation reaction can be made in two ways: time-delay potentiostatic analysis (*2*) and analysis of single potentiostatic current–time curves (*3*).

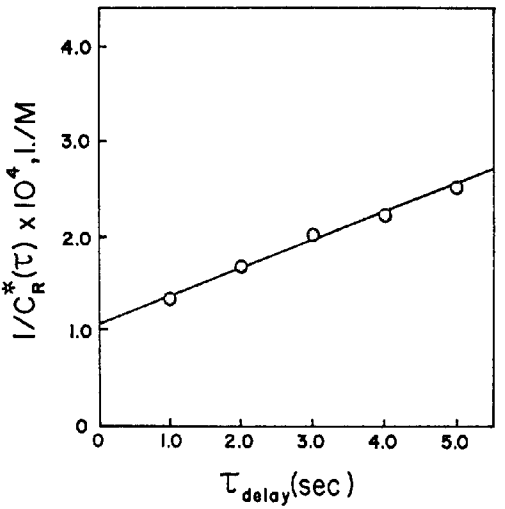


**Figure 4. Kinetic plot from time-delayed potentiostatic data**

**$5 \times 10^{-4}M$ benzil, 0.1*M* NaOH, in 50% methanol. From slope, $k_2 = 3.0 \times 10^3\ M^{-1}\ sec^{-1}$**

Time-delay studies involve a rapid electroanalytical determination of homogeneous reactant concentration at different times after initiating the photolytic reaction. They provide a general method to obtain the time dependence of the electroactive species from which the reaction order can be determined. The basic assumptions necessary in the application of this technique have been discussed previously (*2*). One further assumption made here was that the diffusion coefficient $D_R$ for the radical or radical anion is similar to that for benzil, which can be experimentally measured. Thus, for all subsequent discussion $D_R$ is taken as $4.8 \times 10^{-6} cm^2\ sec^{-1}$, the value for benzil determined by stationary electrode polarography. The applicability of the time-delay potentiostatic technique is limited, with present instrumentation, to the study of reactions having half-lives greater than 5–10 milliseconds (*3*). Faster reactions can be monitored by analysis of single continuous potentiostatic current–time curves following flash-irradiation. This method requires that measurements be made prior to the half-life $t_{1/2}$ for the reaction (*3*), and is limited only at very short times by the instability of the amplifier-potentiostat caused by the flash discharge close to the electrode sensors (*3*).

A series of time-delay potentiostatic current–time observations were carried out on flash-irradiated benzil solutions ($5 \times 10^{-4}M$ benzil, 0.1*M* NaOH, 50% MeOH). The HMDE potential imposed after the delay time was −0.500 V *vs.* SCE, well onto the ketyl radical oxidation step. The total ketyl radical concentration at the delay time can be obtained by application of the Cottrell equation (Equation 5), assuming that the measurement time, $t$, is short compared to the delay time, $\tau$ (*2*).

$$i_d = nFAD_R^{1/2}\, C_R^*/(\pi t)^{1/2} \qquad (5)$$

where: $i_d$ = diffusion controlled electrolysis current (HMDE), $n$ = number of electrons involved, $F$ = Faraday constant, $D_R$ = diffusion coefficient ($4.8 \times 10^{-6}\ cm^2\ sec^{-1}$), $A$ = electrode area, $t$ = time after $\tau$ at which $i_d$ is measured, and $C_R^*$ = bulk solution concentration existing at $\tau$.

(11) S. H. Metzger, Jr., Ph.D. thesis, Univ. of Illinois, Urbana, Ill., 1962.
(12) H. Berg, *Naturwissenschaften*, **48**, 100 (1961).
(13) J. L. Ihring and R. G. Caldwell, *J. Amer. Chem. Soc.*, **78**, 2097 (1956).

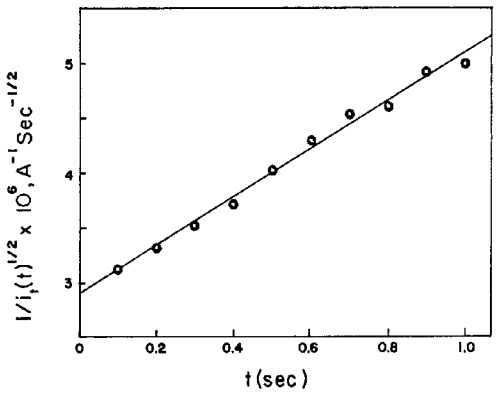


**Figure 5. Second-order kinetic plot from single continuous potentiostatic current–time curve after flash**

**$5.0 \times 10^{-4}M$ benzil, $0.1M$ NaOH, in 50% methanol $k_2 = 4.6 \times 10^3 M^{-1}$ sec$^{-1}$**

$C_R^*(\tau)$ is calculated from experiments with varying delay times. A linear plot of $1/C_R^*(\tau)$ *vs.* time ($\tau$) (Figure 4) indicates a second-order chemical reaction. The rate constant of $(3.0 \pm 1) \times 10^3 M^{-1}$ sec$^{-1}$ obtained is in fair agreement with the value of $9 \times 10^2 M^{-1}$ sec$^{-1}$ reported by Berg (*14*) for the free radical in $0.1M$ NaOH, 40% isopropanol.

Birk and Perone (*3*) have shown that rapid second-order kinetic data may be obtained from single potentiostatic current–time curves. The approach used involves an empirically derived limiting form of the theoretical potentiostatic current–time relationship for the process,

$$O \xrightarrow{h\nu} R \qquad 2R \xrightarrow{k_2} P \qquad (6)$$

$$O \xrightarrow{-ne^-} R$$

which is consistent with the photo-induced disproportionation process studied here, if the back reaction is assumed to be negligible. This should be true (*6*) particularly at short times. This relationship,

$$\frac{1}{i_t(t)^{1/2}} = \frac{\pi^{1/2}}{nFAD_R^{1/2}C^\circ_R} + \left(\frac{k_2\pi^{1/2}}{nFAD_R^{1/2}}\right)t \qquad (7)$$

(where: $C^\circ_R$ is the initial bulk concentration of $R$, $t = 0$), should be valid for second-order kinetics in the limiting case where time is equal to zero, before a concentration gradient is established at the electrode surface. It was shown to be applicable (*3*) at times shorter than $t_{1/2}$. Moreover, the above relationship has been obtained by a more rigorous mathematical derivation (*15*).

Equation 7 provides that a plot of $1/i_t\sqrt{t}$ *vs.* $t$ should be a straight line with a slope depending on $k_2$. In addition, $C^\circ_R$ may be obtained from the intercept, assuming one knows $D_R$, $A$, etc. Typical experimental results ($5 \times 10^{-4}M$ benzil, $0.1M$ NaOH, 50% MeOH) are shown in Figure 5 and the average experimental rate constant found is $(4.6 \pm 1.2) \times 10^3$ $M^{-1}$ sec$^{-1}$. These data are in good agreement with the time-delay results.

(14) H. Berg, 5th International Symposium on Free Radicals, Upsala, Sweden, 1961, preprint #8.
(15) D. Moore and S. P. Perone, unpublished work.

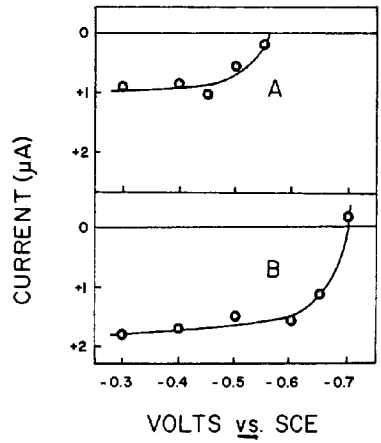


**Figure 6. Current–voltage profile from time-delayed potentiostatic analysis**

***A*. Current measured 5 msec after a 0.3 second time-delay following flash. Sample solution: $5.2 \times 10^{-4}M$ benzil, pH = 8.5, 50% methanol**
***B*. Current measured 5 msec after the flash irradiation, no time-delay. Sample solution: $5.2 \times 10^{-4}M$ benzil, pH = 8.5, 50% methanol**

**Kinetics as a Function of pH.** Electrochemical studies of benzil in alkaline methanol–water solvent (*6*) indicate that the stilbenediolate product of the electrode reduction of benzil is oxidizable in the same general region as the ketyl radical formed by flash irradiation. In addition, the photolytic radical reaction produces the stilbenediolate as one of its products (Equation 3). Therefore, depending on the relative speed of the radical disproportionation as compared to the stilbenediolate rearrangement, the possibility exists of measuring mixed oxidation currents following the flash irradiation.

In very alkaline solution ($0.1M$ NaOH) the stilbenediolate rearranges rapidly (*6*) compared to the radical disproportionation, and therefore does not contribute significantly to observed currents after the flash. As the solution pH decreases, the relative rates change such that the radical is less stable while the stilbenediolate species becomes more stable. The two extremes existing in this situation were reported by Berg (*1*) who observed the ketyl radical oxidation at pH's between 11 and 13.7, and the stilbenediol oxidation at pH 5 to 8 following flash irradiation.

Results obtained in this laboratory indicate that below a pH of about 10 it is possible to differentiate between oxidation of the radical and the combined oxidation of radical plus stilbenediol species, by proper choice of working electrode potential and the time scale of the experiment. For example, Figure 6 shows the anodic portions of current–voltage profiles, at pH 8.5, obtained as a function of time after the flash. Qualitatively these results indicate that at short times after the flash a more easily oxidizable species is present (radical), which is not present at long times. Further evidence is obtained from potentiostatic current–time curves obtained after flash irradiation, at potentials of $-0.600$ V *vs.* SCE and $-0.500$ V *vs.* SCE. Results obtained at $-0.600$ V give a straight line plot of $1/i_t\sqrt{t}$ *vs.* time having a positive slope indicating a second-order chemical reaction, and suggesting that only the radical is oxidized at that potential. However, on the same time scale, results obtained at $-0.500$ V yield a straight line

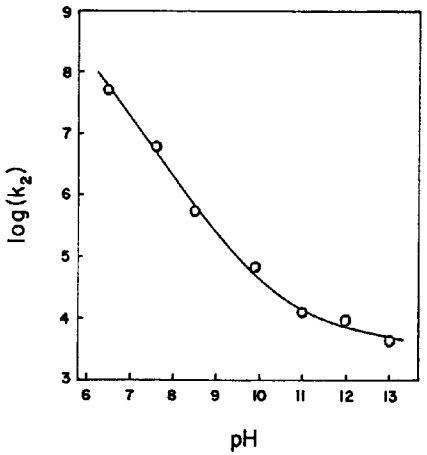


**Figure 7. pH dependence of disproportionation kinetics**

plot having a nearly zero slope. According to Equation 7 a zero slope indicates simple diffusion controlled electrolysis with no kinetic complication. However, this is also what one would expect if both the diol species and radical species were being oxidized, for one diol molecule (two-electron oxidation) is formed for every two radicals (one-electron oxidation) which react. The net change would be zero, and the electrolysis current (−0.0500 V) would appear diffusion-controlled.

On this basis it is possible to obtain kinetic data for the radical disproportionation at pH's < 10 by selecting a potential for potentiostatic experiments which lies between the benzil reduction and stilbenediolate oxidation potentials, and by taking data early during the radical reaction. The last requirement reflects the fact that one cannot completely separate the oxidation of radical from the stilbenediolate oxidation or benzil reduction processes by choice of the electrode potential alone. At the outset of the radical reaction, the solution contains radical, unphotolyzed benzil, but no stilbenediolate. The potentiostatic current (−0.600 V, pH = 8.5) at short times after the flash results from radical oxidation with perhaps some contribution from reduction of unphotolyzed benzil. The slope of the $1/i_t\sqrt{t}$ *vs.* time plot will reflect only the radical disproportionation reaction because the unphotolyzed benzil is essentially at steady state. This is true only at the start of the radical reaction and short times thereafter, for after a sufficient time elapses the stilbenediol species concentration will build up and benzil may no longer be considered at steady state.

Rate constants for the radical disproportionation reaction as a function of pH are given in Table I. Data at pH > 10 were obtained at a HMDE potential of −0.500 V *vs.* SCE, while at lower pH the electrode potential was selected to minimize contributions by the relatively stable stilbenediol species and benzil. These results are limited at short times by instability of the amplifier-potentiostat at the time of the flash discharge (*3*). The potentiostat recovers in a few hundred microseconds so that the faradaic current can easily be measured at times greater than 200 microseconds. However, at shorter times the electrolysis current due to the radical is superimposed on a larger background current (because of the damped amplifier oscillation) and therefore is difficult to measure.

**Table I. Effect of pH on the Ketyl Radical Disproportionation Reaction**

| pH | Buffer[a] | $t_{1/2}$, sec | $k_2$ ($M^{-1}$ sec$^{-1}$)[c] |
|---|---|---|---|
| 13 | 0.1*M* NaOH | 1.3 | $(4.0 \pm 1.2) \times 10^3$ |
| 12 | 0.01*M* NaOH | 1.1 | $(9.4 \pm 3.1) \times 10^3$ |
| 11 | Carbonate | 0.9 | $(1.2 \pm 0.4) \times 10^4$ |
| 9.9 | Glycine–NaOH | 0.2 | $(6.5 \pm 2.2) \times 10^4$ |
| 8.5 | Phosphate | 30 msec | $(5.3 \pm 1.8) \times 10^5$ |
| 7.6 | Phosphate | 3 msec | $(5.9 \pm 2.0) \times 10^6$ |
| 6.5 | Acetate | 300 μsec[b] | $(4.8 \pm 1.6) \times 10^7$ |

[a] Ionic strength maintained at 0.1, adding KCl when necessary. [b] Measurement made after the half-life, $t_{1/2}$. [c] The uncertainty shown reflects the uncertainty in the value of $A$ used in the calculation of $k_2$ (*3*), not the precision of the actual measurement which was ± 15% or better.

## CONCLUSIONS

Following flash irradiation of benzil to produce the radical and/or radical anion species, three disproportionation reactions are possible. Depending on the solution pH and the values of the respective rate constants, any one of the three reactions might predominate. The pH dependence of $k_2$ (shown in Figure 7) shows little change in $k_2$ with changing pH above 10. Below a pH of 10, the experimental rate constant varies ten-fold per pH unit, down to a pH of 6.5. These results are consistent with the idea that at pH greater than 10, the reaction between two radical anions predominates, while in the pH range 6.5 to 10 the reaction between radical and radical anion is more important. One might expect that at pH less than $pK_a$ (for the radical), the rate constant $k_2$ will again become pH-independent, if the radical–radical reaction is most important.

The photo-electrochemical observations made here indicate that photolysis of benzil results in reduction of benzil to its ketyl radical. In contrast, the electrochemical reduction of benzil (*6*) in the same pH range has been shown to produce a stilbenediol or stilbenediolate species rather than the ketyl radical. Therefore, contrary to some previous descriptions (*12, 16, 17*), the photochemical reduction process differs from the electrochemical reduction process.

## ACKNOWLEDGMENT

The authors acknowledge the assistance of Mr. David O. Jones in the development of the LASCR and time-delay circuitry.

RECEIVED for review September 5, 1968. Accepted January 2, 1969. Presented, in part, at the 1968 Eastern Analytical Symposium, New York, N.Y., November 1968. Work supported by Public Health Service, Grant No. CA-07773 from the National Cancer Institute.

(16) R. Kalvoda and G. Budnikov, *Collect. Czech. Chem. Commun.*, **28**, 838 (1963).
(17) E. Bauer, *J. Electroanal. Chem.*, **14**, 351 (1967).

# Polarographic Irreversibility of the Copper(II) Pyrophosphate System

**Gibson W. Higgins**[1]
*Wabash College, Crawfordsville, Ind. 47933*

**Peter E. Sturrock**
*Georgia Institute of Technology, Atlanta, Ga. 30332*

**The polarographic irreversibility of the copper(II) pyrophosphate complex in the presence of $KNO_3$ supporting electrolyte was investigated electrochemically in terms of possible adsorption, a rate-determining chemical reaction, a slow electron transfer step, and double layer influences. It was determined that only nitrate ion is adsorbed in measurable amounts, with the effect of this adsorption appearing in the altered values of the potential drop across the diffuse double layer. For sufficiently alkaline solutions (pH > 5) the charge transfer step is preceded by a slow dissociation of a pyrophosphate ligand. Values for the kinetic product $\vec{v}K$, for this reaction are of the order of $10^{-15}$ at pH 9 after correction for all double-layer effects. The charge on the reducible species varies between −0.41 and −1.6, depending upon the ratio of the concentration of pyrophosphate and copper(II). At pH 5.8 the dissociation reaction is somewhat faster, having a $\vec{v}K$ of about $10^{-3}$. The true heterogeneous rate constant for electron transfer is $1.8 \times 10^{-1}$ cm sec$^{-1}$ at pH 9, and $3.8 \times 10^{-1}$ at pH 3. The rate of electron transfer is therefore always polarographically reversible.**

THE polarographic behavior of complexes of copper(II) with pyrophosphate ion is a function of the pH of the solution and the pyrophosphate ion concentration, in addition to the nature and concentration of the supporting electrolyte. Typical polarograms are given in Figures 1–4. Below a pH of about 4, the complex is reversibly reduced. In the pH 5 region, the wave appears to be somewhat irreversible, and is split into two waves whose relative magnitudes are a function of the ligand concentration. Above pH 9, the first wave is hardly seen except at low ligand concentrations, and the second wave attains the normal value of the diffusion current only after a very long drawn out portion ending at about −1.3 volts *vs.* SCE. Pyrophosphate is a Bronsted base which becomes increasingly protonated as the pH is lowered. This results in lowering both the charge and stability of the complex ions which are related in turn to the electrochemical behavior of the system.

The characteristics of the electrical double layer also affect the polarographic waves. At lower concentrations of $KNO_3$ supporting electrolyte, additional maxima and minima appear on the waves, superimposed, respectively, at approximately −0.2 and −0.6 volt. During the course of this investigation, Payne (*1*) reported the adsorption of $NO^-_3$ on mercury electrodes. This adsorption exerts an influence on the electrical double layer. It has been shown (*2*) that alkali metal cations associate with pyrophosphate ions in alkaline solution by a mechanism thought to be ion-pairing. This influences the double-layer effect on the reduction by altering the net charge on the complex.

[1]Present address, Department of Chemistry, Memphis State University, Memphis, Tenn. 38111

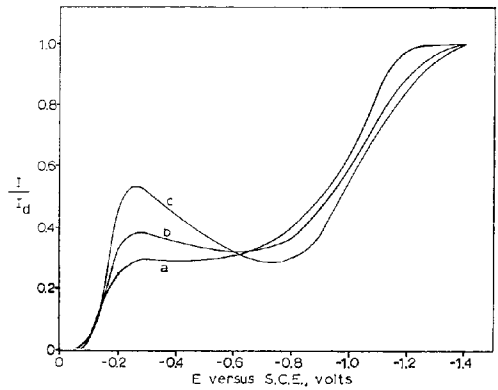


**Figure 1. Polarograms at pH 9.18 for variable $[KNO_3]$, constant [Py] = 2.00 m*F*, $[Cu^{2+}]$ = 1.00 m*F***

*a.* $[KNO_3] = 1.0F$
*b.* $[KNO_3] = 0.5F$
*c.* $[KNO_3] = 0.2F$

In order to study the system, steady-state dc polarographic measurements were employed for conditions under which a preceding chemical reaction could be the rate-determining step. Potential step experiments in which the current and (chronocoulometric) charge transients were measured were employed for kinetic measurements under conditions where the reduction could be assumed to be the rate-determining step. Values are reported for the kinetic parameters for both the chemical and the electrochemical reactions. Double-layer corrections, including the consideration of the specific adsorption of nitrate, are applied to these results. In the case of the polarographic data, the corrections are applied according to the method of Gierst (*3*). A search was made for possible specific adsorption of any ligand or complex species of copper. Chronocoulometry was employed in the case of the copper complexes. Electrocapillary curves, points of zero charge as measured by a streaming mercury electrode, and double-layer capacity measurements were employed to study possible adsorption of the ligand species and the electrolyte.

## EXPERIMENTAL

**Reagents.** All chemicals were J. T. Baker Analyzed Reagent Grade and were used without further purification. Stock solutions of potassium nitrate, sodium pyrophosphate, and copper(II) nitrate were prepared, and combined and diluted in analytical grade volumetric glassware as needed. Bethlehem Instruments triple-distilled mercury was used in the dropping

(1) R. Payne, *J. Phys. Chem.*, **69**, 4113 (1965).
(2) O. E. Schupp, P. E. Sturrock, and J. I. Watters, *Inorg. Chem.*, **2**, 106 (1963).
(3) L. Gierst, "Transactions of the Symposium on Electrode Processes," E. Yeager, Ed., John Wiley and Sons, New York, 1961, pp 109–138.

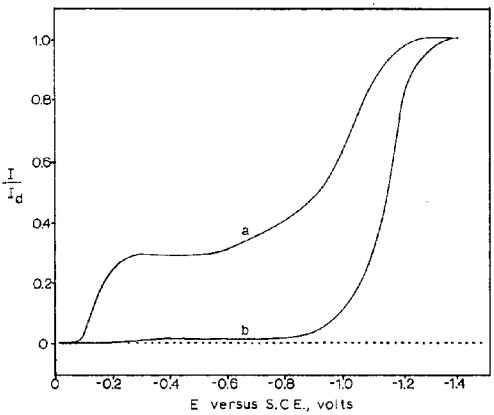


**Figure 2. Polarograms at pH 9.18 for variable [Py], constant [$KNO_3$] = 1.0*F*, [$Cu^{2+}$] = 1.00 m*F***

*a.* [$P_2O_7^{4-}$] = 2.00 m*F*
*b.* [$P_2O_7^{4-}$] = 50.0 m*F*

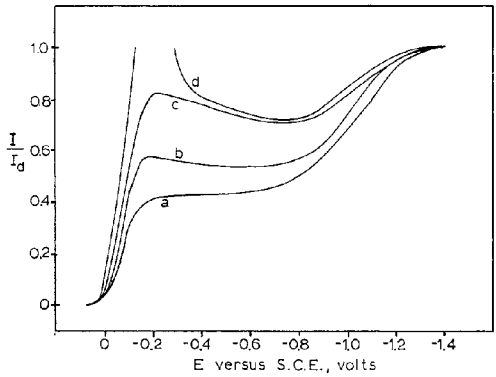


**Figure 3. Polarograms at pH 5.80 for variable [$KNO_3$], constant [Py] = 2.00 m*F*, [$Cu^{2+}$] = 1.00 m*F***

*a.* [$KNO_3$] = 1.0*F*
*b.* [$KNO_3$] = 0.5*F*
*c.* [$KNO_3$] = 0.2*F*
*d.* [$KNO_3$] = 0.1*F*

mercury electrode without further treatment. The copper amalgam employed in some experiments was prepared by exhaustive electrolysis with a mercury cathode in a solution containing a known amount of copper(II) ion. Dilution of the mercury cathode gave an amalgam of known concentration. This concentration was checked polarographically by measuring the diffusion current due to the oxidation of the amalgam in a dropping amalgam electrode.

**Apparatus.** The basic instrument employed was a locally constructed operational-amplifier controlled-potential polarograph. Heath Model EUW-19A operational amplifiers were the active elements of the circuit, schematically represented in Figure 5*A*. The basic controlled-potential circuit is that of the Enke three-electrode polarographic unit (*4*) commercially available from Heath Co., Benton Harbor, Mich. Certain additions were made to the circuit to render the instrument more suitable to the requirements of the techniques employed.

(4) C. G. Enke and R. A. Baxter, *J. Chem. Ed.*, **41**, (4), 202 (1964).

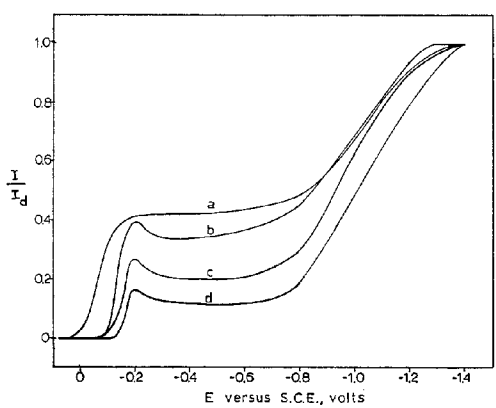


**Figure 4. Polarograms at pH = 5.80 for variable [Py], constant [$KNO_3$] = 1.0*F*, [$Cu^{2+}$] = 1.00 m*F***

*a.* [$P_2O_7^{4-}$] = 2.00 m*F*
*b.* [$P_2O_7^{4-}$] = 50.0 m*F*
*c.* [$P_2O_7^{4-}$] = 100 m*F*
*d.* [$P_2O_7^{4-}$] = 200 m*F*

In most experiments the amplifiers were stabilized with Philbrick K2-PA chopper stabilizers in the zero-current configuration (Philbrick Researches, Dedham, Mass.). Shorting phone jacks were used in the amplifier input circuit to allow the connection of the chopper amplifiers only when desired. Connections to the chopper amplifiers were made through short lengths of shielded low-capacitance cable. The chopper amplifiers themselves were mounted on a separate chassis and were powered from the operational amplifier power supply. Installation of an internal buss-bar common grounding connection within the amplifier chassis decreased the ac noise level considerably. A variable capacitor across the control amplifier of the potentiostat allowed adjustment for optimum risetime without overshoot. Optimum risetime was 10 μseconds into a 10K resistive load, and approximately 40 μseconds into the R-C network formed by the cell and the double-layer capacitance. A fixed capacitance of 100 pF was used across the current follower amplifier to control its oscillation and overshoot and to improve the risetime of the control amplifier. The integrator circuit was modified to allow the integrator to function either as a ramp generator or as a microcoulometer in chronocoulometry experiments.

A locally constructed programmable control module was employed in conjunction with the potentiostat in most experiments. The control circuit, constructed of bistable and monostable multivibrator logic elements, is depicted in block diagram in Figure 5*B*. The assembly was shielded by mounting in a metal box and the circuit was powered by a 12-volt lead storage battery. The module performed a number of operations, including actuation of an electromagnetic drop detacher, application of precisely adjustable and reversible potential steps, starting and stopping of the integrator in coulometry experiments, and oscilloscope triggering after an adjustable time delay.

A triangular sweep generator and ac polarographic adapter were combined in a module constructed around Heath operational amplifiers. This device was employed in some of the preliminary survey work.

Polarograms were recorded on either a Houston Instruments HR 96T X-Y recorder or a Sargent Model SR strip-chart recorder. In relaxation experiments, a Tektronix 561A oscilloscope fitted with a 3A72 dual-channel amplifier, a 2B67 time-base, and a C-12 Polaroid camera, was used to record the transients. The pH was monitored with either a Beckman Research pH Meter or a Coleman Model 12 expanded scale pH meter. A temperature of 25.0 ± 0.1 °C

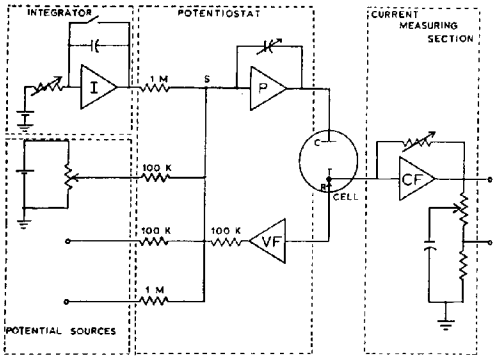


**Figure 5, *A*. Basic potentiostatic circuit**

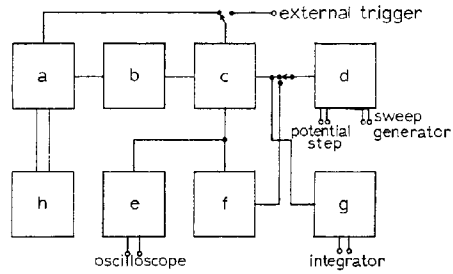


**Figure 5, *B*. Block diagram of controller module**

***a*. adjustable period relaxation oscillator**
***b*. variable time delay–monostable vibrator**
***c*. relay controller–bistable flip-flop**
***d*. relay 1–single or double potential step**
***e*. variable delay oscilloscope trigger–monostable vibrator**
***f*. relay controller–monostable vibrator**
***g*. relay 2–operating switch for electric integrator**
***h*. drop detaching mechanism–solenoid**

was maintained by a thermostated water bath. The cell consisted of a 100-ml Berzelius beaker fitted with a number-10 rubber stopper drilled to accept a DME, a counter electrode (in this case a Pt wire shielded by a glass frit), a deoxygenator, and a reference electrode. The reference electrode was a saturated calomel electrode with a horizontal tip of about 1 mm diameter containing a saturated KCl–agar salt bridge. The DME was constructed of 6-mm borosilicate glass tubing, Tygon tubing, and one half of a Sargent 6- to 12-second capillary. The assembly was affixed to a meter stick to allow reproducible setting of the leveling reservoir. The amalgam electrode employed was constructed entirely of glass. A 30-cm jacketed glass head tube was connected via a 10/30 ST glass joint at the upper end to a 100-cm³ amalgam reservoir. At the lower end of the tube was a 1-mm stopcock and another 10/30 joint for connection to a capillary assembly. The capillary was one half of a Sargent 2- to 5-second DME capillary sealed into the complementary 10/30 glass joint with Varno cement. The amalgam in the reservoir was protected from the atmosphere by a layer of Nujol. The hanging mercury drop electrode was a Metrohm number 410.

## RESULTS AND DISCUSSION

**Adsorption.** AC polarography was employed with sodium pyrophosphate solutions both in the presence and the absence of copper ion to see whether any peak corresponding to either adsorption/desorption or reversible electron transfer could be detected (*5*). No peak was detected.

Employing triangular sweep voltammetry, differential capacities were measured for the DME and for the hanging mercury drop electrode in 1.0*F* $KNO_3$ solutions containing various concentrations of pyrophosphate but no reducible species. The capacitance was independent of pyrophosphate concentration between 0 and −1.5 volts *vs.* the SCE. Observation of the capacity of the hanging mercury drop electrode for periods of time as long as 1000 seconds failed to reveal any capacity decrease which, considering the range of concentrations employed, could be attributable to specific adsorption of pyrophosphate. Mercuric ion was added in some experiments in an attempt to enhance the surface concentration of pyrophosphate by utilization of the diffusion of the mercury(II) pyrophosphate complex to the electrode. This use of the mercury ion was possible because the electrode potential was held constant for several seconds at some value within the diffusion current region for mercury ion, and then a rapid cathodic sweep was applied and the capacitance was calculated directly from the total current flow, as before. After a period of at least 1 second, it was calculated that the Hg(II) diffusion current was completely negligible. No effect upon the capacity was noted.

Potential of zero charge (PZC) values were measured by the streaming electrode technique (*6*). For potassium nitrate solutions which were 1.0*F*, 0.5*F*, 0.1*F*, and 0.05*F*, respectively, the following values were found for the PZC: −0.519, −0.503, −0.478, and −0.462 volts *vs.* SCE. These values are in excellent agreement with those found in the literature (*7*). A series of drop-time electrocapillary curves was obtained for these same $KNO_3$ solutions, but drift in the drop time of the low Hg head DME prevented reproducible data from being obtained and this approach was finally abandoned. Instead, the data of Payne (*8*) for the identical solutions were employed.

Values for the PZC for solutions of sodium pyrophosphate alone were essentially independent of concentration. In fact, an anodic shift of about 5 mV was observed between 0 and 0.2*F*. At the latter value, the PZC was −0.428 volt, 7 mV less than the value obtained for sodium fluoride (*6*). This indicates that essentially no anionic adsorption was occurring. Within experimental error, a drop-time electrocapillary curve confirmed the streaming electrode value for the PZC of sodium pyrophosphate solution.

From the above results, only nitrate ion seems to be adsorbed to any extent. This conclusion also seemed to include the copper complex, but because large initial currents had been encountered in the potential step experiments with the complex in alkaline solution, double-step chronocoulometry was employed as an additional test for possible adsorption of the complex. From the data, two different types of plot, each according to Anson (*9*), were constructed. In the first, the

(5) B. Breyer and H. H. Bauer, "Alternating Current Polarography and Tensammetry," Interscience, New York and London, 1963, Chapter 5.

(6) D. C. Grahame, *J. Amer. Chem. Soc.*, **79**, 2978 (1949).
(7) B. E. Conway, "Electrochemical Data," Elsevier, Amsterdam, 1952, p 221.
(8) R. Payne, *J. Electrochem. Soc.*, **113**, 999–1010 (1966).
(9) F. C. Anson, ANAL. CHEM., **38**, 54 (1966).

**Table I. Values in Moles cm$^{-2}$ of the Surface Excess of Reducible Species in the Copper(II)–Pyrophosphate System**

A. $Q - [t^{1/2} - (t - \tau)^{1/2}]$ Intercept
B. Difference between $Q - t^{1/2}$ and $Q - \theta$ Intercepts

| [Pyrophosphate] | pH | $E_t$, volts | $\Delta E$, volts | A | | B | |
|---|---|---|---|---|---|---|---|
| | | | | $Q_t$, $\mu$ coulombs | $\Gamma \times 10^{10}$, moles cm$^{-2}$ | $Q_t$, $\mu$ coulombs | $\Gamma \times 10^{10}$, moles cm$^{-2}$ |
| 2 m$F$ | 8.98 | 0 | − 0.300 | 0.11 | 0.21 | 0.13 | 0.25 |
| | 5.66 | 0 | − 0.300 | 0.01 | 0.019 | 0.03 | 0.057 |
| | 2.96 | + 0.100 | − 0.300 | − 0.02 | 0.038 | − 0.10 | 0.19 |
| | 9.15 | + 0.100 | − 0.400 | 0.22 | 0.38 | 0.10 | 0.19 |
| | 5.88 | + 0.100 | − 0.400 | 0.03 | 0.057 | 0.15 | 0.28 |
| | 3.26 | + 0.100 | − 0.400 | 0.18 | 0.34 | 0 | 0 |
| | 9.21 | − 0.130 ($E_e$) | − 0.050 | − 0.22 | − 0.42 | 0.01 | 0.02 |
| | | | − 0.090 | − 0.26 | − 0.49 | 0.12 | 0.21 |
| | | | − 0.110 | − 0.22 | − 0.42 | 0.20 | 0.38 |
| | | | − 0.140 | − 0.22 | − 0.42 | 0.24 | 0.46 |
| | 8.98 | − 0.121 ($E_e$) | − 0.050 | − 0.14 | − 0.27 | 0.13 | 0.21 |
| | | | − 0.100 | − 0.12 | − 0.23 | 0.19 | 0.37 |
| | | | − 0.150 | − 0.11 | − 0.21 | 0.06 | 0.11 |
| | | | − 0.200 | − 0.078 | − 0.15 | 0.07 | 0.14 |
| | | | − 0.250 | − 0.070 | − 0.13 | 0.23 | 0.44 |
| | | | − 0.300 | − 0.058 | − 0.11 | 0.36 | 0.68 |
| | | | − 1.000 | 0.065 | 0.12 | | |
| 5 m$F$ | 9.52 | − 0.189 ($E_e$) | − 0.100 | 0.106 | 0.20 | 0.02 | 0.038 |
| | | | − 0.300 | 0.113 | 0.21 | 0.06 | 0.12 |
| | | | − 0.600 | 0.182 | 0.34 | 0.13 | 0.254 |

charge, $Q$, for times greater than the switching time $\tau$, is plotted as a function of time $t$ according to

$$Q(t > \tau) = \frac{2}{\pi^{1/2}} nFAC_{Ox} D^{1/2}[t^{1/2} - (t - \tau)^{1/2}] \quad (1)$$

A finite positive value of the $Q$ intercept obtained by extrapolation toward the origin gives a measure of the amount of electroactive material adsorbed. By employing forward and reverse steps of the same magnitude, the amount of charge required to change the potential of the double layer is effectively canceled. In the second type of plot, $Q$ for $t < \tau$ is plotted *vs.* $t^{1/2}$, according to theory (*10*). For $t > \tau$, $(Q_\tau - Q)$ is plotted on the same graph *vs.* $\theta$, the function of $t$ given in the expression

$$Q_\tau - Q = \frac{2}{\pi^{1/2}} nFAC_{Ox} D^{1/2}[\tau^{1/2} + (t - \tau)^{1/2} - t^{1/2}] \quad (2)$$

Any difference in the absolute magnitudes of the intercepts of these two plots, as obtained by extrapolation to $t = 0$, gives a measure of the adsorption of electroactive species. The results are given in Table I. The maximum amount of adsorption indicated is only $3 \times 10^{-11}$ mole cm$^{-2}$, not enough to exhibit any of the characteristics normally associated with adsorption of electroactive species. In addition, no reaction blocking or alteration of the double layer structure is expected to result from this amount of adsorption. This strengthens the conclusion that, of all the species in the system, only $NO_3^-$ is adsorbed. The result of this adsorption will be demonstrated in the section on double layer corrections of kinetic data.

**Dependence on Mercury Height and Ligand Concentration.** In order to check the possible existence of a kinetic phenomenon, the influence of the mercury height on the polarographic limiting current was measured for a solution which was 1.0 m$F$ in $Cu(NO_3)_2$, 50.0 m$F$ in $Na_4P_2O_7$, and 1.0$F$ in $KNO_3$. The pH was adjusted first to 9.20 with dilute NaOH solution and later to 5.80 with dilute $HNO_3$ solution, and polarograms were obtained for each condition. Corrections were made for the background current with identical solutions, lacking only copper, and back pressure corrections were applied for each mercury column height according to the procedure described by Kolthoff and Lingane (*11*). The results are presented in Table II. In each case, it can be seen that the first wave is a kinetic wave, while the second is diffusion-controlled.

The principal complex species known to exist in alkali-free solutions of pH 9 or greater is $Cu(P_2O_7)_2^{6-}$ (*2*). Foster (*12*) has reported that this species is not directly reduced, but rather undergoes a slow dissociation of a pyrophosphate ligand to give the reducible 1:1 complex. Sturrock (*13*) has shown that protonation of the 2:1 complex increases its reducibility. At pH 5.8 there is at least one proton attached to each ligand. As may be seen by observation of the polarograms in Figures 2 and 4, the limiting current for the first wave at each pH decreases as the concentration of pyrophosphate increases. This may be interpreted as being due to a kinetic wave (*14*) of the type caused by increasing the ligand concentration, L, in the slow forward reaction of the equilibrium

$$ML_2 \rightleftarrows ML + L \quad (3)$$

where ML would be the reducible species. The fact that at higher pyrophosphate concentrations there is still a reduction current for the first wave at pH 5.8 indicates that the kinetic reaction may be somewhat faster in this case.

Thus the mechanism for the first wave appears to consist of two steps, dissociation of a ligand followed by electrochemical

(10) J. H. Christie, G. Lauer, and R. A. Osteryoung, *J. Electroanal. Chem.*, **7**, 60–72 (1964).

(11) I. M. Kolthoff and J. J. Lingane, "Polarography," 2nd ed., Interscience, New York and London, 1952, p 81.
(12) J. N. Foster, Thesis, California Institute of Technology, 1965.
(13) P. E. Sturrock, Thesis, Ohio State University, 1960.
(14) P. Delahay, "New Instrumental Methods in Electrochemistry," Interscience, New York, 1954, Chapter 5.

Table II. Test for Kinetic Waves in the Polarograms of a Solution Containing 1.0 m*F* $Cu^{2+}$, 50.0 m*F* $Na_4P_2O_7$, and 1.0*F* $KNO_3$, pH adjusted with dilute $HNO_3$ Solution

| Wave | $P_{total}$, cm Hg | $P_{corrected}$, cm Hg | pH = 9.20 $i_{limiting}$, μA | pH = 9.20 $i_l/(P_{corr.})^{1/2}$ | pH = 5.80 $i_{limiting}$, μA | pH = 5.80 $i_l/(P_{corr.})^{1/2}$ |
|---|---|---|---|---|---|---|
| | 25.0 | 23.5 | 0.12 | 0.025 | 2.67 | 0.550 |
| First | 36.0 | 34.5 | 0.13 | 0.022 | 2.82 | 0.480 |
| $E_{1/2}$ = − 0.24 volt *vs.* SCE | 49.0 | 47.5 | 0.12 | 0.017 | 2.97 | 0.431 |
| | 64.0 | 62.5 | 0.12 | 0.015 | 3.01 | 0.380 |
| | 25.0 | 23.5 | 5.20 | 0.972 | 4.89 | 1.01 |
| Second | 36.0 | 34.4 | 6.61 | 0.972 | 5.95 | 1.01 |
| $E_{1/2}$ = − 1 volt *vs.* SCE | 49.0 | 47.4 | 8.30 | 0.971 | 7.42 | 1.08 |
| | 64.0 | 62.4 | 10.92 | 0.971 | 9.42 | 1.19 |

reduction of the 1:1 complex. This is the mechanism proposed by Foster (*12*) for the reduction of the most basic form of the complex, but the evidence contained herein demonstrates that some of the protonated forms of the 2:1 complex are also either not reducible or else have their reduction waves influenced by the presence of other ions. The combination of the influence of the pyrophosphate concentration on the reduction current for the first wave and the variation of diffusion current with mercury height indicates that the 2:1 complexes are not directly reducible except either in very acidic solution or when the electrode potential is at least −0.6 volt *vs.* SCE.

In addition to the kinetic effects on the reaction, the double layer also exerts an influence on the reaction, as can be seen from the variations of the current with the concentration of the supporting electrolyte, $KNO_3$, as discussed below. From a combination of the ideas of Foster (*12*) and the present authors, the proposed overall reaction for the first wave is the sum of

$$CuH_j(P_2O_7)_2^{j-6} \underset{\vec{v}}{\overset{\leftarrow v}{\rightleftharpoons}} CuH_m(P_2O_7)^{m-2} + H_{m-j}P_2O_7^{m-j-4} \quad (4a)$$

and

$$CuH_m(P_2O_7)^{m-2} + 2e^- \underset{}{\overset{k_a^\circ}{\rightleftharpoons}} Cu + H_mP_2O_7^{m-4} \quad (4b)$$

By employing the stability constants for the formation of the complex species (*13*), it can be shown that in the presence of a 50-fold excess of the ligand the 2:1 complexes predominate greatly in the bulk solution, so that the reduction current at the lower potentials at either pH must be preceded by the dissociation step.

**Electrochemical Kinetic Parameters.** In all of these experiments, a constant absolute concentration ratio of 2:1 m*F* pyrophosphate to copper was maintained. Potential step experiments upon these solutions employing an amalgam electrode allowed the determination of the apparent exchange current densities, $i_a^\circ$, and the apparent electrochemical rate constants, $k_a^\circ$. The photographs of the oscilloscopic traces were treated according to the method of Oldham and Osteryoung (*15*) for calculation of the zero-time current density, $i_0$. The method principally employed here was the direct drawing of tangents to the current–time curves on the photographs. This method yielded more consistent results than the method of drawing of tangents to curves drawn through transposed sets of $i - t^{1/2}$ points. As pointed out by Delahay (*16*), extrapolation to $t = 0$ corresponds to equilibrium for the chemical step, allowing the calculation of the electrochemical kinetic parameters even if a preceding chemical reaction occurs. As suggested by Allen and Hickling (*17*), the current-overvoltage ($i - \eta$) characteristic was employed in the exponential form

$$B = 2.303 \log \frac{i_0}{1 - \exp(nf\eta)} = 2.303 \log i_a^\circ - \alpha nf\eta \quad (5)$$

where $n$ is the number of electrons involved in the reduction, and $\eta$ is the overvoltage defined by the relation $\eta = E - E_e$, $E_e$ being the formal equilibrium potential. The quantity $f$ is defined by $f = F/RT$. The terms $F$, $R$, $T$, and $\alpha$, the transfer coefficient, have their usual thermodynamic significances. Plots of $B$ *vs.* $\eta$, when extrapolated to $\eta = 0$, have a slope of $\alpha nf$ and an intercept of 2.303 log $i_a^\circ$. The values of $i_a^\circ$ and $\alpha$ resulting from these calculations are listed in Table III, along with the values of $k_a^\circ$ calculated from the expression

$$i_a^\circ = nFk_a^\circ C_{Ox}^{1-\alpha} C_{Red}^{\alpha} \quad (6)$$

For each calculation of $k_a^\circ$, the value of $\alpha$ used was that obtained from the corresponding $B$ *vs.* $\eta$ plot.

The concentrations of the reducible 1:1 species were calculated from the equilibrium constants for the copper–pyrophosphate system as reported by Schupp, Sturrock, and Watters (*2*), even though their determinations were made with alkali cation-free solutions. With the 2:1 ratio of pyrophosphate to copper, appreciable concentrations of the 1:1 complex

Table III. Apparent Electrochemical Kinetic Parameters for the Reduction of the Copper(II) Pyrophosphate Complex

| Salt conc. | pH | $E_e$, volts | $i_a^\circ \times 10^3$, amp $cm^{-2}$ | $k_a^\circ \times 10^2$, cm $sec^{-1}$ | $\alpha$ |
|---|---|---|---|---|---|
| 1.0*F* | 9.34 | − 0.137 | 0.596 | 1.04 | 0.39 |
| | 8.24 | − 0.073 | 2.86 | 4.98 | 0.38 |
| | 5.82 | − 0.029 | 5.04 | 3.98 | 0.39 |
| | 3.02 | + 0.039 | 6.02 | 2.32 | 0.14 |
| | 2.99 | + 0.009 | 6.92 | 3.90 | 0.27 |
| 0.5*F* | 9.60 | − 0.150 | 0.339 | 0.800 | 0.20 |
| | 5.17 | − 0.021 | 7.98 | 6.22 | 0.37 |
| | 3.02 | + 0.006 | 7.31 | 4.30 | 0.36 |
| 0.1*F* | 9.78 | − 0.179 | 4.28 | 10.1 | 0.22 |
| | 5.84 | − 0.063 | 18.5 | 13.7 | 0.74 |
| | 2.98 | + 0.004 | 7.39 | 4.41 | 0.48 |
| 0.05*F* | 8.96 | − 0.143 | 1.93 | 2.48 | 0.58 |
| | 5.77 | − 0.056 | 2.01 | 1.54 | 0.50 |
| | 3.00 | + 0.021 | 1.57 | 0.94 | 0.48 |

(15) K. B. Oldham and R. A. Osteryoung, *J. Electroanal. Chem.*, 11, 397 (1966).

(16) P. Delahay, "Advances in Electrochemistry and Electrochemical Engineering," Vol. 1, P. Delahay, Ed., Interscience, New York, 1969, p 245.

(17) P. L. Allen and A. Hickling, *Trans. Faraday Soc.*, 53, 1626 (1957).

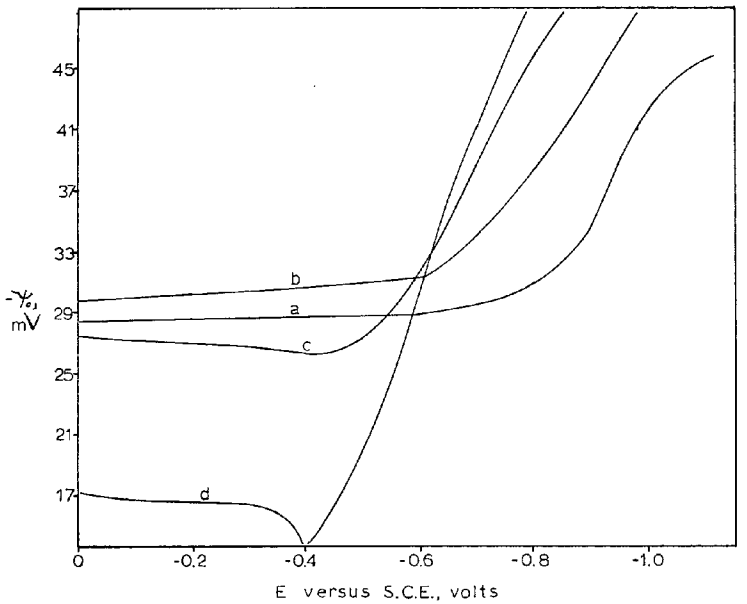


**Figure 6. Plots of $\psi_0$ *vs.* $\phi$ considering specific adsorption for a series of solutions having $[P_2O_7^{4-}] = 50.0$ m*F*, $[Cu^{2+}] = 1.00$ m*F*, pH 9.18**

*a.* $[KNO_3] = 1.0F$
*b.* $[KNO_3] = 0.5F$
*c.* $[KNO_3] = 0.2F$
*d.* $[KNO_3] = 0.1F$

exist in solution. In the case of the pH nine solution, 16% of the copper is calculated to be in the form of the reducible 1:1 complex. In the pH 5.8 solutions, 62% of the copper is in the form of the 1:1 complex. It is also possible to obtain approximate values for the ratio of the two forms of the complex (1:1 to 2:1) from measurements of the ratio of the first and second polarographic plateaus, although the kinetic contribution should lead to a high result. A reasonable check of the pH 9 case is obtained from Figure 1, Curve *a*, by determining that the polarographic value of the ratio 1:1/2:1 is 23%. However, a similar analysis for the pH 5.8 case indicates less than 43% as the 1:1 complex. This discrepancy is probably due to the inapplicability of the literature values of the equilibrium constants to the $KNO_3$ media.

The tabulated values for $k_a^0$ for the intermediate and low pH solutions all either equal or exceed the value $4.5 \times 10^{-2}$ cm $sec^{-1}$ given by Randles (*18*) for the reversible reduction of copper(II) from 1*F* $KNO_3$ solution. It is noteworthy that the reduction reaction appears to have the greatest rate at the intermediate pH. The conclusion of greatest interest, however, is that all of the values of the heterogeneous rate constant are sufficiently large to indicate that in no case is the reduction of the 1:1 complex either polarographically irreversible or the rate determining step of the overall reaction. The criterion for polarographic reversibility, as indicated by Delahay (*14*), is that any reaction with a $k_a^0$ of at least $10^{-2}$ cm $sec^{-1}$ is polarographically reversible.

When double layer corrections were applied to these data some interesting results were obtained. The site of reduction was assumed to be the outer Helmholtz plane, making possible use of $\psi_0$, the potential drop across the entire diffuse double layer. Values for $\psi_0$ were calculated from the Gouy–Chapman theory by employing data of Payne (*8*), who reported the specifically adsorbed charge $q^1$ as a function of electrode charge $q$, and the potential of the electrode as a function of the charge on the electrode at various values of the $KNO_3$ concentration. These data were utilized to obtain values for $\psi_0$ *vs.* $E$ and $KNO_3$ concentration through the following procedure. It was assumed (a) that no specific adsorption of pyrophosphate occurred at any potential more negative than zero *vs.* SCE, and (b) that neither the presence nor the concentration of the pyrophosphate ion influenced the adsorption characteristics of the nitrate ion. A modified form of the Gouy–Chapman equation (*19*) was written as

$$q + q^1 = A' F(c_i, z_i, \psi_0) \tag{7}$$

where $c_i$ and $z_i$ are, respectively, the concentrations and charges, with sign, of the various species present, and

$$A' = \left(\frac{RT\epsilon}{2\pi}\right)^{1/2} \tag{8}$$

$\epsilon$ being the dielectric constant. Values of $q + q^1$ for a particular solution containing definite amounts of the several electrolytes were employed to calculate values for the function $F(c_i, z_i, \psi_0)$. In turn, for each of the same solutions values for the function $F$ were calculated from Equation 7 for integral multiples of $\psi_0 = 10$ mV, and smooth working curves were

(18) J. E. B. Randles and K. W. Somerton, *Trans. Faraday Soc.*, **48**, 951 (1952).

(19) D. L. Chapman, *Phil. Mag.*, **25**, 475 (1913).

Table IV. Range of Values for $i_t^\circ$ and $k_t^\circ$ for Various Values of $z$

Units: $i_t^\circ$ in (amps cm$^{-2}$)
$k_t^\circ$ in cm sec$^{-1}$

| | pH | − 3 | − 2 | − 1 | 0 | + 1 | $\alpha$ |
|---|---|---|---|---|---|---|---|
| $i_t^\circ$ | 9 + | $1.43 \times 10^{-1}$ | $2.80 \times 10^{-2}$ | $7.59 \times 10^{-3}$ | $2.03 \times 10^{-3}$ | $5.48 \times 10^{-4}$ | 0.2 |
| $k_t^\circ$ | | 2.47 | $6.66 \times 10^{-1}$ | $1.81 \times 10^{-1}$ | $4.85 \times 10^{-2}$ | $1.31 \times 10^{-2}$ | |
| $i_t^\circ$ | 3 | | $2.49 \times 10^{-1}$ | $6.93 \times 10^{-2}$ | $1.82 \times 10^{-2}$ | $4.91 \times 10^{-3}$ | 0.3 |
| $k_t^\circ$ | | | 1.4 | $3.82 \times 10^{-1}$ | $1.03 \times 10^{-1}$ | $2.78 \times 10^{-2}$ | |

prepared from these data, so that finally there were as many working curves as there had been different solutions. On the appropriate working curve, each of the values of the function $F$ as calculated from Equation 7 was located, giving a value for $\psi_0$ at each $KNO_3$ concentration and electrode potential $\phi$ of interest, where $\phi$ is defined by

$$\phi = E - E_z \tag{9}$$

$E_z$ being the potential at which $q = 0$. Plots of these values for $\psi_0$ are depicted in Figure 6. Even for positive values of $\phi$, $\psi_0$ remains considerably negative, and varies less with $KNO_3$ concentration than expected.

The zero-time current densities, $i_0$, were replotted as a function of $(\psi_0 - \eta)$ according to a modified form of Equation 5.

$$B = 2.303 \log \frac{i_0}{1 - \exp(nf\eta)} = 2.303 \log i_t^\circ + \alpha_t nf(\psi_0 - \eta) - zf\psi_0 \tag{10}$$

where $\alpha_t$ and $i_t^\circ$ are the so-called true values of the transfer coefficient and exchange current density, respectively. Values for these two parameters were determined from the slope and intercept of plots of $B$ vs. $(\psi_0 - \eta)$, on the assumption that for the range of values of $\eta$ taken, $\psi_0$ remains constant. The validity of this assumption is proven by observation of Figure 6 which indicates that for the potential region within which all of the potential step experiments were performed, the value of $\psi_0$ for a given solution is virtually independent of potential. One other difficulty arose with the use of Equation 10, in that a value must be specified for $z$ in order to calculate $i_t^\circ$. Because the value for $z$, the charge on the reducible species, was thought to be an integer, an attempt was made to determine what $z$ value between +3 and −3 would make $B$ at $\eta = 0$ invariant for a series of solutions identical except for the concentration of $KNO_3$ present. At constant $\psi_0$ and pH, all of the terms in Equation 10 are constant with respect to the concentration of $KNO_3$ except the value of $i_0$. Because of random error in the data and the subsequently calculated parameters, no constant value for $z$ was found at any of the pH values employed. However, it is still possible to calculate a range of values for $i_t^\circ$, and subsequently for $k_t^\circ$, the true value of the heterogeneous rate constant, based on the assumption of a reasonable range of values for $z$. This range of values for $z$ was taken as −3 to +1. The results are presented in Table IV.

Positive values for $z$ at pH 9 are unexpected, both for chemical reasons and because it is seen from the Gierst analysis that the value of $\psi_0$ affects the reduction of the complex and that the charge on the reducible species is negative. By considering ion-pairing, it is possible to postulate 1:1 complex ions with charges of 0 or −1, the most probable species being $CuKP_2O_7^{1-}$. Therefore, the most probable value for the "true" kinetic parameters are those calculated from the assumption that $z = -1$.

For the pH 3 case, no unique value is determinable for $z$.

Experimental values for $\alpha$, both true and apparent, varied principally between 0.2 and 0.5, and seemed to be nearly the same for a given set of experimental conditions, whether or not double-layer corrections were applied. Values appeared to increase somewhat with decreasing $KNO_3$ concentrations, but there was no certain trend in this fashion. Because of the uncertainties about both the nature and determination of $\alpha$, its value is reported here as 0.2 in alkaline solution and 0.3 in acidic solution. The values for the kinetic parameters for the pH 9 case now indicate that the reduction of the 1:1 complex is inherently rather fast. Although admittedly the quality of these double-layer corrections is less than perfect, they still serve to illustrate the effects of various experimental parameters on the reaction, as well as to point out the effects of ignoring these parameters. Moreover, the double-layer corrections confirm, not contradict, the original assumption that the electrochemical reaction is in all cases fast enough not to be the rate-determining step of the overall reaction.

Chronocoulometry was applied as an independent determination of the value of $k_a^\circ$ (*20*). This study was made upon the complex in 1$F$ $KNO_3$ solution at pH 9. Because 16% of the complex was present in the reducible form, it was assumed that once again the kinetic contribution to the current could be ignored for sufficiently small potential steps. A series of $Q = 0$ intercepts, $t_i^{1/2}$, for different sized potential steps allowed the calculation of a series of values for $\lambda$, according to the equation of Christie, Lauer, and Osteryoung (*10*).

$$\lambda = \frac{\pi^{1/2}}{2t_i^{1/2}} \tag{11}$$

Subsequently, as seen in Figure 7, plotting of $\lambda$ vs. $(E - E_t) = \eta$ according to

$$\log \lambda = \log k_a^\circ - 1/2 \log D_{Ox} (-1/2.303)\, \alpha nf\eta \tag{12}$$

and extrapolation to $\eta = 0$ allowed the determination of $k_a^\circ$ as $6.08 \times 10^{-3}$ cm sec.$^{-1}$. A value of $9 \times 10^{-6}$ cm$^2$ sec$^{-1}$ for $D_{Ox}$, the diffusion coefficient of the oxidized species, was calculated from polarography. This value for $k_a^\circ$ agrees with the corresponding one from the potential step method within a factor of 2, tending to confirm the validity of the potential step data.

**Chemical Kinetic Parameters.** From the order of magnitude of the electrochemical rate constant, it was assumed that under polarographic conditions any slow preceding chemical reaction would be rate determining. The reverse chemical reaction would be a second-order process, thus causing the reduction current to decrease with increasing ligand concentration wherever the reaction is slow. This behavior was noted for both pH 9.2 and pH 5.8 solutions of the complex system. General equations for the system are

(20) G. W. Higgins, Thesis, Georgia Institute of Technology, 1966.

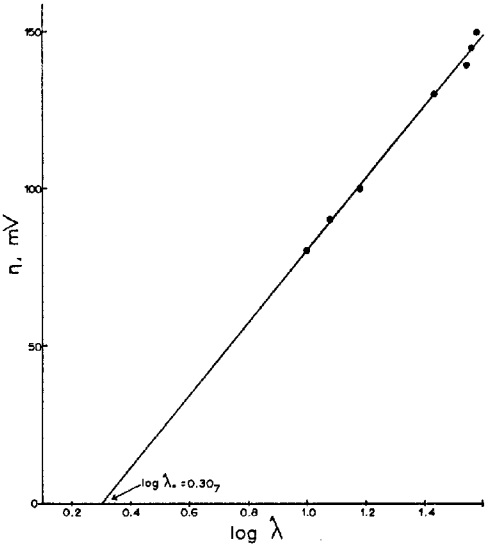


**Figure 7. Chronocoulometric determination of $k_a^\circ$ from λ according to Equation 12**

**Solution had $[KNO_3]$ = 1.0*F*, $[P_2O_7^{4-}]$ = 2.00 m*F*, $[Cu^{2+}]$ = 1.00 m*F*, pH = 9.18**

$$ML_2 \rightleftarrows ML + L \tag{13}$$

$$K' = \frac{\vec{v'}}{\overleftarrow{v'}} = \frac{[ML]\,[L]}{[ML_2]} \tag{14}$$

The $K'$, $v'$, and $v'$ are related to the corresponding first-order parameters in the following manner:

$$\vec{v'} = \vec{v} \qquad \overleftarrow{v'} = \overleftarrow{v}/[L] \qquad K' = K[L] \tag{15}$$

For kinetic polarograms one may write, after Delahay (*14*),

$$I/I_d = \pi^{1/2}\,\lambda \exp(\lambda^2)\, erfc\,(\lambda) \tag{16}$$

where

$$\lambda = (\vec{v'}\,K'\,t)^{1/2} \tag{17}$$

for the 1st order/2nd order reaction indicated above. Equation 16 is derived on the assumption that equilibrium for reaction 13 is far to the left. Because of this assumption, the results of this derivation were only used for systems containing an appreciable excess concentration of the pyrophosphate ligand. By substituting the relations of Equation 15 into 17, the dependence of λ upon pyrophosphate concentration, [Py], may be derived as

$$\lambda = (\vec{v}\,K\,[Py]\,t)^{1/2} \tag{18}$$

Squaring and taking the derivative gives

$$\frac{d(\lambda^2)}{d[Py]} = \vec{v}\,K\,t \tag{19}$$

Values of λ were obtained as a function of $I/I_d$ according to the table of Koutecky (*21*). From the slope of plots of $\lambda^2$ *vs.* [Py] it was possible to determine the kinetic product $\vec{v}K$ uncorrected for double layer effects. The product is not separable by solely polarographic techniques. Application

(21) J. Koutecky, *Chem. Listy*, **47**, 323 (1953).

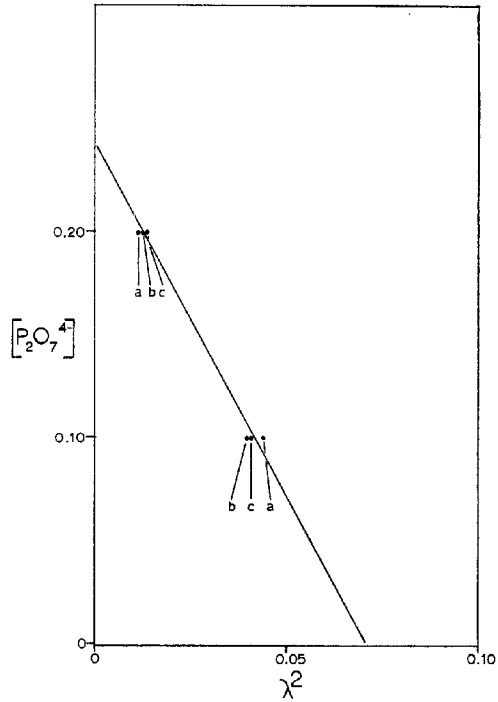


**Figure 8. Determination of $\vec{v}K$ from a plot of $\lambda^2$ *vs.* $[P_2O_7^{4-}]$ according to Equation 19**

**Solution had $[KNO_3]$ = 1.0*F*, $[Cu^{2+}]$ = 1.00 m*F*, pH = 5.80**
***a.*** **E = −0.600 volt *vs.* SCE**
***b.*** **E = −0.500 volt *vs.* SCE**
***c.*** **E = −0.400 volt *vs.* SCE**

of this technique to the pH 5.8 case yielded a value of 0.11 $sec^{-1}$ for $\vec{v}K$ (See Figure 8). For the reaction

$$CuHPy_2^{5-} \rightleftarrows CuPy^{2-} + HPy^{3-} \tag{20}$$

log $K_{ass.}$ = 2.41 (*22*), and calculation of $\vec{v}$ gives a value of about 2.8 $sec^{-1}$, not a fast reaction. Sufficiently accurate data were not obtained for the pH 9 case to permit the calculation of $\vec{v}$.

Because it is not feasible to apply double-layer corrections directly to these results, the Gierst type of analysis was employed. Values of an apparent rate constant $v^*$ were calculated from the polarographic $I/I_d$ according to the formula of Koutecky (*21*). The total potential difference, $\phi$, between the electrode and the solution is given by the relation

$$\phi = \phi' + \psi_o \tag{21}$$

where $\psi_o$ is the potential drop across the diffuse double layer and $\phi'$ is the primary driving force of the reaction. Plots of $v^*$ *vs.* $\phi$ for several values of the $KNO_3$ concentration were placed on the same graph with plots of $\psi_o$ *vs.* $\phi$ at the same values of the $KNO_3$ concentration. In accordance with the Frumkin Equation (*23*)

$$v^* = v^\circ \exp(-\alpha nf\phi') \exp(-zf\psi_o) \tag{22}$$

(22) J. I. Watters and A. Aaron, *J. Amer. Chem. Soc.*, **75**, 611 (1953).
(23) A. N. Frumkin, O. A. Petry, N. V. Nicolaeva-Fedorovich, *Electrochim. Acta*, **8**, 177 (1963).

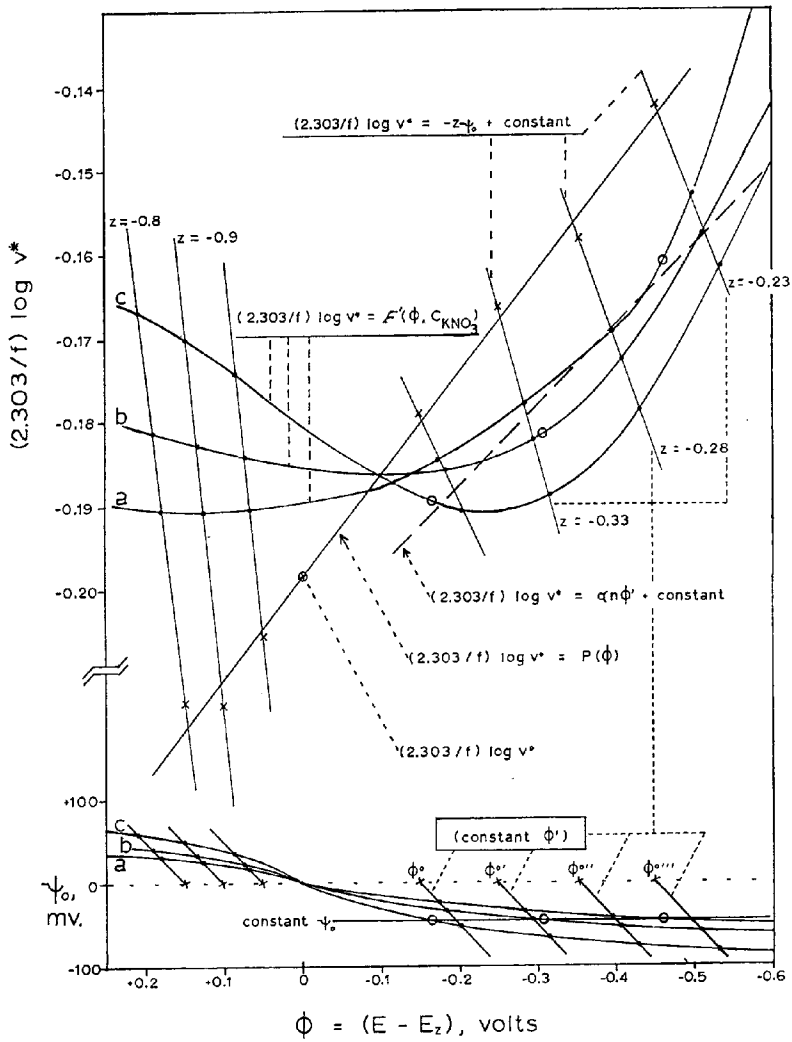


**Figure 9. Polarographic data corrected for the influence of the electrical double layer, according to the method of Gierst**

Solutions had $[P_2O_7^{4-}] = 2.00$ m$F$, $[Cu^{2+}] = 1.00$ m$F$, pH = 9.18
*a.* $[KNO_3] = 1.0F$
*b.* $[KNO_3] = 0.5F$
*c.* $[KNO_3] = 0.2F$

it was desirable to determine separately the dependence of the electrode reaction on $\psi_o$ and $\phi'$. From arbitrarily chosen points, $\phi^o$, along the $\phi$ axis for $\psi_o = 0$, 45° lines were drawn through the $\psi_o$ curves as indicated in Figure 9. These 45° lines represent the condition of constant $\phi'$. The abscissa values of the resulting intersections were then transposed to the respectively corresponding $v^* = F'(\phi, C_{KNO_3})$ curves. Each set of the latter points corresponding to the same $\phi'$ value obeys the relation

$$(2.303/f) \log v^* = -z\psi_o + \text{constant} \qquad (23)$$

Thus, the slope of the line of constant $\phi'$ gives $-z$. The ordinate of the point of intersection of the line of constant $\phi'$ with its corresponding value of $\phi^o$ gives the value of the apparent rate constant, $v^*$, at $\phi = \phi^o$. The locus of several such ordinates is the line $(2.303/f) \log v^* = p(\phi)$, and the extrapolation of this line to $\phi = 0$ gives the value of $v^o$ as $(2.303/f) \log v^o$.

If a horizontal line representing constant $\psi_o$ is drawn through the $\psi_o$ *vs.* $\phi$ curves of a plot such as Figure 9, the abscissa values of the resulting intersections may be transposed to the corresponding $v^*$ *vs.* $\phi$ plots as in the previous case. The locus of the latter set of points is a line representing a constant $\psi_o$ and having the slope $\alpha n$. Thus it is theoretically possible, from polarographic data, to calculate the true overall rate constant, $v^o$, the transfer coefficient for the electron trans-

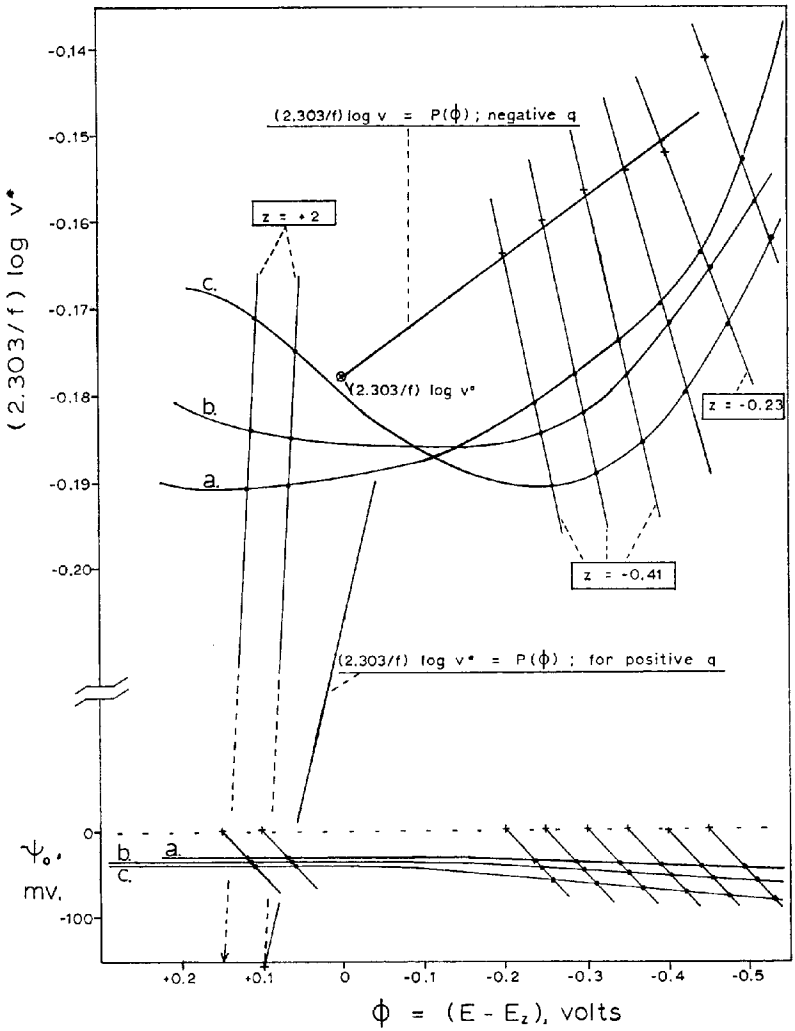


**Figure 10. Polarographic data corrected for the influence of the electrical double layer including specific adsorption of nitrate**

**$[P_2O_7^{4-}]$ = 2.00 m*F*, $[Cu^{2+}]$ = 1.00 m*F*, pH = 9.18**

***a.*** **$[KNO_3]$ = 1.0*F***

***b.*** **$[KNO_3]$ = 0.5*F***

***c.*** **$[KNO_3]$ = 0.2*F***

fer reaction, $\alpha$, the charge on the reducible species, $z$, and the number of electrons involved, $n$, in terms of the influence of both components of the total electrode potential. Plots of the type described were prepared both with and without consideration of the specific adsorption of nitrate.

Figure 10 was constructed from data taken for solutions at pH 9.18 and containing 1.0 m*F* Cu(II), 2.0 m*F* sodium pyrophosphate, and various concentrations of potassium nitrate, and for which the specific adsorption of nitrate has been accounted in the calculation of the potential of the Outer Helmholtz Plane. Figure 9 is the same as Figure 10 except that the specific adsorption of nitrate was ignored in the calculation of the potential of the Outer Helmholtz Plane. For negative values of $\phi$, Figures 9 and 10 lead to essentially the same results. Values of $z$ range between $-0.23$ and $-0.41$. Similar analysis of solutions containing 50.0 and 100 m*F* pyrophosphate, but otherwise the same, give $z$ values of $-1.3$ and $-1.6$, respectively. These results indicate that, in the second wave, both the 1:1 and the 2:1 complexes are reduced and that there exists a high degree of ion pairing between the complexes and potassium ions. The change of $z$ values from $-0.2$ to $-1.6$ with the increasing pyrophosphate concentration strongly suggests that on the average two potassium ions are associated with each pyrophosphate ligand. For positive values of $\phi$, the results obtained from Figures 9 and 10 are in conflict. Figure 10, which considers specific adsorption of nitrate, indicates a $+2$ value for $z$ while Figure 9 indicates a $-1$ value of $z$. Neither of these results seems reasonable and it must be concluded that the calculations of the potential at the Outer Helmholtz Plane, in the presence of specific adsorption, are significantly in error, probably because of the inaccuracy of the assumption that the pyrophosphate ion does not

Table V. Kinetic Parameters Derived from Gierst Analysis of Polarograms

The quantities $z$ and $\alpha$ are dimensionless. The units of $\vec{\nu}K$ and $\nu^0$ depend on the exact order of the forward chemical reaction.

| | | | | Second Wave | | |
|---|---|---|---|---|---|---|
| pH | $[KNO_3]$ | [Py] | z | $\alpha$ | $\nu^0$ | $\vec{\nu}K$ |
| 9 + | | 2.00 m$F$ | − 0.41 | 0.04 | $8.9 \times 10^{-4}$ | 0.089 |
| | 1.0, 0.5, 0.2, 0.1, $F$ | 50.00 m$F$ | − 1.3 | 0.44 | $5.5 \times 10^{-11}$ | $3.4 \times 10^{-16}$ |
| | | 100.0 m$F$ | − 1.6 | 0.37 | $1.1 \times 10^{-9}$ | $2 \times 10^{-13}$ |
| 5.80 | | 2.00 m$F$ | + 0.9 to + 0.6 | $0.05_4$ | $1.7 \times 10^{-4}$ | $3.3 \times 10^{-3}$ |

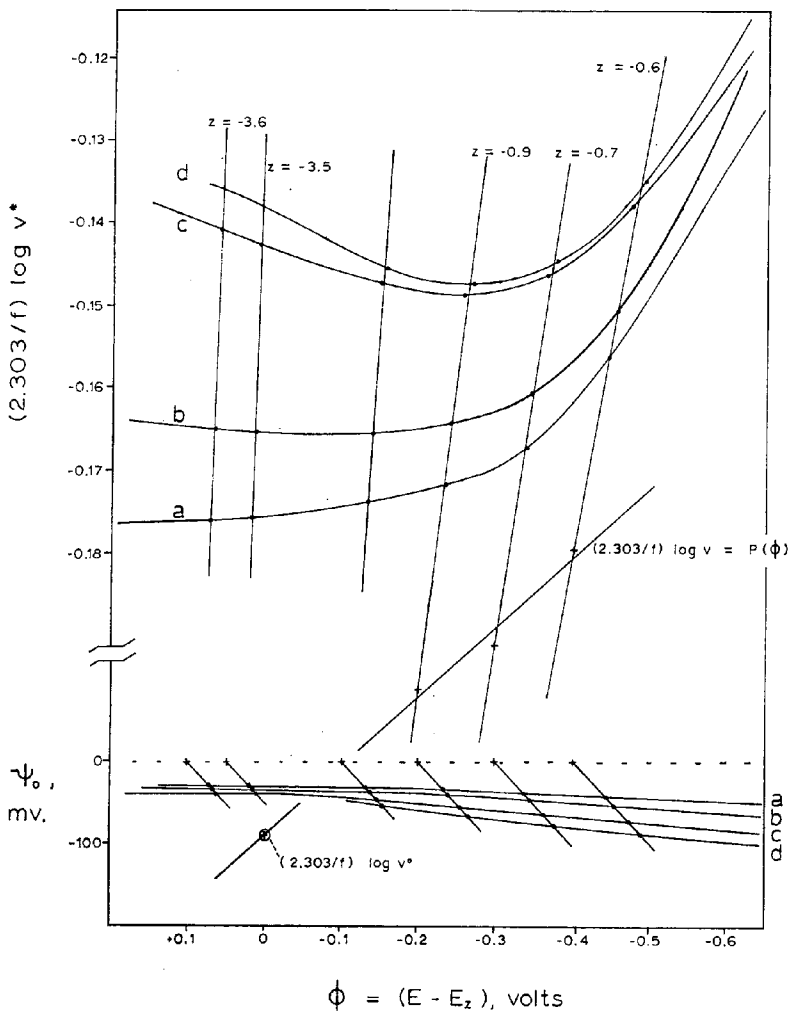


Figure 11. Polarographic data corrected for the influence of the electrical double layer including specific adsorption of nitrate

$[P_2O_7^{4-}] = 2.00$ m$F$, $[Cu^{2+}] = 1.00$ m$F$, pH = 5.80
*a.* $[KNO_3] = 1.0F$
*b.* $[KNO_3] = 0.5F$
*c.* $[KNO_3] = 0.2F$
*d.* $[KNO_3] = 0.1F$

influence the adsorption characteristics of the nitrate ion. It has been demonstrated (*1*, *8*) that the presence of the fluoride ion, also known to be hardly adsorbed at the point of zero charge, has significant influence over the adsorption characteristics of the nitrate ion. Moreover, the fluoride ion is singly charged, whereas the pyrophosphate ion is more highly charged, the average value depending upon the pH of the solution. The presence of multicharged anions, even when not specifically adsorbed, causes the $\psi_0$ *vs.* $\phi$ curve calculated from the Gouy–Chapman theory to be lower for $q > 0$ than the corresponding curve for an equal concentration of singly charged anions, and a series of curves representing $\psi_0$ *vs.* $\phi$ and concentration will be quite close together in the potential region where $q > 0$ (see Figure 10). Any deviation from the assumed adsorption characteristics will therefore cause a significant error in the calculated double layer effects. This difficulty seems to be the cause of the anomalous results for $z$ in the potential region where $q > 0$.

The situation at pH 5.80 is quite different from that at pH 9.18. The mercury pressure dependence of the height of the first wave clearly indicates that this is a kinetic wave, as is verified by the decrease in height of the first wave as the pyrophosphate concentration is increased. However, the dependence of current on concentration of $KNO_3$ indicates that the reducible species is positively charged. This positive value for $z$ is clearly indicated by the region of negative $\phi$ of Figure 11, from the fact that, at any constant $\phi$ value where $q < 0$, the current increases as the value of $\psi_0$ increases because of the decreasing supporting electrolyte concentration. The assumptions concerning the exact nature of the adsorption are essentially inoperative in reaching the conclusion about the sign of $z$, because the same result was obtained from calculations employing two different sets of electrocapillary data, both with and without the consideration of specific adsorption. There is the possibility, however, that the assumptions concerning the reaction site and the thickness of the reaction layer are in error. While the equilibrium constants previously obtained in alkali free solutions cannot be rigorously applied under the present conditions, it seems evident that a surprisingly high degree of ion pairing exists, causing a positively charged species—such as $CuH_2KP_2O_7^+$—to be present. It seems inconsistent to postulate for this case a completely dissociated reactant as would have to be done to explain the positively charged species in the absence of ion pairing.

The kinetic parameters obtained from the Gierst-type analysis of the dc polarograms, considering specific adsorption of nitrate, are summarized in Table V. The quantity $\vec{v}K$ was calculated from the expression (*3*)

$$v^\circ = (\vec{v}K\,D)^{1/2} \qquad (24)$$

where $D$ is the diffusion coefficient. For the reaction in Equation 13, the equilibrium constant $K$ should be multiplied by [Py] to obtain the actual equilibrium constant $K'$ (see Equation 15).

RECEIVED for review September 8, 1968. Accepted January 21, 1969. Research supported in part by PRF grant 1516 A5 to P.E.S. Presented in part, Division of Analytical Chemistry, 153rd National Meeting, ACS, Miami Beach, Fla., April 1967.

# Electrochemical Reduction Products of Chromium(VI) in Molten Lithium Chloride–Potassium Chloride Eutectic

**J. H. Propp[1] and H. A. Laitinen**

*Department of Chemistry and Chemical Engineering, University of Illinois, Urbana, Ill. 61801*

**The electrochemical reduction product of $K_2CrO_4$ dissolved in a LiCl-KCl eutectic containing dissolved $MgCl_2$ is characterized as a single, unstoichiometric compound having the empirical formula $Li_xMg_yCrO_4$ where $x + 2y = 5$. The values of $x$ and $y$ are found to depend upon the conditions of the electrolysis. X-ray powder diffraction shows the compound to have a face-centered cubic structure with an "a" parameter of 4.182 Å. The thermal and pressure stability of the compound are also investigated. The electrochemical reduction of $K_2Cr_2O_7$ or $CrO_2Cl_2$ in the presence of $MgCl_2$ is complicated by chemical attack of the cathode causing a mixture of compounds to be deposited on the electrode surface. Also, oxide ion is released to the bulk melt altering the oxygen to chromium ratio of the Cr(VI) species being transported to the electrode surface.**

PREVIOUS WORK in this laboratory by Laitinen and Bankert (*1*) has shown that the electrochemical reduction of $K_2CrO_4$ dissolved in a LiCl–KCl eutectic results in the formation of an insoluble film on the surface of the platinum cathode. The chemical composition of the film was established to be $Li_5CrO_4$ using spark emission spectrometry. In the presence of divalent cations such as Mg(II) or Ca(II), the reduction potential of chromate was shifted from −1.0 V *vs.* the Pt/Pt(II) reference to −0.2 V and −0.4 V, respectively, and the composition of the insoluble film was altered. Attempts to establish the composition of these new deposits were not successful because of large and erratic blanks which made the spectrometric data unreliable.

In the work presented here, the chemical composition and structure of the reduction product of chromate in the presence of Mg(II) are investigated. Preliminary results are also given for the electrochemical reduction of Cr(VI) species in the presence of Mg(II) which contain a lower oxygen-to-chromium ratio, such as $K_2Cr_2O_7$ and $CrO_2Cl_2$.

## EXPERIMENTAL

**Apparatus.** A Sargent Model IV coulometric current source was used for the constant current generation of the platinum reference electrode and for the constant current electrolytic preparation of the electrode deposits.

The constant current source used for the coulometric determination of the chromium content of the electrode

[1]Present address, Wisconsin State University, Oshkosh, Wis. 54901

(1) H. A. Laitinen and R. D. Bankert, ANAL. CHEM., **39**, 1790 (1967).

deposits and for the chronopoteniometric studies was constructed by use of the Heath Model EUW-19A operational amplifier system and the Heath Model EUA-19-4 operational amplifier stabilizer. The instrument had a current range of approximately 10 $\mu$A to 20 mA and was capable of reverse current chronopotentiometry. The details of its construction are given elsewhere (*2*).

A Tektronix 532 oscilloscope served to record chronopotentiograms and to monitor the potential of the working electrode during the preparative electrolysis studies.

A Beckman Model DU quartz spectrophotometer with flame attachment employing a Beckman Model 4020 oxyhydrogen atomizer burner was used for the flame photometric determination of lithium in the electrode deposit. The lithium emission was detected using a 1P28 photomultiplier tube mounted in a Heath Built Model EUA 20-20 photohead. The resulting photomultiplier current was measured by a Heath Built Model EUA-20-28X log/linear current module attached to a Heath Built Model EUA-20A servo recorder.

X-ray powder patterns of the electrode deposits were made with an 11.47-cm camera using CuK$\alpha$ radiation. The Cu tube was mounted in a Norelco generator.

Other apparatus employed in this laboratory for the manipulation of the molten salt has been previously described (*1*).

**Electrodes.** The Pt/Pt(II) 1*M* reference electrode which has been characterized previously (*3*) was used throughout this work. The construction of 0.5-cm$^2$ platinum flag electrodes used in the chronopotentiometric studies was the same as that described by Laitinen and Bankert (*1*).

A spectrometric carbon rod (1/8 inch in diameter) generally served as the counter electrode in all electrochemical investigations in the melt.

The cathode used for the preparation of the electrode deposit was constructed from 52-mesh platinum gauze. Each gauze was approximately 1.5 cm on a side and could be conveniently attached and detached from a hook on the supporting electrode. This arrangement permitted the electrode to be weighed before and after electrolysis.

**Chemicals.** All solid chemicals used in this study were reagent grade, vacuum-dried and stored over $Mg(ClO_4)_2$ until use. Anhydrous $MgCl_2$ was prepared by slowly heating the hexahydrate in vacuum to 200 °C over a period of 2 days followed by sweeping of anhydrous HCl through the salt for 5 hours at 500 °C. Analysis of the $MgCl_2$ prepared in this manner for chloride indicated it to be 99.5% pure.

The LiCl-KCl eutectic was prepared and purified by Anderson Physics Laboratories, Inc., Champaign, Ill. The method of purification has been previously described (*4*).

Solid chemicals were added to the melt with a small glass spoon; chromyl chloride was added in an argon gas stream.

**Techniques Employed in Preparation and Analysis of Electrode Deposits.** The gauze electrodes which served as the cathode in the electrolytic reductions were cleaned in boiling, concentrated $HClO_4$, rinsed with distilled water, dried at 130 °C for 24 hours, and stored in a desiccator until use. Because it was found that the electrochemical reduction product of chromate in the presence of Mg(II) adhered very strongly to the gauze electrode, the electrode could be weighed before and after the electrolysis to determine the weight of the deposit. The large surface area gauze electrodes minimized solvent entrapment problems by keeping the current density low (1–5 mA/cm$^2$) and the thickness of the deposit relatively thin. After a sufficient amount of deposit had been electrochemically produced on the electrode surface, the gauze was removed from the molten salt, allowed to cool to room temperature, and excess eutectic dissolved with distilled water. The electrode was dried at 110 °C and weighed to the nearest microgram.

Dissolution of the electrode deposit directly from the platinum gauze was accomplished by a perchloric acid oxidation procedure described by Smith (*5*).

Analytical methods for the determination of Cr, Mg, and Li in the above solution were developed because these three elements appeared to be the only metallic constituents of the deposit as determined by Bankert's spectrometric work (*1*).

The method chosen for the chromium determination was that of Meier, Myers, and Swift (*6*). In this method Cr(VI) is determined by coulometrically generated Cu(I) using a biamperometric end point. The method was tested on known samples and found to be accurate to approximately 0.1% relative error at the concentrations involved.

The magnesium content of the solution was conveniently determined by a simple EDTA titration with Eriochrome Black T as the indicator. The accuracy and precision of this determination was experimentally found to be approximately 0.2%.

The lithium content was determined using flame photometry with a relative error of approximately 1.0%. The Li emission was observed at 670.8 m$\mu$.

## RESULTS AND DISCUSSION

**$K_2CrO_4$–$MgCl_2$–LiCl–KCl System.** When $K_2CrO_4$ is electrochemically reduced at constant current in the presence of $MgCl_2$ a green, adherent deposit is formed on the surface of the platinum gauze cathode. The deposit, which is remarkably resistant to acid attack, can be conveniently dissolved by boiling, concentrated $HClO_4$. Bankert had observed (*1*) that the deposit was insoluble in hot, concentrated $HClO_4$. It was found, however, that dissolution took place if the acid were allowed to boil. According to Smith (*5*), 70% $HClO_4$ becomes an effective oxidant for Cr(III) only after it concentrates to its azeotropic composition (72.5%).

Employing the methods described for the determination of Cr, Mg, and Li in the electrode deposit, several gauze electrodes were electrolytically coated with the reduction product and analyzed. It was of interest to determine if and how the composition of the electrode deposit changed with the conditions of the electrolysis. Three parameters could be conveniently varied—the temperature of the molten salt bath, the current density, and the molar ratio of Mg(II) to Cr(VI) dissolved in the melt. In all of these studies the current density was kept low enough so that the potential of the working electrode never exceeded $-0.4$ V *vs.* the Pt/Pt(II) reference.

Table I clearly shows how the composition of the electrode deposit changes with temperature, while holding the current density and the Mg(II) to Cr(VI) molar ratio constant. The lithium content of the deposit is found to increase substantially when the temperature is increased from 400 to 500 °C. Notice that the Mg(II) content decreases as the Li(I) content increases. The relationship between the Mg(II) decrease and the Li(I) increase can be explained if one observes that the oxygen-to-chromium atomic ratio in the deposit appears to remain constant at a number approaching 4.0. The electrode deposit could then be described by the empirical formula $Li_xMg_yCrO_4$ where $x + 2y = 5$. As seen from the table, typical values of $x$ range between 0.3 and 0.5.

It can also be observed in Table I that the total weight percentages of the metallic oxides is nearly equal to 100% in all cases, indicating that the only anion present is oxide. The

(2) J. H. Propp, Ph.D. Thesis, University of Illinois, 1968.
(3) H. A. Laitinen and W. S. Ferguson, ANAL. CHEM., **29**, 4 (1957).
(4) H. A. Laitinen, R. S. Tischer, and D. K. Roe, *J. Electrochem. Soc.*, **107**, 546 (1960).
(5) G. F. Smith, *Analyst*, **80**, 16 (1955).
(6) D. J. Meier, R. J. Myers, and E. H. Swift, *J. Amer. Chem. Soc.*, **71**, 2340 (1949).

**Table I. Composition of Electrode Deposit as Function of Temperature**

| $[K_2CrO_4] = 0.045M$ | | $[MgCl_2] = 0.176M$ | | $I_0 = 1$ mA/cm² | |
|---|---|---|---|---|---|
| Temperature | Wt % $Li_2O$ | Wt % MgO | Wt % $Cr_2O_3$ | Total wt % | Formula |
| 400 °C | 2.29 | 54.21 | 43.19 | 99.7 | $Li_{0.27}Mg_{2.36}CrO_{3.99}$ |
| 450 °C | 3.22 | 53.73 | 43.78 | 100.7 | $Li_{0.36}Mg_{2.25}CrO_{3.93}$ |
| 500 °C | 4.13 | 51.41 | 43.61 | 99.2 | $Li_{0.50}Mg_{2.22}CrO_{3.97}$ |

**Table II. Composition of Electrode Deposit as Function of $MgCl_2$ Concentration**

Temp. = 450 °C; $I_0 = 1$ mA/cm²

| $[K_2CrO_4]$ | $[MgCl_2]$ | Wt % $Li_2O$ | Wt % MgO | Wt % $Cr_2O_3$ | Total wt % | Formula |
|---|---|---|---|---|---|---|
| $0.059M$ | $0.099M$ | 3.98 | 52.02 | 44.74 | 100.7 | $Li_{0.45}Mg_{2.19}CrO_{3.91}$ |
| $0.051M$ | $0.185M$ | 3.05 | 52.44 | 44.25 | 99.7 | $Li_{0.35}Mg_{2.23}CrO_{3.90}$ |
| $0.037M$ | $0.231M$ | 2.63 | 52.54 | 43.89 | 99.1 | $Li_{0.31}Mg_{2.26}CrO_{3.91}$ |

| Electricity passed to prepare electrode deposit, μeq | Cr(III) found, μeq | Difference, μeq | Pt lost as Pt(II), μeq |
|---|---|---|---|
| 70.93 | 74.12 | 3.19 | 1.80 |
| 70.00 | 71.90 | 1.90 | 2.92 |
| 70.00 | 71.48 | 1.48 | 1.24 |

**Table III. Effect of Current Density on Composition of Electrode Deposit**

$[K_2CrO_4] = 0.034M$; $[MgCl_2] = 0.104M$; Temperature = 450 °C

| Approximate $I_0$ | Wt % $Li_2O$ | Wt % MgO | Wt % $Cr_2O_3$ | Total wt % | Formula |
|---|---|---|---|---|---|
| 1 mA/cm² | 2.78 | 52.02 | 43.01 | 97.8 | $Li_{0.33}Mg_{2.28}CrO_{3.95}$ |
| 2 mA/cm² | 2.32 | 53.23 | 42.37 | 97.9 | $Li_{0.28}Mg_{2.37}CrO_{4.01}$ |
| 4 mA/cm² | 2.20 | 52.65 | 42.58 | 97.4 | $Li_{0.26}Mg_{2.33}CrO_{3.96}$ |
| 10 mA/cm² | 2.12 | 52.72 | 42.67 | 97.5 | $Li_{0.25}Mg_{2.33}CrO_{3.95}$ |

| Electricity passed to prepare electrode deposit, μeq | Cr(III) found, μeq | Difference, μeq | Pt lost as Pt(II), μeq |
|---|---|---|---|
| 100.0 | 106.8 | 6.8 | 3.5 |
| 100.0 | 103.2 | 3.2 | 3.0 |
| 100.2 | 103.9 | 3.7 | 3.8 |
| 100.0 | 105.7 | 5.7 | 3.8 |

100% summation also indicates that the Cr(VI) dissolved in the melt underwent a 3-electron reduction to Cr(III); otherwise the chromium content of the deposit could not adequately be described as $Cr_2O_3$.

The results of changing the molar ratio of Mg(II) to Cr(VI) dissolved in the melt while holding the current density and temperature constant are shown in Table II. The Mg(II) content of the deposit is found to increase as the molar ratio of Mg(II) to Cr(VI) in the bulk melt is increased. Again it is observed that the oxygen-to-chromium atomic ratio is 4 to 1, indicating that no oxide was lost to the bulk melt during the electrolysis. It is interesting that the number of microequivalents of Cr(III) found by analysis generally exceeds slightly the number of microequivalents of electricity passed in the preparation of the electrode deposit. The data in Table II appear to indicate that the excess Cr(III) results from a slight chemical oxidation of the Pt. Because it was observed that only a very small loss of Pt occurred during the $HClO_4$ dissolution, most of the chemical attack of the Pt occurred in the melt. This chemical attack, which was not too serious a problem in the present study, could possibly explain the large and erratic blanks observed by Bankert (*1*) when he attempted to analyze by spark emission spectrometry microgram quantities of the deposit plated onto platinum rods. It should be pointed out that in all cases the weight percentages of the three oxides were calculated from a corrected tare weight of the Pt gauze—*i.e.*, account was taken of the loss in weight of the gauze by the chemical reaction. Generally, this correction, while only 0.2 to 0.3 mg of platinum, was of the order of 5% relative, as seen from Tables II and III.

Table III shows that there is only a small change in the composition of the electrode deposit upon changing the current density over a 10-fold range while holding the other two variables constant. No absolute values for the current densities employed can be given because gauzes of indeterminate surface area were used; however, a reasonable estimate of the range of current densities used would be of the order of 1 to 10 mA/cm². The data show a slight decrease in the Li content of the deposit as the current density is increased. This result strongly suggests that Li(I) is not trapped as an impurity,

**Table IV. X-Ray Powder Pattern of $Li_xMg_yCrO_4$**

| $d$(Å) | $I/I_0$ | $hkl$ | $a$(Å) |
|---|---|---|---|
| 2.4024 | 20 | 111 | 4.166 |
| 2.0819 | 100 | 200 | 4.168 |
| 1.4742 | 60 | 220 | 4.172 |
| 1.2585 | 20 | 311 | 4.178 |
| 1.2049 | 30 | 222 | 4.178 |
| 1.0441 | 20 | 400 | 4.182 |
| 0.9584 | 10 | 331 | 4.182 |
| 0.9339 | 30 | 420 | 4.182 |
| 0.8524 | 30 | 422 | 4.181 |
| 0.8038 | 5 | 511,333 | 4.182 |

for if this were the case an increase in current density would tend to increase the Li(I) content in the deposit.

**X-Ray Powder Diffraction Studies.** A typical X-ray powder pattern for the electrode deposit is shown in Table IV. The deposit shows only a single pattern which can be clearly indexed to a face-centered cubic lattice with an "a" parameter equal to 4.182 Å. This lattice is the same as that assumed by pure MgO, and the powder patterns for the deposit and pure MgO are nearly identical. The experimentally determined "a" parameter for pure MgO, however, is 4.213 Å, so the unit cell for the deposit is slightly smaller. Because the deposit is indicated to be a pure compound and not a mixture, it is not unreasonable to assume that the compound is a solid solution of the three oxides $Li_2O$, $Cr_2O_3$, and MgO.

Kordes and Petzolt (*7*) have in fact prepared a series of solid solutions involving $LiCrO_2$ and MgO by high temperature sintering of the two oxides. They found that in the range from 0 to 40 mole % $LiCrO_2$, the sintered mass gave an X-ray powder pattern which was face-centered cubic with the "a" parameter decreasing from the pure MgO value of approximately 4.22 Å to 4.18 Å. Above 40 mole % $LiCrO_2$, the solid solutions exhibited the hexagonal $LiCrO_2$ structure.

Clearly the compounds prepared by Kordes and Petzolt (*7*) would always have a Li-to-Cr ratio of 1; therefore, the electrode deposit cannot be described exactly by any of their compositions. Still there are many similarities between their solid solutions and the electrode deposit, and it would be of interest to attempt to explain the structure of the electrode deposit in terms of the interpretation offered by Kordes and Petzolt (*7*). These authors state that the Li(I) and Cr(III) ions in their compounds randomly substitute for the Mg(II) ions in a MgO lattice. Because the Mg(II) ions are octahedrally coordinated, this interpretation would require that the Cr(III) and Li(I) ions also be octahedrally coordinated.

In order to determine experimentally if the Cr(III) ions in the electrode deposit occupy sites of octahedral symmetry, an ESR spectrum of the powdered deposit was run. A single, broad, symmetrical, Lorentian peak due to Cr(III) was observed. The "g" value calculated from this spectrum was 1.979 which is in excellent agreement with a previously reported value of 1.980 (*8*) for MgO crystals which had been doped with small quantities of Cr(III). This result may be fortuitous, however, because the concentrations of Cr(III) in the two studies differed greatly. Nevertheless, the ESR data, the X-ray data, and crystal field stabilization arguments would tend to favor an octahedral coordination about the Cr(III) ions rather than a tetrahedral one.

If the interpretation of Kordes and Petzolt (*7*) is correct and the Li(I) and Cr(III) ions do randomly substitute for the Mg(II) ions, the unstoichiometric nature of the electrode deposit demands that some of the octahedral sites be vacant. Because the total number of lattice sites available which have octahedral symmetry is the same as the number of oxide ions in the lattice, it becomes a simple matter to determine if all the octahedral sites are occupied by the cations. Table V shows that 6 to 10% of the sites are vacant.

One way to verify the existence of cation vacancies experimentally would be to compare the density calculated from the X-ray data with the experimentally measured density. The density of the electrode deposit calculated from the X-ray parameters is 4.01 g/cm³. By employing a displacement technique using water in a 5-ml pycnometer, the density of the deposit was measured to be 3.88 ± 0.10 g/cm³. The inherent inaccuracies present when trying to measure the density of a powder available only in small quantities makes quantitative interpretation of these data very difficult. Qualitatively, however, it would appear that cation vacancies do exist in the lattice because the measured density is less than that calculated from the X-ray data.

**Table V. Determination of Cation Vacancies in Electrode Deposit**

| No. of oxygen atoms per molecule | No. of cations per molecule | Difference | No. of vacancies per MgO |
|---|---|---|---|
| 4.00 | 3.64 | 0.36 | 0.09 |
| 4.00 | 3.63 | 0.37 | 0.09 |
| 3.94 | 3.62 | 0.32 | 0.08 |
| 3.93 | 3.61 | 0.32 | 0.08 |
| 3.97 | 3.71 | 0.26 | 0.07 |
| 3.98 | 3.74 | 0.24 | 0.06 |

**Table VI. Thermogravimetric Data for $Li_zMg_yCrO_4$**

| Argon atmosphere | | Air atmosphere | |
|---|---|---|---|
| Temp. (°C) | Wt (g) | Temp. (°C) | Wt (g) |
| 25 | 0.11825 | 25 | 0.28340 |
| 320 | 0.11804 | 550 | 0.28340 |
| 615 | 0.11802 | 720 | 0.28340 |
| 700 | 0.11784 | 920 | 0.28337 |
| 805 | 0.11761 | 1000 | 0.28337 |
| 920 | 0.11769 | | |
| 1010 | 0.11774 | | |

**Pressure Stability of the Lattice.** The presence of cation vacancies might be expected to weaken the lattice causing it to rearrange under extreme pressures. To test this possibility the powdered deposit was subjected to pressures of the order of 80,000 atmospheres and X-ray powder patterns of the pressed deposit were compared with those of the unpressed powder. No change was observed in the lattice type or the lattice dimensions, indicating that either the lattice was not affected by the pressure, or if some transition did occur it was reversible when the pressure was released.

**Thermal Stability of $Li_zMg_yCrO_4$.** Platinum gauze electrodes coated with the deposit were heated in argon and air atmospheres to 1000 °C and their weights were recorded as a function of temperature. The thermogravimetric data shown in Table VI indicate that there was no significant weight loss during the heating process and that the oxygen in the air had no effect. In each case the color of the deposit changed from the original bright green to a brownish green. Chemical analysis of one of the heated samples indicated that it contained 2.34% $Li_2O$, 52.50% MgO, and 42.87% $Cr_2O_3$ which corresponds to the original empirical formula, $Li_{0.28}Mg_{2.35}CrO_{3.99}$. Because the analysis corresponded to previous analyses on unheated samples and there was no loss of weight upon heating, it appears that no chemical change occurred. X-ray powder patterns of the electrode deposit shown in Table VII, however, do indicate a change in the structure of the deposit upon heating. At approximately 1000 °C new lines appear in the powder pattern which cannot be ascribed to the original face-centered cubic lattice. Upon further heating to 1400 °C these new lines are clearly defined and can be indexed to a diamond cubic lattice having an "a" parameter of 8.318 Å as indicated in Table VIII. It is also shown in Table VII that the original

(7) V. E. Kordes and J. Petzolt, *Z. Anorg. Allg. Chem.*, **335**, 138 (1965).
(8) W. Low, *Phys. Rev.*, **105**, 801 (1957).

Table VII. X-Ray Powder Pattern of Electrode Deposit as Function of Temperature

| 25 °C to 800 °C | | 1050 °C | | 1400 °C | | | |
|---|---|---|---|---|---|---|---|
| $d$ (Å) | $I/I_0$ | $d$ (Å) | $I/I_0$ | $d$ (Å) | $I/I_0$ | $d$ (Å) | $I/I_0$ |
| 2.3981 | 10 | 4.7995 | 40 | 4.7586 | 50 | 1.1643 | 10 |
| 2.0773 | 100 | 2.5060 | 40 | 2.9284 | 15 | 1.1104 | 5 |
| 1.4721 | 80 | 2.4086[a] | 20 | 2.4973 | 100 | 1.0819 | 20 |
| 1.2561 | 20 | 2.3075 | 5 | 2.0993[a] | 80 | 1.0533[a] | 10 |
| 1.2041 | 30 | 2.0892[a] | 100 | 2.0710 | 80 | 1.0398 | 10 |
| 1.0427 | 20 | 1.6053 | 30 | 1.9068 | 1 | 0.9604[a] | 5 |
| 0.9576 | 10 | 1.4773[a] | 100 | 1.6906 | 1 | 0.9418[a] | 20 |
| 0.9333 | 30 | 1.2602[a] | 40 | 1.5963 | 50 | 0.9302 | 20 |
| 0.8523 | 30 | 1.2064[a] | 40 | 1.4858[a] | 60 | 0.9128 | 5 |
| 0.8035 | 10 | 1.1088 | 1 | 1.4669 | 60 | 0.8596[a] | 20 |
| | | 1.0846 | 1 | 1.4035 | 15 | 0.8491 | 20 |
| | | 1.0456[a] | 10 | 1.2668 | 15 | | |
| | | 0.9582[a] | 3 | 1.2533[a] | 15 | | |
| | | 0.9352[a] | 20 | 1.2149[a] | 15 | | |
| | | 0.8535[a] | 20 | 1.1984 | 15 | | |

[a] Face-centered cubic lines

face-centered cubic lines are diminished in intensity and shifted to higher $d$ spacings during the heating process. Upon indexing the new face-centered cubic lines, an "a" parameter of 4.215 Å is calculated which is significantly larger than the original "a" parameter of 4.182 Å. This value now closely approximates the "a" parameter experimentally measured for pure MgO (4.213 Å). This observation, coupled with the observation that the diamond cubic lines closely match the ASTM pattern for pure $MgCr_2O_4$ as shown in Table IX, appears to indicate that the heating to 1400 °C decomposed the solid solution to a mixture of MgO and $MgCr_2O_4$.

Table VIII. Indexing of Diamond Cubic Powder Pattern

| $d$ (Å) | $\sin^2\theta$ | $s$ | $\lambda^2/4a^2 \times 10^3$ | $hkl$ | $a$ (Å) |
|---|---|---|---|---|---|
| 4.7586 | 0.0262 | 3 | 8.733 | 111 | 8.251 |
| 2.9284 | 0.0691 | 8 | 8.637 | 220 | 8.296 |
| 2.4973 | 0.0952 | 11 | 8.655 | 311 | 8.288 |
| 2.0710 | 0.1383 | 16 | 8.644 | 400 | 8.293 |
| 1.9068 | 0.1632 | 19 | 8.589 | 331 | 8.320 |
| 1.6906 | 0.2076 | 24 | 8.650 | 422 | 8.291 |
| 1.5963 | 0.2328 | 27 | 8.622 | 511,333 | 8.286 |
| 1.4669 | 0.2756 | 32 | 8.613 | 440 | 8.308 |
| 1.4035 | 0.3012 | 35 | 8.606 | 531 | 8.312 |
| 1.2668 | 0.3697 | 43 | 8.598 | 533 | 8.315 |
| 1.1984 | 0.4130 | 48 | 8.604 | 444 | 8.312 |
| 1.1643 | 0.4376 | 51 | 8.580 | 711,551 | 8.324 |
| 1.1104 | 0.4811 | 56 | 8.591 | 642 | 8.319 |
| 1.0819 | 0.5068 | 59 | 8.590 | 731,553 | 8.319 |
| 1.0398 | 0.5659 | 67 | 8.446 | — | — |
| 0.9302 | 0.6855 | 80 | 8.569 | — | — |
| 0.9128 | 0.7121 | 83 | 8.580 | — | — |
| 0.8491 | 0.8230 | 96 | 8.573 | — | — |

Table IX. X-Ray Identification of Heated Electrode Deposit

| $MgCr_2O_4$ (ASTM) | | Electrode deposit | |
|---|---|---|---|
| $d$ (Å) | $I/I_0$ | $d$ (Å) | $I/I_0$ |
| 4.813 | 65 | 4.759 | 50 |
| 2.945 | 13 | 2.928 | 15 |
| 2.512 | 100 | 2.497 | 100 |
| 2.406 | 13 | | |
| 2.083 | 55 | 2.071 | 80 |
| 1.912 | 5 | 1.907 | 1 |
| 1.701 | 3 | 1.691 | 1 |
| 1.603 | 40 | 1.596 | 50 |
| 1.4731 | 55 | 1.4669 | 60 |
| 1.4089 | 13 | 1.4035 | 15 |
| 1.3176 | 1 | | |
| 1.2711 | 13 | 1.2668 | 15 |
| 1.2563 | 9 | | |
| 1.2028 | 9 | 1.1984 | 15 |
| 1.1666 | 9 | 1.1643 | 10 |
| 1.1136 | 3 | 1.1104 | 5 |
| 1.0850 | 11 | 1.0819 | 20 |
| 1.0416 | 5 | 1.0398 | 10 |

Chemical analysis of the deposit heated to 1400 °C substantiates this interpretation. The deposit was found to contain 53.56% MgO, 45.24% $Cr_2O_3$, and no detectable amount of $Li_2O$. Evidently the $Li_2O$ was either volatilized at this temperature or it reacted with the ceramic crucible used to contain the deposit. Work by Deren and Haber (9) supports the observation that $MgCr_2O_4$ is thermally stable at 1400 °C. These workers, while studying the mechanism of formation of $MgCr_2O_4$ when mixtures of MgO and $Cr_2O_3$ were heated in air, observed that the only solid phases present at temperatures above 600 °C were MgO and $MgCr_2O_4$. Deren and Haber also observed that when pure $MgCrO_4$ is heated in air it tends to lose oxygen, which substantiates our observation that no air oxidation occurred during the heating of the electrode deposit.

**$K_2Cr_2O_7$–$MgCl_2$–LiCl–KCl System.** It was of interest to investigate the electrochemical reduction of dichromate in the presence of Mg(II) to see what effect the lower oxygen-to-chromium ratio would have on the composition of the electrode deposit. Several complications make the results of this investigation difficult to interpret. One serious problem is that in the melt dichromate is a much stronger oxidant than chromate. As a result, substantial chemical oxidation of Pt, C, and Au electrodes is observed. In the case of the Pt oxidation the reduction product was identified as $Cr_2O_3$ by X-ray powder diffraction. This result demands that oxide ion be lost to the bulk melt during the chemical reaction. The oxide ion would immediately be consumed to form $CrO_4^{2-}$ and consequently would alter the oxygen-to-chromium ratio of the Cr(VI) species dissolved in the melt.

Table X shows the effect of chemical oxidation on the composition of the electrochemical reduction product of dichromate in the presence of Mg(II). For each of the three electrodes 100 $\mu$eq of electricity were passed and the weight

(9) V. J. Deren and J. Haber, *Z. Anorg. Allg. Chem.*, **342**, 277, 288 (1966).

Table X. Composition of Reduction Product of Dichromate in the Presence of $MgCl_2$

$[K_2Cr_2O_7] = 0.056M$ $[MgCl_2] = 0.180M$
$I_0 = 2$ mA/cm² T = 450 °C

| Order of deposition | Cr(III) due to chemical oxidation, μeq | Wt % $Li_2O$ | Wt % MgO | Wt % $Cr_2O_3$ | Total wt % | Formula |
|---|---|---|---|---|---|---|
| 1 | 41.7 | 1.0 | 13.4 | 79.9 | 94.3 | $Li_{0.07}Mg_{0.32}CrO_{1.85}$ |
| 2 | 4.8 | 2.5 | 32.2 | 61.9 | 96.6 | $Li_{0.21}Mg_{0.98}CrO_{2.59}$ |
| 3 | 2.7 | 2.2 | 46.3 | 47.7 | 96.2 | $Li_{0.24}Mg_{1.83}CrO_{3.45}$ |

Table XI. Composition of Electrochemical Reduction Product of Chromyl Chloride in the Presence of $MgCl_2$

| Electricity passed in electrode preparation, μeq | Cr(III) found on the electrode, μeq | Excess μeq | Platinum lost as Pt(II), μeq |
|---|---|---|---|
| 75.00 | 86.60 | 11.6 | 19.5 |
| 50.00 | 58.19 | 8.19 | 18.2 |

| Wt % $Li_2O$ | Wt % MgO | Wt % $Cr_2O_3$ | Total wt % | Formula |
|---|---|---|---|---|
| 3.67 | 29.63 | 66.61 | 99.9 | $Li_{0.32}Mg_{0.97}CrO_{2.63} \cdot 0.08Cr_2O_3$ |
| 3.76 | 29.21 | 65.18 | 98.1 | $Li_{0.34}Mg_{0.98}CrO_{2.65} \cdot 0.08Cr_2O_3$ |

per cent of each of the three oxides was determined. Note that there was extensive chemical oxidation of the first electrode resulting in a high percentage of $Cr_2O_3$ in the deposit. Subsequent electrodes showed less chemical attack because a portion of the dichromate had been titrated to chromate by oxide ion released in the chemical oxidation.

As a result of this chemical oxidation, it has not been possible to ascribe a specific composition to the electrochemical reduction product. Qualitatively it appears, however, that the oxygen-to-chromium ratio in the deposit is lower than that observed for the chromate reduction.

**$CrO_2Cl_2$–$MgCl_2$–LiCl–KCl System.** As in the case of the dichromate reduction, chromyl chloride was found to be a strong enough oxidant to oxidize Pt to Pt(II). The chemical reduction product was again identified as $Cr_2O_3$ by X-ray powder diffraction. Table XI shows the results of chemical analyses of two typical deposits electrochemically prepared on Pt electrodes. The empirical formulas obtained are written to indicate that the chemical reduction product is $Cr_2O_3$ and that all other chromium on the electrode surface is due to the electrochemical reduction. The formulas indicate that there is a higher oxygen-to-chromium ratio in the deposit than the expected 2-to-1 ratio. This result would be expected if the chromyl chloride chemically attacked the platinum electrode producing $Cr_2O_3$, Pt(II), and oxide ion. The oxide produced would consequently raise the oxygen-to-chromium ratio of the Cr(VI) species dissolved in the melt, causing the oxygen-to-chromium ratio in the reduced product to increase. Considerable work remains to be done in an attempt to overcome the problem of chemical oxidation and obtain a pure electrochemical reduction product.


## ACKNOWLEDGMENT

The authors are indebted to Brian Moores and R. L. Belford for their assistance in obtaining and interpreting the ESR data, and to H. G. Drickamer for his assistance concerning the high pressure studies.

Received for review November 25, 1968. Accepted January 16, 1969. Financial support of this research was provided by the Army Research Office, Contract Number USDA-ARO-D-G586 and USDA-ARO-D-G968.

# Quantitative Determination of 1-Naphthylamine and 2-Naphthylamine in Cigarette Smoke

**Yoshito Masuda and Dietrich Hoffmann**

*Division of Environmental Cancerigenesis, Sloan-Kettering Institute for Cancer Research, New York, N.Y. 10021*

**A method is described for the analysis of 1-naphthylamine (I) and 2-naphthylamine (II) in cigarette smoke. The basic nonvolatiles of the smoke of 300 cigarettes are reacted with pentafluoropropionic anhydride and the resulting neutral components are chromatographed on Florisil. The concentrates of N-pentafluoropropionamides of I and II are analyzed by gas chromatography with an electron capture detector, which has a sensitivity limit of less than 1 ng. $^{14}C$-labelled I and II served as internal standards. The mainstream smoke of an 85-mm U.S. nonfilter cigarette contained 27 ng of I and 22 ng of II. Although the identification of 2-naphthylamine in cigarette smoke represents the first isolation of a known bladder carcinogen from a non-occupational respiratory environment, no biological significance can as yet be attached to this finding.**

THE ISOLATION, identification and quantitative determination of primary amines of polynuclear aromatic hydrocarbons in non-occupational respiratory environments presents a difficult and arduous task. In fact, none of these components was so far detected in urban air (*1*), and only recently Pailer, Hübsch, and Kuhn (*2*) found 1-naphthylamine, an aminofluorene and an aminostilbene in cigarette smoke. Miller and Stedman (*3*) failed to detect 2-naphthylamine in cigarette smoke.

The relatively high reactivity of primary amines, especially of naphthylamines (*4*, *5*), as well as their presumably low concentrations in respiratory environments require special methods and sensitive detection techniques for their analysis. This paper reports the first method for the qualitative and quantitative determination of nanograms of 1-naphthylamine and 2-naphthylamine in cigarette smoke.

## EXPERIMENTAL

**Apparatus.** A Wilkens gas chromatograph Model 1525 with flame ionization detector was used to assess the purity of free primary aromatic amines. A Varian Aerograph Model 1200 with an electron capture detector (tritiated titanium as $\beta$-source) was employed for the quantitative analysis, and a Perkin-Elmer gas chromatograph Model 800 with flame ionization detector for the isolation of unknowns. The $\beta$-radiation of the $^{14}C$-labelled internal standards was counted with a Nuclear Chicago Scintillation System 720. The cigarettes were smoked with a Cigarette Components CSM-10 for the quantitative analysis and with a multiple-unit automatic machine for the isolation of naphthylamines (*6*). The mass spectra were obtained with a Hitachi-Perkin-Elmer RMU-6D by the Morgan-Schaffer Corporation (Montreal, Canada). The energy of the bombarding electrons was kept at 70 eV. The laboratories were illuminated with yellow light (Sylvania Electric Tubes F-40 G.O.) which excludes radiation below 450 m$\mu$.

**Reagents.** All organic solvents were spectrograde, the other chemicals of analytical reagent grade. Pentafluoropropionic anhydride ($n_D^{25}$ = 1.273) was obtained from Peninsular Chemresearch, Inc. and used without further purification. Florisil (60–100 mesh) was obtained from Fisher Scientific Co., basic alumina Woelm (activity III) from Alupharm Chemicals, Gas Chrom Q (80–100 mesh), Chromosorb W (60–80 mesh), Silicon QF-1, DC-200 and Siponate DS-10 from Applied Science Laboratories.

**Internal Standards.** 1-Naphthylamine-1-$^{14}C$ (sp. activity 2.0 mCi/mmol) and 2-naphthylamine-8-$^{14}C$ (sp. activity 3.58 mCi/m mol) were purchased from Mallinckrodt Nuclear, purified before use and their purity ascertained by GLPC. Toluene solutions with 0.4% PPO (2.5-diphenyloxazole) and 0.005% POPOP (p-bis[2(5-phenyloxazole)] benzene) as scintillators gave counting efficiencies of 72.5% for the unquenched $^{14}C$-labelled naphthylamines.

**Pentafluoropropionamides of Naphthylamines.** The electron capture system has been reported to be most sensitive for the detection of certain polyfluorinated organic compounds (*7*). The freshly purified amines were dissolved in dry ether and reacted with magnetic stirring with a 50% excess of pentafluoropropionic anhydride. The solution was kept for 18 hr at room temp., extracted with 2*N* hydrochloric acid, sat. sodium bicarbonate solution and then dried ($Na_2SO_4$). The residue was recryst. from *n*-hexane/benzene (4:1). The yields for the pentafluoropropionamides (PF) of 1-and 2-naphthylamines were better than 95%; the same high yields were observed in the presence of nicotine in an excess of 1000 parts.

*Anal.* *N*-1-Naphthylpentafluoropropionamide mp 132 °C cor. Calcd for $C_{13}H_8F_5NO$:C, 53.98; H, 2.79; F, 32.84; N, 4.84. Found: C, 54.10; H, 3.04; F, 32.65; N, 4.72.

*N*-2-Naphthylpentafluoropropionamide mp 150 °C cor. Calcd for $C_{13}H_8F_5NO$:C, 53.98. H, 2.79; F. 32.84; N, 4.84. Found C, 53.74; H, 3.00; F, 32.55; N, 4.66.

**Gas Chromatography.** The primary amines were purified on basic alumina, recrystallized, and checked for purity by GLPC at 175 °C on 3mm by 2.5-m column filled with 10% Siponate DS-10 on Chromosorb W. The PF of 1-and 2-naphthylamine can be separated at 145 °C on glass columns (3-mm by 1.7-m) filled with 7.5% QF-1 and 5% DC-200 on Gas Chrom Q. The retention times were 7.1 and 9.5 min, respectively. Figure 1 presents the electron capture sensitivity to nanograms of the PF of 1- and 2-naphthylamine.

For the gas chromatographic separation of the *N*-1 and *N*-2 naphthylpentafluoropropionamides from a concentrate from cigarette smoke, a 2-m glass column of 6-mm diameter was used and the liquid phases and support were as described above; the temperature was kept at 160 °C; the column exit was connected with a glass splitter which led 10% of the effluent to a flame ionization detector and the remainder was collected.

**Procedures.** A. ISOLATION OF THE PF OF 1-AND 2-NAPHTHYLAMINES. A total of 12,000 cigarettes were smoked with a multiple unit automatic machine at a rate of one puff per

(1) D. Hoffmann and E. L. Wynder in "Air Pollution, Vol. II", A. C. Stern Ed., Academic Press, New York, 1968, Chapter 20.
(2) M. Pailer, W. J. Hübsch and H. Kuhn, *Fachliche Mitt. Oesterr. Tabakregie*, **7**, 109 (1967).
(3) R. L. Miller and R. L. Stedman, *Tobacco Sci.*, **11**, 111 (1967).
(4) S. F. D. Orr, P. Sims, and P. Manson, *J. Chem. Soc.*, **1956**, 1337.
(5) Q. Quick, R. F. Layton, H. R. Harless, and O. R. Haynes, *J. Gas Chromatogr.*, **6**, 46 (1968).
(6) E. L. Wynder and D. Hoffmann, "Tobacco and Tobacco Smoke, Studies in Experimental Carcinogenesis," Academic Press, New York, N.Y., 1967.
(7) D. D. Clarke, S. Wilk, and S. E. Gitlow, *J. Gas Chromatogr.*, **4**, 310 (1966).

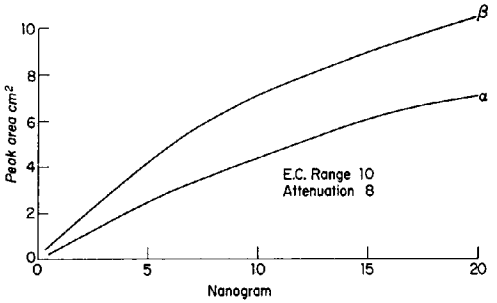


**Figure 1. Linearity curve for *N*-1-naphthylpentafluoropropionamide ($\alpha$) and *N*-2-naphthylpentafluoropropionamide ($\beta$)**

minute of 2-sec duration and an average puff volume of 35 ml; butt length was 23 mm. The mainstream smoke was drawn through a series of 4 wash bottles (500 ml each) filled with 7% HCl in methanol/water (1:1) and immersed in ice water. The traps were washed with methanol and the combined suspensions filtered and concentrated; the filtrate (1 l) was diluted with an equal volume of water, three times extracted with ether, 1 l each, was made basic with 3*N* sodium hydroxide, and seven times extracted with ether (1 l each). The ethereal extract (~30 grams) was dried ($Na_2SO_4$) and concentrated to 250 ml. To this solution was added 100 grams of pentafluoropropionic anhydride under ice cooling and magnetic stirring; the solution was then kept at room temperature for 20 hr. The neutral portion was separated and the basic portion dissolved in 200 ml of ether and treated again with pentafluoropropionic anhydride (20 grams). The combined neutral portions were dried ($Na_2SO_4$) and their residues (~8 grams) dissolved in *n*-hexane/benzene (4:1; 50 ml) for chromatography on Florisil (300 grams) with *n*-hexane, *n*-hexane/benzene (8:1, 4:1, 2:1, 1:1) and benzene as eluting solvents. 250 fractions (25 ml each) were obtained of which all those eluted with *n*-hexane, benzene 1:1 were combined. Their concentrate was rechromatographed on 30

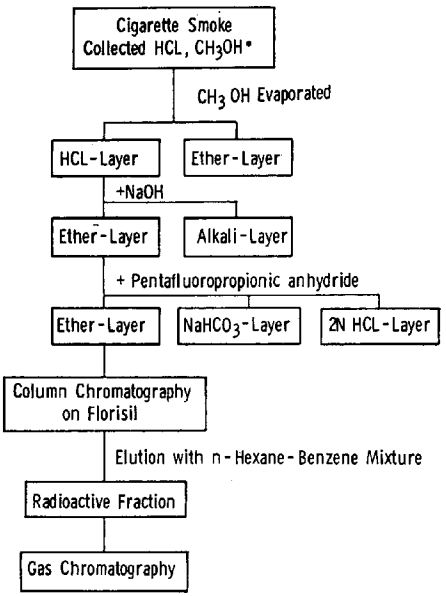


**Figure 2. Analytical separation procedure for 1-naphthylamine and 2-naphthylamine from cigarette smoke**

**internal standard added**

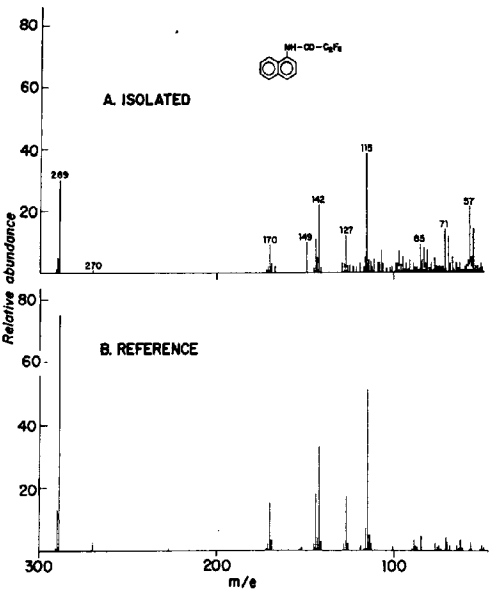


**Figure 3. Mass spectra of *N*-1-naphthylpentafluoropropionamide**

grams of Florisil. Every fifth fraction of 100 fractions (20 ml each) of the *n*-hexane-benzene (2:1, 1:1) and benzene eluates was analyzed for PF by a gas chromatograph with an electron capture detector. The fractions with maxima corresponding to retention times of the PF of 1-and 2-naphthylamine were combined for the isolation of the derivatives.

B. Quantitative Analysis. A total of 300 cigarettes were smoked individually under standard conditions with a Model CSM-10 (*6*). The mainstream smoke was directed through a series of 3 gas wash bottles filled with 150 ml of 3.5% HCl in methanol. The smoke suspensions in the gas wash bottles were combined with the rinsing solvent (~500 ml) and 1.5 $\mu$g of 1-naphthylamine 1-$^{14}$C (or 1.5 $\mu$g 2-naphthylamine-8-$^{14}$C) in 1 ml of toluene was added and filtered. The filtrate and washings were concentrated to 50 ml, diluted with 100 ml of $H_2O$ and extracted three times with 100 ml ether each. The acidic layer was made basic with 3*N* sodium hydroxide and seven times extracted with 100 ml ether. The combined extracts were dried ($Na_2SO_4$), evaporated to about 30 ml and reacted with 1.5 grams of pentafluoropropionic anhydride. After standing for 20 hr, the solution was extracted with 2*N* hydrochloric acid and 5% sodium bicarbonate solution. The ether containing the neutral portion was dried, evaporated, dissolved in 5 ml of *n*-hexane/benzene (4:1) and chromatographed on Florisil (30 grams). The fractions were eluted with *n*-hexane, *n*-hexane/benzene (8:1, 4:1, 2:1, 1:1) and benzene. The eluates with *n*-hexane/benzene 2:1, 1:1 contained in separate fractions the PF of 1-and 2-naphthylamine. The fractions with $\beta$-radioactivity were combined, concentrated to 1–2 ml, and five 1-$\mu$l samples were injected for GLPC analysis. Three aliquots of 100–200 $\mu$l were taken for liquid scintillation counting. Figure 2 summarizes the analytical separation procedure.

## RESULTS AND DISCUSSION

Figures 3 and 4 compare mass spectra of synthetic and isolated *N*-1, and *N*-2-naphthylpentafluoropropionamides. These data and the retention times and retention volumes from two gas chromatography systems served for the identification of 1-naphthylamine and 2-naphthylamine. For the

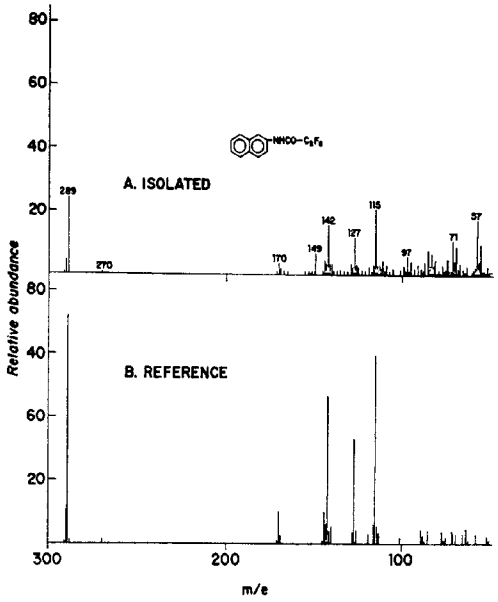


Figure 4. Mass spectra of *N*-2-naphthylpentafluoropropionamide

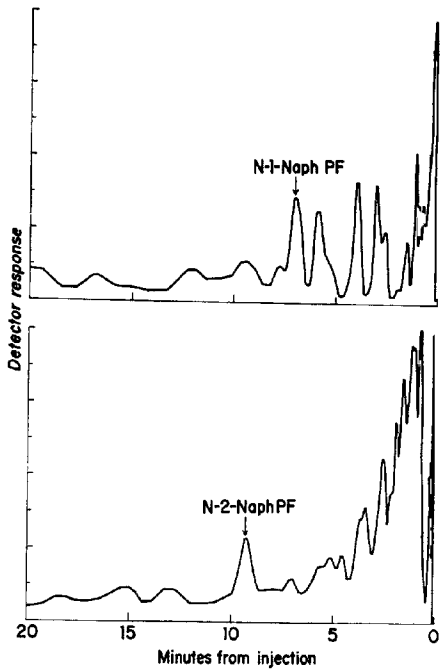


Figure 5. Gas chromatograms for concentrates of *N*-1-, and *N*-2-naphthylpentafluoropropionamide from cigarette smoke

quantitative analysis, three times 300 cigarettes were smoked for each of the amines. From the final gas chromatograms (Figure 5) it was calculated that the smoke from an 85-mm, U.S. blended cigarette without filter tip contained 27 ng of 1-naphthylamine and 22 ng of 2-naphthylamine (Table I).

As experienced before for trace components in cigarette smoke (<1.0 μg/cig), the quantitative analysis (isotope dilution method) cannot be accomplished without losses of less than 20% (*8, 9*). The higher losses for the naphthylamines may be explained by oxidations and condensations of the free primary aromatic amines. It appears, therefore, not unlikely that earlier efforts to identify 1-and 2-naphthylamine were only partially successful (*2,3*), because the investigators did not try to prevent condensations to Schiff's bases during the trapping of the smoke and attempted to isolate micrograms of primary aromatic amines as free bases. During our preliminary investigations we tried to enrich the free naphthylamines from the basic portion by two different ion exchange columns prior to forming the PF-derivatives. However, with this method the overall losses exceeded 90%.

So far, only limited information is available on the pyrosynthesis of naphthylamines. Cigarette smoke contains naphthalene and ammonia (*6, 10*), and one may regard their thermically activated forms as precursors of naphthylamines in the hot zones of a cigarette. α-Aminoacids could also be another type of precursors as was demonstrated by pyrolysis studies (*11*).

To our knowledge, this report presents the first successful identification of a bladder carcinogen in a non-occupational respiratory environment (*1, 6, 10, 12*). The bladder carcinogen 2-anphthylamine, however, is present in cigarette smoke in such a minute amount (22ng/cig) that one cannot at this time attach a biological significance to its identification. The presented data, however, call for an extensive search for other polynuclear aromatic amines in cigarette smoke. If such compounds exist in significantly higher concentration and have a similar carcinogenic potential as 2-naphthylamine, such data may provide an explanation for the epidemiological link between cigarette smoking and bladder cancer (*12*).

RECEIVED for review November 29, 1968. Accepted January 23, 1969. The study was presented at the 22nd Tobacco Chemists' Research Conference in Richmond, Va., October 1968. Work was supported by the American Cancer Society Grant E-231 and in part by the National Cancer Institute Grant 08748.

(8) D. Hoffmann and E. L. Wynder, ANAL. CHEM., **32**, 295 (1960).
(9) D. Hoffmann and G. Rathkamp, *Beitr. Tabakforsch.*, **4**, 201 (1968).
(10) R. L. Stedman, *Chem. Rev.*, **68**, 153 (1968).
(11) Y. Masuda, K. Mori, and M. Kuratsune, *Int. J. Cancer*, **2**, 489, (1967).
(12) U.S. Public Health Service. "The Health Consequences of Smoking." A Public Health Review, 1967 Suppl. 1968, p 104.

**Table I. 1-and 2-Naphthylamine in Cigarette Mainstream Smoke**

| Number of analyses | 1-Naphthylamine[a] (ng per cigarette) | 2-Naphthylamine[a] (ng per cigarette) |
|---|---|---|
| 1 | 29.8 | 21.3 |
| 2 | 25.0 | 23.3 |
| 3 | 26.2 | 20.8 |
| Average | 27.3 | 21.8 |
| Standard deviation | 2.2 | 1.3 |
| Deviation coefficient | 7.9% | 6.0% |
| Recoveries | 60–70% | 65–75% |

[a] Calculated with the isotope dilution method.

# Electrochemical Kinetics of the Ferri–Ferrocyanide Couple on Platinum

**P. H. Daum and C. G. Enke**

*Chemistry Department, Michigan State University, East Lansing, Mich. 48823*

**The current impulse technique was used to study the electrochemical kinetics of the ferri-ferrocyanide couple. The exchange rate of the reaction was strongly dependent on the oxidation state of the electrode surface. The transfer coefficient and the activation energy do not appear to be affected by surface oxidation. All experimental evidence points to a simple first order electron transfer reaction. The results of the investigation were in substantial concordance with those measured by other techniques when surface oxidation effects are taken into account.**

THE CURRENT IMPULSE technique (*1*) is a perturbation method which is especially suitable for the study of rapid electrochemical reactions. The system is perturbed from its equilibrium potential with an extremely short pulse of constant current that charges the electrical double layer capacitance to a new potential several millivolts anodic or cathodic of the equilibrium potential. The relaxation of the double layer charge through the faradaic process is observed by measuring the potential $\eta$ as a function of time. With the absence of mass transport complications, a simple exponential decay law $\eta = \eta_{t=0} \exp(-t/R_f C_d)$ is followed where $R_f$ is the faradaic resistance ($R_f = RT/nFI^\circ$) and $C_d$ is the differential double layer capacitance. The exchange current of the reaction can be calculated directly from the slope of the log ($\eta$)–time curve if the double layer capacitance of the system is known under the exact conditions of the experiment.

This technique offers two methods of determining the double layer capacitance. The log ($\eta$)–time curve can be extrapolated to zero time (defined as the time of the termination of the impulse), and the capacitance can then be calculated from the relationship $C_d = i\tau/\eta_{t=0}$ where $i$ is the magnitude of the applied current pulse and $\tau$ is the pulse duration. It can also be determined directly by measuring the slope of the overpotential time curve while charging the double layer with a constant current from the relationship $i = C_d(d\eta/dt)$.

Studies with the current impulse technique have been limited to the kinetics of the electrochemical reduction of the Hg(I)/Hg system (*2*) which appears to have mechanistic complications, and the resulting data are somewhat anomolous. It seemed desirable to show that the technique is capable of obtaining unambiguous data from a mechanistically simple reaction, and to extend its usefulness to the study of very fast electrochemical reactions at solid electrodes. A system that fulfills these requirements is the ferri-ferrocyanide couple on platinum. It has been the subject of much investigation and is regarded by many as the model of a highly reversible electrochemical reaction without complicating mechanistic effects.

The study of this system with the current impulse technique has presented several intriguing aspects, and has given some new data previously unavailable with other methods. First, the current impulse technique gives an unambiguous estimate of the differential double layer capacitance under the actual conditions of the experiment, a measurement which is not readily available from other techniques with a reaction of this speed. This ability is particularly important in this system because the ferricyanide and ferrocyanide anions are highly charged, and one might expect that the double layer capacitance of platinum would be a strong function of their concentration and the potential. However, this study has revealed no drastic changes in the double layer structure as a function of these variables. Second, these two anions are most certainly associated to a differing degree with the potassium ion of the supporting electrolyte (*3*), and the oxidation of the ferrocyanide ion or reduction of the ferricyanide ion probably involves a change in the number of potassium ions associated with the particular anion. The analyses of the overpotential *vs.* time curves gave no definite information regarding this proposed mechanism. Third, the exchange rates and capacitance values obtained with this system were very much dependent upon the preconditioning of the electrode. The pretreatment of the electrode with hot perchloric acid oxidized the platinum surface, which slowed the apparent exchange rate to a marked degree. When the oxidized electrode was reduced by evolution of hydrogen, the electrode became more active. These two electrode surfaces were reproducible so it was convenient to define two states, an oxidized state and a reduced state. Most of the effort of the present investigation has been directed to the establishment of the kinetic parameters for the reduced electrode system; oxidized electrodes have been measured only to demonstrate that surface oxidation affects the kinetic parameters.

## EXPERIMENTAL

**Instrumentation.** An Intercontinental Instruments PG-33 pulse generator was used as the perturbation source. It has a current output mode capable of a maximum output of 200 mA pulses with rise times of less than 7 nsec, and with durations as short as 30 nsec. In its quiescent state the impedance to ground is a minimum of 10 kohms; this is quite large with respect to the faradaic resistance of the ferri-ferrocyanide couple; thus the cell is essentially at open circuit after termination of the pulse, and relaxation takes place only through the faradaic reaction. A Tektronix 556 Dual Beam Oscilloscope with a 1A5 differential preamplifier was used to measure the potentials. The combination of the main frame and preamplifier has a rise time of less than 11 nsec, a 1 Mohm input resistance, and a maximum sensitivity of 1 mV/cm. The preamplifier has a calibrated voltage which can be subtracted from the input signal, thus allowing the measurement of charging curves at high sensitivities by offsetting the IR drop of the cell. Currents were measured by inserting a calibrated 10-ohm composition resistor in series with the pulse generator and measuring the IR drop of a 1 μsec pulse with the oscilloscope; current values were estimated to be correct to within 2%.

Experiments were initiated by an external trigger pulse which started the oscilloscope sweep; the delayed trigger output of the oscilloscope was then used to trigger the pulse generator. The experimental data were recorded photographically on Kodak Tri-X film using a Tektronix 350/C 35mm camera system. Temperature control for the activation energy studies was maintained with a Tamson TVZ-45 con-

(1) W. D. Weir and C. G. Enke, *J. Phys. Chem.*, **71**, 275 (1967).
(2) W. D. Weir and C. G. Enke, *ibid.*, p 280.
(3) W. A. Eaton, P. George, and G. I. H. Hanania, *ibid.*, p 2016.

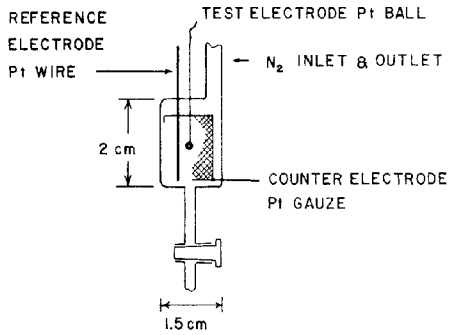


EXPERIMENTAL CELL

**Figure 1**

stant temperature bath fitted with a push-pull external circulator. Temperature control was estimated to be within 0.1 °C of the set point.

**Reagents and Solutions.** Solutions were prepared directly by weight from ACS reagent grade chemicals without further purification. Water was prepared by the redistillation of an alkaline permanganate solution of laboratory distilled water. Nitrogen used to purge solutions of oxygen was dried over calcium chloride, passed through an oven containing copper turnings at 350 °C to remove traces of oxygen, passed through traps containing activated charcoal at liquid nitrogen temperatures, presaturated in a 1*M* KCl solution, and fed to the cell via a glass and Teflon train.

**Cell and Electrodes.** A cell of small dimensions similar to one used by Piersma, Schuldiner, and Warner (*4*), shown in Figure 1, was constructed and fitted to a small shielded box which was attached to male and female BNC connectors. The cell assembly was plugged directly onto the output of the pulse generator, and a short length of BNC cable was connected from it to the input of the oscilloscope. Nitrogen was led from the purification train to the cell assembly *via* a small diameter Teflon tube which was immersed directly into the test solution. A second cell of slightly larger dimensions to accommodate immersion in a constant temperature bath was developed for use in the activation energy studies. It was unshielded and noisier than the first; however both cells demonstrated excellent high frequency response with minimal distortions due to stray inductances and capacitances. System settling times, defined as the time from the start of the impulse to the time at which it is possible to accurately measure the potential, were on the order of 50 nsec. Transient ringing after termination of the impulse was no more than 200 nsec.

A three electrode configuration was used in both cases, because it minimized the IR drop and gave slightly less noise than a two electrode system. The test electrode was made by melting a small diameter platinum wire with a gas–oxygen torch into a small sphere of approximately 0.05 cm² area. The geometric area of the electrode was determined by measurement with a Bausch and Lomb microscope fitted with a micrometer eyepiece, and a calibrated micrometer slide. The area was estimated to be correct to within 2%. The reference electrode was a large diameter platinum wire of approximately 0.5 cm² area arranged so that it was less than 0.5 mm from the test electrode. The area of the reference was large enough so that an insignificant amount of polarization occurred at it

(4) B. J. Piersma, S. Schuldiner, and T. B. Warner, *J. Electrochem. Soc.*, **113**, 1319 (1966).

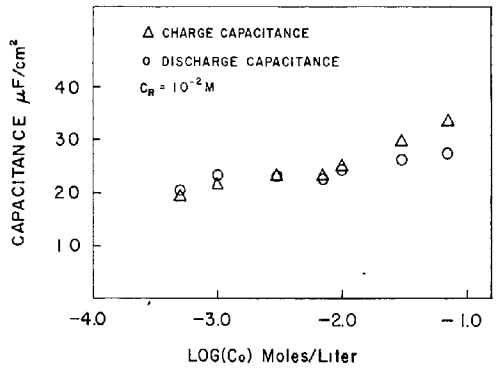


**Figure 2. Plot of differential capacitance from charge and discharge data of current impulse technique, of platinum in 1*M* KCl at 25 °C as a function of log[Fe(CN)$_6^{3-}$]**

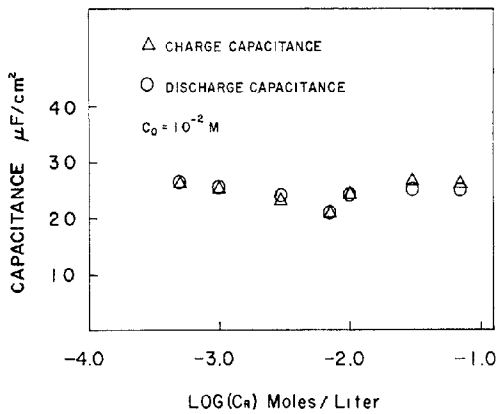


**Figure 3. Plot of differential capacitance from charge and discharge data of current impulse technique, of platinum in 1*M* KCl at 25 °C, as a function of log[Fe(CN)$_6^{4-}$]**

under the conditions of the experiments. The counter-electrode was a cylinder of platinum gauze of approximately 3 cm² area, arranged concentrically about the reference and test electrodes.

Prior to each experiment, the cell and electrodes were allowed to stand in hot perchloric acid for ten minutes. This served both to oxidize the surface of the electrodes and to oxidize any absorbed impurities in the cell electrode system. For the reduced electrode experiments, the cell was rinsed several times with triple distilled water, filled with 1*M* KCl, and the electrodes were reduced for several minutes at hydrogen evolution potentials. For the oxidized electrode experiments, the system was used after the usual rinsing with no further treatment.

## RESULTS AND CONCLUSIONS

**Reduced Electrodes.** The kinetics of the ferri-ferrocyanide couple were measured by holding the concentration of either the ferricyanide or ferrocyanide ion constant at 0.01*M*, and varying the concentration of the complex of the other oxidation state in seven increments from $5 \times 10^{-4}M$ to $7 \times 10^{-2}M$. Exchange rates were measured in 1*M* KCl at a total of thirteen different concentrations, and the data presented below are the

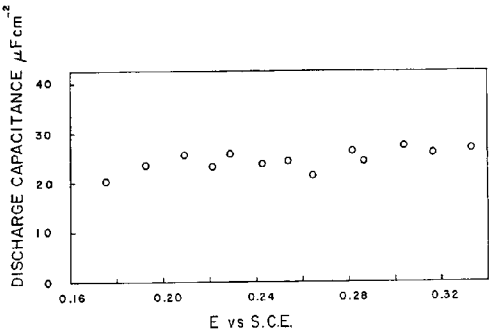


**Figure 4. Plot of differential capacitance from discharge data of current impulse technique, of platinum in 1*M* KCl at 25 °C, as a function of measured potential *vs.* SCE**

averages of at least three separate experiments at each concentration.

Estimates of the differential capacitance were obtained in two ways; the log($\eta$)-time curves were extrapolated to zero time, to give what is known as the discharge capacitance, and in a separate experiment, a pulse of approximately 0.8 $\mu$sec duration was applied to the cell and the capacitance value (denoted hereafter as the charge capacitance) was calculated directly from the slope of the charging curve. The capacitance data are presented in Figures 2 and 3 as functions of log ($C_o$) and log ($C_R$). There is marked agreement between the two estimates of the capacitance at all but the highest concentration, where the measured charge capacitance is significantly higher than the discharge capacitance. This apparent anomoly can be explained by considering a simple electrical model which describes the system. The calculation of the charge capacitance assumes that the charging process is linear with respect to time; this implies that on the time scale of the measurement (approximately one half micro-second) an insignificant amount of the charge is used by the faradaic process which is in parallel with the double layer capacitance. At low concentrations this is a good approximation, and the charging curves are linear; however, as the concentration increases, the exchange current increases and a significant amount of the applied current goes to the faradaic process rather than to the charging process. This causes a progressive decrease in the slope of the charging curve and leads to a high estimate of the double layer capacitance. If the slope of the charging curve could be observed at zero time, then the two estimates would presumably be the same at all concentrations; however, with the present experimental system, the minimum time for an accurate slope measurement was about 500 nsec.

In view of these considerations, it was decided that the discharge capacitance values were a better representation of the true capacitance values at the higher concentrations, since the charging time of 100 nsec for this experiment was considerably less than the 500–800 nsec required for the charging capacitance measurement. Figure 4 shows the discharge capacitance as a function of potential. This figure indicates that the differential capacitance of platinum under these conditions is essentially independent of the potential, and of the concentration of these two ions, or at least that these effects cancel. The capacitance of a series of solutions with a ratio of ferricyanide to ferrocyanide ion concentrations of 1:1 was measured as a function of the total concentration of the two ions, from a concentration of $5 \times 10^{-2}M$ to $3 \times 10^{-3}M$ of each. The differential capacitance remained constant over

**Table I. Values of Apparent Exchange Current Density for Solutions of Varying Concentrations of $K_3Fe(CN)_6$ and $K_4Fe(CN)_6$ in 1.00*M* KCl at 25 °C**

| Concn. $Fe(CN)_6^{3-}$ mole $l.^{-1}$ | Concn. $Fe(CN)_6^{4-}$ mole $l.^{-1}$ | $I_a^\circ$ amp $cm^{-2}$ |
|---|---|---|
| $7.00 \times 10^{-2}$ | $1.00 \times 10^{-2}$ | 0.493 |
| $3.00 \times 10^{-2}$ | $1.00 \times 10^{-2}$ | 0.321 |
| $1.00 \times 10^{-2}$ | $1.00 \times 10^{-2}$ | 0.229 |
| $7.00 \times 10^{-3}$ | $1.00 \times 10^{-2}$ | 0.185 |
| $3.00 \times 10^{-3}$ | $1.00 \times 10^{-2}$ | 0.109 |
| $1.00 \times 10^{-3}$ | $1.00 \times 10^{-2}$ | 0.075 |
| $5.00 \times 10^{-4}$ | $1.00 \times 10^{-2}$ | 0.050 |
| $1.00 \times 10^{-2}$ | $7.00 \times 10^{-2}$ | 0.620 |
| $1.00 \times 10^{-2}$ | $3.00 \times 10^{-2}$ | 0.380 |
| $1.00 \times 10^{-2}$ | $7.00 \times 10^{-3}$ | 0.197 |
| $1.00 \times 10^{-2}$ | $3.00 \times 10^{-3}$ | 0.116 |
| $1.00 \times 10^{-2}$ | $1.00 \times 10^{-3}$ | 0.079 |
| $1.00 \times 10^{-2}$ | $5.00 \times 10^{-4}$ | 0.052 |

that concentration range within experimental error. This indicates that the differential capacitance is essentially independent of the total concentration of the two anions, at least at the potential of an equimolar solution.

Exchange currents, shown in Table I, were calculated by assuming that the observed overpotential time curves followed the simple exponential decay law dictated by pure charge transfer kinetics, $\eta = \eta_{t=0}(-t/R_fC_d)$. The use of this equation presupposes that the contributions of mass transport processes to the observed decay are minimal. There are several criteria which can be applied to test this assumption (5), one of which is:

$$\frac{4nF}{RT}\frac{1}{C_dI_a^\circ} \gg \left[\frac{1}{nF}\left(\frac{1}{C_oD_o^{1/2}} + \frac{1}{C_RD_R^{1/2}}\right)\right]^2$$

where $C_o$, $C_R$, $D_o$, $D_R$, $n$, $F$, $R$, $T$, $C_d$, and $I_a^\circ$ have their usual significance.

At the above concentrations, assuming that $D_o = D_R = 10^{-5}$ cm²/sec, this inequality is satisfied by a factor of 80 in the most favorable case to a factor of 1.5 in the least favorable case. While it appears that the linear form of the equation is not applicable in certain instances, it should be recognized that this inequality determines the condition for pure charge transfer control throughout the entire relaxation time. However, even at low concentrations where the inequality is only marginally satisfied, the decay is essentially charge transfer controlled at short times. If a measurement of the slope of the log ($\eta$)-time curve is made at short enough times, a good estimate of the exchange current can be made.

The reaction order plot shown in Figure 5 was calculated using the discharge capacitance for all of the measurements. It is linear over the entire concentration range and gives a transfer coefficient of 0.50. The heterogeneous rate constant, calculated at a concentration of $10^{-2}M$ for each ion, was found to be 0.24 cm/sec. The exchange current of a solution of $0.01M$ ferrocyanide and $0.01M$ ferricyanide was measured at several temperatures. Log($I_a^\circ$) was plotted as a function of $1/T$, and an activation energy of 3.13 to $\pm 0.2$ kcal/mole was calculated.

**Oxidized Electrodes.** The exchange rate at oxidized electrodes was measured at several concentrations. The apparent heterogeneous rate constant was found to be $0.028 \pm 0.001$ cm/sec, at the 95% confidence level, which is about a factor

(5) P. Delahay, *J. Phys. Chem.*, **66**, 2204 (1962).

Table II. Comparison of Present Kinetic Results with Results of Previous Investigators[a]

| Investigator(s) | Technique | Ref | Apparent transfer coeff | Std rate const. cm sec$^{-1}$ |
|---|---|---|---|---|
| Randles and Somerton | Faradaic impedance | (6) | — | 0.09 |
| Jordan | Hydrodynamic voltammetry | (7) | — | 0.08 |
| Jahn and Vielstich | Rotating disk electrode | (8) | 0.61 | 0.05 (C) |
| Agarwal | Faradaic rectification | (9) | 0.49 | — |
| Wijnen and Smit | Cyclic potential step | (10) | 0.55 | 0.095 (C) |
| Wijnen and Smit | Cyclic coulombic step | (10) | 0.50 | 0.13 (C) |
| Daum and Enke | Current impulse reduced electrode | — | 0.50 | 0.24 |
| Daum and Enke | Current impulse oxidized electrode | — | 0.46 | 0.028 |

[a] Results designated (C) were not reported by the respective authors but are calculated from their data.

of 10 less than that obtained with reduced electrodes. A reaction order plot revealed a transfer coefficient of 0.46 ± 0.02 which compares favorably with that of 0.50 obtained with reduced electrodes. The exchange rate of a 0.01*M* ferricyanide and ferrocyanide solution was measured as a function of temperature, and the activation energy was found to be 3.49 ± 0.5 kcal/mole.

Thus the rate of the ferri-ferrocyanide exchange is greatly reduced by the presence of surface oxidation on the platinum while the transfer coefficient and the activation energy appear to be essentially unchanged. It is not possible to postulate the mechanism by which the surface oxidation affects the reaction rate without further rate studies on a variety of carefully controlled surface oxidation states. Such studies are currently under way in this laboratory.

**Mechanistic Conclusions.** Nothing in the present investigation suggests that the rate of this reaction is affected by anything other than the simple electron transfer step. The linearity of the reaction order plot over the entire concentration range, the independence of the differential capacitance with respect to either the applied current or the potential, and the marked agreement between the charge and discharge capacitance at all but the highest concentrations all support this conclusion. One could propose a mechanism based upon

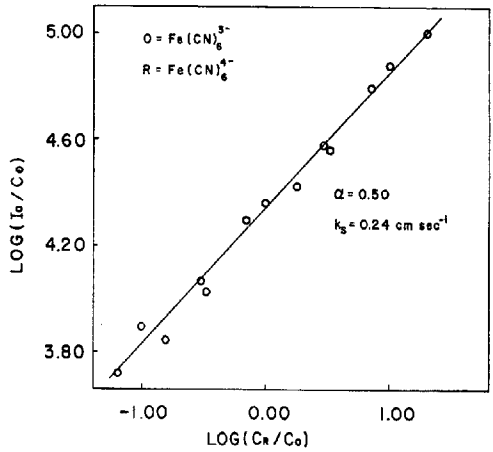


Figure 5. Reaction-order plot for the ferri-ferrocyanide couple on platinum in 1*M* KCl at 25 °C

the association constants measured by Eaton, George, and Hanania (3) of:

$$\left(K_nFe(CN)_6\right)^{n-3} + K^+ + e^- \rightleftharpoons \left(K_{n+1}Fe(CN)_6\right)^{n-3}$$

but if such steps take place, the current impulse technique gives no information to prove or disprove them. The association-dissociation reaction is probably extremely rapid with respect to the electron transfer reaction.

**Comparison of Results.** A comparison of the results of the present investigation with those of previous investigators is presented in Table II. The current impulse technique gives a rate constant for reduced electrodes which is about twice as large as that measured by any of the other techniques, while that measured for oxidized electrodes is substantially less than any of the others. The estimates of the apparent transfer coefficient agree very well except for the value obtained by Jahn and Vielstich with the rotating disk electrode. It is our conclusion that the observed differences in the rate constants are primarily due to differences in electrode conditioning. We have shown that the apparent rate constant is dependent on the amount of surface oxidation, though the measurement of the transfer coefficient is not. The conditioning procedures reported by previous investigators promote varying amounts of surface oxidation as has been verified in this laboratory; so their results are bound to be lower than the ones of the present investigation.

RECEIVED for review October 30, 1968. Accepted February 3, 1969. Work supported by the National Science Foundation, Grant GP-6572. Presented in part at the 155th National Meeting, ACS, San Francisco, Calif., April 1968.

(6) J. E. B. Randles and K. W. Somerton, *Trans. Faraday Soc.*, **48**, 937 (1952).
(7) J. Jordan, ANAL. CHEM., **27**, 1708 (1955).
(8) D. Jahn and W. Vielstich, *J. Electrochem. Soc.*, **109**, 849 (1962).
(9) H. P. Agarwal, *ibid.*, **110**, 237 (1963).
(10) M. D. Wijnen and W. M. Smit, *Rev. Trav. Chem.*, **79**, 289 (1960).

# Improved Resolution in High-Sensitivity Dual-Label Gas Radiochromatography

**Paul J. Thomas and H. J. Dutton**

*Northern Regional Research Laboratory, Peoria, Ill. 61604*

**The simultaneous and independent measurement of carbon-14 and tritium isotopes in compounds separated by gas-liquid chromatography can be performed by automatic serial collection of fractions in vials with subsequent scintillation counting. This paper describes the application of digital computer techniques to speed the analysis of counting data, to improve the sensitivity and resolution of the analysis, and to plot the individual isotopic curves. This improvement is obtained by combining and averaging the results of two to four replicate analyses of a given sample into a single plot of radioactivity vs. chromatographic retention time. With these techniques, samples having an activity of around 1-10 nanocuries/mg can be easily analyzed. The profile of radioactivity vs. chromatographic retention time is superior in its signal-to-noise-ratio, in its resolution of closely spaced peaks, and in its sensitivity to that obtainable with any continuous flow system.**

THE QUANTITATIVE ANALYSIS of either $^{14}C$ or tritium isotopes in compounds separated by gas-liquid chromatography (GLC) has been accomplished by several methods. These include serial collection of fractions for scintillation counting (*1–3*); cumulative collection for continuous integral counting (*3, 4*); continuous ion-chamber monitoring of the effluent vapor (*5–8*); and continuous proportional counting of the effluent, with or without combustion (*9, 10*). Some of these methods are employed in commercially available instruments. Simultaneous analysis for $^{14}C$ and tritium in dual-labeled compounds has required separate combustion and reaction trains for each isotope.

Automatic collection of serial fractions for scintillation counting as described by Dutton (*1, 2*) gives the highest sensitivity for compounds of low specific activity—*i.e.*, 0.5 to 100 nanocuries/mg—because the time of counting is not limited to residence time, as in a differential detector. High sensitivity is primarily caused by the increased time available for counting collected fractions (up to 100 minutes or more) and the resulting improved statistical accuracy. High resolution in this present method can be provided by the close spacing of fractions and the constant time interval of collection. This high resolution has now been improved significantly by the application of modern data-processing techniques available with a high-speed digital computer. These techniques enable us to combine and average the results of two to four repeated analyses on the same sample and then to approximate a true differential curve of the distribution of radioactivity in the column effluent. The shape and resolution of overlapping peaks for radioactivity are nearly as good as those of the thermal conductivity curve. A complete description of this technique and some examples of the results are given below.

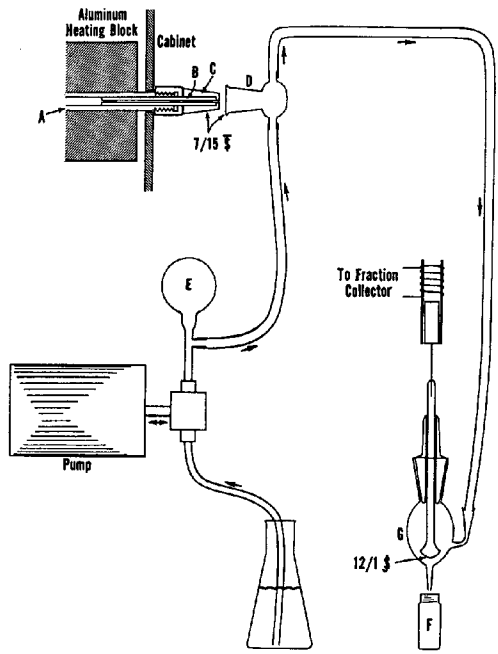


**Figure 1. Modified automatic system for condensation of effluent in scintillation solvent**

Simultaneous analysis of dual-labeled compounds is impossible with ion-chamber monitoring, and it can be performed by proportional counting only after chemical separation of $^{14}CO_2$ and $^{3}H_2$ from the combustion products of the effluent. Because tritium and $^{14}C$ isotopes can be easily resolved by scintillation spectrometry, our procedure is particularly useful for the analysis of dual-labeled compounds in GLC effluents.

## EXPERIMENTAL

**Apparatus.** The system for automatic serial collection of fractions was slightly altered from that described by Dutton (*1, 2*).

An Aerograph Model A-90 gas-chromatographic instrument was modified by the addition of an auxiliary stainless-steel collection tube, A (3-inches × $^{1}/_{2}$-inch o.d. and $^{3}/_{16}$-inch i.d.), enclosed in an aluminum block placed at the top of the detector oven (Figure 1). The aluminum block was maintained at 250° to 260 °C by a 75-W cartridge heater and controller. The effluent streams from both the sample side and the reference side of the thermal conductivity detector cell were

(1) H. J. Dutton in "Advances in Tracer Methodology," Vol. 1, S. Rothchild, Ed., Plenum Press, New York, 1962, pp 147–152.
(2) H. J. Dutton, *J. Amer. Oil Chem. Soc.*, **38**, 631 (1961).
(3) A. Karmen and H. R. Tritch, *Nature*, **186**, 150 (1960).
(4) G. Popják, A. E. Lowe, D. Moore, L. Brown, and F. A. Smith, *J. Lipid Res.*, **1**, 29 (1959).
(5) P. Riesz and K. E. Wilzbach, *J. Phys. Chem.*, **62**, 6 (1958).
(6) L. H. Mason, H. J. Dutton, and L. R. Bair, *J. Chromatogr.*, **2**, 322 (1959).
(7) F. Cacace and Inam-Ul-Haq, *Science*, **131**, 732 (1960).
(8) H. E. Dobbs, *J. Chromatogr.*, **5**, 32 (1961).
(9) R. Wolfgang and F. S. Rowland, ANAL. CHEM., **30**, 903 (1958).
(10) A. T. James and E. A. Piper, *J. Chromatogr.*, **5**, 265 (1961).

brought together through a tee into the interior end of the collector tube. A heavy-walled aluminum tube, *B* ($2^1/_2$-inches × $^3/_{16}$-inch o.d. and $^1/_{16}$-inch i.d.), was inserted to a depth of $1^1/_2$ inches into the exterior end of the stainless steel tube, and sealed to it with a washer made of Teflon (Dupont) and a stainless steel packing nut.

The outer end (*ca.* 1 inch) of the aluminum tube was covered with a sleeve made of Teflon (Dupont), *C*, machined to a $^7/_{15}$ standard male taper. The $^3/_{16}$-inch bore of the sleeve was reduced to $^1/_{16}$ inch at the tip, to cover and insulate the front face of the aluminum tube. A small glass tee, *D*, with a $^7/_{15}$ standard female taper on the short arm was placed over the sleeve made of Teflon (Dupont). The two sides of the long arm of the tee were connected to $^1/_8$-inch o.d. Polyflo tubing. A toluene-base liquid scintillation mixture was introduced through the lower tubing (with a metering pump); liquid and gas flow together out the upper tubing to the fraction collector. An air-filled damping reservoir, *E*, was provided at the pump to smooth the flow. The fraction collector was operated on a time basis by a 0 to 60 second interval timer. Fractions were collected directly in 20-ml scintillation counting vials, *F*. A solenoid-operated glass valve, *G*, connected to the interval timer interrupted the flow of solvent at the collector between fractions. An event marker on the thermal conductivity recorder chart was also connected to the interval timer.

## MATERIALS

$^{14}$C-Labeled methyl esters of palmitic, stearic, oleic, and linoleic acids with specific activities of 70 to 100 microcuries/mg were purchased from New England Nuclear Corp. Tritium-labeled methyl stearate with a specific activity of *ca.* 8.3 microcuries/mg was a remnant from earlier experiments of Jones *et al.* (*11*) in which tritium gas was added to methyl oleate. Small amounts of tritium-labeled methyl esters can also be conveniently prepared by the procedure of Mounts and Dutton (*12*). A standard sample was made by mixing trace amounts of these labeled esters with soybean methyl esters. The final activity was 9 nanocuries of $^{14}$C and 40 nanocuries tritium/mg of esters. The composition of the mixture by weight was not detectably different from soybean methyl esters.

**Procedure.** For the separation of fatty methyl esters, a $^1/_4$-inch o.d. × 10-ft stainless steel column was packed with 15% Hi-Eff IBP (diethylene glycol succinate polyester) on 80/100 mesh Gas Chrom P. (The packing was obtained, precoated and pretested, from Applied Science Laboratories.) The column was maintained at 195° to 200 °C with helium flowing at 100 ml/min. Under these conditions methyl stearate has a retention of 20 to 25 minutes. The interval timer was generally set for about 45 to 50 seconds, and the metering pump was set at about 20 ml/min. Methyl stearate generally fell between fraction numbers 25 and 30; a total of 50 to 80 fractions were collected, depending on the sample.

The filled vials from the fraction collector were counted in either a Packard Tri-Carb or a Beckman Model LS-250 scintillation counter. The latter was equipped with automatic external standardization and automatic quench compensation, as well as a teletypewriter printer and paper tape punch. No significant quenching was noted in any sample collected with the system as described. Both counters were provided with at least two voltage-discriminator channels to provide simultaneous data on $^{14}$C and tritium isotopes. Data from the scintillation counter were transferred to an IBM 1130 computer either directly from the punched paper tape through an IBM 1134 Tape Reader or from hand-punched data cards through an IBM 1440 Card Read-Punch. Interpretation of the teletypewriter character codes required a machine-language subroutine.

Each fraction collected was counted in duplicate and the duplicate counts were compared. If a significant deviation was noted, an error message was printed identifying the fraction number. Dual-labeled samples were resolved by computer programs making use of standard procedures (*13*, *14*) as follows:

(1) The voltage-discriminator "windows" of the scintillation spectrometer were adjusted to achieve a balance between high efficiency and low "spill-over." Counting efficiency for each isotope in each channel was determined as a function of the external standard ratio by counting a series of quenched standards. The function was approximated by a second degree polynomial "quench curve."

(2) The efficiency of each sample counted was determined from its external standard ratio by reference to the quench curves. With our samples in the Beckman Model LS-250, the routinely observed efficiencies were: Tritium, 40% in channel A, 0.5% in channel B; $^{14}$C, 9% in channel A, 67% in channel B. The absolute disintegration rate for each isotope was then determined by solving the following two simultaneous equations:

$$\text{net cpm chn. A} = {}^{14}\text{C eff. chn. A} \times {}^{14}\text{C dpm} + {}^{3}\text{H eff. chn. A} \times {}^{3}\text{H dpm}$$

$$\text{net cpm chn. B} = {}^{14}\text{C eff. chn. B} \times {}^{14}\text{C dpm} + {}^{3}\text{H eff. chn. B} \times {}^{3}\text{H dpm}$$

If a single analysis was done, data from the scintillation counter were reduced to a plot of disintegrations per minute in each fraction *vs.* the relative retention time at the beginning of the fraction; the points were connected by straight lines, and the resulting graph, complete with grid lines, was produced by an IBM 1627 x-y plotter.

Two or more repetitive analyses of the same sample were combined, as follows:

(1) The absolute disintegration rate for each isotope in each fraction of each chromatographic "run" was stored. The maximum count and the minimum count were selected by the program for each run. The minimum count was subtracted from all fractions as a background or baseline correction.

(2) The exact position of the methyl stearate peak, determined by inspection of the recorder chart, was specified to the program in terms of the fraction numbers. Each fraction was then assigned an $x$ value corresponding to its position relative to methyl stearate.

(3) A scale of relative retention values from 0 to 2.5 times that of methyl stearate was divided into 1250 increments. The computer, beginning at 0, calculated a $y$ value at each increment for each of the separate runs by straight-line interpolation between the data points on either side. The calculated values for each separate run were added and divided by the maximum count to give a "per cent of full scale" figure that was recorded by the plotter as a point on the curve. A new point was calculated at every 1/100 inch interval along the $x$ axis, and the plotter connected these points by straight lines. The resulting graph of radioactivity *vs.* relative retention time is, in essence, a radiochromatogram.

Integration of the "peaks" was obtained by summing the $y$ values for each increment between specified values of the relative retention time. The area under each peak as a per cent of the total was then calculated and printed out.

A complete triplicate analysis of a single sample required

(11) E. P. Jones, L. H. Mason, H. J. Dutton, and R. F. Nystrom, *J. Org. Chem.*, **25**, 1413 (1960).
(12) T. L. Mounts and H. J. Dutton, *J. Label. Compounds*, **3**, 343 (1967).
(13) F. A. Blanchard, Mary R. Wagner, and I. T. Takahashi in "Advances in Tracer Methodology," Vol. 4, S. Rothchild, Ed., Plenum Press, New York, 1968, p 133.
(14) M. I. Krichevsky, S. A. Zaveler, and J. Bulkeley, *Anal. Biochem.*, **22**, 442 (1968).

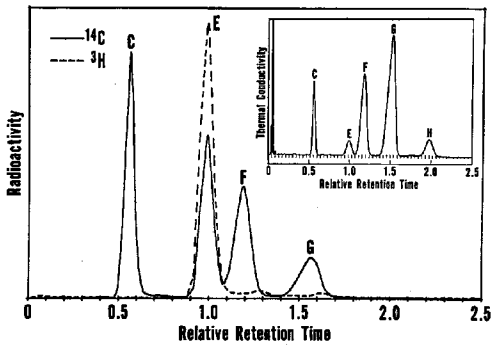


**Figure 2. Computer-plotted profile of radioactivity in the effluent of a gas-liquid chromatograph, averaged from three repeated analyses as described in the text.**

**The sample contained $^{14}C$-labeled methyl palmitate (*C*), methyl stearate (*E*), methyl oleate (*F*), and methyl linoleate (*G*), diluted with soybean oil methyl esters to a final specific activity of 9 nanocuries/mg. Tritium-labeled methyl stearate was added to a final specific activity of 40 nanocuries/mg. Methyl stearate is assigned a relative retention time of 1.0. The thermal conductivity analysis is shown in the insert. H is methyl linolenate**

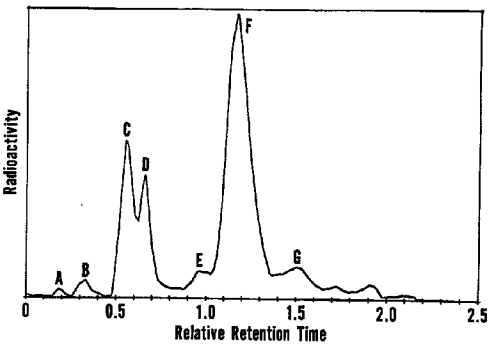


**Figure 3. Profile of radioactivity in the effluent of a gas-liquid chromatograph, obtained as in Figure 2.**

**The sample consisted of methyl esters prepared from the lipids of immature soybean seeds incubated in sodium acetate-1-$^{14}C$ for 15 minutes. The actual measured activity of the total sample before analysis was 845 cpm/mg—*i.e.*, less than 0.5 nanocurie/mg. Methyl stearate is assigned a relative retention time of 1.0. Peaks are identified as follows: methyl laurate (*A*), methyl myristate (*B*), methyl palmitoleate (D); others as in Figure 2. The small peaks after 1.7 are not reproducible and must be assigned to background fluctuations**

3 to 5 hours for gas chromatography and collection of fractions; 24 to 48 hours for liquid scintillation counting (unattended); and less than 15 minutes for data processing and output, starting from the punched tape.

Dual-labeled samples were handled in essentially the same length of time. The plotting routine was simply run twice by using the appropriate data for each isotope. The plots were superimposed on the same chart by using different colored inks. An accurate determination of the isotope ratio could be obtained by plotting $^{14}C$ dpm *vs.* $^{3}H$ dpm for all the fractions collected in a particular peak.

## RESULTS AND DISCUSSION

The important features of the collection system are:

(1) A high temperature is maintained in the gas stream up to the point of its contact with the scintillation solvent.

(2) The holdup volume at all points of the liquid stream is kept to a minimum to eliminate peak tailing. This is especially important in the glass tee, *D*, and the collector valve, *G*.

(3) The joining of the sample and reference streams from the exit of the thermal conductivity cell eliminated about 80% of the noise introduced by gas pressure changes within the cell. This noise was further reduced by the air reservoir at the pump.

The radiochromatogram computed from triplicate analyses of 1- to 2-mg aliquots of the standard sample is shown in Figure 2.

This example illustrates the high resolution achieved by the system we describe. In addition to this standard sample, we have made triplicate analyses of nearly 50 samples, which were isolated from algae and higher plants grown in the presence of carbon dioxide-$^{14}C$, and from seeds incubated in acetate-1-$^{14}C$. Figure 3 shows that useful results can be obtained with specific activities as low as 0.5 nanocurie/mg in a mixture of methyl esters.

In selecting conditions such as fraction spacing, there is a certain degree of "trade-off" between resolution and sensitivity; that is, sensitivity will be increased by collecting fewer fractions with longer intervals; resolution will be correspondingly decreased. The practice of collecting only a single fraction for each peak observed gives very poor resolution and can lead to serious errors of interpretation, because a small amount of material with high specific activity may be mistakenly identified if it overlaps another compound of low specific activity.

When a single run is graphed by plotting the count in each fraction *vs.* its retention time, as we have described, the results are deceptive. The top of each peak will generally fall in a single fraction and will appear as a sharp point. While each point will be plotted with a precision of $\pm 0.002$ relative retention units, its position is significant only to about $\pm 0.03$ units, and compounds differing in relative retention by that amount could not be distinguished. Moreover, with compounds of very low specific activity, the total count in each fraction may be close to the background level. Thus, a noticeable degree of uncertainty may be expected.

This uncertainty could be reduced by repeating the analysis and averaging the two (or more) sets of data. Between repetitions, however, there may be slight changes in the conditions of the chromatographic column, leading to variations in the composition of each fraction collected. The data could not, therefore, be averaged by simply summing the count in corresponding vials for each run and dividing by the number of runs. Such a procedure would at best give no increase in resolution of adjacent peaks; in most cases it would drastically reduce resolution. The logical alternative, and the method we adopted, was to scale the data points on a common axis, interpolate at many increments between points, and average the data at corresponding increments for the several runs.

This procedure, which was possible only with the aid of a digital computer, successfully reduced the "noise" or random error, in the final plot. It also led to an increase in resolution when the fractions of successive runs did not coincide, because the total number of actual data points was increased from perhaps 60 to 180. Peak positions could now be considered significant to a precision of $\pm 0.01$ relative retention units, subject to the limitation described below. Calculations of the percentage of radioactivity in each peak showed an average

deviation of 0.4% when calculated from a single run, and only 0.06% when calculated from a triplicate.

The ultimate capability of the system is demonstrated by Figure 2, which compares the radioactive analysis of a standard dual-labeled mixture, described above, with the corresponding thermal conductivity analysis. This mixture was employed routinely to test the performance of our system. The data shown in the figure are typical of the results obtained when the system was functioning properly. From measurements of the peak widths, and using the general relation that the peak width is inversely proportional to the square root of the number of theoretical plates for the column, we can estimate the resolution of our radioactivity separation. Our estimation is that this resolution corresponds to about 60% of the number of theoretical plates obtained for the nonradioactive separation.

In matching peaks of the thermal conductivity recording with those of the radioactivity profile, it is necessary to make a slight correction for the "time lag." This lag leads to a small uncertainty in the precise position of the radioactive peak; however, this uncertainty is generally smaller than 1 to 2% of the retention time. If a dual-labeled compound is present, the coincidence of the $^{14}C$ peak and the tritium peak is visibly apparent. Therefore, if a small amount of tritium-labeled standard is added to a mixture of $^{14}C$-labeled compounds, peaks may be matched to a precision of 0.5% of the retention time.

On closer examination of dual-labeled compounds, a small separation may be observed due to an isotope effect (*15*). In the analysis shown in Figure 2, the ratio of $^{14}C$ to tritium increased from 0.09 in the first half of the methyl stearate peak to 0.11 in the second half. This increase amounts to a difference in retention time for the two isotopic compounds of roughly 1 part in 300.

When this very slight isotopic effect is taken into account, the precision of determining isotope ratios with this technique is unsurpassed by any other system. Simultaneous independent measurement of carbon and hydrogen cannot be done with ionization detectors. The analysis can be performed with continuous-flow scintillation counters (*16*), or with proportional counters, by combustion of the effluent, splitting of the stream, chemical separation of carbon dioxide from water, reduction of the water to hydrogen, and subsequent measurement of the radioactivity of the carbon dioxide and hydrogen in separate counters (*17*). This procedure introduces many uncertainties in the relative amounts of the two isotopes, since there may be variations in the efficiency at the combustion, reduction, trapping, and counting stages. By contrast, the system we describe measures both isotopes on the same collected fractions, and the efficiency of collection must be identical for both. The efficiency of counting the collected fractions is easily determined with modern scintillation counters (*13*, *14*).

Dual-label radiochromatography offers many advantages for chromatographic analysis. Tritium-labeled internal standards may be added to $^{14}C$-labeled samples, or *vice versa*, to check the coincidence of retention times, the relative specific activities, and the relative collection efficiency of different compounds. The use of tritium-labeled standards for programmed-temperature gas chromatography of fatty ester ozonolysis products, as outlined by Dutton (*18*), can be extended by using $^{14}C$-carboxyl-labeled standards to distinguish aldehydes from aldehyde-esters. Liquid-liquid chromatography should also be amenable to double-labeled isotope analysis with this procedure. The use of computer programs such as we describe greatly shortens the time required for computation and processing of the data and increases the accuracy and credibility of the results. We will provide any or all of these computer programs upon request.


## ACKNOWLEDGMENT

We are grateful to J. O. Ernst and R. O. Butterfield of this Laboratory for helpful advice on computer programming.

RECEIVED for review October 16, 1968. Accepted January 16, 1969. Presented at 156th meeting of the American Chemical Society, Atlantic City, N.J., September 1968. The Northern Regional Research Laboratory is headquarters for the Northern Utilization Research and Development Division, Agricultural Research Service, U.S. Department of Agriculture. Mention of trade or company names is for identification only and does not imply endorsement by the Department.



(15) P. D. Klein, *Sep. Sci.*, **1**, 511 (1966).
(16) G. Popják, A. E. Lowe, and D. Moore, *J. Lipid Res.*, **3**, 364 (1962).
(17) Leon Swell, *Anal. Biochem.*, **16**, 70 (1966).
(18) H. J. Dutton, presented at Pittsburgh Conference on Analytical Chemistry and Applied Spectroscopy, Cleveland, Ohio, March 1968.

# Quantitative Aspects of Nuclear Quadrupole Resonance Spectrometry of Inorganics and Minerals

**Harry D. Schultz and Clarence Karr, Jr.**

*Morgantown Coal Research Center, Bureau of Mines, U.S. Department of the Interior, Morgantown, W.Va. 26505*

**Quantitative nuclear quadrupole resonance (NQR) spectrometric analyses of synthetic mixtures and natural ores are presented, apparently for the first time. Reproducible linear quantitative calibration curves were obtained on several inorganic compounds ($Cu_2O$, $HgCl_2$, $BiCl_3$), using the signals from $^{63}Cu$, $^{65}Cu$, $^{35}Cl$, and $^{209}Bi$. Synthetic mixtures of $HgCl_2$ in NaCl, and $BiCl_3$ in KCl, were analyzed by NQR for weight-per cent $HgCl_2$ and $BiCl_3$, respectively, with good results. In addition, several samples of cuprite ore were analyzed for weight-per cent of $Cu_2O$ from the standard curves. Noted were the influence of various instrument parameters and the physical state of the sample on quantitative NQR spectrometry.**

NUCLEAR QUADRUPOLE RESONANCE (NQR) spectrometry is a relatively new technique for the structure determination of compounds. An NQR spectrometer detects the absorption of energy from quadrupolar nuclei that are located in nonspherical electrical fields. It is similar in many ways to nuclear magnetic resonance (NMR) spectrometry primarily in that an applied RF field is used to effect nuclear spin transitions. With either technique an operator can discern subtle properties of molecular structure, such as geometric isomers in organics or crystal structure differences in inorganics, from the resonance frequencies and intensities of the signals. The most important difference is that NQR uses the built-in electric field gradients in a crystal to observe the frequency of the nuclear spin transitions, whereas NMR requires an externally applied magnetic field. However, several conditions must be met before NQR signals can be observed. In the first place, the compound must contain at least one isotope whose nucleus has a quadrupole moment that is greater than zero ($Q > 0$) and a spin quantum number that is greater than one half ($I > 1/2$). Approximately 130 isotopes meet these requirements (*1*). Second, samples must be solid. If the samples are not solid at ambient temperature, they must be cooled, usually with liquid nitrogen (77 °K) to make them solid. All the inorganic samples discussed in this paper were solids at ambient temperature. Virtually all minerals are solids.

Although NQR spectrometry has been used to advantage in crystal structure determinations of inorganics, it has apparently never been used previously for quantitative analyses of synthetic mixtures or natural ores. In fact, the operating parameters for the instrument and the effect of the physical state of the sample for quantitative use of NQR spectrometry apparently have not been previously determined.

## EXPERIMENTAL

The studies were made on the Wilks Model NQR-1A nuclear quadrupole resonance spectrometer (*1*). The Wilks spectrometer is a transistorized version of the first self-adjusting NQR instrument developed by Dr. George Peterson of Bell Telephone Laboratories in 1965 (*2, 3*).

The spectrometer includes a self-quenched oscillator employing a feedback loop. A servo motor is used to adjust the coherence, thus solving the problem of nonlinearity in the feedback system and its consequent limit of scanning band

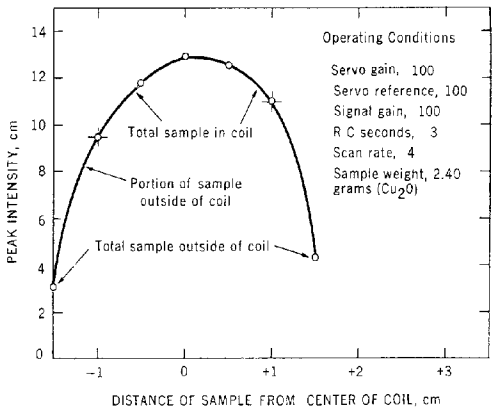


**Figure 1. Effect of sample position in RF Coils**

As the spectrometer is changed in frequency, any variation in noise level is detected and compensated. The resonance signal was recorded on a Leeds & Northrup strip chart recorder.

## RESULTS AND DISCUSSION

**Operating Parameters.** Instrument operating parameters were determined first. The position of the sample in the radio frequency coil was very important for obtaining the maximum sensitivity. Figure 1 shows the top portion of a curve, probably gaussian, obtained by placing a relatively thin layer of $Cu_2O$ at different heights in the radio frequency coil, the resonance of the $^{63}Cu$ being 26.5 MHz at room temperature. The scan rate of 4 represents 8.33 MHz per hour. Figure 1 demonstrates that the strongest resonance was obtained when the sample was positioned in the center of the coil. This is due to the nonlinearity of the RF-field intensity along the axis of the coil. The quantitative aspect of this effect is demonstrated in the S-shaped curve obtained, Figure 2. In this instance, the peak height increased nonlinearly as the total weight of $Cu_2O$ was increased, with the sample vial setting on the plate below the coil. This effect depends on changing the number of quadrupolar nuclei present. Again, the largest increases were observed for that part of the sample near the center of the coil. Consequently, for quantitative NQR analyses, only the coil region should be used, although a weak signal can be obtained on that portion of the sample along the axis immediately outside of the receiving coil. All samples must occupy the same volume within the same portion of the coil,

(1) T. P. Das and E. L. Hahn, "Solid State Physics," Supp. 1, "Nuclear Quadrupole Resonance Spectroscopy," Academic Press, Inc., New York, N.Y., 1958, 223 pp.
(2) P. M. Bridenbaugh and G. E. Peterson, *Rev. Sci. Instrum.*, **36**, 702 (1965).
(3) G. E. Peterson and P. M. Bridenbaugh, *ibid.*, **35**, 698 (1964).

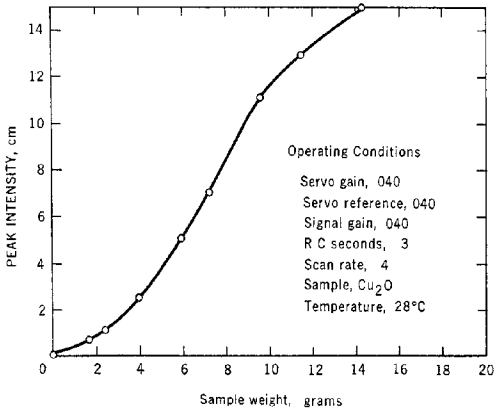


**Figure 2. Effect of quantity of sample in RF Coil**

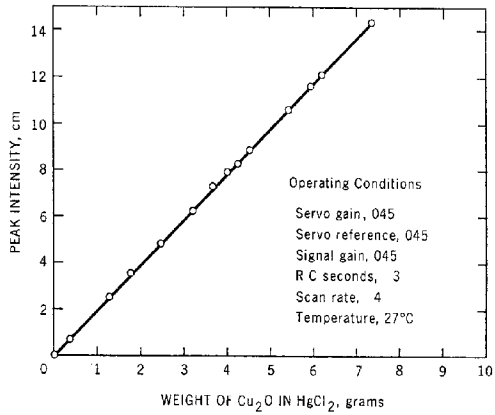


**Figure 3. Calibration curve for $^{63}Cu$ (26.5 MHz) in $Cu_2O$**

for a given quantitative analysis. This may require dilution of the sample by thorough blending with a solid that will not react chemically under these conditions nor contain an isotope that is NQR active in the region used.

The results were reproducible from one day to the next. Reproducible results could be obtained with spectrometer settings other than those shown in the figures.

**Sample Purity.** Impurities in the crystal lattice produce line broadening and reduce a signal intensity. However, this phenomenon is not observed with mechanical mixtures of compounds. To demonstrate this with inorganic compounds, two completely separate $^{35}Cl$ NQR signals were obtained from mixtures of $NaClO_4$ (at 27.8 MHz) and $KClO_4$ (at 29.9 MHz). The mixtures gave signals for the $NaClO_4$ and $KClO_4$ of intensities equal to the signals obtained on the single compounds. The only reference found in the literature on NQR of mixtures was for separate signals for $^{35}Cl$ in a mixture of two solid phases of hexachlorocyclopentadiene (*4*). No quantitative analysis was made on this organic mixture by NQR. In most instances crystal lattice impurities are either negligible, or sufficiently consistent, so that practical calibration curves can be determined. The question of relative lattice impurity can be resolved readily by comparing samples, all of known high purity, from different sources. The effect on the lattice of grinding the samples is shown later in this report.

**Calibration Curves for Pure Inorganics.** Varying amounts of $Cu_2O$, 0.32 to 7.31 grams, were weighed into vials and the total volume was held constant using $HgCl_2$ as the filler material or diluent. In each instance the height of the total sample corresponded to the height of the RF coil. The height of the center line of the split resonance peak was measured in centimeters, and the relationship of peak height to weight of $Cu_2O$ was plotted. Figures 3 and 4 show the results of these determinations. Two excellent linear relationships of 14 points were obtained, one for $^{63}Cu$ at 26.5 MHz and one for $^{65}Cu$ at 24.6 MHz. In addition, linear calibration curves were established for the two signals from $^{35}Cl$ in $HgCl_2$ observed at 22.4 and 22.5 MHz using $Cu_2O$ as diluent, as shown in Figure 5, and for $^{209}Bi$ in $BiCl_3$ observed at 37.5 MHz using $Bi_2O_3$ as diluent, as shown in Figure 6. Linear calibration curves were thus obtained with four different nuclides ($^{63}Cu$, $^{65}Cu$, $^{35}Cl$, $^{209}Bi$), two different nuclides in the same environment ($^{63}Cu$ and $^{65}Cu$ in $Cu_2O$), and the same nuclide in two nonequivalent environments ($^{35}Cl$ in $HgCl_2$).

Shoji Kojima *et al.* (*5*) studied the integrated intensity *vs.*

(4) M. Hayek and D. Gill, *J. Chem. Phys.*, **47**, 3680 (1967).

(5) S. Kojima, S. Ogawa, M. Minematsu, and M. Tanaka, *J. Phys. Soc. Jap.*, **13**, 446 (1955).

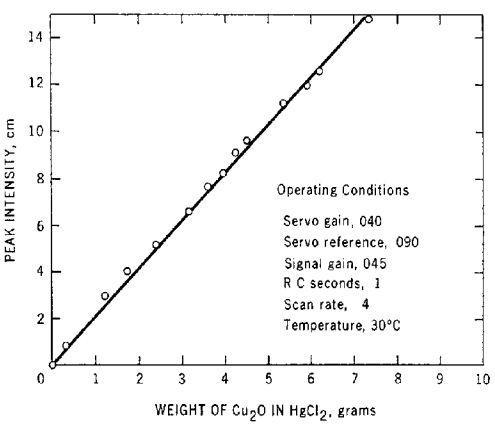


**Figure 4. Calibration curve for $^{65}Cu$ (24.6 MHz) in $Cu_2O$**

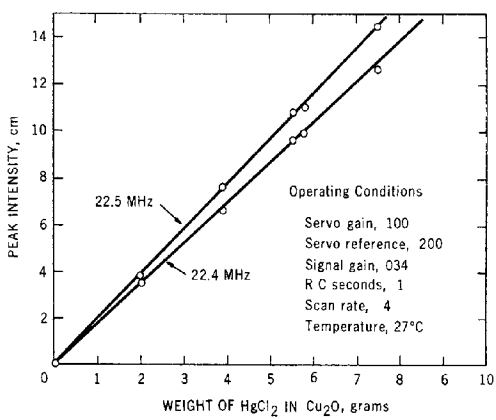


**Figure 5. Calibration curve for $^{35}Cl$ in $HgCl_2$**

**Table I. Quantitative NQR Analysis of Synthetic Mixtures**

| Wt of $BiCl_3$ in KCl, g | Total wt of mixture, g | $BiCl_3$ wt % | Wt of $BiCl_3$, g, from 37.5 MHz calibration curve | $BiCl_3$, wt % from 37.5 MHz calibration curve | Difference, wt % |
|---|---|---|---|---|---|
| 1.20 | 4.23 | 28.4 | 1.05 | 24.8 | + 3.6 |
| 2.56 | 4.86 | 52.7 | 2.63 | 54.1 | − 1.9 |
| 3.77 | 5.20 | 72.5 | 3.82 | 73.5 | − 1.0 |

| Wt of $HgCl_2$ in NaCl, g | Total wt of mixture, g | $HgCl_2$ wt % | Wt of $HgCl_2$, g, from calibration curves | | $HgCl_2$, wt %, from calibration curves | | Difference, wt % | |
|---|---|---|---|---|---|---|---|---|
| | | | 22.4 MHz | 22.5 MHz | 22.4 MHz | 22.5 MHz | 22.4 MHz | 22.5 MHz |
| 1.04 | 3.55 | 29.3 | 1.10 | 1.00 | 31.0 | 28.2 | − 1.7 | + 1.1 |
| 2.41 | 4.73 | 51.0 | 2.45 | 2.30 | 51.8 | 48.6 | − 0.8 | + 2.4 |
| 3.92 | 5.07 | 77.3 | 3.90 | 3.87 | 76.9 | 76.3 | + 0.4 | + 1.0 |

**Table II. Quantitative NQR Analysis of Cuprite Mineral Samples**[a]

| Sample source | Weight of sample, grams | Weight of $Cu_2O$ in cuprite, grams (from 26.5 MHz) | $Cu_2O$ in cuprite, wt % | |
|---|---|---|---|---|
| | | | 26.5 MHz | 24.6 MHz |
| Butte, Montana No. 1 | 5.01 | 1.00 | 20.0 | |
| | 4.58 | 1.15 | 25.1 | 29.5 |
| Butte, Montana No. 2 | 3.07 | 1.00 | 32.6 | 33.9 |
| | 4.57 | 1.70 | 37.1 | |
| Bisbee, Arizona | 4.03 | 0.90 | 20.9 | 21.2 |
| | 4.58 | 0.65 | 14.2 | |
| | 2.29 | 0.35 | 15.3 | |
| Ajo, Arizona | 6.89 | 7.00 | 101.6 | 99.1 |
| | 6.89 | 7.05 | 102.3 | |
| | 6.79 | 6.95 | 102.4 | |
| | 5.70 | 5.60 | 98.2 | 99.4 |
| | 6.79 | 7.05 | 103.8 | |

[a] Physical state of sample: solid chunks.

amount of *p*-dibromobenzene impurity in α-phase *p*-dichlorobenzene. They observed a decrease in integrated intensity commencing at a concentration of impurity of 0.1%, and they plotted a linear decrease in peak area measurements up to 1% impurity. The instrument used was a continuous wave spectrometer described by Wang (*6*). Area measurements were taken from the recorded derivative curve. Our perimeter area measurements obtained by enclosing the split resonance signal in a hand drawn envelope gave calibration lines of less reproducibility and linearity than peak height measurements.

In day-to-day work with calibration curves, it was occasionally desirable to compensate for instrumental drift by checking the signal intensity of a few standard samples and adjusting the servo reference and gain accordingly before proceeding to unknown samples. Signal intensities would then automatically fall at the appropriate point on the calibration curve.

The calibration curves indicate that the quench frequency is reproducible, and therefore peak height measurement is acceptable for quantitative analyses. Considering the rather large amount of data collected to establish the calibration curves, the reproducibility of the quench frequency is shown by the excellent linearity of the lines, the reproducibility of the calibration lines, and the reproducibility of the specific points on the line. The reproducibility of the individual points on the calibration line was approximately 0.1 cm on successive scans. If the quench frequency varied randomly, these observations could not be made. Investigations of the stability of the quench frequency, using an oscilloscope, were

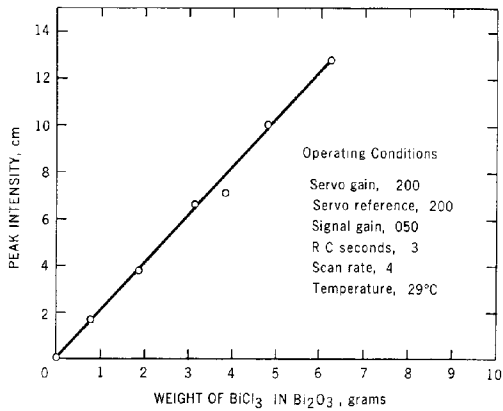


**Figure 6. Calibration curve for $^{209}Bi$ (37.5 MHz) in $BiCl_3$**

conducted at several resonant frequencies. The results indicated that the quench frequency was stable at a given resonant frequency as long as the quench gain and quench reference controls were not varied. Naturally, for the determination of any specific calibration curve, the quench gain and reference are held at a constant value.

Synthetic mixtures of $BiCl_3$ in KCl, and $HgCl_2$ in NaCl, were analyzed using resonances of $^{209}Bi$ at 37.5 MHz, and $^{35}Cl$ at 22.4 and 22.5 MHz for the mercury compound. In each instance the compound under investigation and the diluent were weighed, thoroughly blended, and placed into vials. The filler material was in each instance a different compound than

(6) T. C. Wang, *Phys. Rev.*, **99**, 566 (1955).

Table III. Effect of Grinding on Cuprite

| Sample source | Physical state of sample | Weight of sample, grams | Weight of $Cu_2O$ in cuprite, grams (from 26.5 MHz) | $Cu_2O$ in cuprite, wt % (from 26.5 MHz) |
|---|---|---|---|---|
| Butte, Montana No. 1 | Solid chunks | 4.58 | 1.15 | 25.1 |
| | Grind 5 min. | 4.15 | 0.25 | 6.0 |
| Ajo, Arizona | Solid chunks | 6.79 | 7.05 | 103.8 |
| | Grind 5 min. | 6.42 | 4.80 | 74.8 |
| | Grind 10 min. | 5.96 | 1.75 | 29.4 |
| | Grind 15 min. | 5.82 | 0.23 | 3.9 |

the one used in determining the calibration curve. This was necessary for a genuine evaluation of the accuracy of the analytical method. The total volume was held constant for each mixture. The height of the resonance signal was directly proportional to the weight of the compound in the sample. The results for six different samples are summarized in Table I. These results suggest that NQR quantitative analysis of synthetic mixtures is comparable in accuracy to other spectrometric methods such as infrared analysis.

**Analysis of Mineral Samples.** Several different samples of the mineral cuprite were analyzed for $Cu_2O$ content. The results of 17 analyses of four different cuprite ores are summarized in Table II. When two or more vials were filled to a line (representing the calibration volume) with small, solid pieces of an ore sample, and the peak height was determined as a measure of the weight of $Cu_2O$ in the cuprite ore, the analyses showed the same $Cu_2O$ content within a few weight-per cent. In 5 representative instances, the 24.6 MHz values were also determined to demonstrate good agreement with the 26.5 MHz values.

There was a decrease of the $^{63}Cu$ signal at 26.5 MHz (Table III) as the result of grinding in a tungsten carbide vial. This is attributed to the alteration of the crystal lattice system of $Cu_2O$. The X-ray diffraction pattern of ground cuprite showed broadening in the back reflection region as contrasted to the normal X-ray diffraction pattern of unground cuprite and synthetic $Cu_2O$. The apparent reason for this broadening is slight disorder in the crystal lattice system created by the vigorous grinding with the tungsten carbide vial. A detailed grind study on minerals and inorganics is in progress, employing several different grinding methods. The conclusions will be reported in a separate publication. Preliminary results indicate no reduction in signal intensity of cuprite if an agate vial or hand grinding with mortar and pestle is employed. Obviously some ore samples must not be subjected to vigorous grinding before the analysis. This presents no analytical problems because an average value can be determined from several different selections of small pieces of ore, or a mild grinding method can be employed. This is demonstrated for five different selections of small pieces of the high-purity Ajo, Ariz., ore (Table II). All samplings consistently gave values close to 100% $Cu_2O$. In this regard, NQR analysis is faster and much simpler than infrared analyses in which samples must be ground until reproducible absorptivities are obtained.

In addition to the mineral cuprite, the resonance of $^{121}Sb$ in the mineral stibnite ($Sb_2S_3$) was detected at 45.1 MHz on two different ore samples. Pure $Sb_2S_3$ of the same crystal structure as the mineral was not available for determining a calibration curve. Identity of crystal structure is shown readily by identical frequency values for the NQR signals. Work is in progress on other minerals and inorganics.

The results reported here indicate that quantitative NQR analysis of ores and other natural mixtures for various specific inorganics and minerals gives reproducible results that are comparable to other spectrometric methods in accuracy and has considerable promise for future development.


## ACKNOWLEDGMENT

We are grateful to John J. Renton, Geology Department, West Virginia University, for providing X-ray diffraction data on samples.

RECEIVED for review November 6, 1968. Accepted February 6, 1969. Presented at the Division of Analytical Chemistry, 156th Meeting, ACS, Atlantic City, N.J., September 1968. The equipment is named in this report for identification only and does not necessarily imply endorsement by the Bureau of Mines.

# Cation Exchange Separation–X-Ray Spectrometric Determination of Scandium in Plutonium

**E. Arnold Hakkila, Ronald G. Hurley, and Glenn R. Waterbury**

*The Los Alamos Scientific Laboratory, University of California, Los Alamos, N.M. 87544*

A RAPID METHOD was required for determining scandium present in concentrations between 0.05 and 0.4% in alloys with plutonium. X-ray fluorescence methods were considered because generally they are specific, rapid, and easy to use. Scandium intensities measured with a helium-path spectrometer from plutonium-containing solutions were approximately 10 cps for 1 mg of scandium per ml, indicating the required sensitivity of 0.05% could not be obtained without separations. Precipitating agents such as fluoride, hydroxide, or oxalate, normally used to separate rare earths, did not quantitatively precipitate scandium. Ion exchange separations were then considered.

Korkisch and Ahluwalia (*1*) studied the cation exchange behavior of various ions from hydrochloric acid–organic solvent media. Although scandium and plutonium were not investigated, studies with uranium(VI) and cerium(III) suggested application of cation exchange filter papers to remove scandium from plutonium(VI) solutions in hydrochloric acid–organic solvent media. Applications of ion exchange filter papers to the separation of trace elements from aqueous media prior to X-ray fluorescence measurements were reported by Campbell, Spano, and Green (*2*).

## EXPERIMENTAL

**Apparatus and Reagents.** A Philips Electronics Corp. vacuum X-ray spectrograph equipped with a chromium target X-ray tube, LiF analyzing crystal, and a flow proportional detector with P-10 gas was used for X-ray measurements. Adequate intensities for the $K\alpha$ X-ray of scandium were obtained operating with an air path (20 cps per $\mu$g of scandium). Therefore, helium or vacuum path operation were considered unnecessary.

Reeve-Angel SA-2 cation exchange filter papers were cut to 15/16-inch diameter, and discs, selected at random, were weighed to assure that weights ranged between 60 and 70 mg. The exchange capacity of a disc was calculated to be 1.5 to 2 mg of scandium. The filtering apparatus consisted of a 125-ml Erlenmeyer flask, a modified size 000A Hirsch funnel, and a glass chimney held in place over the Hirsch funnel with a No. 35 pinch clamp. The flow rate was adjusted to approximately 50 cc/min using a controlled air leak to the vacuum.

The plutonium metal was prepared by a Los Alamos electrorefining process (*3*) and contained 100 ppm of americium, less than 200 ppm of other detected metallic impurities, and no scandium. Scandium solutions were prepared from 99.9% pure scandium oxide.

**Solvent System.** The studies of Korkisch and Ahluwalia (*1*) with uranyl and cerous ions indicated that the following hydrochloric acid–organic solvent systems might be used for separating scandium from plutonyl ion: (1) 90% isopropanol–0.3 to 1.2*M* hydrochloric acid, (2) 90% 1,2-propanediol–0.5 to 1.2*M* hydrochloric acid, (3) 90% acetic acid–0.6 to 1.2*M* hydrochloric acid, (4) and 90% acetone–0.1 to 1.2*M* hydrochloric acid. Good separations of scandium from plutonium were obtained only with the acetone–hydrochloric acid system at low acid concentrations. The optimum hydrochloric acid concentration for the separation of 100 $\mu$g of scandium from plutonium was determined by analyzing a set of solutions in which the final acidity varied from 0.05 to 0.9*M*. Lanthanum was added to serve as internal standard in each test.

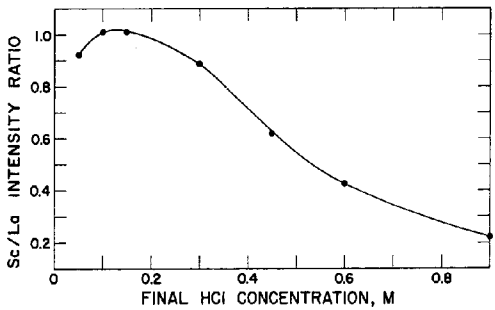


**Figure 1. Effect of acid concentration on Sc/La intensity ratio (100 $\mu$g Sc)**

The scandium and lanthanum were adsorbed onto SA-2 filter papers and the scandium and lanthanum X-ray intensities measured. The data (Figure 1) showed that the scandium/lanthanum intensity ratio did not vary appreciably for hydrochloric acid concentrations between 0.1 and 0.2*M*; therefore, an acidity of 0.1*M* was selected for all further work.

**Internal Standard.** Approximately 90 to 95% of the scandium was adsorbed onto SA-2 filter papers in six passes from solutions containing 100 $\mu$g of scandium in 50 ml of 90% acetone–0.1*M* hydrochloric acid. The adsorption was reduced if strongly absorbed cations were present in amounts greater than a few hundred micrograms. An internal standard technique was utilized, therefore, to reduce the effect of variable adsorption of scandium. The internal standard selected was lanthanum which had adsorption and chemical properties similar to those of scandium. In addition, lanthanum has the longest wavelength $L\alpha_1$ X-ray of the rare earth elements. The distribution coefficient for lanthanum in acetone–0.1*M* hydrochloric acid is $>10^3$ (*1*); the distribution coefficient for scandium was not measured. Cation exchange studies of scandium and rare earths in sulfuric acid (*4*) showed that scandium was not adsorbed as strongly as the rare earths. This may also be the case in the organic–hydrochloric acid system.

(1) J. Korkisch and S. S. Ahluwalia, *Talanta*, **14**, 155 (1967).
(2) W. J. Campbell, E. F. Spano, and T. E. Green, ANAL. CHEM., **38**, 987 (1966).
(3) J. A. Leary and L. J. Mullins, U.S. At. Energy Comm. Rept. LA-3356-MS, 1965.
(4) F. W. E. Strelow and C. J. C. Bothma, ANAL. CHEM., **36**, 1217 (1964).

**Table I. X-Ray Lines that Overlap the $L\alpha_1$ Line for Lanthanum and the $K\alpha$ Line for Scandium**

| Element | X-Ray | Diffraction angle, degrees $2\theta$, LiF | Relative intensity |
|---|---|---|---|
| La | $L\alpha_1$ | 82.85 | 100 |
| Ce | $L\eta$ | 81.15 | 10 |
| Pt | $L\alpha_1$ (n = 2) | 81.38 | 100 |
| Sb | $L\gamma_{2,3}$ | 81.86 | 10 |
| Pt | $L\alpha_2$ (n = 2) | 82.28 | 10 |
| Cs | $L\beta_4$ | 82.88 | 20 |
| Nd | $Ll$ | 83.23 | 30 |
| Cs | $L\beta_1$ | 83.53 | 80 |
| Sb | $L\gamma_2$ | 83.99 | 10 |
| Sc | $K\alpha$ | 97.66 | 100 |
| Sn | $L\gamma_1$ | 96.32 | 40 |
| Sb | $L\beta_1$ | 96.49 | 80 |
| La | $Ll$ | 96.54 | 30 |
| Te | $L\beta_3$ | 96.67 | 30 |
| Sb | $L\beta_2$ | 97.27 | 60 |
| Ta | $L\alpha_1$ (n = 2) | 98.17 | 100 |
| Te | $L\beta_4$ | 98.26 | 20 |

**Effect of Sample Size.** The range of sample sizes that could be analyzed by the recommended method was investigated by determining known amounts of scandium between 0 and 400 μg in 100, 200, 500, or 1000 mg of plutonium. Ratios of scandium intensity to lanthanum intensity (Figure 2) showed that the method tolerated only small variations in sample size; the intensity ratio decreased as the plutonium content or sample size increased. This was caused by incomplete oxidation of the plutonium(IV) which also was adsorbed. The adsorbed plutonium displace the more weakly cationic scandium and tended to partition the lanthanum and the scandium on the filter paper. By proper preparation of standards, the method was readily applied to determination of as little as a few ppm of scandium in 1-gram samples of plutonium.

**Recommended Procedure.** Weighed 100 ± 10 mg samples of plutonium were dissolved in hydrochloric acid and 2 ml of 70% perchloric acid. Five hundred micrograms of lanthanum were added, and the solutions were fumed to incipient dryness at a temperature of 225 °C. The residue was dissolved in 5.0 ml of 1*M* hydrochloric acid, and 46 ml of acetone were added. The solution was passed through an SA-2 cation exchange filter paper six times at a flow rate of 50 ml per min. The paper was washed with 5 to 10 ml of 90% acetone–0.1*M* hydrochloric acid and dried under an infrared lamp. The dried paper, held between two layers of 0.25-mil Mylar in the Philips standard sample holder, was irradiated using a chromium target X-ray tube operated at 48 kV and 28 mA. The intensities of the $K\alpha$ X-ray for scandium and the $L\alpha_1$ X-ray for lanthanum were determined by measuring the number of counts accumulated in 10.00 seconds while the sample was rotated under the X-ray beam. The sample was inverted and the intensities from the back of the disc were measured in the same manner. The scandium-to-lanthanum intensity ratio was calculated from the total counts accumulated from fronts and backs of the papers (without background corrections), and the scandium content was determined by comparing the intensity ratio to ratios obtained for standards prepared by separating known amounts of scandium from 100 mg of plutonium.

## RESULTS AND DISCUSSION

**Reliability.** The reliability of the method was determined by repeated analyses of solutions containing known quantities of scandium and 100 mg of high purity plutonium. Fourteen samples were analyzed at each scandium concentration. The data showed that the relative standard deviation of the method was approximately 2% for determining 50 to 400 μg of scandium. The standard deviation for measuring a blank was 0.15 μg, indicating that the lower limit of reliable measurement was approximately 0.5 μg (5 ppm for 100-mg samples). The method was unbiased.

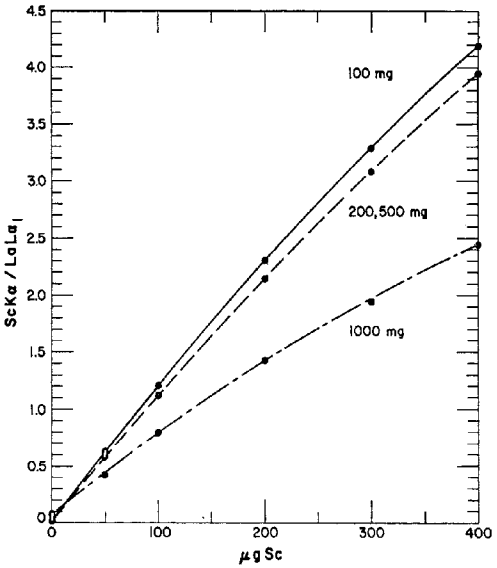


**Figure 2. Effect of sample size on Sc/La intensity ratio**

**Interferences.** Expected interferences in this method were: X-ray line overlap by elements adsorbed on the ion exchange resin, and swamping of the resin by elements which had greater distribution coefficients than that for scandium. Because of the limited exchange capacity of the discs, microgram amounts of strongly absorbed cations were expected to interfere.

Overlap interference may be caused by elements that have X-ray lines within approximately two line half-widths (1.9° $2\theta$) of the $K\alpha$ X-ray for scandium or the $L\alpha_1$ X-ray for lanthanum, providing these elements are retained on the resin. Possible interfering X-rays are listed in Table I. Only first order lines having a relative intensity of 10 or greater are listed, except for tantalum and platinum which have intense second order $L\alpha_1$ lines near the lines used in the analysis.

Of these elements, the effects of cesium, neodymium, and platinum on the determination of scandium were studied. Results showed that no greater than 50 μg of cesium, 100 μg of neodymium, or 500 μg of platinum can be tolerated. The second order X-ray for platinum was not completely eliminated using the pulse height analyzer.

The decrease in scandium/lanthanum intensity ratio with increasing sample weight (Figure 2), as discussed previously, indicated that lanthanum is more tightly adsorbed on SA-2 papers than is scandium. It would be expected, therefore, that cations such as other rare earths would tend to partition scandium and lanthanum. To study the effect of a typical rare earth on the determination of scandium, a series of samples was prepared to contain 0 or 100 μg of scandium, 500 μg of lanthanum, 100 mg of plutonium, and between 100 and 5000 μg of cerium. The results show that greater than 100 μg of cerium interferes.

In addition to cerium, the effects of sodium ($K_d > 10^3$), aluminum ($K_d > 10^3$), calcium ($K_d > 10^3$), nickel ($K_d > 10^3$), terbium ($K_d > 10^3$), thorium ($K_d > 10^3$), cobalt ($K_d = 500$),

copper ($K_d = 3$), cadmium ($K_d = 2$), iron ($K_d < 1$), zinc ($K_d < 1$), gallium ($K_d < 1$), bismuth ($K_d < 1$), and uranium ($K_d < 1$) on the separation of scandium from plutonium were studied. These elements were selected to include mono- to tetravalent elements having $K_d$ values in the range between 1000 (strongly adsorbed) and $< 1$ (weakly or not adsorbed). These studies showed that 100 $\mu$g of elements having $K_d >$ 1000 can be tolerated in the determination of scandium. For copper, which has a $K_d$ value of 3, 1 mg can be tolerated. For those elements having $K_d$ of 2 or less, 100 mg did not interfere.

Although the method applies specifically to the determination of scandium in plutonium, it can be readily adapted to determining other strong cations, such as rare earths, or scandium in other materials that are not adsorbed on cation exchange membranes. One analyst can separate and measure eight samples in duplicate per day.


### ACKNOWLEDGMENT

The authors are indebted to Dr. C. F. Metz, who supervised this work, for valuable suggestions, and to Miss H. L. Barker for performing some of the separations and X-ray measurements.

RECEIVED for review November 15, 1968. Accepted January 8, 1969. The Los Alamos Scientific Laboratory is operated under the auspices of the Atomic Energy Commission.


# Infrared Spectra of Compounds Separated by Thin Layer Chromatography Using a Potassium Bromide Micropellet Technique


**W. J. de Klein**

*Laboratory of Organic Chemistry, State University of Leiden, Leiden, The Netherlands*


COMBINATION of thin layer chromatography (TLC) and infrared spectroscopy (IR) is an interesting and promising extension of both techniques. The separation of the components of a mixture by TLC and examination of the resulting spots by IR is one of the most useful ways of identifying the unknown compounds.

Several procedures have been described in the literature. These include scraping of the sample from the support, followed by filtration, centrifugation or elution of the sample from the support material (*1*) or followed by packing the support into a Pasteur type pipet and elution of the compound into the tip of the pipet, evaporation of the solvent and dissolution of the compound in a solvent which is suitable for IR measurement (*2*); and scraping the support surrounding the spot from the chromatoplate, building a dam of KBr powder onto the tip of the spot, and eluting the compound directly onto the KBr powder (*3*).

Experience has shown that the method of Sturn, Parkhurst, and Skinner (*1*) is not directly suited to the infrared experiment for it was developed as a combination with ultraviolet spectroscopy which permits a much larger dilution. The method of McCoy and Fiebig (*2*) is rather time consuming (40–85 minutes) and suffers from the restriction that spectra can only be measured in a solvent. Rice's method (*3*) is a rather promising technique but is limited by the skill of the individual worker for considerable loss occurs when the elution solvent spills from the support on to the glass plate.

A method is now described which is rapid and generally applicable for it uses the KBr technique and gives relatively high recovery. Garner and Packer (*4*) have described a similar technique employing Harshaw's Wick-Stick.


(1) P. A. Sturn, R. M. Parkhurst, and W. A. Skinner, ANAL. CHEM., **38,** 1244 (1966).
(2) R. N. McCoy and E. C. Fiebig, *ibid.*, **37,** 593 (1965).
(3) D. D. Rice, *ibid.*, **39,** 1906 (1967).
(4) H. R. Garner and H. Packer, *Appl. Spectrosc.*, **22,** 122 (1967).




**Figure 1. The shape of the KBr wall around the tip of the spot depends somewhat on the size of the spot. The upper spot is small and requires a relatively larger envelope**

### EXPERIMENTAL

Glass plates (5 × 20 cm) were coated with a 250-$\mu$ layer of either silica gel (Merck HR), or silica gel containing an inorganic fluorescent indicator and gypsum (Merck GF 254), or aluminium oxide (Merck GF 254). The plates were air dried and heated as described. They were then stored in an air-tight box. Glass plates coated with cellulose (Merck, Fertigplatten F, thickness 80 $\mu$) were used in some experiments.

One to fifty micrograms of a compound in solution were applied to the plates with a micropipet (Camag AG, Muttenz, Schweiz). The plates were developed in the usual manner in covered chromatographic tanks. The walls of the tanks were not paper covered for vapor saturation. Location of separated components was done by irradiation with ultraviolet radiation at 254 or 350 m$\mu$. The spots were outlined by scratching the support.

After evaporation of the elution solvent, the TLC support was removed around the spot. The glass around the spot was carefully cleaned with tissue paper or wash leather. A wall of KBr powder was built around the tip of the spot and an open space of 1–2 mm left between the spot and the KBr wall (Figure 1). This wall can easily be built by lightly tapping a Pasteur pipet, containing finely divided KBr powder, with the

**Table I. Dependence of Recovery and Contamination on Type of Compound and Solid Support**

| Compound | Type of support | Amount of material brought upon plate (μg) | % Recovery[a] | Ordinate expansion[b] | Contamination around 1100 $cm^{-1}$[c] |
|---|---|---|---|---|---|
| *o*-Nitrophenol | Silica gel | 20 | Medium | 3 × | Some |
| *o*-Nitrophenol | Aluminium oxide | 25 | None | 10 × | Some |
| *o*-Nitrophenol | Cellulose | 25 | Low | 6 × | Considerable |
| *p*-Nitrobenzaldehyde | Silica gel | 40 | High | 1 × | None |
| *p*-Nitrobenzaldehyde | Silica gel | 20 | High | 1 × | None |
| *p*-Nitrobenzaldehyde | Silica gel | 4 | High | 1 × | Hardly detectable |
| *p*-Nitrobenzaldehyde | Aluminium oxide | 4 | High | 1 × | Hardly detectable |
| *p*-Nitrobenzaldehyde | Cellulose | 4 | Low | 5 × | Hardly detectable |
| Benzophenone | Silica gel | 10 | High | 1 × | Hardly detectable |
| Benzophenone | Silica gel | 5 | High | 1 × | Some |
| Benzophenone | Silica gel | 2 | High | 2 × | Considerable |
| Benzophenone | Aluminium oxide | 10 | High | 1 × | Not detectable |
| Benzophenone | Aluminium oxide | 5 | High | 1 × | Not detectable |
| Benzophenone | Cellulose | 5 | Medium | 2, 5 × | Not detectable |
| Phenyl acetic acid | Silica gel | 20 | Medium | 3 × | Considerable |
| Phenyl acetic acid | Aluminium oxide | 20 | None | 10 × | Hardly detectable |
| Phenyl acetic acid | Cellulose | 20 | Low | 3 × | Some |

[a] High recovery 100–70%, medium 70–40%, low 40–0%.
[b] Ordinate expansion was used when % T of strongest band was less than 45%.
[c] When contaminated interpretation of spectra was most difficult around 1100 $cm^{-1}$.

capillary end pointing away from the spot. The wall can be adjusted with a micro spatula if necessary. Care should be taken not to contaminate the KBr with the support material.

A solvent in which the compound is readily soluble was now added to the spot. It is best to use an a-polar solvent, alcohols or other strongly complexing solvents should not be applied. The compound was concentrated into the tip of the spot by moving the solvent slowly over the length of the spot. It is essential that the solvent spill over the edges of the spot that lie within the semicircle of KBr. The solvent now spreads rapidly over the glass surface and is sucked up by the KBr powder. Because the solvent carries the compound into solution, the compound is thus transferred from the spot to the KBr powder. When the solvent reaches the powder, no additional solvent is added in order to avoid spilling the solvent beyond the KBr powder. Elution volumes normally used were 100–150μl. The solvent was allowed to evaporate and the KBr powder was collected and transferred to a micro KBr disk (*5*).

In this experiment a lead disk of 1 mm thickness with a bore of 1.5 mm i.d. was used. Five milligrams of KBr are needed to fill this disk. The pellets were pressed in an ordinary commercial KBr press at 8–9 tons pressure under vacuum.

The IR spectra were obtained in the usual manner using a KBr lens beam condenser and a beam attenuator. The spectra were taken on a Perkin-Elmer 225 or Hitachi EPIG 2.

## RESULTS AND DISCUSSION

Experimental results are given in Table I. The percentage recovery was estimated from the intensities of the bands of the IR spectra. As can be seen from the table the direct elution technique is sensitive to: (a) the type of compound to be eluted, compounds that form strong hydrogen bonds show a poor recovery; (b) the support material used, different support materials show different recoveries; (c) contamination of the spectrum of the eluted compound with that of the support material. This contamination is both dependent on the support material used and the compound that is eluted.

From a point of easy recovery silica gel can best be used in this technique. On the other hand spectra of compounds that have been eluted from silica gel generally show more contamination with the solid support than those eluted from aluminium oxide or cellulose.

All three supports show their strongest absorption around 1100 $cm^{-1}$. The absorption of the 1100 $cm^{-1}$ band of silica gel is much stronger than that of aluminium oxide or cellulose. This is one reason why spectra show contamination by silica gel quicker than by aluminium oxide or cellulose. Comparing this technique with that mentioned by Rice (*3*), the same amount of contamination was always found. This indicates that contamination mainly results from the difficulty of thoroughly cleaning the glass plate around the spot and from (colloidal) solution of the support into the solvent used. Contamination partly imposes on this technique the lower limit of amount of compound that can be treated. This limit ranges from 1–2 μg for relatively nonpolar compounds to 10–20 μg for strongly hydrogen-bonded compounds.

Compounds that contain —OH and —COOH groups that can readily hydrogen-bond to the solid support suffer from a low percentage recovery. A slight improvement can be effected when the thickness of the solid support layer is reduced from 0.25 mm to 0.1 mm. However, generally the amount of material to be separated on the plate also has to be reduced in this case, thus giving no overall gain in amount of material that can eventually be brought into the KBr pellet.

The solvent that is used to elute the compound on to the KBr powder should be relatively a-polar and dry for strongly polar solvents—*e.g.*, alcohols, DMSO, and DMF—cause strong contamination of the spectrum with solid support, especially with silica gel. In our experiments chloroform, ether, and acetone gave good results.

Silica gel GF 254 and aluminium oxide GF 254 contain 10–13% gypsum as binder. The presence of gypsum in this amount had no effect on the quality of the spectra.

RECEIVED for review October 18, 1968. Accepted December 6, 1968.

(5) W. J. de Klein and K. Ulbert, ANAL. CHEM., **41**, 682 (1969).

# Radiochemical Determination of Technetium-99 in Environmental Water Samples

**Norbert W. Golchert and Jacob Sedlet**

*Argonne National Laboratory, Argonne, Ill., 60439*

THIS NOTE describes a radiochemical procedure for the determination of technetium-99, a pure beta emitter (0.29 MeV maximum energy) with a half-life of $2.12 \times 10^5$ years, at levels as low as 0.5 dpm per liter of water. Most separation procedures in the literature are designed to separate much larger quantities of technetium, usually from fission products. Typical of these are the procedures collected by Anders (*1*). Where macroquantities are available, as in the determination of technetium for the measurement of nuclear fuel burnup (*2, 3*), chemical–instrumental methods are employed. These methods cannot be used at the low technetium concentrations found in the environment. Separation procedures that are designed for low concentrations are those for urine (*4*) and rain (*5*), but the former method does not provide adequate separation from some interfering activities and does not have adequate sensitivity, while in the latter method the technetium recovery is low and uncertain. Parallel studies that might be modified for analytical work are the search for long-lived technetium in minerals (*6*), the determination of technetium from the spontaneous fission of uranium-238 in pitchblende ores (*7, 8*), and the search for technetium produced in molybdenum ores by cosmic-ray neutrons (*9*).

There is no published procedure for the determination of technetium-99 that is applicable to the analysis of large numbers of environmental water samples. With the increasing availability and use of gram to kilogram quantities of this fission product, such a procedure is needed. The present work provides a method for the determination of small amounts of technetium-99 in aqueous solutions, especially in naturally-occurring water.

## EXPERIMENTAL

**Reagents.** Tri-isooctylamine (TIOA), Bram Metallurgical Chemical Co., Philadelphia, Pa., reagent grade CP, was used without further purification to form 5% (V/V) solutions with xylene. The ruthenium carrier was prepared by dissolving 10 grams of C. P. ruthenium trichloride, A. D. MacKay, Inc., New York, N.Y., in 6*N* HCl and diluting to 500 ml with 6*N* HCl. The ruthenium concentration was about 10 mg/ml.

**Tracers.** Technetium-99 was obtained from Oak Ridge National Laboratory as an aqueous solution of ammonium pertechnetate. The concentration was determined by four-pi beta counting. Appropriate dilutions of the initial solution were prepared in 1*M* $NH_4OH$ for routine use. In some cases, technetium-95m, produced by cyclotron irradiation of niobium with helium-3 or helium-4 ions, was used and measurements were made by gamma-ray counting.

**Equipment.** Beta counting was done by a Sharp Laboratories (now Beckman Instruments, Fullerton, Calif.) Low-Beta Counter operated in the Geiger region on a 99.05% helium-0.95% isobutane gas mixture at 1050 V. The average background for the 2-in. diameter detector, which contained a gold-plated 0.9 mg/cm² Mylar window, was 0.75 cpm. The electrodeposition cell used in this work was an enlarged model of the one described by Schwendiman and Healy (*10*).

**Sample Pretreatment.** Water samples are acidified immediately after collection at the rate of 5 ml concentrated $HNO_3$/l to inhibit hydrolysis of cations.

**Procedure.** Ten milliliters of 12*N* NaOH, 5 ml of 5% NaOCl, and 2 ml of Ru(III) carrier are added to one liter of the water sample. The solution is evaporated to about 50 ml, 10 ml of absolute alcohol is added, and the evaporation continued until 20–25 ml remain. The solution is centrifuged and the precipitate washed with $H_2O$. The combined supernatant and wash solutions are acidified with concentrated HCl and stirred for 15 min to decompose the NaOCl. Five milligrams of Fe(III) is added, and the hydroxide is precipitated from the hot solution by the dropwise addition of concentrated $NH_4OH$. The solution is centrifuged and the supernate is retained. The precipitate is dissolved in a minimum of concentrated HCl, 5 ml of $H_2O$ is added, and the hydroxide is precipitated as before. The precipitate is centrifuged and the supernate combined with the initial supernate. The ferric hydroxide precipitation is repeated on the combined supernatant–wash solution. The supernate is then made 1*N* in HCl, 10 mg of Cu(II) and 100 mg of thioacetamide are added, and the solution is heated on a hot water bath for 30 min. The precipitate is centrifuged; then 10 ml of 1*N* $H_2SO_4$, 0.5 ml of 50% $H_2O_2$, and 2 ml of xylene are added, and the mixture is heated on a hot water bath for 15 min. The cooled solution is shaken in a separatory funnel with 15 ml of 5% TIOA in xylene for 1 min. The aqueous phase is discarded and the TIOA solution washed with 10 ml of 1*N* $H_2SO_4$ containing 1 drop of 50% $H_2O_2$. The wash solution is discarded, 15 ml of 2*N* NaOH are added, and the phases mixed for 1 min. The phases are separated and the TIOA solution contacted once more with 15 ml of 2*N* NaOH. The two portions of NaOH solution are transferred to the electrodeposition cell with a small volume of water and the technetium is deposited onto stainless steel at 100 mA and 3.0 V for at least 5 hr. The steel disk is washed with water and alcohol, dried, and counted for beta activity.

## RESULTS AND DISCUSSION

Water samples were acidified with nitric acid to prevent hydrolysis of trace elements. Because the levels of activity were very low, it was necessary to use a large volume and concentrate the sample for analysis. Direct evaporation of these nitric acid solutions would result in loss of technetium

(1) E. Anders, "The Radiochemistry of Technetium," AEC Report, NAS-NS-3021, Nov. 1960.
(2) R. J. Meyer, R. D. Oldham, and R. P. Larson, ANAL. CHEM., **36**, 1975 (1964).
(3) R. E. Foster, Jr., W. J. Maeck, and J. E. Rein, *ibid.*, **39**, 563 (1967).
(4) W. Fairman and J. Sedlet, AEC Report, TID-7696, 10, Oct. 1963.
(5) M. Attrep, Jr., M. S. Thesis, The University of Arkansas, Fayetteville, Arkansas, 1962.
(6) G. E. Boyd, and Q. V. Larson, *J. Phys. Chem.*, **60**, 707 (1956).
(7) B. T. Kenna and P. K. Kuroda, *J. Inorg. Nucl. Chem.*, **23**, 142 (1961).
(8) B. T. Kenna and P. K. Kuroda, *ibid.*, **26**, 493 (1964).
(9) G. Goldstein, Ph.D. Thesis, The University of Tennessee, Knoxville, Tennessee, 1965.
(10) L. C. Schwendiman and J. W. Healy, *Nucleonics*, **16** (6), 78 (1958).

**Table I. Loss of Technetium in Various Steps of Procedure**

| Step | Per cent Tc lost |
|---|---|
| Evaporation | < 1 |
| Ruthenium dioxide precipitation | 15 |
| Ferric hydroxide scavengings | 1 |
| Copper sulfide precipitation | 3 |
| Copper sulfide dissolution | < 1 |
| Extraction and back-extraction | 1 |
| Electrodeposition | < 1 |

**Table II. Decontamination Factors for Technetium Procedure**

| Tracer | Decontamination factor |
|---|---|
| $^{54}$Mn | $2 \times 10^4$ |
| $^{60}$Co | $8 \times 10^4$ |
| $^{65}$Zn | $2 \times 10^4$ |
| $^{90}$Sr-$^{90}$Y | $1.8 \times 10^4$ |
| $^{95}$Zr-$^{95}$Nb | $1 \times 10^5$ |
| $^{106}$Ru-$^{106}$Rh | $1.3 \times 10^4$ |
| $^{125}$Sb | $6 \times 10^4$ |
| $^{131}$I | $5 \times 10^3$ |
| $^{137}$Cs | $1 \times 10^5$ |
| $^{144}$Ce | $3 \times 10^4$ |
| $^{233}$U | $> 10^4$ |
| $^{239}$Pu | $> 10^4$ |

as the volatile heptoxide. For this reason, evaporations were carried out from a sodium hydroxide solution, although ammonium hydroxide would work equally well. Other experiments showed that technetium was retained if it was first reduced to the nonvolatile lower oxidation states, but reduction was not used in the procedure because of other complications.

The initial ruthenium separation was necessary to obtain adequate decontamination from ruthenium activities. Trace quantities of ruthenium existed in the samples in a number of different oxidation states (or chemical forms). The ruthenium was converted to a single species by employing an oxidation–reduction cycle in order to obtain reproducible and adequate ruthenium decontamination. All the ruthenium was oxidized by the sodium hypochlorite to ruthenium(VII) and then reduced to the insoluble ruthenium(IV) oxide by the alcohol. This step alone provided a ruthenium decontamination of several hundred and could be repeated, if large quantities of ruthenium activity were present.

After the insoluble ruthenium dioxide was removed, the remaining sodium hypochlorite was decomposed to prevent it from interfering with the copper sulfide precipitation by oxidizing the sulfide. The subsequent iron scavenging steps provided additional decontamination. It was more effective to dissolve and reprecipitate the ferric hydroxide than to wash the precipitate.

According to Anders (*1*), copper sulfide will carry technetium(VII) quantitatively, as technetium heptasulfide, from 0.2 to 3*N* acid. Most authors precipitate the sulfide from nitric acid. However, copper sulfide will dissolve in hot 2*N* nitric acid, and at lower nitric acid concentrations if large quantities of ammonium nitrate are present. The sulfide ion is oxidized to elemental sulfur under these conditions. To avoid this problem, the copper sulfide was precipitated from hydrochloric acid solution.

The method of dissolving the copper sulfide is one of the significant innovations used in this procedure. Copper sulfide is generally dissolved by repeated treatment of the precipitate with ammoniacal hydrogen peroxide (*4–8*). A more effective and cleaner dissolution is obtained by treating the precipitate with 50% hydrogen peroxide in 1*N* sulfuric acid and heating the mixture at 90 °C for 15 minutes. The xylene is present to dissolve elemental sulfur, which is usually produced, and thus frees any copper sulfide trapped in small sulfur particles, thereby allowing complete reaction. Any remaining peroxide is beneficial in maintaining the technetium as pertechnetate. Tracer studies showed that no technetium was lost by volatilization of the heptoxide.

Extraction of pertechnetate into the 5% TIOA in xylene solution is rapid and effective. Equilibrium is established within seconds for both the extraction and back-extraction. Although TIOA extracts numerous species, most cations require much higher acid concentrations or the formation of complexes (*11*). Back-extraction was effected by a simple change in pH to a basic solution. Although the extraction into the TIOA is quantitative, about 90% of the technetium is back-extracted with an equal volume of NaOH solution. The two back-extractions removed 99% of the activity from the TIOA.

The cathode of the electrodeposition cell was a 1.5-in. stainless steel disk, 25 mils thick, with the technetium deposited in a circle of $1^1/_8$-in. diameter using a platinum anode. The deposition half-time is 27 minutes. Previous experience with the electrodeposition of technetium revealed several problems. Electrodeposition of technetium metal onto platinum required solutions greater than 2*N* in sulfuric acid (*12*) and deposition times of three days for quantitative deposition. Electrodeposition from sodium sulfate solutions results in the hydrated dioxide (*13*, *14*). Although not observed with macroamounts of technetium, small solubility losses, about 5%, occurred while washing the electrolyte from the disk when sodium sulfate solutions were used to deposit trace quantities. Electrodeposition from sodium hydroxide solutions onto stainless steel eliminated the solubility problem, allowed quantiative deposition in about four hours, and provided a source with the highest possible efficiency for the counting system. The deposition of technetium from sodium hydroxide has been extensively studied by Matsuura and Yumoto (*15*).

The procedure as presented is a carrier-free radiochemical procedure. Recoveries were determined by adding technetium-99 tracer to one of a pair of samples and analyzing both in an identical manner. The inherent weakness in any carrier-free radiochemical separation procedure is that it is assumed that the factors that influence recovery are the same in all samples. Several alternatives to a carrier-free procedure were considered and rejected. If technetium-95m is used as an isotopic tracer, conversion electrons give sufficient beta counts to mask the technetium-99 activity at low levels. About $10^3$ dpm of technetium-95m give about 50 beta cpm. Rhenium could be used as a non-isotopic carrier because of the chemical similarity between technetium and rhenium, and the technetium recovery assumed to be identical with that of rhenium. This approach was rejected because the inevitable fractionation between rhenium and technetium would make it impossible to obtain accurate chemical yields (*1*). The carrier-free approach, in the case of low-level samples, is at least equal to the alternatives, and the reproducibility of the recovery is determined primarily

(11) G. H. Morrison and H. Freiser, "Solvent Extraction in Analytical Chemistry," John Wiley and Sons, Inc., New York, N.Y., 1957.
(12) W. D. Box, *Nucl. Appl.*, **1**, 155 (1965).
(13) G. E. Boyd, Q. V. Larson, and E. E. Motta, *J. Amer. Chem. Soc.*, **82**, 809 (1960).
(14) R. E. Voltz and M. L. Holt, *J. Electrochem. Soc.*, **114**, 128 (1967).
(15) N. Matsuura and H. Yumoto, *Radioisotopes (Tokyo)*, **8**, 28 (1959).

by the care taken by the analyst to follow instructions. The over-all chemical recovery, as determined by periodic checks with known amounts of technetium-99, is 79.6% ($\sigma$ = 3.4%). Stepwise losses are summarized in Table I. Excluding evaporation, electrodeposition, and counting time, the analysis takes about three hours.

The counting efficiency for electrodeposited technetium-99 in the beta counter is 41%. For a 1000-minute count, the limit of detection is 0.5 pCi ($2.7 \times 10^{-11}$g)/liter at the 99% confidence level, about the same as the sensitivity by activation analysis (*6*). The relative error of a single determination is 30% at 0.5 pCi/l, 22% at 1 pCi/l, 14% at 5 pCi/l, and 13% above 10 pCi/l.

Decontamination factors were determined in the following manner. An appropriate quantity of the tracer to be checked was added to the initial sample and the entire separation procedure run. The resulting sample was then beta counted, in the same manner as a routine sample, and the counts due to the added tracer were converted to dpm by using efficiencies of the counter as determined by the procedure outlined by Bayhurst and Prestwood (*16*). The ratio of the dpm added to the dpm recovered is then the decontamination factor for the particular isotope added.

The decontamination factors in this procedure for a number of typical isotopes are presented in Table II. The isotopes chosen either represent families of elements or are frequently present in typical samples. The decontamination factors are adequate for the samples encountered.

One problem that occurs with any procedure for the separation of technetium-99 at very low levels is how to establish that the observed radioactivity is from technetium-99. At these levels there is no nuclear property that can be used to identify technetium-99. The half-life is too long for practical measurement, there are no gamma-rays, and beta spectrometry is at best impracticable. Most evidence is indirect. What is known is that the observed activity followed the chemistry of technetium and that the half-life of the beta emitter, from a series of counts, is long. One method that has been used in this laboratory with excellent success is to characterize technetium-99 by measurement of the absorption half-thickness of its beta particle, 7.2 mg/cm$^2$ of aluminum in our counters. Counts are taken over the first few half-thicknesses with appropriate absorbers and compared to a technetium-99 source counted in the same manner. This technique has been used successfully with as little as 2 cpm of technetium-99.

Surface water samples, collected on a weekly basis, have been analyzed for technetium-99 by this procedure since the fall of 1965. Of some 150 samples analyzed, approximately 80% of the results have been below the limit of detection. The positive values ranged from 0.5 pCi/liter to 49.4 pCi/liter with an average of 4.65 pCi/liter.

An attempt was made to adapt the extraction step of Foster, Maeck, and Rein (*3*) to our problem. Their extraction of pertechnetate with tetrapropylammonium hydroxide from basic solution provides an excellent separation of technetium from essentially all other fission products. Unfortunately, the high salt concentrations encountered in evaporated water samples reduced the technetium extraction to 13% in spite of a scale-up in volume by a factor of five.

RECEIVED for review May 3, 1968. Accepted January 23, 1969. A preliminary report of this study was presented to the Division of Nuclear Chemistry and Technology, 153rd National Meeting, American Chemical Society, Miami Beach, Florida, April 1967. The work was done under the auspices of the U.S. Atomic Energy Commission.

(16) B. P. Bayhurst and R. J. Prestwood, *Nucleonics*, **17** (3), 82 (1959).

# Solvent Sublation of Iron(III) Chloride by Tri-*n*-Octylamine

**Jacob Elhanan and Barry L. Karger**

*Department of Chemistry, Northeastern University, Boston, Mass. 02115*

RECENTLY solvent sublation, a subdivision of the general method of adsorption bubble separation processes (*1*), has been successfully demonstrated by Karger and coworkers (*2, 3*) as a new tool in low concentration analytical separations. The technique was originally introduced by Sebba (*4*) as an auxiliary method to ion flotation. In solvent sublation gas bubbles generated in an aqueous phase are used to extract material selectively into a water immiscible organic phase. The aqueous phase will normally contain ionic nonsurface active solute in the presence of an oppositely charged surfactant.

Several mechanisms of mass transfer from the aqueous to the nonaqueous phase are possible. The surfactant may adsorb at the gas–liquid interface as the bubbles travel through the aqueous phase. Being oppositely charged to the solute in the water, the surfactant may then form an ion pair with the solute at the gas–liquid interface, with the subsequent extraction of the ion-pair complex into the organic phase. Alternatively, a solute-surfactant ion pair may form in solution and be subsequently adsorbed at the gas–liquid interface. Nonsurface active soluble species may also be carried into the organic phase by bulk liquid surrounding the bubble being dragged into the nonaqueous layer. Solubilization of such nonsurface active species in the organic layer will depend on the interaction of the species with the organic solvent, free surfactant molecules, or solute-surfactant ion pairs. The controlled aspects of solvent sublation provide an opportunity to follow closely the various stages associated with this extraction technique.

In the present work, the solvent sublation of ferric ion from hydrochloric acid–dioxane aqueous solutions into anisole by tri-*n*-octylamine was studied. The choice of this system was largely determined by the established data available on the liquid–liquid solvent extraction of group VIII metals from

(1) B. L. Karger, R. B. Grieves, R. Lemlich, A. J. Rubin, and F. Sebba, *Sep. Sci.*, **2**, 401 (1967).
(2) B. L. Karger, A. B. Caragay, and S. B. Lee, *ibid.*, **2**, 39 (1967).
(3) A. B. Caragay and B. L. Karger, ANAL. CHEM., **38**, 652 (1966).
(4) F. Sebba, "Ion Flotation," Elsevier, Amsterdam, 1962, Chap. X.

acidic media (*5–8*). Thus, Good and Bryan (*5*) studied the solvent extraction of Fe(III) from HCl aqueous solutions into hydrocarbon solvents with high molecular weight amines. They concluded that the tetrachloroferrate ion, $FeCl_4^-$, is the species involved in the extraction process. A limiting mole ratio of 1:1 of Fe(III)/amine corresponding to the stoichiometric structure $R_3NH^+ FeCl_4^-$ was also established in the organic phase. The extraction process was suggested to proceed *via* the following mechanism:

$$Fe^{3+}_{(aq)} + 4Cl^-_{(aq)} \rightleftarrows FeCl_4^-{}_{(aq)}$$

$$R_3NH^+Cl^-_{(org)} + FeCl_4^-{}_{(aq)} \rightleftarrows R_3NH^+FeCl_4^-{}_{(org)} + Cl^-_{(aq)}$$

## EXPERIMENTAL

The extraction vessel was a 280-mm × 45-mm glass column fitted with a 34-mm medium porosity, Kimble No. 28280 glass frit. Nitrogen gas travelled into the column through the frit at a constant flow rate of 20 ± 0.1 ml per minute. The flow was regulated by a Moore 63 BUL low flow controller and was measured by a manometer and soap bubble meter connected in parallel (*2*). To avoid spurious evaporation effects, the nitrogen gas was presaturated with water. Analysis of the $^{59}Fe$ tracer was performed in a well-type scintillation counter, Nuclear Chicago Model 1810. Potentiometric determination of the amine content of the organic phase was accomplished using an L & N pH meter Model 7664. Centrifugation of the samples was carried out in a Model CL International Clinical Centrifuge.

All chemicals used were Analytical Grade. The tri-*n*-octylamine hydrochloride was supplied by Eastman Kodak and had a melting point of 72–74 °C. Anisole, from Matheson, Coleman, and Bell, was redistilled and the fraction boiling between 152–154 °C was collected. Dioxane was supplied by Fisher and was employed without further treatment.

**Procedure.** Stock solutions of 2.43 × $10^{-2}M$ of aqueous $FeCl_3$, $10^{-2}M$ of tri-*n*-octylamine hydrochloride in dioxane, and 1–10*M* of aqueous hydrochloric acid were prepared. Determination of HCl concentration was carried out by titration with standardized aqueous NaOH. Anisole and each of the aqueous acid concentrations were presaturated with one another before use in order to minimize mutual solubility effects. It should be noted that no significant change in volume was produced in this presaturation step. Also, no significant volume change was noted when the presaturated organic phase was re-equilibrated with a presaturated aqueous phase that contained 3.31% v/v of dioxane.

A 140-ml solution of the desired aqueous HCl concentration was pipetted into the sublation column followed by 5 ml each of aqueous $FeCl_3$ and tri-*n*-octylamine hydrochloride in dioxane stock solutions and 1 ml of $^{59}Fe$ tracer. Nitrogen gas was then slowly generated into the solution to cause a thorough mixing of the components. Twenty-five milliliters of anisole were then carefully pipetted along the wall of the column, and the gas which was regulated at the precise flow rate of 20 ± 0.1 ml per minute was bubbled for the required period of time. Replicate solvent sublation experiments were run in each case. At the end of each run, aliquots of the organic and the aqueous phases were removed and centrifuged. Equal volumes of each phase were then counted for Fe(III) distribution. The per cent iron in the organic phase was calculated as

$$\frac{\text{activity in the organic phase} \times 100}{\text{activity in the organic phase} + \text{activity in the aqueous phase} \times R}$$

where *R* is the volume ratio of the aqueous to the organic phase. In these experiments the *R* value was equal to 6.04. Reproducibility in Fe(III) analyses was found to be ± 5%.

For the determination of the amine concentration in the organic layer, 10 ml of this phase were twice equilibrated with equal volumes of 1*M* aqueous NaOH. A 5-ml sample was then analyzed for the amine content after dilution with methanol by potentiometric titration with aqueous perchloric acid. Reproducibility in amine analyses was found to be ± 0.5%.

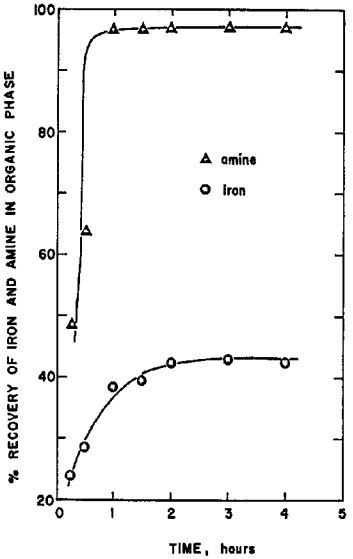


**Figure 1. Per cent recovery of iron and amine *vs.* sublation time**

**Concentrations in initial aqueous phase: HCl 9.6*M*, dioxane 3.31% v/v, tri-*n*-octylamine hydrochloride 2.72 × $10^{-4}M$, $FeCl_3$ 6.86 × $10^{-4}M$**

## RESULTS AND DISCUSSION

In the first series of experiments the extent of extraction of Fe(III) and tri-*n*-octylamine hydrochloride into the organic phase as a function of gas bubbling time with a constant acidity in the initial aqueous phase of 9.6*M* HCl and a constant flow rate of 20 ± 0.1 ml/min was studied. The results are presented in Figure 1. In the second series of experiments the extraction of the two components as a function of HCl concentration in the initial aqueous phase with a constant sublation time of 180 minutes was investigated. The results are illustrated in Figures 2 and 3. The concentrations of Fe(III) and tri-*n*-octylamine hydrochloride in the initial aqueous phase in each series of experiments were 6.86 × $10^{-4}M$ and 2.72 × $10^{-4}M$, respectively.

The results are presented in terms of per cent extraction and the mole ratio of Fe(III) to amine in the organic phase, in lieu of the normally used distribution coefficient, *K*. This choice is determined by the fact that the sublation process depends on kinetic factors, such that the extraction is time dependent, whereas *K* is obtained at equilibrium.

Assuming $R_3NH^+ FeCl_4^-$ is the only species extracting into the anisole phase, a limiting mole ratio of 1:1 of Fe(III)/amine should be established in this phase (*5*). Also upon complete removal of the amine into the organic phase, 40% of iron should be recovered in the anisole under the concentrations

(5) M. L. Good and S. E. Bryan, *J. Amer. Chem. Soc.*, **82**, 5636 (1960).
(6) M. L. Good and S. E. Bryan, *J. Inorg. Nucl. Chem.*, **20**, 140 (1961).
(7) M. L. Good and S. E. Bryan, *ibid.*, **24**, 1683 (1962).
(8) D. E. Chalkley and R. J. P. Williams, *J. Chem. Soc.*, **1955**, 1920.

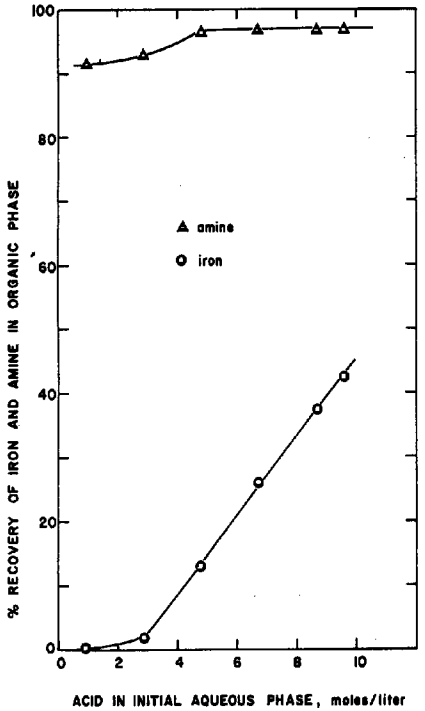


**Figure 2. Per cent recovery of iron and amine *vs.* acidity in initial aqueous phase**

**Concentrations in initial aqueous phase: dioxane 3.31% v/v, tri-*n*-octylamine hydrochloride $2.72 \times 10^{-4}M$, $FeCl_3$ $6.86 \times 10^{-4}M$. Sublation time, 3 hours**

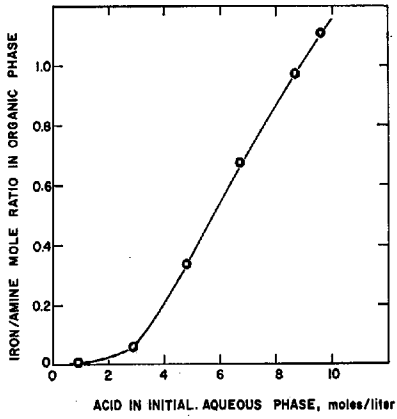


**Figure 3. Iron/amine mole ratio in organic phase *vs.* acidity in initial aqueous phase**

**Concentrations in initial aqueous phase: dioxane 3.31% v/v, tri-*n*-octylamine hydrochloride $2.72 \times 10^{-4}M$, $FeCl_3$ $6.86 \times 10^{-4}M$. Sublation time, 3 hours**

selected for this study. The results in Figure 1 show that a constant content of tri-*n*-octylamine into anisole corresponding to 96.7% recovery and a constant concentration of Fe(III) equivalent to 43% recovery and 1.1:1 mole ratio of Fe(III)/amine in the organic phase are achieved. This per cent extraction for Fe(III) at long times is within experimental error of the expected value assuming a 1:1 complex.

Most interestingly, the iron to amine mole ratio was found to have an initially large value at 15 minutes of 1.3:1. Upon continued sublation, a gradual change in this ratio occurred until the constant value was reached at equilibrium. To explain the initial mole ratios of Fe(III) to amine in the organic phase being greater than 1:1, we must examine the species which are extracted into the anisole.

Assuming that the tetrachloroferrate ion, $FeCl_4^-$, is the only Fe(III) anionic species existing in the aqueous phase at the experimental acidity, then the only ion pairs, containing the surface active tri-*n*-octylamine, that are likely to extract by adsorption at the gas–liquid interface are $R_3NH^+ Cl^-$ and $R_3NH^+ FeCl_4^-$ (*5*). However, removal into the organic phase of nonsurface active, water soluble species, such as ionic $FeCl_4^-$ and molecular $HFeCl_4$, is also possible. According to Lemlich (*9*), a small amount of bulk liquid surrounds each bubble rising through the aqueous phase and is dragged upward along with the bubble. Miller (*10*) has been able to obtain photographic evidence that water is also dragged through the liquid–liquid interface as the bubble traverses this interface. Clearly this extracted bulk water provides a means by which $FeCl_4^-$ and $HFeCl_4$ can be brought into the anisole phase.

Once in this phase these water soluble species can become solubilized by interactions with other species already present in the anisole. It is reasonable to expect formation of a Fe(III)-amine complex within the organic phase possibly *via* the interaction of ionic $FeCl_4^-$ with an $R_3NH^+ Cl^-$ ion pair in the usual ion exchange mechanism (*5*). In addition, Chalkley and Williams (*8*), in their study of the extraction of Fe(III) from acidic solutions of $FeCl_3$ with ethyl and isopropyl ethers, concluded that removal of molecular $HFeCl_4$ from the aqueous phase is possible through a hydrogen bond formation with the ethereal oxygen of the organic solvent. It is thus entirely reasonable to expect that in the sublation system the transported $HFeCl_4$ will remain in the organic phase through such hydrogen bond formation with anisole and perhaps any dioxane that is also removed into the organic phase. This effect may explain in part the incorporation of Fe(III) in the organic phase in a mole ratio of iron to amine in excess of 1:1.

The decrease in the iron to amine mole ratio in the nonequilibrium state with sublation time may be partially explained by the increased removal of HCl into anisole as sublation proceeds (*5–7*). Ryan (*11*) attributes this effect to the competition of HCl molecules with the metallic species for complexation with organic molecules, presumably *via* hydrogen bond formation in the organic phase.

Figures 2 and 3 present the extraction of Fe(III) and tri-*n*-octylamine as a function of acidity in the initial aqueous phase with a constant sublation time of 180 minutes and a flow rate of 20 ± 0.1 ml/min. An examination of Figure 2 indicates again that the sublation of the species into the organic phase involves more than one process. The amine content in anisole reaches a maximum value of 96.7% recovery, corresponding to an Fe(III)/amine mole ratio of 0.34:1, at 4.8*M* HCl concentration in the initial aqueous phase. However, the Fe(III) content and the iron/amine mole ratio in the organic phase

(9) R. Lemlich, *A.I.Ch.E. (Amer. Inst. Chem. Eng.) J.*, **12**, 802 (1966).
(10) M. W. Miller, Ph.D. Thesis, Northeastern University, Boston, Mass., August, 1968.
(11) J. Ryan, *Inorg. Chem.*, **2**, 348 (1963).

continue to increase above this HCl concentration. The increase in per cent iron removal seems to depend on the concentration of the $FeCl^-_4$ species in the aqueous phase which in turn is governed by the chloride ion concentration in this phase (*5*). The results in Figures 2 and 3 indicate that the removal of tri-*n*-octylamine hydrochloride ion pair in addition to the simultaneous sublation of Fe(III)-amine complex is possible. This conclusion supports our previous assumption that the formation of Fe(III)-amine species may also occur within the organic phase.

The solvent extraction—*i.e.*, intimate mixing of the two liquid phases by shaking—of Fe(III) at 9.6*M* HCl concentration in the initial aqueous phase was also investigated and compared to solvent sublation in the equivalent system. A 250-ml separatory funnel was vigorously shaken for an equivalent period of 180 minutes even though equilibrium is known to be established in a matter of a few minutes (*5*). The values 43% and 96.8% for the recovery of iron and amine, respectively, in the organic phase were obtained. Because the values agree with the corresponding solvent sublation results, it was concluded that at the state of equilibrium the distribution of the species is the same and independent of the extraction technique employed. This result indicates that over the long run, bulk water dragged up into the anisole layer and re-extracted into the aqueous medium can create the liquid–liquid equilibrium state under the conditions of these experiments. However, the rate of approach to equilibrium as well as the mechanistic details of the extraction process differ for the two methods. If desired, advantage can be taken of the slow extraction rate for separation purposes (*2*) in solvent sublation.

RECEIVED for review September 9, 1968. Accepted January 21, 1969. This work was supported by Grant WP 01129-02 from the Federal Water Pollution Control Administration, U.S. Department of Interior.

# Derivative Spectroscopy and Its Application to the Analysis of Unresolved Bands

**I. G. McWilliam**[1]

*Central Research Laboratories, Imperial Chemical Industries of Australia and New Zealand Ltd., Newson Street, Ascot Vale, Victoria 3032, Australia*

IT IS RECOGNIZED that the first derivative of a spectral or chromatographic band is very sensitive to change in the band shape. This fact can be used both for qualitative (*1–3*) and quantitative (*4*) analysis. To date, however, no work has been reported on the application of the derivative technique for quantitative analysis where two components overlap to such an extent that even the derivative curve shows no clear separation of the peaks.

The present work reports on the application to this problem of an oscillating plate differentiator used in conjunction with a Grubb-Parsons type S.4 infrared monochromator (*5*).

**Production of Derivative Spectra.** It has been shown elsewhere (*5*) that derivative spectra can be produced by interposing an oscillating beam-deflecting plate in the optical path of a monochromator (see Figure 1). Several similar devices have also been reported recently (*6, 7*).

Referring to Figure 1, a relatively simple expression can be derived relating the angle of rotation of the plate, $i$, the plate thickness, $t$, the refractive index of the plate, $n$, and the effective displacement of the slit, $\Delta s$. The displacement from the normal of the emerging ray, and of the extrapolated incident ray, at the rear face of the plate will be $t \tan r$ and $t \tan i$, respectively. Hence

$$\Delta s = (t \tan i - t \tan r) \cos i$$

$$= t (\sin i - \sin r \cdot \frac{\cos i}{\cos r}$$

$$= \frac{t}{n}\left(n - \frac{\cos i}{\cos r}\right) \sin i$$

For small values of $i$, $\Delta i$ (in radians)

$$\Delta s \simeq \frac{t}{n}(n - 1)\, \Delta i$$

For most practical purposes, the error introduced by the approximation is very small. Taking $n$ as 1.55, the error in $\Delta s$ is less than 0.3% for $i = 5°$, 1.6% for $i = 10°$, 6% for $i = 20°$ and still only 13% ($\Delta s$ is underestimated) for $i = 30°$.

The corresponding wavelength variation depends on the optical geometry of the instrument. For a prism instrument it is of the form

$$\Delta i \simeq \text{const.} \tan i \left(\frac{\Delta n}{\lambda \Delta \lambda}\right) \lambda \Delta \lambda$$

where $i$ is the angle of the incident ray on the prism. Because variation in the term $(\Delta n/\lambda\Delta\lambda)$ is relatively small over a fairly wide wavelength range [0.00066–0.0009 for a sodium chloride prism over the range 2–20 $\mu$ (*8*)], the above expression reduces to

$$\Delta i \simeq \text{const.}\ \lambda \Delta \lambda$$

**Application to the Quantitative Analysis of Unresolved Bands.** The present application of the derivative technique to the analysis of unresolved bands is based on measurement of the maximum and minimum of the first derivative curve.

[1]Present address, Chemistry Department, Monash University, Wellington Road, Clayton, Victoria 3168, Australia

(1) C. S. French and A. B. Church, *Carnegie Inst. Wash. Yearbook*, **54**, 162 (1954–55).
(2) A. T. Giese and C. S. French, *Appl. Spectrosc.*, **9**, 78 (1955).
(3) T. Kambara, K. Saitoh, and K. Ohzeki, ANAL. CHEM., **39**, 409 (1967).
(4) G. L. Collier and F. Singleton, *J. Appl. Chem.* (London), **6**, 495 (1956).
(5) I. G. McWilliam, *J. Sci. Instrum.*, **36**, 51 (1959).
(6) R. E. Drews, *Bull. Amer. Phys. Soc.*, **12**, 384 (1967).
(7) A. Gilgore, P. J. Stoller, and A. Fowler, *Rev. Sci. Instrum.*, **38**, 1535 (1967).

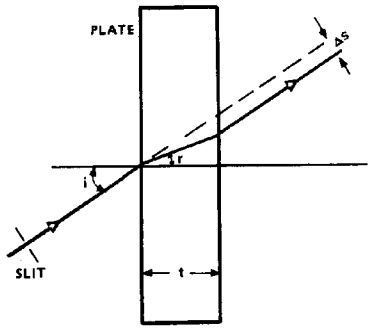


**Figure 1. Displacement of slit position by beam-deflecting plate**

In Figure 2 the first curve represents a symmetrical band or peak due to a minor component. The derivative curve, immediately below, is symmetrical and the ratio of the maximum and minimum of the first derivative is equal to unity. This ratio, which is a measure of the symmetry of the original peak, is termed here the peak ratio.

The second curve in Figure 2 represents a compound peak formed by the overlap of the major peak and a second symmetrical peak, displaced slightly from the center of the major peak, due to a minor component (broken curves). As can readily be seen, for a compound peak which is not symmetrical, the peak ratio will differ from unity, and can therefore be used as a measure of the amount of one component in the other.

The separation range over which the peak ratio concept in its simple form is viable can be defined with the help of published derivative curves (*2*). (These curves are, unfortunately, not sufficiently accurate to provide reliable peak ratio *vs.* concentration plots, although their general trend agrees well with the experimental curves which are discussed below.) As the peak separation increases, the derivative curve becomes more complex, the degree of complexity depending on the relative heights, widths, and separation of the two components. For two Gaussian peaks of equal width, it would appear that the peak ratio (as defined here) can be used unambiguously as a measure of impurity content up to a maximum peak separation of about $2\sigma$, where $\sigma$ is the standard deviation, provided that the impurity peak height does not exceed about 25% of the major peak (*2*). With closer peaks, as in the examples below, higher percentages can be tolerated.

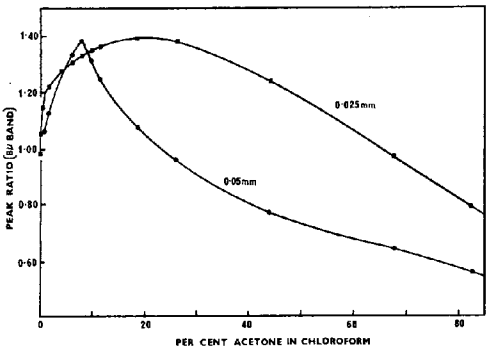


**Figure 3. Peak ratio *vs.* concentration curves for acetone in chloroform (8 $\mu$ bands)**

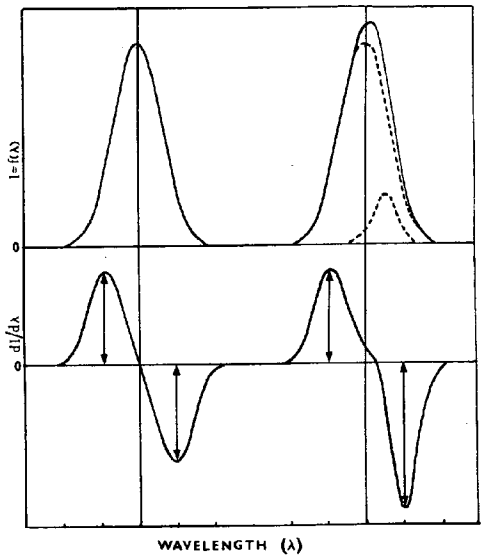


**Figure 2. First derivative curves for a symmetrical peak and for a compound peak containing a displaced impurity band**

The 8 $\mu$ bands of acetone and chloroform, whose peak maxima differ by 0.04 $\mu$ (a separation of about 0.04 $\sigma$), provide the first example of the use of the technique. In Figure 3 the peak ratio for the 8 $\mu$ acetone–chloroform peak is shown as a function of concentration at two sample thicknesses. The derivative curves were obtained using a sodium chloride plate 4.5 mm thick and an angular oscillation of 3°.

Several points are evident from Figure 3. First it is seen that the peak ratio is markedly dependent on the sample thickness. This results from the fact that the transmission derivative $dI/d\lambda$, is used rather than $d(\log I)/d\lambda$ (*4*, *8*). However, this has the advantage that any ambiguity caused by the double-valued nature of the peak ratio *vs.* concentration curve can be overcome by measuring the ratio at two sample thicknesses. The ratio is independent of incident radiation intensity, and it was found that the ratio for 1.63% acetone in chloroform (1.24) was unaffected by reducing the Nernst current from 0.9 to 0.6 A.

(8) W. A. Roth and K. Scheel, Eds., "Landolt-Bornstein Physikalisch-Chemische Tabellen II," Vol. 2, Julius Springer, Berlin, 1923, p 913.

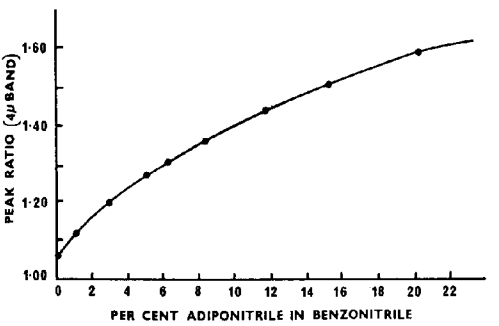


**Figure 4. Peak ratio *vs.* concentration curve for adiponitrile in benzonitrile (4 $\mu$ bands)**

Second, the sensitivity of the method in this particular example is greatest over the range 0–5% acetone, and it is possible to determine 1% acetone in chloroform to ± 0.05% with the unresolved 8 $\mu$ band.

Third, whereas the peak ratio for pure chloroform is close to 1.00, the ratio for pure acetone is much lower due to the asymmetrical shape of the acetone peak. It should also be noted that, although a perfectly symmetrical peak will give a peak ratio of 1.00 (assuming negligible distortion due to instrumental factors), the reverse does not necessarily apply.

A second example is shown in Figure 4. This is the analysis of adiponitrile in benzonitrile with only the unresolved 4 $\mu$ CN bands (separation 0.06 $\mu$). Because the derivatives are obtained by operating the instrument in the single-beam mode, some interference may occur in this particular case due to overlap of the CN and atmospheric carbon dioxide bands. Provided, however, that the carbon dioxide concentration remains constant, its only effect will be to modify the shape of the peak-ratio *vs.* concentration curve. (Alternatively, of course, the instrument could be purged to eliminate this interference.) Conversely, it is possible to modify the shape of these curves, and therefore the sensitivity of the method, by the addition of a known amount of interfering material.


### ACKNOWLEDGMENT

The author gratefully acknowledges the encouragement and assistance of Dr. J. H. Beynon and Mr. M. St.C. Flett, Research Department, Imperial Chemical Industries Ltd., Manchester, England, where this work was carried out.

RECEIVED for review November 18, 1968. Accepted December 23, 1968.


# Anion Determination with Ion Selective Electrodes Using Gran's Plots

## Application to Fluoride


**Arnaldo Liberti and Marco Mascini**

*Istituto Chimica Analitica, Universitá di Roma, Rome, Italy*


WITH THE RECENT introduction of ion selective electrodes, very sensitive analytical tools have become available for many ions. The construction and the operation of these electrodes is similar to glass pH electrodes and as they are both indicators of single ion activities in aqueous solution should be valuable for a large number of physico-chemical investigations. Since the evaluation of concentration is frequently of more interest than activity, a number of procedures have been suggested to express the millivolts response in terms of concentrations.

Though the described procedure can be extended to most electrodes, the present experimental work and discussion refer to a fluoride ion electrode which has been extensively used by various authors for fluorine determinations in bone (*1*), tungsten (*2*), chromium plating baths (*3*), urine (*4*), enamel of teeth (*5*), saliva (*6*), and others (*7–8*).

The procedures which have been suggested can be grouped as follows: preparation of fluoride solution at an ionic strength close to the samples under investigation to build up a reference calibration curve for the indicator electrodes; dilution of the samples 1 : 1 with a solution of high ionic strength [total ion strength adjustment buffer, TISAB (*7*)] and use of a reference calibration curve; titration of the fluoride ion with thorium or lanthanum (*8–9*); the use of linear null-point potentiometry (*10*).

The titration procedure has been recommended by Lingane (*8*) to obtain higher precision but a number of limitations have been noted: the equivalence point is not the point of maximal slope, but has to be determined in careful titrations of precisely known amounts of fluoride in the particular medium used; the titrations are quite time consuming as equilibria are rather slow to be obtained, namely, near the equivalence point; thorium and lanthanum salts are not primary standard and require standardization.

The procedure described in this paper makes use of Gran's plots (*11–12*); this method, permitting the weighing of several data points is more accurate than a single point direct potentiometry measurement and yields satisfactory results for a number of applications.

### THEORY

To a sample solution in which a fluoride and a reference electrode are immersed, known amounts of standard fluoride solutions are added and the potential difference is measured. The potential of the indicator electrode according to the Nernst equation is:

$$E = E_o - \frac{2.3RT}{F}\log\frac{(C_oV_o + CV)}{V_o + V} - \frac{2.3RT}{F}\log\gamma + E_j \qquad (1)$$

where $E$, $E_o$, and $E_j$ are, respectively, the equilibrium potential, the normal potential, and the liquid junction potential. $C_oV_o$ and $CV$ are, respectively, the concentration and volume of the sample solution, and of the standard solution; $\gamma$ is the activity coefficient of the fluoride ion.

From Equation 1 is obtained:

$$(V_o+V)\times 10^{-E\frac{F}{2.3RT}} = 10^{-(E_o+E_j)\frac{F}{2.3RT}}\times\gamma\times(C_oV_o+CV) \qquad (2)$$


(1) L. Singer and W. D. Armstrong, ANAL. CHEM., **40**, 613 (1968).
(2) B. A. Raby and W. E. Sunderland, *ibid.*, **39**, 1304 (1967).
(3) M. S. Frant, *Plating*, **54**, 702 (1967).
(4) L. Singer, W. D. Armstrong, and J. J. Vogel, Abstract, 45th General Meeting of Inter. Assoc. Dental Research, p 77, March 1967.
(5) B. Richardson and H. G. McCann, *ibid.*, p 77.
(6) P. Gron, F. Brudevold, and H. G. McCann, *ibid.*, p 79.
(7) M. S. Frant and J. W. Ross Jr., ANAL CHEM., **40**, 1169 (1968).
(8) J. J. Lingane, *ibid.*, **39**, 881 (1967); **40**, 935 (1968).
(9) T. S. Light, Pittsburgh Conference on Analytical Chemistry and Applied Spectroscopy, March 1967.
(10) R. Durst, ANAL. CHEM., **40**, 931 (1968).
(11) G. Gran, *Analyst*, **77**, 661 (1952).
(12) F. J. Rossotti and H. Rossotti, *J. Chem. Educ.*, **42**, 375 (1965).

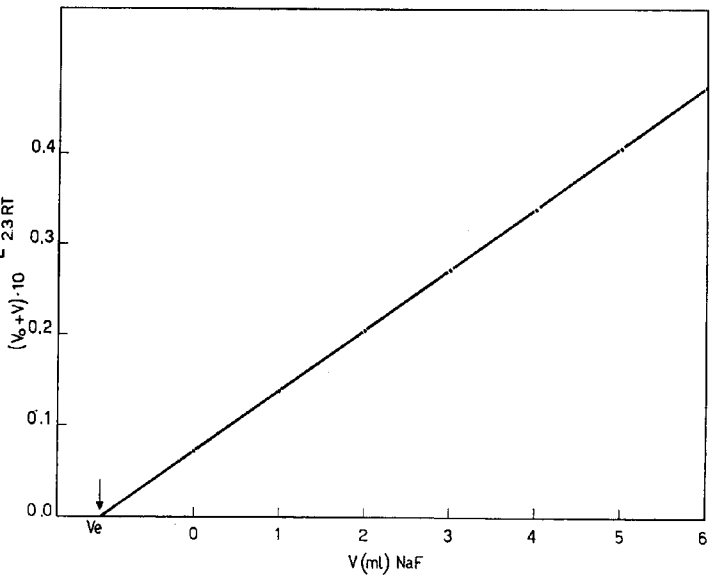


**Figure 1. Determination of fluoride of 20 ml of 5.5 × $10^{-5}M$ fluoride and $1M$ $NaNO_3$**

**Fluoride standard solution added was $10^{-3}M$ NaF and $1M$ $NaNO_3$**

If the sample and the standard solutions are prepared in such a way that the ionic strength is kept quite high and almost constant, $\gamma$ and $E_j$ do not change appreciably, and by plotting $(V_o + V)\,10^{-E\frac{F}{2.3RT}}$ *vs.* $V$ a straight line is obtained which intercepts the abscissa for a $V_e$ value where $C_oV_o = -CV_e$, (Figure 1). The initial fluoride concentrations is obtained from $C_o = CV_e/V_o$. The determination of the unknown concentration of fluoride is thus carried out in a simple manner by adding a standard fluoride solution.

## EXPERIMENTAL

**Apparatus and Reagents.** A model 94-09 fluoride ion electrode (Orion Research Inc.) and a conventional fiber type calomel electrode Beckman 39170 were employed with the Beckman Research pH meter 1019. A polyethylene beaker was used as titration cell; solutions were magnetically stirred. The standard fluoride solutions were made from NaF reagent grade Carlo Erba.

**Procedure.** A 20-ml sample $1M$ in sodium nitrate with a fluoride concentration in the range $10^{-2}$–$5.10^{-6}M$ was taken. The standard solution $1M$ in sodium nitrate which had a fluoride concentration 10–100 greater than the sample under investigation, was added in 1 ml at a time up to 10 ml. The solution was stirred and the potential, which was attained rapidly, was recorded. The variation of potential from the beginning to the end of the addition was about 30–90 mV. In Table I some of the analytical results are collected; they are compared with the ones obtained by using the TISAB procedures. Figure 1 reports the Gran's plot for the determination of 20-ml solution containing 20.7 $\mu$g of fluoride by addition of standard fluoride solution.

**Determination of Fluorides in Mineral and Waste Water.** The determination of fluoride in mineral and waste water is of great importance. All procedures involve a preliminary distillation of fluorides and a colorimetric determination. The specificity of the fluoride electrode permits the satisfactory use of the above procedure. Table II shows some results obtained in the analysis of mineral waters where the fluoride concentration is usually in the microgram per milliliter range; the samples were $1M$ in $NaNO_3$ and a solution $10^{-3}M$ in NaF and $1M$ in $NaNO_3$ was added. This analysis has also been carried out with the TISAB procedure. It is important to point out the additional information which can be obtained on the state of the fluoride ion in solution when ions which form strong complexes with fluoride such as $Al^{3+}$ or $Fe^{3+}$ are present. This information may be quite useful when the fluoride ion is utilized for biological purposes. When all points of the Gran's plot lie on a straight line, it means that the concentration of the binding ions is negligible or lower than the concentration of the fluoride: the intercept on the abscissa yields the concentration of free fluoride ion. If the concentration of the binding cations is larger than fluoride concentration, the first points, due to small additions of standard fluoride solution, do not lie on a straight line. By drawing a line through the values corresponding to larger additions and by extrapolation on the volume axis, a negative fluoride concentration is obtained, which means the absence of free fluoride ions (Figure 2).

To obtain the total fluoride concentration, it is necessary to add competing ions, as citrate ions, which may replace the

**Table I. Determination of Fluoride in Solution by the Gran's Plot and the TISAB Procedure**
**(Sample Solution, 20 ml)**

| Sample taken | | Found, $\mu$g | | Error, % | |
|---|---|---|---|---|---|
| | | Gran's | | Gran's | |
| $M$ | $\mu$g | plot | TISAB | plot | TISAB |
| $5.0 \times 10^{-6}$ | 1.90 | 1.97 | 2.47 | +3.5 | +30 |
| $1.00 \times 10^{-5}$ | 3.80 | 3.88 | 3.0 | +2 | −21 |
| $2.63 \times 10^{-5}$ | 10.0 | 9.9 | 9.4 | −1 | −6 |
| $3.69 \times 10^{-5}$ | 14.0 | 13.7 | 14.8 | −2 | +6 |
| $1.00 \times 10^{-4}$ | 38.0 | 38.0 | 39.6 | 0 | +4 |
| $1.00 \times 10^{-3}$ | 380 | 382 | 372 | +0.5 | −2 |
| $1.00 \times 10^{-2}$ | 3800 | 3820 | 3720 | +0.5 | −2 |

**Table II. Determination of Fluoride Content in Mineral Waters by Gran's Plot and TISAB Procedure**
**(20-ml Sample Solution)**

| Sample | Gran's plot, $M \times 10^5$ | TISAB, $M \times 10^5$ |
|---|---|---|
| A | 5.3 | 5.1 |
| B | 4.2 | 4.5 |
| C | 6.4 | 6.7 |
| D | 5.45 | 5.3 |

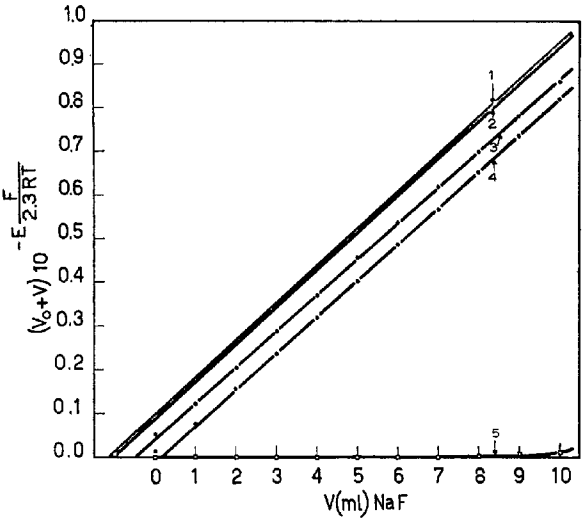


**Figure 2. Gran's plot relative to fluoride determination in the presence of aluminum ions**

**All samples were 20-ml solutions, 1 ppm in fluoride and 1*M* $NaNO_3$. Standard fluoride solution was $10^{-3}M$ NaF and 1*M* $NaNO_3$**

**(1) No $Al^{3+}$ added**
**(2) 0.10 ppm Al**
**(3) 0.33 ppm Al**
**(4) 1.0 ppm Al**
**(5) 10 ppm Al**

fluoride from the complexes. In this case to 10 ml of sample are added 10 ml of a buffer complexing solution which is 2*M* in $NaNO_3$, 0.5*M* in $CH_3COOH$, 0.5*M* in $CH_3COONa$, and 0.1*M* in sodium citrate. The standard solution is 1*M* in $NaNO_3$, 0.25*M* in $CH_3COOH$, 0.25*M* in $CH_3COONa$, 0.05*M* in sodium citrate and $10^{-3}M$ in NaF; it is thus possible in a simple way to have information concerning the total and the free fluoride concentration. The former is determined by using Gran's plot in the presence of the buffer complexing solution and the latter only with the neutral salt.

**Determination of Fluorides in Polluted Air.** The procedure can be successfully applied for the determination of fluoride in a polluted air providing a sufficient fluoride amount is collected. Air is made to bubble into a standard impinger containing 0.1*N* NaOH. To 20 ml of the adsorbing solution are now added 2 ml of 2*N* acetic acid: the fluoride and reference electrode are inserted and the standard fluoride solution $5 \times 10^{-4}M$ NaF, 0.1*N* in acetic acid, and sodium acetate are added and the emf is measured; 0.1 ppm fluoride can be measured with about 5% error.

**Titrations of Slightly Soluble Salts.** Gran's plot can be successfully applied to locate the end point in precipitation titrations, namely, when the equivalence point is affected by the solubility of the salt. In Figure 3 are reported the experimental graphs relative to the potentiometric titration of 20 ml of $10^{-2}M$ $Ca^{2+}$ with NaF 0.1*M*.

The usual plot, potential *vs.* volume of fluoride added, does not permit accurate location of the equivalence point because of the high solubility of calcium fluoride; to obtain more reliable results, the addition of organic solvents to decrease the solubility of $CaF_2$ has been suggested (*8*). This limitation is overcome by Gran's plot: the equivalence point is obtained by extrapolation through the points obtained when fluoride is present in excess, thus depressing the solubility effect.

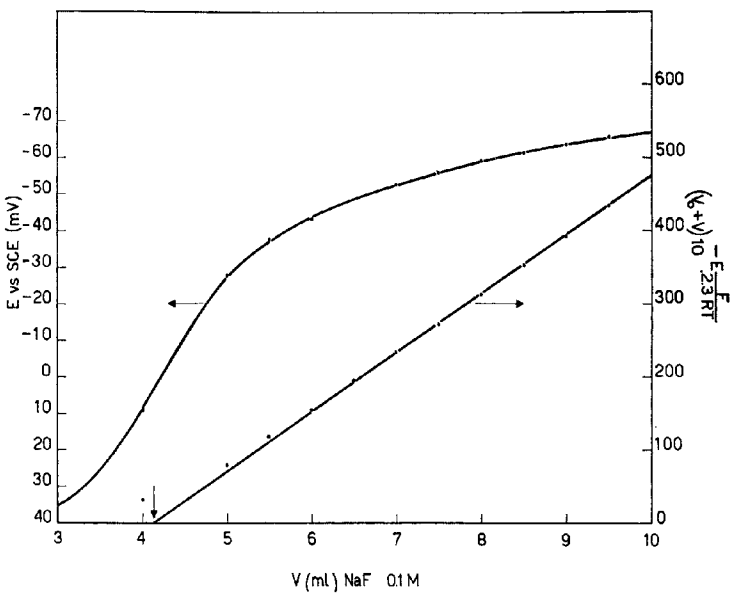


**Figure 3. Potentiometric titration of 20 ml of $Ca^{2+}$ 0.01 with NaF 0.100*M***

**Upper curve is usual potential–volume plot and the lower is Gran's plot**

In this case Equation 1 is modified to the following which is valid after the equivalence point:

$$E = E_o - 2.3RT \log \frac{C(V - V_e)}{V_o + V} - \frac{2.3RT}{F} \log \gamma + E_j \quad (3)$$

and thus:

$$(V_o + V)10^{-E\frac{F}{2.3RT}} = 10^{-(E_o + E_j)\frac{F}{2.3RT}} \times \gamma \times C(V - V_e) \quad (4)$$

The extrapolation of the straight line described by the experimental points $[V,(V_o+V)10^{-E\frac{F}{2.3RT}}]$ intercepts the abscissa for a value $V = V_e$.

## DISCUSSION

Fluoride concentration may be directly determined by adding a sodium fluoride solution and by using Gran's plot to locate the equivalence point. It is assumed that the liquid junction potential and activity coefficient of the fluoride ion do not change appreciably under the conditions of the experiment. If the solution contains only fluoride ions in the microgram per milliliter range, then the small additions of fluoride solution have little effect on these values. In more general cases, however, it is necessary to have the sample and the standard fluoride solution at the same ionic strength; this goal is reached by making both solutions 1 $M$ in any salt such as $NaClO_4$ or $NaNO_3$ or by using an acetate buffer.

The procedure described is more accurate than the direct measurement of the electrode potential and of the other suggested procedures; it is carried out quite rapidly because no slow equilibria are involved when a fluoride solution is added. It can be used to measure fluoride concentration as low as $10^{-5}$–$10^{-6}M$ which corresponds almost to the sensitivity of the fluoride electrode. In this range fluoride cannot be determined by titration with $La^{3+}$ or $Th^{4+}$, which are the most accurate and sensitive titration procedures. It is noteworthy to mention that the response of the membrane electrodes is more rapid when going from dilute to concentrated solutions than in the other direction.

The discussions of this paper have been concerned with the fluoride electrode; they may be applied to any selective electrode providing a linear relationship exists between electrode response and logarithm of the concentration.

RECEIVED for review October 9, 1968. Accepted December 16, 1968.

# AIDS FOR ANALYTICAL CHEMISTS

## Qualitative Thin-Layer Chromatography of Some Irritants

**William D. Ludemann, Martin H. Stutz, and Samuel Sass**

*Chemical Research Laboratory, Edgewood Arsenal, Md. 21010*

THIS REPORT describes a method developed for the qualitative analysis (and identification) of some irritant agents used at one time or another by military and law enforcement agencies. These agents include α-bromobenzyl cyanide (brombenzylcyanide, CA), *o*-chlorobenzalmalononitrile (CS), α-chloroacetophenone (CN), diphenylaminechloroarsine (DM), and diphenylcyanoarsine (DC). All are considered effective irritants.

As there are no published methods for the identification of these compounds as a group of chemical agents, a need existed for such a method. This is especially true today with the increasing use of chemicals in combating crime, preventing personal attacks, and in controlling civil unrest, where one (or a combination) of these agents might be used for riot control. Also included here are qualitative thin-layer chromatographic procedures for the analysis of individual irritant samples which allow detection of the most common impurities associated with the compounds.

## EXPERIMENTAL

**Adsorbents and Equipment.** Adsorbents used were silica gel-G (Merck-Brinkmann Instruments, Inc.) and acid alumina (Woelm-Alupharm Chemicals). The binder used with the acid alumina adsorbent was Ultracal 30 (a modified calcium sulfate, United States Gypsum Corp.).

Desaga thin-layer chromatographic apparatus, including a variable thickness applicator (Brinkmann Instruments, Inc.), was used to apply the adsorbents to standard (50 × 200 mm) glass plates in thicknesses of either 250 or 500 μ. The chromatoplates were prepared in the usual manner (after Stahl).

Slurry compositions used in the chromatoplate preparation are shown in Table I. Only the neutral silica gel-G plates were activated; these were heated at 105 to 110 °C for 30 minutes and stored over silica gel (desiccant). All plates were allowed to equilibrate over silica gel overnight before use.

**Standard Irritants.** Irritant samples were obtained from various internal agencies located at Edgewood Arsenal.

Physical Properties of Irritants

CA, brownish liquid, b.p. decomposes at 242 °C
CS, white to cream solid, m.p. 93–95 °C
CN, pale yellow crystals, m.p. 54–55 °C
DM, yellow to green solid, m.p. 195 °C
DC, white to pink solid, m.p. 30 °C

**Detection Reagents.** *o*-Dianisidine (Eastman Organic Chemicals), Technical grade, 0.1% solution in ethyl alcohol.

4-(4′-Nitrobenzyl)pyridine (K and K Laboratories), 5% solution in acetone.

Quinone (Eastman Organic Chemicals), White Label, 0.5% solution in methyl alcohol.

Sodium perchlorate, 5% solution in aqueous potassium acid phthalate (92.11 mg/100 ml of water), adjusted to pH 5.0 with 1 $N$ sodium hydroxide.

Iodine, resublimed.

*m*-Dinitrobenzene (Eastman Organic Chemicals), White Label, 1% solution in ethyl alcohol.

Sodium hydroxide (Baker), C.P., 20% aqueous solution.

Cupric acetate (Baker), C.P., 0.1% solution in water containing one drop of acetic acid per 50 ml.

## PROCEDURES

Sample aliquots are applied to the plates by conventional means in amounts of 5 to 50 μg per spot on the 250-μ layers and 50 to 100 μg per spot on the 500-μ layers. The chromatoplates are developed in solvent-saturated chambers (lined with filter paper) at a room temperature of 25 ± 2 °C. On com-

Table I. Slurry Compositions Used for Chromatoplate Preparation

| Plate | Adsorbent layer thickness, μ | Adsorbent weight, g | Binder weight, g | Slurrying solvent | |
|---|---|---|---|---|---|
| | | | | Solvent | Volume, ml |
| Acid alumina | 250 | 60 | 6 | Water | 45 |
| Acid alumina | 500 | 138 | 13.8 | Water | 92 |
| Basic silica gel-G | 250 | 30 | — | NaOH, 1 *N* | 60 |
| Silica gel-G | 250 | 30 | — | Water | 60 |
| Silica gel-G | 500 | 60 | — | Water | 115 |

Table II. Composite of CA, CS, and CN. DM and DC Included for Comparison

(Adsorbent, acid alumina; solvent, 5% chloroform in benzene)

| Compound | $R_f$ | Quinone | NaOH, 5% | 4-(4′-Nitrobenzyl) pyridine | *o*-Dianisidine, sulfuric acid |
|---|---|---|---|---|---|
| α-Bromobenzyl-cyanide (CA) | 0.65 | Yellow | Darker yellow | Red-violet | — |
| *o*-Chlorobenzal-malononitrile (CS) | 0.55 | Blue | Reddish spot, blue ring | Yellow-orange | — |
| α-Chloro-acetophenone (CN) | 0.50 | — | Brownish | Blue | — |
| Diphenylcyano-arsine (DC) | 0.30 | — | — | — | Rose |
| Diphenylamine-chloroarsine and its oxide (DM) | 0.00 | — | — | — | Orange |

pletion of development (100 mm), the plates are air-dried before further treatment.

CA, CS, and CN (dissolved in chloroform or carbon tetrachloride) are separated from one another on an adsorbent layer of acid alumina, using a mixture of 5% chloroform in benzene. After the developed chromatoplate is air-dried, the spots are first visualized with a spray of methanolic quinone and they are noted and marked (CN gives no color under these conditions). On subsequent spraying with the aqueous sodium hydroxide, all three compounds are visualized. Further confirmation is obtained on the same plate with sprays of 4-(4′-nitrobenzyl)pyridine and buffered sodium perchlorate. CA shows an immediate coloration. The plate is heated at 105 °C for 10 min., cooled to room temperature, and sprayed with piperidine. The color and location of the spots are noted and marked as they appear, since the colors fade. Color can be renewed by a second and third spraying with piperidine (but with less sensitivity).

For determining CS, CN, and the impurities associated with the parent compounds, an acid alumina chromatoplate is used. The developing solvent is 25% dichloromethane in benzene. Exposure to iodine vapors visualizes all of the components. A subsequent spray with 4-(4′-nitrobenzyl)pyridine detects all of the components with the exception of *o*-chlorobenzaldehyde.

For qualitatively evaluating a known CA sample, silica gel-G is used as adsorbent with benzene as the developing solvent. The nitrobenzylpyridine reagent, followed by perchlorate, heat, and piperidine spray will detect all of the significant impurities with the exception of benzylcyanide and benzyl dicyanide. A spray of *m*-dinitrobenzene followed by a spray of 20% sodium hydroxide visualizes these two compounds (preferably on a separate chromatoplate).

For separating and detecting DM and DC, an adsorbent layer of silica gel-G with a developing solvent of 20% acetone in chloroform is employed. Visualization of components is achieved by spraying first with *o*-dianisidine, then with cupric acetate, and finally with 50% sulfuric acid.

DM is separated from its impurities on a basic silica gel-G adsorbent layer using 10% ethyl acetate in methanol as a developing solvent. Visualization is as previously described.

In case a sample is completely unknown (except for the fact that it is an irritant), a group of spot tests are performed prior to chromatography. The sample is spotted, in triplicate, on a silica gel-G plate. Each individual spot is then treated with one of the reagent systems above—that is, with quinone, with the 4-(4′-nitrobenzyl)pyridine reagents, and with the *o*-dianisidine reagents. From the results obtained in these spot tests, the chromatographic system (or systems) best suited for the positive identification of the unknown is chosen.

## RESULTS AND DISCUSSION

CA, CN, and CS were readily separable from one another on an acid alumina plate in conjunction with a developing solvent of 5% chloroform in benzene. When the plate was sprayed with quinone (*1*), CA produced a yellow spot and CS a blue spot. The authors found that a subsequent spray with 5% sodium hydroxide intensified the yellow color for CA, converted the CS spot to a red with a blue ring, and visualized CN as a brown spot. On the same plate, the nitrobenzyl pyridine spray showed CA as a red spot and on subsequent spray with buffered perchlorate, heating at 105 °C, and spraying the cooled plate with piperidine, CA became red-violet; CS, yellow-orange; and CN, blue. A reduction in sensitivity occurs when the nitrobenzyl pyridine and its series of reagents is applied after the aqueous sodium hydroxide spray. These results including $R_f$ values are summarized in Table II.

Qualitative separation of CS and CN from their degradation products and impurities was accomplished on acid alumina using 25% dichloromethane in benzene solution as the developing solvent. Visualization was accomplished by means of the 4-(4′-nitrobenzyl)pyridine reagent system. $R_f$ values and color of spots are shown in Table III.

CA was separated from its impurities and degradation products on silica gel-G with benzene as developing solvent. Spots were initially visualized and noted by using the 4-(4′-nitrobenzyl) pyridine reagent system. Benzyl cyanide and benzyldicyanide were subsequently detected on the plate by spraying first with

(1) A Silvestri, Defense Development and Engineering Laboratories, Edgewood Arsenal, Md., private communication, Nov. 1967.

1% ethanolic *m*-dinitrobenzene and then with 20% sodium hydroxide. For detecting 1 μg or less of these two impurity components, the *m*-dinitrobenzene–sodium hydroxide sprays were best utilized on a separate chromatogram. The composite information for CS, including $R_f$ and detection color, is shown in Table IV.

The above system was also useful for preparative purification of CA when a 1-mm thickness adsorbent layer was employed(*2*).

DM and DC in fresh, anhydrous methanol solutions were separable on silica gel-G using 20% acetone in chloroform. Spots were detected at a lower limit of 10 μg using sprays of *o*-dianisidine and cupric acetate followed by sulfuric acid. DM and DM oxide were separable on basic silica gel-G employing 10% ethyl acetate in methanol as the developing solvent. The same detection reagents were applicable to this system. If the methanol solutions of DM were not chilled or the solutions were older than 10–15 min. only the DM oxide was found. These results are summarized in Table V. DM and DC are also separated from CA, CS, and CN in the acid alumina–5% chloroform in benzene system. These results are included in Table II.

For the identification of irritant, it was preferable to collect vapor or aerosol samples, and subsequently dissolve or extract with ethanol. Extraction was both from aerosol filters or contaminated cloth. CA reacted with dry alcohol (10 to 20% per day under ambient conditions); therefore solutions should be kept reasonably fresh.

Numerous thin-layer chromatographic systems were investigated before the methods described above were selected. In addition to the adsorbents used in the selected methods, the following were also investigated for possible use as chromatographic media to separate the irritants: neutral cellulose, basic cellulose, silver nitrate-impregnated silica gel-G, cellulose : silica gel-G mixtures, porous glass, and basic alumina. A large number of individual solvents and solvent mixtures were tested as developing solvents with the above adsorbents. This extensive test program was necessitated by the large difference in the polarities of the two groups of compounds to be separated.

Although emphasis has been placed on standard thin layers (250 μ) in this report, the same systems were successfully scaled up to thicker layers (500 μ and greater) for preparative chromatography. In these instances, preparative samples were obtained for use as colorimetric and infrared standards (except diphenylaminechloroarsine). It was also possible to scale down the systems for micro-detection (micro-slides) since all the detection reagents described were sensitive to 1 μg or less of agent.

The TLC separations of α-bromobenzyl cyanide, *o*-chlorobenzalmalononitrile, α-chloroacetophenone, and diphenylcyanoarsine were sufficiently clean to allow probable quantitation by spectrophotometric or densitometric procedures.

(2) M. H. Stutz, W. D. Ludemann, and S. Sass, ANAL. CHEM., **40**, 258 (1968).

**Table III. Composite of CA, CS, CN and Some Impurities**
**(Adsorbent, acid alumina; solvent, 25% dichloromethane in benzene)**

| Compound | $R_f$ | 4-(4′-Nitrobenzyl) pyridine |
|---|---|---|
| *o*-Chlorobenzaldehyde | 0.71 | [a] |
| α-Bromobenzylcyanide | 0.58 | Red-violet |
| *o*-Chlorobenzalmalononitrile | 0.53 | Yellow-orange |
| α-Chloroacetophenone | 0.45 | Blue |
| Malononitrile | 0.29 | Yellow |
| Acetophenone | 0.00 | Yellow |

[a] Detected with iodine vapors.

**Table IV. Composite of CA and Its Impurities**
**(Adsorbent, silica gel-G; solvent, benzene)**

| Compound | $R_f$ | 4-(4′-Nitrobenzyl) pyridine | *m*-Dinitrobenzene and NaOH |
|---|---|---|---|
| Benzylbromide | 0.73 | Blue | — |
| Dibrombenzylcyanide | 0.67 | Tan | — |
| α-Bromobenzylcyanide | 0.52 | Red-violet | — |
| Unknown | 0.43 | Violet | — |
| Benzyldicyanide | 0.40 | — | Violet |
| Benzylcyanide | 0.29 | — | Violet |
| Unknown | 0.11 | Violet | — |
| Unknown | 0.04 | Blue | — |
| Phenylbromo-acetamide | 0.00 | Blue | — |

**Table V. Composite of DC, DM, Diphenylamine-chloroarsine Oxide, and Diphenylamine**

| Compound | $R_{f1}$[a] | $R_{f11}$[b] | *o*-Dianisidine, sulfuric acid |
|---|---|---|---|
| Diphenylcyano-arsine | 0.65 | | Rose |
| Diphenylamine-chloroarsine | 0.35 | 0.23 | Orange |
| Diphenylamine- | 0.08 | 0.15 | Green |
| Diphenylamine-chloroarsine oxide | | 0.38 | Orange |

[a] System I. Adsorbent, silica gel-G; solvent, 20% acetone in chloroform.
[b] System II. Adsorbent, basic silica gel-G; solvent, 10% ethyl acetate in methanol.

RECEIVED for review September 16, 1968. Accepted November 27, 1968.

# A Simple Micropelleting Technique

**W. J. de Klein and K. Ulbert**[1]

*Laboratory of Organic Chemistry, State University of Leiden, Leiden, The Netherlands*

PELLETING TECHNIQUES are long established in chemical spectroscopy. Dies of various diameter have been described in the literature (*1*, *2*) or are available commercially. Micro samples require a special pelleting technique. The usual procedure is to use a metal disk holder, drill a hole in its center, and fill it with the material to be pressed. In most cases a steel disk holder is used which has the disadvantage of needing a special and expensive die—*e.g.*, the Perkin-Elmer Ultra Micro die.

A simple method is described which can be carried out with a normal die. The first part of this paper describes a method that can usefully be employed in infrared spectroscopy, where the metal disk holder is used to hold the micro pellet in the beam of infrared radiation. The second part describes an adaptation which offers the possibility to withdraw the pellet from the metal holder in cases where the metal may influence other types of measurement—*e.g.*, conductivity measurements on the pressed material.

The disk holder is a circular piece of lead, 16 mm in diameter, 1 mm thick with a hole of 1–1.5 mm drilled in its center. It is prepared in the following way. A piece of lead is rolled into a flat bar of 1 mm thickness. From this bar lead pellets of 16-mm diameter are punched with a hollow punch. A round steel pin with a sharp point serves to make a hole of the required diameter in the center of the lead pellet. This hole is carefully cleaned with a file and pipe-rag. The disk holder is now put on the upper die of the die-assembly (type RIIC D-0.3, for 16-mm pellets) which is turned upside down to facilitate manipulation with the lead disk holder. Next, the lower die is placed on the lead disk holder and firmly pressed by hand to ensure complete flatness of the lead disk holder and good contact between the lead and the upper die. (A poor contact would spill sample material when filling the hole.) The lower die is removed and the pellet holder is now ready to be filled. It is our practice, when preparing KBr pellets, to first fill the hole of the holder with a small amount of pure KBr powder so that the bottom of the hole is just covered. Now the hole is filled with KBr containing the sample—*e.g.*, eluted from a TLC-spot. A hole of 1.5 mm in diameter requires about 5 mg KBr. The KBr is tamped into the hole with a small rod with a flat end—*e.g.*, a broken sewing needle. When the hole is filled with the sample containing KBr a small pile of pure KBr is built over the orifice of the hole. (If some sample containing KBr is left over it can of course also be used to build the pile.) The amount of pure KBr needed to build a 1.5-mm high pile over a hole with a bore of 1.5-mm diameter is about 10 mg. This pile is indispensable for it serves to press the KBr into a clear pellet and prevents the hole from being pressed together when pressing the pellet. The pile is thus comparable with the steel pin used in most micro dies.

The lower steel die is put on and firmly pressed by hand onto the KBr pile. The bottom piece of the die assembly is put on and the whole die is turned and put into a press in its normal way.

[1]On leave from the Institute of Macromolecular Chemistry, Czechoslovak Academy of Sciences, Prague 6, Petriny, Czechoslovakia.

(1) F. E. Resnik, L. S. Harrow, J. C. Holmes, M. E. Bill, and F. L. Greene. ANAL. CHEM., **29**, 1874 (1957).
(2) F. Bissett, A. L. Bluhm, and L. Long, *ibid.*, **31**, 1927 (1959).

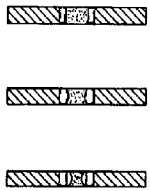


**Figure 1. *a*. Insert and sample lie in the lead pellet; *b*. deformation of the Teflon (Du Pont) insert under pressure causes a deformation of the pressed material; *c*. the pellet as it lies loose in the lead holder after pressure has been released**

A vacuum is applied for about 2 minutes and a pressure of 8–9 tons/cm² is applied for 3–4 minutes. In this way micro pellets of excellent optical transparency can be fabricated. Good quality infrared spectra were obtained in this way with the 1.5-mm diameter pellet holder from 1–4 μg solid material using a refracting beam condenser with KBr optics.

With an ordinate scale expander good spectra could be obtained with less than 1 μg of solid sample. When applying pressures higher than 8–9 tons/cm² the pellet holder is deformed and the hole is squeezed together thus considerably reducing the diameter of the pellet. At a pressure of 8–9 tons the original bore of 1.5 mm is squeezed together by less than 10% when a KBr pile of adequate body is used.

When it is necessary to withdraw the pellet from the holder the following adaptation is made. The modification is based on the use of a Teflon (Du Pont) insert which is placed in the hole and has the same height as the lead holder (Figure 1*a*). The sample is slightly precompressed in the insert with the flat-ended rod. The die is assembled as described above and a pressure of about 10 tons/cm² is applied. Under pressure the insert is deformed as shown in Figure 1*b*. After releasing the pressure the Teflon insert recovers to almost the original shape with the diameter only slightly smaller (Figure 1*c*). The pellet now lies loose in the Teflon holder and can be pushed out easily. For most applications the distortion of the cylindrical shape is of no harm.

The ratio of the insert's wall thickness to its diameter and height must be found by trial and error. It depends to a certain degree on the sample used as the pellet and on the precompression.

This method was used in preparing micropellets from the iodine complex of the leucobase of Bindschädlers' green (organic semiconductor). The following dimensions of the lead holder and Teflon insert were used: lead holder, diameter 13 mm, thickness 1 mm; and Teflon insert, o.d. 2.1 mm, i.d. 1.5 mm, length 1 mm. The applied pressure was 10 tons/cm². The resulting pellet had a diameter of 1.4 mm (1.35 mm in the middle part, thus having a hyperbolic shape distortion.) It appeared to be possible to press metal electrodes from lead or gold powder on the surface of the pellet. This was done in one operation as the pellet was pressed. It also appeared possible to make electrodes on the surface of the pellet by a metal evaporation technique; this has to be done before removing the pellet from the holder to protect the side surface of the actual pellet from becoming metallized. In this way the conductivity of the sample as a pellet could be measured.

RECEIVED for review October 4, 1968. Accepted December 6, 1968.

# Diamond-Windowed Cell for Spectrophotometry of Molten Fluoride Salts

**L. M. Toth, J. P. Young, and G. P. Smith**

*Oak Ridge National Laboratory, Oak Ridge, Tenn. 37830*

SPECTROPHOTOMETRY has proven a very useful tool for studying ionic species in molten fluoride salts. However, these media are corrosive toward common optical window materials and progress up to now has been based on the application of liquid holders that do not have windows (*1*, *2*). For example, the captive liquid cell (*2*) consists of a cylindrical container with holes below the liquid level through which the light beam passes. Surface tension prevents the liquid from running out through these holes. For solutions other than molten fluorides, a variety of liquid holders without windows have been used when conventional containers were not practical and which might be modified for molten fluoride spectroscopy.

Despite their utility, windowless cells have several limitations among which are the following: the gas–liquid interface through which the light passes is curved and the curvature varies with temperature, melt composition, and other factors. Because of this curvature, it is difficult to obtain an accurate value for the path length, particularly when the path length is short. Furthermore, light transmission across this curved surface is not rectilinear and to minimize its effect on the spectra, the cells must be positioned at the focus of the spectrometer beam. Even under these conditions, the accurate reproduction of a given baseline cannot be guaranteed. Evaporative losses from windowless cells can cause difficulties at high temperatures when the system contains a volatile component. Finally, with most designs of windowless cells, homogenization of the melt by agitation is not practical. (The only exception with which we are familiar is the reflection cell (*3*) in which the light beam is transmitted vertically through the horizontal liquid surface and reflected back by a metal mirror immersed in the melt; but this design introduces a variety of new problems.)

For molten fluoride spectroscopy, some of the limitations of windowless cells were circumvented by Cocks, Schroeder, and Schwartz who designed a cell with diamond windows (*4*). Diamond is inert toward a wide variety of molten fluorides and has good to excellent optical transmission properties over the near infrared, visible, and ultraviolet regions. However, this particular cell design suffered from three disadvantages. First, it was difficult to fill, empty, and clean. Second, it was elaborately constructed. Third, the window mounting placed stresses on the diamonds that enhanced the possibilities for breakage. On the whole the cell was not suitable for routine measurements but it demonstrated the feasibility of using diamond windows in contact with fluoride melts.

In an effort to use diamond windows on a more or less routine basis for molten fluoride spectroscopy, we designed a cell of simple construction that can be easily taken apart for cleaning. This cell is described here. It has a graphite body and is, of course, limited to use with systems that are inert toward carbon, but there is a wide variety of such systems.

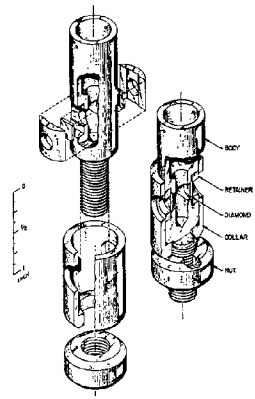


**Figure 1. Two views of the diamond-windowed cell**

**Exploded and partially cutaway view to the left, assembly cutaway view to the right**

This design has been tested in practice and found to perform well.

**Design of the Cell.** The construction of the diamond cell is displayed in Figure 1. All parts except the windows are machined from dense, reactor grade, Type ATJ graphite. In use, the cell is suspended in a heated inert-atmosphere chamber as described below.

The fluid is contained in a cylindrical body with a 0.50-inch outside diameter. The upper part of this body has a 0.375-inch inside diameter drilled to a depth of 0.688-inch. The lower part of the body has a 0.188-inch inside diameter drilled to an additional depth of 0.625-inch. A horizontal hole of 0.188-inch diameter, capped off by the diamond windows, allows passage of the light beam. The distance between windows is 0.25 inch.

The windows are held in place firmly but without significant stresses by a graphite framing arrangement shown in Figure 1. The frame consists of two retainer plates (one for each window) a cylindrical sleeve which holds the retainer plates in place, and a graphite nut, which screws on to the bottom of the body and holds the sleeve in place. Positioning of a window is achieved by means of a horizontal groove in the body, to fix the vertical position, and a vertical groove in the retainer plate to fix the horizontal position. The depth of each groove is one-half the window thickness, which is nominally 1 mm, while the width of each groove is, of course, the same as the width of the window, nominally 5 mm square.

With the above arrangement, the windows do not achieve a gas-tight seal with the cell body, but fluid leakage around the windows does not normally occur because most molten fluoride salts do not wet graphite. The possibility of such leakage constitutes a potential limitation in the use of this cell but in practice we have had no leakage problems. The advantages of this arrangement are simplicity of design, ease of assembly and disassembly, and no significant danger of window breakage due to loading stresses.

We find that the procurement of diamond windows cut to precise dimensions is particularly expensive, and the above design permits appreciable variations in the window dimensions away from their nominal values. For example, one of

(1) J. P. Young and J. C. White, ANAL. CHEM., **32**, 799 (1960).
(2) J. P. Young, *ibid.*, **36**, 390 (1964).
(3) J. Greenberg and L. J. Hallgren, *Rev. Sci. Instrum.*, **31**, 444 (1960).
(4) G. G. Cocks, J. B. Schroeder and C. M. Schwartz, "The Spectroscopy of Fused Salts," Battelle Memorial Institute Rept. No. BMI-1185, Columbus, Ohio, Feb–April 1957.

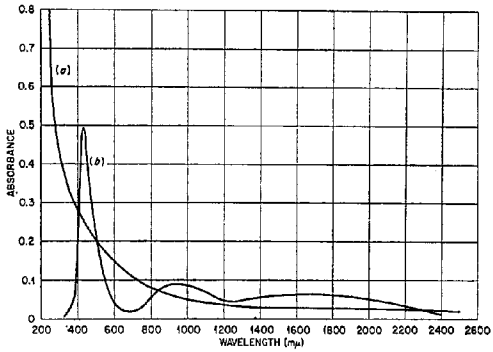


**Figure 2. Curve (*a*) apparent absorbance of diamond-windowed cell containing a transparent molten fluoride, LiF–$BeF_2$ (66–34 mol %) at 550 °C and referenced against a neutral density screen with an absorbance of about one. Curve (*b*), absorption spectrum of a dilute solution of $NiF_2$ in the above LiF–$BeF_2$ melt at 550 °C**

**The absorbance of cell plus solvent has been subtracted from that of the solution to give the solute absorbance**

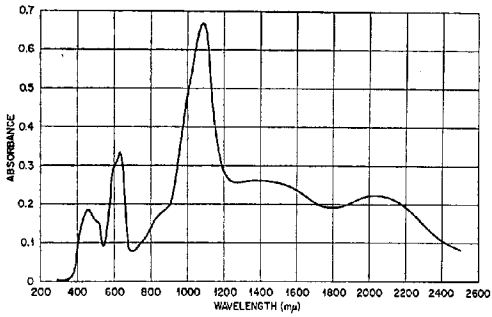


**Figure 3. Absorption spectrum of a dilute solution of $UF_4$ in molten LiF–$BeF_2$ (66–34 mol %) at 550 °C**

**The absorbance of the cell plus solvent has been subtracted from that of the solution to give the solute absorbance**

the plates we are now using is 5.0 × 4.3 × 1.3 mm as opposed to the design dimensions of 5.0 × 5.0 × 1.0 mm.

A metal cap, not shown in the figures, welded co-axially to a ⅛-inch diameter support rod, is slipped over the top of the graphite body and held in place by a metal pin. This pin passes through small holes in the cap and body. (The latter holes will be seen in Figure 1.) The support rod is used to suspend the cell in the inert-atmosphere chamber.

It is necessary to enclose this cell in a nonoxidizing atmosphere to prevent atmospheric reaction with the cell and windows at high temperatures, and generally, it is also necessary to control the composition of the gas phase to prevent reaction with the melt. For this purpose we have used an inert-atmosphere furnace described previously (*5*) for use with captive liquid cells. This furnace fits the cell compartment of a Cary Model 14 spectrophotometer and can easily be modified to fit a Cary Model 14H spectrophotometer for service at high temperature.

The diamonds used in our work are Type IIa because they have particularly good transmission characteristics in the ultraviolet. Type I diamonds, which are more common than Type IIa, are satisfactory in the near infrared and visible regions but absorb in the ultraviolet. Therefore it might be economically advantageous to use Type I diamonds for measurements restricted to these regions. Further information on the optical properties of diamonds is reported in the book edited by Berman (*6*).

Although cost is a seriously limiting factor in the use of diamond windows, it is not as excessive as often supposed, and we recommend that costs be investigated before rejecting the use of diamonds on this basis. Particularly if routine work is planned, the reusability of diamond, compared with less corrosion resistant materials, will prove an economic saving.

**Procedure.** The graphite pieces of the cell are cleaned in an ultrasonic bath to remove loose graphite dust and then heated in a vacuum at 800 °C to drive off adsorbed gaseous impurities. The cell is assembled in a helium-filled drybox containing about 1 ppm by volume of water vapor, and loaded with approximately two grams of prepared salt in the form of a few large pieces. For this work it has been found convenient to purify and mix the solutions in metal containers. These are then cooled to room temperature and the solids kept in an inert atmosphere until needed.

The loaded cell is fitted with the holder rod and placed in a metal transfer container where it is sealed in an inert atmosphere during transfer to the spectrometer furnace. The transfer and melting of the sample has been previously described (*5*).

After a spectrum of the molten solution has been recorded, the furnace cell assembly is inverted to drain the salt from the window region into the top portion of the cell. The furnace is cooled to room temperature and the solid piece of salt easily picked out. Because of the nonwetting characteristics of most fluorides in contact with graphite, no residual salt remains in the window region. Upon removal of the nut and sleeve, the retainers and diamonds literally fall away from the cell body so that any piece can be cleaned separately in preparation for another spectrum.

**Performance.** We follow a practice, common in molten salt spectrophotometry, of measuring the absorbances of the cell plus solvent and the cell plus solution separately as functions of wave length against an air reference. The absorbance of the solute is determined by subtracting these absorbance curves.

The absorbance of a diamond-windowed cell containing a molten LiF–$BeF_2$ (66–34 mol %) mixture (referred to here as $L_2B$) was about one absorbance unit in the near-infrared region when measured against air with a Cary Model 14 spectrophotometer. A large fraction of this apparent absorbance is due to beam clipping and is not a serious problem because of the high absorbance measuring capabilities of the Model 14. In practice, most of this constant background absorption was compensated for by attenuating the reference beam with a neutral density screen. Figure 2 shows the complete absorbance curve for $L_2B$ in the cell at 550 °C as measured with an attenuated reference beam. The $L_2B$ solvent is transparent in the wavelength range investigated (*7*) so that the gradually rising absorption and eventual effective cut off near 240 mμ is due to absorption by the diamond windows.

(5) J. P. Young, *Inorg. Chem.*, **6**, 1486 (1967).
(6) R. Berman, ed., *Physical Properties of Diamonds*, Clarendon Press, Oxford, 1965, p 295.
(7) J. P. Young in "Characterization and Analysis in Molten Salts," Gleb Mamantov, Ed., Marcel Decker, New York, N.Y., 1969.

To illustrate the capabilities of the method, we show typical spectra in Figures 2 and 3. Figure 2 shows the spectrum of pure $L_2B$ plus cell (discussed above) and the solute spectrum of a dilute solution of $NiF_2$ in $L_2B$ at 550 °C. This spectrum is similar to that observed in windowless containers (*8*). Figure 3 shows the solute spectrum of a dilute solution of $UF_4$ in $L_2B$ at 550 °C. The weak band at 2.03 $\mu$ in this spectrum of U(IV) was not observed in previous measurements with a windowless cell (*5*) because it could not be distinguished from a gradual variation in the baseline. The existence of such a band has been predicted (*9*, *10*) and its observation with the diamond-windowed cell helps confirm the value of this device.


ACKNOWLEDGMENT

We gratefully acknowledge the assistance of F. Davis, W. Longaker, and D. Allen of the Field Engineering Staff in helping with cell design problems and S. M. Horszowski of the Diamond Research Laboratory, Johannesburg, South Africa who supplied the diamonds used here. We also wish to thank G. G. Cocks and C. M. Schwartz for their comments and advice.

RECEIVED for review October 24, 1968. Accepted January 16, 1969. Research sponsored by the U.S. Atomic Energy Commission under contract with the Union Carbide Corporation.


(8) J. P. Young, *Inorg. Chem.*, in press.
(9) D. Cohen and W. T. Carnall, *J. Phys. Chem.*, **64**, 1933 (1960).
(10) J. G. Conway, *J. Chem. Phys.*, **31**, 1002 (1959).

# Technique for Obtaining Absorption Spectra of Insoluble Metal Chelate Polymers


**P. S. Shetty and Quintus Fernando**

*Department of Chemistry, University of Arizona, Tucson, Ariz. 85721*


MANY METAL CHELATES that are obtained from dithio-oxamide, $(CSNH_2)_2$, (rubeanic acid) and certain transition metal ions are polymeric and are potentially useful for a variety of purposes. One of the more important uses of rubeanic acid and its derivatives is the detection and determination of metal ions in low concentrations. The electronic spectra of these polymeric metal chelates provide analytically useful information, but cannot be readily obtained. Vaeck (*1*) measured the reflectance spectrum of nickel rubeanate adsorbed on paper, and Jacobs and Yoe (*2*) in their studies on the composition of nickel rubeanate used gum acacia as a protective colloid to prevent the coagulation of the polymeric nickel chelate. A simple method of obtaining the absorption spectra of polymeric metal chelates is proposed and its application to the study of the absorption spectrum of nickel rubeanate is described.

The method consists of the electrodeposition of a film of the nickel chelate of rubeanic acid from an organic solvent on the surface of an electrode made of conducting glass which is transparent in the visible region of the spectrum. The conditions under which the film is electrodeposited can be used to control the thickness of the film. The absorption spectrum of the metal chelate film is recorded against air, and corrected for the absorbance of the conducting glass electrode.

## EXPERIMENTAL

**Reagents.** Rubeanic acid was obtained from Eastman Organic Chemicals, Rochester, N.Y., and nickel perchlorate from G. F. Smith Chemical Company, Columbus, Ohio. All other compounds used in this work were of reagent grade purity.

**Apparatus.** A dc power supply, capable of supplying a variable voltage up to 500 V at 100 mA was used for the electrodeposition. The electrodes consisted of a platinum anode and a conducting glass electrode, (No. 7740), manufactured by Corning Glass Works, Corning, N.Y. A metal oxide film was permanently bonded by the manufacturer to one side of the glass, and it transmitted approximately 75% of the light in the visible region of the spectrum. All absorption spectra in the visible region were obtained with a Cary Model 14 recording spectrophotometer. The infrared spectra in KBr were recorded with a Perkin-Elmer 337B grating spectrophotometer.

**Method.** The electrodeposition was carried out in a water-cooled double-walled glass vessel containing an isopropanol solution of the metal chelate which was prepared by mixing $2 \times 10^{-4}M$ isopropanol solutions of nickel perchlorate and rubeanic acid in a 1 : 2.5 ratio. The total volume of the metal chelate solution was made up to 125 ml with isopropanol.

The conducting glass electrode was rinsed with $2M$ nitric acid and washed thoroughly with ethanol. Before the electrodeposition was carried out, the absorption spectrum of the electrode *vs.* air was recorded. The platinum anode and the conducting glass cathode were placed in the metal chelate solution, the distance between the two electrodes was adjusted to obtain an appropriate current value, and electrodeposition was commenced. The solution was stirred by means of a magnetic stirrer throughout the course of the electrodeposition which usually lasted for about half an hour to obtain a sufficient quantity of an adherent film of a purple-blue nickel rubeanate. The absorption spectrum of the metal chelate film was recorded *vs.* air and corrected for the absorbance of the conducting glass.

## RESULTS AND DISCUSSION

The manner in which the following parameters affected the nature of the deposited metal chelate was investigated: voltage, current, time of deposition, concentration of the metal chelate, acidity of the medium, surface active agents, and water added to the isopropanol medium.

In all the experiments, the initial current was 1 mA and the voltage was varied from 20 to 300 V. The rate of formation of the deposit increased with increasing voltage, but the current decreased with time as the thickness of the deposit increased. The presence of small amounts of water (up to

(1) S. V. Vaeck, *Anal. Chim. Acta*, **10**, 48 (1954).
(2) W. D. Jacobs and J. H. Yoe, *ibid.* **20**, 332 (1959).

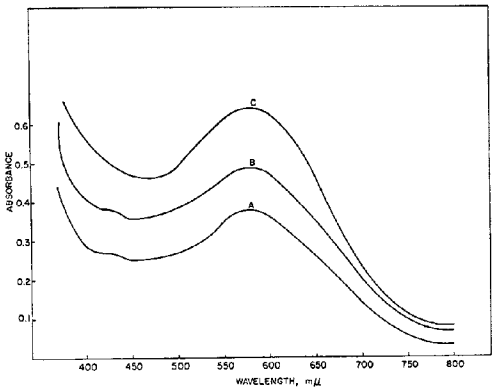


**Figure 1. Absorption spectrum of nickel rubeanate**

*A.* **Isopropanol solution containing $8 \times 10^{-5}M$ $Ni(ClO_4)_2$ and $2 \times 10^{-4}M$ rubeanic acid**

*B.* **Thin film electrodeposited from an isopropanol solution containing $8 \times 10^{-5}M$ $Ni(ClO_4)_2$ and $2 \times 10^{-4}M$ rubeanic acid**

*C.* **Thick film electrodeposited under the same conditions as in *B***

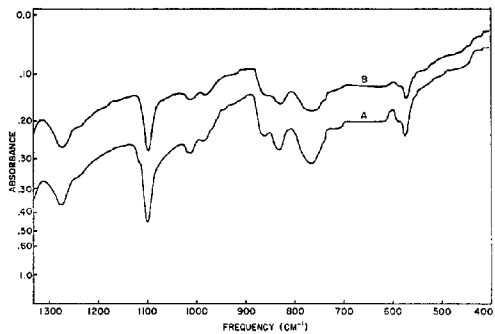


**Figure 2. Infrared spectrum of nickel rubeanate**

*A.* **Obtained by precipitation**

*B.* **Electrodeposited from isopropanol**

1% v/v) increased the rate of formation of the deposit. When about 10% v/v was present in the isopropanol solution, the deposit became flaky and nonadherent. Addition of small amounts of gum arabic (0.001%) did not affect the nature of the deposit although the rate at which the deposit formed was decreased.

The acidity of the metal chelate solution in isopropanol was varied by the addition of small quantities of acid or base; a pH meter reading with a glass-saturated calomel electrode pair gave an indication of the acidity of the solution. It was possible to deposit the nickel rubeanate when the pH meter readings were between 0.8 and 2.4, but above 2.5 no deposit was formed. The lower the pH meter reading of the solution, the slower the rate of formation of the deposit. The infrared and visible spectra of the metal chelate deposited confirmed that the same complex was obtained in all the experiments.

When all other experimental parameters were kept constant, the amount of the metal chelate deposited was governed by the time of electrodeposition. The concentration of the complex affected the rate of electrodeposition. The optimum concentration range of the metal complex was between $2 \times 10^{-4}M$ and $4 \times 10^{-5}M$. At lower concentrations the rate of deposition was much too slow, whereas at higher concentrations there was a tendency for the complex to precipitate and form a nonadherent deposit.

The above experiments have established that a uniform, adherent film of nickel rubeanate can be deposited on a conducting glass electrode under the following conditions: The potential range between 50 and 100 V, an initial current of 0.5–1.2 mA (which can be adjusted by varying the distance between the conducting glass and platinum electrodes), the acidity of the solution between 2.0 and 2.2 (as indicated by the pH meter reading) and the concentration of the nickel rubeanate complex between $2 \times 10^{-4}M$ and $4 \times 10^{-5}M$. The deposit is insoluble in water and in most common organic solvents. The absorption spectrum of the deposited film has a strong absorption band at 585 mμ. The position of this band does not change with the thickness of the film and is identical with the strong band found in the solution spectrum of nickel rubeanate in isopropanol containing the same concentration of acid (Figure 1). It must be emphasized, however, that nickel rubeanate precipitates within a few minutes after mixing the isopropanol solution of nickel perchlorate and the rubeanic acid. The solid nickel rubeanate complex was prepared by the addition of 4 ml of $5 \times 10^{-3}M$ $Ni(ClO_4)_2$ in isopropanol to 10 ml of $5 \times 10^{-3}M$ rubeanic acid in isopropanol, and the total volume of the solution made up to 250 ml with isopropanol. The mixture was allowed to stand for 24 hours, centrifuged, washed, and dried at 100 °C. For purposes of comparison, an infrared spectrum of this complex in KBr was obtained and was found to be identical with the infrared spectrum in KBr of the film of nickel rubeanate that was scraped from the surface of the conducting glass (Figure 2). These results confirm that the composition of the electrodeposited complex and that obtained by precipitation from solution is essentially the same.

The rubeanic acid complexes of Pb(II), Cu(II), Mn(II), and Zn(II) could also be deposited in the form of uniform adherent films with the same technique. Certain transition metal chelates of azo dyes were also electrodeposited readily. In some of these cases, however, it appears that the hydroxy complexes of the metal chelates are electrodeposited.

The proposed method for obtaining the absorption spectra of polymeric metal chelates has several advantages. For example, the effect of the degree of polymerization on the absorption spectrum of the polymer can be studied. Also, the reflectance and the absorption spectrum of metal chelate films can be measured simultaneously.

RECEIVED for review November 15, 1968. Accepted December 20, 1968. Work supported by a NASA Institutional Grant.

# A Modified Differential Scanning Calorimeter Technique Utilizing a Quenched Polymer Reference Material

**Carl R. Foltz and Paul V. McKinney**[1]

*Armstrong Cork Company, Lancaster, Pa. 17604*

A MODIFIED DSC PROCEDURE has been developed (*1*) in the course of making a quantitative examination of the effect of annealing of poly(vinyl chloride) near the glass transition temperature (*2*). In this modified procedure a quenched specimen of the polymer which is under investigation has been used as the reference material replacing the usual inert reference material. In the DSC two sample holders are provided, one for the reference material and one for the sample under investigation. Both are subjected to a linear temperature program and the heat flow rate into each is continuously monitored. The difference in power required to maintain the programmed temperature in the two cells is charted. By using a quenched sample of the polymer as reference, the instrument charts directly differences in energy requirements between it and the sample specimen which previously had received special conditioning. Thus the difference in energy between the two physical states of the sample is measured directly. With this technique it is possible to measure small energy differences which in the usual procedure appear as minor inflections on the slope of the $T_g$ curve or as irregularities prior to the start of the glass transition.

## EXPERIMENTAL

**Apparatus.** The instrument used in this investigation was the Perkin-Elmer Differential Scanning Calorimeter (DSC) described in detail by Watson *et al.* (*3*) and O'Neill (*4*).

**Procedure.** The following procedure was adopted. Equal weights (20 mg) of the polymer sample were prepared in matched aluminum containers and placed in the reference and sample holders. They were then heated to a temperature above the glass transition temperature in order to eliminate previous thermal history effects. Quenching to room temperature by application of a direct air stream completed the effort to attain identically conditioned sample and reference specimens prior to the annealing process. The capsule containing the quenched reference specimen was then removed from the DSC and maintained at room temperature to preserve the quenched state. The test specimen remaining in the DSC sample holder was rapidly brought to a selected annealing temperature and maintained for the selected period of time. Following this annealing period, the test specimen was quenched to room temperature. The quenched reference specimen was then returned to the DSC. Final scanning provided the thermogram displaying the energy difference between the quenched and annealed polymer specimens. All curves were obtained by scanning at a rate of 20 °C/min and the DSC instrument was calibrated for peak area using the recrystallization transition of ammonium thiocyanate (*5*).

[1]Present address, 620 Great Road, Princeton, N.J.

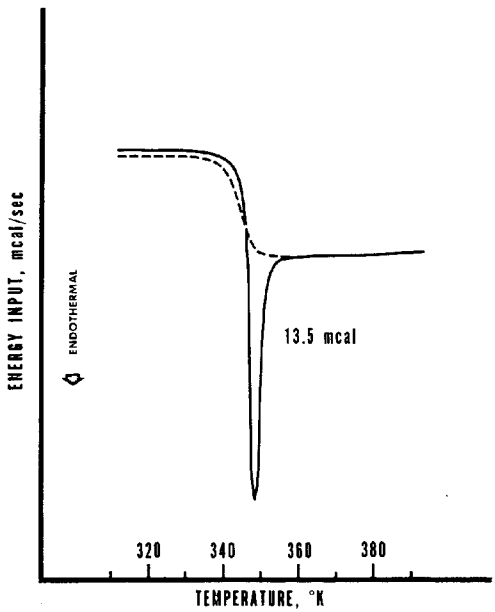


**Figure 1. Normal DSC thermogram**

**Quenched (-----) and annealed (——) curves superimposed. PVC copolymer (Exon 487) 20-mg sample**

## RESULTS AND DISCUSSION

An example of conventional DSC thermograms using an inert reference material is shown in Figure 1. The dashed line is the usual $T_g$ curve for the amorphous polymer after heating well above $T_g$ and quenching. The solid line is for a specimen of the same polymer aged (annealed) for a long period in storage. The curves are superimposed to illustrate the difference produced at the $T_g$ by aging. Both curves depict the abrupt change in specific heat typical of the glass transition while the aged specimen displays an added peak.

The results obtained for the same polymer by the modified DSC procedure, Figure 2, display the same difference in energy at the glass transition but without the complicating shift associated with the specific heat increase. The peak area for a 20-mg specimen by conventional DSC procedure is 13.5 m-cal and by the modified procedure is 14.1 m-cal. These values are in satisfactory agreement for such a small transition energy change. If desired, greater accuracy in defining peak area can be achieved by superimposing the thermogram representing the quenched state of both reference and sample specimens (quenching both from above $T_g$ to room temperature and rescanning after obtaining the initial thermogram) rather than employing the ruled line technique. However, the difference in defined peak area for the two techniques is small when both reference and sample polymer specimens are weighed to an accuracy of ±0.01 mg and the DSC differential

(1) C. R. Foltz, M.S. Thesis (Physics), Franklin and Marshall College, Lancaster, Pa., 1968.
(2) P. V. McKinney and C. R. Foltz, *J. Appl. Polym. Sci.*, **11**, 1189 (1967).
(3) E. S. Watson, M. J. O'Neill, J. Justin, and N. Brenner, ANAL. CHEM., **36**, 1233 (1964).
(4) M. J. O'Neill, *ibid.*, **36**, 1238 (1964).
(5) J. J. Keavney and E. C. Eberlin, *J. Appl. Polym. Sci.*, **3**, 50 (1960).

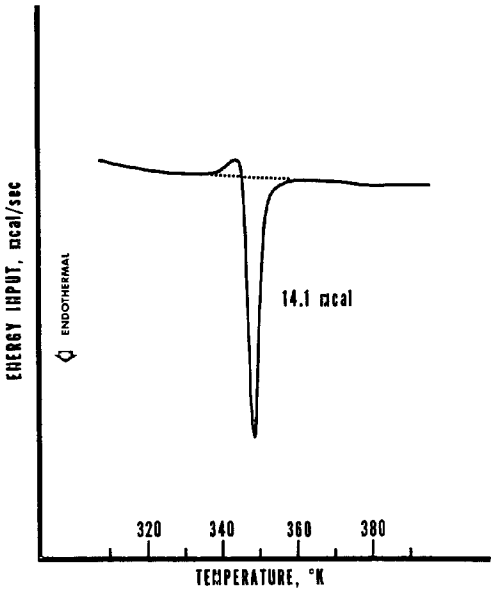


Figure 2. Modified DSC technique

Thermogram of annealed specimen *vs.* quenched specimen as reference. PVC copolymer (Exon 487) 20-mg sample. ------ Ruled line defining peak area

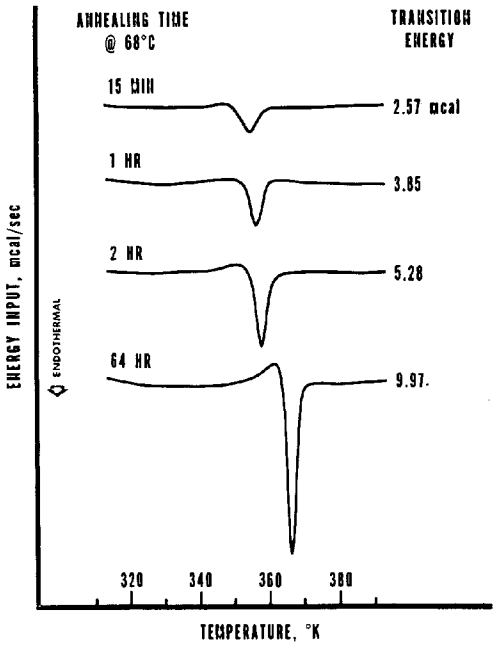


Figure 3. Annealing study of PVC homopolymer (Opalon 630) employing modified DSC technique

Twenty-milligram sample

temperature calibration is initially adjusted to produce essentially a straight line in the scan of quenched polymer reference *vs.* quenched polymer sample.

The data in Figure 3 illustrate the value of this modified DSC procedure in detecting small differences. Four measurements on the PVC homopolymer Opalon 630 annealed at 68 °C (ten degrees below its quenched state $T_g$) for, respectively, 15 min, 1 hr, 2 hr, and 64 hr are shown. In the conventional DSC procedure, the values at 15 minutes and 1 hour, if noted at all, would be difficult to estimate because no peak appears on such a thermogram, but only an inflection on the slope of the $T_g$ curve.

The slight displacement of the initial portion of the two curves in Figure 1 is real and represents a difference in specific heat between annealed and quenched specimens, the specific heat of the annealed specimen being less than that of the quenched specimen. The slight exothermal rise before the peak in Figures 2 and 3 results from the difference in temperature at which the transition starts in the two forms of the polymer. In Figure 1 it is evident that the quenched polymer begins absorbing additional energy a few degrees in temperature before the annealed specimen. Because it is placed in the reference cell in the DSC, the increase in specific heat of the quenched specimen is endothermal for the reference cell but appears as an exothermal energy change of the sample specimen up to the temperature that the two curves in Figure 1 cross. These data for PVC can be compared with similar differences in specific heat between annealed and quenched polymer specimens below $T_g$ which have been reported by Karasz *et al.* (*6*) for poly(2,6-dimethyl-1,4-phenylene ether). In the case of PVC small changes in physical properties in addition to specific heat can be expected on annealing and such changes have been reported for rigid PVC by Phillips (*7*). A theoretical consideration and analysis of the time factor in measurement of the glass transition by scanning procedure can be found in the study of polystyrene by Wunderlich and associates (*8*).

ACKNOWLEDGMENT

The authors thank the assisting faculty of Franklin and Marshall College for their kind cooperation in helping to organize the original thesis from which this article has been prepared.

RECEIVED for review December 2, 1968. Accepted January 22, 1969. Permission to publish and financial support granted by Armstrong Cork Company.

(6) F. E. Karasz, J. M. O'Reilly, H. E. Bair, and R. A. Kluge, Polymer Preprints, Vol. 9, 155th National Meeting of the American Chemical Society, San Francisco, April 1968, p 822.
(7) R. Phillips, R. L. Cox, and C. A. Heilberger, Preprints, 26th Antec, Society of Plastics Engineers, May 1968, p 216.
(8) B. Wunderlich, D. M. Bodily, and M. A. Kaplan, *J. Appl. Phys.*, **35**, 95 (1964).

**10 kHz ..... 220 MHz**

( 15 octaves without tuning or bandswitching )

**M500L ..... 3 watts, 10 db**

**M5000L ..... 10 watts, 30 db**

**M402L ..... 50 watts, 40 db**

**M404L ..... 200 watts, 50 db**

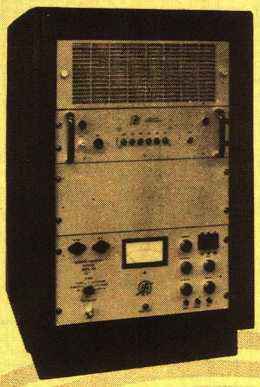

M402L

All IFI broadband power amplifiers are designed to produce up to twice rated power into matched load when driven by typical lab type signal generators. They offer high tolerance to load mismatch and feature complete internal damage protection and ultimate operating convenience and reliability.

**IDEAL SOURCES FOR:**

**RFI/EMI Susceptibility Testing**
**NMR and ENDOR excitation**
**Antenna test systems**
**Electronic countermeasures**
**Filter attenuation measurements**
**Insertion loss measurements**
**Ionospheric sounding**
**RF component testing**
**Wideband communications systems**

*Special models available for higher power, wider bandwidth and unique user requirements. Call your IFI representative, or the factory collect.*

INSTRUMENTS FOR INDUSTRY ifi INC

**INSTRUMENTS FOR INDUSTRY, INC.**
151 Toledo St., Farmingdale, L.I., N.Y. 11735
516-694-1414

Circle No. 169 on Readers' Service Card

## NEW CATALOG describes 15 Mettler top-loading balances

Mettler's high-speed, easy-to-use, top-loading balances are fully described in a new catalog. Included are units with performance levels ranging from semi-analytical to 11-kilo high capacity. All are precise, rapid-reading and offer improved precision-to-capacity relationships.

Most unusual is the new Model P160. It features a reversible scale for weight loss studies and gravimetric titrations. Most versatile is the widely-used P1200. Its 1200-gram capacity and ±10-milligram readability make it ideal for the vast majority of routine weighings.

All Mettler top-loaders can be used for five different types of weighings. Included are weighing of unknowns, batching, check-weighing, weighing-in, and below-balance weighing.

Request Bulletin P from Mettler Instrument Corporation, 20 Nassau Street, Princeton, New Jersey 08540.




Mettler®

Circle No. 56 on Readers' Service Card

See ACS Laboratory Guide for All Products/Sales Office

Analytical Chemistry

**APRIL 1969**

Valid through August 1969

**NEW PRODUCTS, NEW CHEMICALS, MFG. LITERATURE:**

401 402 403 404 405 406 407 408 409 410 411 412 413 414 415
416 417 418 419 420 421 422 423 424 425 426 427 428 429 430
501 502 503 504 505 506 507 508 509 510 511 512 513 514 515
601 602 603 604 605 606 607 608 609 610 611 612 613 614 615
616 617 618 619 620 621 622 623 624 625 626 627 628 629 630
631 632 633 634 635 636 637 638 639 640 641 642 643 644 645

**ADVERTISED PRODUCTS:**

| | | | | | | | | | | | | | | |
|---|---|---|---|---|---|---|---|---|---|---|---|---|---|---|
| 1 | 26 | 51 | 76 | 101 | 126 | 151 | 176 | 201 | 226 | 251 | 276 | 301 |
| 2 | 27 | 52 | 77 | 102 | 127 | 152 | 177 | 202 | 227 | 252 | 277 | 302 |
| 3 | 28 | 53 | 78 | 103 | 128 | 153 | 178 | 203 | 228 | 253 | 278 | 303 |
| 4 | 29 | 54 | 79 | 104 | 129 | 154 | 179 | 204 | 229 | 254 | 279 | 304 |
| 5 | 30 | 55 | 80 | 105 | 130 | 155 | 180 | 205 | 230 | 255 | 280 | 305 |
| 6 | 31 | 56 | 81 | 106 | 131 | 156 | 181 | 206 | 231 | 256 | 281 | 306 |
| 7 | 32 | 57 | 82 | 107 | 132 | 157 | 182 | 207 | 232 | 257 | 282 | 307 |
| 8 | 33 | 58 | 83 | 108 | 133 | 158 | 183 | 208 | 233 | 258 | 283 | 308 |
| 9 | 34 | 59 | 84 | 109 | 134 | 159 | 184 | 209 | 234 | 259 | 284 | 309 |
| 10 | 35 | 60 | 85 | 110 | 135 | 160 | 185 | 210 | 235 | 260 | 285 | 310 |
| 11 | 36 | 61 | 86 | 111 | 136 | 161 | 186 | 211 | 236 | 261 | 286 | 311 |
| 12 | 37 | 62 | 87 | 112 | 137 | 162 | 187 | 212 | 237 | 262 | 287 | 312 |
| 13 | 38 | 63 | 88 | 113 | 138 | 163 | 188 | 213 | 238 | 263 | 288 | 313 |
| 14 | 39 | 64 | 89 | 114 | 139 | 164 | 189 | 214 | 239 | 264 | 289 | 314 |
| 15 | 40 | 65 | 90 | 115 | 140 | 165 | 190 | 215 | 240 | 265 | 290 | 315 |
| 16 | 41 | 66 | 91 | 116 | 141 | 166 | 191 | 216 | 241 | 266 | 291 | 316 |
| 17 | 42 | 67 | 92 | 117 | 142 | 167 | 192 | 217 | 242 | 267 | 292 | 317 |
| 18 | 43 | 68 | 93 | 118 | 143 | 168 | 193 | 218 | 243 | 268 | 293 | 318 |
| 19 | 44 | 69 | 94 | 119 | 144 | 169 | 194 | 219 | 244 | 269 | 294 | 319 |
| 20 | 45 | 70 | 95 | 120 | 145 | 170 | 195 | 220 | 245 | 270 | 295 | 320 |
| 21 | 46 | 71 | 96 | 121 | 146 | 171 | 196 | 221 | 246 | 271 | 296 | 321 |
| 22 | 47 | 72 | 97 | 122 | 147 | 172 | 197 | 222 | 247 | 272 | 297 | 322 |
| 23 | 48 | 73 | 98 | 123 | 148 | 173 | 198 | 223 | 248 | 273 | 298 | 323 |
| 24 | 49 | 74 | 99 | 124 | 149 | 174 | 199 | 224 | 249 | 274 | 299 | 324 |
| 25 | 50 | 75 | 100 | 125 | 150 | 175 | 200 | 225 | 250 | 275 | 300 | 325 |

**RUSH: I have an immediate use for these advt. products I've circled above:**

_____ _____ _____ _____ _____

_____ _____ _____ _____ _____

Name _____

Position _____

Company _____

Address _____

Zip _____

FIRST CLASS
Permit No. 1538
New York, N. Y.

**BUSINESS REPLY CARD**
NO POSTAGE STAMP NECESSARY IF MAILED IN THE UNITED STATES

POSTAGE WILL BE PAID BY

**ANALYTICAL CHEMISTRY**

**PUBLISHER'S DATA CENTER, INC.**

**132 WEST 31ST STREET**

**NEW YORK, N. Y. 10001**

your free copy . . .

# THE ORION GUIDE TO SPECIFIC ION ELECTRODES

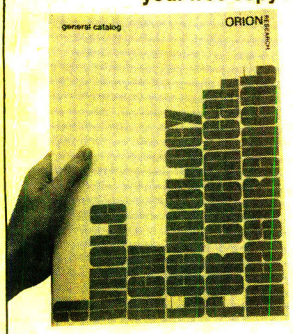


- theory section
- technical data on 21 specific ion electrodes, including four new solid-state electrodes — lead, copper, thiocyanate, sodium
- applications information on direct measurements, titrations, and recovery methods
- detailed information on:
  - *reference electrodes for specific ion electrode measurement*
  - *standardizing solutions*
  - *instrumentation for digital measurement, printout, control and multiple electrode switching*
- bibliography of journal articles

**Orion Research Incorporated**
**11 blackstone street**
**cambridge, massachusetts 02139**

Circle No. 63 on Readers' Service Card

See ACS Laboratory Guide for All Products/Sales Office

Name _____

Position _____

Company _____

Address _____

Zip _____

FIRST CLASS
Permit No. 1538
New York, N. Y.

**BUSINESS REPLY CARD**
NO POSTAGE STAMP NECESSARY IF MAILED IN THE UNITED STATES

POSTAGE WILL BE PAID BY

**ANALYTICAL CHEMISTRY**

**PUBLISHER'S DATA CENTER, INC.**

**132 WEST 31ST STREET**

**NEW YORK, N. Y. 10001**

Analytical Chemistry

**APRIL 1969**

Valid through August 1969

**NEW PRODUCTS, NEW CHEMICALS, MFG. LITERATURE:**

401 402 403 404 405 406 407 408 409 410 411 412 413 414 415
416 417 418 419 420 421 422 423 424 425 426 427 428 429 430
501 502 503 504 505 506 507 508 509 510 511 512 513 514 515
601 602 603 604 605 606 607 608 609 610 611 612 613 614 615
616 617 618 619 620 621 622 623 624 625 626 627 628 629 630
631 632 633 634 635 636 637 638 639 640 641 642 643 644 645

**ADVERTISED PRODUCTS:**

| | | | | | | | | | | | | | | |
|---|---|---|---|---|---|---|---|---|---|---|---|---|---|---|
| 1 | 26 | 51 | 76 | 101 | 126 | 151 | 176 | 201 | 226 | 251 | 276 | 301 |
| 2 | 27 | 52 | 77 | 102 | 127 | 152 | 177 | 202 | 227 | 252 | 277 | 302 |
| 3 | 28 | 53 | 78 | 103 | 128 | 153 | 178 | 203 | 228 | 253 | 278 | 303 |
| 4 | 29 | 54 | 79 | 104 | 129 | 154 | 179 | 204 | 229 | 254 | 279 | 304 |
| 5 | 30 | 55 | 80 | 105 | 130 | 155 | 180 | 205 | 230 | 255 | 280 | 305 |
| 6 | 31 | 56 | 81 | 106 | 131 | 156 | 181 | 206 | 231 | 256 | 281 | 306 |
| 7 | 32 | 57 | 82 | 107 | 132 | 157 | 182 | 207 | 232 | 257 | 282 | 307 |
| 8 | 33 | 58 | 83 | 108 | 133 | 158 | 183 | 208 | 233 | 258 | 283 | 308 |
| 9 | 34 | 59 | 84 | 109 | 134 | 159 | 184 | 209 | 234 | 259 | 284 | 309 |
| 10 | 35 | 60 | 85 | 110 | 135 | 160 | 185 | 210 | 235 | 260 | 285 | 310 |
| 11 | 36 | 61 | 86 | 111 | 136 | 161 | 186 | 211 | 236 | 261 | 286 | 311 |
| 12 | 37 | 62 | 87 | 112 | 137 | 162 | 187 | 212 | 237 | 262 | 287 | 312 |
| 13 | 38 | 63 | 88 | 113 | 138 | 163 | 188 | 213 | 238 | 263 | 288 | 313 |
| 14 | 39 | 64 | 89 | 114 | 139 | 164 | 189 | 214 | 239 | 264 | 289 | 314 |
| 15 | 40 | 65 | 90 | 115 | 140 | 165 | 190 | 215 | 240 | 265 | 290 | 315 |
| 16 | 41 | 66 | 91 | 116 | 141 | 166 | 191 | 216 | 241 | 266 | 291 | 316 |
| 17 | 42 | 67 | 92 | 117 | 142 | 167 | 192 | 217 | 242 | 267 | 292 | 317 |
| 18 | 43 | 68 | 93 | 118 | 143 | 168 | 193 | 218 | 243 | 268 | 293 | 318 |
| 19 | 44 | 69 | 94 | 119 | 144 | 169 | 194 | 219 | 244 | 269 | 294 | 319 |
| 20 | 45 | 70 | 95 | 120 | 145 | 170 | 195 | 220 | 245 | 270 | 295 | 320 |
| 21 | 46 | 71 | 96 | 121 | 146 | 171 | 196 | 221 | 246 | 271 | 296 | 321 |
| 22 | 47 | 72 | 97 | 122 | 147 | 172 | 197 | 222 | 247 | 272 | 297 | 322 |
| 23 | 48 | 73 | 98 | 123 | 148 | 173 | 198 | 223 | 248 | 273 | 298 | 323 |
| 24 | 49 | 74 | 99 | 124 | 149 | 174 | 199 | 224 | 249 | 274 | 299 | 324 |
| 25 | 50 | 75 | 100 | 125 | 150 | 175 | 200 | 225 | 250 | 275 | 300 | 325 |

**RUSH:** I have an immediate use for these advt. products I've circled above: _____ _____ _____ _____

# Coleman Photofluorometer®

## . . . the *working* tool for fluorescence analysis

The Coleman Photofluorometer is the practical tool for routine fluorescence analysis in the laboratory.

Simple and easy to use, it has proved its value over years of use in clinical and control laboratories having a large number of routine analyses.

Its sensitivity range covers all practical applications — quinines, quinoline, vitamins, porphyrins, steroids, metal complexes, etc. The instrument permits quantitative determination of fluorophors (quinine, for example) down to 3 parts in 10 billion.



The Photofluorometer achieves its sensitivity without photomultipliers or other elaborate, trouble-prone circuits. This forthright simplicity encompasses all aspects of the instrument's operation:

—samples insert directly into the instrument's optical system,

—readings are taken directly from the meter scale,

—a simple lens-and-aperture system prevents decay of sensitive substances by allowing exposure to irradiation only during the actual reading.

Low priced, the Coleman Photofluorometer provides an economical approach to routine fluorescence in the working laboratory.

*Send for Bulletin A-298*

*Write to Coleman Instruments Division, The Perkin-Elmer Corporation, 42 Madison St., Maywood, Illinois 60153*

**Visit Our Booth—FASEB Meeting**

**PERKIN-ELMER**

Circle No. 31 on Readers' Service Card

# We ask you:

# Is this the face of an ordinary pH meter?

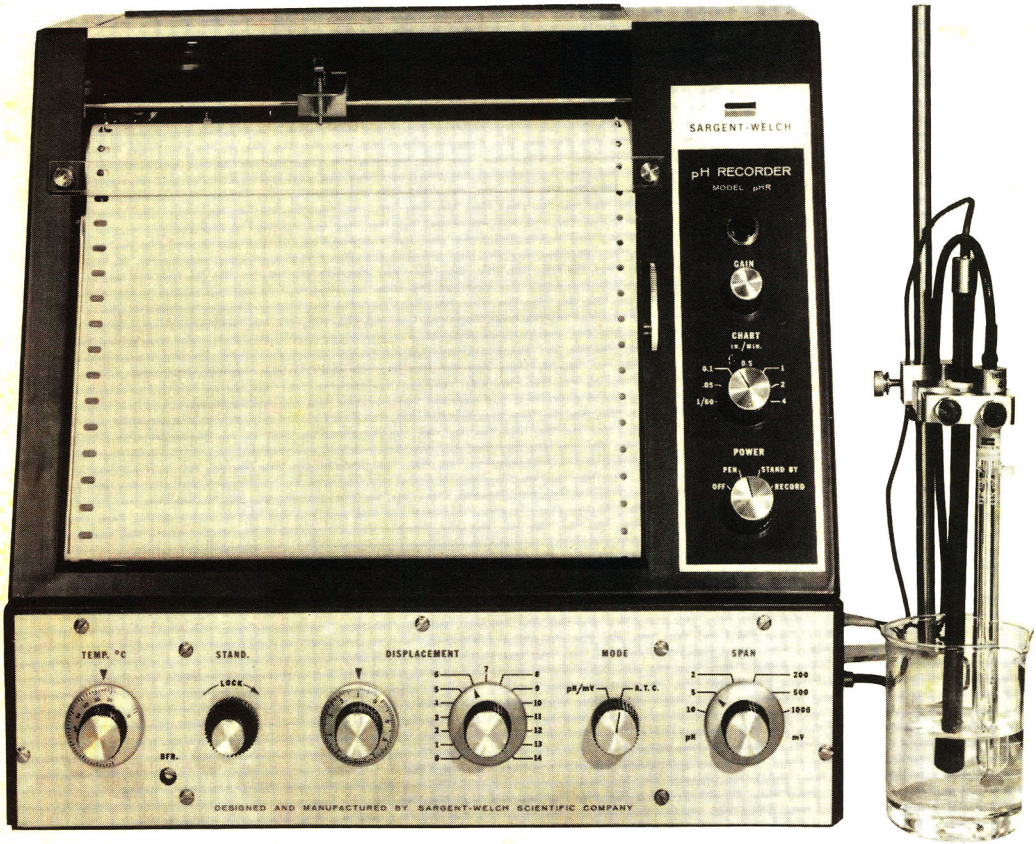


Even a good, "ordinary" pH meter can have an expanded reading range of any 2, 5, or 10 pH span between 0 and 14 pH.

But how many pH meters can also *record* these same spans — at 7 different chart speeds from 1/60 to 4 inches per minute?

This one can. Because it's a pH recorder. Our new Model pHR.

**Circle No. 74 on Readers' Service Card**

And, when optionally equipped, it can also perform as an electrometric titrator, or a pH-stat, or a pH/emf-actuated controller.

The multi-duty pHR does it all with all the accuracy you could ask for. Its basic price: $1250.

There are a lot more performance specifications for the Model pHR that you'll want to get your hands on.

Just call your Sargent-Welch representative or write to us. 9-211

**SARGENT-WELCH**

*Scientific instruments, apparatus, chemicals.*
Sargent-Welch Scientific Company
4647 Foster Ave.; Chicago, Ill. 60630

Chicago/Anaheim/Birmingham/Cincinnati
Cleveland/Dallas/Denver/Detroit
Springfield, N.J./Toronto/Montreal/Vancouver

**See ACS Laboratory Guide for All Products/Sales Office**

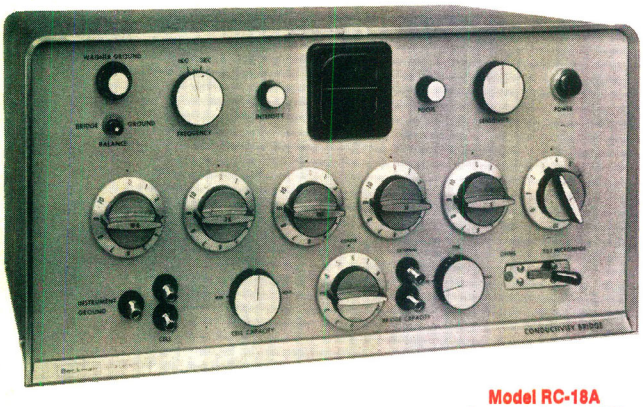

Model RC-18A
Accurate to ±0.05%

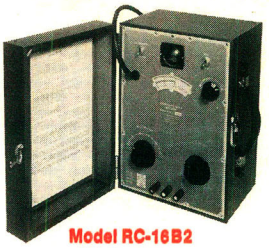

Model RC-16B2
1% Accuracy

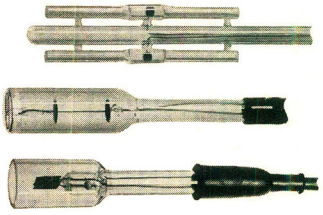

Laboratory Conductivity Cells

# FOR ACCURATE MEASUREMENTS OF SOLUTION CONDUCTIVITY

**RC-18A CONDUCTIVITY BRIDGE** — Provides compactly and economically in one housing, an oscillator that provides both 1,000 and 3,000 Hz bridge current, decade and ratio resistors that comprise the bridge, decade and continuously variable capacitors that facilitate reactive balance, a modified Wagner ground balance, a sharply tuned high-gain amplifier, and a 2" CRT null detector. Accuracy of the bridge is ±0.05% of the reading above 300 ohms while below this value it is limited by the resolution of the last decade dial. Sensitivity exceeds 0.005%. The overall instrument range is 0-111,111 ohms in steps of 0.1 ohms and 0-11,111 micromhos in steps of 0.01 micromho.

**RC-16B2 CONDUCTIVITY BRIDGE** — Line operated, compact, general purpose laboratory instrument with uniform 1% accuracy over the *whole* range of the instrument and sensitivity at least three times better. Extremely wide range: 0.2 to 2,500,000 ohms and 0.4 to 5,000,000 micromhos. True AC Wheatstone Bridge measuring circuit requires no adjustments to readout in absolute ohms. "Eye" tube null indicator for clear indication of electrode polarization. When used with conductivity cells of appropriate cell constants, the entire range of electrolytic conductivity from that of ultra-pure demineralized water to concentrated strong acids is easily covered.

**LABORATORY CONDUCTIVITY CELLS** —Choose from a complete range of pyrex glass dip cells with cell constants within ±1% of nominal value for use with the RC-16B2.

Jones type cells with cell holders and constant temperature bath available for use with the RC-18A.



**ELECTROLYTIC CONDUCTIVITY IS OUR BUSINESS** and we'd like to tell you about our other bridges, cells and accessories designed exclusively for laboratory solution conductivity measurements. A set of three highly informative pamphlets are available just for the asking. Write today to .....

Beckman INSTRUMENTS, INC.

**CEDAR GROVE OPERATIONS**

89 COMMERCE ROAD
CEDAR GROVE, NEW JERSEY • 07009

INTERNATIONAL SUBSIDIARIES: Geneva; Munich; Glenrothes, Scotland; Tokyo; Paris; Capetown; London; Mexico City.

Circle No. 9 on Readers' Service Card

See ACS Laboratory Guide for All Products/Sales Office

# NEW PRODUCTS

Equipment
Apparatus
Instruments

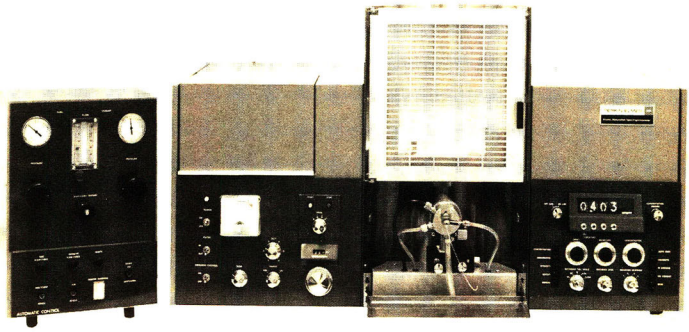

**Model 403 atomic absorption spectrophotometer** uses advances in integrated circuit electronics and materials technology to establish new standards of operating speed, convenience, and simplicity. Lamps, automatically set to the correct current, can be interchanged in five seconds. The burner is corrosion proof and flashback proof, and the flame is lit at the touch of a button. Readout, directly in concentration, appears on four illuminated digits, and zero absorbance is automatically set. Working curves are straightened with a curvature corrector. Throwing two switches converts the system from atomic absorption to flame (or lamp) emission. Model 403 can make use of Model TR-1 typewriter readout. The Perkin-Elmer Corp., Main Ave., Norwalk, Conn. 06852 **401**

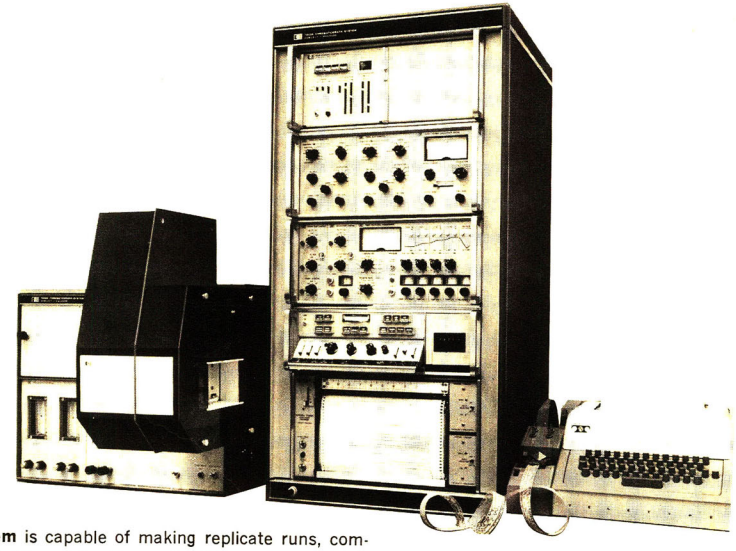

**Model 7600A chromatographic system** is capable of making replicate runs, completely unattended, of as many as 36 different liquid samples. The system consists of four stages. Sample measurement and injection employs standard syringes and chemically inert, vapor-tight sample bottles. The GC analysis stage is completely automatic and features plug-in design, multiple detectors, and directly calibrated temperature controllers. Readout, both analog and digital, produces both the full size chromatogram and area count and retention time for each peak and total area count of all peaks in an individual sample. The data reduction and computation stage produces a computer-compatible punched tape record of the GC analysis. Hewlett-Packard, Avondale Division, Route 41, Avondale, Pa. 19311 **402**

## SPECIAL EVAPORATOR
—All Glass-Teflon System

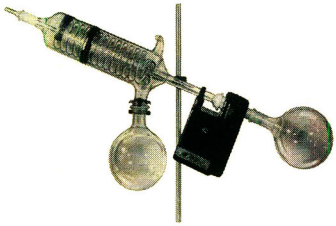

For high vacuum rotary and flash evaporation. All Teflon and glass construction to eliminate O-ring problems and contamination due to metal corrosion, metallic ions and stopcock grease. Extra high quality motor gives smooth rotating movement, avoids splashing and entrainment of solids, minimizes foaming. Maintains 0.9 mm vacuum during continuous addition or batch operation. Choice of condensers available.

*Write for Catalog SMI-25 and name of your nearest dealer.*

smi scientific manufacturing industries

1165 67TH ST., OAKLAND, CALIF. 94608
Phone 654-8616 (Area 415)

## CALIBRATED DISPENSERS

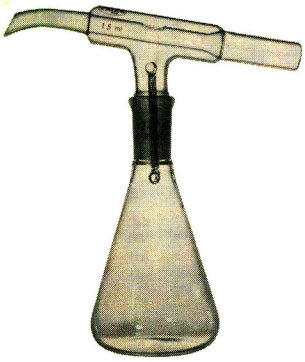

Patented, all-in-one pre-calibrated delivery heads. Dispenser automatically and accurately measures a specific volume of liquid, then rapidly delivers in repeated operations. Size of delivery head used determines volume dispensed. Accurate to ± 1%. Heads calibrated 1 to 100 cc in ½ cc increments. Especially useful for handling volatile, toxic, or otherwise dangerous materials.

*Write for Catalog SMI-30 and name of your nearest dealer.*

smi scientific manufacturing industries

1165 67TH ST., OAKLAND, CALIF. 94608
Phone 654-8616 (Area 415)

Circle No. 78 on Readers' Service Card


## New Products

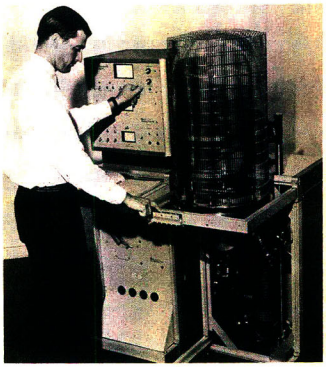

**Innovac** is a completely new diffusion-pumped vacuum system. The system's cantilevered structure permits interchangeability of baseplates and fixturing for production requirements. The high vacuum valve, called Thrust-Seal, consists of two plates which shield the O-ring from abrasion with the valve housing during rotation. The O-ring extrudes to sealing position only after the valve is closed. A unique spherical cold trap called a Cryosphere is used. The upper hemisphere is a high-capacity liquid nitrogen reservoir, while the lower half has two circular orifices which allow a 2200 liters/sec conductance. A verticle Teflon (Du Pont) baffle between the two orifices provides a positive anti-creep barrier. Varian Associates, 611 Hansen Way, Palo Alto, Calif. 94303 **403**

### Water and Waste Analysis Systems

Series 260–1 analysis systems test for any or all of 48 different water and waste elements from acidity to zinc. The user can custom-select any or all of the tests needed for his individual requirements and add more at a later date. Each system consists of a photometer, a complete procedure handbook of officially approved methods, and an optional automatic-zeroing titration outfit. Delta Scientific Corp., Lindenhurst, L. I., N. Y. 11757 **404**

### Permanent Chromatographic Packings

Durapak, for both gas and liquid chromatography, is a permanent, no-bleed, liquid coated substrate which was developed utilizing a unique concept of bonding between the liquid and support materials. Rapid overload recovery, fewer active sites than conventional coatings, and no puddling in the column are among the features of Durapak. Waters Associates, 61 Fountain St., Framingham, Mass. 01701 **405**


NEW

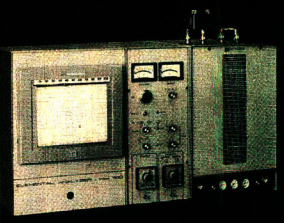

## NUMEC-Carlo Erba Elemental Analyzer
determines C, H, N, or O automatically

**Model 1100 simultaneously analyzes 23 micro samples as a batch in six hours and records the results—without interruption, without an operator, without opening the reactor tubes.**

- Determines C, H and N automatically
- Rapid switching for O analysis
- Conversion to oxygen determination requires no change in technique, sampling or calculation; no change in reactors, no stabilization time
- Accepts solid or liquid samples
- Automatic combustion
- Choice of either static or dynamic mode of operation
- Precision better than ± 0.3%

**Price $9,500**

**NUMEC®**
Instruments Department
NUMEC® is a subsidiary of Atlantic Richfield Co.
155 Washington Ave., Vandergrift, Pa. 15690
Phone: 412 • 567-6736

Circle No. 190 on Readers' Service Card

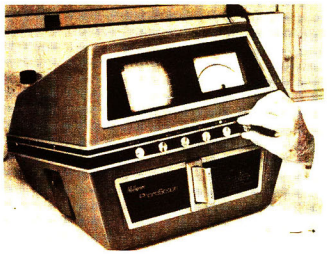

**The PhoroScope Densitometer** reads and analyzes electrophoresis separation patterns. A stained cellulose acetate strip is inserted in a sliding frame and pushed in. Instantly, a light trace pattern appears on the oscilloscope screen. Integrated areas under each peak are read directly on the meter, giving the percentage for each fraction in the separation. The only moving internal part is an oscillating mirror that sweeps the phoretogram with a swath of light. The verticle deflection plates of the cathode ray tube respond to the varying optical density of the fractions, and the horizontal sweep is keyed to the oscillations of the mirror. The meter has an expanded scale for more precise readings of fractions less than 20%. Millipore Corp., Bedford, Mass. 01730 **406**

### EPR Spectrometers

The new E-line EPR spectrometer systems provide insight into chemical compounds and radical intermediates which have unpaired electrons. There are five E-line spectrometer systems available. All feature high sensitivity and a dynamic microwave power range of 1 nanowatt to 200 milliwatts. Each spectrometer consists of an electronic console, a microwave bridge, an electromagnet, and related power supplies. Modular construction provides for the addition of accessories. Varian, 611 Hansen Way, Palo Alto, Calif. 94303 **407**

### Cadmium Ion Activity Electrode

Model 94-48 directly determines cadmium in a variety of aqueous and nonaqueous solutions. It is ideal for continuous monitoring in manufacturing processes, in the production of alloys, and in checking industrial waste waters for cadmium pollution. The electrode, consisting of a solid-state sensing element mounted in an unbreakable, chemical-resistant body, can be used in solutions from pH 1 to 14, and is free from interferences from most common ions. Orion Research Inc., 11 Blackstone St., Cambridge, Mass. 02139 **408**


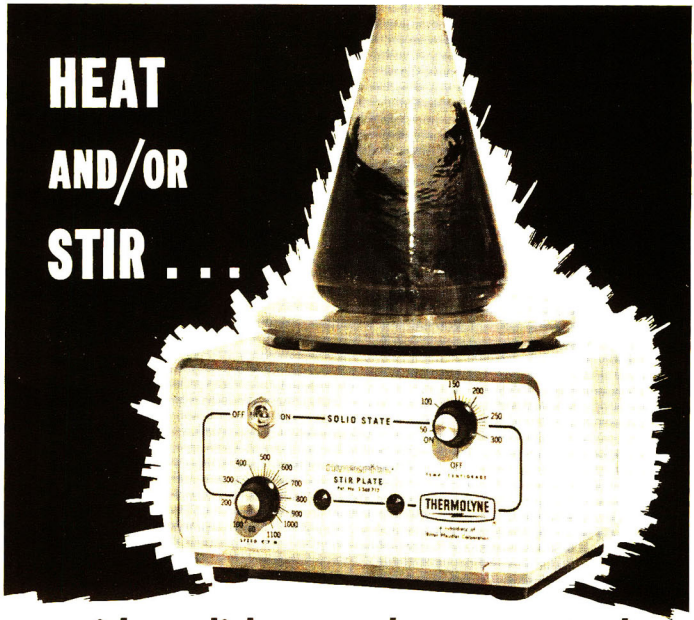


**with solid-state heat control and Nucerite top plate**

**NUCERITE TOP PLATE** — a ceramic-metal (Inconel) combination with noncorrodible advantages of glass and supporting strength of Inconel . . . with ceramic sealed heating element.

**SOLID STATE TEMPERATURE CONTROL** — Control is assured with demand type bi-metallic thermostat and triac. This control will give virtually indefinite contact life. Pilot light shows when temperature level is reached. Temperature accuracy-plus/minus 3°F.

**FAST HEAT-UP** — Maximum temperature of 320°C (600°F) is reached in 3-4 minutes. Nucerite top plate gives broad and even heat distribution. Unit cools rapidly for storing.

**UNIQUE SPEED CONTROL** — Constant speed motor and mechanical control (not rheostat) offer fluctuation-free, constant speed stirring action - 60 to 1100 RPM . . . no stalling at low speeds. Separate on-off switch permits duplication of tests.

**MODERN, LOW SILHOUETTE DESIGN** — A height of 4⅞", width of 7⅝" and depth of 7¼" means solid tip-proof operation. 6½" dia. top plate gives efficient heating. Pastel green vinyl covered steel case and dark green top are resistant to substances that affect ordinary stir-plates.

**NUCERITE STIR-PLATE** — Model SP-11715 complete ___**$125.00**

Model HP-11415B, identical except without stirring features; matched in color and compatible in size _____**$34.50**





Write today for FREE catalog

THERMOLYNE
SYBRON CORPORATION

**2555 Kerper Blvd. Dubuque, Iowa 52001**

Circle No. 80 on Readers' Service Card




it helps to have instruments capable of performing a wide variety of tasks. The versatile **MP-System** gives you the basic building blocks common to most electronic instruments. Interconnect the precision modules with patch cords and they will perform most electro- and photometric instrument functions.*

**NEED ASSISTANCE?**

Our 114 page manual answers most questions. It contains detailed descriptions, practical applications and set-ups. A new lab manual by L. P. Morgenthaler explains operational amplifiers and their use in chemical instrumentation. In addition, the bi-monthly MPI **Applications Notes** keeps you up-to-date on **new** uses.

**ECONOMICAL**

Simplicity, solid state circuitry and good design have been combined to permit the lowest price consistent with high performance.

***coulometry, polarography, pH titrations, spectrophotometry, colorimetry, filter fluorometry, conductimetry, temperature measurement, etc.**

MPI

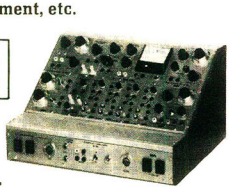

**McKEE-PEDERSEN INSTRUMENTS**

BOX 322, DANVILLE, CA 94526

**Circle No. 54 on Readers' Service Card**


## New Products

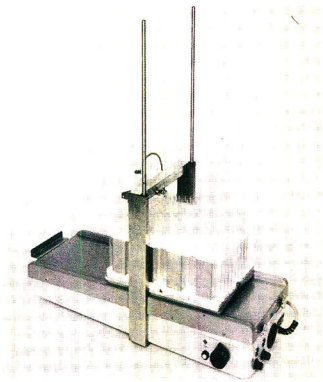

**A fraction collector** with assembly-line design features a rectangular tray with provisions for extension tracks at both ends for adding additional test tubes. The instrument is light enough to be portable, corrosion-resistant, spill-proof, and operates at temperatures as low as —20 °C. It has a distributor that travels in either of several zig-zag or meandering patterns and an optional multiple distributor that collects from as many as ten columns simultaneously. The collector counts drops or measures volume photoelectrically for any pre-set period of time. Brinkmann Instruments Inc., Cantiague Rd., Westbury, N. Y. 11590 **409**



**Model 4329A high resistance meter** has 30 resistance ranges with center-scale indication from $1 \times 10^{6}$ to $1 \times 10^{15}$ ohms in a 1, 2.5, 5 sequence. The full range, from low end of the lowest scale to high end of the highest, is from $5 \times 10^{5}$ to $2 \times 10^{16}$ ohms. Center scale accuracy is ±5%. The meter is used to determine the resistivity of liquids, plastics, ceramics, and other materials, and for applications where leakage currents are of concern. Model 4329A also functions as a picoammeter with eight full scale ranges from $20 \times 10^{-6}$ to $20 \times 10^{-13}$ ampere, and with ±5% accuracy. An optional module, Model 16008A resistivity cell, makes it possible to measure volume and surface resistivity of materials in sheet form. Hewlett-Packard Co., 1501 Page Mill Rd., Palo Alto, Calif. 94304 **410**





Ready now! A new, comprehensive bulletin describing Milton Roy's special line of products for use in gas or liquid chromatography and other critical laboratory applications. Helpful technical data on:

- **Hydrogen Generators**
- **Instrument Pumps**
- **Deuterium Generation**
- **Hydrogen Purifiers**
- **Low-capacity Controlled Volume Pumps**
- **Gas Analyzers**

Find out how these products can bring better performance and greater economy into your laboratory. Send today for your copy of the new bulletin. Write to Milton Roy Company, P.O. Box 12169, St. Petersburg, Florida 33733.

**MILTON ROY COMPANY**

ST. PETERSBURG, FLORIDA

**Circle No. 60 on Readers' Service Card**

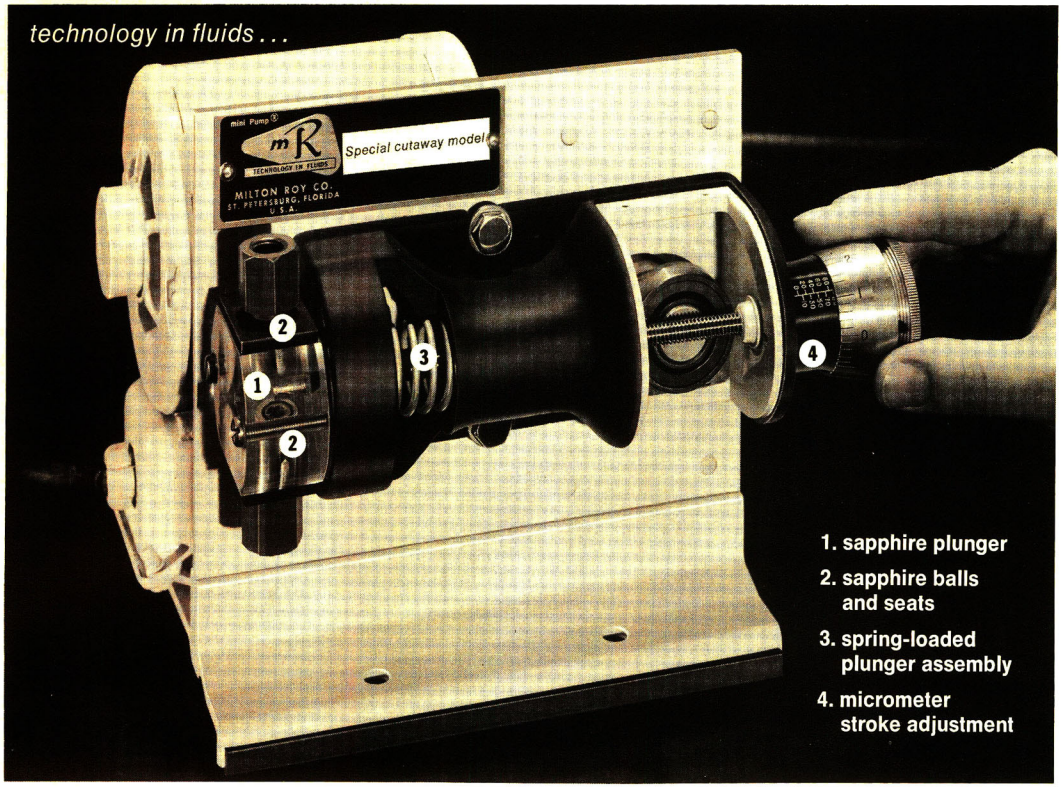


# look into the advantages of the instrument miniPump® for liquid chromatography

Instrument miniPumps serve as critical components in many major-make analyzers for metering small volumes of liquids at pressures to 1000 psig with constant repetitive accuracy of ±0.3%.

Superior miniPump performance results from precise reciprocating action achieved with a unique spring-loaded plunger assembly actuated by a cam. Plunger travel is continuously adjustable with a micrometer stroke control that permits capacity changes as close as 0.2% of stroke.

For optimum pump service, single-crystal sapphires are used for the plunger and for the seats and balls in the double-ball check valves. The superfinished plunger will not distort, score, or corrode, and permits O-ring sealing to prevent contamination of the liquid being pumped. A special stainless steel alloy makes the entire liquid end highly chemical resistant. Use of dry, antifriction bearing surfaces results in oil-less operation.

Capacity ranges are from 16 to 460 milliliters/hour for the simplex models, duplex units available. Prices are only $348 for simplex models, $608 for duplex, F.O.B. Factory.

Check into all the advantages of the Instrument miniPump by writing today for Bulletin 25.002 to Milton Roy Company, P.O. Box 12169, St. Petersburg, Florida 33733. Plants also at Philadelphia, Pa.; Rochester, Minn.; Peterborough, Ontario; Runcorn-Cheshire, England. Sales and service offices worldwide.

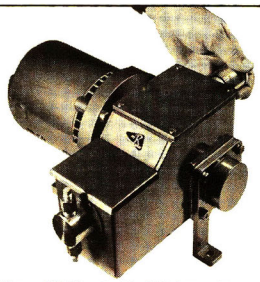

**Milroyal D Controlled Volume Pump** is another proven component for critical analyses applications. Laboratory capacities from 30 to 7150 ml/hour. Discharge pressures to 1000 psig (some models to 3000 psig). ±1.0% repetitive accuracy. Simplex and Multiplex models. Prices from $282, F.O.B. Factory. Ask for Bulletin 36.001.

MILTON ROY COMPANY
ST. PETERSBURG, FLORIDA
mR TECHNOLOGY IN FLUIDS

Circle No. 59 on Readers' Service Card



# The new shape in portable mixers

**now comes to you from Eastern**

The shape of things to come in portable mixers for industry is exemplified today by this new Eastern mixer series.

- **Much more rugged:** Heavy-duty outboard bearing carries radial mixer shaft load . . . single reduction internal gears for greater strength, longer life and quieter operation.
- **Much more flexible:** Standard Nema Frame Motors . . . selection of direct drive or gear reduction . . . choice of agitator assemblies.
- **Much more versatile:** Special coupling assures positive drive and quick shaft removal . . . adjustable type swivel clamp for mixer positioning.
- Send for the new Series 500 Bulletin.

LFE EASTERN INDUSTRIES
A Division of Laboratory For Electronics, Inc.
100 Skiff Street, Hamden, Connecticut 06514

Circle No. 114 on Readers' Service Card

See ACS Laboratory Guide for All Products/Sales Office


## New Products

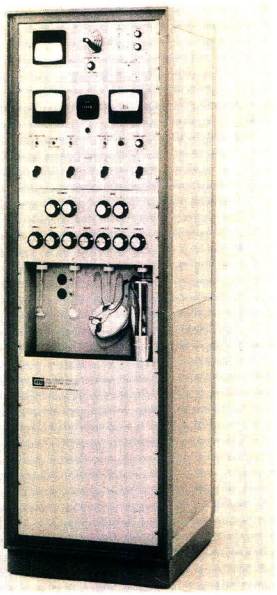

**Model 2100 Orr surface-area pore-volume analyzer** utilizes the classical low-temperature gas-adsorption, B.E.T. technique. Under controlled conditions, a single layer of gas molecules is adsorbed on the surface of the solid being analyzed and the quantity of gas required to form this layer is established. Through calculations, the cross-sectional area of the adsorbed gas is translated into surface area in $m^2$/gram. By analyzing a complete adsorption or desorption isotherm, pore size, volume, and area distribution can be determined. Micromeritics Instrument Corp., 800 Goshen Springs Rd., Norcross, Georgia 30071 **411**

### Interferometer

A two-inch Mach-Zehnder interferometer is used to determine complex density fields without disturbing the flow field by conventional probes. The instrument measures $2\frac{1}{2}' \times 3\frac{1}{2}'$ with a test section length of 18″. The assembly is guaranteed to produce interference fringes at the screen of $\frac{1}{4}$ wave length or better, and exhibits exceptional stability over long periods of time. The interferometer is easily adjusted either by hand or entirely by remote control. It can also be used for Schlieren and Shadow-graph methods by using a simple attachment. Light sources which can be supplied include Hg–arc, super pressure Hg, synchronized flash, and lasers. Intertech Corp., 262 Alexander St., Princeton, N. J. 08540 **412**


# Record weight changes at pressures as low as $10^{-10}$ TORR



- Sensitivities down to **1/10th MICROGRAM**
- Loads up to **100 GRAMS**
- Precision up to **ONE PART/10 MILLION** of sample

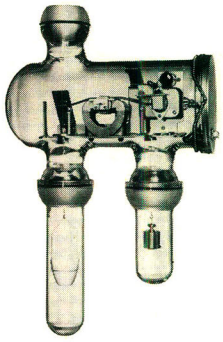

## RECORDING ELECTROBALANCES®

**THOUSANDS NOW IN USE**

- OUTGASSING STUDIES
- SPACE SIMULATION
- THRUST MEASUREMENT
- ADSORPTION ISOTHERMS
- REACTION RATES
- THIN FILM MONITORING

**Phone or Write for details**

CAHN DIVISION
VENTRON INSTRUMENTS CORP.
7500 Jefferson St., Paramount, Calif. 90723
(213) 634-1935
27 Essex Rd., Dartford, Kent, U.K., Ph. 21540

Circle No. 103 on Readers' Service Card

See ACS Laboratory Guide for All Products/Sales Office

# A 60 Second "GUIDE TO PHOENIX SCIENTIFIC INSTRUMENTS"

For many years now PHOENIX has been a pioneering force in the engineering and development of sophisticated instrumentation for the scientific and industrial community.

This "Guide" was developed to show the scope of our company's products and their applications. A Phoenix instrument could be the answer to your research or development problems. A call or letter will bring a PHOENIX Sales Representative to discuss types and applications.

**SAMPLE**

**ANALYSIS**

**LIQUID CHROMATOGRAPHY**
- BIOLYZER
- VARIPUMP
- PKU ANALYZER
- MICRO-ANALYZER
- SAMPLE INJECTORS
- ACCESSORIES

**CONCENTRATION MEASUREMENT**
- COLORIMETERS, UV AND VISIBLE
- RECORDING DIFFERENTIAL REFRACTOMETER
- AEROSOL PHOTOMETERS

**CHARACTERIZATION**

**SPECTROPHOTOMETRY**
- DUAL WAVELENGTH SCANNING, SPLIT BEAM

**LIGHT SCATTERING**
- BRICE-PHOENIX PHOTOMETER
- LOW-ANGLE PHOTOMETER

**OPTICAL CONSTANTS**
- SPHERE PHOTOMETER
- DIFFERENTIAL REFRACTOMETER
- COLORIMETERS

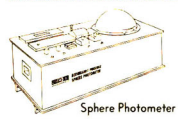
Sphere Photometer


Colorimeter

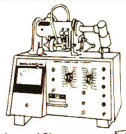
Aerosol Photometer

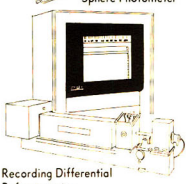
Recording Differential Refractometer

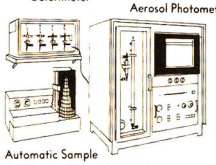
Automatic Sample Injector, Varipump & M-7800

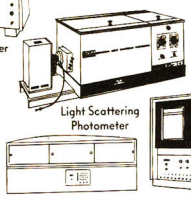
Low Angle-Light Scattering Photometer

Light Scattering Photometer

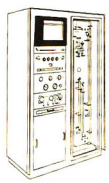
Biolyzer

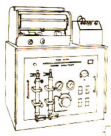
PKU Analyzer

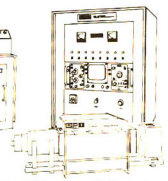
Dual Wavelength Scanning Spectrophotometer

**PPI PHOENIX PRECISION INSTRUMENT COMPANY**

A Division of cenco INSTRUMENTS CORP.

3803-05 North Fifth Street, Phila., Pa. 19140, U.S.A. • Phone: 215-228-7417 • CABLE PPICO


Circle No. 68 on Readers' Service Card


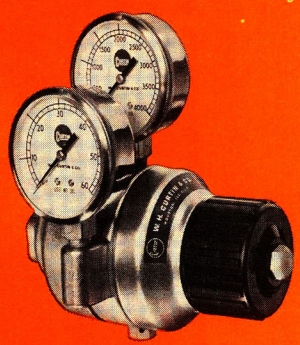

**PRESSURE REGULATORS**
Single and two stage

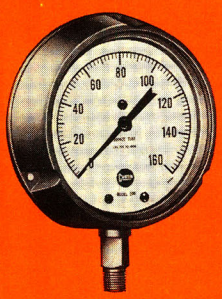

**PRESSURE AND VACUUM GAUGES**

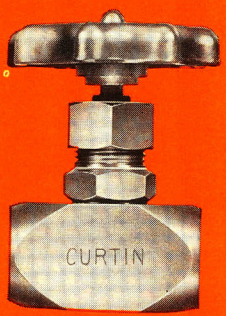


**VALVES**
Brass and Stainless Steel

**SAMPLE CYLINDERS**
10 ml to 5 gal
Carbon and Stainless Steel

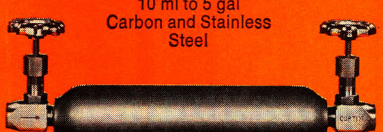

CURTIN

To obtain your copy of Curtin's complete catalog of pressure regulators, pressure and vacuum gauges, sample cylinders and valves, write Curtin Scientific Company, P. O. Box 1546, Houston, Texas 77001.

**CURTIN SCIENTIFIC COMPANY**

SCIENTIFIC APPARATUS • CHEMICALS • LABORATORY FURNITURE

HOUSTON • TULSA • LOS ANGELES • NEW ORLEANS • ATLANTA • SAN FRANCISCO • DALLAS
MIDLAND, MICH. • JACKSONVILLE • WASHINGTON • WAYNE, N. J. • MEXICO CITY • MONTERREY
GEO. T. WALKER & CO. DIVISION • MINNEAPOLIS, MINNESOTA

2598


Circle No. 110 on Readers' Service Card

See ACS Laboratory Guide for All Products/Sales Office

# Cut your budget in half with a Tecam® bath



Never before have such a unique combination of features been offered in a standard range of low cost constant temperature baths.

Just look:

• All stainless steel construction • Temperature sensitivity ±0.1°C • Operating range 0–100°C • Ultra-quiet in operation • Integral thermometer and bath stirrer • Circulation pump available.

*Write or telephone today for full technical details.*

TECHNE

Techne Incorporated
661 Brunswick Pike, Princeton
N.J. 08540/Dial 609.452.9275

Circle No. 79 on Readers' Service Card

CELL RECONDITIONING SERVICE CELL RECONDITIONING SERVICE CELL RECONDITIONING SERVICE CELL RECONDITIONING SERVICE CELL RECONDITIONING SERVICE CELL RECONDITIONING SERVICE CELL RECONDITIONING SERVICE CELL RECONDITIONING SERVICE CELL RECONDITIONING SERVICE CELL RECONDITIONING SERVICE CELL RECONDITIONING SERVICE CELL RECONDITIONING SERVICE

# ATTENTION INFRA-RED SPECTROSCOPISTS

## HERE'S HOW NOT TO DO IT YOURSELF

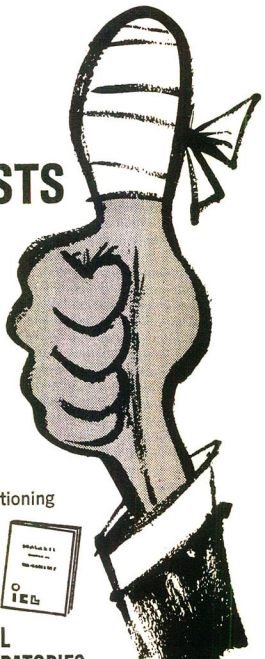

ICL, recognized leaders in the manufacture of infra-red cells and crystals is also widely known for its **CELL RECONDITIONING SERVICE** that's fast, expert and low-cost.
Now, you can free yourself from this frustrating maintenance problem as have many universities and companies in the chemical, oil and rubber industries.
Follow the leaders to ICL for a cell reconditioning service that's sure to save time, temper and treasure.



Write for catalogs and price lists on Crystals, Sealed Liquid Cells, Long Path Cells and Cell Reconditioning Service.

ICL INTERNATIONAL CRYSTAL LABORATORIES
122 Coit Street, Irvington, N. J. 07111
Phone (201) 373-4242

CELL RECONDITIONING SERVICE CELL RECONDITIONING SERVICE CELL RECONDITIONING SERVICE CELL RECONDITIONING SERVICE CELL RECONDITIONING SERVICE CELL RECONDITIONING SERVICE CELL RECONDITIONING SERVICE CELL RECONDITIONING SERVICE CELL RECONDITIONING SERVICE CELL RECONDITIONING SERVICE CELL RECONDITIONING SERVICE CELL RECONDITIONING SERVICE

Circle No. 12 on Readers' Service Card

See ACS Laboratory Guide for All Products/Sales Office


## New Products

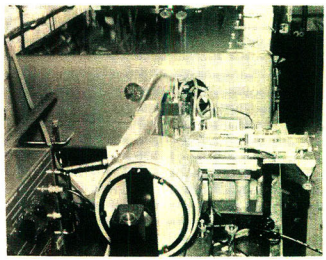

**Model 501SF rapid-scanning spectrometer** is adapted to kinetic studies such as stopped-flow reactions and reactions of light-sensitive materials. By scanning over a broad wavelength range, intermediates in a reaction can be detected, and significant wavelengths for quantitative study can be rapidly selected. The 501SF measures up to 800 spectra per second in the UV, visible, and IR; interchangeable detectors and sources are available for ranges between 2200 Å and 15 $\mu$. Both adsorption and emission spectra can be measured. Through the reversible optical system, absorbing samples can be illuminated with either monochromatic or undispersed light. Front-surface optics make feasible IR studies of nonaqueous solutions. The Warner & Swasey Co., 32-16 Downing St., Flushing, N. Y. 11354 **413**

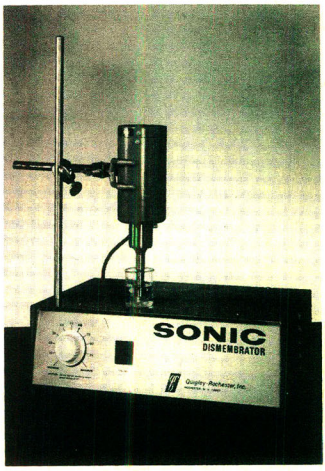


**An advanced ultrasonic probe,** the Sonic Dismembrator, features automatic tuning, variable power output, and titanium tips and accessories. The unit operates at 20 kHz and produces approximately 625 accoustical W/sq. inch at the tip. The unit has been tested with electron microscopy for biological effectiveness on organelles of both plant and animal cells. Quigley-Rochester, Inc., 250 N. Goodman St., Rochester, N. Y. 14607 **414**

# IN SECRET
## find out all you want to KNOW

Without alerting vendors' reps or competition, go straight to CHEMICAL MATERIALS CATALOG for all the product and supplier facts you need. In secret session, CMC speeds your CPI process planning. 3-way index gives you immediate reference to over 100 suppliers' catalogs describing more than 8,000 chemicals and raw materials. Or refer to over 1,300 brand names, trade names and trademarks identified by product use and supplier. It's all right on home ground! Right on your desk! It's all in CMC!

REINHOLD PUBLISHING CORP.
SUBSIDIARY OF
LITTON PUBLICATIONS, INC.
Division of Litton Industries

CHEMICAL MATERIALS CATALOG cmc

430 PARK AVENUE, NEW YORK, N.Y. 10022
**Circle No. 11 on Readers' Service Card**

# ANALYTICAL STANDARDS

**46 Kits Available from a Stock of 322 Standards**

HYDROCARBONS • ALCOHOLS
AMINES • KETONES • PESTICIDES
PHENOLS • ESTERS • MERCAPTANS
SULFIDES • TEFLON PERMEABLE GASES

Excellent for all applications where high purity analytical standards are needed for use with spectrophotometers, gas chromatographs, NMR, thin layer and paper chromatography.

Purified and analyzed to meet the most stringent requirements, these standards* are supplied in "kits" containing 15 to 21 standards of a series together with the technical data necessary for effective use.

*Primary Air Pollution standards (Teflon permeable gases) are supplied individually.

*Call or write for detailed literature*

PSC **PolyScience Corporation**
2101 DEMPSTER ST. EVANSTON, ILL. 60201 312 475-2909

**Circle No. 53 on Readers' Service Card**
See ACS Laboratory Guide for All Products/Sales Office

# Our Multipoint Has More Standard Features Than Others Have Options

Where else can you get manual point advance, five chart speeds, two print rates, infinite resolution conductive plastic potentiometer, plus MV, volts, T/C or RTD inputs as standard features?

And look at these exclusive options: print-on-alarm that will scan and record only off-normal inputs; programmed printing that electrically selects points to be printed and deleted; automatic dual range, which allows mixing inputs of two T/C types or DC volts and T/C on one recorder.

Learn more about this Multipoint. Write or call: Esterline Angus • Division of Esterline Corporation • Box 24000 • Indianapolis, Indiana 46224 • Phone 317/244-7611.

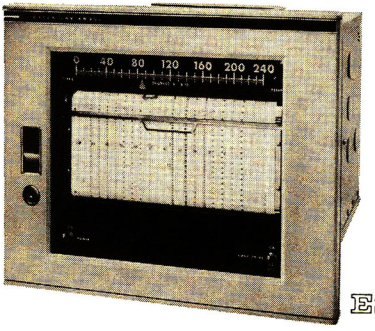


ESTERLINE ANGUS

**Circle No. 5 on Readers' Service Card**

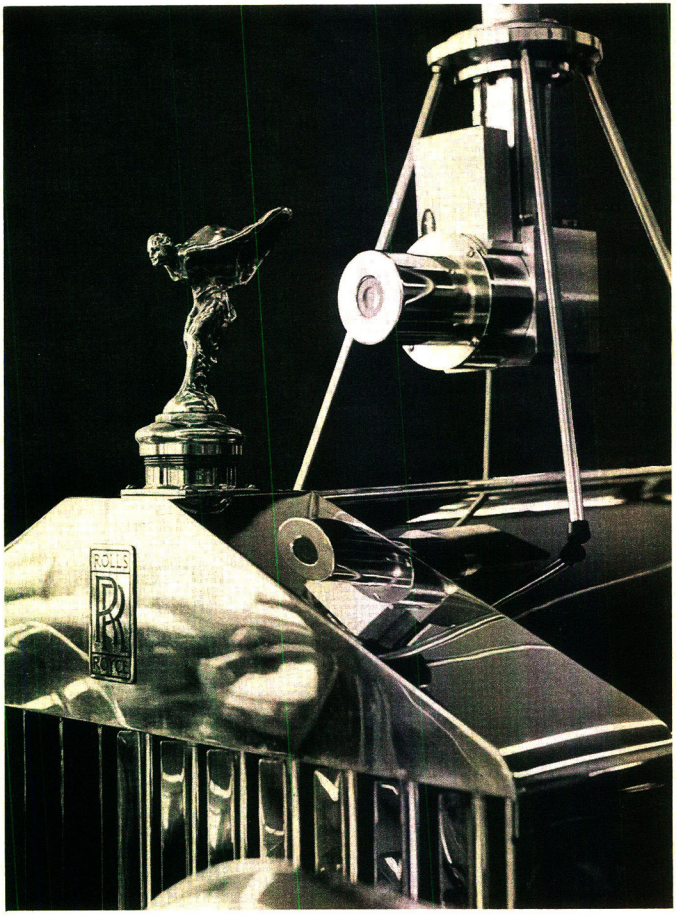


*Analysis of hood ornament with new Kevex-ray unit*

**INSTANT NONDESTRUCTIVE CHEMISTRY WHEN DEPENDABILITY COUNTS**

Nondispersive x-ray analysis is about the only way to analyze up to 81 elements:

- simultaneously
- rapidly and in real time
- with high sensitivity (ppm - 100%)
- high accuracy and precision
- absolute specificity
- nondestructively
- in the laboratory or field
- analog or digital readout
- with a modest investment ! ! !

kevex

898 Mahler Road
Burlingame, California 94010
Telephone: (415) 697-6901

Circle No. 76 on Readers' Service Card

## New Products

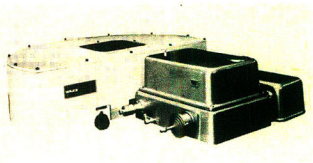

**Model 44 infrared goniometer** is a precision optical-mechanical instrument designed to replace the fore-optics of a single-beam spectrometer. This combination enables precise ATR measurements to be made which lead to accurate values of the sample's extinction coefficient and refractive index. The unit consists of a Nernst glower and focusing mirrors mounted on a rotating platform. The light strikes an ATR crystal which is placed in intimate contact with the sample, and whose axis of rotation is coincident with the axis of the platform so that the image of the source remains focused on the entrance of the monochromator. The mean angle of incidence can be calibrated to better than 0.1°. Wilks Scientific Corp., 140 Water St., Box 441, South Norwalk, Conn. 06856 **415**

### Recycle Accessory for Chromatography

The RAC-100 is capable of providing ultra-high resolution when used with the ALC-100 analytical liquid chromatograph or the GPC-300 gel permeation chromatograph. By continuously recirculating the sample in the mobile phase, the RAC-100 enables a single chromatographic column to function as a multi-column system. This provides maximum resolution with a minimum number of columns. The accessory also facilitates the preparative scale separation and collection of high-purity single species fractions. Waters Associates Inc., 61 Fountain St., Framingham, Mass. 01701 **416**

### Viscosity Measurements

A new Thermosel system permits viscosity measurements of materials up to 500°F with temperature accuracy within 1% of the control temperature. Sample size is between 5 and 15 ml. The basic Thermosel components are a thermo-container, a removable melt chamber and spindle, and an SCR temperature controller. Viscosity measurements are in centipoise. Coaxial cylinder geometry provides defined shear rate conditions on each test sample with sample negligible temperature gradients. Brookfield Engineering Laboratories, Inc., Stoughton, Mass. 02072 **417**

# STIRRED REACTORS

**PARR**
Series
4500

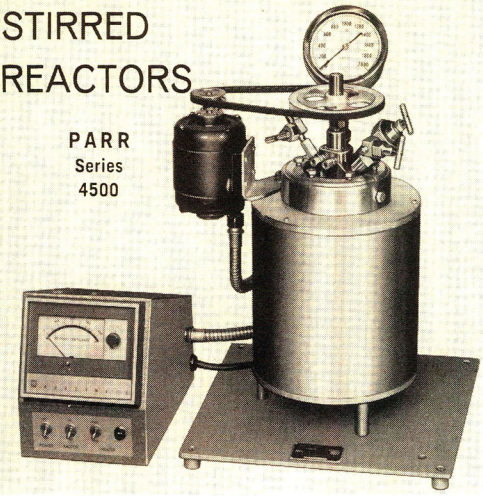

- Convenient bench-scale units provide complete facilities for applying heat and pressure to any chemical reaction.
- One and two liter sizes.
- Pressures to 2000 psig.
- Temperatures to 350° C.
- Automatic temp. control.
- Available in all principal corrosion resistant alloys.

*Ask for Specification 4500*

**PARR INSTRUMENT COMPANY**
**211 Fifty-Third St. Moline, Illinois 61265**

Circle No. 65 on Readers' Service Card

# MASS SPECTROMETRY STANDARDS




**PCR'S MASS SPEC KIT** provides a series of perfluorinated alkyl triazines with molecular weights up to 1185 permitting their use as standards up to m/e 1500 by the peak matching technique. Also included are standard lots of PFK and Heptacosafluorotributylamine.

Eight fluorocarbon standards — 2 grams each
Catalog No. 01 18723 01 — $215.00

For more information call or write PCR, Department 68-4, P.O. Box 1466, Gainesville, Florida 32601.
Phone: 904-376-7522

CALGON CORPORATION
PENINSULAR CHEMRESEARCH
CALGON CORPORATION
SUBSIDIARY OF MERCK & CO., INC.

Circle No. 66 on Readers' Service Card

# no detergent cleans as clean as ALCONOX except LIQUI-NOX

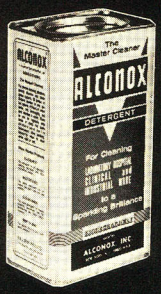


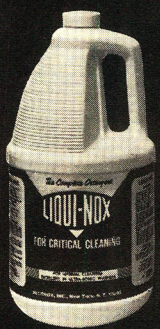


**Liqui-Nox and Alconox . . . advanced cleaning products that prove all detergents are *not* alike. In our own labs they are tested, compared, improved, made to be consistently superior to any other detergent available.**

**TOTAL CLEANING POWER**—for glassware, porcelain, metals, plastics
**SEQUESTERING**—high efficiency in hard or soft water
**WETTING**—reduce surface tension for effective, thorough rinsing
**NON-CORROSIVE**—safe for any material
**SOLUBLE**—dissolve completely in hot or cold water—no residue
**MILD**—baby-gentle to the hands

**ALCONOX**—Powder detergent for manual cleaning or ultrasonic washers . . . *The world's biggest seller!*

**LIQUI-NOX**—Liquid detergent for manual cleaning or ultrasonic washers . . . *Phosphate-free!* Ideal for tissue culture or Bio-Chemical Laboratories.

**ALCONOX and LIQUI-NOX for the *cleanest* clean!**
And we'll prove it. Write today for FREE samples and analysis chart. You'll convince yourself that no detergent cleans as clean as Alconox (except Liqui-Nox). Contact your local Laboratory Supply Dealer.




**ALCO TABS** Detergent tablets for syphon-type washers
**ALCO JET** For machine washing
**ALCONOX** Powder detergent for manual cleaning
**LIQUI-NOX** Liquid detergent for manual cleaning

**ALCONOX INC.**
215 PARK AVENUE SOUTH
NEW YORK, N.Y. 10003

Circle No. 6 on Readers' Service Card

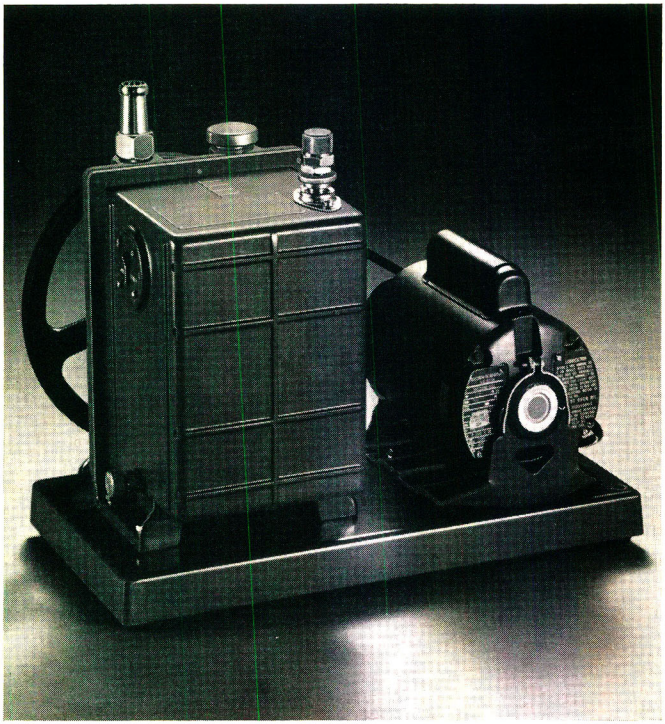

# UNMATCHED PERFORMANCE

**Pump for pump, WELCH DUO-SEAL vacuum pumps . . .** are the quietest, most efficient, vibration-free, long lasting oil-sealed rotary vacuum pumps available. Many thousands of Model 1402B (illustrated) are included in the more than one quarter million Welch **Duo-Seal** pumps now in service in research and industry — some since 1935, never returned for repair and still meeting the original vacuum guarantee.

Welch **Duo-Seal** vacuum pumps will outperform all others because of exclusive features, such as the unique **Duo-Seal**, and superior manufacturing standards which assure the most precise running clearance in the industry — features which provide faster pump down to the low millitorr range.

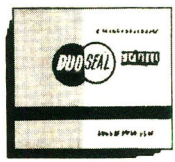


**Call 312/677-0600 or write for new Welch Duo-Seal catalog which fully describes and illustrates the entire Duo-Seal line.**

WELCH
DUO-SEAL®
VACUUM PUMPS

SARGENT-WELCH SCIENTIFIC COMPANY
7300 N. LINDER AVENUE • SKOKIE, ILLINOIS 60076
SKOKIE, ILL.–SPRINGFIELD, N.J.–SAN CARLOS, CALIF.

**DUO-SEAL—*the dependable pump***

Circle No. 172 on Readers' Service Card

See ACS Laboratory Guide for All Products/Sales Office



## New Products



**Model 445 autoranging digital picoammeter** measures currents over nine ranges from $10^{-9}$ ampere full scale to $10^{-2}$ ampere. The three-digit display permits a resolution of $10^{-12}$ ampere. The instrument uses MOS-FET input followed by a differential transistor amplifier stage and a transistor output stage. Negative feedback is used for stability and accuracy. The A to D converter is a dual-slope integrating type composed almost entirely of integrated circuits. Time stability is better than 0.5% of full scale per week, temperature stability is better than 0.05% of full scale per °C. Offset current is less than $10^{-13}$ ampere. Keithley Instruments, Inc., 28775 Aurora Rd., Cleveland, Ohio 44139 **418**

### Differential Electrometer Amplifier

Model 604 was designed primarily for use as a differential electrometer amplifier, with $10^{14}$ ohms input resistance, low 20 mV input noise, excellent stability, and immunity to ac pickup. Model 604 is readily used as a millivoltmeter and, when coupled with the guarded Model 6041 differential current shunt, as a picoammeter. Model 604 uses a completely overload protected, all solid state MOS FET input which provides its high input resistance, low noise, and excellent stability. The solid-state circuit eliminates tube microphonics and provides improved reliability. Keithley Instruments, Inc., 28775 Aurora Rd., Cleveland, Ohio 44139 **419**

### Self-Contained Quantometer

Model 127 is a complete spectrochemical analysis system contained in one cabinet. The system includes a source unit, spectrometer, air conditioner, power supplies, control circuits, vacuum pump, and readout system. It connects directly to 220 V, 60 Hz mains and requires no other accessories for operation. Modular in design, the QVAC contains a one-meter focal length spectrometer and is designed to be operated as a vacuum unit with a self-contained argon sample stand. Various source unit and data readout configurations are available for simultaneous detection of up to 60 elements. Applied Research Laboratories, 9545 Wentworth St., Sunland, Calif. 91040 **420**

# TSI TAPES AND LABELS

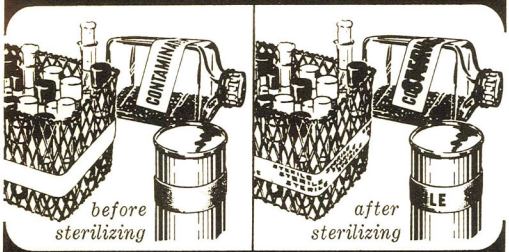


**show "STERILE" after service in an autoclave**

TSI (Time Sterile Indicator) Tapes and Labels are impregnated with a special chemical to change color after autoclaving. Their pressure-sensitive adhesive sticks to any surface, leaves no messy residue. A variety of tapes are available for use with standard and high vacuum autoclaves as well as high temperature ovens. Special TSI Conversion Labels articulate the change from contaminated to sterile. TSI indicators can be imprinted with any wording you desire. Write for complete information.

**TSI**®

All Time Tape products are Bacteriostatic for your Safety

AVAILABLE THROUGH LABORATORY DEALERS.

**PROFESSIONAL TAPE CO., INC.**
363 EAST BURLINGTON ROAD
RIVERSIDE, ILLINOIS 60546

Circle No. 73 on Readers' Service Card

# LO-TEMP BATH HEATS, COOLS $462.



Double the range of the average visibility bath! Waco's Lo-Temp Bath maintains temperature at any level from —10°C to +65°C, ±.01°C . . . ideal where precise temperature control is required. Plenty of testing room, too. Coils fit snugly against the bottom. Use the entire volume of the jar. Self-contained unit is only 20½" wide, 27½" high.

No. 882 Waco Lo-Temp Refrigerated Bath, complete with Pyrex jar 12" diam., for 115V, 50/60 cycle AC. **$462.**

*Write for WACO Bath Bulletin for complete information*

Laboratory Supplies and Equipment.

**wilkens-anderson co.**
4525 W. Division St., Chicago, Ill. 60651

Circle No. 85 on Readers' Service Card
See ACS Laboratory Guide for All Products/Sales Office

# Klett . . .

## Photometers

**Klett-Summerson Photoelectric Glass Cell Colorimeter**

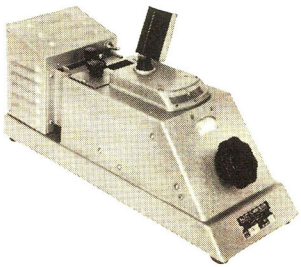

No. 900-3

**The Klett Fluorimeter**

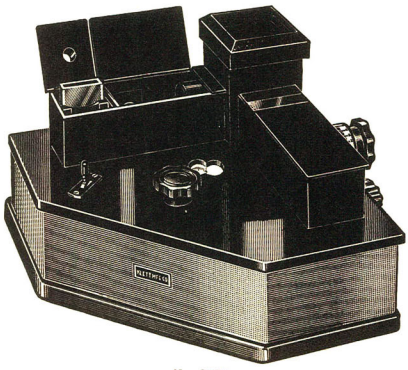

No. 2070

**Designed for the rapid and accurate determination of thiamin, riboflavin, and other substances which fluoresce, in solution. The sensitivity and stability are such that it has been found particularly useful in determining very small amounts of these substances.**

**KLETT SCIENTIFIC PRODUCTS**

PHOTOELECTRIC COLORIMETERS • BIO-COLORIMETERS
COLORIMETER-NEPHELOMETERS • COLONY MARKER
• KLETT REAGENTS • GLASS CELLS

**Klett** Manufacturing Co., Inc.
179 EAST 87TH STREET, NEW YORK, N. Y.

Circle No. 52 on Readers' Service Card
See ACS Laboratory Guide for All Products/Sales Office

# Unlimited Volume Syringe Pump

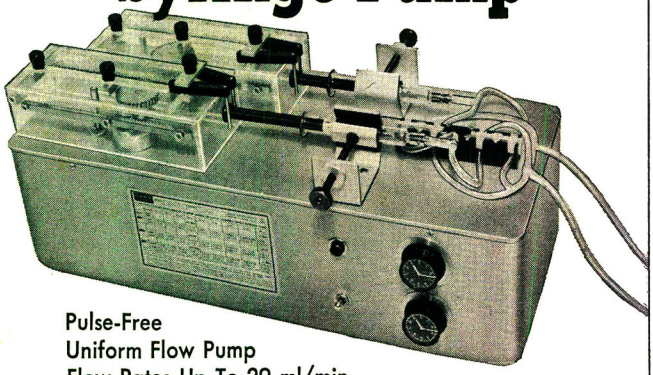

Pulse-Free
Uniform Flow Pump
Flow Rates Up To 29 ml/min

Dial any flow rate from 0.007 to 29 ml/min for pulse-free uniform flow. Pumps continuously at precise flow rate desired. Unique design eliminates transients, even from valving. Add small volumes to streams on a continuous basis, or feed samples to analytical instruments. Use in chemistry, tissue culture, bacteriology, pilot plant studies, process applications. Write for complete data — Sage Model 220 Pump. $985.00

**SAGE INSTRUMENTS, INC.**
Subsidiary of Orion Research Incorporated
230 Ferris Ave., White Plains, N. Y. 10603 ■ 914 949-4121

Circle No. 186 on Readers' Service Card

See ACS Laboratory Guide for All Products/Sales Office



# Convenient, Low Cost Culligan Deionizers

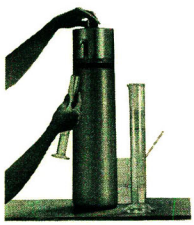

## D-25 LABORATORY DEIONIZER

Designed specifically for uses requiring small quantities of high quality water. The D-25 produces water containing as little as 0.5 ppm of dissolved minerals from source water having up to 700 ppm of dissolved solids. Capacity is 2,500 grains per regeneration, flow rate 48 gallons per hour. D-25 is regenerable, eliminates costly throw away cartridges.

## EXCHANGE SERVICE SYSTEM

Provides a constant supply of deionized water. Exchange Service Deionizer produces water containing as little as .04 ppm of dissolved minerals from source water having up to 850 ppm of dissolved solids. Systems can be engineered to meet a wide range of water quality and capacity requirements. We replace exhausted deionizer systems with regenerated deionizer units to provide uninterrupted flow of deionized water.



For complete information, call your local Culligan Man— or contact Culligan Inc., Northbrook, Illinois 60062, Phone (312) 272-1000.

Culligan®
THE WORLD-WIDE WATER CONDITIONING PEOPLE

Circle No. 35 on Readers' Service Card


## New Products

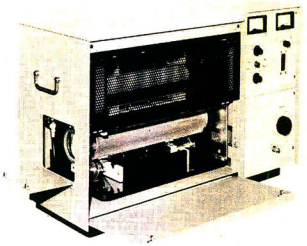

**Model LTA-600JB low temperature plasma unit** has an RF energy input of 500 W. This energy ionizes a gas (oxygen, helium, etc.) which, when excited, breaks down the molecular structure of the sample under test. The inorganic portion of the sample is left intact while the organic portions are drawn off by the vacuum chamber within the unit. The system is effective in the removal of photoresist from a semiconductor wafer during the manufacturing process. The LTA-600JB employs a test chamber that will hold a sample container three inches in diameter and 20 inches in length. Tracerlab, 2030 Wright Ave., Richmond, Calif. **421**

### Electronic Calculator

Model 700 is a third-generation programmable calculator which has a capacity of 12 digits plus a two-digit exponent (range −98 to +99) with a unique dual Nixie-type two-register display. Model 700 is self-contained with a simple keyboard for input and control, from which it learns programs by storing the keystroke sequence in a built-in 8192-bit core. Programs are run from the core, and, for permanent storage, may be transferred to magnetic tape using a built-in cassette recorder and snap-in tape cassettes. A rear-panel connector provides for plug-in addition of a Selectric output writer. Add time is 300 $\mu$sec and trig functions are completed in 250 msec each. Wang Laboratories, Inc., 836 North St., Tewksbury, Mass. 01876 **422**

### Correction

In the description of Model JLC-5AH amino acid analyzer, February issue, page 157A, the statement concerning fractionation should read that fractionation *is possible*. The analyzer is available from Japan Electron Optics Laboratory Co., Ltd., New Tokyo Bldg., 3-2 Marunouchi, Chiyoda-ku, Tokyo, Japan.

# New Model R-20A NMR Spectrometer gives you the best combination of high performance, versatility, simplicity and price. Now!

The Hitachi Perkin-Elmer Model R-20A, a new permanent magnet NMR Spectrometer, represents the state-of-the-art in high performance NMR. It offers full nuclei capability, including $^{13}$carbon, fluorine, phosphorus and boron. And you can get it now. No promises. No waiting.

Its external-locked, thermostatted permanent magnet assures field and resolution stability. This, in combination with the unique RF frequency sweep and all-nucleus field locking, permits wide linear spectral scans, optimized for each nucleus. You don't need complex magnet power supplies or heat-dissipation equipment. You get the analytical results you need. Fast.

A built-in oscilloscope makes preliminary adjustment and initial viewing of spectra convenient. Resolution is set easily using a simple meter deflection technique.

The signal enhancement accessory is the best in the business.

Check these features:

- ☐ signal-to-noise ratio 25:1
- ☐ highest specified resolution
- ☐ reproducibility: 0.2 Hz
- ☐ extended low-temperature range
- ☐ wide field sweeps and offsets with excellent stability
- ☐ solid state electronics.

Additional features include calibrated charts for all nuclei, precise chemical shift determination with frequency counter, and frequency sweep homo/hetero nuclear spin decoupling for simplifying complex spectra. Monthly rental on 5-year lease: $748.65.

For further information, write: Instrument Division, Perkin-Elmer Corporation, 702 Main Avenue, Norwalk, Conn. 06852.

PERKIN-ELMER



Circle No. 174 on Readers' Service Card

See ACS Laboratory Guide for All Products/Sales Office

# Spectroscopists:




# See a good movie, courtesy MC&B Spectroquality.®

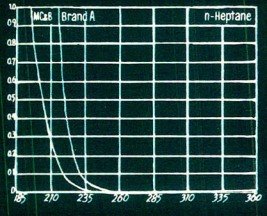


Typical curves show superiority of Spectroquality when compared to other solvents sold for spectrophotometric use.

We spend a lot of time purifying MC&B Spectroquality solvents so you won't have to. You can see the results of our extra effort in the comparison at the left. Spectroquality means maximum transparency, freedom from excessive residues and moisture. Next time, instead of wasting your time on an involved purification procedure or settling for an inferior solvent, select MC&B Spectroquality and see a good movie with the time you save.

MC/B

*Matheson Coleman & Bell*
*Manufacturing Chemists*
*Norwood, Ohio; Los Angeles, Calif.;*
*East Rutherford, N.J.*

## NEW CHEMICALS

### NBS Standard Reference Materials

The NBS Office of Standard Reference Materials has recently made available several new standards and the renewal of a low-carbon steel standard. The new standards are binary alloys of the tungsten–molybdenum and gold–silver systems intended for elemental microanalysis, and also a neutron flux monitor wire standard.

The tungsten–molybdenum microprobe standard, designated SRM 480, is a composite of a core of W-20 wt% Mo alloy wire embedded in a pure Mo rod onto which a layer of pure W has been electroplated.

The gold–silver microanalytical standard, SRM 481, consists of a series of binary alloy wires that range in nominal composition from 100% Au to 100% Ag by steps of 20 wt%.

SRM 953, Neutron Flux Monitor Wire is a cobalt-in-aluminum wire, 0.5 mm in diameter, of ultra-high homogeneity for which an accurate determination of the cobalt content is provided. The homogeneity is within ±0.001 wt % of Co.

The renewal steel standard, SRM 131b, is a low-carbon silicon steel certified for its carbon content only. It nominally contains 20 ppm by weight of carbon, and is supplied in units of approximately 100 grams. Standards are available from the Office of Standard Reference Materials, Rm. B308, Chemistry Bldg., National Bureau of Standards, Washington, D.C. 20234

### High Purity Inorganic Chemicals

Included in a second group of ULTREX™ ultra-pure salts now available are ammonium acetate, ammonium sulfate, calcium carbonate, lithium carbonate, magnesium acetate, potassium chloride, potassium phosphate (monobasic), sodium bromide, sodium carbonate, sodium chloride, and strontium carbonate. They are packed in 100-gram vials, each of which will be accompanied by a detailed certificate of analysis. A typical analysis of ULTREX Potassium Chloride would include data on: loss on drying, nonmetallic elements, and over 20 metallic impurities. Suggested applications include analytical standardization, biochemical studies, inorganic research, single crystal growth, and enzyme purification. J. T. Baker Chemical Co., Dept. J., Phillipsburg, N. J. 08865




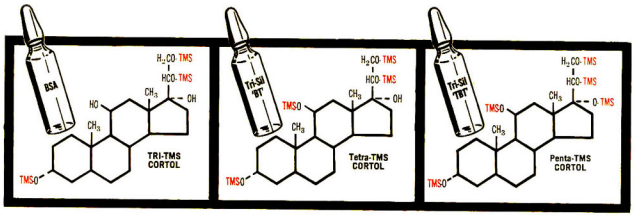


# KIT FOR THE SELECTIVE SILYLATION OF STEROIDS

**According to the method of Chambaz & Horning[1].**

With this new set of reagents you have a reliable and reproducible method for preparing volatile and stable derivatives of steroids and related compounds for gas phase analysis; knowing in advance just which active sites you will derivatize. This method will also be valuable for studies of derivative formation in synthetic work, structural determinations and separations other than gas phase.

Recent Studies [1,2,3,4] have shown that various hydroxyl sites on steroids may be selectively converted to trimethylsilyl derivatives depending upon their relative steric hindrance. The conclusions reached in these studies were supported by GLC data and confirmed by Mass spectrometry. These sites fall into three distinct classes: unhindered, moderately hindered and highly hindered. Three reagents have been developed for the selective silylation of these sites: Tri Sil TBT will silylate all three types of sites; Tri Sil BT will silylate the moderately hindered and unhindered; BSA will silylate the unhindered groups.

An additional reagent, 'MOX', may be used to form methoxime (MO) derivatives with ketones[5], eliminating the possibility of enol-TMS ether formation in Keto-steroids.

Three useful solvents, especially prepared for silylation reactions are included in the kit; acetonitrile, dimethylformamide and pyridine.

**No. 38300 Steroids Silylation Kit.....56.00 each**

(We will quote attractive prices for large volume users of this kit or its components)

Consists of the following, available separately at prices shown:

No. 49016 TRI-SIL 'TBT', pkg of 10x1 ml ampules..20.00

No. 49015 TRI-SIL 'BT', pkg of 10x1 ml ampules...15.00

No. 38836 BSA, pkg of 10x1 ml ampules.....12.50

No. 45950 MOX, 10 ml hypovial.....12.00

No. 20062 Acetonitrile, silylation grade, 50 ml hypovial ..... 2.50

No. 20672 Dimethylformamide, silylation grade, 50 ml hypovial..... 2.50

No. 27530 Pyridine, silylation grade, 50 ml hypovial 2.50

**Ask for our technical bulletin "Steroids Silylation Brochure."**

**References:**

1. E. M. Chambaz & E. C. Horning, Analytical Letters, 1, 201-211 (1968).
2. E. M. Chambaz & E. C. Horning, Analytical Biochemistry, in press.
3. B. Maume, W. E. Wilson and E. C. Horning, Analytical Letters, 1, 401 (1968).
4. E. M. Chambaz, G. Maume, B. Maume & E. C. Horning, Analytical Letters, 1, 749-761 (1968).
5. W. L. Gardiner and E. C. Horning, Biochim. Biophys. Acta, 115, 425 (1966).

PIERCE CHEMICAL COMPANY
P. O. Box 117 Rockford, Illinois 61105
PHONE 815/968-0747 TWX 910-631-3419

**Circle No. 69 on Readers' Service Card**

**See ACS Laboratory Guide for All Products/Sales Office**

# Gas chromatographers:

# Win

## your own copy of The Rubber Handbook

PORAPAK® microporous polymer GC column packings are still so new and revolutionary that even *we* don't know everything they can separate. So we want to learn what *you* have done with Porapak.

Send us a chromatogram of an unusual GC separation you've made with Porapak. If yours is one of the three most interesting received this month, we'll reward you with a copy of *The Rubber Handbook* for your own home or office.*

Since its development just three years ago, Porapak has become one of the most widely used packing materials in gas chromatography. Reasons: No liquid phase needed; stability at high temperatures; no bleeding; sharp, symmetrical peaks with excellent baseline stability; easy column packing. We now offer eight types of Porapak, including two deactivated grades, for the widest range of polar and non-polar compounds with boiling points as high as 300°C.

Now—how about that chromatogram of a separation you couldn't have made without Porapak?

Send your chromatogram to the address shown below, and tell us where to ship your prize.

4253

James L. Waters, President
WATERS ASSOCIATES INC.
61 Fountain Street
Framingham, Mass. 01701

WATERS ASSOCIATES

*P.S.: If your chromatogram isn't among the month's winners, you'll still get a pleasant "thank you" gift.

**Circle No. 171 on Readers' Service Card**

**Circle No. 143 on Readers' Service Card**

# New 2 Kg optical projection balance ...0.1g accuracy, fast, rugged

New Torbal PL-12 top loader (2000g capacity, tare to capacity *plus* 325g, 0.1g accuracy) provides optical projection readout... fast, easy-to-read, foolproof weighing.

*Easy reading* of optical projection with high-quality optics, coated first-surface mirrors, high illumination.

*Easy-to-operate* internal weight handling to achieve weighing by substitution with 100 gram increments to 1 kilogram.

*Long-lasting accuracy*—rugged, thanks to superior friction-free torsion-band weighing mechanism; no knife edges to dull or chip.

*Fast weighing*—with no friction to overcome or to build up over the life of the balance, dash pot can be adjusted to attain rest point immediately without undue oscillation.

As is typical in Torbal optical balances, minor changes in level do not change the zero point. Long-lasting accuracy of the Torsion construction has been proved by continuous weighings (over 1,750,000 operations) 24 hours a day for 6 months. Also available in an explosion proof model.




WRITE FOR FREE BROCHURE.

**THE TORSION BALANCE CO.** Dept. A Main Office and Factory: Clifton, N. J.; Sales Offices: Birmingham, Ala.; Chicago, Ill.; San Mateo, Cal.; Pittsburgh, Pa.; Plants and Offices in Montreal, Quebec; London, England and Waterford, Ireland

TORBAL

Circle No. 199 on Readers' Service Card

See ACS Laboratory Guide for All Products/Sales Office



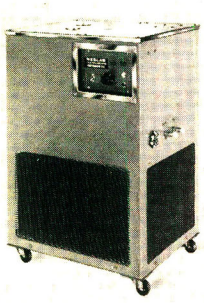

# WHY WASTE 3,839,800* gallons of water yearly?

**HX-50**
**Capacity: 1.4 KVA**
**Flow: 8 gpm (max)**
**Pressure: 20 psi max**
**Temp. Control: ± 0.3°C**

If you use tap water to cool EPR and NMR magnets, electrophoresis units or other heat producing equipment, you can waste almost 4 million gallons of water a year! You can also suffer from temperature and pressure instability, clogged filters, water shut off and other problems.

A Neslab HX series Refrigerated Recirculating Heat Exchanger will operate with less effort and considerable increase in the reproducibility of results. It saves plenty of water, too . . . a mighty important consideration in this era of water shortages.

We offer several models with cooling capacities from 1.4 to 10 KVA and a variety of output pressures and temperature controls. Priced from $900.

*Based on 8 gpm 24 hr. operation

NESLAB Instruments, Inc.

Temperature Controlled Liquid Systems

871 Islington St., Portsmouth, N.H. 03801

Circle No. 115 on Readers' Service Card

See ACS Laboratory Guide for All Products/Sales Office


## MANUFACTURERS' LITERATURE

**Moisture Monitor.** Aquanal, an instrument for measuring parts per million moisture in gases, is described in a recent brochure. Technical Services Dept., Engelhard Minerals & Chemicals Corp., 113 Astor St., Newark, N. J. 07114 **601**

**Thin Layer Chromatography.** The evaluation of thin layer chromatograms by using a chromatogram spectrophotometer is the topic of this reprint. Carl Zeiss, Inc., 444 Fifth Ave., New York, N. Y. 10018 **602**

**Phosphorus Intermediates.** The properties, reactions, and uses of phosphorus trichloride, phosphorus oxychloride, and phosphorus pentasulfide are detailed in an illustrated, 20-page brochure. Stauffer Chemical Co., 299 Park Ave., New York, N. Y. 10017 **603**

**Laser System Accessories.** A complete range of laser-quality optical coatings, components, and mounts are featured in a six-page short-form catalog. Spectra-Physics, 1250 W. Middlefield Rd., Mountain View, Calif. 94040 **604**

**Digital Products.** Generic block diagrams and explanations of general experiments as well as a selection guide of data handling equipment are included in a new multi-section literature package. Ortec Inc., 200 Midland Rd., Oak Ridge, Tenn. 37830 **605**

**Distillation Applications.** Several applications of the Auto Annular distillation system are offered in a four-page data sheet. Nester/Faust Manufacturing Corp., 2401 Ogletown Rd., Newark, Del. 19711 **606**

**Laboratory Equipment.** Included in this 1969 catalog are plastic labware, wide mouth Erlenmeyer flasks, and a chemical resistance guide. Nalge Co., Nalgene Labware Division, P. O. Box 365, Rochester, N. Y. 14602 **607**

**Glass Apparatus.** Cryogenic equipment, distillation–extraction apparatus, custom glass apparatus, and vacuum equipment are among the items included in an eight-page booklet. Pope Scientific, Inc., 13600 W. Reichert Ave., Menomonee Falls, Wis. 53051 **608**

HAAKE

# ROTOVISCO

ROTATING VISCOMETER



For measurement of such properties as:

Viscosity, Structural Viscosity, Dilatancy, Pseudo-Plasticity, Modulus of Elasticity, Relaxation Time, and Yield Value

**SPECIFICATIONS**
**Measuring Range:**
Viscosity 1 to $10^{10}$cP
Shear Stress 5 to $10^{7}$ Dyne/cm²
Shear Rate .01 to $10^{4}$ sec⁻¹
Temperature Range —60° to +400°C

**SPECIAL FEATURES**
30 rotor speeds, three torque ranges selected electrically, provision for external recorder, extremely wide measuring range, provision for making measurements under pressure, or continuous in-line.

*Call or write for detailed literature*

PSC **PolyScience Corporation**
2101 DEMPSTER ST. EVANSTON, ILL. 60201 312 475-2909

Circle No. 92 on Readers' Service Card
See ACS Laboratory Guide for All Products/Sales Office

# NEW POWER AND PRECISION FOR VISCOUS MIXTURES

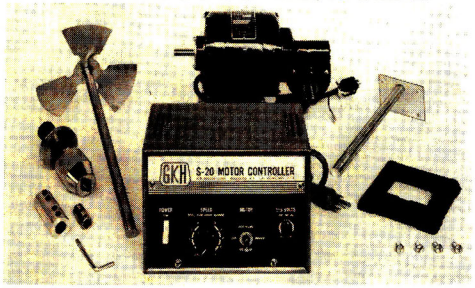


## The HELLER 6T60 Heavy-Duty Stirrer for only $177!

The new Heller 6T60 gives precise speed control with a 1/20 HP motor having seven times the torque of the famous GT21 Lab Stirrer, of which more than 25,000 have been sold. Solid-state motor controller provides adjustable speed with automatic correction for changing viscosity and line voltage fluctuations. Two output shafts are rated 0-1800 RPM at 1.8 inch-lbs. torque and 0-180 RPM at 12 inch-lbs. torque through 10:1 gearhead. High-range control doubles maximum speeds at reduced torque. Controller operates on standard 100-130 volt 50-60 Hz AC. Price includes motor, controller, 6" stainless steel propeller, coupling, 3-jaw chuck, motor mounting bracket and base plate with rod for lab stand clamp, and regular motor base plate for shelf or wall mounting. Heller GT21 1/40 HP mixer includes chuck, propeller, paddle, pulley and mounting accessories for $117. For details, write for Bulletin 639.

*Available through leading lab supply dealers*

GKH G. K. HELLER CORP.
Box 14746 • Las Vegas, Nevada 89114
249-06 Jericho Turnpike • Bellerose, L.I., N.Y. 11426

Circle No. 19 on Readers' Service Card
See ACS Laboratory Guide for All Products/Sales Office

# Thin Layer Chromatography at a Modest Price

## New TLC adsorbents for the researcher on a budget

### SILICA GEL GA & HA

**Separation** of (left to right) cholesterol, palmitic acid, tripalmitin, methyl palmitate, cholesteryl palmitate, mixture (spotted twice) on **Silica Gel HA.** Solvent: hexane/ethyl ether/acetic acid, 90/10/1 by volume.



| | Catalog No. | Price |
|---|---|---|
| Silica Gel GA (10% $CaSO_4$ binder) | 16262 | $ 6.00/lb. |
| | 16263 | 21.00/4 lb. |
| Silica Gel HA (no binder) | 16264 | 6.00/lb. |
| | 16265 | 21.00/4 lb. |

### ALUMINUM OXIDE GA & HA

**Separation** of (left to right) vitamin A (pure), vitamin D (pure), vitamin E (pure), mixture of A, D, and E, vitamin A (commercial), vitamin D (comm.), vitamin E (comm.) on **Aluminum Oxide GA.** Solvent: pure benzene.

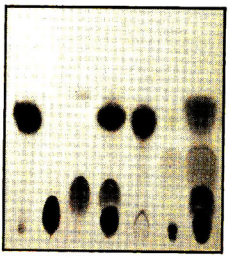

| | Catalog No. | Price |
|---|---|---|
| Aluminum Oxide GA (10% $CaSO_4$ binder) | 16710 | $ 6.00/lb. |
| | 16711 | 21.00/4 lb. |
| Aluminum Oxide HA (no binder) | 16713 | 6.00/lb. |
| | 16714 | 21.00/4 lb. |

Write for our 1969 Catalog #12

APPLIED SCIENCE Laboratories, Inc.
P. O. Box 440 • State College, Pa. 16801

West Coast Branch:
11135 Inglewood Ave. • Inglewood, Calif 90304

Circle No. 94 on Readers' Service Card

**NEW from PHARMACIA**

# SEPHADEX® LH-20

## extends gel filtration to organic solvents

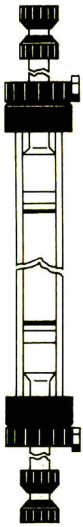

Pharmacia Fine Chemicals now introduces the *first* lipophilic derivative—Sephadex LH-20—to extend the use of Sephadex to organic solvents. Since it swells in water, polar organic solvents and in mixtures of these solvents, Sephadex LH-20 makes it possible to apply the conventional Sephadex gel filtration technique in fields such as lipid chemistry, polymer chemistry and other areas of organic chemistry and biochemistry where organic solvents must be used.

**Sephadex Solvent-Resistant Columns**

The only laboratory columns especially designed for use in chromatographic separations with organic solvent systems. The columns are equipped with two specially designed adjustable flow adaptors for use with various bed heights and for ease of sample application. The columns have the advantage of allowing either descending, upward flow or recycling chromatography as one of their many features.

RANGE OF APPLICATION

| Solvent | Approx. solvent regain ml solvent/g dry gel | Approx. bed volume ml/g dry gel |
|---|---|---|
| Dimethylformamide | 2.2 | 4 |
| Water | 2.1 | 4 |
| Methanol | 1.9 | 3.5-4.0 |
| Ethanol | 1.8 | 3.0-3.5 |
| Chloroform* | 1.8 | 3.0-3.5 |
| n-butanol | 1.6 | 3 |
| Dioxane | 1.4 | 2.5-3.0 |
| Tetrahydrofuran | 1.4 | 2.5-3.0 |
| Acetone | 0.8 | 1.5 |

*Containing 1% ethanol. Particle size: 25-100 μ

EXAMPLE OF SPECIFIC APPLICATION

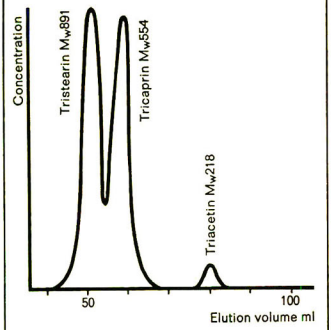


Separation of glycerol esters in chloroform. Bed dimensions: 2.5x32 cm. Sample: 2 ml containing 4 mg of each substance. Flow rate: 0.6 ml/min.

For additional technical information, including the booklets *Sephadex LH-20* and *The Sephadex Solvent-Resistant Columns*, write to:

**PHARMACIA FINE CHEMICALS INC.**
800 Centennial Avenue
Piscataway, New Jersey 08854
Pharmacia (Canada) Ltd., 110 Place Crémazie, Suite 412, Montreal 11, P. Q.

*(Inquiries outside U.S.A. and Canada should be directed to PHARMACIA FINE CHEMICALS, Uppsala, Sweden.)*

Circle No. 116 on Readers' Service Card

See ACS Laboratory Guide for All Products/Sales Office

## Manufacturers' Literature

**Instrumentation Technology.** A 28-page catalog lists instrumentation publications in all areas of science and industry. Instrument Society of America, Publications Dept., 530 William Penn Place, Pittsburgh, Pa. 15219 **609**

**Radioactive Sources.** A 20-page brochure lists 265 reference and radiation sources. Information concerning half-life, principal photon energies, and calibration accuracy is included. New England Nuclear Corp., 575 Albany St., Boston, Mass. 02118 **610**

**Permselective Membranes.** Ultra-thin synthetic permeable membranes and their properties are described in Bulletin GEA-8685, 12 pages. General Electric Co., Distribution Services, Bldg. 6, 1 River Rd., Schenectady, N. Y. 12305 **611**

**Laboratory Automation.** The Spectro-System 100/200 family of laboratory data processing systems is described in a 20-page illustrated booklet. Varian Data Systems, 611 Hansen Way, Palo Alto, Calif. 94303 **612**

**Ge(Li) Detectors.** A 16-page guide for the selection and use of lithium drifted germanium gamma ray detectors in specific applications is available. Nuclear Diodes, Inc., P. O. Box 135, Prairie View, Ill. 60069 **613**

**Power Supplies.** Power supplies, laboratory instruments and systems, test equipment, and OEM applications are included in a comprehensive 56-page catalog. Lambda Electronics Corp., 515 Broad Hollow Rd., Melville, N. Y. 11746 **614**

**Organometallics.** A four-page brochure lists organometallics available in research and development quantities. The major categories are organotins, organoantimony, organophosphorus, organosilicon, tin soaps, and Grignard reagents. M&T Chemicals Inc., Rahway, N. J. 07065 **615**

**Radioactive Sources.** A 14-page catalog describes sources and standards for research and industrial uses including fluorescence spectroscopy, ionization, solid state detector calibration, and gaging applications. Included are sections on $^{63}Ni$ and $^{85}Kr$. Isotope Products Laboratories, 920 N. Citrus Ave., Los Angeles, Calif. 90038 **616**



*Do bad TLC plates get you bearish ?*

**Problem:** You buy one of those robust glass TLC plates that you can "even write on" and **find** the adsorbent's bound to the substrate like chewing gum to the sole of your shoe.

***Solution:*** *Only one major supplier makes TLC plates the way you do (drag slurry) with a functional layer the first prerequisite . . .* ***ANALTECH.***

**Problem:** You buy one of those delicate plastic plates that you can cut-up with a pair of cuticle scissors and **find** the adsorbent layer's mighty skimpy.

***Solution:*** *Only one major supplier can make plastic plates with coating thicknesses exceeding 500 microns and without additional binders . . .* ***ANALTECH.***

**Problem:** You prefer to make your own plates but you need such a wide variety of adsorbents and plate sizes.

***Solution:*** *Only one major supplier makes stock plates sizes from 2.5 x 7.5 cm to 20 x 40 cm with a choice of 70 adsorbents, and all available when you need them . . .* ***ANALTECH.***

**Fact:** Analtech has been making a larger variety of precoated TLC plates for a longer time than any other company in the world. If you have a very, very special TLC plate problem—send us the specifications. If we can't make your TLC plates, chances are no one can. **ANALTECH,** Inc., 100 South Justison Street, Wilmington, Del. 19801 or call (302) 656-4436.

ANALTECH, INC.

Circle No. 26 on Readers' Service Card

See ACS Laboratory Guide for All Products/Sales Office

# What's a good HIGH PRESSURE connection?

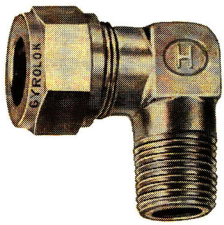


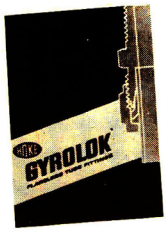


Hoke's Gyrolok tube fitting has a pretty good track record. If you've ever witnessed our burst test demonstration, you've seen a ½" stainless fitting hold heavy wall tubing to a burst pressure of over 34,000 lbs.

Our beautiful new catalog contains two pages of pressure data on tubing plus a staggering variety of fitting shapes, sizes & materials.

*Your Hoke distributor has a copy awaiting your call. We even have a limited supply ourselves.*

**GYROLOK**
FLARELESS TUBE FITTINGS

HOKE MFG. CO • 1 TENAKILL PARK • CRESSKILL, N.J.

Circle No. 7 on Readers' Service Card
See ACS Laboratory Guide for All Products/Sales Office



**LOW, LOW PRICES ON QUALITY**

# ABSORPTION CELLS

*Fully Fused—No Cemented Seams To Dissolve In Acids*

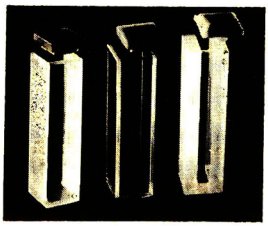

**CUVETTE ADD-A-MIXER** *used for adding small volumes of enzyme solution to reaction mixtures in spectrophotometer cuvettes.* *$2.50 ea.*



*520 types* **Cuvettes** *available in Glass, Special Glass, Quartz, Matched Sets, specials to order.*



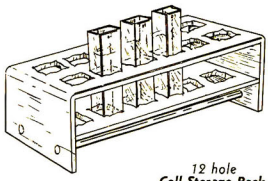

*19 hole* ***Cell Storage Rack*** *$8.50 ea.*

**CUVETTE WASHER-DRYER** *The only fast way to wash and dry cuvettes without scratching or breaking. Completely assembled (without filtering flask) $16.00 ea.*

*To order, write*

**PRECISION CELLS, INC.**
401 BROADWAY
NEW YORK 10013
Tel: 212-226-1373
*Catalog 67/3 E available*

Circle No. 192 on Readers' Service Card
See ACS Laboratory Guide for All Products/Sales Office



# NEW in Column Chromatography

## Aluminum Oxide W 200 Constant initial Activity

A fully standardized Alumina which is an asset for all chromatographic work

We guarantee
for all three types
acid, basic, and neutral

Constant initial Activity
Constant Deactivation Behavior
Constant Reproducibility




From now on: No difference between production lots. It pays to move over to Aluminum Oxide W 200

Never before initial activity, deactivation behavior, and inner surface were so uniform with all three types of alumina.

We kicked the guess-work out of chromatography. No guess: the price is low.

Aluminum Oxide W 200 acid
Aluminum Oxide W 200 basic
Aluminum Oxide W 200 neutral

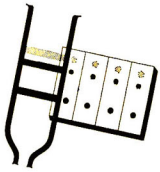

For information and price list write to:

**Alupharm Chemicals**
P. O. Box 30628
New Orleans, La. 70130
Tel. JA 5-3477

Circle No. 86 on Readers' Service Card

*Our Ad is not Perfect . . . . . but our*

CELLS

*are . . . . . and we have all types of*

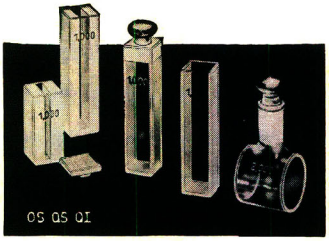

Standard . . . Flow-through . . .
Constant-temperature . . . . . .
Anaerobic . . Special design Cells.

SUPRASIL — INFRASIL — SPECIAL OPTICAL GLASS
(far uv-ir) (uv-ir) (near uv-visible)

Also available

*ULTRAVIOLET LIGHT SOURCES*

Deuterium Lamps
(30–60 watts — air cooled)
(150 watts — water cooled)
Mercury Vapor Lamps
Hollow Cathode Lamps
Power Supplies

Write for literature to

**HELLMA CELLS, INC.**

Box 544, Borough Hall Station, Jamaica, N. Y. 11424
Tel.: (212) 544-9534

Circle No. 123 on Readers' Service Card
See ACS Laboratory Guide for All Products/Sales Office

JOIN THE
PETROLEUM DIVISION
OF THE A.C.S.

Members receive Preprints of the Division's Spring and Fall meetings, the Directory, and are eligible for a discount on ACS meeting abstracts. Dues are $5.00/year ($6.50 foreign).

*Mail This Application to*

Petroleum Division, ACS
Dr. J. Y. Beach, Treasurer
Chevron Research Company
P. O. Box 1627
Richmond, California 94802

Please enroll me as a member of the Petroleum Division. I am now a member of the ACS. I enclose $5.00 ($6.50 foreign)

Name _____

ACS Mail Address _____

_____ Zip _____

Company Affiliation _____

_____

New members will also receive the two most recent available issues of Symposia Preprints in addition to current Preprints.

ANALYTICAL CHEMISTRY
CUMULATIVE INDEXES

These complete author and subject indexes of all articles and major features in ANALYTICAL CHEMISTRY will simplify your use of the journals:

I. ANALYTICAL CHEMISTRY Collective Index, Vols. 1–15, 1929–1943 $ 2.25 **2943**

II. ANALYTICAL CHEMISTRY Collective Index, Vols. 16–30, 1944–1958 $ 9.00 **4458**

Indexes I & II Bound together $11.50 **2958**

III. ANALYTICAL CHEMISTRY Five-Year Collective Index, Vols. 31–35, 1959–1963 $ 7.00 **5963**

To: Dept. B
Special Issues Sales
American Chemical Society
1155 Sixteenth St. N.W.
Washington, D.C. 20036

☐ 2943 ☐ 4458 ☐ 2958 ☐ 5963

From:

_____
Name

_____
Street

_____
City State Zip Code

_____
Company name

☐ Bill me ☐ Bill company ☐ Check enclosed

## CHEMTRIX SSP-3

# digital polarographic system

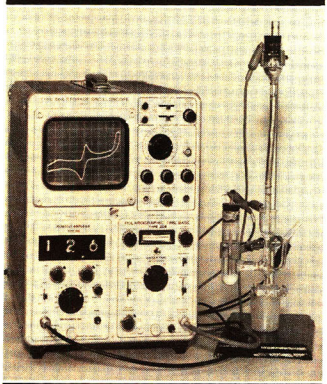

*with image storage and digital readout, for the added dimension in organic and inorganic chemical analysis*

Single-sweep polarography reaches a new dimension with the Chemtrix SSP-3 three electrode Polarographic Anlayzer System.

Precision adjustment of reference and measurement levels with 10-turn potentiometers, and digitally displayed amplitude readout takes the guesswork out of measuring peak current ($I_d$). Analysis of organic or inorganic matter normally takes less than a minute, with image storage display for detailed waveform examination.

Write or call for information on this and other Chemtrix polarographic equipment today, and ask for our booklet *"Applications of Single-Sweep Polarography with the Storage Oscilloscope"*.

Model SSP-3
Polarographic Analyzer System . . . $3190
Type 310
Digital Readout Amplifier,
available separately . . . . . $1195

**Other Chemtrix Instruments**

Model SSP-2
Three-Electrode Polarographic
System . . . . . $2790
Type 800
Waveform Source for
Electrochemistry . . . . . $795
No. A-111
Glassy Carbon Electrode, for
anodic voltammetry . . . . . $19.50

**CHEMTRIX, INC.**
*Instrumentation for Science*
P.O. Box 725 Beaverton, Oregon 97005
(503) 648-1434

Circle No. 29 on Readers' Service Card

See ACS Laboratory Guide for All Products/Sales Office




**Liquid Chromatography.** Technical Reprint LC–R/D–968 describes principles, applications, and instrumentation for analytical liquid chromatography. Waters Associates, 61 Fountain St., Framingham, Mass. 01701 **617**

**Operational Power Supply Technology.** The capabilities of modern dc regulators for the control of voltage or current are discussed in a 12-page monograph. Kepco, Inc., 131-38 Sanford Ave., Flushing, N. Y. 11352 **618**

**Instruments and Apparatus.** Catalog 69, 94 pages, describes and illustrates over 400 scientific instruments and apparatus items. Eberbach Corp., P. O. Box 1024, Ann Arbor, Mich. 48106 **619**

**Light Measurement.** Spectral energy measurements from 200 to 1200 nanometers are discussed in an eight-page technical brochure. Measurement units, modes, and applications are included. International Light Inc., Dexter Industrial Green, Newburyport, Mass. 01950 **620**

**Direct Printout System.** An eight-page brochure discusses the CRS-160 digital readout system that can be used with all mass spectrometers, regardless of type or model. Infotronics Corp., 7800 Westglen, Houston, Tex. 77042 **621**

**Power Supplies.** A complete listing of the company's power supplies and discussions of circuit principles, operating features, performance measurements, and special applications of regulated dc power supplies are included in an 82-page catalog and handbook. Hewlett-Packard Co., Jersey Division, 100 Locust Ave., Berkeley Heights, N. Y. 07922 **622**

**Recorders.** Two direct writing recorders, a low frequency four-channel and a versatile two-channel, featuring Permanent-Magnet Moving-Coil measuring elements and Recti Graph movement are described and illustrated in an eight-page catalog. Esterline Angus, P. O. Box 24000, Indianapolis, Ind. 46224 **623**

**NOVA Computer.** A 16-page brochure discusses small computers and describes the hardware, input, output, facilities, instruction set, and software for the NOVA. Data General Corp., 275 Cox St., Hudson, Mass. 01749 **624**


## ACCURATE MOISTURE ANALYSIS

*fibers • grains • semi-liquids • solids*

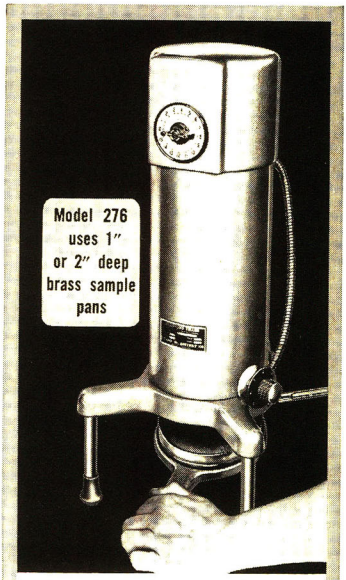


Control costs and maintain consistent quality through accurate moisture analysis.

Dietert-Detroit Moisture Tellers are widely used in industry for research and analysis of foodstuffs, chemicals, fibers, foundry sands, soaps, tobacco, ceramics and similar materials. Complete range of models available.

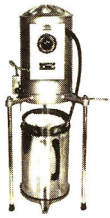

**MODEL 278A-12** is equipped with two 8" dia. x 12" deep sample pans, to accommodate bulky samples such as wool.

**HARRY W. DIETERT CO.**
*CONTROL EQUIPMENT*
9330 Roselawn Avenue • Detroit, Michigan 48204
Telephone: 933-9790 (Area Code 313)

Please send Moisture Teller Catalog and prices.

Name_____
Company_____
Address_____
City_____ State_____

Circle No. 36 on Readers' Service Card

# TRACE INORGANICS IN WATER ADVANCES IN CHEMISTRY SERIES NO. 73

Twenty-one papers from a symposium by the Division of Water, Air, and Waste Chemistry of the American Chemical Society, chaired by Robert A. Baker. Includes:

Five surveys on broad topics—

- Transport properties of electrolytes
- Anions in aqueous solution
- Effects of trace inorganics on the ice/water system
- Aluminum species in water
- The role of hydrous Mn and Fe oxides in fixation of metals in soils and sediments

Eleven papers on analytical developments, such as:

- Atomic absorption (3 papers)
- Atomic fluorescence
- Flame emission
- Neutron activation

And five research reports.

396 pages with index Cloth (1968) **$12.50**

**Set of L.C. Cards free with library orders.**

Other books in the **ADVANCES IN CHEMISTRY SERIES** on inorganic chemistry include:

**No. 72 Mass Spectrometry in Inorganic Chemistry.** A basic tool for chemical manipulations, the mass spectrometer is a conventional monitor for any stage in a research problem to help establish what is going on. 21 Research reports. 329 pages with index
**Cloth (1968) $12.00**

**No. 71 Lanthanide/Actinide Chemistry.** The two series share similarities in chemical properties, magnetism, and radiant energy absorption and emission characteristic of *f*-electron species. But important differences exist—oxidation states, bonding, and complex ion formation. Lanthanides—13 papers; actinides—12 papers. 359 pages with index
**Cloth (1968) $11.00**

**No. 62 Werner Centennial.** Four biographical papers on Alfred Werner, systematizer of coordination chemistry, and 38 papers that report current research and survey progress in his field since he died 50 years ago. 661 pages with index
**Cloth (1967) $17.50**

**No. 54 Advanced Propellant Chemistry.** Primarily directed toward the search for new oxidizers. Twenty-six papers survey theory of advanced oxidizers, oxygen oxidizers, fuels and binders, fluorine systems, and liquid systems. 290 pages with index
**Cloth (1966) $10.50**

**No. 49 Mechanisms of Inorganic Reactions.** Ten lectures by top authorities with extensive discussion prepared and presented by 20 more authorities. Topics include ion association in octahedral complexes, bridging groups in electron transfer reactions, kinetic patterns of ligand reactivity, acid-base reactions in fused salts. 266 pages with index
**Cloth (1965) $10.00**

**No. 42 Boron-Nitrogen Chemistry.** Thirty-two papers on theoretical and preparative aspects of molecules containing B-N bonds, including many heterocyclic ring compounds. 330 pages with index
**Cloth (1964) $10.00**

**No. 39 Nonstoichiometric Compounds.** Twenty-three papers survey the field and give new work on structural aspects of nonstoichiometric oxides, hydrides, chalcogenides, and miscellaneous compounds. 253 pages
**Paper (1963) $9.00**

**No. 37 Reactions of Coordinated Ligands and Homogeneous Catalysis.** Directs attention to changes in ligand groups when they attach to metal ions and to the role of coordination compounds in organic syntheses. 255 pages
**Paper (1963) $9.50**

**No. 36 Free Radicals in Inorganic Chemistry.** Surveys methods for investigating inorganic free radicals and details studies on several species, including the new difluoramine radical. 175 pages with index
**Paper (1962) $7.50**

**No. 32 Borax to Boranes.** Twenty-eight papers from symposia sponsored by the Boron Committee of the ACS Division of Inorganic Chemistry during the peak years of interest in boron chemistry. Covers history and personalities in the field, chemistry of boron and its compounds, including the superfuels. 244 pages
**Paper (1961) $8.00**

**No. 21 Ozone Chemistry and Technology.** Sixty papers from the International Ozone Conference cover: ozone chemistry, high concentration ozone, organic chemistry of ozone, ozone analysis and technology, atmospheric ozone, formation in electrical discharge, toxicity, sterilization and water purification, reaction kinetics. 465 pages
**Cloth (1959) $10.00**

**No. 19 Handling and Uses of Alkali Metals.** Nineteen articles on the chemistry, manufacture, and use of the alkali metals; five are devoted solely or partly to lithium, two to potassium, the remainder to sodium. 177 pages
**Paper (1957) $7.00**

**All books postpaid in U.S. and Canada, plus 20 cents foreign and PUAS**

Order from **SPECIAL ISSUES SALES**
**AMERICAN CHEMICAL SOCIETY**
**1155 SIXTEENTH ST., N.W.**
**WASHINGTON, D.C. 20036**

# HANOVIA makes photochemical lamps for all kinds of lab-scale reactions.

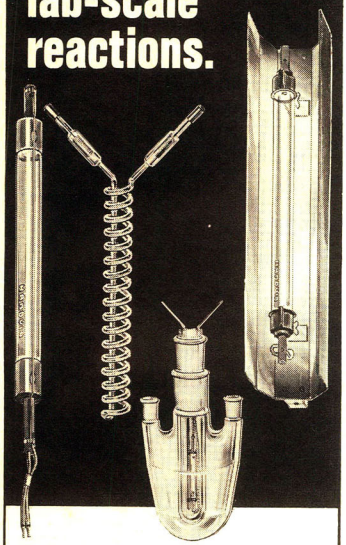

## Now let's talk about your requirements.

If you're interested in exploring improved yields and reaction efficiencies through photochemistry, Hanovia can supply Mercury Vapor lamps, immersion wells and accessories made to your specific requirements.

*We can supply the following from stock:*

| Lamp Model | Arc Length In. | Watts | Radiation Output, Watts |
|---|---|---|---|
| 608A | 2.9 | 100 | 11.5 |
| 654A | 4.5 | 200 | 25.2 |
| 679A | 4.5 | 450 | 175.8 |
| 673A | 4.5 | 550 | 202.7 |

Hanovia lamps are scaled to fit readily into conventional apparatus, and are also available as low-pressure custom made arcs that provide sources of radiation of short wave uv without the heat of the medium and high pressure arcs. For more information on Hanovia laboratory, pilot plant and industrial photochemical systems, contact:

* ENGELHARD HANOVIA, INC. *
HANOVIA
LAMP DIVISION
100 Chestnut St., Newark, New Jersey 07105
842A

Circle No. 113 on Readers' Service Card

See ACS Laboratory Guide for All Products/Sales Office


## Manufacturers' Literature

**Teaching Aids.** Among the items included in a new 16-page catalog are atomic, molecular, and crystal models, charts, math models, and templates. Dyna-Slide Co., P. O. Box 1009, Evanston, Ill. 60204 **625**

**Data Conversion Service.** A new concept for converting graphical data to digital form for computer entry is discussed in a four-page brochure. CompuScan, Inc., 125 Fort Lee Rd., Leonia, N. J. 07605 **626**

**Glassware.** Combined Catalog 69, 1528 pages, consists of a General Section, an Interjoint Section covering interchangeable glassware, and a cross-referenced index. Scientific Glass Apparatus Co., Inc., Bloomfield, N. J. **627**

**Computing System.** The EAI 7800 analog/hybrid computing system is described and illustrated in Bulletin No. 852519, 18 pages. Electronic Associates, Inc., West Long Branch, N. J. **628**

### Company Periodicals

*Requests for copies of the following publications, catalogs, etc., should be sent directly to the address shown. Business or professional letterheads are requested.*

**Osmometry News,** February, 1969. The measurement of deuterium oxide in biological fluids is the feature article this month. Advanced Instruments, Inc., 45 Kenneth St., Newton Highlands, Mass. 02161

**Aminco Laboratory News,** Vol. 24, No. 3. A review of mercury porosimetry as a method of measuring pore-size distributions in porous materials is presented. American Instrument Co., 8030 Georgia Ave., Silver Spring, Md. 20910

**The Spex Speaker,** Vol. 13, No. 4. An article discussing microsampling techniques in laser Raman spectroscopy is offered. Spex Industries, Inc., 3880 Park Ave., Metuchen, N. J. 08840

**Current Peaks,** Vol. 1, No. 1. The key features in the first issue of this new periodical are an outline of the sophomore chemistry courses at UCLA and a discussion of the uses of single purpose gas chromatographs. Carle Instruments, Inc., 1141 E. Ash Ave., Fullerton, Calif. 92631


Measures and Records DC voltage current and resistance

Volts, Ohms, Milliamps

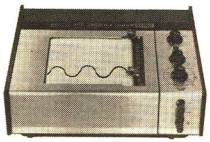

VOM 5—$675

For Spectrophotometer readout and other analytical instrument recording on 5″ chart with 5 variable chart speeds

Volts, Ohms, Milliamps

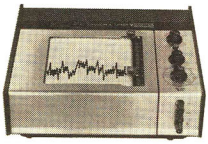

VOM 6—$745

With Built-in Event Marker; Full Scale Zero Set; High Off-Balance Impedance; and ½ second Full Scale Response

Volts, Ohms, Milliamps

write for bulletin

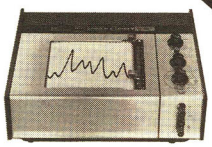

VOM 7—$910
VOM 8—$995
(log-linear)

BAUSCH & LOMB
GRAPHICS DIVISION
4950 TERMINAL AVENUE
BELLAIRE, TEXAS 77401
(713) 667-7403 CABLE HOINCO

Circle No. 130 on Readers' Service Card

# NEW BETHLEHEM GLASS TUBING SCORER!



A radical departure from the conventionally designed glass knife. For scoring borosilicate glass tubing. The handle is of solid clear plastic. A tungsten carbide cutting blade, triangular in design with three cutting edges is inserted and clamped into the handle. The blade is reversible and actually provides six usable cutting edges in all. Blades are replaceable. Cutting edge 1½″—overall length 6″—shipping weight 1 lb. KN3 Knife ..... $24.00

**BETHLEHEM APPARATUS COMPANY, INC.**

Hellertown, Pa. 18055 Phone 215 838-7034

Circle No. 25 on Readers' Service Card See ACS Laboratory Guide for All Products/Sales Office

micromeritics

**HIGH SPEED SURFACE AREA ANALYZER**

**3 to 5 analyses per hour . . . semi-automatic . . . for production and quality control, development!**

**MODEL 2200**

**measures surface areas from 1.0 to 1,500 m²/gm**

provides typical accuracies within 3%, maintains repeatability to less than 0.5% variation / no in-process calculations, direct digital read-out / simple, fast, accurate operation / low initial and operating cost / new, unique concept using modified B. E. T. low temperature nitrogen gas adsorption method / tabletop size 19½″ W by 18½″ D by 23½″ H / price $3750, complete with accessories.

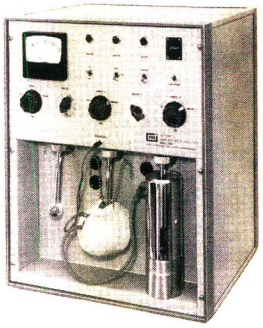

*Write for complete descriptive literature, technical information and details on obtaining sample analysis of your material.*

INSTRUMENTS AND TECHNICAL SERVICE FOR THE MATERIALS INDUSTRY

**micromeritics instrument corporation**

800 goshen springs rd. norcross, georgia 30071

(metro atlanta) phone (404) 448-8282

Circle No. 58 on Readers' Service Card


## Manufacturers' Literature

**Resonance Lines,** Vol. 1, No. 1. This new periodical presents articles concerning atomic absorption instrument principles and applications. Cary Instruments, 2724 S. Peck Rd., Monrovia, Calif. 91016

**The Polarogram,** No. 4, Jan. 1969. A method is presented for determining nitrates in water by using single-sweep polarography. Chemtrix, Inc., P. O. Box 725, Beaverton, Ore. 97005

**Analytical Advances,** Vol. 2, No. 1. Model 9100A electronic calculator and its applications to analytical problems are presented in this issue. A second article discusses flame detector–electrometer relationships in gas chromatography. Hewlett-Packard, Avondale Division, Route 41, Avondale, Pa. 19311

**Electron Optics News,** January, 1969. This new periodical will cover the fields of electron microscopy, electron microprobe X-ray analysis, and low energy electron diffraction. The feature article this month presents a resolution test for electron microscopes. Perkin-Elmer, Ultek Division, P. O. Box 10920, Palo Alto, Calif. 94303

**Instrument News,** Vol. 19, No. 3. Among the topics included in this issue are an analytical data system for thermal analysis and an on-line computer system for high resolution mass spectrometry. The Perkin-Elmer Corp., Main Ave., Norwalk, Conn. 06852

**Matters of Fact,** Vol. 3, No. 1. A discussion of a method for the separation of trypanosomes is included in this issue. Reeve Angel, 9 Bridewell Place, Clifton, N. J. 07014

**Scientific Instrument News, Chromatograph Series,** Vol. 2, No. 1. Pyrolysis gas chromatography is the topic discussed in this issue. Shimadzu Seisakusho Ltd., 18 Nishinokyo-Kuwabaracho, Nakagyo-ku, Kyoto, Japan

**Scientific Instrument News, Thermal Analysis Instrument Series,** Vol. 1, No. 1. Differential thermal analysis at both the micro and the macro levels is discussed. Shimadzu Seisakusho Ltd., 18 Nishinokyo-Kuwabaracho, Nakagyo-ku, Kyoto, Japan

# NEW IN TLC

Alupharm Chemicals presents

## Four New Silica Gels Woelm TLC

excellent separation
constant $R_F$ values
better results

Silica Gel Woelm TLC
Silica Gel F Woelm TLC
Silica Gel G Woelm TLC
Silica Gel GF Woelm TLC

Highly competitive prices
Write for price list and quantity discounts to

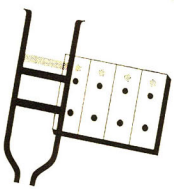

**Alupharm Chemicals**
P. O. Box 30628
NEW ORLEANS, LA. 70130
Tel. JA 5-3477

Circle No. 87 on Readers' Service Card

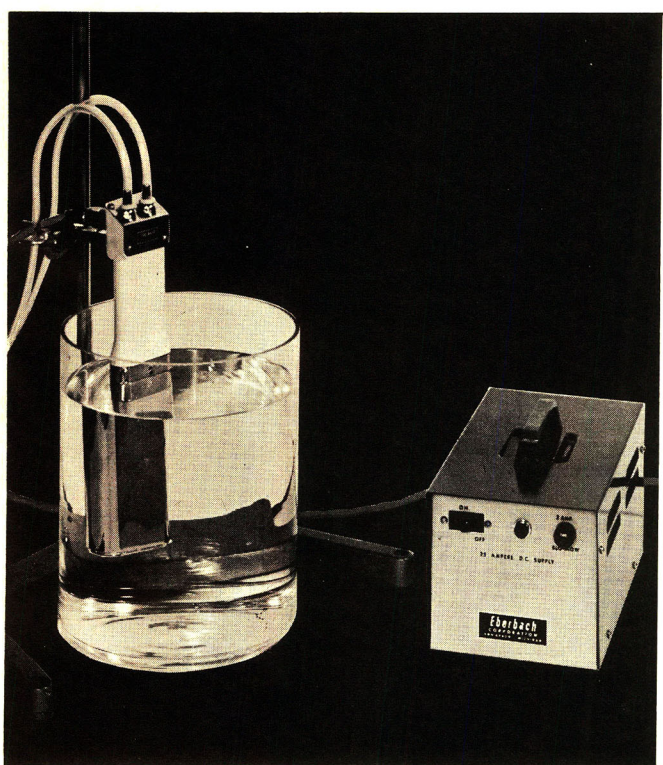

## PORTABLE THERMOELECTRIC IMMERSION COOLER

*cools liquid in laboratory baths*

You can lower temperature, even produce sub-zero temperature, in laboratory baths with the compact, space saving portable Eberbach Immersion Cooler.

It operates on the Peltier effect in semiconductor thermocouples. When direct current of proper polarity is applied to the thermocouples, heat is extracted from the outer metal shell and moves to the central heat sink from which it is removed by a flowing coolant (tap water). Direct current is supplied by the Power Supply Unit shown, which operates from 115 volt, 50/60 cycle input, drawing 165 watts. Thermal pumping rate is 175 BTU per hour when bath and coolant temperature are the same.

Catalog No. 9900
Thermoelectric Immersion Cooler
Assembly with DC Power Supply,
115 volt 50/60 cycle . . . . . $250.00

Eberbach CORPORATION

P.O. BOX 1024 ANN ARBOR, MICHIGAN 48106

Circle No. 13 on Readers' Service Card

# LABORATORY SUPPLY CENTER

ε-Aminocaproic, L-& DL-Aspartic, Glutaric & Iodoacetic Acids
2,3-Butanedione Monoxime • Dimethyl Glyoxime & Sodium Salt
1,2-Diethoxyethane • 2,2′-Diquinolyl • Dithiooxamide • Dulcitol
o-Ethylphenol • α-Ketoglutaric Acid • Methyl Butyrate • Morin
p-Nitrobenzenesulfonyl Chloride • Orcein • Orcinol & Hydrate
Phloroglucinol C.P. • Purine • Salicylaldoxime • Salicin
Sodium Dithionate & Tetrathionate • Sodium Tetraphenylboron
Triphenylphosphine & Oxide • Triphenylstibine • Uracil • Xylose

Write for list K-68 of other chemicals

Tel. 201 696-1700 TWX: 710 988-5831 Zip Code 07440

**EASTERN CHEMICAL CORPORATION** BOX K PEQUANNOCK, N. J.

**Specialists in Distillation**
**PODBIELNIAK**
Custom Glassblowing
Distillation Columns — Vacuum Jacketed
Heli-Pak Packings — Corrosion resistant metals
Evacuated Vessels — Dewars
**Podbielniak, Inc.**
203 Gateway Road, Bensenville, Ill. 60106
Tel.: (312) 766-1816

**The UNIVERSITY of MINNESOTA offers in July and September 1969**

**TWO COURSES IN INFRARED SPECTROSCOPY**

- **Techniques of Infrared Spectroscopy July 22–26**
- **Chemical Interpretation of Infrared Spectra July 28–August 1**

Conducted by Molecular Spectroscopy Laboratory, Department of Chemistry with Professors Bryce Crawford, Stuart Fenton and John Overend directing. Guest Lecturers will be Lionel J. Bellamy, W. J. Potts and Clara D. Smith. Registrants should have basic training in chemistry (especially knowledge of organic nomenclature), but not necessarily experience in spectroscopy.

**A COURSE IN X-RAY DIFFRACTION AND SPECTROSCOPY**

- **September 1–13**

X-RAY DIFFRACTION AND SPECTROSCOPY courses will be offered by the Department of Geology and Geophysics, University of Minnesota, between September 1 and 13, 1969. Instructors will include Professors Tibor Zoltai, Paul Weiblen, George Rapp, and Morris Nicholson. The two courses will start with a common series of lectures during the first week and separate instruction during the second week. The laboratory exercises in the two options will emphasize repectively x-ray diffraction and electron microprobe analysis techniques and practices.

FOR information and registration form, write to the departments above or: Department of Conferences and Institutes, Nolte Center for Continuing Education, University of Minnesota, Minneapolis, Minnesota 55455

**STOP BUMPING**
**in BOILING LIQUIDS**
Prevent superheating and boiling loss.
Speed distillation. Safe. Efficient.
WRITE FOR LITERATURE
**HENGAR GRANULES**
A division of Henry Troemner, Inc.
6815 Greenway Ave., Phila., Pa. 19142
Phone (215) 724-0800

**ANALYTICAL SERVICES**
MASS SPECTROMETRY
Organics — Gas Analysis — $N^{15}$, $O^{18}$, $H^2$, $He^3$ Isotopes
COMBINED GC-MS
THERMAL ANALYSIS-DTA-TGA-DSC
**WEST COAST TECHNICAL SERVICE**
1049 S. San Gabriel Blvd.
San Gabriel, California 91776
(213) 287-0926

**Your specialist in AGATE**  **Mortars with pestles**

| Ø | 2″ | 3″ | 4″ | 5″ | 6″ | 8″ |
|---|---|---|---|---|---|---|
| ccm | 10 | 25 | 50 | 100 | 250 | 500 |
| $ | 3– | 7– | 13– | 24– | 55– | 150– |

Orders over 150—free any U.S. place. For further data about agate parts (balls, ball mills a.s.o.) please contact:

**C. GIESE KG. establ. 1890**
**P. O. B. 2556c**
**658 Idar-Oberstein, Germany**

**CABLE ADDRESS: SACTEX** **PROMPT SHIPMENT**

**Lithium Metaborate $LiBO_2$ Anhydrous***

Faster fusions at lower temperatures. Less damage to platinumware. Lower blanks. Easier dissolution after the fusion. Photometric and titrimetric measurements may be made directly on the dissolved fusions.

*It is imperative that ANHYDROUS $LiBO_2$ be used for fusions to prevent expansion when heated!

**SOUTHWESTERN ANALYTICAL CHEMICALS** BOX 485 — AUSTIN, TEX AREA 512 444-3626
*—literature on request*

**ANALYTICAL AND CONSULTING SERVICES**

- Mass Spectrometric Analysis of Inorganic Solids and H/D, $C^{13}/C^{12}$, $N^{15}/N^{14}$, $O^{18}/O^{16}$, and $S^{34}/S^{32}$
- Radiochemical and Atomic Absorption Analyses at Trace Levels
- Gas Chromatographic Analysis of Trace Radioactive and Stable Gases

**ISOTOPES**
A TELEDYNE COMPANY
50 Van Buren Avenue, Westwood, N. J. 07675
Phone: (201) 664-7070

**MASS SPECTROMETRIC ANALYSIS**
Thin films-solid state materials.
Bulk and trace analysis of all solid materials.
Concentration gradients of diffused impurities.
Resolution 5000.
Sensitivity to parts per billion.
GCA Technology Division, division of GCA Corporation, Bedford, Mass., Tel. (617) 275-9000.
Attn: Director of Marketing

**now even better for Fluoride**
**AMADAC-F** ™
Convenience-packaged mixture of lanthanum chelate of 3-aminomethylalizarin-NN-diacetic acid, buffers and stabilizers, affords accurate, sensitive and convenient quantitative colorimetric method for fluoride.
50 g. (for 100 detns.), with bibliography and complete instructions.....$15

BURDICK & JACKSON LABORATORIES, INC. 616 722-2310
MUSKEGON, MICHIGAN 49442

*LaMotte Chemical*
**Chestertown, Maryland 21620**
*Manufacturers of chemical testing equipment and accessories since 1919*
**Write Dept. AC for free catalog**

**CALL ALPHA FOR METAL ANALYSIS**
Optical emission, x-ray, atomic absorption equipment; metallographic, wet chemical facilities. 48-hour service.
■ Tin/Lead Solder Pot Samples ■ High Purity Metals & Alloys ■ Non-ferrous Alloys ■ Precious Metals ■ Scrap ■ Electroplating Baths & Deposits.
**ANALYTICAL DIVISION Alpha Metals, Inc.**
56 Water Street, Jersey City, N.J. 07304 • 201 • 434-6778

Rates Available on Request

**Analytical Chemistry**

**Anne Forrest, Production Manager**

**430 Park Avenue**
**New York, N. Y. 10022**
**212-MU 8-8600**

# INDEX TO ADVERTISERS IN THIS ISSUE


**Wm. Ainsworth & Sons, Inc.** ..... 42
Buchen Advertising, Inc.
**Air Reduction Co., Inc.** .....35:109
Fuller & Smith & Ross, Inc.
**Alconox, Inc.** ..... 133
Alden Advertising Agency, Inc.
**Amersham/Searle, Div. of G. D. Searle & Co.** ..... 41
Sidney Clayton Associates, Inc.
**°Analtech, Inc.** ..... 142
Allyn H. Jacobson
**H. Reeve Angel & Co., Inc.** ..... 4
Eckstein-Stone, Inc.
**Applied Research Laboratories** ..... 103
Jordan Advertising & Marketing Services, Inc.
**Applied Science Laboratories, Inc.** ..... 141
Science Advertising Associates
**°Aztec Instruments, Inc.** ..... IFC
A.B.W. Toft & Co.

**°Bausch & Lomb, Inc.** ..... 91
Wolff Associates, Inc.
**°Beckman Instruments, Inc., Cedar Grove Operations** ..... 122
Lescarboura Advertising, Inc.
**°Beckman Instruments, Inc., Scientific Instrument Div.** .....49–50:85:110
Hixson & Jorgensen, Inc.
**Beckman Instruments, Inc., Spinco Div.** 1
Hixson & Jorgensen, Inc.
**°Bel-Art Products** ..... 94
Gallard Advertising Agency, Inc.
**°Bendix Corp.** .....17:24
MacManus, John & Adams, Inc.
**°Bethlehem Apparatus Co., Inc.** ..... 148
Beaumont, Heller & Sperling, Inc.
**°Bio-Rad Laboratories** ..... 71
Bonfield Associates, Inc.
**Brinkmann Instruments, Inc.** .....79:86
The Shaller-Rubin Co., Inc.
**°Buchler Instruments, Inc.** ..... 116
Selvin & Jaffe
**Burrell Corp.** ..... 56

**°Cahn Instrument Co.** ..... 128
Haas, Zimmerman, Ostrowe
**°Carle Instruments, Inc.** ..... 66
Cochrane Chase & Co.
**°Fred S. Carver, Inc.** ..... 90
J. C. Bull, Inc.
**°Cary Instruments, A Varian Subsidiary** 101
Chiat/Day Advertising, Inc.
**Chemical Materials Catalog** ..... 131
Persons Advertising, Inc.
**°Chemtrix, Inc.** ..... 145
Hugh Dwight Advertising, Inc.
**Coleman Instruments Corp.** .....63:78:120
Mandabach and Simms, Inc.
**°Corco Chemical Co.** ..... 48
Charles D. Karlsruher
**°Cosmos Scientific Co.** ..... 44
Valerie Taylor Associates
**Culligan, Inc.** ..... 136
Alex T. Franz, Inc.
**°W. H. Curtin & Co.** ..... 129
Robinson-Gerrard, Inc.

**Harry W. Dietert Co.** ..... 145
Watkins-Rogers, Inc.
**°Digital Equipment Corp.** ..... 106
Kalb & Schneider, Inc.
**°Du Pont Co.** ..... 53
Rumrill-Hoyt, Inc.

**EG&G, Inc.** ..... 75
Culver Advertising, Inc.
**°Eastern Industries** ..... 128
Hepler & Gibney, Inc.
**°Eastman Kodak Co., Eastman Organic Chemicals** .....64–65
Rumrill-Hoyt, Inc.
**Eberbach Corp.** ..... 149
Drury, Lacy, Inc.
**°Engelhard Hanovia, Inc., Hanovia Lamp Div.** ..... 147
Keyes, Martin & Co.
**Carlo Erba, S.p.A.** ..... 6
Publicitas
**Esterline Angus, Div. of Esterline Corp.** 131
Caldwell-Van Riper, Inc.

**°Fabri-Tek Instruments, Inc.** ..... 25
Ralph Timmons, Inc.
**°Farrand Optical Co., Inc.** .....37:43
Taube/Violante, Inc.
**°Fisher Scientific Co.** .....20:58
Fuller & Smith & Ross, Inc.
**Floridin Co.** ..... 84
Marsteller, Inc.
**Fluoroware** ..... 6
Colle & McVoy Advertising Agency, Inc.

**°Gilford Instrument Laboratory, Inc.** ... 5
Garber-Evans Advertising, Inc.
**Glas-Col Apparatus Co.** ..... 80
Fensholt Advertising, Inc.
**°Gow-Mac Instrument Co.** ..... 97
Leonard M. Sive & Associates
**Greiner Scientific Corp.** ..... 60
Fairfax, Inc.
**Gulf General Atomic, Inc.** ..... 99
Barnes-Champ Advertising

**°Hamamatsu TV Co., Ltd.** ..... 152
Sanreisha, Ltd.
**°Hamilton Co.** ..... 39
Swain/Mealer, Inc.
**°Harvard Apparatus Co., Inc.** ..... 108
Frederick E. Allen Advertising
**°Heath Co.** ..... 114
Advance Advertising Service, Inc.
**°G. K. Heller Corp.** ..... 141
Feeley & Wheeler, Inc.
**°Hellma Cells, Inc.** ..... 144
**°Hewlett-Packard Co., Avondale Div.** ..18-19
Richardson, Thomas & Bushman, Inc.
**°Hewlett-Packard Co., Palo Alto** ..... 57
Lennen & Newell, Inc.
**Heyden & Sons, Ltd.** ..... 34
**°Hoke, Inc.** .....8:143
Tek-Mark, Inc.
**°Houston Instruments Div. of Bausch & Lomb, Inc.** ..... 147
Ray Cooley & Associates, Inc.

**Illinois Water Treatment Co.** ..... 52
Cummings, Brand, McPherson Associates, Inc.
**Infotronics Corp.** ..... 55
Robinson-Gerrard, Inc.
**°Instrumentation Laboratory, Inc.** ..... 36
Pazolt & Co.
**°Instrumentation Specialties Co., Inc.** ... 72
Graham Printing & Advertising Service
**Instruments for Industry, Inc.** ..... 119
Beecher Associates, Inc.
**°International Crystal Laboratories** .... 130
Raymond-Nicholas Advertising

**Japan Electron Optics Laboratory Co.** ... 61
Asian Advertisers, Inc.
**°Johns-Manville** ..... 59
Cunningham & Walsh, Inc.

**°Keithley Instruments, Inc.** ..... 54
The Bayless-Kerr Co.
**Kevex Corp.** ..... 132
Martel Scroggin Advertising
**Klett Mfg. Co., Inc.** ..... 135
**°Kontes Glass Co.** ..... 21
Garceau, Hallahan & McCullough, Inc.

**E. Leitz, Inc.** ..... 9
L. W. Frohlich & Co.
**°The London Co.** ..... 77
Ritchie & Sattler, Inc.

**Manostat Corp.** ..... 60
Fairfax, Inc.
**McKee-Pedersen Instruments** ..... 126
Dave Comstock Advertising
**McPherson Instrument Corp.** ..... 112
Culver Advertising, Inc.
**°Merck & Co., Inc.** ..... 89
Rumrill-Hoyt Co., Inc.
**E. Merck, AG** ..... 31
Deutsche Anzeigen GMBH
**°Mettler Instrument Corp.** ..10:40:88:102:119
Mort Barish Associates, Inc.

**Micromeritics Instrument Corp.** ..... 148
George and Glover
**Milton Roy Co.** .....126:127
Beaumont, Heller & Sperling, Inc.

**°Nalge Co., A Div. of Ritter Pfaudler Corp.** ..... 76
Wolff Associates, Inc.
**°Neslab Instruments, Inc.** ..... 140
Goodhue/Gunther Advertising, Inc.
**°Nester/Faust Mfg. Corp.** .....92:93
Allyn H. Jacobson
**New England Nuclear Corp.** ..... 6
Kalb & Schneider, Inc.
**Norton Plastics & Synthetics Div.** ..... 47
Northlich, Stolley of Akron, Inc.
**Nuclear-Chicago Corp. (Texas-Nuclear Division)** ..... 98
Winn-McLane Associates, Inc.
**Numec Instruments Dept., Sub. of Atlantic Richfield Co.** .....70:124
Delta Advertising

**°Orion Research, Inc.** ..... 120
Visual Research & Development

**°Packard Instrument Co., Inc., A Subsidiary of Ambac Industries, Inc.** 12
Ross Llewellyn, Inc.
**Parr Instrument Co.** ..... 133
F. Willard Hills
**Peninsular ChemResearch, Inc.** ..... 133
Advertising Associates of Jacksonville, Inc.
**°Perkin-Elmer Corp.** ...38:52:82:100:117:137
Gaynor & Ducas, Inc.
**°Pharmacia Fine Chemicals, Inc.** ..... 142
Cummins, MacFail & Nutry, Inc.
**°Phoenix Precision Instrument Co.** ..... 129
Product Promotions Agency, Inc.
**°Photovolt Corp.** ..... 96
Mohr & Co., Inc.
**°Pierce Chemical Co.** ..... 139
Advertising Design
**°Polyscience Corp.** .....131:141:152
**°Precision Cells, Inc.** ..... 143
**°Precision Sampling Corp.** ..... 32
William U. Stracener
**Precision Scientific Co.** ..... 83
Tri-State Advertising Co., Inc.
**Preprints, Publications of ACS Div. of Petroleum Chemistry** ..... 144
**Princeton Applied Research Corp.** ....104–105
Mort Barish Associates, Inc.
**Professional Tape Co., Inc.** ..... 135
Robert Peterson Advertising Agency

**Regis Chemical Co.** ..... 154
Foley Advertising, Inc.
**Will Ross, Inc. (Matheson Gas Prod.)** 51
Cooper, Strock & Scannell, Inc.
**Will Ross, Inc. (Matheson, Coleman & Bell)** ..... 138
Cooper, Strock & Scannell, Inc.

**°Sage Instruments, Inc.** ..... 136
Mohr & Co., Inc.
**°Sargent-Welch Scientific Co.** .....16:121
Sidney Clayton & Associates, Inc.
**Sargent-Welch Scientific Co.** ..... 134
Armstrong-Desmond Advertising, Inc.
**°Schleicher & Schuell Co.** ..... 33
Wildrick & Miller, Inc.
**°Scientific Glass Apparatus Co., Inc.** .. 22
**Scientific Manufacturing Industries** .... 124
Smith & Reynolds

**Techne, Inc.** ..... 130
**Technical Operations, Inc.** ..... 95
Creamer, Trowbridge, Case & Basford, Inc.
**°Technicon Corp.** ..... 7
Mediad, Inc.
**Texas Nuclear Div., Nuclear Chicago Corp.** ..... 98
Winn-McLane Advertising
**°Thermolyne Corp.** ..... 125
E. R. Hollingsworth & Associates


*°See ad in ACS Laboratory Guide*

## INDEX TO ADVERTISERS IN THIS ISSUE


°Arthur H. Thomas Co. ..... 117
°The Torsion Balance Co. ..... 140
Michel-Cather, Inc.
°Tracor, Inc. ..... OBC
Winn-McLane Associates, Inc.

°Ultra Carbon Corp. ..... 111
The Jaqua Co.

°Varian Associates
Cary Instruments Div. ..... 101
Chiat/Day Adv., Inc.
AID Div. ..... 115
Aerograph Div. ..... 23
Botsford, Constantine & McCarty, Inc.

°Wang Laboratories, Inc. ..... 62
Impact Advertising, Inc.
°Waters Associates, Inc. ..... 14:139
Thomas R. Sundheim, Inc.
Whitey Research Tool Co. ..... IBC
Falls Advertising Co.
John Wiley & Sons, Inc. ..... 67:68:69
Ed McLean Co., Inc.
°Wilkens-Anderson Co. ..... 135
Mandabach and Simms, Inc.
°Wilks Scientific Corp. ..... 73
A.B.W. Toft & Co.
M. Woelm ..... 143:149
Linder Presse Union GMBH

°Carl Zeiss, Inc. ..... 81
Michel-Cather, Inc.

LABORATORY SUPPLY CENTER .... 150
Alpha Metals, Inc.
Burdick & Jackson Laboratories, Inc.
Eastern Chemical Corp.
GCA Corp., Technology Div.
C. Giese KG.
Isotopes, Inc., A Teledyne Co.
LaMotte Chemical Products Co.
Podbielniak, Inc.
Southwestern Analytical Chemicals
Troemner, Inc.
University of Minnesota
West Coast Technical Service



*Advertising Management for the American Chemical Society Publications*
REINHOLD PUBLISHING CORP., a Subsidiary of Litton Publications, Inc., Division of Litton Industries, Inc. Thomas N. J. Koerwer, Advertising Sales Director, ACS Publications; Alfred E. Gall, Advertising Production Director, 430 Park Ave., New York, N.Y. 10022 (Area Code 212) 688-8600. Cable Address: REINPUB NYK

Note: Effective May 1, Reinhold Publishing Corp. will be located at 600 Summer St., Stamford, Conn. 06904. Telephone: 203-348-7531.

SALES DEPARTMENT

J. Barry Stanford
*Advertising Sales Manager, AC*

SALES REPRESENTATIVES

New York 10022 . . . J. Barry Stanford, Frank Ryan, Murray Strelitz, Reinhold Publishing Corp., 430 Park Ave., 212-688-8600

Philadelphia 19107 . . . James A. Byrne, Reinhold Publishing Corp., 12 So. 12th St., 215-922-0346

Chicago 60603 . . . Eugene P. Eldridge, Reinhold Publishing Corp., 10 So. La Salle St., 312-726-1282

Cleveland 44114 . . . Michael Hayes, Reinhold Publishing Corp., East Ohio Bldg., 1717 East 9th St., 216-771-4011

Los Angeles 90045 . . . Clay S. Holden, Lynn Gaskill, Reinhold Publishing Corp., 8939 So. Sepulveda Blvd., 213-776-0552

San Francisco 94109 . . . Clay S. Holden, Lynn Gaskill, Reinhold Publishing Corp., 415-421-8080

Denver 80203 . . . Robert H. Heidersbach, Roy McDonald Associates, Inc., 846 Lincoln St., 303-825-3325

Houston 77006 . . . Frank N. Vickrey, Roy McDonald Associates, Inc., 3130 Southwest Freeway, 713-529-6711

Tulsa 74114 . . . Max C. Nelson, Roy McDonald Associates, Inc., 2570 South Harvard Ave., 918-742-9961

Great Britain and Western Europe . . . Brayton Nichols, The American Magazine Group, 44 Conduit Street, London, W. 1, England

Japan . . . Sumio Oka, International Media Representatives, Ltd., 2-4, 6-chome, Akasaka, Minatoku, Tokyo, Japan

PRODUCTION DEPARTMENT

Anne Forrest
*Advertising Production Manager*
*Analytical Chemistry*


*°See ad in ACS Laboratory Guide*


HAAKE

# CONSTANT TEMPERATURE CIRCULATORS

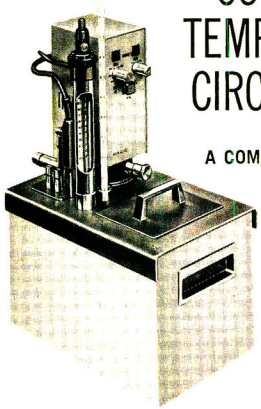

A COMPLETE LINE TO MEET ALL REQUIREMENTS

High, Intermediate, or Low Temperature

Open Baths • Closed Systems • Immersion Types

Rugged • Compact Easy to Operate

CONTROL TO ± .002°
OPERATING RANGE FROM —60° to +350°C

Excellent for use with refractometers, viscometers, calorimeters, spectrophotometers, distillation columns, auto analyzers, column chromatography, blood pH equipment, etc.

*COMPLETE LINE OF COOLING ACCESSORIES AVAILABLE*

*Call or write for detailed literature and list of dealers*

PSC PolyScience Corporation

2101 DEMPSTER ST. EVANSTON, ILL. 60201 312 475-2909

Circle No. 137 on Readers' Service Card

See ACS Laboratory Guide for All Products/Sales Office



# HTV's PHOTOMULTIPLIER TUBES




| | |
|---|---|
| R106 | Side-on, 1600 to 6500Å spectral response, Ultraviolet and visible region use |
| R136 | Side-on, 1600 to 8000Å spectral response, Wide range spectral sensitivity |
| R166 | Side-on, 1600 to 3200Å spectral response, Solar blind use |
| R196 | Side-on, 4000 to 12000Å spectral response, Visible and infrared region use |

*Many other photomultipliers made specially for your instruments.*

## INFRARED VIDICON TUBES



For use in infrared T. V. cameras; Spectral response covers 4000 to 24000Å; 500-TV lines resolution; Heater power is 0.95 watt.
N156=1 inch dia., 6 inches long
N157=1 inch dia., 5 inches long

photon is our business

OUR PRODUCTS
PHOTOTUBES■ PHOTOMULTIPLIER TUBES ■ PHOTOCONDUCTIVE CELLS ■ SPECIAL VIDICONS ■ INDUSTRIAL T.V. CAMERAS

## HAMAMATSU TV CO., LTD.

HEAD OFFICE = 1126 ICHINO-CHO, HAMAMATSU CITY, JAPAN
TELEX: 4225-185 JAPAN CABLE: HAMA TV HAMAMATSU JAPAN
EAST COAST = N. Y. OFFICE: c/o KINSHO-MATAICHI CORP.
80 PINE STREET, NEW YORK 5, N. Y., USA PHONE: DIGBY 4-6226
WEST COAST = AGENT: CALIFORNIA EASTERN LABO., INC; 1540
GILBRETH ROAD, BURLINGAME, CALIF. 94010 PHONE: 697-6670

Circle No. 46 on Readers' Service Card

See ACS Laboratory Guide for All Products/Sales Office

# Most Used ...because it's most useful.

It leads in editorial pages (230) and advertising pages (240). No wonder it generates far more inquiries (68,000) from laboratory chemists, life scientists, physicists, and engineers than any other guide.

The LAB GUIDE is where manufacturers say, "Here we are. Compare us with all our competitors, and our products with theirs."

It's the true one-stop buying source.

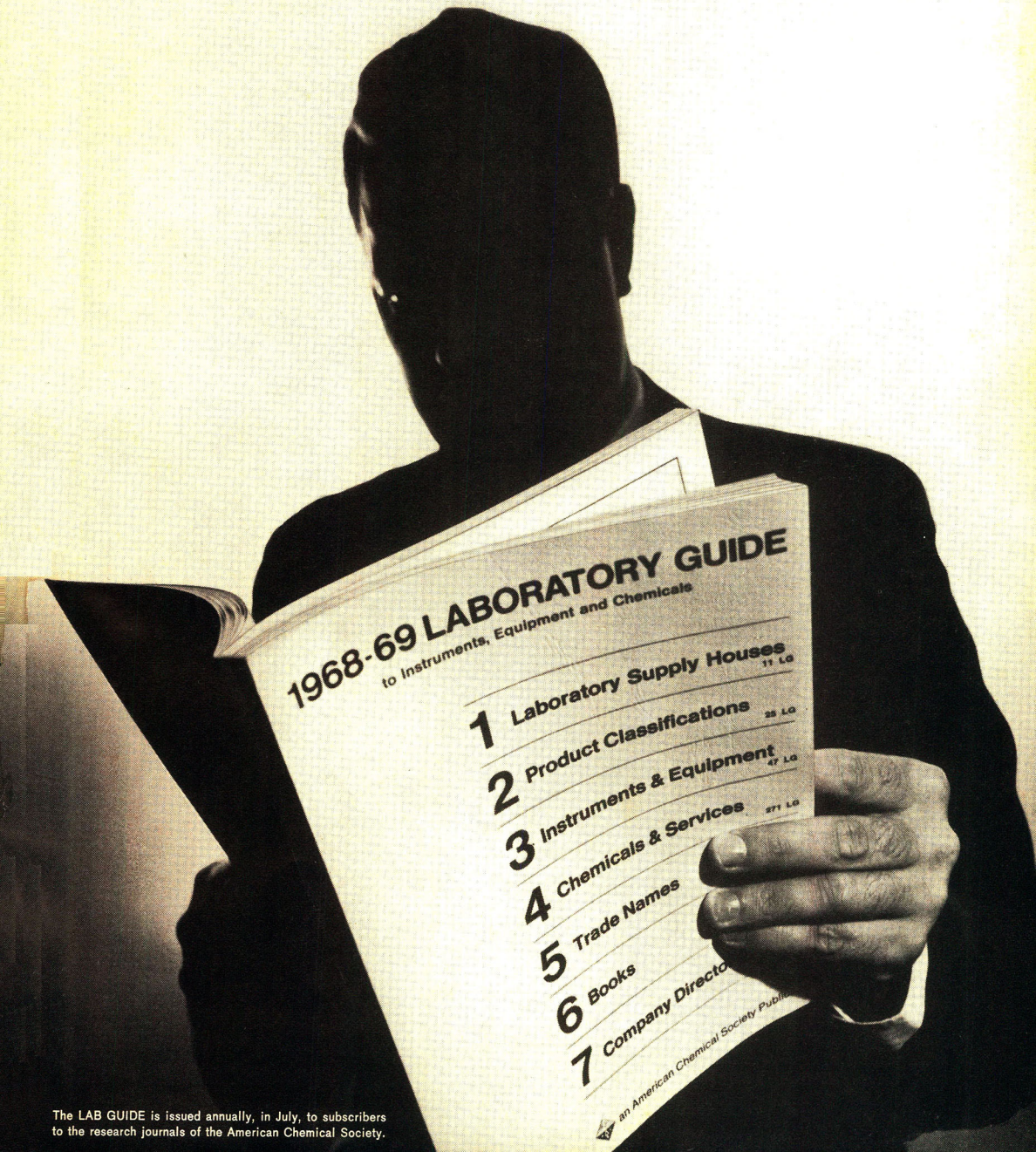


The LAB GUIDE is issued annually, in July, to subscribers to the research journals of the American Chemical Society.

now from regis

gas chromatography
kits
For Complete Analysis Of
- Monosaccharides
- Protein Amino Acids
- Purines & Pyrimidines
- Urinary Steroids

reagents
- **Regisil** . . . a new potent silylating agent for preparing trimethylsilyl derivatives for GC
- **TPC Resolving Agent** . . . for separation and measurement of amine and amino acid enantiomorphs
- **N-Heptafluorobutyrylimidazole** . . . for preparing volatile derivatives suitable for electron capture detection

And other unique GC reagents

accessories
- Pre-tested column packings
- Stationary phases
- Solid supports
- Other GC materials & supplies

For more information write for Regis GC literature.

*See us at Booth D-125, 53rd FASEB Meeting*

1101 N. Franklin
Chicago, Ill. 60610
REGIS

Circle No. 33 on Readers' Service Card

# FUTURE ARTICLES

**Polarographic Reduction of the Molybdate–Chlorate System in Biphthalate Medium**

Demetrios Kyriacou

**Analysis of Microsamples by Single Exposure Spark Source Mass Spectrometry**

P. Chastagner

**Electrochemistry of 8, 8′-Diquinolyldisulfide**

J. J. Donahue and J. W. Olver

**The Correction and Simulation of Polychromatic Optical Spectra**

John R. Morrey

**Quantitative Infrared Determination of Ammonium Ion in Hydroxylamine Sulfate**

Everett S. Whitehead

**Determination of Atmospheric Concentrations of Sulfuric Acid Aerosol by Spectrophotometry, Coulometry, and Flame Photometry**

F. P. Scaringelli and K. A. Rehme

**Computer Methods in Analytical Mass Spectrometry. Structure Codes in Processing Mass Spectral Data**

L. R. Crawford and J. D. Morrison

**A Reaction Rate Method for Ammonia and Blood Urea Nitrogen Utilizing a Pentacyanonitrosyloferrate Catalyzed Berthelot Reaction**

Theodore E. Weichselbaum, John C. Hagerty, and Harry B. Mark, Jr.

**Direct Spectrophotometric Determination of Sulfate in Natural Waters by Formation of the Ferric Sulfate Complex**

Reiner Goguel

**Spectrophotometric Determination of Iron with 2-Pyridyl-2′-Hydroxymethane Sulfonic Acid**

E. E. H. Pitt and V. M. Stanway

**Oxygen Distribution in Asphalts Used for Bituminous Paving**

W. E. Kuykendall, J. S. Hislop, and R. N. Traxler

**Preparative Thin-Layer Chromatography and High Resolution Mass Spectrometry of Crude Oil Carboxylic Acids**

W. K. Seifert and R. M. Teeter

**Computerized Learning Machines Applied to Chemical Problems. Investigation of Convergence Rate and Predictive Ability of Adaptive Binary Pattern Classifiers**

P. C. Jurs, B. R. Kowalski, T. L. Isenhour, and C. N. Reilley

**Computerized Learning Machines Applied to Chemical Problems. Multicategory Pattern Classification by Least Squares**

B. R. Kowalski, P. C. Jurs, T. L. Isenhour, and C. N. Reilley

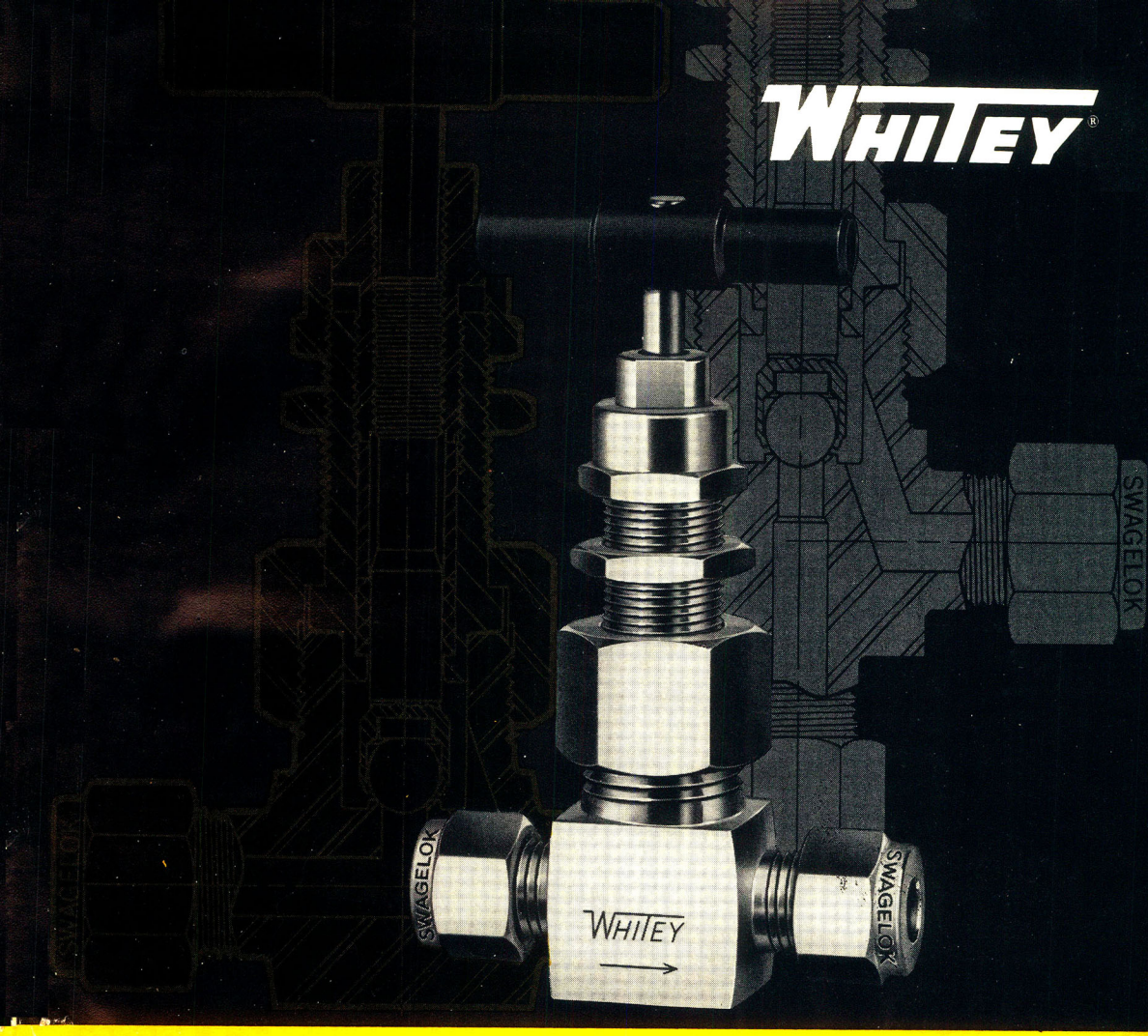


# This new WHITEY Valve was designed for reliability under the most severe service conditions!

This new WHITEY Ball Tipped Union Bonnet Valve is Teflon packed below the stem threads for trouble-free service.

A hardened Ball Stem Tip forms a bearing joint with the stem, which eliminates rotation between the ball and seat at closure. Thus, galling and scoring of the valve seat is prevented which allows repetitive, leak-tight shut-off.

WHITEY Ball Tipped Valves are designed for corrosive applications and for shut-off service on non-lubricating fluids such as gases, acids, solvents and many other chemicals.

*OTHER FEATURES INCLUDE*: 0.156″ orifice ● Adjustable Teflon packing while in service ● Low dead space ● Safety backseat ● 316 stainless steel barstock body and bonnet ● Metal to metal bonnet seal ● Universal mounting nut ● Color coded handles available ● SWAGELOK Tube Fitting or female pipe connections ● Pressures to 5000 psi ● Temperatures to 450°F ● 100% factory tested.

Whitey Research Tool Co./5679 Landregan Street/Emeryville, California 94608

Circle No. 84 on Readers' Service Card

SWAGELOK, T.M. CRAWFORD FITTING COMPANY • TEFLON, T.M. DuPont
©1969 by WHITEY RESEARCH TOOL CO./all rights reserved

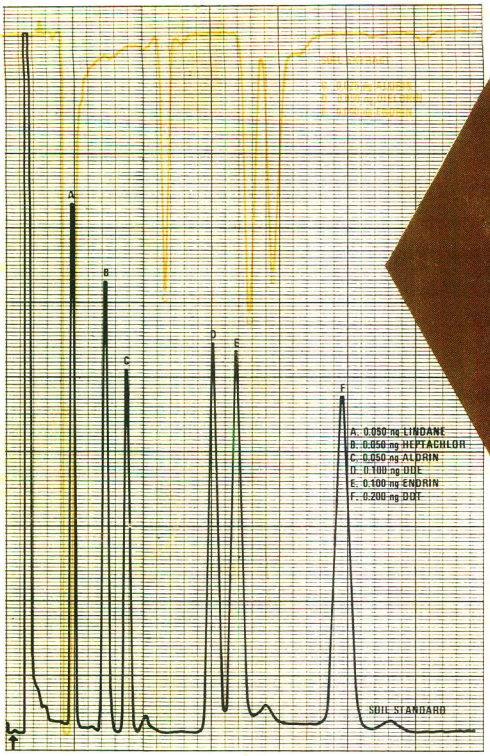


The above chromatogram was made with a MICRO TEK MT220 with quadruple inlets and two EC detectors.

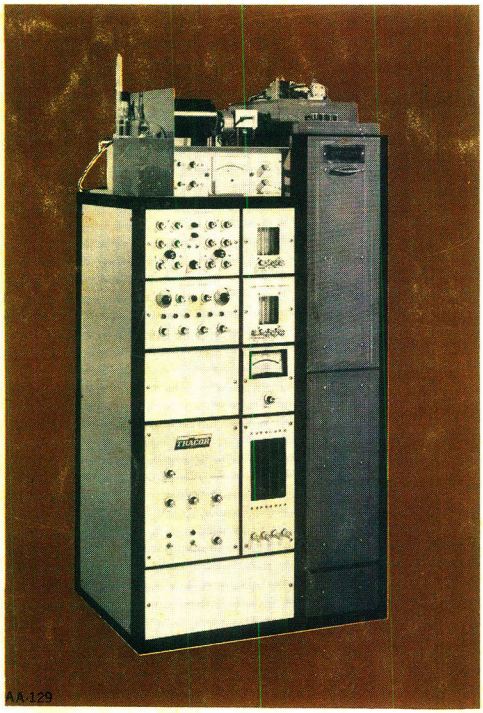


AA-129

# TAKE THE TWO BEST ELECTRON CAPTURE DETECTORS IN THE WORLD

If you come close to our sensitivity, you already have a Micro Tek high temperature EC system. If you equal it, you probably have one or more mounted on the ultimate chromatograph, the MT 220.

Micro Tek first demonstrated the superior performance of a nickel source (patent pending). Now all manufacturers offer it. But **only** MICRO TEK has the unique high temperature electron capture detector with "concentral" geometry which provides a $Ni^{63}$ sensitivity **superior to tritium** . . . the reverse of all others.

MICRO TEK's "concentral" geometry is the answer. It permits operation at higher DC voltages with reduced drift and improved sensitivity in either DC or Pulse Modes.

**MICRO TEK'S SECOND GENERATION DESIGN OF $Ni^{63}$ DETECTOR PROVIDES YOU:**

- Highest Sensitivity of any EC Detector
- DC or Pulsed Modes with continuously variable pulse height, width and rate
- Leak-tight system suitable for series operation with other detectors (FPD, CCD, etc.)
- Unsurpassed base line stability
- High temperature operation to 400° C.

For further information on how our $Ni^{63}$ or other superior detector technology can solve your problems, for sample examination or instrument demonstrations, contact

**Analytical Instruments Division**
**6500 Tracor Lane, Austin, Texas 78721 AC 512 926-2800**

***The Detectors Make the Difference***

TRACOR™

Circle No. 82 on Readers' Service Card

See ACS Laboratory Guide for All Products/Sales Office

- 3 F.O. 2512